Urban Landslide Hazard Mapping: A Case Study in Orinda, California, USA

SPECIAL PUBLICATION NO. 31

J. DAVID ROGERS, Ph.D., P.E, P.G., C.E.G., C.HG, F.ASCE, F.GSA

DAN WANG, Ph.D.

RUNE STORESUND, D.ENG, P.E., G.E., F.ASCE, SM.NAFE

ISBN 979-8-218-34276-0

90000>

9 798218 342760

Downloaded from http://pubs.geoscienceworld.org/aeg/eeg/article-pdf/31/1/i/6130855/i1558-9161-31-1-i.pdf
by AEG RBAC user

Urban Landslide Hazard Mapping: A Case Study in Orinda, California, USA

J. DAVID ROGERS*

Department of Geological Engineering, Missouri University of Science and Technology, Rolla, MO 65409

DAN WANG*

Department of Geological Engineering, College of Environment and Civil Engineering, Chengdu University of Technology, Chengdu 610059, Sichuan, China

RUNE STORESUND

Storesund Consulting, Kensington, CA 94707

PREFACE

In the early 1990s, Dr. J. David Rogers and his team of geologists at the consulting firm Rogers/Pacific in the San Francisco Bay Area began to compile a database that included a map catalog of the geology lying beneath the rolling hills of Orinda, CA to gain a better understanding of the physical factors most often responsible for triggering landslides. These physical parameters were split into four general groups: 1) sites that had never previously been involved in active landsliding; 2) hillside sites that had been involved in prehistoric slope movements but never modified to increase their stability; 3) sites that had never previously experienced slope instability; and 4) sites that failed after multiple attempts to bolster their stability, usually through the application of mechanical stabilization and drainage.

It took their team of geologists nine months to carefully record the various geologic units nestled along the northeastern flank of the Berkeley Hills coincident with the Alameda-Contra Costa County boundary. Rogers/Pacific, Inc. was charged with studying both the developed and undeveloped slopes within the newly incorporated City of Orinda, which had slightly more than nine square miles of landslide-prone hillsides. Wary of the legal challenges that might accompany such an ambitious undertaking, most geotechnical firms felt they could not afford to tie up at least six professional geologists and engineering geologists for so long a period, especially while having to operate across private property lines to produce the nation's first geohazard map that would include all of the legal boundaries and recorded easements.

It turned out that only about 13% of Orinda's exposed slopes had been developed by mass grading or engineered retention structures. Underdeveloped portions of Orinda were infamous for having spawned hundreds of stability problems on a remarkable range of scales (between a few cubic yards upwards of one million cubic yards. These included road closures of commuter highways and the Bay Area Rapid Transit District's (BART) commuter trains, which began operations in 1972. Materials were excavated to reconfigure the twin-tunnel portals of the proposed Orinda BART Station between the east and westbound lanes of State Highway 24. After the first week of excavation in 1969, insipient landslide movements began appearing, alerting everyone to significant unforeseen problems. These unexpected slides were slowly creeping towards Highway 24 and the BART Station. Costs of the right-of-way improvements eventually required six years and $360,000 to complete the first round of landslide repairs. BART had previously agreed to share the cost of any "remedial grading" with the California Department of Transportation (CALTRANS) for ten years after the initial completion of all BART improvements, just in case any of the sloping areas failed unexpectedly.

*The first two authors contributed to this book equally.

Downloaded from http://pubs.geoscienceworld.org/aeg/eeg/article-pdf/31/1/i/6130855/i1558-9161-31-1-i.pdf
by AEG RBAC user

The staff at Rogers/Pacific studied a wide range of landslide mapping options before selecting the type they would perform. Orinda's Town Council felt that their property owners expressed the most interest in some sort of map that would summarize what was known or inferred about all of the mapped geohazards easements and property lines and their respective scales. They reasoned that the best example locales for landslides are those with the highest activity levels, measured over the longest time spans.

Rogers/Pacific made their argument that funding an in-depth study of the comparable risk of future mass movements might be based on pre-existing conditions (areas where landslides had previously formed) in the recent geologic past overlain on a present-day County property/parcel map as one of the operable "database maps," along with orthophoto topographic map as a companion base map that would record and illustrate recognizable changes in land use, such as site grading and drainage, and highway improvements that any property owner should be able to afford (typically less than $5 in 1993).

By using a recorded public document such as a parcel map, all of the city's property owners and building officials would have affordable access to pay a small fee to reproduce detailed maps of their respective lots and boundaries, as would the various city, school districts, regional park district, public utilities, transportation agencies, and adjoining lands of Alameda and Contra Costa Counties, much of which remains rural and unincorporated.

Orinda had suffered more landslide-induced property damage over the previous 100 years than any other community in the USA. The Orinda area was studied by the U.S. Geological Survey's Engineering Geology Branch between 1956 and 1993. The Lafayette-Orinda-Moraga (Lamorinda) area was also covered by historic stereo-pair aerial photography dating back to 1928. The most desired information for property owners was the perceived threat of prehistoric movement, which abounded, especially beneath blankets of eroded soils, colluvium (slope wash), and alluvium. The landslide maps represent an in-depth study of the comparable risk of future mass movements based on pre-existing conditions beneath the ground surface (where landslides have previously formed).

In summary, this book is a pioneering work that not only provides crucial geological information but also sets a benchmark for geohazard mapping and urban planning. It serves as a valuable resource for professionals, policymakers, and property owners, highlighting the importance of geological awareness in mitigating the risks associated with landslides and surficial deposits in urban areas.

Downloaded from http://pubs.geoscienceworld.org/aeg/eeg/article-pdf/31/1/i/6130855/i1558-9161-31-1-i.pdf
by AEG RBAC user

CONTENTS

Downloaded from http://pubs.geoscienceworld.org/aeg/eeg/article-pdf/31/1/i/6130855/i1558-9161-31-1-i.pdf
by AEG RBAC user

Downloaded from http://pubs.geoscienceworld.org/aeg/eeg/article-pdf/31/1/i/6130855/i1558-9161-31-1-i.pdf
by AEG RBAC user

Downloaded from http://pubs.geoscienceworld.org/aeg/eeg/article-pdf/31/1/i/6130855/i1558-9161-31-1-i.pdf
by AEG RBAC user

Downloaded from http://pubs.geoscienceworld.org/aeg/eeg/article-pdf/31/1/i/6130855/i1558-9161-31-1-i.pdf
by AEG RBAC user

INTRODUCTION

This special publication summarizes the processes employed in the preparation of a state-of-the-art map of landslides and other surficial deposits within the city limits of Orinda, CA. This mapping has been prepared in a digitized georeferenced format. The base map for the mapping was prepared at an original scale of 1 in. = 300 ft (1 cm = 36.0 m), based on orthophoto topographic base maps prepared from aerial photos imaged in June 1991. We note that an orthophoto is a photo image that has been corrected so that its scale is uniform across the image. A topographic map is made from photographs, but the photos themselves are not rectified. These are two distinct products, and orthophotos are not used to produce topographic maps. When topographic maps are produced from aerial photographs, it is implied or could be described as being photogrammetrically derived.

This effort was one of the most detailed municipal assessments of earth movement ever attempted in the San Francisco Bay-Delta area. These were also the first landslide maps in the United States produced on assessor's parcel maps, so end users could easily percieve-property boundaries and street addresses, which are shown on the base maps. Orthophoto topographic maps were also prepared to aid related engineering, planning, emergency preparedness, and environmental studies.

The landslide maps were originally produced (early 1990s) on a DXF format AutoCad 11 software file base, along with hard copy reproducible transparencies at the original scale of 1 in. = 300 ft (1 cm = 36.0 m). This scale was intended to be compatible with the tax assessor parcel maps maintained by the Contra Costa County Department of Public Works (County). The County parcel base maps delineate each lot and its respective street address. These maps are available to the public in a number of configurations: in full-size single sheets at a scale of 1 in. = 300 ft (1 cm = 36.0 m); in a bound volume containing all of the maps at half scale (1 in. = 600 ft [1 cm = 72.0 m]); and in georeferenced electronic files.

Limitations Inherent to Reconnaissance Geologic Mapping

By necessity of scale, the landslide and surficial deposits mapping was accomplished on a reconnaissance level, usually without on-site verification, subsurface sampling, or review of geotechnical reports that may have been prepared for historic development within the City of Orinda (City). That said, all known published references were reviewed for relevance to this project. Given these limitations, all of the mapping is subject to revision by more detailed, site-specific work performed by licensed professionals familiar with the engineering geology of Orinda.

If local geoscience consultants disagree with the various interpretations, they may employ independent field investigations to verify or disclaim the existence of landslides. By far, the best method to investigate deep-seated prehistoric slope movements is by using down-hole logging of large-diameter (bucket auger) borings. In this method, an engineering geologist can view the three-dimensional structure to either confirm or disprove the existence of prehistoric slides (Lebarre, 1936; Scullin, 1994; and Johnson and Cole, 2001).

This volume seeks to point out the economic utility of urban landslide mapping, first by way of historic experience with earth movement in the Orinda area and a brief summary of the underlying geologic framework. The balance of this volume seeks to explain the methodologies employed by engineering geologists and geotechnical consultants in preparing the accompanying landslide hazard maps.

Downloaded from http://pubs.geoscienceworld.org/aeg/eeg/article-pdf/31/1/i/6130855/i1558-9161-31-1-i.pdf
by AEG RBAC user

PURPOSE OF STUDY

The purpose of this study was to provide City staff and residents a definitive map of surficial geomorphic features covering the City of Orinda at a scale useful to individual parcel owners. These maps can also be utilized by City staff to assist in engineering, planning, and disaster relief/response concerns, as well as by real estate interests and the general public.

An example of earth-movement-related distress common to Orinda is that of recurring settlement or extension of pavement and buried utilities along the lateral margins of dormant landslides. Due to contrasting consistency and creep susceptibility of landslide deposits (Rogers and Chung, 2016), structures constructed across slide boundaries tend to exhibit long-term manifestations of imperceptibly slow earth movement, commonly termed slope "creep" (Sharpe, 1938b). Although less visible than storm-related earth movement, this style of distress causes the greatest property loss in Orinda, often requiring perpetual maintenance.

Another purpose of the landslide maps is to aid in planning-level decisions associated with future development. For instance, if a development application were contemplated on a parcel shown to be an active landslide, City staff would likely require a more extensive geologic analysis of the site. In other cases, a review of the slide maps might reveal a benign site in terms of geologic hazards, allowing the building official the option of waiving a geologic report as part of a building permit application (although a foundation engineering report might still be required).

Individuals contemplating the purchase of private parcels should also derive benefit from the maps by apprising themselves of potential geologic hazards before purchasing a parcel. These individuals can inform themselves about the types of geologic hazards City staff will require to be addressed by an engineering geologic consultant before that consultant's services are engaged.

These regional maps are not intended to replace or supersede a site-specific study prepared for a parcel. In such cases, the maps simply provide an overview (or notification, as the case may be) for private geotechnical consultants working within the City's jurisdiction as to the hazards that they should be aware of, should consider, or will be required to address in their respective consultations.

The stated intent of the landslide maps is to make qualitative suggestions for planning purposes and to lay the burden-of-proof of such mapped features on the applicants/parcel owners or their consultants. No other purpose is envisioned, such as property devaluations, condemnation, or re-zoning, although the geologic information contained in the maps could be utilized in planning-level decisions.

Electronic Georeferenced Files

The mapping effort was intended to be compatible with the tax assessor parcel base maps employed within the County. The assessor parcel maps are prepared on a base scale of 1 in. = 300 ft (1 cm = 36 m) and were initially digitized in 1990. The assessor parcel maps clearly delineate the areal limits of property lines and the street addresses of each parcel.

Concurrent with this study, in 1994–95, the City entered aerial photographic images of the county tax assessor parcel maps and storm-water discharge data onto geographic information system (GIS) overlays compatible with the County's Intergraph GIS base. The City then purchased the computerized assessor's base maps so that they could manipulate their landslide, topography, and flood-related databases in-house. In this manner, additional "layers" of information were progressively added or annotated, as the need arose.

IMPACT OF EARTH MOVEMENT ON DEVELOPMENT OF ORINDA

Introduction

Since the very earliest development of Orinda in the late 1800s, the area has been plagued by landslides. These slides generally occur in the winter and spring months during years of extranormal precipitation (Kachadoorian, 1956, 1959; Radbruch and Weiler, 1963; and Nilsen and Turner, 1975). The significance of rainfall in initiating landslides depends on cumulative antecedent moisture, which is moisture that has occurred within the previous 60 days (2 months) prior to a particular storm, as well as additional precipitation in the preceding days and months. Peak 24-hour (period 1981–2020), peak 30-day (period 1895–2020), and peak 3-year (1895–2020) running averages are presented in Table 1.

Let us now consider the development of Orinda and the roles landslides and earth movements have played in that development.

The First Roads

In July 1850, Contra Costa County was partitioned into road districts (Sorrick, 1986), a few months before California achieved statehood. Two roads crossed the Orinda area: County Road No. 5 connected the Moraga redwood groves with Martinez (via Lafayette), while Road No. 6 connected the Victor Castro adobe (on what is now El Cerrito Plaza) around San Pablo Ridge, up San Pablo Creek to Lauterwasser Creek (in Orinda), thence up over the Miner Road divide into Lafayette through Elam Brown's ranch (upper Happy Valley), and

Downloaded from http://pubs.geoscienceworld.org/aeg/eeg/article-pdf/31/1/i/6130855/i1558-9161-31-1-i.pdf
by AEG RBAC user

Table 1. *Comparison of 1-day, 1-month, and 3-year highs in rainfall in the Orinda area 1895–2020.*

Peak 24-Hour Events (24 Hours)*	Peak 30-Day Events (Avg over 30 Days)**	Peak 3-Year Running Averages**
Oct 1962 (8.40 in./21.3 cm)	1955-12 (18.77 in./47.7 cm)	1981–83 (65.37 in./166.0 cm)
Jan 1982 (6.98 in./17.7 cm)	1911-01 (17.61 in./44.7 cm)	1980–82 (56.26 in./142.9 cm)
Oct 2009 (4.70 in./11.9 cm)**	1986-02 (16.72 in./42.5 cm)	1994–96 (46.60 in./118.4 cm)
Dec 2014 (4.14 in./10.5 cm)**	1916-01 (16.54 in./42.0 cm)	1939–41 (45.43 in./115.4 cm)
Jan 1967 (3.95 in./10.0 cm)	1909-01 (16.36 in./41.6 cm)	1996–98 (43.12 in./109.5 cm)
Jan 2006 (3.32 in./8.4 cm)**	2017-01 (15.34 in./39.0 cm)	1967–69 (42.58 in./108.2 cm)
Nov 1982 (3.31 in./8.4 cm)**	1998-02 (15.25 in./38.7 cm)	1979–81 (40.23 in./102.2 cm)
Oct 1991 (3.31 in./8.4 cm)**	1914-01 (14.68 in./37.3 cm)	1968–70 (39.45 in./100.2 cm)
Feb 1987 (3.22 in./8.2 cm)	1983-03 (14.66 in./37.2 cm)	1950–52 (37.94 in./96.4 cm)
Jan 1982 (3.19 in./8.1 cm)	1962-10 (14.50 in./36.8 cm)	2004–06 (36.27 in./92.1 cm)
Dec 1981 (3.17 in./8.1 cm)	1970-01 (13.39 in./34.0 cm)	1940–42 (35.39 in./89.9 cm)
Nov 1984 (3.11 in./7.9 cm)	1907-03 (13.36 in./33.9 cm)	1973–75 (32.70 in./83.1 cm)
Dec 1969 (3.10 in./7.9 cm)	2005-12 (13.23 in./33.6 cm)	1995–97 (27.81 in./70.6 cm)
Feb 1986 (3.08 in./7.8 cm)	1902-02 (13.17 in./33.5 cm)	1982–84 (26.47 in./67.2 cm)
Jan 2000 (3.02 in./7.7 cm)	2014-12 (13.12 in./33.3 cm)	1983–85 (21.61 in./54.9 cm)

* This is a Berkeley rainfall record. McCarty and Bryant (1962) and Brown (1982) reported rainfall in excess of 16 in. (40.6 cm) over 48 hours during the October 1962 storm, which makes it the 24-hr storm-of-record, with the January 1982 storm delivering approximately 8+ in. (20+ cm) over 31 hours.
** Oregon State PRISM daily data from 1981 to 2020.

finally to the Moraga-Martinez Road near Jonah Bernell's home (in lower Happy Valley).

Orinda was initially settled by emigrants traveling up San Pablo Creek, from the direction of present-day El Sobrante and Richmond. The first road serving Orinda appears to have been cut sometime around 1850, along old County Road No. 6, described above. At the drainage divide between Happy Valley and Lauterwasser Creek, another road was soon graded northward, towards the Felipe Briones adobe, along what is now Bear Creek Road. Later in the 1850s, this road was extended to Martinez through the Briones Rancho and christened Briones Road. The Briones Road followed Bear Creek, climbing the watershed divide along the north fork and dropping into upper Alhambra Creek watershed, and then following that watercourse into Martinez. This route serves as the main entry into Briones Regional Park from the Bear Creek side and can still be driven upon between its terminus with Alhambra Valley Road (just west of the latter's intersection with Reliez Valley Road) and the East Bay Regional Park gate (approximately 3 mi [4.8 km]). Old Briones Road can then be followed by foot through Briones Regional Park.

Contra Costa Road Ordinance of 1852

Contra Costa County enacted its first road ordinance in 1852, requiring all males 18 to 45 years of age to contribute 5 days of road work per year, or have a substitute work for them, when the supervisors or overseers of the county road districts needed them (Young, 1954; Sorrick, 1986). "Road work" at that time consisted of building and maintaining key wooden bridges, as well as infilling ruts, which often formed during wet winters. It is likely that the County's action was made in response to heavy storm damage during the winters of 1849–50 and 1852–53, the effects of which are well documented, in the gold fields of the Sierra Nevada's Mother Lode as well as in Contra Costa County (Purcell, 1940).

During heavy winter rains, Contra Costa roads became so mired in mud as to be impassable prior to the advent of paving in the 20th century. Purcell (1940) reported that during the extreme winter storms of 1861–62, a total of more than 15 in. (38.1 cm) of rain was recorded in Martinez in a single week. Up until 1862, lower Pacheco Creek (which was fed by Walnut, Marsh, and upper Pacheco Creeks) had been a navigable channel for ocean-going ships! In 1862, the channel was permanently filled with silty sand, as were most of the principal watercourses serving the gold fields (Gilbert, 1917).

Using the County's rainfall correlations developed for the period 1873–1973 (Contra Costa County, 1977), we could expect Orinda to receive about 70 percent greater rainfall than Martinez, suggesting Orinda likely received about 25 in. (63.5 cm) of rainfall in the same period (January 4–11, 1862). This is the greatest precipitation event since establishment of historic rainfall records in the late 1800s (see Appendix 4).

The Telegraph Road and Public Highways (1858–60)

The first road connecting Orinda to Walnut Creek was cut in 1858 as part of the Oakland to Antioch telegraph line, servicing the bustling coal communities of eastern Contra Costa County and continuing onto the Comstock Lode mines in western Nevada. Known as the "Telegraph Road," this route ascended the crest of the East Bay Hills via Claremont Canyon, thence down the draw now served by Fish Ranch Road to the canyon floor presently occupied by Highway 24 (State Route 24), and

Downloaded from http://pubs.geoscienceworld.org/aeg/eeg/article-pdf/31/1/i/6130855/i1558-9161-31-1-i.pdf
by AEG RBAC user

thence to the intersection with roads leading to San Pablo and Martinez, known as the "Orinda Crossroads."

From the crossroads, the road climbed St. Stephen's Hill, following the current alignment of Mt. Diablo Boulevard through Lafayette and then over Saranap Ridge into Walnut Creek. In September 1859, a stagecoach began service, and settlers were soon claiming land adjacent to this new road. In May 1860, the road was declared a public "highway" (Sorrick, 1986). In 1860–61, the national Pony Express route used this alignment when their riders missed the Sacramento–San Francisco boat and were obliged to use the Benicia Ferry. The road's name was changed to "Summit Road" when an inn was constructed at the watershed divide between Fish Ranch Road and Claremont Canyon, at an elevation of 1,315 ft (401 m) above sea level.

California & Nevada Railroad Succumbs to Landslides (1894)

The earliest documented landslide problems in Orinda were recorded along the old California & Nevada Railroad, a narrow-gauge line built between Oakland and Orinda in 1888–90 (Willes, 1966).

According to Hanson (1988), distortion of the graded roadbed during winter rains in 1889–90 greatly hampered the construction of the original line between San Pablo and Bryant (Orinda Crossroads). During the severe rains of 1893–94, approximately 4 mi (6.4 km) of right-of-way were destroyed in the north Orinda area (Figure 1). This was a calamity for the fledgling railroad, which was unable to recover financially (Hanson, 1988). Moraga Way, between Orinda Crossroads and Moraga, was originally graded for the California & Nevada Railroad as their rail right-of-way in 1893. The California & Nevada Railroad sold its holdings to the Atchison, Topeka & Santa Fe Railway before the rails were laid from Orinda Crossroads to Moraga (Figure 2a and b). In 1922, this right-of-way became one of the first paved highways in Contra Costa County.

The High-Level Tunnel and Old Tunnel Road (1903)

By the end of the 1860s, residents on the eastern side of the East Bay Hills began to promote the construction of a tunnel approximately 500 ft (152 m) long that would advance through Grizzly Peak Ridge and improve entry into and out of Contra Costa County from Oakland. In 1871, a franchise was formed that excavated 300 ft (91.4 m) of the required 500 ft (152 m) before running out of funds.

In 1882, the tunnel idea re-surfaced, helped in part by some fatal accidents on the steep grade over Grizzly Peak Ridge. In 1895, County supervisors approved a survey on 0.75 mi (1.2 km) of alignment on the Contra Costa side of the abandoned tunnel excavation. In 1895, the Merchant's Exchange Club of Oakland (a forerunner of today's Chamber of Commerce) began promoting the excavation of a tunnel beneath the steep divide (Figure 3a and b). Lobbying both counties' Boards of

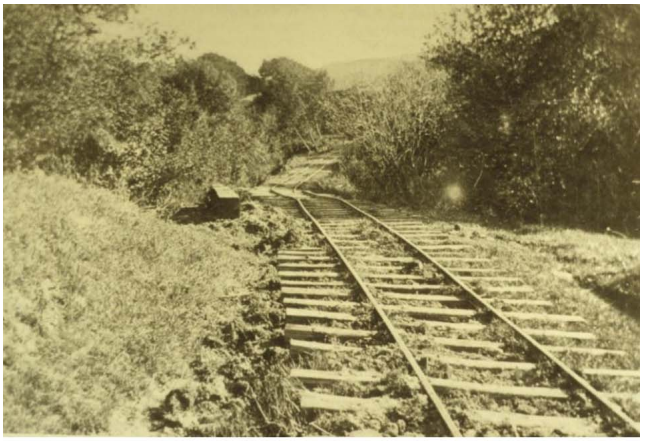

Figure 1a. Four miles (6.4 km) of the California & Nevada Railroad tracks south of Frenchman's Curve (what is now Kennedy Grove at San Pablo Dam) were impacted by massive earth movements during the wet winter of 1893–94. The fledgling railroad never recovered from these losses.

Figure 1b. Note how the rail line was initially built with a less expensive narrow gauge of 3 ft (0.9 m). The intention was to later upgrade to a standard gauge (4 ft 8.5 in. [1.4 m] width) as more business developed (Contra Costa County Historical Society).

Figure 2a. The California & Nevada Railroad's Narrow Gauge Consolidated Engine No. 3 at Bryant Station, the end of the line in 1892 (Willes, 1966).

Downloaded from http://pubs.geoscienceworld.org/aeg/eeg/article-pdf/31/1/i/6130855/i1558-9161-31-1-i.pdf
by AEG RBAC user

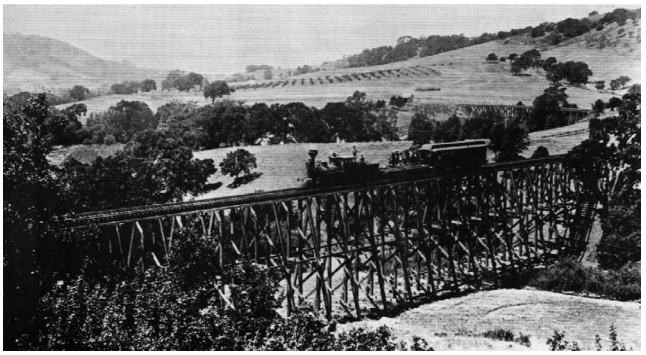

Figure 2b. One of the California & Nevada Railroad's classic timber trestles, spanning an ephemeral stream that now bounds the 18th Fairway of the Orinda Country Club golf course graded in the mid-1920s (Willes, 1966).

Figure 3a. Steam-powered shovel excavating Old Tunnel Road just west of Orinda Crossroads around 1902. With the completion of the old Broadway High Level Tunnel the following year, this became the primary link with Oakland between 1903 and 1937 (Contra Costa County Historical Society).

Figure 3b. Eastern portal of what came to known as the "High Level Tunnel" was excavated off-and-on for over 6 years (1897–1903). It officially opened on November 4, 1903. The new tunnel was 1,100 ft (335.3 m) long and two narrow (wagon-width) lanes in wide, and it eliminated 320 ft (97.5 m) of rise from the grade of the old Telegraph Road (Willes, 1966).

Supervisors, by 1897, the Merchant's Exchange agreed to fund 1/5 of the tunnel's cost, with Alameda and Contra Costa Counties each contributing 2/5 of the new tunnel's projected length. This arrangement went through a series of false starts and cost adjustments associated with increased cost of excavation more deeply into the ridge because the rock was less weathered with distance from either portal. In addition, the tunnel muck had to be transported farther away from the portal on the bay side, which was considerably higher elevation that resulted in steeper grades approaching the eastern portal (from OrindaCrossroads)

More Storms and Slide Damage (1912–15)

Despite completion of the new tunnel in 1903, soil conditions along the road alignment were so treacherous that the road became difficult to maintain through heavy storms. In 1912, a section of the road between Fish Ranch (near what is now the Gateway exit on Highway 24) and the tunnel's east portal failed, closing the road for more than 6 months (this was the same location where sliding plagued the highway in the early 1940s, described later). A 20-man crew was kept busy trying to repair the road, which re-opened in June 1913 (Sorrick, 1986). During the closure, the tunnel floor was lowered by 2 ft (0.6 m) to provide increased clearance for gas-powered vehicles and paved with asphalt.

In the winter of 1914–15, the road failed again. This time the slide was so large that it necessitated closure of the road for almost an entire year, re-opening in July 1916. Scrutiny of the aerial photos of Old Tunnel Road taken in February 1928 suggests that the entire eastern slope below the tunnel's Contra Costa (eastern) portal appears to be an ancient bedrock landslide (later confirmed by Louderback, 1930), portions of which appear to have been reactivated by road cuts made for Old Tunnel Road around the turn of the 20th century.

Establishing Connecting Roads to Orinda (1923–29)

In 1903, the first tunnel was completed (Figure 2), forming a paved link between Oakland and Walnut Creek along the route now occupied by Highway 24. This became the main thoroughfare into and out of Orinda. Between 1910 and 1922, automobile traffic increased by a staggering 1,900 percent! In 1919, Contra Costa residents passed a $2.6 million (1919 dollars) highway construction bond issue by a 20 to 1 margin (Dalton, 1954). Between July 1919 and mid-1923, 73 mi (117.5 km) of concrete roadway and 37 mi (59.5 km) of macadam-surface roadways were constructed in Contra Costa County. These included many of the transportation corridors still in use today: State Route 21 down the San Ramon Valley (now Interstate 680), a highway between Martinez and Albany,

Downloaded from http://pubs.geoscienceworld.org/aeg/eeg/article-pdf/31/1/i/6130855/i1558-9161-31-1-i.pdf
by AEG RBAC user

via Richmond (following the Carquinez Straits), and Route 75 (most of what later became State Route 24) between Walnut Creek and Oakland.

An interesting feature of these early highways was the use of 8-ft-wide (2.4-m-wide) concrete traffic lanes separated by a 4-ft-wide (1.2-m-wide) macadam divider strip (shown in Figure 4). As can be appreciated from the picture, slow-moving vehicles were passed at the driver's own risk. Many of these early highways were so well built that they were not replaced until the late 1950s (Dalton, 1954).

The introduction of the automobile to middle citizens in the 1920s, coupled with this new all-weather highway alignment into Orinda, brought the first real estate boom to Orinda. The town's first gas station and restaurant opened in 1920. Luring residents to sunny Orinda from the Oakland–East Bay plain necessitated an improved vehicular corridor. The highway between the Orinda Cross Roads and the 1903 tunnel was overlaid with asphalt in 1926–27 and enlarged to an 18-ft-wide (5.5-m-wide) concrete pavement section in 1931. This was when the highway was named "Mount Diablo Boulevard" and designated as Sign Route 24 of the State Highway System by act of the State Legislature (Young, 1954).

Other roads leading into Orinda were completed around this same time. These included Wildcat Canyon Road, with connection to El Toyonal. It had been graded in 1882 as a toll road alternative to the Telegraph Road. After the failure of the initial Contra Costa tunnel excavations in 1887, the County appropriated funds to extend "Wagner Road" (through Wagner Ranch) up over the hills, from El Toyonal, crossing the crest of San Pablo Ridge at Inspiration Point (in what is now Tilden Park), and then across and along Wildcat Valley, crossing the crest of Grizzly Peak Ridge in the saddle now occupied by Summit Reservoir (on the Berkeley-Kensington border), operated by East Bay Municipal Utility District (EBMUD). This route became known as the "Berkeley Road," and it flourished through the 1890s. Between 1935 and 1937, the present alignment was excavated and paved after the East Bay Regional Park District was formed and Tilden Park was being developed.

Figure 4. View along the uphill grade of Old Tunnel Road, between the Orinda Crossroads and the old tunnel. In 1921, the old grade was paved with two lanes of concrete and a gravel median to accommodate passing of slower vehicles, like the wagon pictured here. A few years later, the entire right-of-way was overlain with asphalt).

Old San Pablo Dam Road was constructed and paved by Contra Costa County in cooperation with the East Bay Water Company (predecessor of EBMUD) between 1920 and 1923, when San Pablo Dam was under construction. In 1956, San Pablo Dam Road was re-configured to a high-speed alignment utilizing federal funds for secondary highways and a county-wide bond measure. The cut slopes along this alignment have been plagued by differential erosion and occasional deeper-seated landslides ever since.

As mentioned previously, the old California & Nevada Railroad grade connecting Orinda Crossroads to Moraga (Moraga Way) was paved in 1922, and became the main road between Lafayette and Moraga, replacing the old Jonas Hill Road in 1926–27. In 1944, the wooden flumes route was renamed "Moraga Road."

Early Subdivisions (1876–1926)

The town's first subdivision was laid out in 1876. Termed "Orinda Park," it was located about 2 mi (3.2 km) north of what is now State Route 24, along either side of Camino Pablo. However, the envisioned real estate boom did not materialize for another 50 years. Consumer interest in Orinda was influenced by the introduction of affordable automobiles like the Model T.

The early subdivisions included: Orinda Park Terrace (1921) in the El Toyonal area; Encinas de Moraga (1922) along the west side of Moraga Way, just south of the Crossroads; Lake Cascade Dam (1922); commercial lots for Orinda Village (1923); Hacienda Homes (1923) north of the Country Club; the 159-acre (0.6-km^2) Orinda Country Club development (1924 onward), containing Orinda Units 1 through 9; and the Oak Springs Units 1 through 4 on the slopes southwest of the Orinda Crossroads (along either side of Beatricia, Barbara, and Oak Roads), commencing in 1925–26. Other tracts followed later, such as the Charles Hill Circle area, subdivided by Vernon Hardy in 1935.

The style of land development in the 1920s and 1930s was inexpensive and accomplished without much regard for engineering or geologic input. Local pioneer/entrepreneurs, like Miguel de Laveaga, simply graded the roads portrayed in their "paper subdivisions" with "Fresno scrapers," commonly employed by farmers using four-mule pulls (Figure 5a).

Virtually all of the early subdivisions and Country Club were constructed in this manner, with 0.5-cubic-yard (0.4-m^3) increments of soil shaved off a hillside and dumped in a lower area in one continuous motion. Prior to 1950, no attempt was made to physically "key" the fills into the adjacent sloping ground or to mechanically

Downloaded from http://pubs.geoscienceworld.org/aeg/eeg/article-pdf/31/1/i/6130855/i1558-9161-31-1-i.pdf
by AEG RBAC user

Figure 5a. Grading of the first roads for a new subdivision near Orinda Crossroads around 1922. Most of the early roads were graded by four-mule teams pulling 0.5 cubic yard (0.38 m^3) "Fresno graders," or scrapers, as shown here. Prior to 1950, there was very little mechanical compaction of fill soils (Orinda Historical Society).

Figure 5b. Grading of the 18th fairway of the Orinda Country Club in 1924 with horse or mule-drawn Fresno scrapers. In those days, no attempt was made to excavate "shear keys" into the native slopes. Many of these slopes were underlain prehistoric landslides (Orinda Historical Society).

compact the fill lifts being placed (Figure 5b). Many of these early grading projects experienced slope instability decades later.

Landslide at Lafayette Dam (1928) and EBMUD Service (1934)

During construction of Lafayette Dam in September 1928, a large landslide occurred within the downstream shell of the embankment, causing a 2-year delay in its completion. It appears that the earthen structure had been founded on relict landslide and colluvium deposits infilling the canyon floor. These soft foundation materials subsequently gave way under the newly imposed weight and loading of the dam's earth fill embankment). The failure drew national attention and was termed "excessive settlement" by the EBMUD (Bowers, 1928; Engineering News Record, 1928, 1929a, 1929b).

In 1934, EBMUD began utility service to Orinda, following completion of the Mokelumne Aqueduct in 1931 between the Lafayette, San Pablo, and Upper San Leandro storage reservoirs. This distribution system included a series of tunnels. One of these is approximately 3 mi (4.8 km) long between Lafayette and San Pablo Reservoirs and runs beneath the Orinda hills just north of Charles Hill Circle. This tunnel is 8 ft (2.4 m) in diameter and was completed in 1929 (Danehy, 1969). The EBMUD Mokelumne Aqueduct feeding into the East Bay was enlarged in 1947–49 and again in 1960–63, tripling the original capacity of the aqueduct.

Broadway Low Level Tunnels, a New Highway, and Bus Service (1934–41)

In 1928, Contra Costa and Alameda Counties agreed to form Joint Highway District (JHD) 13. JHD 13 contemplated the construction of a modern high-speed highway extending from Oakland to Walnut Creek. Studies for a pair of low-level tunnels began in early 1928, with University of California, Berkeley (Cal Berkeley) geology professor George D. Louderback serving as the principal geologic consultant for the feasibility studies (Louderback, 1930). After considering input from this body, in 1931, the State Legislature appropriated funds to construct a state highway from Walnut Creek to the Contra Costa (eastern) portals, including new low-level vehicular tunnels.

The twin Broadway Low Level Tunnels (renamed the Caldecott Tunnels in 1960) were situated 310 ft (94.5 m) lower than the 1903 tunnel, extending 3,160 lineal feet (963 m), with an inside diameter of 22 ft (6.7 m); these tunnels were lined with concrete and provided with a forced-air ventilation system capable of supplying fresh air during traffic jams. The original twin bores were situated 150 ft (45.7 m) apart. The first contract was awarded to Six Companies, Inc., comprised of Kaiser, Bechtel, Shea, Morrison-Knudsen, and Warren Brothers. These firms had just completed the Boulder Canyon Project, which included Hoover Dam. The Boulder Canyon Project cost, $156 million, and it was the largest line-item appropriation ever approved by the U.S. Congress prior to 1931.

During tunnel excavation, Six Companies and the JHD became embroiled in a claims dispute over the need for additional steel supports. After a workman's death in a fault zone encountered in the north bore, Six Companies sued for additional compensation, but Joint Highway District No. 13 prevailed in the court proceedings. At this juncture, the job was about two-thirds complete.

Downloaded from http://pubs.geoscienceworld.org/aeg/eeg/article-pdf/31/1/i/6130855/i1558-9161-31-1-i.pdf
by AEG RBAC user

When the highway district re-advertised the partially completed job, maverick contractor George D. Pollack of Sacramento was the only bidder, and he completed the project on time and on budget in the fall of 1937, much to everyone's surprise (Gerwick and Woolery, 1983).

In November 1937, the twin Broadway Low Level Tunnels were officially opened, bringing a high-speed four-lane highway to Orinda (Figure 6). This event revived the dismal real estate activity of the depression years (1929–40). The lots subdivided some 10 to 15 years earlier could now serve commuters using their own automobiles.

In 1940, Rhodes States, Inc., bus lines inaugurated service from Orinda to Oakland and points beyond. This line was assumed by Greyhound Bus Lines 1 year later. In 1941, the Sacramento Northern Railroad ended passenger service along their short line running from Sacramento to Oakland via Concord, Walnut Creek, and Moraga. They began running a bus service between St. Mary's College and the Oakland Key System (or Key Route) terminal at the eastern terminus of the San Francisco–Oakland Bay Bridge. The Key System featured a morning and evening commuter stop in Orinda. A commuter parking area for bus riders emerged in the years following World War II and enjoyed widespread use until the Bay Area Rapid Transit (BART) District began passenger service along their new lines in 1972–73.

An upturn in defense-related construction, the increasing affordability of cars, and half-hour commute times to Oakland and Berkeley attracted buyers by the dozens, most searching for affordability over ambiance. Orinda did not open its first grocery store until 1943. In 1941, the Orinda Improvement Association was formed as a successor to Hacienda Homes and was the first entity of its type to impact almost every aspect of the community's development style.

Figure 6. View looking east from Pleasant Hill Road at the newly completed State Route 24 in November 1937. The original alignment was three full lanes of asphalt, designed for speeds of 50 mph (80 kph). The middle lane was for passing. A fourth lane was added in 1943 between the Broadway Tunnels and St. Stephen's Hill (Contra Costa County Historical Society).

The First Orinda Slide (1936–37)

In 1934, one of the largest road cuts made for State Highway 75 (re-designated as Highway 24 in 1952) was completed about 0.5 mi (0.8 km) west of the Orinda Crossroads (Figure 7). The highway district's engineers had unknowingly severed the toe of an enormous relict landslide, nestled in the plunging axis of a prominent anticlinal fold. In the severe storms of October 1936 and those that followed in 1937–38 (McGlashan and Briggs, 1939), this relatively fresh cut slope failed, blocking the new highway and the requiring the excavation of a 30-ft-high (9.1-m-high) cut slope on the opposite side of the canyon to accommodate temporary diversion of traffic until the debris could be removed (Herlinger and Stafford, 1952). This extra space along the south side of the highway later proved to be useful when the slide reactivated and enlarged itself dramatically in December 1950.

One of the biggest cut slopes for the new route undermined a dormant landslide, which reactivated in 1941

Figure 7. Aerial oblique view of Orinda Crossroads taken on January 17, 1935. This image looks southwest along State Route 75 (today's Highway 24) while under construction.

Downloaded from http://pubs.geoscienceworld.org/aeg/eeg/article-pdf/31/1/i/6130855/i1558-9161-31-1-i.pdf
by AEG RBAC user

(Figure 7, arrow A). The opposing cut was made in the toe of the same slide, which accounts for its failure just a few years later. The remaining hill was removed as part of the emergency work that began in December 1950 to construct a temporary bypass for commuter traffic (Figure 7, vicinity of arrow B) (photo from California Department of Transportation [Caltrans]).

Contra Costa's "Moving Mountain" (1941–43)

The original 1937 alignment for State Route 75 (which became Highway 24 in 1952) was comprised of four lanes from the Broadway Low Level Tunnel connecting with a new four ()-lane alignment of Broadway Tunnel Road down to Orinda Crossroads, east of which a three-lane alignment was utilized (shown in Figure 6). In 1940, the highway alignment west of the Orinda Crossroads was widened to incorporate macadam shoulders on the steep uphill grade. The following year (1940–41) brought more rain, which precipitated landsliding from fresh cuts along the north side of the 1937 widening. These—slides emanated from the fractured strata in the apex of a tightly folded anticline with a southeasterly plunge. The anticline feature is about 0.25 mi (0.4 km) east of the present Siesta Valley exit of westbound Highway 24.

The State Division of Highways excavated a 30-ft-high (9.1-m-high) cut slope along the opposite (south) side of Broadway Tunnel Road to provide a temporary detour around the moving mountain slide area (Herlinger and Stafford, 1952). The higher cut along the westbound lanes continued to ravel and erode, undercutting portions of the slope extending far above Tunnel Road. The slope problems were exacerbated by a string of intermittent springs emanating from the highly fractured strata in the apex of the fold. These aided in the downslope movement of loose earthen debris. Westbound lane closures became so chronic that the local newspaper labeled it "Contra Costa's Moving Mountain" (Contra Costa Standard, 1943). The slide is clearly seen in the January 1937 aerial photo (Figure 7) as well as the July 1945 aerial photos for the State Division of Highways.

In June 1943, the County awarded a contract to lower the grade at O'Neil's Crest (between Siesta Valley and the Orinda Crossroads) and use this fill to raise the highway grade across Thomas Hill (on the ridge west of Siesta Valley) to help buttress the over-steepened cut slopes made to accommodate widening of State Route 75 to four traffic lanes. In this same contract, State Route 75 was also widened to four lanes between the Orinda Crossroads and the crest of Charles Hill, between Lafayette and Orinda. The additional lane helped to mitigate traffic problems associated with the three-lane configuration initially employed east of the Orinda Crossroads beginning in 1937.

The Great Orinda Slide of 1950

On Saturday morning, December 9, 1950, an enormous landslide affected State Highway 75 at the same location as the 1943 slide (Figures 8 and 9). The slide mass was about 300 ft (91.4 m) wide and extended more than 800 ft (244 m) uphill. It began blocking traffic around 10:30 a.m., and within 3 hours, it had covered the four-lane highway to an average depth of 30+ ft (9.1 m+) (Figure 9b). The workday traffic load in 1951 was 35,000 vehicle trips per day. The effect on commuters could have been much worse if not for the fact that the previous detour had been constructed in 1943 (Herlinger and Stafford, 1952). In total, 9,000 cubic yards (6,786 m^3) of earthen slide debris had to be trucked offsite to re-establish a "shoo-fly" detour around the toe of the slide, similar to that constructed in 1937. This bypass was completed in just 8 days (Figure 8b). The temporary bypass was re-opened at 5:00 a.m. on Monday, December 19. It seemed incredible that commuters were only inconvenienced for 1 week. They were given four detours, which added 15 to 25 mi (24 to 40 km) to their respective commutes (along old San Pablo Dam Road, Wildcat Canyon Road, or southerly detours through Moraga and across the southern Oakland Hills).

The 1950 Orinda slide made headlines across America (Figure 8a), and photos of the slide are still reproduced more than any other photograph of a California landslide. The mitigation measures undertaken by the State Division of Highways were unconventional for that era, insofar as they centered on an interconnected system of subdrains and drainage interception ditches.

Within hours of its occurrence, state highway engineers who specialized in combating landslide problems were promptly summoned from Sacramento. Their initial inspections suggested that the first priority should be draining the slide debris as much as practicable before attempting to remove it from the highway corridor. This was because the enormous mass of material provided lateral support for the troubled slope, much of which was saturated earthen debris.

On December 14, crews from the State Highway Materials and Research Department in Sacramento set up their first drill rig to begin installing horizontal subdrains at roadside level, employing a 7-day-work-week in the hopes of slowing the slide's downslope movement in the shortest possible time (Figures 10 and 11).

Horizontal drains were a very practical means of installing *in situ* subdrainage that had been pioneered by the Ransome Construction Company of San Leandro in the late 1930s. Ransome developed a drilling rig that employed a reversible air motor with a hollow crankshaft to deliver water to a rotating cutting bit through a string of hollow rods. They were then drilled at a low uphill inclination between 1 and 10 degrees from horizontal. They

Downloaded from http://pubs.geoscienceworld.org/aeg/eeg/article-pdf/31/1/i/6130855/i1558-9161-31-1-i.pdf
by AEG RBAC user

Figure 8a. Aerial oblique photo of the Orinda landslide that appeared in the *San Francisco Examiner* on Sunday, December 10, 1950 (photograph by Bob Bryant). The slide blocked the principal arterial transportation corridor serving Contra Costa County communities east of the Oakland-Berkeley East Bay Hills.

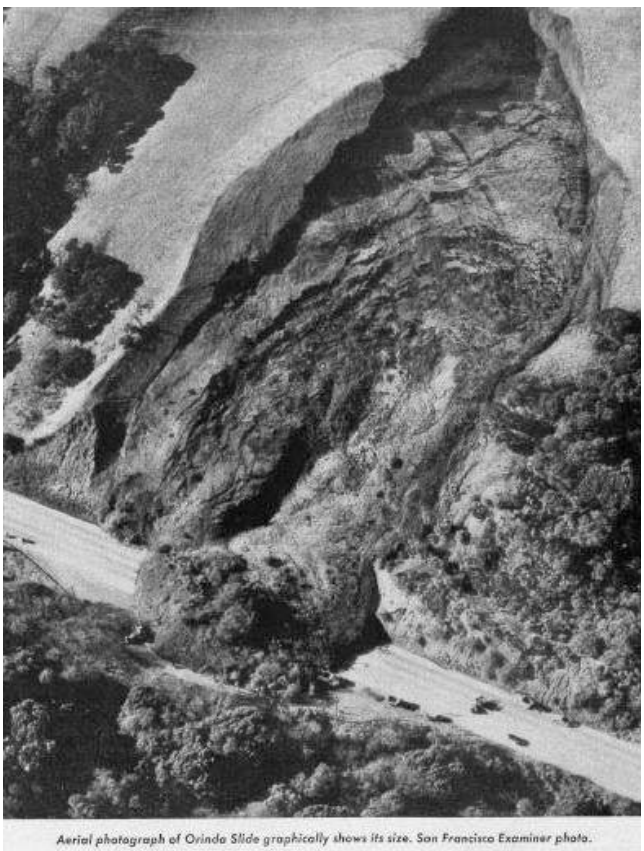

were often used in combination with vertical relief wells as part of several slope stabilization schemes in the early 1940s in the Oakland Hills (described in Forbes, 1947).

The State Division of Highways crews began drilling horizontal subdrains in 1939, and their original method was to employ modified fishtail bits drilling 4-in.-diameter (10-cm- diameter) holes so 2-in.-diameter (5-cm-diameter) steel pipe with 3/8-in.-diameter (1-cm-diameter) perforations could be inserted in the cavity (Smith and Stafford, 1957). The perforated casing came in lengths between 16 and 24 ft (4.9 and 7.3 m). In 1949, the industry began shifting to the use of rock roller bits used in the petroleum industry because these were readily available in a variety of diameters (Stanton, 1948). The industry came to call these drains "hydraugers," a term adopted by most agencies that employed these methods (Root, 1955a & 1955b).

Fourteen horizontal drains were completed during the initial emergency response phase of the restorative work. This initial network included 2,000 lineal feet (610 m) of horizontal subdrains extending into and

←

Figure 8b. Aerial oblique view of the Orinda landslide after it spilled onto the highway on Saturday, December 9, 1950, following 9 in. (23 cm) of rain in 7 days. In this view, crews are just beginning to excavate 9,000 cubic yards (6,786 m^3) of slide debris to construct a temporary bypass (or "shoo-fly") 50 ft (15.2 m) wide and 600 ft (182.9 m) long around the toe of the slide (Sorrick, 1986).

Downloaded from http://pubs.geoscienceworld.org/aeg/eeg/article-pdf/31/1/i/6130855/i1558-9161-31-1-i.pdf
by AEG RBAC user

Figure 9a. Another aerial view of the December 1950 Orinda landslide. The highway was closed for 10 days while the State Division of Highways constructed a temporary bypass of the 350-ft-high (106.7 m) slide. This bypass followed the 1903 right-of-way of Old Tunnel Road (Sipe Collection, Contra Costa County Historical Society).

Figure 9b. Ground view looking northeast at the debris that spilled onto the four-lane highway in December 1950. Note the displaced trees that were carried down the slope. The slide repair took an entire year to complete (Sipe Collection, Contra Costa County Historical Society).

underneath the landslide debris from the pre-slide level of the highway and four drains beneath the temporary bypass to enhance its stability and drainage of the debris blocking the main highway (shown on Figure 12b). This lowest network of drains resulted in an aggregate maximum flow of 85,000 gallons (108 m^3) per day, which pleased the state engineers because they felt that de-watering would have the most cost-effective impact on long-term slope stability.

Figure 10a shows a tracked shovel excavating slide debris that blocked Highway 24, while bulldozers are

Figure 10a. Overview of the early stages of exploration and mitigation in the spring of 1951, after the slope had been allowed to dry out (Sipe Collection, Contra Costa County Historical Society).

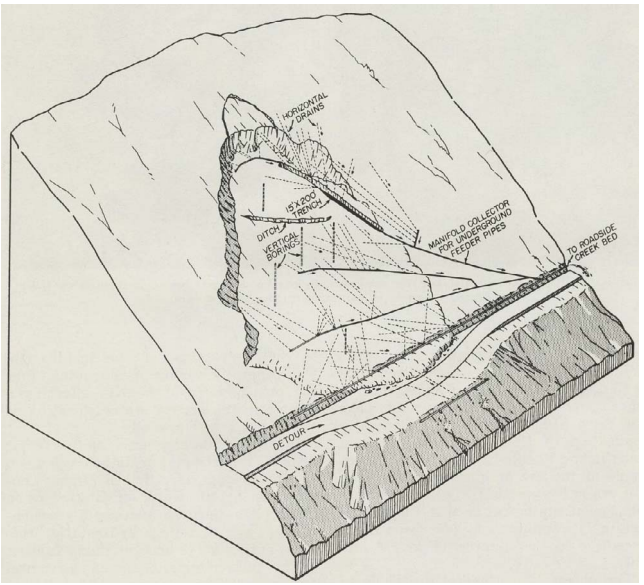

Figure 10b. Block diagram illustrating the dewatering scheme employed by the State Division of Highways in 1951 to stabilize the Orinda slide. In total, 95 hydrauger (horizontal) drains and three manifold collectors were installed for a total length of 10,000 ft (3,048.0 m). This system of subdrainage recorded daily outflows of up to 135,000 gpd (511,000 liters/d), which appear to have stabilized the slope (Baker and Marshall, 1958).

beginning to blaze switchbacks for a temporary access road on a 20 percent grade to support exploratory drilling and installation of hydrauger subdrains. Note the graded road about 65 ft (20 m) above the highway at far right. This temporary haul road was graded to allow access to Orinda Crossroads without blocking highway traffic. At the time, this was the largest landslide the

Downloaded from http://pubs.geoscienceworld.org/aeg/eeg/article-pdf/31/1/i/6130855/i1558-9161-31-1-i.pdf
by AEG RBAC user

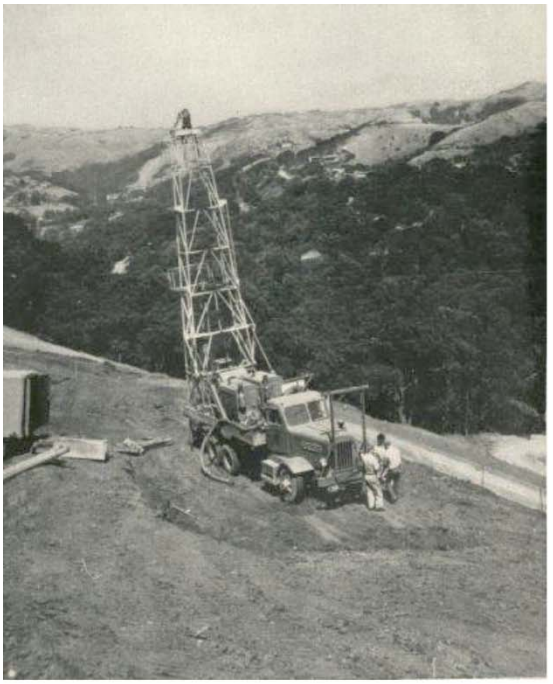

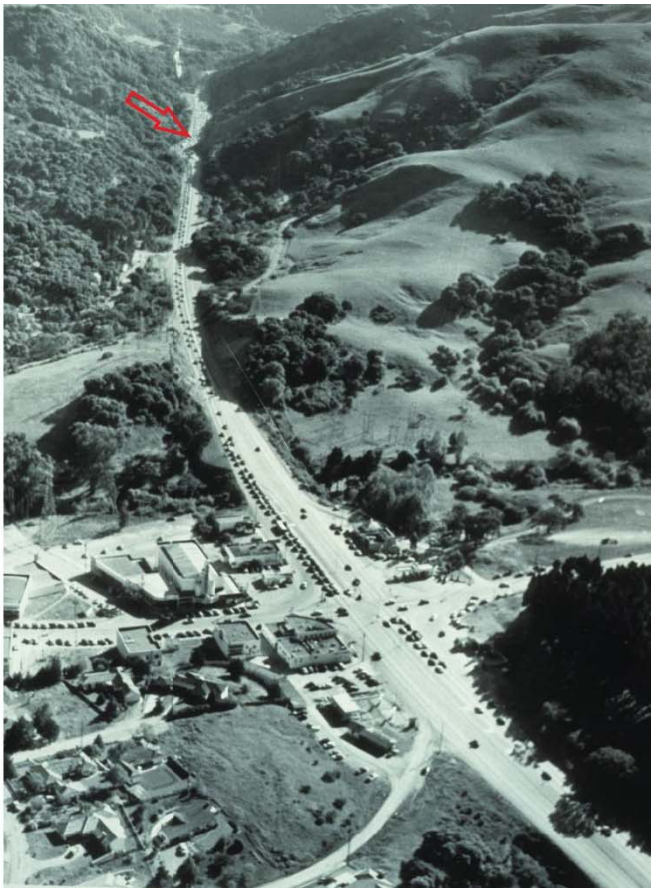

Figure 11a. Vertical Boring No. 4 at the second switchback of the bench road blazed on the Orinda landslide during the summer of 1951 (Herlinger and Stafford, 1952).

Figure 11b. Aerial view looking up the grade of State Route 75 west of Orinda Crossroads in 1951, during corrective grading and de-watering of the slide mass. The eastbound afternoon commute is passing through the temporary bypass around the Orinda slide (arrow). A traffic light at Orinda Crossroads created severe rush-hour traffic until the Route 24 freeway was completed in 1960 (Contra Costa County Historical Society).

State of California had ever repaired while maintaining traffic flow 24 hours per day on a state highway with four or more lanes of traffic.

When this initial phase was complete, the state highway engineers gathered at the Division of Highways District 4 office in San Francisco to consider their long-term repair options. The active portion of the slide now encompassed about 250,000 cubic yards (191,000 m^3) of material (Figure 10a and b). It was decided to leave the landslide debris on the highway until the fall of 1951 to allow it to drain, dry out, and shrink as much as possible. They feared that the excavation of the toe area might trigger retrogressive slides of between 100,000 cubic yards (76,400 m^3) and 200,000 cubic yards (152,800 m^3), which might compound the cost of maintaining this key arterial highway. At that time, the 24-hour traffic volume on a normal Monday commute day was just over 35,000 vehicles per day. About 55 percent of the residents of central and western Contra Costa County commuted to jobs in San Francisco and Oakland (Herlinger and Stafford, 1952). The likelihood of triggering another slide of similar scale was of significant concern to everyone involved.

Another complication was performing all of the corrective work during peak traffic cycles associated with morning and afternoon commutes. It soon became apparent that the plan for excavation and haulage of saturated slide debris was inefficient. The debris was so wet and sticky that it adhered to the earth-moving equipment and left a muddy trail on the highway lanes, which had to be shared with thousands of commuting vehicles each day. In response to these concerns, it was decided that no off-haulage would be allowed during peak commute hours. This ban also applied to deliveries of large earth-moving equipment.

Separate haul roads up to Siesta Valley and down to the Orinda Crossroads were quickly graded parallel to the existing highway (Figures 10a, 11a, and 11b), with a cross-over to the south side of the highway just above San Pablo Creek. These haul roads were only used during non-peak hours. During the summer and fall of 1951,

Downloaded from http://pubs.geoscienceworld.org/aeg/eeg/article-pdf/31/1/i/6130855/i1558-9161-31-1-i.pdf
by AEG RBAC user

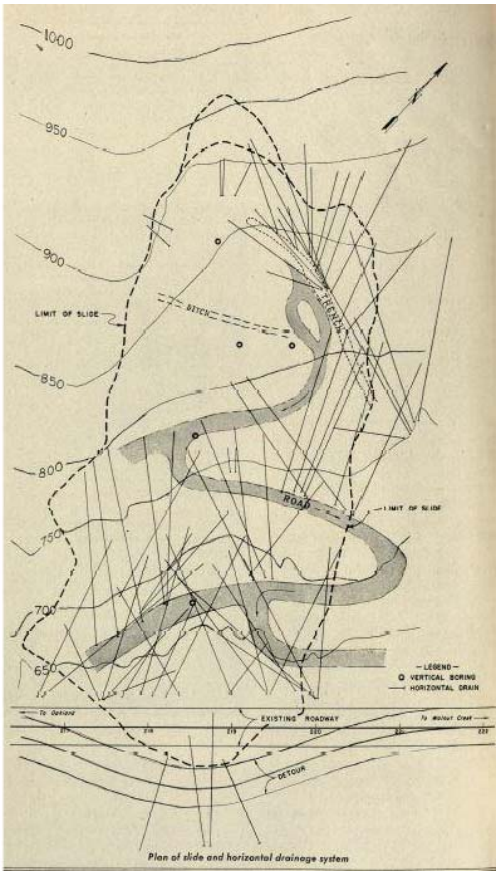

Figure 12(a). Head-on view of the December 1950 landslide area, showing the switchbacks of the bench access road and the over-excavation of the slide's lateral margins (Caltrans).

Figure 12(b). As-built plan of topography, bench access road, exploratory borings, horizontal subdrains (hydraugers), and surface interceptor drains comprising the slide repair (Caltrans).

another 71,000 cubic yards (54,244 m^3) of slide debris was removed from the site by off-haulage. Some of the fill was used to enlarge embankments supporting San Pablo Dam Road (widened to its present right-of-way in 1956–57) and in reclamation of portions of the old Kaiser Sand & Gravel quarries across the highway, in south Siesta Valley (above today's Gateway Valley exit). This same area was utilized for disposal of tunnel muck from the third bore of the Caldecott Tunnels in 1960–62.

The state highway engineers decided to pioneer a temporary bench access road 14 ft (4.3 m) wide on a near-constant 20 percent grade with three switchbacks up the face of the active landslide mass. This temporary haul road extended more than 700 ft (213 m) above the highway. This path allowed State Division of Highways crews to drill five borings in the center of the slide mass to evaluate the strength and consistency of the debris and the depth to intact bedrock beneath the slide (Figures 10b, 11a, and 12a). This access way also allowed the drilling of more horizontal drains through saturated horizons beneath the exposed slope (Figures 11a and 12a and 12b).

It was eventually decided that all of the finish slopes within the landslide area should be laid back to 2:1 horizontal-to-vertical inclinations (26.7 degrees from horizontal) to enhance long-term stability (Herlinger and Stafford, 1952). This was considered to be adequate if sufficient subdrainage were installed as an integral part of the repair scheme (Figures 10b and 12b).

The foremost construction problem was how to deal with incipient landslides at the crest of the slope, 335 to 800 ft (102 to 244 m) above the highway, shown in Figure 12a and 12b. The engineers found that the eastern half of the 1950 landslide was underlain by a series of dormant landslides comprised of disaggregated siltstone and shale that had the consistency of a loose soil, uncharacteristic of what they expected to encounter in such tall, steep hillsides. These materials could absorb large volumes of water that could cause them to lose shear strength and behave like a plastic material prone to sliding.

The State Division of Highways design team was led by A.W. Root, head of the Foundations Section of the state's Division of Highway's Materials & Research Laboratory in Sacramento (Root, 1938). Root later wrote a

Downloaded from http://pubs.geoscienceworld.org/aeg/eeg/article-pdf/31/1/i/6130855/i1558-9161-31-1-i.pdf
by AEG RBAC user

treatise on "Prevention of Landslides" for Special Report 29 on *Landslides and Engineering Practice*, published by the National Academy of Sciences (Root, 1958).

Root initially felt that as-graded slopes would not be stable on a 2:1 slope inclination and pressed for the removal of as much of the active slide debris as practicable. This was expensive due to difficult site access and the length and gradients of potential off-haul paths southwest and northeast of the slide. Root altered his opinion as more and more hydrauger drains were installed in the troubled slope, slowing it to a complete standstill by mid-1951. At that time A.W. Root was considered one of the most experienced geotechnical engineers on highway slope stability in the United States.

As the repairs kept workmen out on the troubled slope for almost 2 consecutive years the project the State Division of Highways concurred with Root's advice and supported his advice backed Root's recommendations at every juncture and backed him up on every detail he recommended (Root, 1955b). His novel recommendations actually resulted in conservative recommendations that were heeded, except for several letters from a Contra Costa County supervisor appealing to the state Division of Highways to "get Highway 24 repaired before the summer season!."

Two decades later, Cal Berkeley Professor J. Michael Duncan (1971) back-calculated the average soil strength parameters of the weathered Orinda Formation and estimated that the formational materials degraded to an angle of internal friction (phi) of about 20 degrees with an effective cohesion of only 20 pounds per square foot (psf) (1 kPa) after the slide begins moving downslope as a semi-coherent mass.

The decision was made to begin excavation in the spring (Figure 10a and 10b) and install an interconnected system of horizontal drains with buried collector lines to convey moisture out of the slide mass within impervious drains and pipes, as well as install a system of concrete-lined surface interceptor drains (for spring flows as well as storm runoff).

The most difficult challenge was to lay back the most unstable materials (such as the Orinda Formation) in the headscarp area along the eastern crown of the slide. This required winching of bulldozers using steel cables so they could gently drift the loosened soil downslope, where it was loaded into 10-wheel dump trucks and hauled to one of the waste-disposal areas.

Throughout the summer and fall of 1951, a total of 11,700 lineal feet (3,556.2 m) of slotted well casing was inserted into 95 horizontal subdrains colloquially known as "hydraugers" (Figure 12b). These subdrains succeeded in intercepting up 35,000 gallons (172 m^3) of seepage per day. Because the active slide mass was 30 ft (9.1 m) to 50 ft (15.2 m) deep, only 71,000 cubic yards (54,244 m^3) of material were removed, leaving the remaining soils on a 2:1 slope (horizontal to vertical), as shown in Figure 12a. Armco steel bin retaining walls were assembled by filling with them with free-draining gravel at the toe of the slide to buttress the remaining slide debris that was left in place.

In addition to the 9,000 cubic yards (6,876 m^3) of slide debris removed to construct the shoo-fly bypass in December 1950, 62,000 cubic yards (47,368 m^3) of additional debris were scalped from the troubled slope, including the debris covering the highway (Figure 10a and 10b). These excavations took about 3 months in the mid-summer and early fall of 1951. The novel slide repair was completed on schedule, in just over 1 year.

The spectacular nature of the 1950 Orinda slide generated considerable public awareness of geologic hazards in the East Bay Hills. In the 1952–53 fiscal year, the State Division of Highways installed more than 23,000 lineal feet (7,010 m) of horizontal drains in stabilizing landslides and slip-outs along California highways. All of these were drilled and installed by State Division of Highways drilling crews, not by commercial contractors.

In 1957, the State Division of Highways undertook the largest highway cut excavation in the world for Interstate 80, which was dubbed the "Carquinez Cut" (Smith and Cedergren, 1962). Cost and schedule overruns on that project hastened the hiring of engineering geologists to aid in the design layout of highway alignments. Prior to this, geologists had only been employed by the Bridge Department to help assess bridge foundations, despite a national trend towards engaging geologic input in slope characterization, described by Huntting (1945).

Post–World War II Building Boom (1946–66)

The second Contra Costa real estate boom began following World War II, with the bulk of Orinda's growth occurring 1946–66. The newly formed Central Contra Costa Sanitary District began operation in 1946, servicing Orinda among other central county hamlets. Previously open hillside land was quickly subdivided, with lots extending from newly bulldozed roads that were soon paved with asphalt. Most of the "paper lots" created near the Orinda Crossroads area in the 1920s were also sold. By 1950, the adjacent ranchlands were quickly being carved up as subdivisions (Figure 13), utilizing progressively larger earth-moving machinery to create building pads that were impractical to construct decades earlier with mule-powered Fresno scrapers (Figure 4).

Orinda's lack of a commercial district was less of an issue as high-speed highways were developed because they dramatically reduced commute times from what they had been before the war. Many blue-collar employees moved to central Contra Costa County in search of

Downloaded from http://pubs.geoscienceworld.org/aeg/eeg/article-pdf/31/1/i/6130855/i1558-9161-31-1-i.pdf
by AEG RBAC user

Figure 13. Aerial oblique view of the Orinda Crossroads area, taken in January 1957, when the first housing tracts on Warford Mesa were being graded in the right foreground (Pacific Aerial Surveys).

affordable housing, warmer weather, and larger lots. Orinda's draw seemed to be more focused on professionals, drawn by the country ambiance, riding stables, and the country club.

Adoption of Title 21 of the California Administrative Code (1950)

In 1950, the California State Legislature enacted California Administrative Code Title 21-Public Works: Department of Public Works, Architecture, Highways, Toll Bridge Authority (California State Legislature, 1950), which required materials testing, including soil compaction tests, for public buildings, streets, and trench backfill of buried utilities in public rights-of-way. Materials testing firms reconfigured themselves to perform soil mechanics tests. The requirements of Title 21 signaled the beginning of a new era in soil mechanics and foundation engineering as well as pavement design in California.

The First Grading and Excavation Codes (1952)

In 1952, it was southern California's turn to be impacted by destructive rainstorms. In January, a freak storm passed over Los Angeles and then made a U-turn and dropped even more rainfall on the second storm cycle, which triggered mudslides and flood damage across the hillside subdivisions of coastal inland portions of Los Angeles. The damage was so sudden and severe that it prompted the Los Angeles City Council to order the city's Department of Building & Inspection to develop the nation's first grading and excavation ordinance a few months later (Scullin, 1966). That same year, Cal Berkeley launched an ambitious soil mechanics and foundation engineering program that soon became one of the most prestigious in the world. By 1969, they supported nine full-time faculty specialists, which established it as the largest geotechnical program of any university in the world.

The Freeway Era Begins in 1953

By 1951, the average daily traffic count on State Route 24 reached 35,000 vehicles per day (vpd), up 7,000 from the year before (Figure 14). This was a reflection of the residential building boom that began accelerating in 1949. Traffic counts had reached 3,500 vpd in 1931, climbing to more than 14,000 a decade later (1941), on the eve of World War II. By 1947, the commuter traffic count exceeded 23,000 vpd (Young, 1954). A new traffic light installed at Orinda Crossroads was backing up rush-hour traffic all the way to the

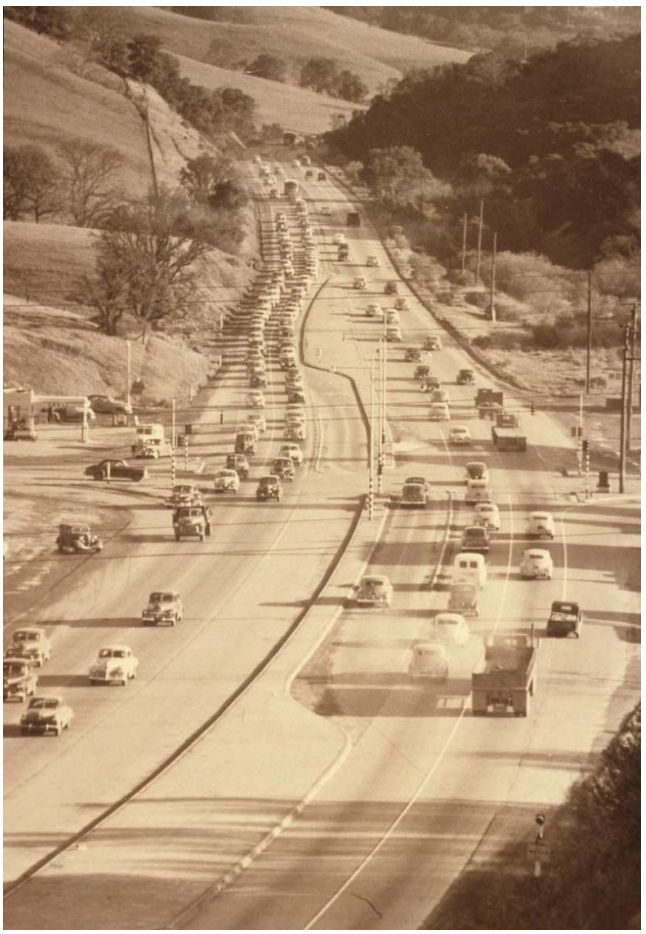

Figure 14. Afternoon rush hour at Orinda Crossroads, circa 1953. By 1951, 35,000 motorists were commuting up the grade each day, an increase of 7,000 over the previous year. The impact of residential construction in central Contra Costa County was beginning to be felt (Contra Costa County Historical Society).

Downloaded from http://pubs.geoscienceworld.org/aeg/eeg/article-pdf/31/1/i/6130855/i1558-9161-31-1-i.pdf
by AEG RBAC user

Broadway (Caldecott) Tunnels, more than 2 mi (3.2 km) distant (Figure 14).

In September 1953, the State Division of Highways let a contract for a major grade separation (overpass system) at the Orinda Crossroads, developing Contra Costa's first "freeway" with a cloverleaf interchange when it opened in March 1955. In the process of designing the interchange, the Orinda Chamber of Commerce suggested eastbound off-ramp cuts still in use today, which were utilized in lieu of a bridge (Betz, 1993).

While San Pablo Creek was being excavated for installation of a concrete box culvert to carry it beneath the new highway (Figure 15), the entire hillside (within the Mulholland Formation) above the cut began moving towards the highway right-of-way (Figure 16). Quick reaction on the part of the contractor averted a disaster similar to that which had befallen the highway in December 1950 (Young, 1954). They stopped excavating the slope and began installing hydrauger drains. As soon as the horizontal drains pierced the Moraga Thrust fault, large volumes of water were released, and within 72 hours, the slide ceased moving.

Highway 24 Serves as a High-Speed Commuter Link (1956–64)

The demand for East Bay housing reached an all-time high after 1955, when the interstate highway program was launched. In 1952, Route 75 between Walnut Creek and Oakland was re-designated State Route 24. In 1955, construction of the freeway corridor between Oakland and Walnut Creek began, and the Lafayette Bypass between Pleasant Hill Road and Sunnybrook Drive opened in June 1956.

Figure 15. Grading activities for the Highway 24 freeway in the Orinda Crossroads area in late 1958. In the center foreground, a large concrete box culvert is being constructed to convey the flow of upper San Pablo Creek beneath the interchange (Pacific Aerial Surveys).

Figure 16. Aerial view of grading activities for the Orinda Crossroads interchange along Highway 24 in early 1959. The large cuts for the new freeway can be seen in the foreground, while the box-like structure for San Pablo Creek is barely discernible just left of the highway (Pacific Aerial Surveys).

Construction proceeded westward through Lafayette and Orinda through the late 1950s (Figures 15 and 16). When it officially opened in March 1960 (Figure 17), the highway created a high-speed link between the Caldecott Tunnels and Walnut Creek.

In August 1960, the Lower Broadway Tunnels were renamed the "Caldecott Tunnels" in honor of Berkeley Mayor Thomas E. Caldecott, who served as president of the board of directors of California Joint Highway District No. 13, which sponsored the design and construction of the original twin tunnels in the early 1930s.

A third bore of enlarged diameter was excavated north of the original twin tunnels between 1960 and 1964 (Degenkolb, 1960; Black and Degenkolb, 1964). Much of the material excavated from this bore was disposed of in Fish Creek Canyon (north of the tunnel's east portal) and in Gateway Valley (about 0.75 mi [1.2 km] east of the tunnels). The long-anticipated fourth Caldecott Tunnel bore was not completed until 2013.

The high-speed connection we know today as Highway 24 came later. As originally designated, Highway 24 proceeded down Broadway Tunnel Road to Ashby Avenue, connecting with the Eastshore Freeway in Emeryville. Commuters bound for Oakland continued southwest from the tunnels, taking a four-lane version of Broadway Avenue into Oakland. It was along this alignment that the cut slope experienced repeated failures between 1935 and 1947, described by Forbes (1947).

The Grove-Shafter Freeway, connecting the Nimitz Freeway to the Caldecott bores, was completed as part of the highway re-alignments to accommodate BART in 1966–71. The Highway 24 freeway had the greatest

Downloaded from http://pubs.geoscienceworld.org/aeg/eeg/article-pdf/31/1/i/6130855/i1558-9161-31-1-i.pdf
by AEG RBAC user

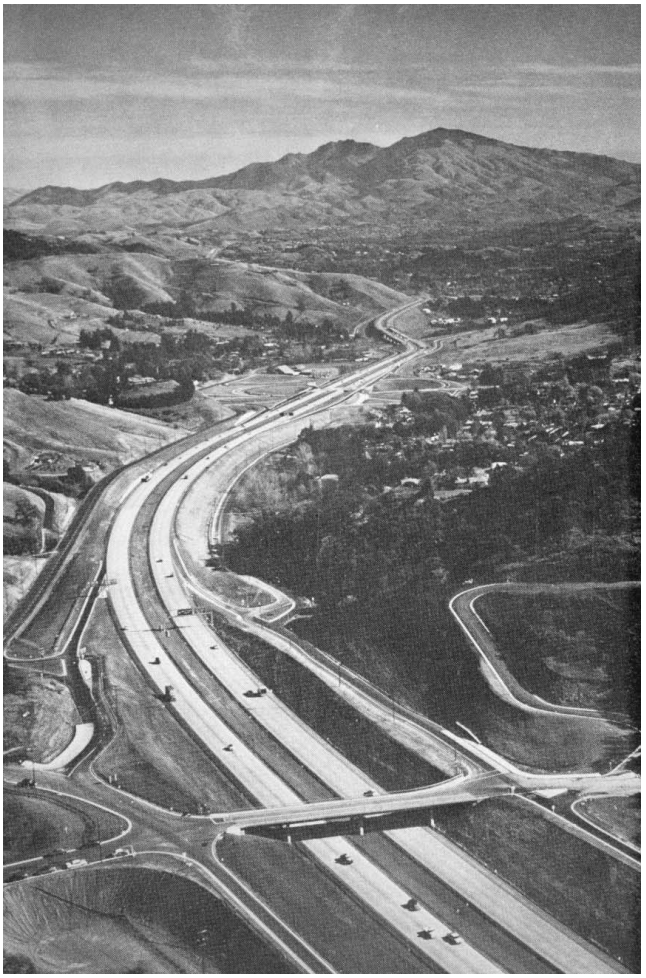

Figure 17. Aerial oblique view of the Highway 24 freeway above St. Stephen's Hill, as viewed in 1960. The new alignment for Tahos Road, shown at right, failed in the storms of the late 1960s).

impact on Orinda's character, separating the downtown into two districts north (Orinda Village) and south (Orinda Crossroads) of Highway 24.

Warford Mesa Subdivided (1955)

In the summer of 1955, A. R. Muth and Sons began grading for Warford Mesa Unit 1, just uphill and northeast of the Orinda Crossroads. During the summer and fall of 1955, lower Muth, Bates, and Warford Terrace Drives (connecting the other two streets) were also graded.

Soil compaction reports filed at the time (October 1955) noted that a "...fairly elaborate drainage system to stabilize the hillside" had been implemented by the State Division of Highways in the Warford Terrace area in the past "five to eight years" (1947 to 1950). The drainage work described consisted of a series of horizontal wells, or "hydraugers," a landslide repair technique commonly employed by the State Division of Highways during that era (Stanton, 1948; Root, 1955b).

The 1948 base map used by Kachadoorian (Figure 18) shows "wooden flumes" (likely built during World War II (when steel and concrete were less available in the mid-1940's) that conveyed discharge from the hydrauger subdrains down to the road's northwestern shoulder. After viewing the sub-drain troughs and recognizing the potential for seepage and increased pore pressures the Engineer-of-Record warned their client about the risks of future drainage issues and saturation cycles do to the significant complex existence of the state's drainage system. The tract's original soils report Hersey Inspection Bureau, (1955) opined that the cost of repairing the slopes might exceed the property values and recommended that the developer might consider setting some of the wettest and steepest areas of the project aside as as "unimproved parkland."

December 1955–January 1956 Storms

In late December 1955, a disastrous series of "El Niño" storms struck northern California, flooding many areas, including portions of the East Bay Hills. The storm dumped record amounts of rainfall on other parts of northern California (State of California, 1956). Flooding was the most visible problem, as most subdivisions had been constructed with little regard for "off-site impacts." Another series of storms struck the Orinda area in January 1956. This precipitation fell on -saturated ground, leading to high runoff conditions and additional flooding of lowland areas (Hoffmann and Rantz, 1963).

Erosion damage to the Warford Mesa tract was extensive, especially to recently graded embankments constructed to support relatively flat building pads. Flooding problems were exacerbated when culverts clogged with silt and organic debris eroded from the recently graded slopes. Hall Drive was closed, as was El Toyonal in about half a dozen locations. Highways under construction were also impacted by eroded cut slopes.

Federal Housing Administration Land Planning Bulletin No. 3 (1956)

In 1956, the Federal Housing Administration (FHA) issued Land Planning Bulletin No. 3 (FHA, 1956, which established minimum standards for excavation and grading of residential subdivisions, including: maximum inclinations of cut and fill slopes, requirements for mid-slope drainage interceptor terrace drains, and certification of 95 percent of standard Proctor soil compaction (ASTM D698). Developers seeking federal assistance had to comply with the FHA standards and present soils and foundation engineering reports as documentation of compliance.

Downloaded from http://pubs.geoscienceworld.org/aeg/eeg/article-pdf/31/1/i/6130855/i1558-9161-31-1-i.pdf
by AEG RBAC user

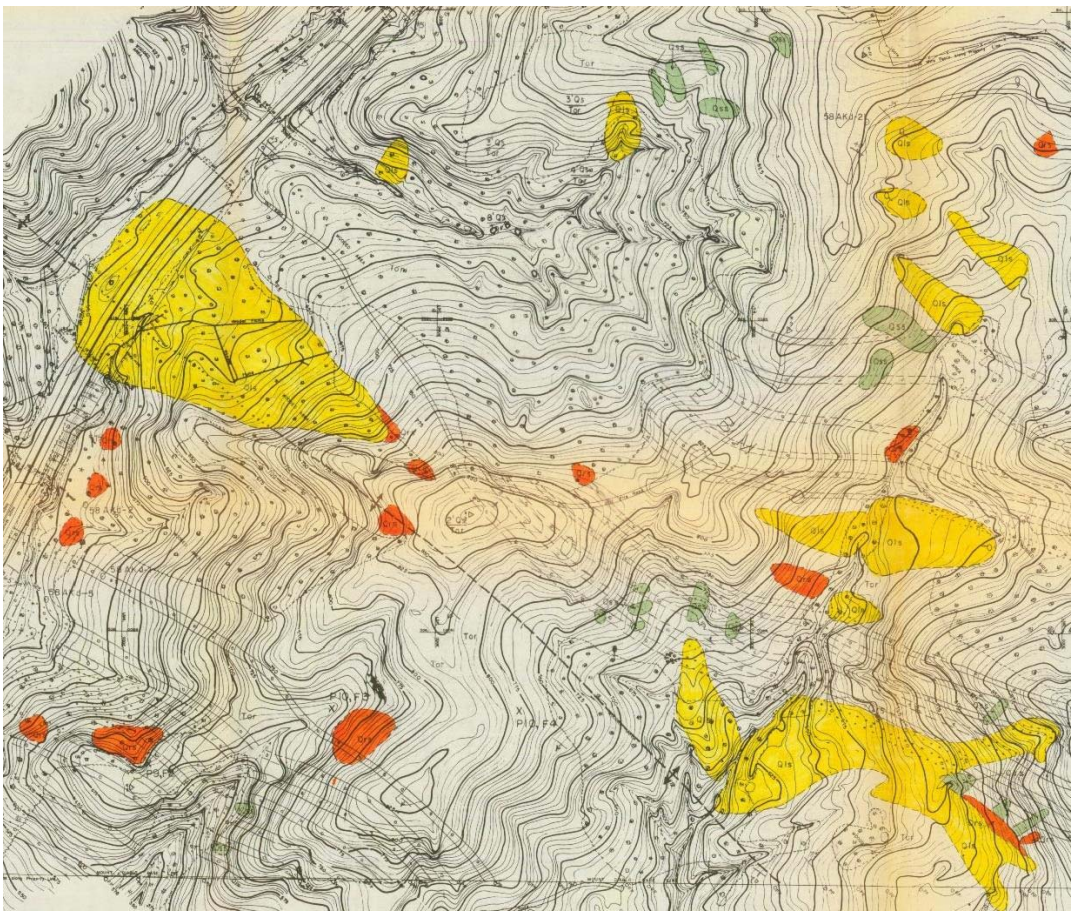

Figure 18. A portion of Kachadoorian's 1956 landslide map of Warford Mesa was prepared before the area was graded for residential development (Kachadoorian, 1956). The yellow areas are active landslides prior to July 1956; the green areas are soil slides that activated prior to June 1956, and the orange spots are slides that occurred after July 1956. The corrective subdrainage placed by the Division of Highways is noted beneath the largest yellow area, along Highway 24 at upper left (also see Figure 47).

U.S. Geological Survey Mapping of Landslides in Orinda for the FHA (1956–60)

Alarmed by geotechnical damage losses in the December 1955/January 1956 storms, the Warford Mesa development's insurer, the Federal Housing Administration (FHA), decided to withhold approval of the Warford Mesa tracts until the subdrainage improvements could be installed by the State Division of Highways (Figure 18). FHA declined to approve further hillside developments in the Warford Mesa area until an independent study by the U.S. Geological Survey (USGS) could be conducted and reported to FHA.

In February 1956, the USGS began conducting a preliminary investigation of the Warford Mesa subdivisions along Bates, Muth, and Warford Terrace Drives, which had fared poorly in the recent storms. FHA felt that further engineering geologic study was warranted before federal agencies should be expected to provide insurance for the proposed developments. They indicated there was ample evidence of surficial erosion and shallow landsliding triggered by the recent storms (Figure 19).

In the summer of 1956, the USGS began assigning specialists from their Engineering Geology Branch to the San Francisco Bay Region. This initial cadre of geologists included Dorothy Radbruch, Manuel G. "Doc" Bonilla, Reuben Kachadoorian, George Plafker, and Fred Taylor. One of their first assignments was the studies being requested by the FHA, which included Warford Mesa in Orinda.

The USGS studied the underlying geology and slope stability problems in the Warford Mesa area, and the results were summarized by Reuben Kachadoorian in a publication titled *Engineering Geology of the Warford Mesa Subdivision*, released in 1956 as a USGS Open-File Report (OFR). The 13-page study (Kachadoorian, 1956) included a preliminary landslide map (shown in Figure 18).

Manuel G. "Doc" Bonilla of the USGS began mapping landslides in the South San Francisco area. His

Downloaded from http://pubs.geoscienceworld.org/aeg/eeg/article-pdf/31/1/i/6130855/i1558-9161-31-1-i.pdf
by AEG RBAC user

Figure 19. Storm damage of March–April 1958 between lower Bates and Muth Avenues (Kachadoorian, 1959). The fill at center of photo had been placed in late 1955. The slope beneath this fill had been mapped as a landslide by "Doc" Bonilla of the USGS in 1956.

study area included an entire quadrangle (70 square miles) and resulted in a report titled *Landslides in the San Francisco South Quadrangle, California*, which was released as a USGS Open-File Report in 1960 (Bonilla, 1960). These were the first reconnaissance-level studies of potential landslide hazards in the San Francisco Bay area.

USGS geologists mapped the proposed development area south of Highway 24 at a scale of 1 in. = 200 ft (1 cm = 24.0 m), highlighting sandstone and conglomerate outcrops across the area. The USGS geologists found a repeating series of conglomerates (30 percent) and sandstones (15 percent), with the remainder (55 percent) of the bedrock formations composed of softer claystone beds. A 6-ft-thick (1.8-m-thick) bed of volcanic ash was also noted by Kachadoorian (1956, 1959).

Montmorillionite Discovered in the Orinda Formation (1956)

Probably the most alarming of the USGS findings summarized in Kachadoorian's 1956 report were the mineralogical analyses, which indicated that the average percentage of montmorillonite clay within the "Orinda Formation" at Warford Mesa was 45 to 50 percent, with some specimens exhibiting as much as 95 percent montmorillonite. These clays are often derived from weathering of volcanic ash in a semiarid environment. The presence of such large amounts of montmorillonite was a startling discovery because these are the natural materials of lowest shear strength that are often associated with destructive landslides (Skempton, 1964; Tembe et al., 2010).

Named after Montmorillon in France, montmorillonite is the most reactive of a family of swelling clay minerals called "smectites." Smectites can chemically absorb up to 800 percent moisture when compared to their dry weight (Grim, 1968). Such large absorption of water serves to make these materials extremely slippery and have low shear strength when saturated. As little as 5 percent of such clay, by weight, can control the behavior of whatever other material is present (Mitchell, 1993). A colloquial corollary would be a bowl of guacamole with uncrushed pits. Although the pits might dominate the volume and weight of the mass, the strength of the mixture is controlled by the "guacamole sauce" filling the voids and forming a deformable matrix between the stiff pits.

USGS Studies Are Ignored and Hillside Development Suffers (1957–67)

Kachadoorian's mapping suggested the widespread existence of landslides, particularly occupying the larger ravines (Figures 19 and 20a and 20b). With the report thereby completed, the FHA granted necessary approvals for insurance coverage, which allowed approval of

Figure 20a. Photograph of Warford Mesa taken in 1956 by Kachadoorian.

Figure 20b. The same view in 1992 by Rogers. This is a typical example of "topographic healing" of exposed landslide scarps and cut slopes in relatively soft Tertiary-age lacustrine and shallow-marine sediments.

Downloaded from http://pubs.geoscienceworld.org/aeg/eeg/article-pdf/31/1/i/6130855/i1558-9161-31-1-i.pdf
by AEG RBAC user

the loans necessary to fund what became known as the "Warford Mesa Tracts" (Contra Costa County Subdivision Tracts 2245, 2470, 2472, 2475, 2925, 3083, and 3286).

Realizing that FHA was withholding approval for insurance, banks withheld their development loans, and by early 1956, Muth & Sons were faced with a partial shutdown of their development activities. In February 1956, Muth consented to retain Hersey Inspection Bureau to provide recommendations on repairing the troubled slopes along Warford Terrace. Hersey's engineers recommended employment of additional hydraugers and "French drains," which were gravel-filled trenches intended to convey excess soil moisture away from the slopes, and thereby lower the antecedent moisture. Upon FHA and Contra Costa County approval, the remaining tracts were excavated by mass-mechanized-grading techniques developed by Bay Area contractors.

Unfortunately, the focus of the engineer's design efforts appears to have been the construction of lot pads, with little appreciation of the underlying geologic structure. Despite the voluminous amount of engineering data generated for these hillside subdivisions, there was no mention of the engineering geologic studies undertaken by the USGS, nor of the landslides they had mapped, and upon which fill had been placed to unintentionally create what turned out to be 21 high-risk building pads.

Landslides of March–April 1958

March and April 1958 witnessed six consecutive weeks of precipitation (see Table 1 and Appendix 4), which culminated in another series of disasters along watercourses and hillsides (Harding, 1969). The troublesome slopes along Warford Terrace gave way first, undermining the corner of an existing house and damaging three other lots (Hersey Inspection Bureau, 1958). It was the first in a series of slides between Warford Mesa and Muth Drive that would plague the area for the next 25 years.

On April 3, a large portion of Hall Drive began to move towards newly built homes on Easton Court (described in Kiersch, 1969). Mr. and Mrs. Robert Pfeiffer had just purchased a new home on Easton Court the previous October (1957) when the entire hillside began to lift and carry their home downslope. Hall Drive had been graded without benefit of soils engineering during the land boom of early 1946 but was permanently closed in 1958 (Figure 21a, 21b, and 21c).

Subsequent investigations by other geotechnical consultants suggested that both Hall Drive and Easton Court had been graded upon an extensive relict landslide complex (with multiple slide planes), which had partially reactivated during the storms of 1951–52 (Kiersch, 1969; Kiersch and Waggoner, 1991). The Pfeiffers sued their insurance company [Pfeiffer v. General Insurance 185 F. Supp. 605, N.D. Cal (1960)], as did other Contra Costa residents living adjacent to stream banks that failed in the same storm [Hughes v. Potomac, 18Cal Rptr 650/199 Cal App 2nd 239 (1962)] (Kiersch,1969). Both homeowners prevailed in their respective lawsuits, creating often-cited cases for insurance liability due to earth movement (Olshansky and Rogers, 1987). Despite the past history of slope stability problems, both homes remain occupied.

Figure 21a. Ground view of the Hall Drive landslide above the former Pfeiffer residence on Easton Court, as seen in July 1971. Hall Drive has been closed at this location since 1958 (Fred Taylor, USGS).

Hall Drive failed at the same location during the storms of October 1962 and again in February 1983 (see Figure 21a). Other slides affected 15 Hall Drive, somewhat below the Pfeiffer slide (at 23 Hall Drive), in 1969, 1983, and 1986. In 1984, Contra Costa County installed a retaining wall at 15 Hall Drive. Though re-graded in 1991, Hall Drive remains closed at the Pfeiffer slide (just uphill of its intersection with Easton Court), with access being from Glorietta Boulevard on the northeast and Moraga Way on the southwest.

FHA and Contra Costa County Adopt Grading Ordinances (1960)

In the wake of the 1955 and 1958 storm damage, Lamorinda (Lafayette-Moraga-Orinda) businessman Don Doudy lobbied county supervisors to adopt a grading ordinance similar to those adopted by the FHA, which insures mortgages made by private lenders. In September 1960, the FHA implemented its own standards for cuts and fills in the area served by its San Francisco office.

The new FHA guidelines called for fill slopes to be no steeper than 2:1 (horizontal to vertical), while cut slopes could be as steep as 1.5:1 (horizontal to vertical). No mechanical compaction test methodology was specified, only specifying that such determinations "should be made." The FHA guidelines emanated from those

Downloaded from http://pubs.geoscienceworld.org/aeg/eeg/article-pdf/31/1/i/6130855/i1558-9161-31-1-i.pdf
by AEG RBAC user

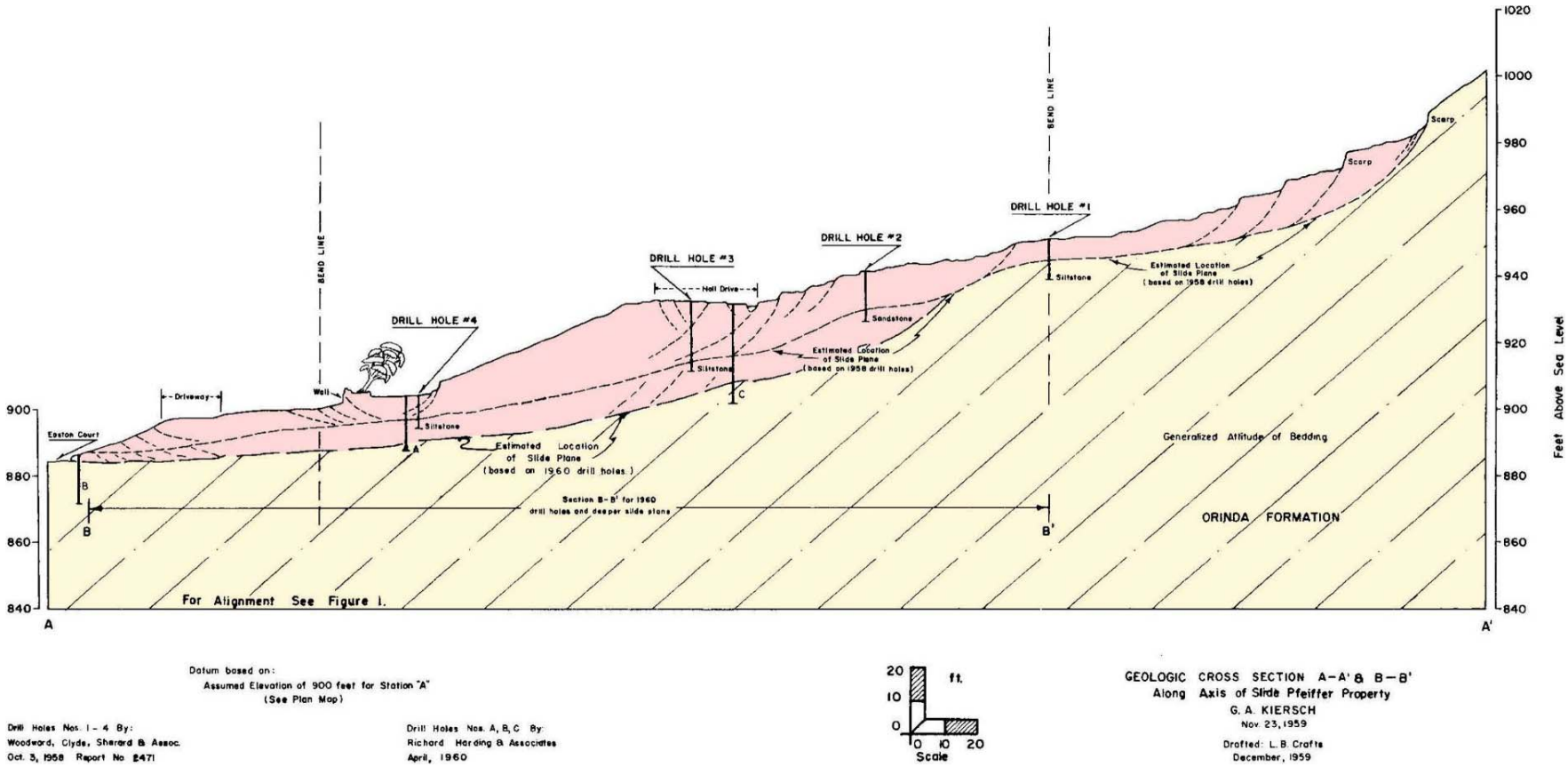

Figure 21b. Geologic cross section through a pair of coalescing slump-earthflow landslides that damaged the Pfeiffers and their neighbors' homes on Easton Court, as well as permanently closing Hall Drive in April 1958 (from Kiersch, 1969). The relatively shallow depth of the active rupture surface (between 5 and 16 ft [1.5 and 4.9 m]) caused significant damage to the Pfeiffer home, shown here. Note that the fill wedge for Hall Drive (graded the previous year) coincided with the deepest portion of the slide.

Downloaded from http://pubs.geoscienceworld.org/aeg/eeg/article-pdf/31/1/i/6130855/i1558-9161-31-1-i.pdf
by AEG RBAC user

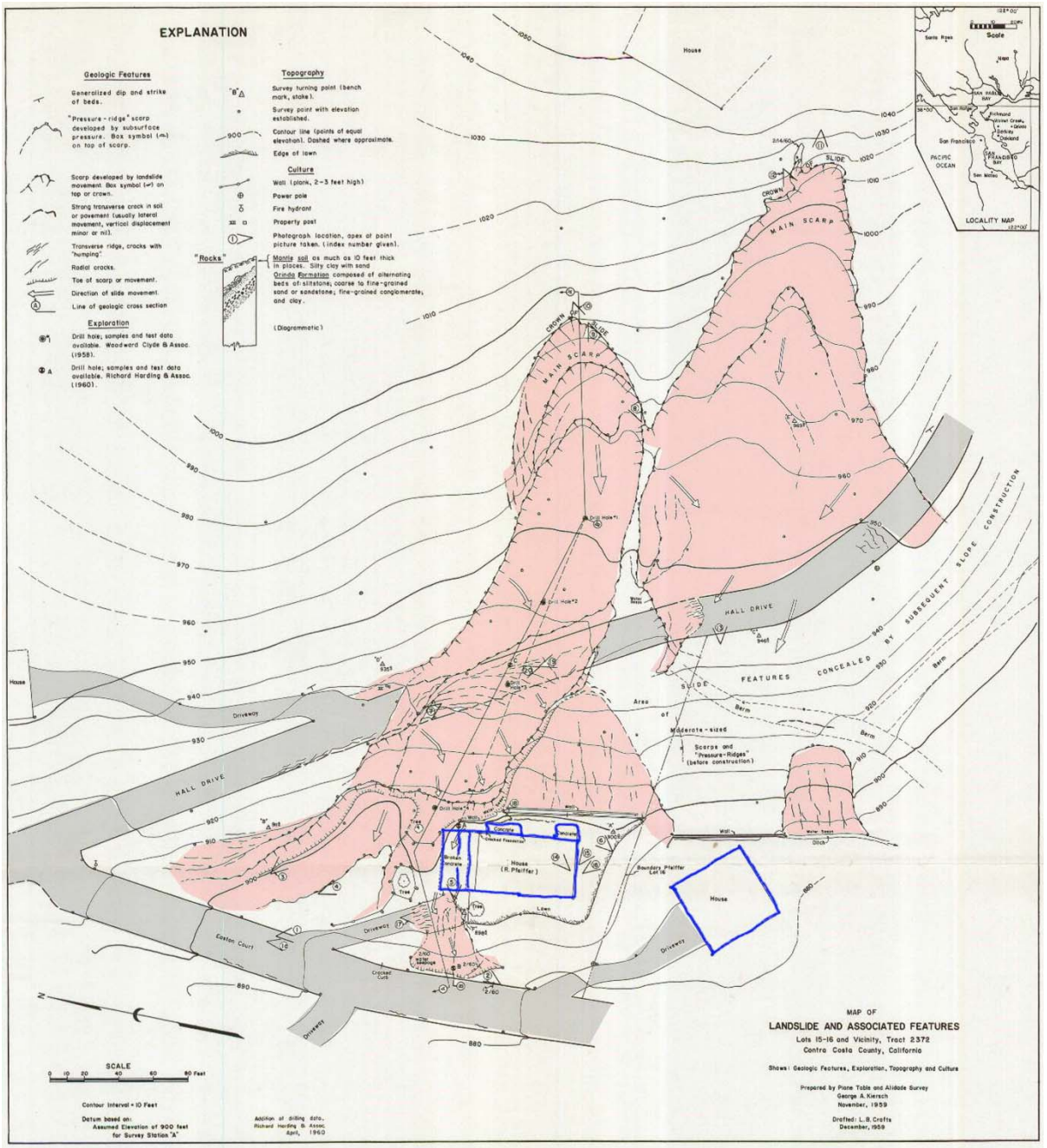

Figure 21c. Topographic map of the landslides that impacted the Pfeiffer residence on Easton Court in April 1958. The Pfeiffer home (outlined in blue ink) was later repaired, but Contra Costa County Public Works decided to close Hall Drive because of the expense of repairing both slides (modified from Kiersch, 1969).

initially adopted by the City of Los Angeles in 1952, which were similar to the excavation and grading ordinances adopted by the City and County of San Francisco in 1956 and Alameda County in 1958.

In the summer of 1960, Contra Costa County sent representatives of their Building & Inspection Department down to Los Angeles to discuss the practical aspects of their new excavation and grading code. One of these visitors was Bob Geise, who became the county's Chief Building Official for many years. Contra Costa's first grading ordinance was adopted on November 30, 1960. San Mateo and Contra Costa Counties were the third and fourth agencies to adopt grading standards in the San Francisco Bay area.

Contra Costa County's implementation in 1961 arrived too late to have a significant impact upon Orinda, but it

Downloaded from http://pubs.geoscienceworld.org/aeg/eeg/article-pdf/31/1/i/6130855/i1558-9161-31-1-i.pdf
by AEG RBAC user

had a beneficial impact on the mass-grading techniques subsequently employed in Moraga by Utah Mining and Development Corporation, described in Rogers (1988b).

Landslides Impact Orinda Once Again (1962–63)

In early 1962, a total of 11.32 in. (28.8 cm) of rainfall was recorded at St. Mary's College during 15 days of rain between February 6 and 20. These showers triggered numerous slump-earthflow slides (Radbruch and Weiler, 1963). These events were followed in October by the largest short-term precipitation event ever recorded in the San Francisco Bay area. Between October 10 and 14, a total of 13.82 in. (35.1 cm) of rain was recorded at St. Mary's College, with 8.40 in. (21.3 cm) in 24 hours between 5:00 p.m. on October 12 and 13. McCarty and Bryant (1962) declared the storm a 100-year recurrence event for 24 hours in Oakland.

These storms were followed by a series of winter storms in January 1963, which affected much of coastal California (Rantz and Harris, 1963). The October 1962 storms also set a 48-hour record for Orinda, dumping 16 in. (40.6 cm) of rain in 2 days, beginning around midnight on October 10.

These intense storms triggered several slope failures (Radbruch and Weiler, 1963). The eight-lane alignment for Highway 24 between the Orinda Crossroads and the Caldecott Tunnels was then under construction (August 1962 through February 1965). A cut slope made on the north side of Highway 24 in 1957 west of Acalanes Road slumped out onto El Nido Ranch Road, revealing jagged exposures of the underlying bedrock (Figure 22).

Oak Road was washed out where it crossed a draw between Camino Encinas and what later became Knickerbocker Lane. Loss of this right-of-way removed vehicular access to the "paper lots" of Oak Springs Units 3 and 4, subdivided back in 1926. Oak Road was not repaired in this location until 1991. Another dramatic closure occurred along Camino Del Monte between Las Piedras and Alta Vista. This stretch of road has never been reopened.

December 1964–January 1965 Storms

Intense storms in December 1964 and January 1965 brought record amounts of rain to northern California (Waananen et al., 1971), causing unprecedented levels of flood-induced erosion damage (Robinson, 1965). The Warford Terrace slide, largely unrepaired since 1958, reactivated. This time, it enlarged considerably over that which had occurred in 1958, impacting the properties at 4 Warford Terrace, 28 Muth Drive, and 30 Muth Drive (Provenzano, 1965). By late February 1965, the slide had enlarged itself even more, damaging the home under construction at 39 Muth Drive (Figure 23a and 23b). The County red-tagged the structure and forced its dismantling (the lot remained vacant for several decades). Emergency repairs were enacted to retard further sliding. These repairs included the drilling of additional hydrauger drains. This same slide reactivated again in February 1983, enlarging itself even more (Provenzano, 1983; Seidelman & Associates, 1983).

Figure 22. Cut-slope failure in January 1963 along the north side of Highway 24 at El Nido Ranch Road, just west of Acalanes Road. The slide involved strata from the eastern facies of the Orinda Formation. The cut had been graded just 4 years prior to the failure (Fred Taylor, USGS).

Figure 23a. The December 1964-January 1965 cut slope failure between Warford Terrace and Muth Drive pushed new concrete retaining walls into the backs of the three homes then under construction. (Roger G. Fry).

Improved Grading Ordinances Make Their Presence Felt (1963–65)

In January–February 1963, southern California was hit hard by a protracted series of storms, which caused

Downloaded from http://pubs.geoscienceworld.org/aeg/eeg/article-pdf/31/1/i/6130855/i1558-9161-31-1-i.pdf
by AEG RBAC user

Figure 23b. This view shows the same home but looking upslope at the dormant Warford Terrace landslide in August 1970. The incomplete homes languished for the next 6+ years until the failing slope was repaired across six adjoining lots using compacted fill with subdrains and new retaining walls (Contra Costa County).

considerable flood damage in the greater Los Angeles area. These events happened to coincide with a 10-year effort to develop minimum universal standards for various aspects of excavation and grading of earth materials, which became "Appendix Chapter 70 on Excavation and Grading" introduced in the 1964 Uniform Building Code (UBC) published by the International Congress of Building Officials (ICBO) in Whittier, CA (Scullin, 1966, 1983). The adoption of Appendix Chapter 70 at the local level brought more conservative standards than those of the original 1952 Los Angeles Code, similar to what Contra Costa County had adopted in late 1960. These changes included dropping maximum fill slope inclinations from 1.5:1 (33.67 degrees) to 2:1 (26.5 degrees) and laying back cut slopes from a maximum of 1:1 (45 degrees) down to 1.5:1 (33.67 degrees).

The new code was advanced by the City of Los Angeles Department of Building & Safety. It adopted a more prescriptive style of regulations and was officially adopted by ICBO in April 1963, and it first appeared in the 1964 UBC. Its adoption was by municipal city councils or county boards of supervisors, usually on the recommendation of their departments of building and safety.

Los Angeles and Orange Counties soon implemented similar standards, creating the most comprehensive grading ordinances up to that time. This became the new standard for all the government entities using the UBC (most of the states west of Missouri). In June 1965, the FHA office in San Francisco also amended their grading and excavating standards to align with the new standards adopted in southern California. The FHA standards now called for cut and fill slopes to be no steeper than 2:1 (horizontal to vertical) and for all fill soils deeper than 5 ft (1.5 m) to be compacted within specifications determined by maximum densities derived from the modified Proctor test method (ASTM.D 1557).

Construction of the BART Berkeley Hills Tunnels (1964–67)

In 1962, a referendum creating the BART District was approved by voters in Contra Costa, Alameda, and San Francisco Counties. By late 1964, plans had been drawn up to enclose the new BART alignment within the centerline of Highway 24 from Orinda to Walnut Creek. In order to accommodate the new BART right-of-way, the recently completed freeway had to be widened dramatically, placing the new Orinda Station and parking lots between the eastbound and westbound lanes of a new dilated freeway interchange at Orinda Crossroads (Figure 24a).

The accommodation for BART at the Orinda Crossroads also provided a staging area for construction of BART's 3.1-mi-long (5-km-long) Berkeley Hills twin tunnels. BART letthe first of $3.1 million (1960s dollars) in exploration contracts for the tunnels in November 1963, and diamond drill cores were drilled and recovered for testing and analysis through May 1964 (Rogers, 2001a). The design of the new BART tunnels was awarded to Bechtel Corporation in 1963. The new bores were to be 450 ft (137.2 m) lower than the Caldecott highway tunnels (Figure 24b). Between May and October 1964, exploratory adits were excavated at both tunnel portals to explore ground conditions (Bechtel Corporation, 1965; Brown et al., 1981).

Figure 24a. The kingpin element of BART's Concord Line is the 3.2-mi-long (5.1-km-long) Berkeley Hills Twin Tunnels, which cross the seismically active Hayward Fault, which creeps as much as 0.35 in./yr (9 mm/yr), depending on location (some locations known as "salients" exhibit no creep). This line began operating on May 21, 1973. This shows an eastbound train emerging from the Orinda Tunnels twin portals just west of the Orinda BART station in 1978. The Hayward Fault Zone is 980 ft (298.7 m) wide and begins about 1,000 ft (304.8 m) from the western portals. In 2017–23, the lining of the twin tunnels was refitted to adjust for the creep offset between 1966 and 2017.

Downloaded from http://pubs.geoscienceworld.org/aeg/eeg/article-pdf/31/1/i/6130855/i1558-9161-31-1-i.pdf
by AEG RBAC user

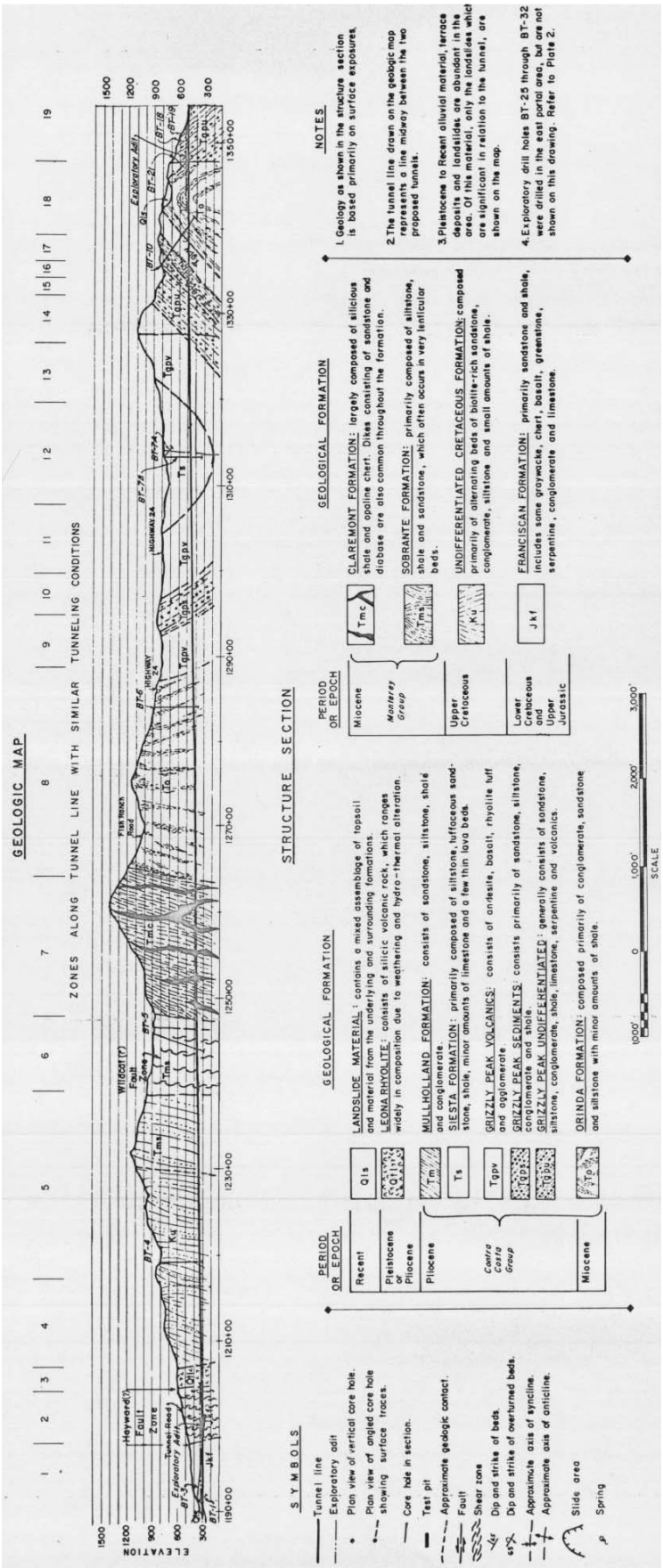

Figure 24b. Initial characterization of geologic conditions to be encountered along the BART Berkeley Hills Twin Tunnels, as initially envisioned in late 1964. These data were collected from four preliminary reports released in 1964. These reports contained geodata collected from reconnaissance mapping of cut slopes and outcrops exposed in the Berkeley Hills, subsurface data gleaned from the Claremont water tunnel excavated in 1927–29 for the East Bay Municipal Utility District, borings for the three Caldecott Tunnels (collected in 1928–34 and 1957–60), vertical and angled exploratory borings and core samples along the proposed alignments of the two tunnels (which were 100 ft [30.5 m] apart, and exploratory adits excavated at the proposed portals. The western portal crossed the tectonically active Hayward Fault Zone and was over 1,285 ft (391.7 m) long, while the eastern portal was 1,000 ft (304.8 m) long. In total, 12 geologic formations were recognized along the proposed tunnel alignment based on the geologic nomenclature of Case (1963). The tunnels were to be 17.5 ft (5.3 m) in diameter and approximately 3.1 mi (5.0 km) long (from Bechtel Corporation, 1965).

Downloaded from http://pubs.geoscienceworld.org/aeg/eeg/article-pdf/31/1/i/6130855/i1558-9161-31-1-i.pdf
by AEG RBAC user

The temporary support and final linings for the twin tunnels were designed by Bechtel Corporation and submitted to BART's Board of Consultants for technical review. In March 1965, a $31 million (1965 dollars) construction contract was awarded to J. F. Shea, Kaiser Industries, and Macco Corporation, in joint venture (Demoro, 1967). Twin headings were undertaken at the Oakland and Orinda portals in May 1965 and were holed through by March 1967 (Content, 1967). Upon completion of the twin tunnels in 1967, the east portal staging area in Orinda was converted into the spacious parking lots for the Orinda BART Station.

The First Orinda BART Station Landslide (1966)

In early 1966, the staging area for the Orinda tunnel portals was excavated north of Highway 24 and 3/8 mi (0.6 km) west of Camino Pablo. These excavations were intended to accommodate the circuitous re-alignment of westbound Highway 24, looping around the new BART station complex (Rogers, 2001a). The new alignment required extensive excavation into the hillsides northeast of the Orinda tunnel portals (950 to 2,500 ft [289.6 to 762.0 m] northeast of the 1950 Orinda landslide). As a part of this highway re-alignment, the concrete culvert carrying San Pablo Creek beneath the new highway right-of-way and BART (originally built in 1953–54) was extended to its present length of over 1,300 lineal feet (396.2 m), which reduced its design capacity.

BART had agreed to pay 100 percent of the cost of the highway re-alignment because Highway 24 had only been completed 4 years earlier. State highway engineers had specified 1.5:1 (horizontal to vertical) cut slopes, extending some 200 ft (61m) above the new westbound alignment. Unfortunately, the proposed cuts truncated prehistoric landslides (Figure 25b) and Case's (1963) proposed trace of the Moraga Thrust (fault), a short distance northwest of the eastern tunnel portal's staging area. By the late summer of 1966, the entire hillside behind the new cuts began to give way without any contribution from rainfall events (Figure 25a). It soon became apparent that the volume of material involved was considerable, and that the back-slope failure was unexpectedly out-of-control. The new highway right-of-way was in jeopardy of being closed at any time.

Figure 25a. Tensile scarp that suddenly formed several hundred yards upslope of recent cut along Highway 24 to accommodate the new Orinda BART Station in the summer of 1966 (Dorothy Radbruch, USGS).

Figure 25b. Overview of massive cuts in the Mulholland Formation being excavated along the northern side of Highway 24 in the summer of 1966, just west of the future Orinda BART Station (Fred Taylor, USGS).

Caltrans engineers decided to lay back the cut slope to a lower inclination, a technique that had proven to be successful in two of California's largest slides: in 1957 at the Carquinez Cut on Interstate 80 (then U.S. Highway 40) and in 1960 at the Mulholland Cut on the San Diego Freeway (Interstate 405) in Los Angeles (Smith and Cedergren, 1962; California Division Highways, 1967). Scrapers were dispatched to the site, and the slope was laid back to a 2:1 inclination (Figure 25b), similar to what had been accomplished on the Orinda slide repair in 1950–52.

As the enormous section of hillside was being excavated, Caltrans geologists monitored the tension cracks above the cut. They found some fissures extending several hundred feet (tens to hundreds of meters) behind the cut face (Figure 25a). Despite their attempts to unload the mass, the slope above the laid-back cuts continued to move (Figure 25b), likely due to decreased effective stresses within the underlying Mulholland Formation (Rogers, 1979). No matter what methods the engineers tried, the slope problems seemed to be enlarging in the heat of a summer without rainfall!

A subsequent look at the cut slopes by USGS geologists (in September 1966) and later by Caltrans geologists revealed that the problem area seemed to be aligned with the un-mapped Moraga Thrust fault. This feature separates gray-colored strata of the Mulholland

Downloaded from http://pubs.geoscienceworld.org/aeg/eeg/article-pdf/31/1/i/6130855/i1558-9161-31-1-i.pdf
by AEG RBAC user

Formation from the brown-colored units of the Grizzly Peak Volcanics, higher on the slope (Figure 25b).

In 1962–63, Jim Case of the USGS discovered and mapped the Moraga Thrust fault through this area. He also showed the Mulholland beds to be overturned by drag folds along the thrust, as part of his doctoral studies at Cal Berkeley (Case, 1963). This work was part of an ongoing project that had assigned Case to work with USGS engineering geologist Dorothy Radbruch (1969), who knew the landslide history of the area.

In all of these massive slope failures along a busy commuter freeway, Caltrans found themselves facing an uncomfortable dilemma: BART was obliged to pay 100 percent of the costs for the re-alignment of Highway 24 and all of the slide repairs associated with the "initial construction," which was not proceeding as expected. However, their contract only covered 50 percent of maintenance costs for the first 10 years after the completion of BART (1972–82). From 1982 onward, Caltrans would be limited to working from their own funds. With BART "on the hook" for 100 percent of any near-term repair costs, Caltrans opted for the most conservative repair they could envision.

They decided that the entire hillside area along either side of the Moraga Thrust would be excavated to create an artificial debris and water storage basin, about 600 ft (182.9 m) long, situated alongside the new highway alignment. In this way, it was hoped that future debris would be trapped in the basin and would not impinge on the paved right-of-way, where it could quickly become a traffic hazard. The new design required excavation of 2.4 million cubic yards (1.83 million m^3) of additional material with finished cut slopes of between 2:1 and 3:1 (horizontal to vertical) inclination, extending as much as 240 ft (73.2 m) above the highway (Rogers, 1979, 2001a).

More Slide Problems (1967–73)

In the midst of all this remedial construction, the new excavations were deluged by fierce storms during the last week of January 1967 (described below). So, the mass grading was not completed until the early fall of 1968. The new BART station landslide repair was tested by another round of storms that struck the area during the winter of 1968–69 and again in 1969–70 (see rainfall data in Appendix 4). Despite their conservative slope layback, the new cut slopes began experiencing retrogressive back-slope failures. Drainage interceptor benches were destroyed, but the length and breadth of the excavated "valley" provided valuable storage space for the newly loosed slide debris.

During the winter of 1972–73, large tension cracks developed high on the cut slope, within the Grizzly Peak Volcanics. Numerous springs and seeps began appearing on the cut slope along the approximate outcrop of the Moraga Thrust fault. Most of the secondary failures were likely associated with elevated groundwater (pore) pressures developed along the hanging-wall side of the fault, which separates the Grizzly Peak Volcanics from the Mulholland Formation (Rogers, 1979). The fact that such fresh exposures of bedrock could weather quickly and lose appreciable shear strength was something of a novelty. The site soon became a favorite stop for Cal Berkeley's geology and geotechnical engineering field trips. Then, without any forewarning, in February 1978, another spectacular failure befell the repaired area (described later, in chronological order).

Storm Damage of January 1967

Between 1959–65, the Warford Mesa tracts evaluated by the USGS for the FHA in the mid-1950s were being graded to support single family residential homes. Tract development began in 1956 with those lots closest to Orinda Crossroads and proceeding to the crest of the ridge along Tahos Road by 1963–64. Home construction generally followed a short time thereafter, with the last tract homes being completed in 1965–66.

The absence of any solid engineering geologic input was soon made apparent when the recently graded slopes were subjected to sustained precipitation. During the last week of January 1967, an intense El Niño–style storm passed through the East Bay, delivering more than 6 in. (15.2 cm) of rain on Orinda in a 41-hour period, commencing at 4:00 a.m. on January 20. Dozens of homes along Warford Terrace, Muth Drive, Wanda Lane, Austin Court, Tahos Road, and Silverwood Court were either lost or severely damaged by new landslides (mostly retrogressive slump blocks and slump-earthflows). Slope failures also occurred along the high-speed alignment for San Pablo Dam Road graded in 1957 (Harding, 1969), shown in Figure 26, and along the newly completed Bear Creek Road (Waltz, 1967), a short distance north of town.

The storms of January 1967 were the first to impact the upper Warford Mesa tracts since grading had been completed in mid-1963. One new home on upper Tahos Road was destroyed (Figures 27 and 28a and 28b), while one of the neighbors' homes was salvaged and moved to another location. The homes on Warford Terrace and Muth Drive were only 5 years old, while those near the corner of Muth Drive and Austin Court were only 3 years old. The Muth/Austin slide behind the Preston home was repaired in 1967–68, but it reactivated during the 1969 storms (also see discussion of 1983 storm damage).

Lawsuits were soon filed alleging that the recent earth movements should have been foreseen. This initiated an infamous series of lawsuits for earth movement that stretched into the 1990s. Research associated with the lawsuits referenced the old studies of the USGS in 1956 (Reuben Kachadoorian was even subpoenaed in Alaska

Downloaded from http://pubs.geoscienceworld.org/aeg/eeg/article-pdf/31/1/i/6130855/i1558-9161-31-1-i.pdf
by AEG RBAC user

Figure 26. Failure of road-fill prism along San Pablo Dam Road, during the storms of January 1967. The fill had been placed in 1956–57 without recognizing that the foundation was part of an extensive relict bedrock landslide complex. The slip-out was repaired but failed again in February 1983 (Ron Rigor, Contra Costa County).

Figure 27. Overview of the Tahos Road landslide of January 1967, after damaged portions of the residences had been demolished and removed from the area (Fred Taylor, USGS).

for questioning in a 1973 lawsuit). The verdict was unnerving: Virtually all of the landslide mapping accomplished by the USGS geologists had been ignored by the developer's consultants! The worst problems appear to have been embankments where compacted fill was often placed on dormant prehistoric landslides that soil technicians and geotechnical engineers were not trained to recognize. The absence of engineering geologic expertise was similar to what had occurred on upper Tahos, Muth Drive, and Austin Court a few years earlier. Surcharging the old slides with fill often triggered more extensive landslides the first time manufactured "rice paddy" lot pads absorbed appreciable amounts of moisture (schematically shown in Figure 24a, 24b, and 24c).

In the interim (1968), more mass grading was accomplished to support new construction of subdivisions along Knickerbocker Lane and Candlestick Road, within

Figure 28a. Close-up of structural damage accompanying the Tahos Road landslide of January 1967, as viewed on May 9 (Ron Rigor, Contra Costa County).

Figure 28b. Profile of damaged homes along upper Tahos Road, as seen on April 27, 1967 (Ron Rigor, Contra Costa County).

lower Gateway Valley, which was being used as a local landfill within the old Kaiser sand and gravel quarry.

Storms of February 1969

Between February 22 and 28, 1969, it rained for 7 consecutive days following a wet January (a 3-week average of 8.5 in. [21.6 cm]). This was followed by storms of even greater intensity the following December (see monthly rainfall tabulations in Appendix 4). During this cycle, more homes and roads were damaged or destroyed than in any previous year up until that time. Lower Tahos Road was closed, as was Warford Terrace and several parts of El Toyonal, Cañon Drive, Normandy Road, and 43 Valencia Road, between Altamont and Don Gabriel. A good-sized slide began near the cul-de-sac of La Encinal Drive, failing again in February 1970 and January 1982 (and repaired in 1983).

Other landslides of note reported by the USGS (Taylor and Brabb, 1972; Fleming and Taylor, 1980)

Downloaded from http://pubs.geoscienceworld.org/aeg/eeg/article-pdf/31/1/i/6130855/i1558-9161-31-1-i.pdf
by AEG RBAC user

included those along Diablo View (off Miner Road), along Spring Road, off upper Wanda Lane onto Highway 24, between Bates/Warford Terrace and Muth Drive (Figures 29a, 29b and 30), Camino Pablo at Orinda Village, Moraga Way between the Orinda Crossroads and Moraga, and at 33 Marston Road. Alice Lane was so damaged that the subdivisions under construction (by Cork Harbor Development) went bankrupt, and the road was closed until development resumed in the late 1980s. More landslides occurred at 15 Hall Drive and 23 Hall Drive, close to the former Pfeiffer home (Figure 21a, 21b, and 21c).

One of the most publicized slides occurred between Donald Drive and Cedar Lane (Figure 30). The slide repair behind the Preston home at the inside corner of Muth Drive and Austin Court was of insufficient effort to dispel further movement, and, according to County records, Preston's entire lot began creeping downslope in March 1969 (Figures 31 and 32). The Preston home was moved off site, and the lot remained vacant for more than 20 years.

Figure 30. Landslide between Cedar Lane (foreground) and Donald Drive, which occurred in early March 1969. Fill had been unknowingly placed on a dormant landslide. The debris slumped and flowed, filling the valley at right (Reuben Kachadoorian, USGS).

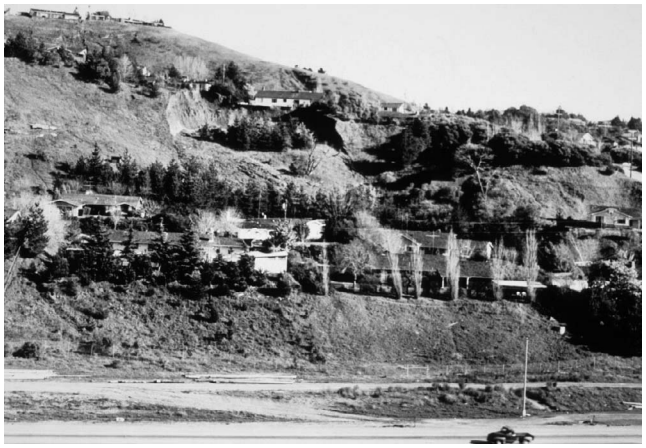

Figure 29a. Rotational slump landslide emanating from the embankment along the north side of Bates Boulevard moving towards Muth Drive in the early spring of 1969 (Fred Taylor, USGS).

Figure 29b. Crown scarp of the 1969 Bates Boulevard–Muth Drive landslide. Note the exposed shell of the swimming pool behind the Bufton residence at left (Ron Rigor, Contra Costa County).

Grading Codes Amended Again (1969–70)

The disastrous effects of the 1967 and 1969 storm damage prompted Contra Costa County to amend their 1960 grading ordinance, summarized in Table 2. Despite a lively debate fostered by local builders, the County Board of Supervisors adopted a series of amendments in mid-1969 that more-or-less mirrored the more conservative limitations adopted in southern California in the late 1960s (Scullin, 1966, 1983). According to County records, other landslides in Orinda triggered during the

Figure 31. View looking northwest down Austin Court in 1969. The street had dropped about 2 ft (0.6 m), indicating the landslide of 1967 had retrogressed into the bedrock cut area. Note asphalt quick-patches installed by Contra Costa County Public Works (Ron Rigor, Contra Costa County).

Downloaded from http://pubs.geoscienceworld.org/aeg/eeg/article-pdf/31/1/i/6130855/i1558-9161-31-1-i.pdf
by AEG RBAC user

Figure 32. Moving 80 degrees to the left, we see the Preston home at the corner of Austin and Muth Drive. Over 2 years, this slide block had dropped 8 to 10 ft (2.4 to 3.1 m), necessitating the home's removal (Fred Taylor, USGS).

Table 2. *Differences between Contra Costa County grading ordinance (Contra Costa County, 1960) and the 1991 Uniform Building Code.*

Contra Costa County Building Regulations (Article 716-8)	Uniform Building Code (UBC) Chapter 70 Excavation & Grading (1991 edition)
Cut slopes up to 40' high without drainage terraces Art 716.8.204 (Fill slopes same as UBC)	No cut or fill slopes greater than 30 feet high without mid-slope terrace Sec. 7012.(a)
Fills need only be compacted to 90% of Caltrans Test Method 216F/33,000 ft-lbs Art 716-8.402	All fill to be compacted to 90% of ASTM D-1557-91/56,200 ft-lbs @ Sec. 7002 & 7010(d)
Drainage terraces not less than 5 feet wide Art 716-8.416	Drainage terraces not less than 6 feet wide Sec. 7012(b)
Allows for 85% relative compaction within 8" of slope face Sec 716-8.404	Mandates minimum of 90% compaction at all locations Sec. 7010(d)
Drainage terraces to be between 1% and 3% slope Sec 716-8.608	Drainage terraces to be sloped a minimum of 5% Sec. 7012(b)
Allows for uncompacted fills to be sloped up to 3:1 Sec 716-8.412	Does not allow for any fill to be placed at less than 90% compaction Sec. 7010 (d)
Does not specify paving of drainage terraces	Specifies concrete pavement on terraces, minimum width, thickness, depth, and maximum tributary drainage area Sec. 7012(b)
No requirements for subdrainage	Requires subdrainage as necessary to insure long-term stability Sec 7012(c)
No specific methodology specified for classification of expansive soils.	Specifically mandates use of UBC Test 29-2, Expansion Index Test, in order to classifdy expansive soils. Sec. 2904(b)
No specific requirements for foundations in expansive soils.	Mandates special design consideration be presented to the building official for all soils with an Expansion Index greater than 20. Sec. 2904(b)

winter of 1969–70 included those along Casa Vieja, Normandy Road, La Encinal, and Cañon Drives.

Winter Storms of 1972–73

The BART system opened for business on September 11, 1972. An extreme frost struck the East Bay Hills during the winter of 1972–73, followed by another El Niño storm sequence during the last week of January 1973, which triggered destructive debris flows in the San Francisco Bay area (Rodine, 1974).

The January 1973 storms were sudden and intense, with most of the damage being caused by shallow debris flows and surficial erosion. An exception was the localized failure of the landslide repair northwest of the Orinda BART Station, completed in 1966–68. Some debris from this failure spilled onto the westbound on-ramp of Highway 24, forcing Caltrans to regrade the toe area and construct a series of concrete-lined drainage interceptor ditches.

In other parts of Orinda, the rain was sufficient to permanently close portions of Donald Drive on Mulholland Hill, and it eroded several hundred cubic yards (cubic meters) of graded material along Stein Way, a short road constructed in 1966 between Moraga Way and undeveloped lots along Oak Road that had been stranded by landslide damage in January 1963. Other parts of Oak Road also gave way again. Recent cut slopes made by Caltrans for the Gateway Boulevard on/off-ramps also failed during this storm, as did those along Mt. Diablo Boulevard near El Nido Ranch Road.

Minimum Grading Code Standards Adopted Statewide (1974)

The new grading ordinances were so successful in mitigating seasonal storm damage that the State of California amended their Health & Safety Code in 1973 to require all cities and counties to enforce the Excavation & Grading chapter of the 1973 UBC or its equivalent, beginning in March 1974. In those days, a new version of the UBC was issued every 3 years, and most building departments adopted these new versions within a year of their introduction if they were issuing a fair number of building permits each year. Communities with lower population densities or an absence of building activity did not tend to adopt new building code standards as promptly.

Comparison of Contra Costa County Grading Ordinance and Uniform Building Code (1970–97)

Contra Costa County's grading ordinance remained largely unchanged for three decades after their adoption of County Ordinance 69-59 in 1969, which was incorporated into Article 716-8 of the County's Building Regulations. Between 1970 and 1997, the UBC incorporated a number of changes, which licensed professionals were supposed to treat as minimum industry standards. Some of these differences are noted in Table 2.

The 1969 County Ordinance 69-59 reduced maximum cut and fill slope inclinations to 2:1 (horizontal to vertical); the minimum slope across graded pads was increased to 2 percent; drainage terraces were to be a minimum of 5 ft (1.5 m) wide and sloped between 1 percent and 3 percent; fills with less than 90 percent relative compaction could not be steeper than 3:1; and the

Downloaded from http://pubs.geoscienceworld.org/aeg/eeg/article-pdf/31/1/i/6130855/i1558-9161-31-1-i.pdf
by AEG RBAC user

compaction standard was relaxed to 85 percent within 8 in. (20.3 cm) of the slope face.

In the 1970 UBC, 2:1 cut and fill slope inclinations were also adopted, as was the 2 percent gradient across graded building pads. However, UBC Sec. 7012(b) specified more drainage terraces than Contra Costa County's code, and it called for a minimum 5 percent slope on drainage terraces to promote self-cleansing (Scullin, 1983, 1993).

Zander Drive and Other Landslides of 1969–70

Between October 14 and 17, 1969, an early-season storm struck the East Bay Hills, dropping several inches (tens of centimeters) of rain, followed on December 10 by 3.10 in. (7.9 cm) of rain in less than 24 hours. By early February 1970, a portion of Zander Drive near its summit with Rheem Boulevard on the Orinda-Moraga border was the scene of a deep-seated bedrock slide that destroyed three and damaged two upscale homes (Figures 33 and 34a and 34b).

The Zander Drive landslide (Figure 33) was similar to other recent slides in Warford Mesa in that it was triggered by the placement of engineered fill on an unrecognized prehistoric landslide. The largest slides were triggered by the cumulative accumulation of precipitation over several consecutive years. When groundwater levels rose to a sufficient level, the entire slide mass began to translate downhill along a preexisting landslide slip surface.

The County employed a novel *in situ* sub-drainage-centered repair designed by Ned Clyde Construction in 1970. The repair consisted of leaving the slide mass in place but installing large-diameter cylindrical shafts backfilled with gravel, intended to drain the slide mass in place. The moisture that collected within the drain caissons was discharged through a series of 2-in.-diameter (5-cm-diameter) hydrauger drains, like those employed by Caltrans in the repair of the 1950 Orinda landslide.

Economic impacts were a major consideration in completing the Zander Drive repair because the County had to bear 100 percent of the repair costs. In the previous winter (1968–69), the County had been declared a disaster area, and federal assistance had paid for 70 percent of the landslide repair costs. The costs associated with the drainage-only repair were about 15 percent of what would have been required to excavate a

Figure 33. Aerial oblique view of the Zander Drive landslide in January 1970, showing the five homes that were imperiled. A truck-mounted drilling rig can be seen a slight distance left of the "S" in the annotation "Slide Area." It was excavating one of the "drainage caissons" intended to intercept subsurface seepage.

Downloaded from http://pubs.geoscienceworld.org/aeg/eeg/article-pdf/31/1/i/6130855/i1558-9161-31-1-i.pdf
by AEG RBAC user

Figure 34a. Temporary shoring beneath the Vetterli residence at 82 Zander Drive, as seen on March 16, 1970, looking east (behind the home). A deep-seated bedrock slide was slowly creeping northward, undermining the ridge-crest neighborhood (Ron Rigor, Contra Costa County).

Figure 34b. View looking easterly along the southern shoulder of Zander Drive on March 16, 1970. The crown scarp of the landslide extended across the paved right-of-way, requiring temporary support of buried utilities, shown in the foreground (Ron Rigor, Contra Costa County).

conventional remove-and-replace mass-grading repair. Two homes situated on the central down-dropped portion of Zander Drive were moved off their lots, which remained vacant for many years thereafter.

Despite these repairs, the Zander Drive landslide reactivated in February 1983. This may have been due to a failure of the hydrauger outlets connected to the vertical shaft drains. This time, the failure was covered by federal disaster assistance funds, and Contra Costa County Public Works was able to complete a permanent conventional repair in 1985–86. The County submitted their repair plans and slope stability calculations for external peer review.

The old UBC allowed an exception in Section 7012(d) for the building official to relax the 2 percent runoff gradient on graded pads to as little as 1 percent slope in flat-lying areas. There was considerable effort to retract this exception, as the basis for its inclusion (depth of fill and height of cuts) have no bearing on whether runoff can flow across a graded building pad (Scullin, 1993). Many agencies, such as Orange County in southern California, require a minimum 5 percent slope extending 5 lineal feet (1.5 m) away from the exterior walls of homes built in areas with expansive surface soils, like Contra Costa County.

USGS and Housing and Urban Development Landslide Hazard Mapping in the San Francisco Bay Area (1970–77)

The USGS–Housing and Urban Development (HUD) combined San Francisco Bay Region Environment and Resources Planning Study paid for the preparation of reconnaissance-level bedrock geology and landslide hazard maps of the San Francisco Bay area, initially at 1:62,500 scale (about 1 in. = 5208 ft [1 cm = 625.0 m]). The first of the true landslide maps was by E. E. Brabb, E. H. Pampeyan, and M. G. Bonilla, titled *Landslide Susceptibility in San Mateo County* (Brabb et al., 1972).

These were followed by special bulletins dealing with landslide mapping and correlations between rainfall and historic activity, which culminated in the following documents: T. H. Nilsen and B. L. Turner, 1975, *Influence of Rainfall and Ancient Landslides (1950–71) in Urban Areas of Contra Costa County, CA*: USGS Bulletin 1388, 18 p., 1 pl.; T. H. Nilsen, F. A. Taylor, and E. E. Brabb, 1976, *Recent Landslides in Alameda County, CA (1940–71): An Estimate of Economic Losses and Correlations with Slope, Rainfall, and Ancient Landslide Deposits*: USGS Bulletin 1398, 21 p., 1 pl.; and T. H. Nilsen, F. A. Taylor, and R. M. Dean, 1976, *Natural Conditions that Control Landsliding in the San Francisco Bay Region: An Analysis Based on Data from the 1968–69 and 1972–73 Rainy Seasons*: USGS Bulletin 1424, 35 p., 1 pl. The landslide maps contained in these bulletins were also released at a scale of 1:62,500, or about 1 in. to 5208 ft (1 cm = 625.0 m).

The key products of the HUD program were 57 7.5-minute USGS landslide quadrangle maps prepared by Dr. Tor Nilsen, termed Preliminary Maps of Landslides and Surficial Soil Deposits, and released as open-file reports, beginning in 1975 (method described in Nilsen and Brabb, 1977). In the late 1970s, these HUD products were re-released by the Association of Bay Area Governments (ABAG) as Basic Data Contributions. Most of these maps are now out-of-print but have been scanned and are available from private sources/suppliers.

Downloaded from http://pubs.geoscienceworld.org/aeg/eeg/article-pdf/31/1/i/6130855/i1558-9161-31-1-i.pdf
by AEG RBAC user

Drought of 1975–78

Following the 1973 storms, California experienced its most severe 3-year drought of the 20th century, between 1975 and 1978. Extra-normal rainfall, experienced throughout much of the 1960s, had served to elevate local groundwater tables. As the drought persisted, embankments began to sink or settle as the water table dropped, due to desiccation and consolidation of fine-grained soils. Portions of upper Rheem Boulevard began creeping downslope, while the big landslide on Zander Drive settled sufficiently to sever the buried storm drain outfall lines constructed by the County in 1970 (Figure 32). The only new construction of much consequence was the Moraga Country Club development, not far from Miramonte High School, and the Orinda Downs project above Sleepy Hollow.

Storms of February 1978 and Phase 2 of the Orinda BART Slide Repairs

The state's worst 3-year drought of the 20th century ended in early February 1978, when winter storms returned with a vengeance. The massive cut slope graded by Caltrans in 1967–68 to accommodate the Orinda BART Station had partially reactivated in 1973, leaving several deep tension cracks. On February 13, a mass of 200,000 to 250,000 cubic yards (152,800 to 191,000 m^3) (Walkinshaw, 1978) swept downslope, spilling onto the westbound on-ramp of Highway 24 (Figures 35 and 36).

Figure 35. Aerial oblique view looking northwesterly at the Orinda BART Station landslide on February 2, 1978. The landslide filled up the debris catchment area designed by Caltrans back in 1973. The entire catchment area was more-or-less filled, and some debris reached the westbound onramp of Highway 24 but was removed in 1.5 days. The landslide was evaluated by Caltrans, and federal disaster funds from the Federal Emergency Management Agency (FEMA) were secured to construct a mass-grading slide repair several years later (Caltrans District 4).

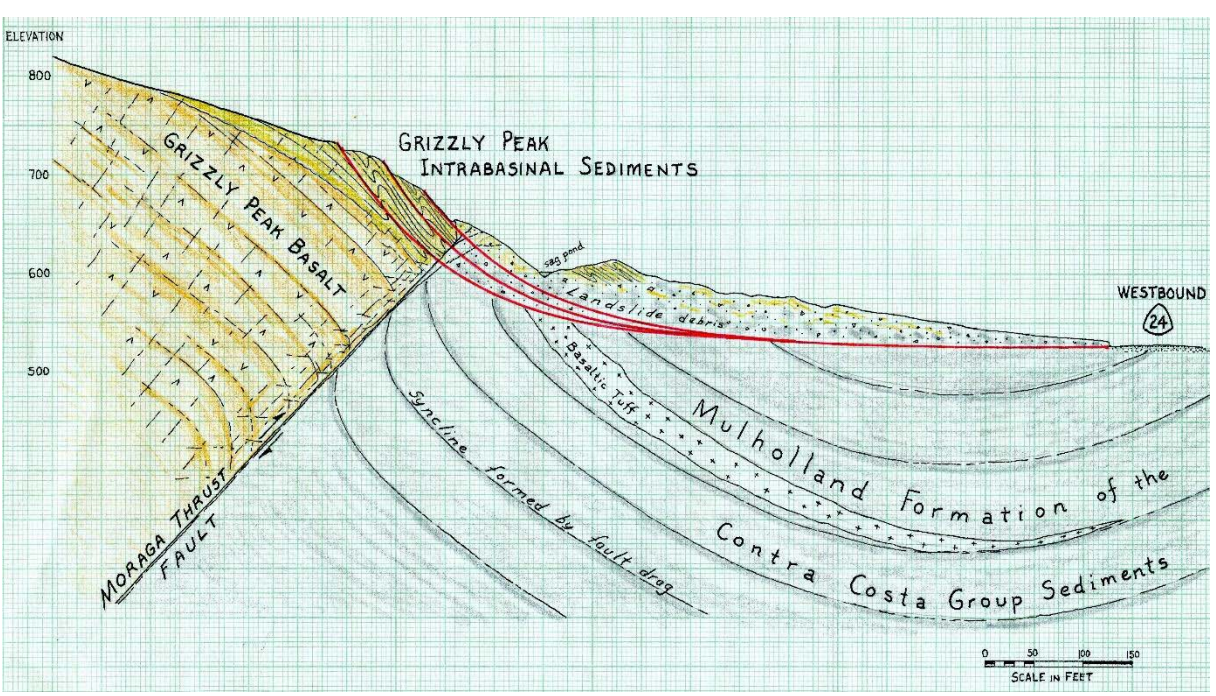

Figure 36. Geologic section through the 1978 Orinda BART Station landslide (from Rogers, 1979). Note structural and hydrogeologic influence of deformation along the Moraga Thrust fault, exposed in a series of the crown scarps.

Downloaded from http://pubs.geoscienceworld.org/aeg/eeg/article-pdf/31/1/i/6130855/i1558-9161-31-1-i.pdf
by AEG RBAC user

Rogers (1979) installed instrumentation at the headscarp of the slide area in 1978 as part of a USGS-funded study measuring shallow slope creep of intact hillsides and active landslides (Goodman et al., 1981). Rogers also excavated an exploratory trench across the Moraga Thrust where it was exposed in the headscarp of the 1978 slide.

Rogers noted that the slide was structurally controlled, slipping along lignite beds caught within steeply dipping recumbent folds on the up-thrown side of the Moraga Thrust (Figure 36). Most of the slide debris was comprised of Grizzly Peak intra-basinal sediments, which included freshwater marls (Curtis, 1978). The lower half of the slide was comprised of soft gray-colored beds from the Mulholland Formation, which exhibited increasing percentages of montmorillonite clay. The Mulholland Formation also contained a bed of basaltic tuff (weathered volcanic ash), which likely contributed to the shrink-swell behavior of the expansive clay (Curtis, 1978).

In order to protect Highway 24 and the BART Station parking lot, Caltrans designed a protective berm 30 ft (9.1 m) high across the toe of the slide, parallel to the westbound on-ramp. This berm was constructed in the fall of 1978 for a cost of $250,000 (1978 dollars). A year later, Caltrans let the Phase II contract for $480,000 (1979 dollars) to construct a conventional remove-and-replace graded repair of the BART Station slide mass. Extensive under-drainage measures were included in the 1979 repair because shearing along the Moraga Thrust had created an effective groundwater barrier due to the lower permeability of the lacustrine clays and weathered volcanics underlying the slopes west of the thrust.

Aside from some localized failures and erosional raveling in 1983, the 1979 slide repair performed satisfactorily. Because of the 1964 cost-share agreement between BART and Caltrans, they shared 50 percent of the costs of repairs for 10 years, which ended up including all the major slide repairs in 1978 and 1979 (Walkinshaw, 1979).

Geologic Hazard Abatement Districts (1979)

In 1979, State Senator Bob Beverly of Rancho Palos Verdes sponsored legislation allowing the establishment of special "Geological Hazard Abatement Districts," or GHADs (1979 Cal State 118, codified as Cal PRC 26500-26601). GHADs are intended to serve as special assessment districts formed to abate actual or threatened geohazards, such as landslides, land subsidence, soil erosion, or other natural or unnatural movements of land. A succinct summary is contained in Robert B. Olshansky's article "Geological Hazard Abatement Districts" in the July 1986 issue of *California Geology* (Olshansky, 1986).

The first GHADs formed in California were the Abalone Cove and Klondike Canyon Landslides adjacent to the Portuguese Bend Landslide in Rancho Palos Verdes in Los Angeles County. Abalone Cove includes 25 homes on a creeping 80-acre landslide and more than 75 residences uphill of the active slide, which could be threatened by the landslide. This district was established on July 19, 1985.

Petitions for GHADs require signatures from owners of at least 10 percent of the real property involved, or by resolution of the local legislative body, such as the City of Orinda. The application is accompanied by a formal "Plan of Control" written by a Certified Engineering Geologist (CEG) in the State of California. If more than 50 percent of assessed valuation of the proposed district objects to district formation, then the process is abandoned.

GHADs have also been employed to provide for preventative maintenance for new or recently constructed developments, such as those at Canyon Lakes in San Ramon and Blackhawk in Danville, formed in 1985. These GHADs were initially funded by the developers. In other instances, the formation of GHADs can be used as a condition of approval by local governing agencies. One example is the Castlegate GHAD, which was formed in Orinda in 1996 before any of the homes were occupied. These San Francisco Bay area GHADs were primarily focused on operations and maintenance of drainage improvements, as well as aging effects, such as slope creep, surficial erosion, and expansion and contraction triggered by shrink-swell cycles of expansive soils.

In 2001, a California Association of GHADs (www.ghad.org) was formed to pool resources and disseminate GHAD-related documents, such as best practices, white papers, legal opinions, and press releases. By 2017, there were 37 GHADs operating in California. GHADs have also been discussed as a possible mechanism for operation and maintenance of waterside flood protection systems, such as berms, bank protection, seawalls, levees, or retention/debris basins (ENGEO, 2008).

Storms of January 3–5, 1982

In late 1981, 24 in. (61 cm) of rainfall impacted the Orinda area, creating antecedent soil moisture (rainfall occurring during previous 60 days) well above normal levels. Just after the New Year, an El Niño cycle storm of approximately 34-hour duration struck the San Francisco Bay area, beginning around 7:00 p.m. on January 3, 1982 (Brown, 1982). This was the largest short-duration (24 to 48 hours) storm ever recorded in many parts of the San Francisco Bay area. The storm failed to supersede the October 1962 storm in the East Bay Hills, when Orinda received between 8 in. and 9.8 in. (20–25 cm) of rain in a little over 31 hours (Ellen and Wieczorek, 1988). In the Orinda area, the return frequency for the 24-hour event was believed to have been somewhere between 25 and 50 years (Brown, 1982).

Downloaded from http://pubs.geoscienceworld.org/aeg/eeg/article-pdf/31/1/i/6130855/i1558-9161-31-1-i.pdf
by AEG RBAC user

As large as the storm was, its effects were magnified by the wet weeks preceding its arrival, which increased the antecedent soil moisture levels. In addition, the storm's duration of >30 hours was most unusual (the normal storm duration in the San Francisco Bay area is about 1.5 hours [90 minutes]). The storm track triggered destructive debris flows and earthflow slides (Smith and Hart, 1982; Cannon and Ellen, 1985). In the Orinda area, there were 26 damaging landslides recorded by the USGS, but only four new landslides south of Highway 24. Debris flows were concentrated in Siesta Valley, Warford Mesa, and the Claremont Avenue drainage, between La Encinal and Camino Pablo (Wieczorek et al, 1988).

Besides natural debris flows, there were about a dozen slope failures associated with excavation and grading practices undertaken prior to the adoption of the county's first grading ordinance in 1960. These included steep cut slopes common in the El Toyonal area, which experienced surficial sloughing (Figure 37). Cañon Drive, off lower El Toyonal, was closed for several months due to the wash-out of road fill where a clogged culvert diverted runoff as sheet flow across the roadway, triggering rapid erosion of the fill wedge supporting the paved right-of-way (Figure 38a and 38b).

Several sections of La Encinal Drive were also threatened by wash-outs of side-cast road fill. Upper El Toyonal Road, connecting to Wildcat Canyon Road, was also hard hit, and this connector was closed to the public (because the cost of its repair exceeded its traffic utilization index). Several of the most visible slides occurred along Highway 24, below the end of Beatrice Road and above Gateway Boulevard, along the paved entry to the former Kaiser quarry owned by Edward J. Daly.

The style of damage was generally limited to excessive runoff-related phenomena, mostly by plugged culverts, runoff-induced erosion of road shoulder fills, and shallow debris sloughing of road cuts. Channel erosion along the region's principal creeks was also noted; in some cases, as much as 2 vertical feet (0.6 m) of downcutting were recorded downstream of hardened hydraulic structures, such as crossroad culverts.

Figure 38a. Washout of fill wedge supporting Cañon Road in January 1982. This was exacerbated by blockage of under-sized crossroad culvert. The road was closed for 4 months (J. David Rogers).

Figure 38b. Washout of non-engineered fill prism along Cañon Drive (a private drive extending off lower El Toyonal) during the storms of January 3–5, 1982 (J. David Rogers).

Figure 37. Surficial sloughing of an over-steepened cut slope along Cañon Drive following the storms of January 3–5, 1982. This view of the site was documented after the foliage had been cut to allow local residents to access their homes by walking (J. David Rogers).

Record Storms of 1982–83

The winter rains of 1981–82 delivered 44 cumulative inches (111.8 cm) of rainfall in Orinda. This was followed by another 41 in. (104.1 cm) during the 1982–83 season (see 12-month totals in Appendix 4). Normal rainfall (based on the period of record 1950–71) for the Orinda Crossroads area is 22 to 24 in. (55.9 to 61.0 cm) per season (Rantz, 1971; Nilsen and Turner, 1975. By the second week of February 1983, the cumulative 12-month precipitation reached its greatest level in the 20th century (and

Downloaded from http://pubs.geoscienceworld.org/aeg/eeg/article-pdf/31/1/i/6130855/i1558-9161-31-1-i.pdf
by AEG RBAC user

was an all-time high for 18-, 24-, 30-, 36-, and 48-month running averages, dating back to 1849). This time, the effects were cumulative, due to months and months of heavy rainfall, dating back to October 1980.

The largest landslides Contra Costa County had experienced in historic time were slowly drawn out of dormancy by the cumulative precipitation over the previous 3 years. So great was the effect that portions of relict bedrock slides dormant for an unknown period of time began reactivating for the first time. A bedrock slide with a volume of approximately 235,000 cubic yards (179,540 m^3) reactivated above Stein Way (Figure 39), severing the road and threatening three recently built homes on the northeast (downslope) side of the road. Review of the 1946 USGS aerial photos suggests that the Stein Way slide was a partial reactivation of similar movements that had occurred in the early 1940s. Though quite large, the Stein Way landslide was only a remnant of a much larger prehistoric slide complex, extending up the crest of San Pablo Ridge (shown on Map Sheet Q-10 in Appendix 2).

Other less spectacular but damaging landslides occurred between Bel Air and Parklane Drives, along lower Hall Drive, at Easton and Hall Drives, on Overhill Drive near Broadview Terrace, along the south side of Bates Drive, and below homes on Scenic Drive and Knickerbocker Lane. Some of the more notorious landslides of the past also reactivated. These included the Tahos Drive landslide, which had destroyed several homes on upper Tahos Road in 1967 (Figures 26 and 27), damaging homes along Silverwood Court when it reactivated.

The Austin Court Landslide, active in 1967 and 1969 (Figure 30), reactivated and enlarged itself, severing the court's utilities and clipping the corner of the residence at 65 Muth Drive (this slope and home were subsequently repaired). Particularly disconcerting was the apparent enlargement of the Austin Court Landslide, evidenced by a new headscarp extending across Muth Drive (Figure 40), above its intersection with Austin Court (Figures 41 and 42). Here, the road dropped about 6 in. (15.2 cm), severing three buried utilities beneath Muth Drive.

Reviews of the original grading plans revealed that the 1983 slippage must extend a considerable distance into the underlying bedrock. By 1983, the slide mass had enlarged to an area of approximately 5 acres (0.02 km^2). The broken utilities were repaired, and Austin Court was repaved in October 1985. Two new homes were constructed on the court in 1985 and 1989, but it is not known how these structures fared. In 1993, the senior author mapped slide-related features for the Contra Costa County Department of Public Works, who also

Figure 39. Aerial oblique view of the Stein Way landslide looking towards Moraga Way. The landslide reactivated in March 1983 (this image was taken in February 1984). Note the deranged drainage and number of isolated sag ponds (J. David Rogers).

Figure 40. Headscarp separation of the Austin Court landslide, cutting across Muth Drive, as seen in 1983. Note the offset curb and asphalt patches for repairs of severed water, gas, and sewer utilities beneath the pavement (J. David Rogers).

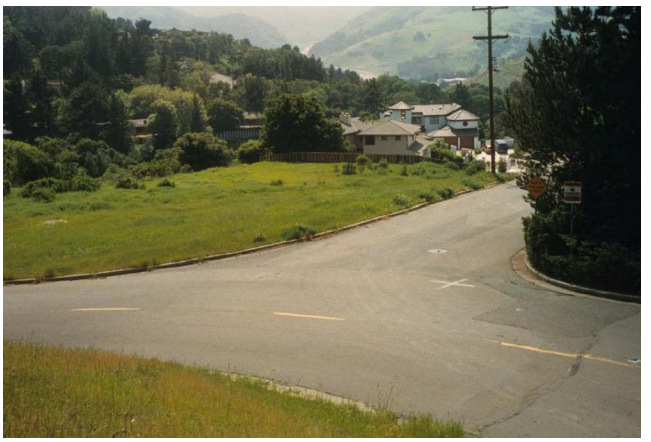

Figure 41. Overview of Austin Court, as seen in December 1988. Two homes have been removed at left center of image, along the downhill side of the court (J. David Rogers).

Downloaded from http://pubs.geoscienceworld.org/aeg/eeg/article-pdf/31/1/i/6130855/i1558-9161-31-1-i.pdf
by AEG RBAC user

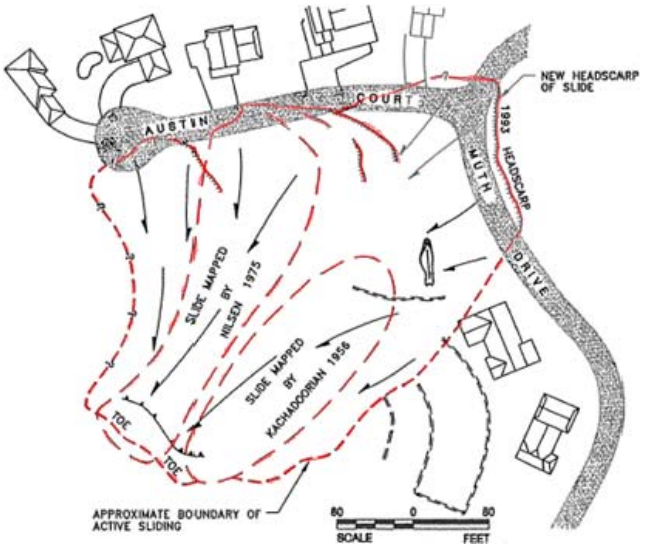

Figure 42. Landslide map of the area below the intersection of Austin Court and Muth Drive by Rogers/Pacific, Inc. (1994).

provided low-level aerial imagery of their storm-damaged areas (Figure 42).

The Warford Terrace Landslide, dating from early 1965 and 1967, was patched up in 1968, but it reactivated in 1983, impacting properties on Warford Terrace and Muth Drive. Lawsuits filed against homeowner's insurance carriers by residents on Warford Terrace resulted in court awards for damages in 1988. Relict slide deposits had been mapped beneath the area by Kachadoorian in 1956 (Figure 20) but were more-or-less ignored by civil and geotechnical consultants engaged in site development in the mid-1960s.

A steel-bin retaining wall was built by Caltrans to support El Nido Ranch Road in 1967. In 1983, it was undercut by a cut-slope failure along the north side of Highway 24. A dramatic debris-flow failure occurred in the valley below Charles Hill Circle, impacting several residences. Countless other slides occurred during the winter of 1982–83.

As in past years, most of these landslides occurred within fills that had been unintentionally placed on dormant landslide features. These included the reactivation and enlargement of the Zander Drive slide, smaller slides between Tara Road and Southwood Drive, below Bates Drive, and upper Warford Terrace, below Knickerbocker Lane, between Valley Drive and Glorietta Boulevard, along Overhill Road, along lower Hall Drive, and below Ardith Drive, among others too numerous to mention, including future Orinda Mayor Bill Dabel's home on Poco Paseo (Bruggers, 1989c).

Road Closures in 1983

Long-term road closures triggered by the 1983 storms affected El Toyonal between La Encinal and Loma Vista (closed for 2.5 years), upper El Toyonal between Vista del Orinda and Wildcat Canyon Road (never re-opened), Zander Drive (closed for 3.5 years), and Parklane (closed for 3 months). The slides on Stein Way, Zander Drive, Parklane, lower Hall Drive, Overhill Road, Tara Road, Charles Hill Circle, El Nido Ranch Road, upper Hall Drive, Warford Terrace, below Silverwood Court, and along Wildcat Canyon Road were eventually repaired with some engineering geologic input. Wildcat Canyon Road was repaired by Contra Costa County at several locations. To those who worked on these evaluations, it seemed like the entire area suffered earth movement damage of one form or another.

More Lawsuits and Grading Code Amendments (1983–89)

The storm damage experienced in 1981–82 and 1982–83 was of record levels, as much as $5 to $7 billion (1980s dollars) in the San Francisco Bay region. This caused planners, politicians, and engineers to consider the long-term consequences and potential policy changes (Olshansky and Rogers, 1987).

Despite public agencies' statutory immunity for issuance or denial of building permits (California Government Code 816.4), public agencies and utilities found themselves embroiled in a plethora of inverse condemnation lawsuits, where plaintiffs alleged that a civic improvement or public use of a road, easement, stream, or watercourse was a "substantial factor" in precipitating earth movement–induced property damage (Olshansky, 1989).

Even if public entities successfully defended the suits, there was an additional surcharge in dollars spent on legal defense. Like Los Angeles in 1963, many local agencies began adopting more restrictive measures for hillside development than those originally mandated by the County. Local entities in Contra Costa County that adopted more restrictive grading ordinances included Walnut Creek (1976 and 1983), San Ramon (1985), Martinez (1986), Danville (1987), and Clayton (1989). In 1987, Moraga adopted a restrictive open space ordinance that addressed grading concerns.

By 1984, most San Francisco Bay area geotechnical consultants decided to reduce maximum slope inclinations to 3:1 horizontal to vertical (18 degrees) for cuts and fills comprised of Orinda formation materials, sediments of the Contra Costa Group, or their age-synchronous equivalents in the Sycamore Basin south of Mt. Diablo and east of Danville–San Ramon (Rogers, 1988b). The "3-on-1 slope standard" gradually spread across the East and North Bay areas and was employed on major grading projects with expansive clay soils of low strength when saturated, like the soils in Pittsburg, Clayton, and Pleasanton, beginning in the early 1990s.

Downloaded from http://pubs.geoscienceworld.org/aeg/eeg/article-pdf/31/1/i/6130855/i1558-9161-31-1-i.pdf
by AEG RBAC user

Once again, the shift towards more conservative standards came a bit late for Orinda, but the information existed in the 1960s, suggesting that 3:1 inclinations performed much better than steeper slopes, based solely on local performance (Figure 43).

Orinda Incorporates (1985) and the Rains Return (1986)

Orinda finally incorporated as an independent city of California on July 1, 1985. Just when it seemed like the worst storm-related calamities of the 20th century were something of the past, another extra-normal storm sequence struck the East Bay Hills in mid-February 1986, bringing 15 in. (38.1 cm) of rain to Orinda in a little over 6 days (Rogers, 1986). This time, most of the damage was divisible into (1) runoff-related erosion/debris flows and (2) reactivation of 1983 slides that had not been modified by corrective grading or subdrainage.

Runoff-related failures impacted a number of homes between El Toyonal and La Encinal Drives, on lower Tahos Road at Wanda Lane, below Juniper Drive, below Camino Sobrante at Mira Loma, below Barbara Road north of Stein Way (a different landslide from that in 1983), and on parcels along lower Hall Drive. Old cut slopes along lower Tahos Road and between Juniper Drive and Hidden Valley also failed (Figure 44), temporarily closing these streets.

Much of the damage occurred within colluvial-filled bedrock ravines (a mechanism discussed later) and along unimproved stream channels. This style of damage was most prevalent in the upper watersheds, such as: the natural channel below Tappan Lane and Bear Ridge Road; along Lauterwasser Creek below Van Ripper Lane, along Miner Road and Tiger Tail Court, and below Southpoint Road; along the west branch of Upper San Leandro Creek, parallel to Don Gabriel Way, and near Del Rey School; along Glorietta Creek, just above Rheem Boulevard and parallel to Valley Drive; and Upper San Leandro Creek, along Brookwood Road just upstream of the 1,300-ft-long (396.2-m-long) concrete box culvert (shown in Figure 15).

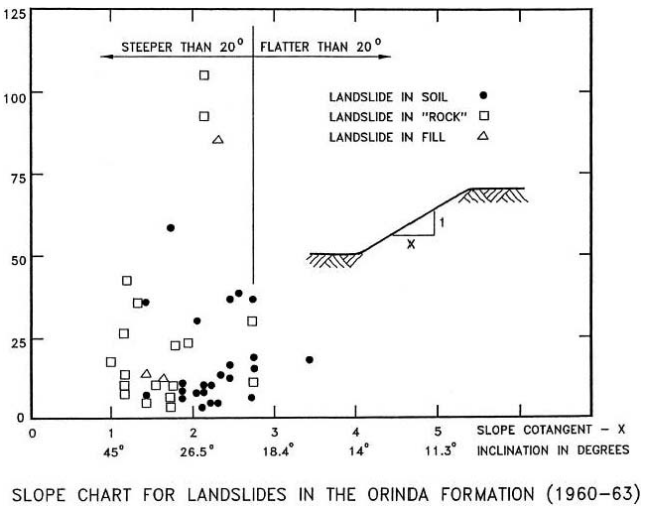

Figure 43. Measurements of slope inclinations for active landslides flooring in the Orinda Formation between 1960 and 1963, compiled by the University of California at Berkeley Professor J. Michael Duncan (1971).

Figure 44. Raveling cut slope between Juniper Drive and Hidden Valley Road, just east of St. Stephen's overcrossing of Highway 24. This was typical of the storm damage incurred in February 1986 (J. David Rogers).

Flooding along lower San Pablo Creek below San Pablo Dam was the worst since February 1936, when much of the same area was inundated (Purcell, 1940). Damage along upper San Pablo Creek was also extensive, although flood levels were never as severe as those experienced downstream of the reservoir, which began spilling overflow on the fifth day of the storms (February 19). The creek banks along upper San Pablo Creek along Glorietta Boulevard and Moraga Way also experienced numerous slope failures, as did some of the homes on the higher slopes, such as lower Hall Drive.

The UBC Relaxes Requirements for Drainage Terraces (1988)

In the 1988 edition of the UBC, the provision regarding terrace drains (Section 7012[a]) was amended to delete all requirements for drainage terraces, or "runoff interceptor ditches," on cut or fill slopes of 3:1 (horizontal to vertical) or flatter (Scullin, 1993). The reasoning offered by proponents of this change were that "flatter slopes were not as susceptible to erosion." This change also emanated from concerns about long-term liability exposure associated with the failure of drainage interceptor ditches, when left in an unmaintained state for many years. Many of the attorneys representing civil engineers in storm damage claims began viewing drainage terraces as "liability triggers."

Downloaded from http://pubs.geoscienceworld.org/aeg/eeg/article-pdf/31/1/i/6130855/i1558-9161-31-1-i.pdf
by AEG RBAC user

This change was welcomed by most developers in the East Bay, who assumed they would save on the expense of drainage interceptor ditches. (In 1988, paved interceptor ditches cost about $26 per lineal foot installed.) However, in situations where precipitation fell on newly graded slopes, there were often disastrous results, as reported in Contra Costa County by Scullin (1993).

Adoption of California Building Code (1988)

The California Building Code (CBC) was approved and incorporated into the UBC in 1988. It was simply the UBC with the addition of California's more stringent seismic design parameters, as determined by the California Building Standards Commission (CBSC). The CBSC reviews and approves building standards proposed and adopted by state agencies, administers California's building code adoption processes, and resolves conflict, duplication, and overlap in building standards. Since 1988, almost every municipality in California has adopted the CBC, while a few entities have adopted more conservative versions, such as the San Francisco Building Code.

Drought of 1986–92

The severe storms of February 1986 were followed by 6 years of lower-than-normal annual cumulative precipitation. The winter of 1990–91 saw the lowest levels of winter precipitation recorded during the 20th century, although droughts in the late 1940s and early 1960s were of comparable magnitude (see 60-month running averages in Appendix 4).

In March 1991, a series of storms staved off what had been, up until that time, a record low season for water storage in northern California reservoirs. As the drought became prolonged, local utilities issued mandates declaring 15 to 25 percent reductions in water consumption. Many people let their yards go dry for the first time, and localized settlement of foundations became commonplace. Settlement of road fills also began to plague highway departments, occasionally sufficient to sever some of the buried utilities!

During extended droughts, desiccation cracking may progressively extend deeper and deeper into the ground, negatively affecting foundations through asymmetric bearing capacity. When sudden storm outbursts occur, surface runoff would soon appear beneath houses, with runoff flowing freely through the network of desiccation cracks developed in the expansive soils.

Storm of January 12–13, 1993

On January 12–13, 1993 a brief, but intense storm rolled across the San Francisco East Bay, dumping 4.5 to 7.5 in. (11.4 to 19.0 cm) of water in a little over 15 hours on select parts of the East Bay (with intense bursts of precipitation in Pinole, Hercules, Rodeo, Walnut Creek, Danville, and Alamo). The storms of February 1986 had been close to a 10-year recurrence frequency (where a 10-year recurrence frequency storm has a one-in-ten chance of happening in any given year, based on a period of record from 1946 to 1979). For a 24-hour event, it was not especially rare, but as a 7-day event, it was significant because it increased the antecedent soil moisture levels (Rogers, 1986).

The January 1993 storm caused considerable erosive damage to old road cuts in the Lamorinda area but had a greater impact on other East Bay areas, such as Pinole and Vallejo. Portions of Moraga Road and Pleasant Hill Road were also impacted by this storm.

USGS Landslide Hazard Mapping in the San Francisco Bay Area (1980–94)

During the 1980s and into the 1990s, the USGS Engineering Geology and Regional Geology Branches continued to prepare relevant products addressing landslide hazards in the San Francisco Bay area. Some of these products were published in the 1982 storms volume, USGS Professional Paper 1434, while some articles appeared in other USGS publications, such as D. K. Keefer and A. M. Johnson, 1983, *Earth Flows: Morphology, Mobilization, and Movement*: USGS Professional Paper 1264, 56 p. (Keefer and Johnson, 1983). Other articles appeared in *GSA Reviews in Engineering Geology* volumes and, occasionally, in field guides (W. M. Brown, III [Editor], 1989, Landslides in central California. In *28th International Geological Congress, Field Trip Guidebook T381*: Washington, D.C., American Geophysical Union, 98 p.).

Other USGS efforts during this time were focused on establishing debris-flow thresholds (S. H. Cannon and S. Ellen, 1985, Abundant debris avalanches: *California Geology*, Vol. 38, No.12 [December], pp. 267–272); the establishment of a demonstration debris-flow hazard warning program in the Santa Cruz Mountains (see D. K. Keefer et al., 1987, Real-time landslide warning during heavy rainfall: *Science*, Vol. 238 [Nov. 13], pp. 921–925); practical techniques for reducing landslides (W. J. Kockelman, 1986, Some techniques for reducing landslide hazards: *Bulletin of the Association of Engineering Geologists*, Vol. 23, No. 1, pp. 29–52); and long-term monitoring and instrumentation of a landslide test site established by the USGS in La Honda in 1975 (Wieczorek et al., 2007).

These reconnaissance-level map products contained information on a regional scale (usually 1 in. = 2,000 ft [1 cm = 240.0 m]) that could be useful in initial attempts to understand basic structure and stratigraphy sufficiently to model many hazards, like seismic site response. However, a good practice is that information taken from older

Downloaded from http://pubs.geoscienceworld.org/aeg/eeg/article-pdf/31/1/i/6130855/i1558-9161-31-1-i.pdf
by AEG RBAC user

publications should be cross-checked with the latest available information from sources such as the USGS. This is because new interpretations of gross structure have been revealed over the past few decades, especially with regard to cognizance of blind thrusting and construction of balanced structural geologic cross sections. For example, in 1994, Russ Graymer, Davey Jones, Earl Brabb, and Ed Helley released a new edition of *Preliminary Geologic Map of the Niles 7.5-Minute Quadrangle* as USGS Open-File Report 94-132, on three sheets. This map is typical of a second generation of reconnaissance-level geologic maps, which include interpretations of geologic structure, blind thrusting, and stratigraphic nomenclature that were seldom recognized in the baseline products released in the 1970s.

Adoption of International Building Code (1997)

The International Code Council (ICC) is based in Falls Church, VA. It was formed in 1994 by combining the three model American building codes published by the Building Officials Code Administrators (BOCA), founded in 1915; the International Conference of Building Officials (ICBO), organized in 1927; and the Southern Building Code Congress International (SBCCI), established in 1940. The ICC produced the first edition of their International Building Code (IBC) in 1997, intended to be the new national standard for the United States.

The 1997, the IBC was based on the 1997 edition of the UBC, but without the Chapter 33 Appendices for Excavation & Grading (these amendments are part of the California Building Code). Amendments to the new IBC were issued every 3 years: in 2000, 2003, 2006, 2009, 2012, 2015, 2018, and 2021. By 2021, all 50 states and Washington, D.C., the U.S. Department of Defense, and the National Park Service had adopted the IBC or parts of it into government regulations. Many agencies in the San Francisco Bay area continue to enforce the old Chapter 33 Appendices of the IBC.

GEOLOGY OF ORINDA

Previous Geologic Work

Early Geologic Studies (1902–14)

The geology of the greater Orinda area has long been a subject of discussion and study by engineering geologists and geotechnical engineers. Like most of the East Bay Hills, geologic conditions are complex and vary significantly across the San Francisco Bay-Delta region, because it is a seismically active borderland.

The geology of the Orinda area has been studied in great detail over the last 125 years. In 1902, Professors Andrew Lawson and Charles Palanche published the first monograph on the geology of the Berkeley Hills, including portions of Orinda. This early work recognized the Wildcat and "Pinole" faults, but not the Hayward Fault. Dibblee's (1980) Pinole Fault does not correspond with that of Lawson (1914).

This monograph was followed by additional work of Lawson (1914) presented in a folio titled *Geology of the San Francisco Bay Area* published by the U.S. Geological Survey. Around the same time, Cal Berkeley paleontology Professor Bruce Clark (1913) compiled the first definitive study of regional stratigraphy, tracing the relative geologic ages of various sedimentary beds across the Orinda area with mapping on the 1897 Concord 15-minute quadrangle.

Recognition of the Contra Costa Basin (1951)

Professor Scott Creely of San Jose State University came to the Lamorinda area for Navy officer training at St. Mary's College during World War II (1941–45). While stationed there, Creely was intrigued by the local geology and the fossils exposed along St. Mary's banks, which parallel present-day Bollinger Canyon Road. In 1951, Creely and fellow Cal Berkeley graduate students Burdette Ogle and Don Savage presented the first formal interpretation of the stratigraphy of what they christened the "Contra Costa Basin" (Savage et al., 1951). The basin they identified was a land-locked depression that entrapped local sediments in the Lamorinda area approximately 4 to 10 million years ago (Figure 45).

The original work in 1951 included the designation of the Mulholland Formation, named after its prominent exposures on Mulholland Ridge in Moraga, behind the old Donald Rheem estate. This unit underlies roughly a quarter of Orinda's incorporated area. For the next three decades, Creely, Savage, and Ogle (Creely et al., 1982) continued to refine their understanding of the local geology, culminating with the most definitive work up through 1982. The accepted stratigraphic nomenclature for sedimentary and volcanic units described within the Contra Costa Basin is shown in Figure 46.

Post-War Studies of Orinda Geology (1950–94)

Several geologists from San Francisco Bay area universities and governmental agencies have also studied the Orinda area. These include: Ben Page (1950) of Stanford University, who described the geology of the Caldecott Tunnels; N.L. Taliaferro of Cal Berkeley, who taught geologic field studies in the Berkeley Hills for over 30 years; and California State Geologist Oliver Bowen (1951), who published the first cross section through the Berkeley Hills along Highway 24.

Downloaded from http://pubs.geoscienceworld.org/aeg/eeg/article-pdf/31/1/i/6130855/i1558-9161-31-1-i.pdf
by AEG RBAC user

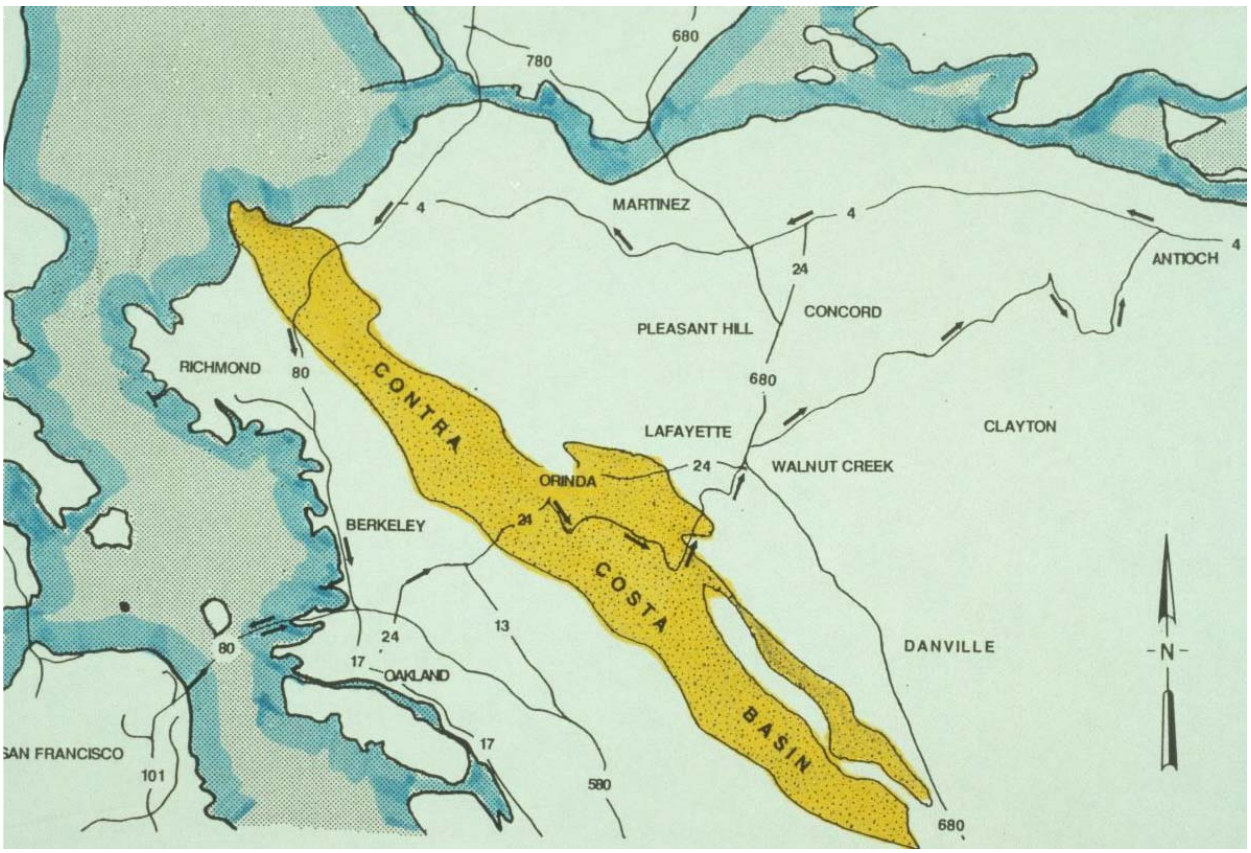

Figure 45. Map showing areal limit of outcrops comprising the Contra Costa Basin of Creely, Savage, and Ogle in 1951 (map from Rogers, 1986).

Garniss Curtis (1919–2012) served on the geology faculty at Cal Berkeley from 1951 to 1992. He continued Professor Tucky Taliaferro's work with students mapping the geology of the Berkeley Hills and was recognized as an expert in the geologic structure, stratigraphy, and active landslides in the Orinda area. A long-time Orinda resident, Curtis supervised or served on all the committees overseeing dissertations that included reconnaissance geologic mapping of the Berkeley Hills between the late 1950s and early 1990s. These studies included the mapping dissertations of James Case in 1960–63 and J. Ross Wagner in 1967–78. Professor Curtis also served as a consultant to BART on the Berkeley Hills Tunnels and made several inspections of the geologic exposures revealed in the tunnel walls and roof while the bores were being excavated in 1964–67.

After mapping the hills of Lamorinda for his doctorate in geology at Cal Berkeley in the early 1960s, James Case was hired by the USGS, where one of his earliest projects was working with Dorothy Radbruch on compiling structural data such as regional joint trends, which were described in an USGS open-file report (Radbruch and Case, 1967).

In 1971, Brabb et al. (1971) prepared the first geologic map of Contra Costa County, which incorporated much of the unpublished data obtained by a number of oil companies. This compilation was regarded as the County's "official" geologic map for several decades. In the early 1970s, Ross Wagner (1978) mapped the Tertiary-age strata in considerable detail as part of his Ph.D. studies at Cal Berkeley, which were funded by the USGS. Dibblee (1980) appears to have utilized much of Wagner's mapping in many of his reconnaissance geologic maps published by the USGS in the early 1980s.

In 1982, Creely, Savage and Ogle published a definitive summary of the stratigraphic relationships within the Contra Costa Basin (Creely et al., 1982) (Figure 46). Graham et al. (1983, 1984) explored the structural evolution of the Oakland–Berkeley Hills terrain, reconstructing the geologic history of the East Bay Hills in the Orinda area. Crane (1988) presented more modern interpretations of regional structure, which incorporated balanced structural cross sections and deep exploration data gleaned from the petroleum industry.

Follow-ons to Crane's pioneering work on regional structural interpretation include Jones and Curtis (1991) at Cal Berkeley; Wakabayashi et al. (1992) of Earth Science Associates; Jones (1992); and Jones and Brabb (1992). In 1994, Graymer et al. (1994) released the *Preliminary Geologic Map Emphasizing Bedrock Formations*

Downloaded from http://pubs.geoscienceworld.org/aeg/eeg/article-pdf/31/1/i/6130855/i1558-9161-31-1-i.pdf
by AEG RBAC user

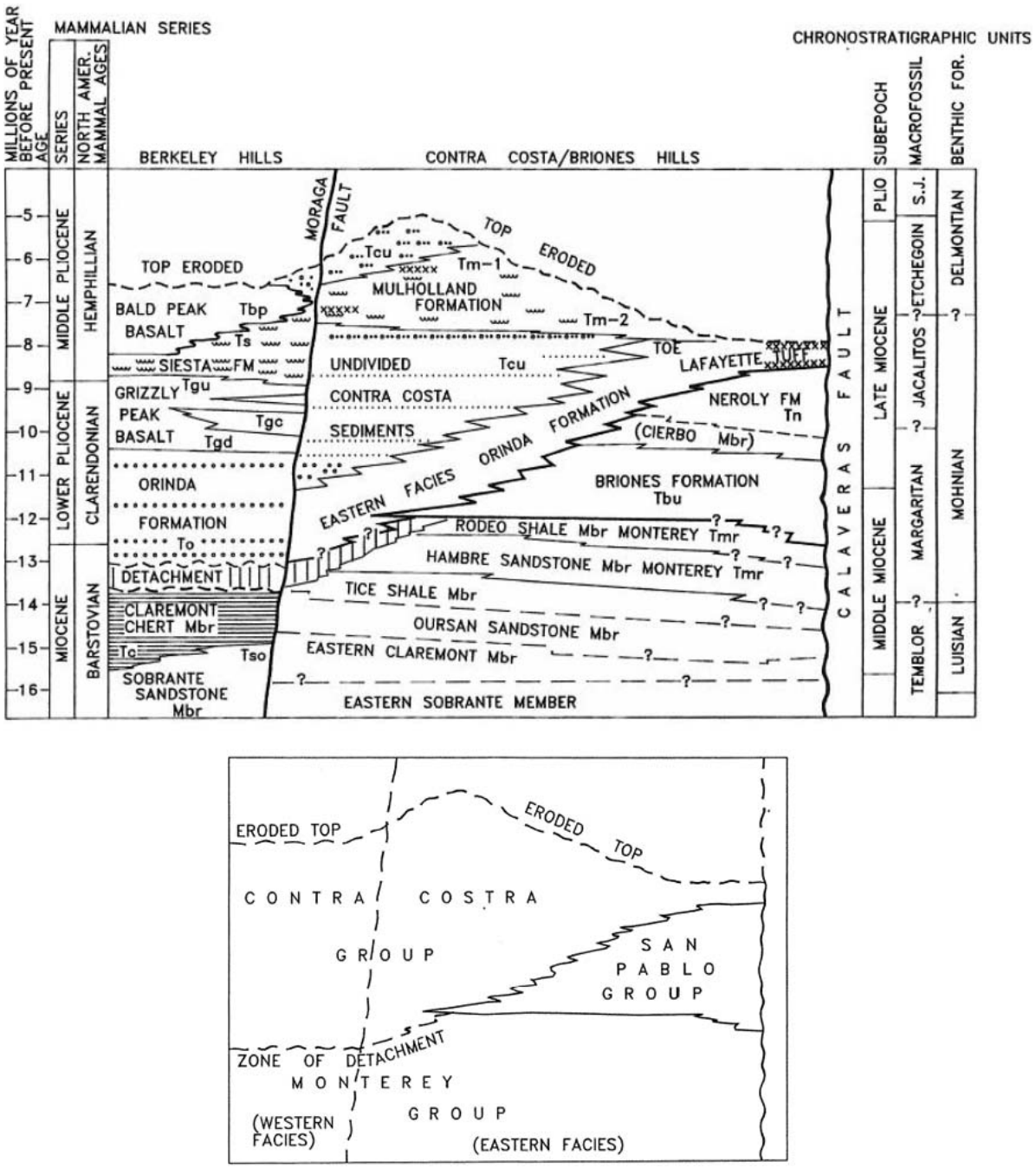

Figure 46. Schematic stratigraphic correlation section through the central Contra Costa Basin, based on interpretations by Rogers/Pacific, Inc., (1994), Creely et al. (1982), and Wagner (1978).

in Contra Costa County, California: A Digital Database, which was a pioneering effort.

Slope Stability Studies

Cal Berkeley graduate student Edward Thomas (1939) studied debris and earthflows generated from colluvial-filled bedrock ravines for his master's thesis Cal Berkeley. He was likely influenced by Sharpe's (1938a, 1938b) recent monographs on landslides, representing the first American text dealing specifically with that subject, which remained in print for more than 30 years. Thomas went onto a distinguished career with the State Division of Highways.

Many of Thomas' ideas were subsequently evaluated by Cal Berkeley Professor J. E. Kessell (1943), who

Downloaded from http://pubs.geoscienceworld.org/aeg/eeg/article-pdf/31/1/i/6130855/i1558-9161-31-1-i.pdf
by AEG RBAC user

studied debris flows emanating from seemingly stable hillslopes in Marin County in the early 1940s. Unlike Thomas, Kessell failed to recognize the controlling influence of underlying bedrock topography on the initiation of such slides (Reneau et al., 1984).

Between 1921 and 1957, California's first engineering geologist, Stanford-trained J. Hyde Forbes, also studied several of the more notorious slope stability problems in the East Bay Hills. These included the cut slopes graded in 1934 for Broadway Boulevard leading up to the Broadway Lower Level (today's Caldecott) Tunnels. Forbes (1947) reported on the rapid erosion and failure of these cut slopes, and his article generated considerable response.

One of those respondents was Earl Buckingham, a long-term resident of Moraga who worked for the Oakland City Engineers office between 1933–68. In a pair of discussions, Buckingham (1947, 1962) described landslide repair techniques employed in the Oakland area in the 1930s and 1940s, most of which proved to be successful. The City of Oakland was a pioneer in the use of hydrauger drains, retaining the Ransome Company of San Leandro to emplace horizontal drains as early as 1939.

USGS geologist Reuben Kachadoorian began studying the Warford Mesa subdivision area under contract with the FHA in 1956. Kachadoorian spent 19 days mapping in the Warford Mesa area in June and July 1956. He mapped exposed strata on a scale of 1:1,200 (1 in. = 100 ft [1 cm = 144.0 m]) topographic base map provided by EBMUD (Figure 47). Later that year, Kachadoorian turned in his preliminary engineering

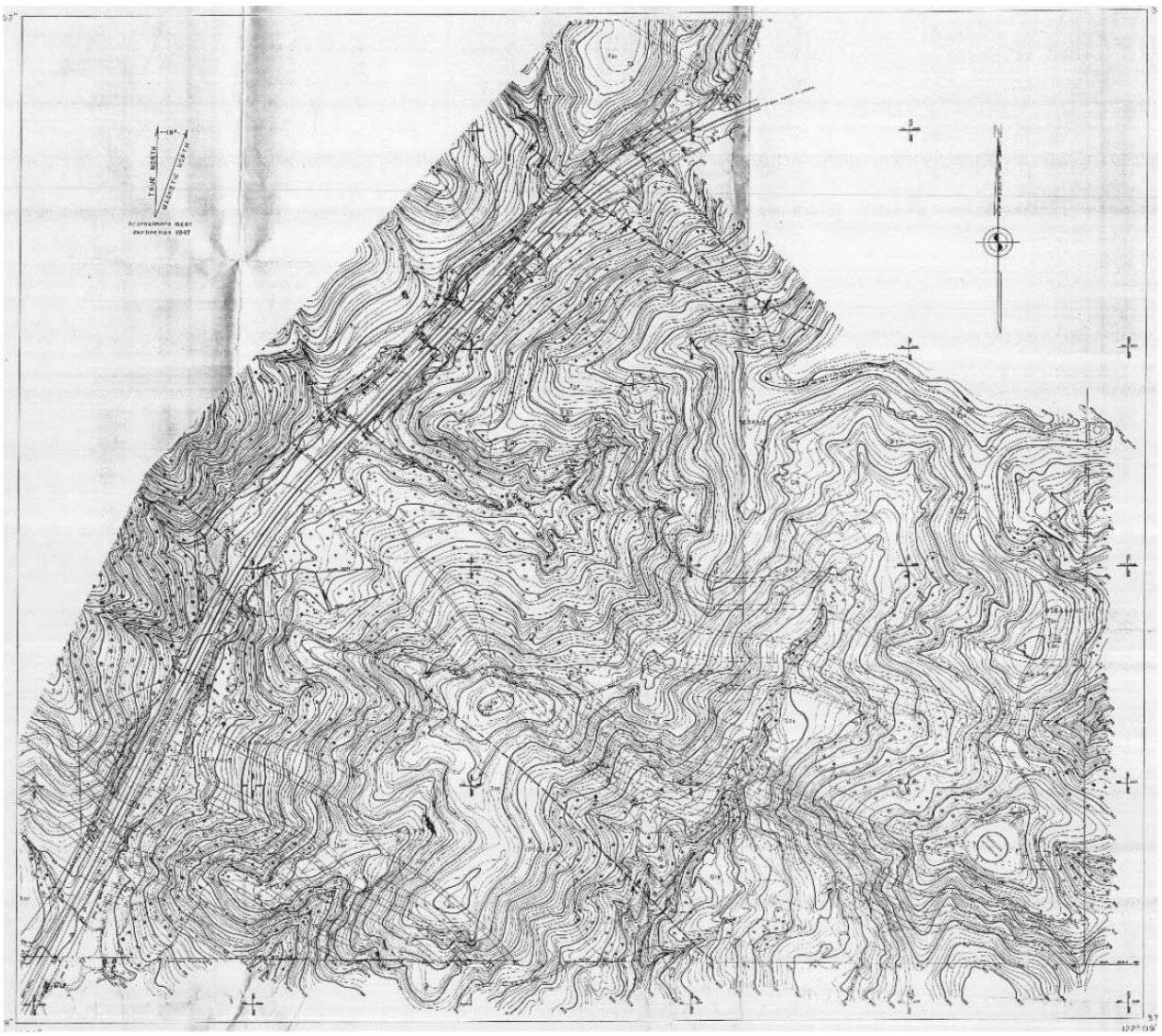

Figure 47. Portion of Reuben Kachadoorian's engineering geologic map of the Warford Mesa area of Orinda prepared in June–July 1956. He meticulously mapped individual beds of pervious conglomerates, which he associated with ephemeral springs that appeared to influence slope stability.

Downloaded from http://pubs.geoscienceworld.org/aeg/eeg/article-pdf/31/1/i/6130855/i1558-9161-31-1-i.pdf
by AEG RBAC user

geology report to FHA. The following year, he performed further analyses of the soil mineralogy using X-ray (XRD) diffraction tests and soil strength parameters (mostly direct shear tests (ASTM D 2080), as well as monitoring for storm-related damage during the spring of 1958. These additional data were incorporated into his master's thesis in geology at Stanford University (Kachadoorian, 1959).

Beaty (1956) also reported on the occurrence of shallow landslides in the San Francisco Bay region. Of the hundreds of slides he studied, he found that 70 percent occurred on shaded, northerly to northeast-facing slopes, a factor confirmed in the Lamorinda area by Radbruch and Weiler (1963).

USGS geologist Dorothy Radbruch worked in the Engineering Geology Branch of the USGS and had served as Kachadoorian's field assistant in Orinda during the summer of 1956. Between 1960 and 1963, Radbruch and Louise Weiler revisited Orinda to follow up on the earlier work done for the FHA in the area. The results of their study were published in 1963, and this publication (Radbruch and Weiler, 1963) remains one of the benchmark documents describing landslide processes common to the East Bay Hills.

The day after the Great Alaska Earthquake of March 27, 1964, Reuben Kachadoorian and two of his USGS colleagues were dispatched to Anchorage, AK. Overcome by the sheer magnitude of the challenges posed by that state's natural hazards, Kachadoorian and many of his professional colleagues later transferred to the new Alaskan Geology Branch of the USGS, where they achieved considerable notariety as pioneering figures in seismo-tectonic aspects of earthquake engineering.

Dorothy Radbruch assumed the role of senior engineering geologist at the USGS office in Menlo Park. In 1969, she published a geologic map of the Oakland East Quadrangle (Radbruch, 1969) and compiled an excellent summation of the engineering geologic problems associated with the area, drawing from the files of local geotechnical consultants and public agencies. The 1969 study was a companion to a similar study she had published in 1957 titled *Areal and Engineering Geology of the Oakland West Quadrangle* (Radbruch, 1957). Both of these studies contained a wealth of background information, which included detailed tables of cited sources.

Waltz (1967) studied shallow earthflow landslides in the East Bay for his research in applied geology at Stanford University. He performed some pioneering work in addressing methods to measure the elliptical form of landslide slip surfaces and compare length-to-width ratios (described later). Waltz focused on developing field measurement techniques at 10 different field sites, stretching from the Dublin Pass area northward into the Pinole Hills. Besides a field site on Mulholland Ridge, Waltz looked at cut-slope failures along the newly graded Bear Creek Road on the north side of Orinda after the January 1967 storm sequence closed down Bear Creek Road until repairs were completed several months later.

J. Michael Duncan (1971) was a professor of geotechnical engineering at Cal Berkeley from 1966 to 1984. In 1971, he began synthesizing the data collected by Radbruch and Weiler, using slope stability back-analysis techniques to craft useful predictions about long-term stability and scale factors suggested by Radbruch and Weiler in their data on failed slopes (Figure 43) collected in 1962–63.

Twenty years later, Duncan's evaluations of Radbruch and Weiler's data were revisited by employing back-analyses that included four ranges of soil plasticity as the principal variable (Duncan and Stark, 1992). They concluded that the best approximations of soil strength parameters came from published correlations of soil friction (Φ') for fully softened and residual conditions, that depend on the soil plasticity index (P.I.) to back-calculate effective cohesion (c') by assuming the lowest predictions (e.g. a factor of safety = 1.0). They found that analyses using the geometry of the observed rupture surfaces did not improve their results. The authors also concluded that back-analyses could not be made without making some key assumptions based on engineering judgment.

Several reconnaissance-level slope stability evaluations and landslide maps have been prepared by government agencies. Nilsen and Turner (1975) followed with broad-brush reconnaissance-level (approximately 1 in. to 1 mile [1 cm = 633.6 m]) mapping of landslide-prone deposits of Contra Costa County and attempted to relate their occurrence with rainfall recorded between 1951 and 1971. Shortly thereafter, Tor Nilsen (1975a, 1975b) produced a series of larger-scale 1:24,000 ($1'' = 2{,}000$ ft [1 cm = 240.0 m]) landslide and surficial deposit maps on USGS 7.5-minute quadrangle topographic maps, which became "benchmark standards" for assessing landslide hazards in the San Francisco Bay area after 1975.

In 1984, Marc Seeley completed an engineering geologic study of the Mulholland Formation in Moraga, close to the Orinda border. He utilized Wagner's and Creely's stratigraphic nomenclature (the same used herein) and mapped landslides, debris flows, and colluvial-filled bedrock ravines across either side of Mulholland Ridge (Donald Drive) and east to Campolindo Ridge (just east of Rheem Boulevard) (Seeley, 1984). A feature of particular interest was Seeley's mapping of a colluvial-filled ravine above the cul-de-sac of Camino Ricardo in Moraga. This hillside failed as one large bedrock landslide during the storms of February 1986, severely impacting the undeveloped lots at the end of the street (Rogers, 1986).

Rogers (1979, 1986) and Rogers et al. (1989) examined the slope stability and slope morphology aspects of

Downloaded from http://pubs.geoscienceworld.org/aeg/eeg/article-pdf/31/1/i/6130855/i1558-9161-31-1-i.pdf
by AEG RBAC user

the Lamorinda area. In 1988–89, Rogers/Pacific, Inc. (1989) mapped the landslide features in Moraga on a scale of 1:6,000 (1 in. = 500 ft [1 cm = 60.0 m]) as part of the town's new General Plan Amendment. This data set included the identification of 23 types of landslide deposits using geographic information system (GIS) software, referred to the open-source U.S. Army Corps of Engineers GIS program (GRASS), in cooperation with the Department of Urban and Environmental Planning at Cal Berkeley (Rogers, 1997).

State Landslide Mapping Project (1983–Present)

In 1983, Assembly Bill 101 was approved by the California State Legislature and signed by the governor into law. Acting in response to the well-publicized landslide losses of that year (described earlier), state lawmakers tasked the California Division of Mines and Geology, todays California Geological Survey to implement a Landslide Hazard Identification Program (LHIP), with the hope that the identification of landslide-prone slopes in urban areas would encourage more responsible planning and hillside development in the future. Areas of known landslide susceptibility and likely future development were targeted in the San Francisco Bay region and the greater Los Angeles Basin/Metro area.

The State's LHIP completed mapping of 24 specific areas in California, a special map of landslides in the Santa Cruz Mountains triggered by the 1989 Loma Prieta earthquake, and averaged 10 or more new areas under study each year (California Division of Mines and Geology, 1992).

The California Geological Survey's (CGS) Landslide Hazard Identification Maps typically include four products: a relative landslide susceptibility map; a landslides and related slope features map; a geologic map (which may be omitted); and a relative debris-flow susceptibility map (which is also optional). These products are mapped and produced at a scale of 1:24,000, or 1 in. to 2,000 ft (1 cm = 240.0 m). Over the years, the California Geological Survey has prepared landslide inventories covering parts of over 400 7.5-minute quadrangles, statewide (Wills et al., 2017). These are available for viewing and are downloadable by quadrangle name at: https://maps.conservation.ca.gov/cgs/informationwarehouse/landslides/.

Some of the earliest areas mapped were the Briones Valley and western half of the Walnut Creek quadrangles, which cover most of Orinda north of the Orinda Crossroads and Overhill Drive. These were issued in 1994–95. Mapping of the Oakland West and East quadrangles has not been undertaken because engineering geologic maps were produced for those areas by the USGS (Radbruch, 1957, 1969).

Limitations Inherent in Reconnaissance Landslide Mapping

In any kind of reconnaissance-level engineering geologic mapping, there exists a considerable degree of subjective interpretation. The factors shaping interpretation are usually professional training, local experience with landslides, and availability and quality of baseline data, such as aerial photos and the resolution of topographic maps. Because of these variables and exposure to various types of subsurface information, engineering geologists seldom agree on the extent and number of landslides within a given area. This does not mean that one geologist is "right" and another "wrong," only that we should expect to see interpretive differences influenced by the experience and training of such geologists, especially in stratigraphy and structural geology.

TOPOGRAPHY OF ORINDA

The City of Orinda is located within the central Coast Range geomorphic province of California. The area is bounded by northwest-trending ridges with southwest-sloping bedrock slopes. Ridge tops rise to elevations of between 850 and 1,500 ft (259.1 and 457.2 m), dropping to as little as 320 ft (97.5 m) in the valley floor at the upstream end of San Pablo Reservoir. As a consequence, maximum relief across the city is approximately 1,300 vertical feet (396.2 m).

Slope profiles are noticeably perturbed by past landsliding, which is the predominant physical process shaping the East Bay Hills of Lamorinda. Virtually all of the ridge tops are structurally controlled by more resistant sandstone or lenses of pebble conglomerate. Most of the sediments strike southeast-northwest, are tightly folded, and dip to the southwest or northeast.

Most of the upper hillslopes exhibit a convex to straight slope profile indicative of long-term subaerial exposure, but the units are also rather soft and erodible. Below this upper slope, most of the natural watercourses are noticeably incised, and numerous inset terraces attest to rejuvenation of the local stream system, most likely triggered by tectonic uplift. Numerous workers have concluded that the northeast-facing slopes (on the shady sides of the ridges) tend to support a greater degree of vegetation, as well as landslides (Beaty, 1956; Radbruch and Weiler, 1963; and Rogers, 1986).

Most of the upper slopes include conspicuous coalescing earthflows, composed of clayey debris, which translate on slopes as slight as 6 degrees (Kessell, 1943; Rogers, 1986). Most bedrock swales that have developed in the upper slopes contain varying amounts of colluvium and coalescing earthflow debris of unknown age. Based on aerial photography dating back to 1928, it would appear that portions of these earthflows tend to reactivate about

Downloaded from http://pubs.geoscienceworld.org/aeg/eeg/article-pdf/31/1/i/6130855/i1558-9161-31-1-i.pdf
by AEG RBAC user

once every 10 to 15 years on average, moving a short distance downslope each time (Rogers/Pacific, Inc., 1989). The earthflows are most prominently displayed along the northeastern, or obsequent (anti-dip), slopes, such as those in the old Wagner Ranch area, above the intersection of San Pablo Dam and Wildcat Canyon Roads.

Lower slopes are typified by erosive incision of local stream channels, suggestive of recent downcutting. This downcutting tends to sculpt the steepest slopes and often triggers deeper bedrock landslides. The age of the largest slides appears to be early Holocene–late Pleistocene (between 7,000 and 14,000 years old). However, the surfaces of these old slide masses are actively eroding and crisscrossed by younger, smaller slides, which are easier to recognize than their parent masses. The bedrock slide terrain seen on the southwest side of the city limits (from Moraga Way to Gateway and Lost Valleys) exhibits evidence of multiple sequences of landsliding, which appear to be of late Pleistocene age (>11,000 years before present).

REGIONAL GEOLOGY STUDIES

Stratigraphy

Previously published geologic maps of the Orinda area can be divided into two basic groups: those that lumped the bedrock strata into one homogeneous assemblage and those that attempted to identify the various sequences of deposition. Typically, one could only recognize the individual units after working in the area for some period of time. This why we have included geologic maps denoting the outcrop patterns of each stratigraphic unit.

Kachadoorian (1956), Case (1963), Radbruch and Case (1967), Brabb et al. (1971), Dibblee (1980), and Crane (1988) comprise the group who lumped the sediments of the Contra Costa Basin into one homogeneous unit, which they termed "Tps," or Tertiary–Pliocene age (undifferentiated) sediments. Wagner (1978) chose to follow the stratigraphic nomenclature originally devised by Savage et al. (1951). He subdivided the Mulholland Formation into two divisible units, the lower (Tm-1) and upper (Tm-2) facies.

In areas where the demarcation between the Mulholland Formation and older sediments is vague or so transitional as to be indistinguishable, Wagner labeled the beds as undifferentiated Contra Costa Group sediments (Tcc). Wagner's (1978) nomenclature has been retained by workers particularly familiar with the Lamorinda area, including: Creely et al. (1982), Liniecki (1982), Seeley (1984), Rogers (1986), Rogers/Pacific (1989). Seeley (1984) and Liniecki-Laporte and Andersen (1988) subdivided Wagner's units of the Mulholland Formation in vicinity of Mulholland Ridge.

Margaret Liniecki's (1986) M.S. thesis provides considerable details on the facies characteristics (including estuarine and fluvial) as well as paleo-environmental interpretations of the Mulholland Formation. In 1988, she and her advisor David Andersen concluded that no depositional connection existed between the proto–Sierra Nevada and the Contra Costa Basin during late Miocene time (8.5 to 5.5 Ma), which was open to the ocean on its western margins. There had to have been some sort of topographic barrier along the eastern side of this coastal basin.

Ross Wagner's (1978) Ph.D. thesis and geologic maps vary from Creely et al. (1982) in that he selected the term "Grizzly Peak" member to describe the Moraga Volcanics, previously termed the "Moraga Formation" by Radbruch (1969) and Creely et al. (1982). This was at the request of Wagner's major field advisor Garniss Curtis.

This volume utilizes Wagner's nomenclature, which was recommended by Garniss Curtis. For the purposes of this study, a "Composite Geologic Map of Orinda" (Figure 48) was prepared by utilizing the outcrop mapping and stratigraphic nomenclature of Wagner (1978) and Creely et al. (1982), with the structural interpretations of Crane (1988), which overlay Dibblee's (1980) mapping.

Alluvium (Qal)

The alluvium infilling these uplifted bedrock valleys can reach substantial thicknesses (upwards of 100 ft [30.5 m] according to Pape, 1978; Rogers, 1988a). This locally derived alluvium generally consists of deposits of silty clay and clayey silt.

Terrace Deposits (Qt)

Stream terraces preserved in the Orinda area are few in number. Inset terraces within Holocene channels are commonplace (Pape, 1975; Rogers, 1988a) and may attest to geomorphic responses to weather pattern changes through the Holocene (Cooke and Reeves, 1976; Reid, 1989; and Bull, 1991). Channel incision throughout the past century is indicated throughout Contra Costa County and is discussed elsewhere in this volume.

There are a number of knickpoints and waterfalls along the natural watercourses. The largest of these is about 7 ft (2.1 m) high along Brookside Creek. The scale of mapping performed for this study (1:3,600) was not sufficiently large to attempt the mapping of channel features except for the largest terraces, most commonly associated with the remains of temporary landslide dams.

Mulholland Formation (Tm)

The Mulholland Formation is the youngest formation comprising the Contra Costa Group of sediments (Figure 49) that outcrops in Orinda. It was deposited in a

Downloaded from http://pubs.geoscienceworld.org/aeg/eeg/article-pdf/31/1/i/6130855/i1558-9161-31-1-i.pdf
by AEG RBAC user

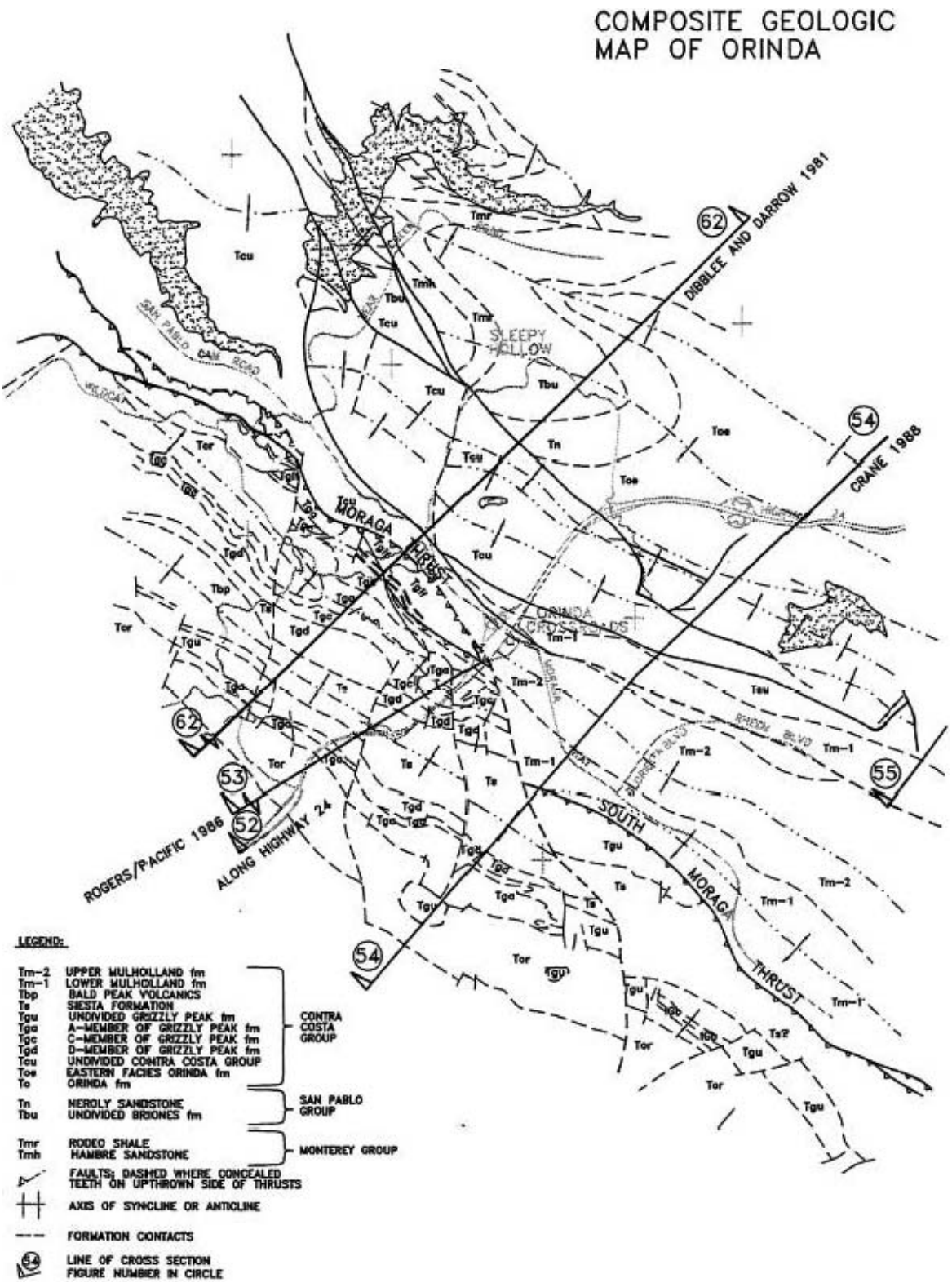

Figure 48. Composite geologic map of Orinda, CA, based on the interpretations of Wagner (1978), Creely et al. (1982), and Crane (1988).

Downloaded from http://pubs.geoscienceworld.org/aeg/eeg/article-pdf/31/1/i/6130855/i1558-9161-31-1-i.pdf
by AEG RBAC user

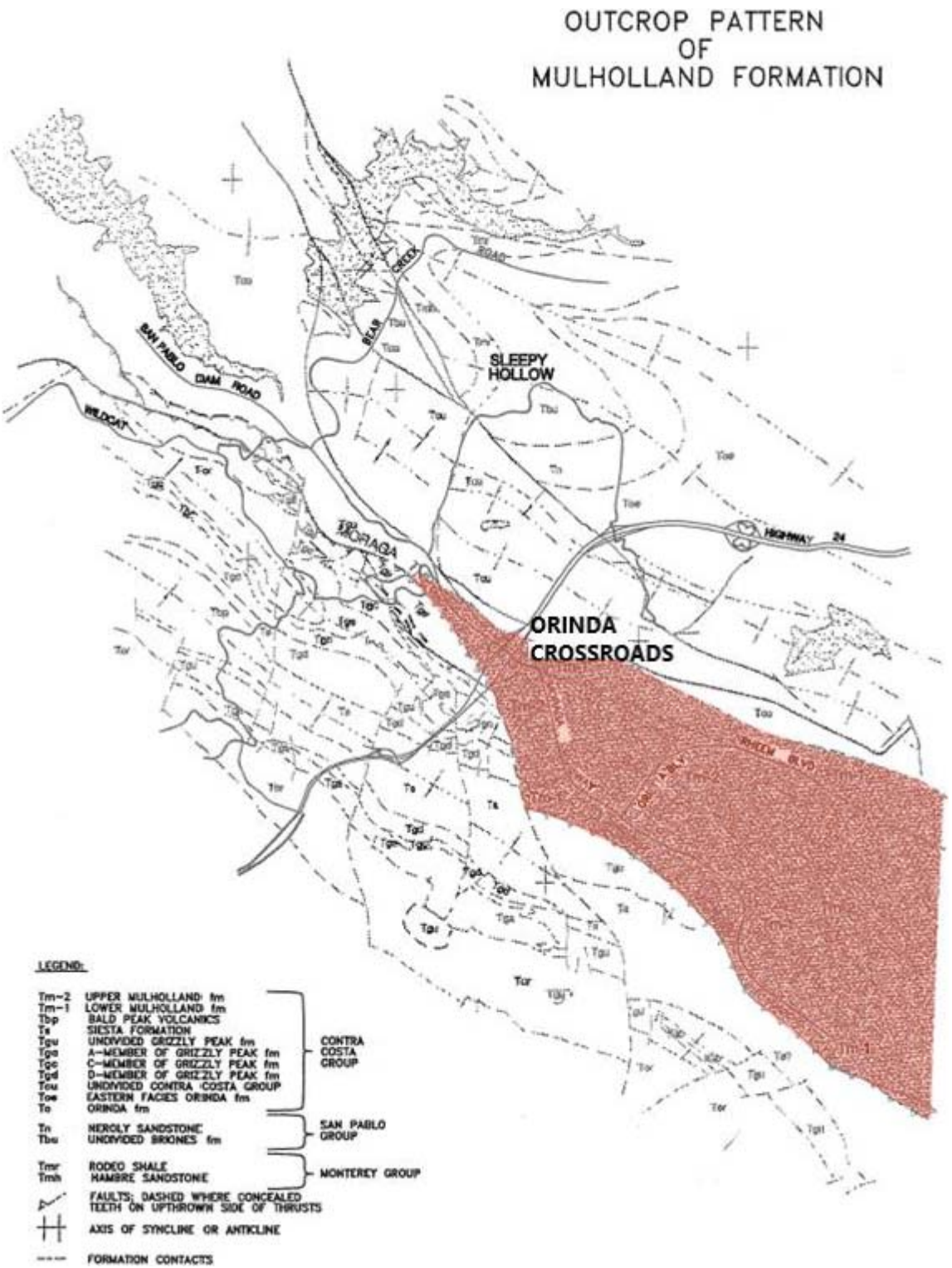

Figure 49. Outcrop pattern of the upper and lower facies of the Mulholland Formation. Note how this unit pinches out north of Orinda Crossroads.

landlocked basin 6 to 10 million years ago (Figure 46). It was named by Savage et al. (1951) for prominent exposures in a tight synclinal fold capping Mulholland Ridge, which is traversed by Donald Drive.

The Mulholland Formation is a sequence of well-bedded sedimentary rocks that crop out in one major belt across the southern half of Orinda (Figure 49). According to Wagner (1978), the Mulholland Formation

Downloaded from http://pubs.geoscienceworld.org/aeg/eeg/article-pdf/31/1/i/6130855/i1558-9161-31-1-i.pdf
by AEG RBAC user

is divisible into two distinct zones, which he delineated as the older, lower Mulholland (Tm-1); and younger, upper Mulholland (Tm-2).

The upper Mulholland beds (Wagner and Seeley's "Tm-2") are typified by massive olive-colored mudstones with lenticular beds of pebble to cobble conglomerate, likely deposited in fluvial and lacustrine/deltaic conditions.

Across the southwestern half of Orinda, the lower Mulholland beds (Wagner's Tm-1) dominate the landscape. The lower Mulholland Formation consists of dark gray shale, claystone, and siltstone deposited in shallow-water lacustrine conditions (the "Lake Mulholland" of Graham, et al., 1984) some 7.8 to 7.0 million years ago (Creely et al., 1982). Sandstone beds within the lower Mulholland Formation have varying thickness. When thick, these beds can be noticeably resistant to erosion, and they account for some of the steepest ridges east of Rheem Boulevard and south of Glorietta Boulevard. The trend of these prominent ridgelines parallels the strike, or structural grain, of the formation.

The lower Mulholland beds overlie the younger upper Mulholland beds where the former have been overturned in tectonic drag, along the footwall of the Moraga Thrust (Case, 1963; Wagner, 1978). The exposures of Mulholland beds become increasingly pinched approaching the Orinda Crossroads area from the southeast. This situation was observed to good effect in the significant excavations undertaken for the Orinda BART Station in 1967–73, the Orinda BART Station slide repair (1979), the Stein Way slide repair (1984), and the Oak Road slide repair (1991).

The Mulholland beds are best discerned from adjacent "undifferentiated" Contra Costa Group sediments by their ordered, well-bedded aspect, by the general absence of any "red beds," and the unit's tendency to be a ridge former (Creely et al., 1982).

This contrast can be easily appreciated by walking along the East Bay Regional Park bike path in Moraga, leading from the intersection of St. Mary's Road and Rheem Boulevard, in an easterly path towards Lafayette (along the 1912–57 right-of-way of the Sacramento Northern Railroad). The lower third of the formation generally consists of lacustrine (lake) sediments, nicely exposed in the steep cuts along Bollinger Canyon Road, known as "St. Mary's Banks."

In places, a blind thrust fault running parallel to Rheem Boulevard (Crane, 1988) separates the lower (Tm-1) and upper Mulholland (Tm-2) beds, as depicted in the geologic cross section presented in Figure 50. The Rheem Fault appears to parallel Rheem Boulevard and forms a less-resistant zone that floors in Rheem Valley, extending from St. Mary's College/Bollinger Canyon north to Glorietta Boulevard.

Contra Costa Group Undifferentiated (Tcu)

The southeastern quarter and northern half of Orinda are underlain by undifferentiated fluvial sediments of the Contra Costa Group. Their outcrop pattern is shown in Figure 51. This unit was designated as "Tcu" by Wagner (1978) and "Tccu" by Creely et al. (1982). As mentioned previously, Dibblee (1980) and Crane (1988) included

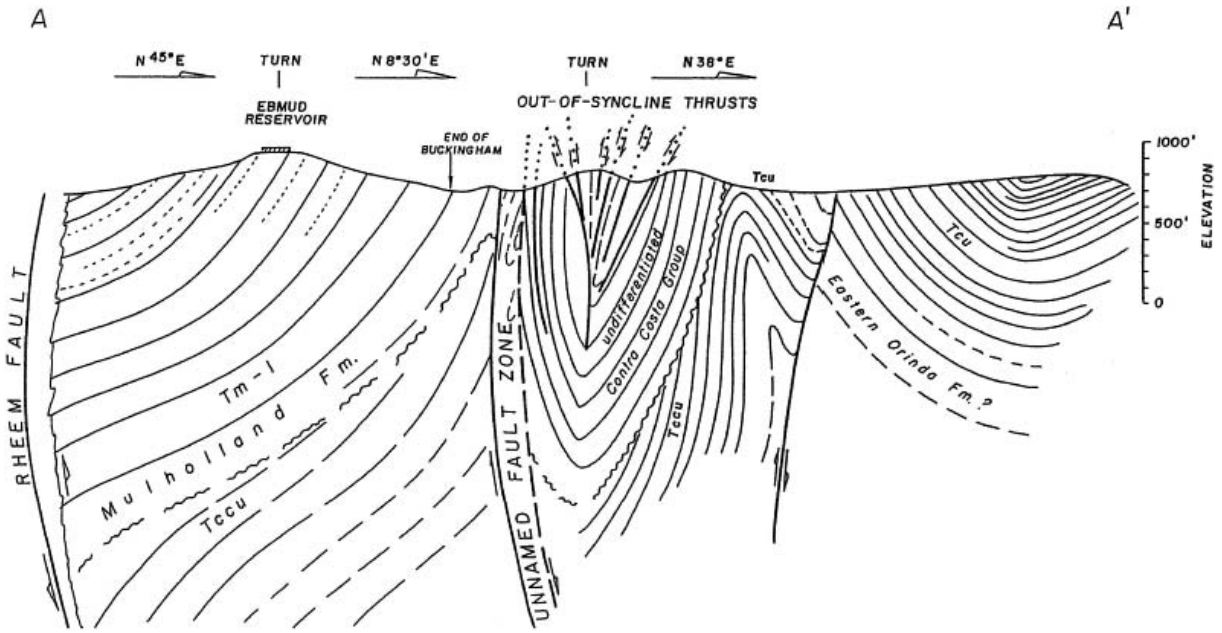

Figure 50. This section runs from the summit of Rheem Boulevard (between Rheem Valley and St. Mary's College), crosses Fayhill Reservoir atop Campolindo Ridge, and then turns northeast, cutting across the hills just beyond the end of Buckingham Drive.

Downloaded from http://pubs.geoscienceworld.org/aeg/eeg/article-pdf/31/1/i/6130855/i1558-9161-31-1-i.pdf
by AEG RBAC user

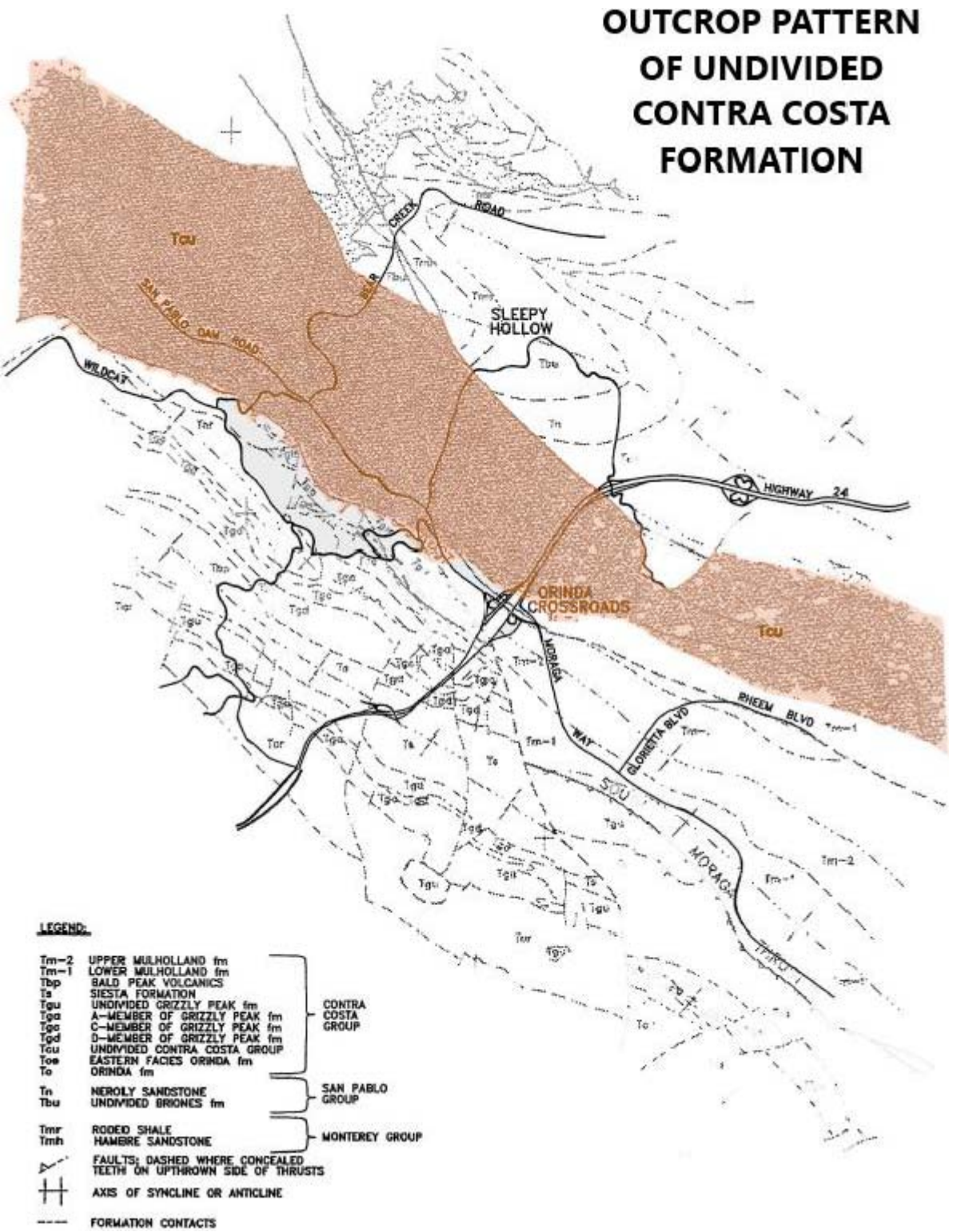

Figure 51. Outcrop pattern of undivided Contra Costa Formation sediments.

these beds as part of their "Tps" (for Tertiary- to Pliocene-age sediments), as with the other sedimentary sequences within the Contra Costa Group.

The undifferentiated Contra Costa Group (or Wagner's Eastern Contra Costa Group west of the Calaveras Fault) consists of sediments with a wide variety of

Downloaded from http://pubs.geoscienceworld.org/aeg/eeg/article-pdf/31/1/i/6130855/i1558-9161-31-1-i.pdf
by AEG RBAC user

characteristics. The unit generally follows a series of pebble conglomerates, sandstones, and mudstones, similar to the type Orinda Formation, west of the Moraga Thrust. Wagner (1978) asserted that the conglomerates contain predominately Franciscan debris but locally contain some pieces of Monterey chert and Briones shell breccia. The base of the formation is around 8.2 million years old, as determined from fossils and plagioclase within the uppermost bed of the Lafayette Tuff (Wagner, 1978).

For the most part, the contact between the younger Mulholland Formation and the older, undifferentiated basin sediments is conformable. However, according to Creely et al. (l982), a slight angular discordance exists in the Rheem Valley area, just north of St. Mary's College. Crane (1988) subsequently interpreted this discordant contact as a blind thrust, with the footwall beds of the older undifferentiated Contra Costa sediments overturned in drag folding parallel to the thrust. These thrusts are shown in Crane's (1988) structural cross section through Orinda, a portion of which is reproduced herein as Figure 52.

In Orinda, the distinction between the lower Mulholland beds and the underlying undifferentiated sediments of the Contra Costa Group appears to be transitional and conformable, so Crane's (1988) interpretation offers the most plausible explanation for the discordant contact in the Campolindo Homes development of eastern Moraga. The Crane interpretation also fits well with the regional context of local geologic structure, representing an area of intense crustal shortening during roughly the past 5 million years since the close of deposition within the Contra Costa Basin.

Siesta Formation (Ts)

The Siesta Formation was designated by Lawson (1914) to describe soft gray sandstone, claystone, and thin-bedded limestones exposed in the Siesta Valley area, east of Grizzly Peak Ridge. Its outcrop pattern is highlighted in Figure 53. Most of the formation is caught within a faulted synclinal structure (Figures 53 and 54), running the length of Siesta Valley (north of Highway 24) and south of Highway 24, through Gateway Valley and on into Lost Valley. It also forms the slope between the Moraga Thrust and the volcanic rocks forming the ridgeline behind Miramonte High School.

Siesta Formation sediments appear to have been deposited in a landlocked freshwater basin. The unit is typified by locally high percentages of montmorillonite, which likely influence the existence of some significant bedrock landslides within the Siesta and Gateway Valley

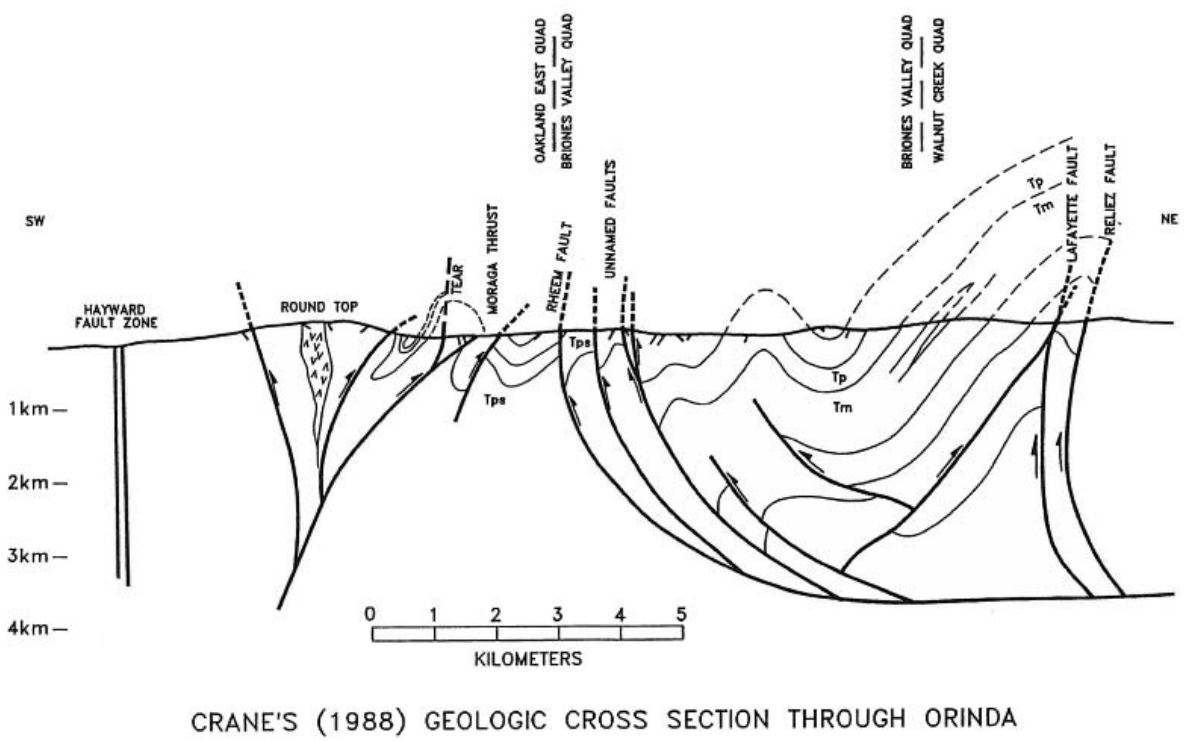

Figure 52. Crane's (1988) interpretive cross section through south Orinda; its trend is shown on Figure 48. The multiple faults are accommodating crustal closure along an ENE-WSW axis.

Downloaded from http://pubs.geoscienceworld.org/aeg/eeg/article-pdf/31/1/i/6130855/i1558-9161-31-1-i.pdf
by AEG RBAC user

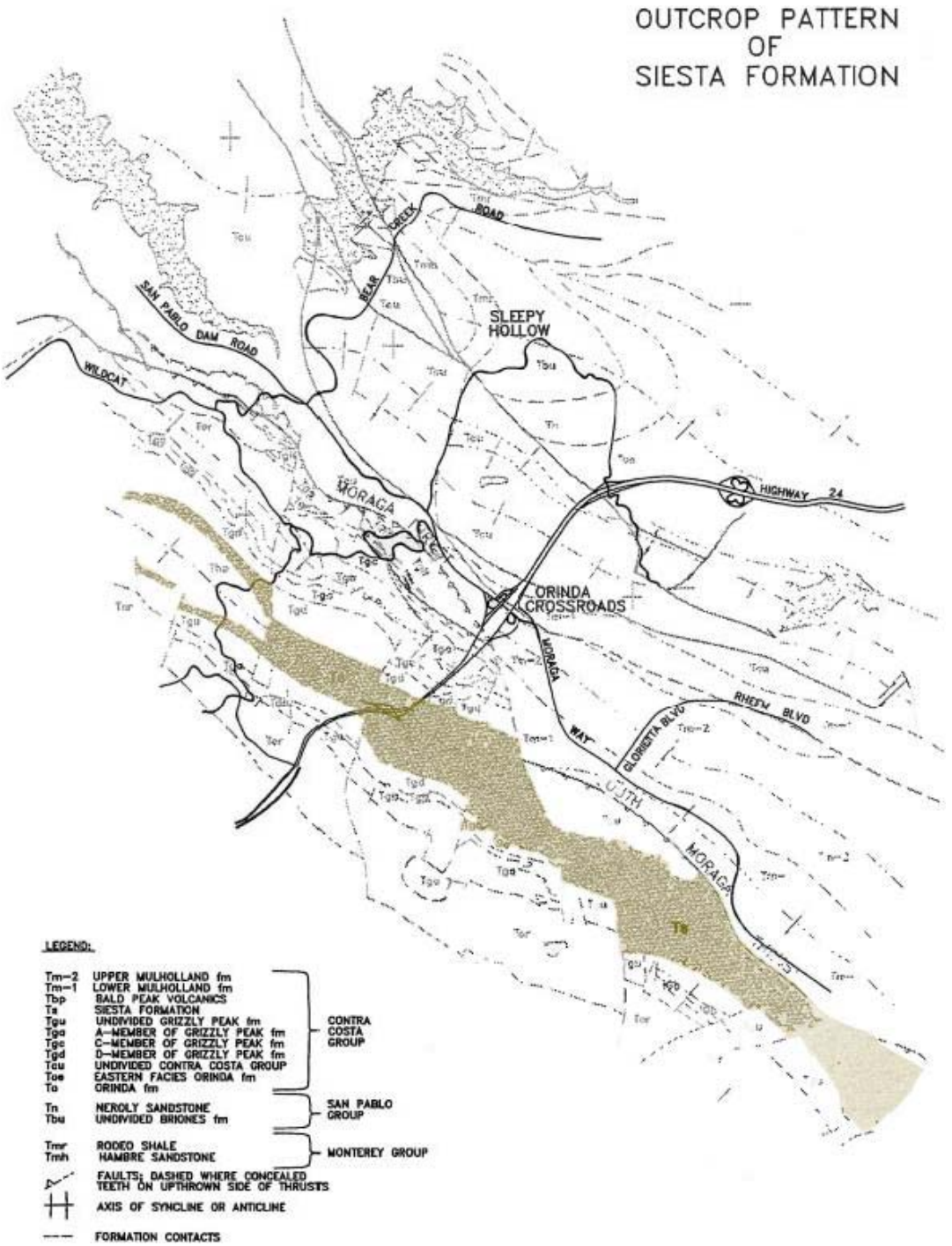

Figure 53. Outcrop pattern of the Siesta Formation, which underlies the southwestern part of the city.

areas. Locally contemporaneous volcanic activity and the closed nature of the unit's depositional basin may also account for the high percentages of smectite clays. Cut slopes steeper than 3:1 have never fared well in the Siesta Formation (Rogers/Pacific, Inc., 1992 a&b).

The Siesta Formation forms an onlapping (transitional) contact with the older Grizzly Peak (also termed the Moraga Formation by other workers) units on the west side of the Siesta Valley Syncline and is conformable with Grizzly Peak units on the east side of the syncline (the nature of this contact is well exposed in cuts along the north side of Highway 24). Wagner (1978) estimated the Siesta Formation's thickness at approximately 1,300 ft (396.2 m). This suggests that there were

Downloaded from http://pubs.geoscienceworld.org/aeg/eeg/article-pdf/31/1/i/6130855/i1558-9161-31-1-i.pdf
by AEG RBAC user

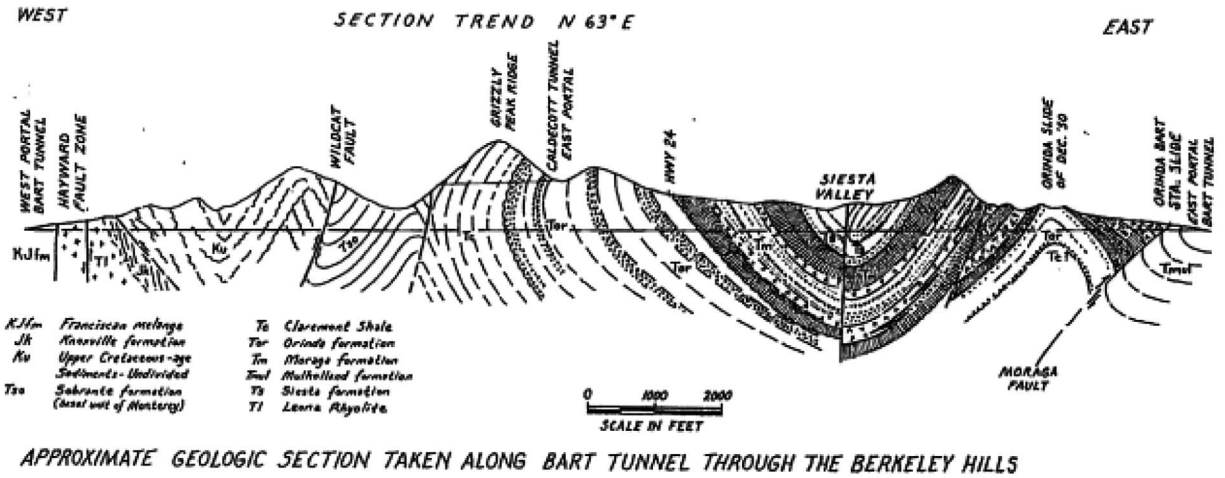

Figure 54. Generalized geologic cross section from the Hayward Fault to Orinda along the 3.2-mi-long (5.1-km-long) Berkeley Hills BART Tunnels (from Rogers, 2001a).

ongoing tectonic compression and folding at the time of deposition.

The age of the Siesta sediments was based on potassium-argon (K-Ar) dating of bounding volcanic strata (see Figure 46) by Garniss Curtis at Cal Berkeley. Wagner (1978) reported Curtis' dates to be approximately 8.6 Ma at the base and 7.7 Ma in the basal member of the Bald Peak Volcanics, which overlies the Siesta Formation.

Grizzly Peak (Moraga) Formation (Tg)

The Grizzly Peak formation was named by Lawson and Palanche (1902) and Lawson (1914) for exposures east of the Cal Berkeley campus, and this terminology was retained by Wagner (1978). Case (1963), Radbruch (1969), and Creely, et al. (1982) defined the same unit as "Moraga formation" (Figure 46) or "Moraga Volcanics." The Grizzly Peak terminology is utilized herein because Wagner (1978) studied the formation in sufficient detail to divide the formation into five distinct units. The outcrop pattern of the Grizzly Peak/Moraga formation in the Orinda area is presented in Figure 55.

The Grizzly Peak formation is composed of locally derived basalt flows resting conformably on the Orinda Formation. The nature of this "baked contact" is seen vividly in the prominent road cut along the north side of Highway 24 at the Fish Ranch Road exit, just east of the Caldecott Tunnels. Wagner (1978) estimated that the formation reaches a maximum thickness of approximately 2,000 ft (609.6 m) in the area bounding either side of Highway 24 and thins rapidly to the northwest and southeast. Wagner (1978) cited Curtis' K-Ar age dating of the formation at between 8.6 and 9.8 Ma (Figure 46).

Wagner (1978) described the formation as being composed of two major units of basaltic lava flows (Figure 54), interbedded with thin basaltic tuffs, and separated by a unit composed of pyroclastics and conglomerate beds. One of the pyroclastic units is a rhyolite tuff (volcanic ash).

Wagner (1978) and Curtis (1978) determined that most of the Grizzly Peak (Moraga) Volcanics emanated from vents in the vicinity of Round Top, about 1 mi (1.6 km) southeast of the Caldecott Tunnels (now part of the East Bay Regional Park system). Some other vents, lying somewhat to the north, may also have contributed.

Wagner's C unit of the Grizzly Peak formation (Tgc in Figure 55) consists, in part, of fluvial, or river-laid, conglomerates, in which the clasts were derived from older rocks east (Great Valley Sequence) and west (Franciscan Formation) of the old Contra Costa Basin (Figure 45). These conglomerate beds are thickest on the eastern side of the basin and tend to pinch out west of the Moraga Thrust. Rogers (1979) identified minor accumulations of thinly bedded lapilli tuffs, freshwater marl, lignite, siltstone, and conglomerate in these intrabasinal sediments, where they were exposed in excavations for the Orinda BART Station landslide. These sediments would appear to have been part of Wagner's C unit (Tgc).

Orinda Formation (To)

The term "Orinda formation" was originally designated by Lawson and Palanche (1902) to describe the basal member of their Berkeleyan series overlying the

Downloaded from http://pubs.geoscienceworld.org/aeg/eeg/article-pdf/31/1/i/6130855/i1558-9161-31-1-i.pdf
by AEG RBAC user

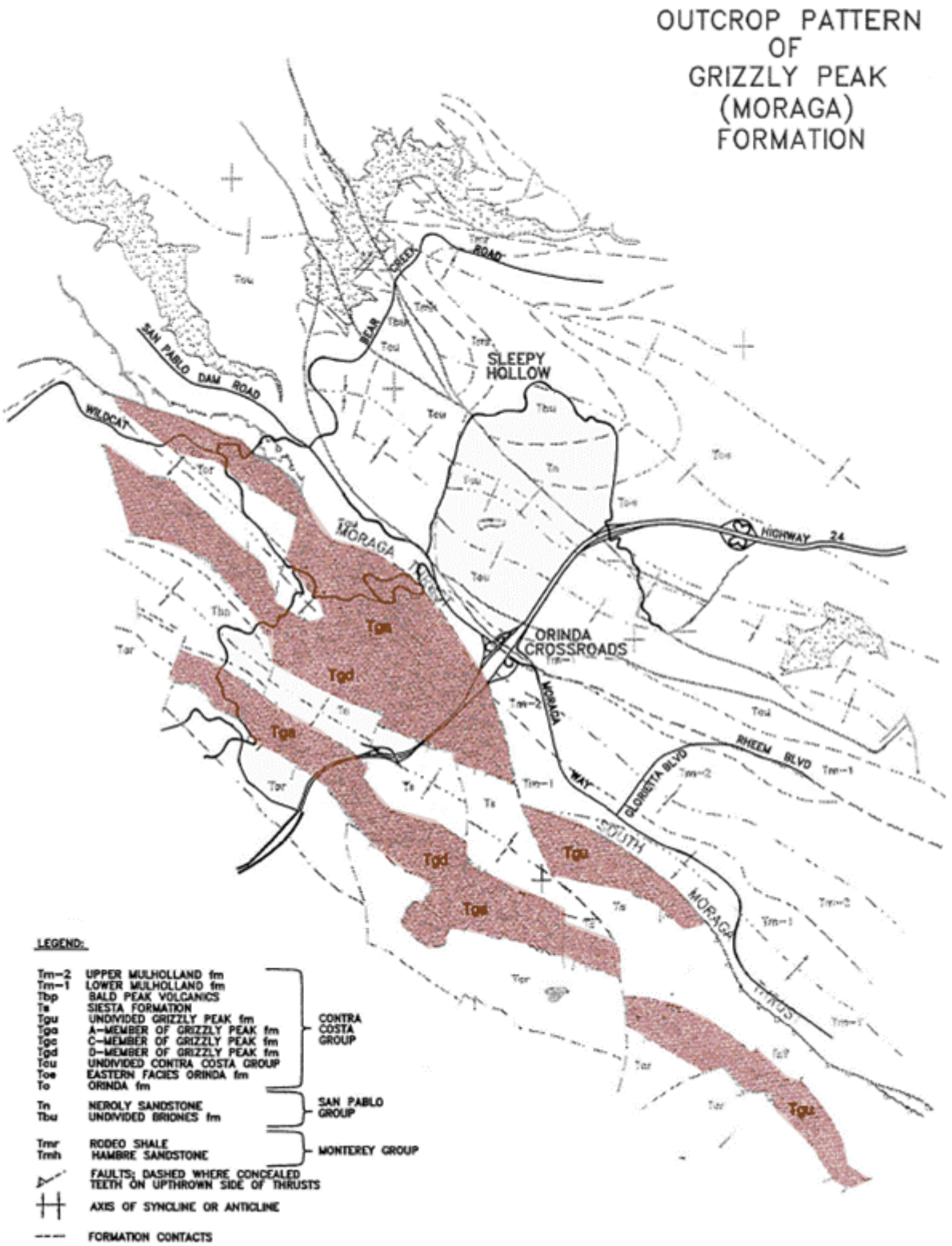

Figure 55. Outcrop pattern of the Grizzly Peak Formation, also referred to as the "Moraga Volcanics."

Monterey series. Later, Lawson (1914) recognized that the Orinda formation had a freshwater depositional genesis and even contains lignites and weathered tuff. Lawson (1914) excluded the Orinda formation from the Berkeley Group and redesignated the Moraga (Grizzly Peak) formation as the base of the Berkeley Group. Clark (1921) assigned the Orinda sediments to the lower Pliocene Epoch.

Downloaded from http://pubs.geoscienceworld.org/aeg/eeg/article-pdf/31/1/i/6130855/i1558-9161-31-1-i.pdf
by AEG RBAC user

After World War II, the Orinda formation was re-evaluated in some pioneering work by three Cal Berkeley geology graduate students: Don Savage, Burdette Ogle, and Scott Creely (Savage et al., 1951). The term "Orinda Formation," as used today, refers to the basal member of the Contra Costa Group, west of the Moraga Thrust. Its outcrop pattern, and that of Wagner's Eastern Orinda facies, is highlighted in Figure 56.

Previous workers have lumped late Miocene– and early Pliocene–age continental sediments of the Contra Costa Basin, Sycamore Basin (south of Mt. Diablo), Meganos Basin (northeast of Mt. Diablo), and even Santa Clara Basin (San Jose area) into a single label of "Orinda formation," or "Orinda-equivalent" assemblages, in deference to its early recognition as a late Tertiary–age unit of freshwater origin, lying unconformably upon the Monterey formation (middle Miocene–age) marine sediments.

Since the term "Monterey formation" is widely applied to upper middle Miocene–age marine sediments along the entirety of the California Coastal borderland (Kleinpell, 1938), geologists were tempted to apply "Orinda-age" to those younger sediments of continental (non-marine) origin. Hence, the term "Orinda formation" has been applied to many of the units deposited within the Contra Costa Basin. In this book, the term "Orinda Formation" is restricted to the basal sedimentary unit of the Contra Costa Group (Figure 46).

The Orinda Formation is typified by a repeating series of conglomerates, sandstones, and mudstones that lie just above the Monterey formation. In most places, this contact is semi-conformable, but it is typified by interformational shearing (e.g., along Grizzly Peak Boulevard, according to Wagner, 1978).

The coarse conglomerates that typify the Orinda Formation within the Berkeley Hills suggest that it was deposited as an alluvial fan that interfingered with marine sediments to the east (Wagner, 1978). Clasts contained within the conglomerates emanated from both the Franciscan and Great Valley Sequences, likely exposed in proto-highlands lying west of the Hayward Fault (Buwalda, 1929; Wagner, 1978; and Graham et al., 1983, 1984).

Age dating of fossil invertebrates suggests that basal members of the unit could be as old as 12 to 13 Ma (Wagner, 1978). Curtis' dating of the overlying Grizzly Peak (Moraga) Volcanics at 9.8 Ma would appear to bound the age of the formation, west of the Moraga Thrust fault (Figure 46).

Eastern Facies of the Orinda Formation (Toe)

Wagner (1978) introduced the modifier "Eastern" to the Orinda Formation to describe the basal member of the Contra Costa Group west of the Calaveras Fault and east of the Moraga Thrust. The generalized outcrop pattern of the eastern facies is shown in Figure 56. The eastern Orinda Formation is well exposed throughout Upper Happy Valley and St. Stephen's Hill, as well as the slopes east of Tahos Road.

The composition of the eastern facies is virtually identical to that exposed west of the Moraga Thrust: conglomerates, sandstones, and mudstones. The conglomerate beds contain predominately Franciscan clasts, with minor amounts of Briones shell breccia (Wagner, 1978). Wagner felt that the source area of these clasts was from proto–western highlands (same as the source for the Orinda type section). Franciscan highlands comprising the Diablo Range (south of what is now the Livermore-Amador Valley) may also have contributed detritus, before being faulted 12 mi (19.3 km) northwest, along the Calaveras Fault (Wagner, 1978).

Wagner (1978) reported that the age of the eastern facies is somewhat younger than the type section (west of Orinda Crossroads), being only 8.2 Ma at the base, and it is conformably overlain by Mulholland beds dated at "younger than 8.2 million years" (age of the top of the Lafayette Tuff).

Nature of the Contact with the Underlying San Pablo Group

The undifferentiated Contra Costa Group sediments and eastern facies of the Orinda Formation appear to lie conformably and unconformably upon marine sediments of the older San Pablo Group, from Interstate 680 (parallel to the Calaveras Fault south of Walnut Creek) northwestward, along the north side of Happy Valley in Lafayette, and extending to the St. Stephen's Drive and Sleepy Hollow areas in north Orinda (Figure 57).

The undifferentiated strata are approximately conformable with the Lafayette Tuff of Wagner (1978). Wagner (1978) also mapped a bed of volcanic ash, which he termed the "Sleepy Hollow Tuff," approximately 1,000 stratigraphic feet (304.8 m) above the base of the Briones Formation beds, just north of Sleepy Hollow (within the Happy Valley syncline). Numerous landslides have been associated with soils derived from this tuff bed.

Within the Orinda area, the undifferentiated strata generally consist of a repeating series of thinly bedded conglomerates, sandstones, and mudstones that appear very similar to the older Orinda Formation beds exposed west of the Moraga Thrust fault. These strata appear to have been deposited within the landlocked Contra Costa Basin 7.8 to 10 million years ago (Creely et al., 1982).

San Pablo Group of Sediments

Originally identified by Merriam (1898) as an upper Miocene–age marine unit, the term "San Pablo Group"

Downloaded from http://pubs.geoscienceworld.org/aeg/eeg/article-pdf/31/1/i/6130855/i1558-9161-31-1-i.pdf
by AEG RBAC user

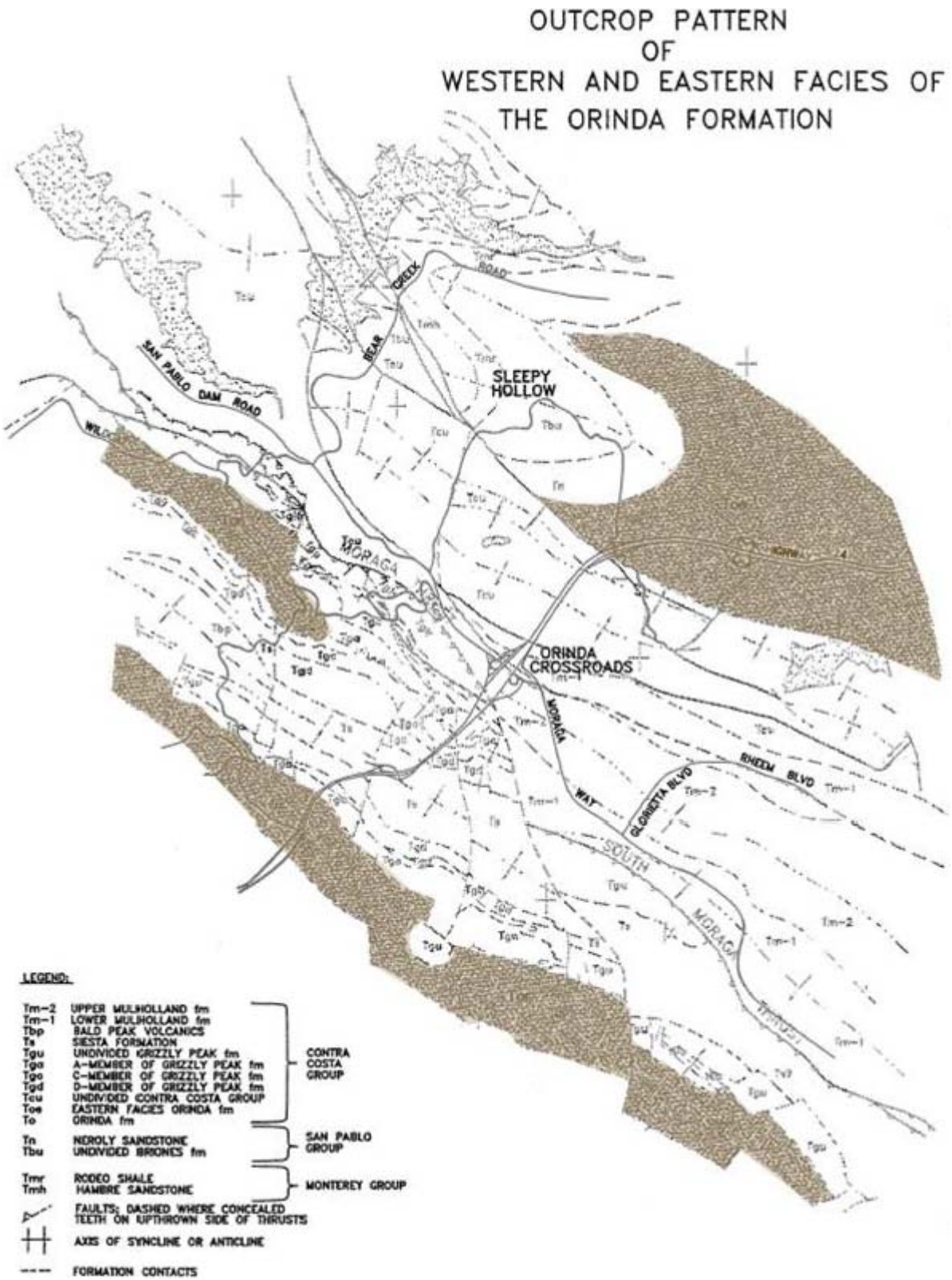

Figure 56. Outcrop map of the western and eastern facies of the Orinda Formation.

Downloaded from http://pubs.geoscienceworld.org/aeg/eeg/article-pdf/31/1/i/6130855/i1558-9161-31-1-i.pdf
by AEG RBAC user

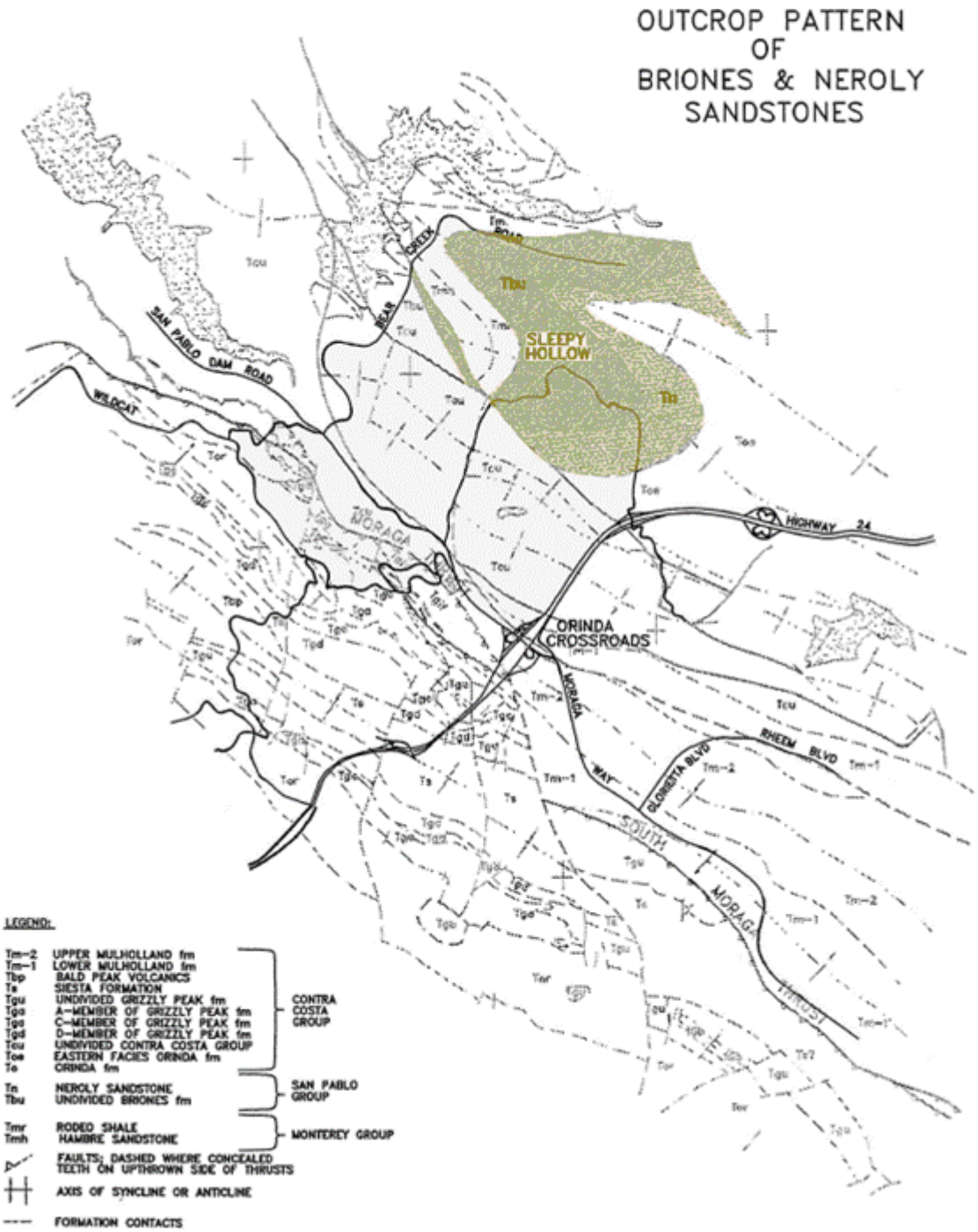

Figure 57. Outcrop pattern of the Briones and Neroly sandstone units within Orinda.

was subsequently applied by Lawson (1914). Later, Clark (1930) subdivided the group into three units, in ascending order: the Briones (basal member), Cierbo, and Neroly formations. Wagner (1978) studied the Cierbo formation closely and concluded that it should be included within the lower portion of the Neroly formation, thereby paring the group down to two distinct units, the Neroly and the Briones, which is the nomenclature applied in this volume (Figure 57).

The San Pablo Group is a series of marine sediments deposited within a feature known as the "San Pablo Embayment," which extended along a northwest-southeast axis and stretched from the Moraga Thrust on the west to an eastern shore in the vicinity of what is now the Mt. Diablo piercement structure. (San Pablo Group sediments are well exposed in Markley Canyon of the Black Diamond Mines Regional Preserve, initially described by Bowen [1951].)

Downloaded from http://pubs.geoscienceworld.org/aeg/eeg/article-pdf/31/1/i/6130855/i1558-9161-31-1-i.pdf
by AEG RBAC user

The San Pablo Group is believed to be of upper Miocene age, lying between the Monterey formation and Contra Costa/Sycamore Basin sediments.

Neroly Formation (Tn)

The Neroly Formation is the youngest member of the San Pablo Group (Figure 42), initially identified by Clark (1930). It lies directly beneath Contra Costa Group sediments between the Moraga Thrust and Calaveras Fault (Figure 46). Its outcrop pattern is seen as a discrete belt of rocks traversing a portion of eastern Orinda, shown in Figure 57.

The Neroly Formation consists of fine-grained andesitic sandstones and reddish siltstone with minor andesitic pebbly conglomerate. The andesitic source rock for the Neroly Formation would appear to have been the late Tertiary volcanics in the Sierra Nevada Mountains, 60 to 100 mi (96 to 160 km) to the east (Mt. Diablo did not begin to push upward until about 4 Ma).

Louderback (1930) suggested that the Mehrten Formation (andesitic volcanic, lahars, and agglomerates) of the Sierra Nevada foothills was the source of the Neroly Formation, a view that has remained unchallenged (Wagner, 1978).

The Neroly is interfingered with the underlying Briones Formation and overlying Contra Costa Group sediments, but, in other localities, it lies in unconformable contact on older strata (Wagner, 1978).

Because of its out-of-area source, and therefore relative lack of montmorillonite, the Neroly Formation spawns fewer landslides than either of the formations bounding it, tending to foster steeper, but more stable hillslopes.

Briones Formation Undifferentiated (Tbu)

The Briones Formation was designated by Lawson (1914) in his San Francisco folio. Lawson originally included the Briones formation within the Monterey Group, which it closely resembles south of Walnut Creek. Trask (1922) demonstrated that, stratigraphically and faunally, it is more closely aligned with the San Pablo embayment, and it has been assigned as the basal member of the San Pablo Group ever since.

In the northeast part of Orinda, the Briones Formation outcrops as a belt of rocks within a major anticlinal structure (Dibblee and Darrow's Miner Ranch Anticline) in Sleepy Hollow and as a steeply folded syncline in the Orinda Downs area (Wagner's "Happy Valley Syncline"). The Briones Formation outcrops immediately beneath the Neroly Formation. In this area, the Briones strata lie conformably upon members of the underlying Monterey Formation.

Within northeast Orinda, the Briones beds appear as a fine-grained feldspathic sandstone, almost a lithic wacke, similar in appearance to the underlying Monterey Formation. The Briones material appears to have been derived from two source areas, the proto-highlands west of the Hayward Fault (the same source as for the Orinda Formation) and within the proto–Diablo Range, south of Livermore-Amador Valley. It is presumed that strike-slip faulting along the Calaveras Fault has shifted the Contra Costa "block," west of the Calaveras Fault, to its present position, approximately 14 mi (22.5 km) north of where it was originally deposited.

The lower half of the undifferentiated Briones Formation contains punky siltstone beds highly susceptible to sliding, but it grades into fine- to medium-grained sandstone higher in the section. The sandstone facies are thinly bedded and tend to foster extensive accumulations of colluvium, infilling bedrock ravines.

Approximately 1,000 ft (304.8 m) above the base of the formation, Wagner (1978) identified a biotite-bearing rhyolite tuff within the formation in the Sleepy Hollow area, which he termed the "Sleepy Hollow Tuff." Outcrops of this marker bed define the structure of the Happy Valley Syncline through Sleepy Hollow, and it also outcrops east of San Pablo Dam. The K-Ar dating of this tuff yielded an age of approximately 14 Ma.

Monterey Formation Sediments

Wagner (1978) identified two members of the Monterey Formation in the Happy Valley Syncline area, cutting across Sleepy Hollow and Orinda Downs. Wagner (1978) listed this portion of the Monterey Formation as his "eastern facies," exposed in the core of the Sobrante Anticline, north of Orinda. These Monterey Formation rocks are the oldest strata exposed in Orinda and were deposited in marine embayments that used to occupy most of what we now know as the Great Central Valley, as well as most of the coastal borderland.

Rodeo Shale Member of the Monterey Formation (Tmr)

The Rodeo shale was initially identified by Lawson (1914), who named it after type exposures along Rodeo Creek. Lawson recognized it as a member of the Monterey Formation, underlying the Briones Formation. This stratigraphic assignment has remained unchanged.

Wagner (1978) retained Lawson's nomenclature, identifying the shale near its type locality and carrying it south, through the Upper Pinole and Bear Creek drainages, into northeast Orinda (Figure 51). Folded by the Happy Valley Syncline, which traverses Sleepy Hollow, the shale exerts structural control on upper Lauterwasser Creek in the Sandhill Road area.

The Rodeo shale usually consists of reddish-colored shale beds, which are intensely fractured, somewhat chalky and cherty, and generally stained with iron oxide.

Downloaded from http://pubs.geoscienceworld.org/aeg/eeg/article-pdf/31/1/i/6130855/i1558-9161-31-1-i.pdf
by AEG RBAC user

Wagner (1978) was the first to note locally fine feldspathic sandstones interbedded within the shale. The Rodeo shale is locally associated with slope instability (Saul, 1973), and it tends to spawn expansive clay soils downslope of its outcrops (U.S. Department of Agriculture, 1977).

The Hambre sandstone is generally recognized as a well-sorted, fine-grained, feldspathic sandstone. In places, Wagner (1978) identified interbeds of yellow limestone. In the Bear Creek drainage, the Hambre sandstone is locally interbedded with reddish claystone.

Hambre Sandstone Member of the Monterey Formation (Tmh)

The Hambre sandstone was also designated by Lawson (1914), who assigned it as a member of the Monterey Formation. Conformably underlying the Rodeo shale, the Hambre sandstone reaches a maximum thickness of about 1,200 ft (365.8 m).

In Orinda, the Hambre sandstone member of the Monterey Formation outcrops along a narrow band on the west side of upper Sleepy Hollow, beneath parts of Tarry Lane, Tappan Lane, Bear Ridge Road, and Tappan Way. Its outcrop area is highlighted in Figure 58.

The Hambre sandstone is not generally associated with widespread slope-stability problems, but it sheds ample accumulations of colluvial slope wash. Exposures of this colluvium can be seen in the creek channel below Bear Ridge Road and upper Tappan Lane, where it reaches thicknesses of up to 40 ft (12.2 m). Much of this material was eroded by zero- and first-order streams during the winter storms of January 1982 and February 1986.

GEOLOGIC STRUCTURE OF ORINDA

Introduction

The dominant structural feature of the Orinda area is the nearby Hayward Fault (Graham et al., 1983, 1984), which borders the western foot of the East Bay Hills, 4 mi (6.4 km) west of the Orinda Crossroads. The East Bay Hills have been uplifted by regional compressional forces directed toward the northeast-southwest (Graham et al., 1983, 1984; Jones and Brabb, 1992). This compression has produced northwest-striking, southwest-dipping thrust faults and related anticlines and synclines (Figure 48). These features are, therefore, the principal geologic structures in the region.

The compressional folds exhibited throughout the Berkeley Hills were recognized before the turn of the 20th century (Lawson and Palanche, 1902) and presented in the San Francisco Folio of the USGS Atlas by Lawson (1914). Bowen (1951) reviewed stratigraphic and structural data generated by the Caldecott Tunnel excavations (Page, 1950) and compiled the most oft-reproduced structural cross section through the Berkeley Hills, along the alignment of Highway 24 (Figure 59). Thirty-five years later, Rogers (1986) prepared a similar section along the Berkeley Hills BART tunnels (Figure 54).

Moraga Thrust Fault

Case (1963) was the first to identify the Moraga Thrust fault as a discordant contact between younger Mulholland beds and older Grizzly Peak volcanic sequences lying above and just west of Orinda Crossroads. Rogers (1979) reported on his trenching of the Moraga Thrust in 1978 where it was exposed in the headscarp of the 1978 Orinda BART Station landslide. The Moraga Thrust has not been deemed potentially active by the USGS or the California Geological Survey (Phelps et al., 2008).

Rogers trenched the Moraga Thrust at the headscarp of the Orinda BART Station landslide in 1978 and above Monte Vista Road near Orinda Hill in 1984. At the north Orinda site, Rogers/Pacific, Inc. (1984) was unable to discern evidence of surface fault rupture where the trace had been mapped by Wagner (1978). Crane (1988) suggested that the Moraga fault is a back-thrust emanating from the Hayward Fault at depth, a view adopted by Borchardt and Rogers (1991) and Jones and Brabb (1992).

Geologic Structure South of Highway 24

Crane (1988) drew a deep regional cross section through Orinda about 0.75 mi (1.2 km) southeast of the Orinda Crossroads that is reproduced herein as Figure 52. Crane's section was the first to account for most of the anomalies of geologic structure long recognized in the area. He suggested that the Wildcat Fault and Lawson's old Pinole fault are ancillary features of the active Hayward rift, and that Gateway/Siesta Valley is an overturned syncline. A tear fault borders the eastern side of this synform and appears to emanate from the underlying Moraga Thrust. The wedge of material caught between the tear and the thrust has been squeezed into an anticlinal structure. This lies immediately west of the Moraga Thrust and was responsible for the December 1950 Orinda slide, shown in Bowen's (1951) cross section (Figure 59).

The dominant structural feature of south Orinda is the Mulholland Syncline, the axis of which forms Mulholland Hill (Hall Drive and Donald Drive traverse this ridge). Wagner (1978) showed this synclinal axis to become progressively overturned with proximity to the Moraga Thrust (moving northwestward, towards the Orinda Crossroads). In the vicinity of the Orinda

Downloaded from http://pubs.geoscienceworld.org/aeg/eeg/article-pdf/31/1/i/6130855/i1558-9161-31-1-i.pdf
by AEG RBAC user

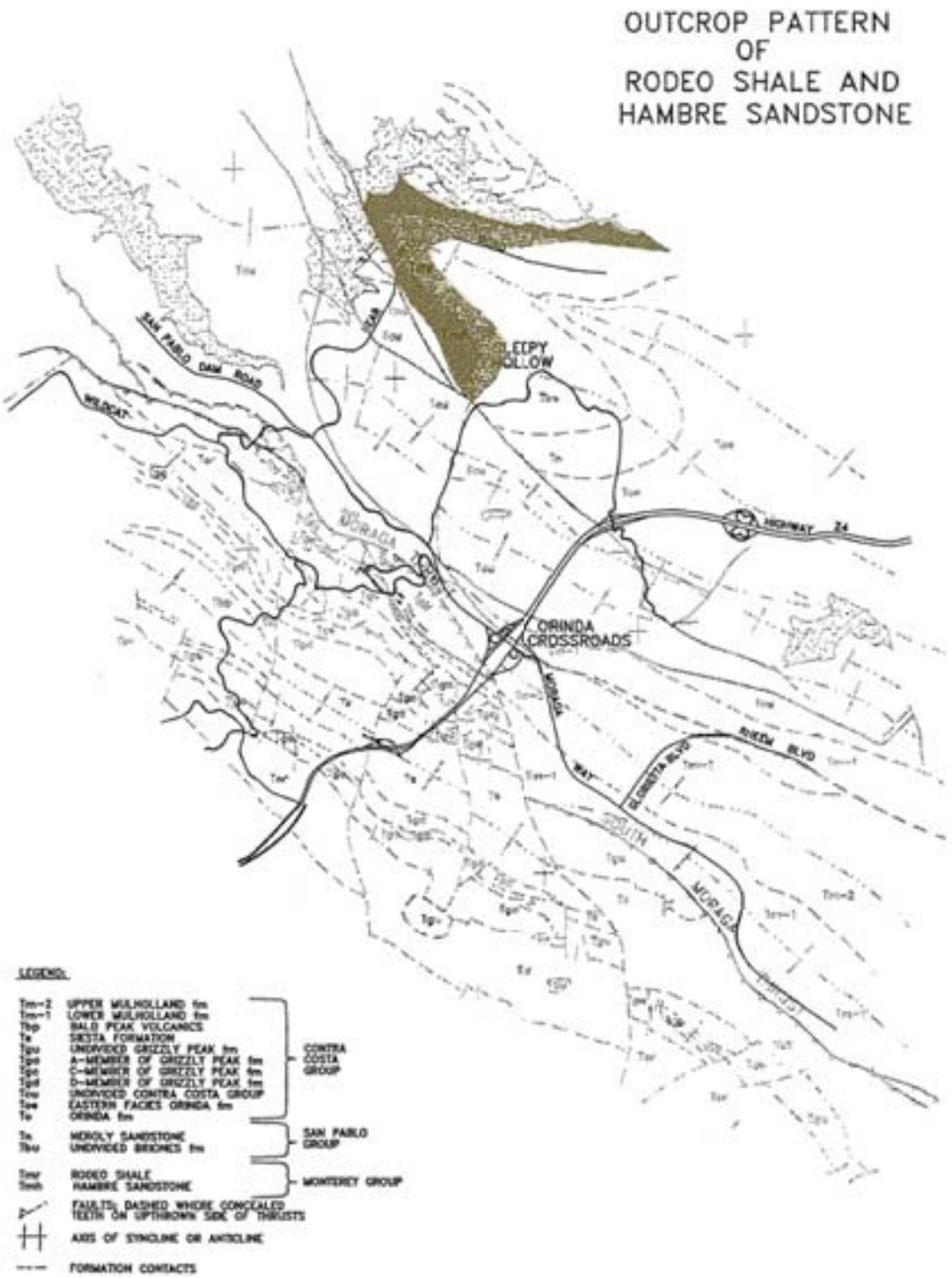

Figure 58. Outcrop map of the Rodeo Shale and Hambre Sandstone members of the Monterey Formation.

Downloaded from http://pubs.geoscienceworld.org/aeg/eeg/article-pdf/31/1/i/6130855/i1558-9161-31-1-i.pdf
by AEG RBAC user

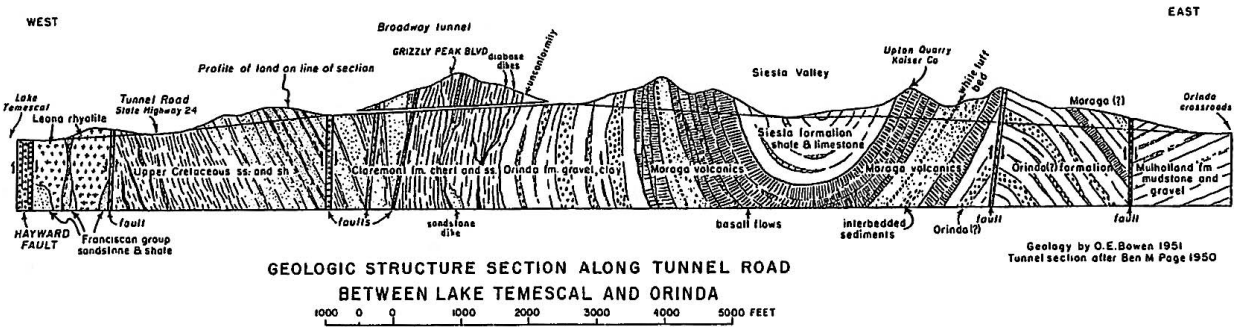

Figure 59. Geologic section across the Berkeley Hills along State Highway 24, prepared by State Geologist Oliver Bowen (1951). Note the three faults identified at the eastern end.

Crossroads (at Highway 24), the Mulholland beds are overturned, due to fault drag on the footwall side of the Moraga Thrust (Figure 35). Along the east side of San Pablo Ridge, just south of Highway 24, the older Mulholland beds (Tm-1) lie ABOVE the younger beds (Tm-2) (this is in the area prone to sliding below Knickerbocker Lane and extending southeasterly, towards Lost Valley; see Map Sheet Q-10 in Appendix 2).

Crane also showed what may be an older thrust, lying parallel to and downslope of the Moraga Thrust, forming the prominent valley bottom that is presently occupied by upper San Pablo Creek and Moraga Way. This is reflected in the cross sections reproduced in Figures 52 (Crane) and 54 (Rogers).

Considerable drag folding has been associated with low-angle horse-tailing thrusts emanating from the Moraga Thrust (Wagner, 1978; Seeley, 1984) in vicinity of the 1978 Orinda BART Station landslide. Rogers (1979) also noted out-of-syncline thrusting emanating from a back-thrust feature partially exposed in the slide's head-scarp (Figure 35). Although many assume the Moraga Thrust fault is near-vertical, it actually dips about 35 degrees south-southwest. Figure 60 presents some of the common seismo-tectonic features observed in discontinuous outcrops along the presumed trace of the Moraga Thrust fault north of Orinda Crossroads.

The rolling upland east of Moraga Way is a broad asymmetric syncline (Figure 52) lying between the

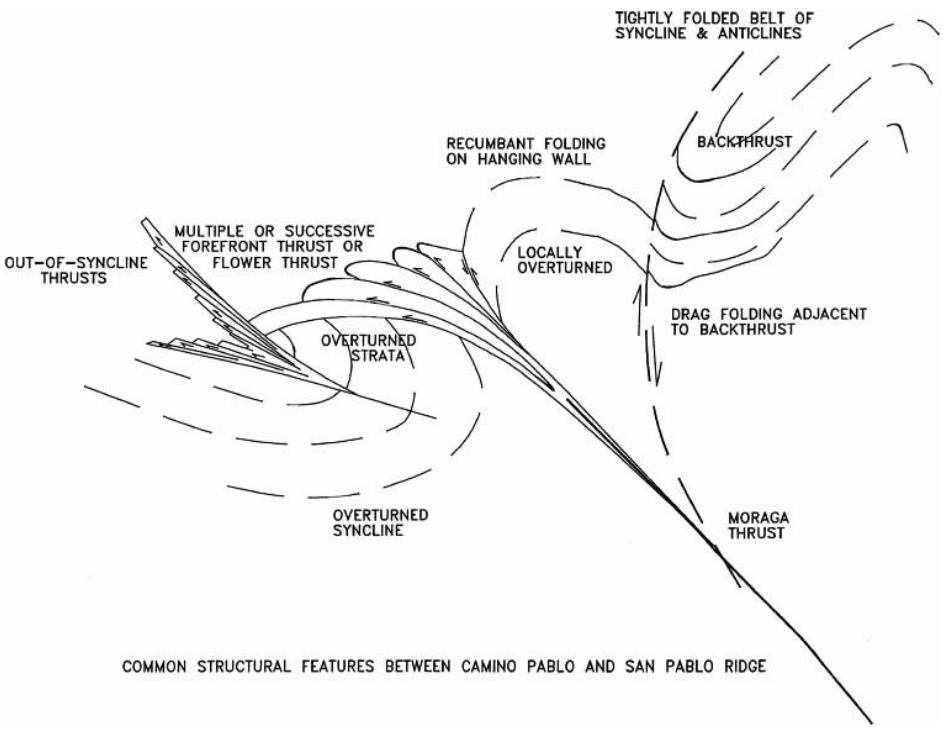

Figure 60. Seismo-tectonic features associated with the Moraga Thrust fault, which parallels the western flank of San Pablo Dam Road north of Orinda Crossroads.

Downloaded from http://pubs.geoscienceworld.org/aeg/eeg/article-pdf/31/1/i/6130855/i1558-9161-31-1-i.pdf
by AEG RBAC user

Moraga Thrust and the Rheem Thrust, which emanates from the deeper Calaveras Fault, some 5 mi (8.0 km) to the east (shown in Figure 52). A series of thrusts parallels the Rheem Thrust, uplifting and folding the soft sedimentary strata (Figure 52). The southeastern quadrant of Orinda lies on the northeast limb of the northwest-southeast–trending Mulholland Syncline and west of the inactive Lafayette Fault.

In places, a steeply dipping fault parallel to Rheem Boulevard (Crane, 1988) separates the lower (Tm-1) and upper Mulholland (Tm-2) beds, as depicted in the accompanying geologic map (Figure 49) and cross section through southeast Orinda (Figure 50). Crane (1988) called this feature the Rheem Fault, and it forms a less-resistant zone, controlling the position of Rheem Valley, from St. Mary's College/Bollinger Canyon northward to Glorietta Boulevard.

Another unnamed fault parallels the Rheem Fault, about 1 mi. (1.6 km) to the east, shown in Figures 50 and 52. This unnamed fault forms a slightly discordant boundary between the Mulholland Formation and the older strata of the undifferentiated Contra Costa Group, which underlies the eastern half of Orinda south of Highway 24, as well as Orinda north of Highway 24 and east of the Moraga Thrust. This outcrop pattern can be appreciated in Figure 48. In some areas, these faults represent weaker zones of material that is more easily eroded by the natural watercourses.

The Lafayette and Reliez faults of Crane (1988) are just two in a series of high-angle, right-lateral, strike-slip faults that appear to be emanating from the Calaveras Fault, and they extend into the Lamorinda area, just east of Fairview and Merriewood Schools in Lafayette. These faults appear to be contemporaneous with the other thrusts emanating from the Calaveras Fault (Figure 52), such as the steeply dipping Rheem Fault, which parallels Rheem Boulevard in Moraga.

Neither the strike-slip faults nor thrust faults are presently considered active (Phelps et al., 2008). Several smaller, strike-slip faults locally cut across bedding at high angles to the larger regional faults. These smaller faults appear to be related to compressional release adjacent to the Rheem and unnamed faults, which have uplifted the eastern half of Orinda above the adjacent terrain. These style of short strike-slip fault is also called a "tear fault." None of these faults has been considered to be an active geologic structure north of Highway 24, but neither have they been subjected to careful paleoseismic age dating, because the Moraga Thrust is not presently zoned as "tectonically active."

The area north of Highway 24 is more tectonically segmented than that south of the freeway. The Moraga Thrust, likely emanating at depth as a back-thrust feature of the Hayward Fault Zone, dominates the terrain west of Camino Pablo. The thrust daylights in the slope approximately 300 (91.4 m) to 3,000 ft (914.4 m) upslope of Camino Pablo. In some areas, natural springs mark the demarcation, but in most places, the contact is marred by relict landslide deposits.

A Detailed Look at San Pablo Ridge West of Orinda Village

Stylized sections through the El Toyonal slopes west of Camino Pablo are presented in Figures 61, 62, and 63. These sketches portray typical scenarios for late Pleistocene evolution of San Pablo Ridge west of Orinda Village, based on examination of trenches and borings in the area over the past 50+ years. The "horse-tailing" feature of the Moraga Thrust (Figure 61) creates multiple shear surfaces, which typically appear more youthful progressing upslope.

The underlying Mulholland beds are overturned by drag folding driven by crustal shortening accommodated by the Moraga Thrust. Large bedrock slides have buried the active thrust features that likely underlie the lower slope. These landslide detachment surfaces serve as groundwater aquicludes and discontinuities of low shear resistance, which tend to spawn deep-seated bedrock landslides, as shown in Figures 61 and 62.

In some areas, there is considerable evidence to suggest the presence of an older, proto-Moraga Thrust plane, daylighting below the Moraga Thrust, somewhere close to the bed of San Pablo Creek (Figure 62). This fault was also suggested by Crane (1988) and is shown in Figures 50 and 52. The presence of a second thrust would help to account for the excavation and grading challenges experienced during construction of the original Highway 24 underpass in 1953–54 (described previously) and the 1,300-ft-long (396.2-m-long) culvert extension for San Pablo Creek in 1964–65.

Conspicuous bedrock benches are noted at many locations along the El Toyonal hillslope, and their likely genesis is from serving as old headscarp evacuation scars, as shown in Figures 62 and 63. In translation of these massive blocks, their stratigraphy is little altered from the surrounding, regional trends. This has been the principal reason that some geologists have failed to recognize their existence, despite the disturbed slope profile. Substantial efforts to explore surface fault rupture features along the projected trace of the Moraga Thrust have proven futile. It was only after such a mammoth slide moved that the anastomosing features of the Moraga Thrust could be explored in detail (Rogers, 1979).

Figures 61–63 depict Holocene-age conditions along San Pablo Ridge over the last 6,800 years. This has been a period of progressive drying, and most of the region's prehistoric bedrock landslides have become increasingly

Downloaded from http://pubs.geoscienceworld.org/aeg/eeg/article-pdf/31/1/i/6130855/i1558-9161-31-1-i.pdf
by AEG RBAC user

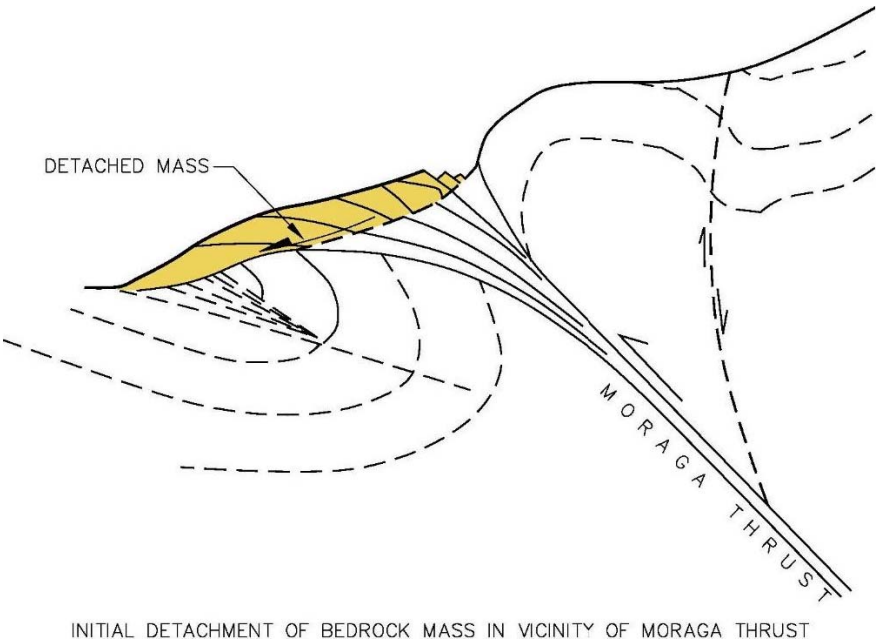

Figure 61. Schematic section through the horse-tail structures of the Moraga Thrust, evidenced by multiple shear interfaces. These appear more recent progressing upslope. The shaded mass represents the initial detachment of a bedrock landslide along potentially active fault traces.

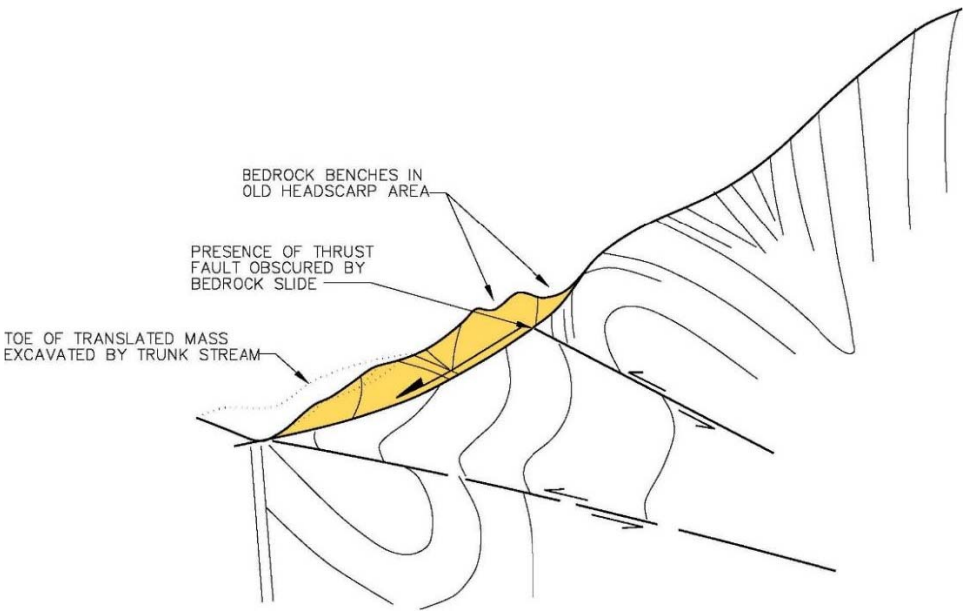

Figure 62. Schematic section through a mature bedrock landslide influenced by elevated pore-water pressures developed on thrust planes. These shear surfaces often serve as aquicludes, reducing the effective stress along old detachment surfaces.

dormant during that interval. The toes of the largest slides are buttressed by alluvium and stream terrace deposits, and the headscarp evacuation areas are smoothed over and often infilled with colluvium (Figure 63). A few strategically placed trenches or borings within these benches often reveal deep accumulations of colluvium, from the natural infilling of the old headscarps. The age of this colluvium varies greatly, from more than 100,000 years just below Orinda Hill to relatively recent elsewhere. Other slope features, lying above these old slides, also appear to be structurally influenced, as sketched in Figures 62 and 63.

Although most of the mega-landslides are currently dormant, numerous smaller slides perturb the slopes of San Pablo Ridge when sufficient cumulative rainfall occurs over 3 or more consecutive years. The volcanic

Downloaded from http://pubs.geoscienceworld.org/aeg/eeg/article-pdf/31/1/i/6130855/i1558-9161-31-1-i.pdf
by AEG RBAC user

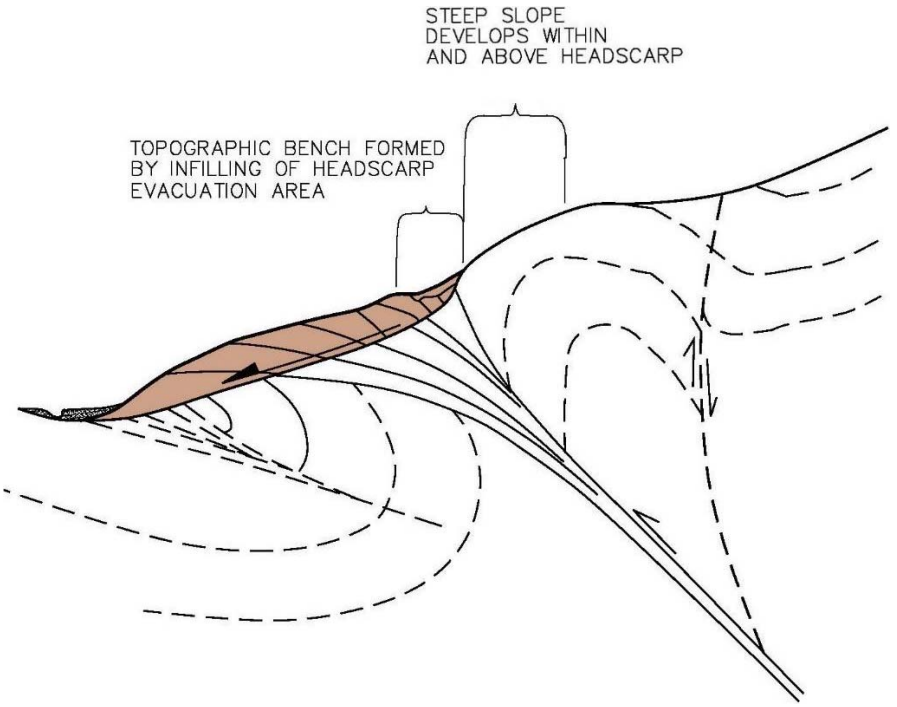

Figure 63. Schematic view of underlying conditions that influence the hillslope morphology. Most of the discontinuous asymmetric topographic benches are associated with faulting and/or deep-seated landslides.

strata and intra-basinal conglomerates of the Grizzly Peak/Moraga formation comprise the slopes along El Toyonal and Claremont Road (Figure 48). In most instances, these units serve as seepage aquifers, which may foster localized land slippage. Residents on Tres Mesas have formed their own water district by pumping from these units.

Area North of Highway 24 and East of Camino Pablo

Faults border the rest of the blocks identified in the north half of Orinda (Figure 48). Dibblee and Darrow (1981) utilized petroleum exploration wells to construct their cross section through north-central Orinda and the Miner Ranch area, reproduced here as Figure 64. While Dibblee and Darrow showed the Franklin and Reliez Faults as thrusts, the Briones Hills are represented as a repeating series of simple folds, cut by vertical strike-slip faulting.

Crane's (1988) release of modern structural interpretations emanating from Chevron's work in the area countered the old tenants of thought, which were dominated by strike-slip faulting until the early 1990s. Crane (1988) suggested that most of the compressional shortening within the area was absorbed through blind thrusts that are usually semi-parallel to bedding. As in the area south of the Highway 24 freeway, erosion along the thrusts influences the structural trends of the prominent valleys, including those occupied by San Pablo Creek and Camino Pablo, described previously.

Most of north Orinda east of the Moraga Thrust is underlain by undifferentiated Contra Costa Group (Tcu)

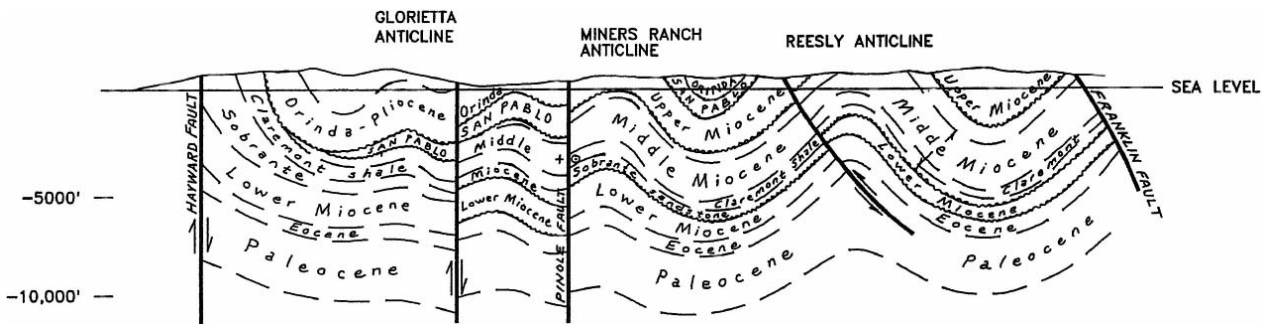

Figure 64. Schematic section cutting northeasterly through north Orinda hills showing the Hayward, Moraga, Pinole, and Franklin Faults, as interpreted by Dibblee and Darrow (1981).

Downloaded from http://pubs.geoscienceworld.org/aeg/eeg/article-pdf/31/1/i/6130855/i1558-9161-31-1-i.pdf
by AEG RBAC user

rocks (Figure 51), which Wagner showed to be in faulted contact with older units of the San Pablo Group, east of St. Stephen's Hill, Lake Cascade, and Sleepy Hollow (Figure 48). The older strata are enclosed with a major anticline that strikes and plunges to the northwest, bordering, and likely contemporaneous with, the Happy Valley Syncline.

Advancing northward from Highway 24, these units include the eastern facies of the Orinda Formation (Figure 56), the Neroly sandstone, and undifferentiated Briones formation (Figure 57). Unlike the younger strata of the Contra Costa Group, these units were deposited in a shallow epicontinental sea, which Graham et al. (1984) has termed the "San Pablo Embayment."

Neotectonics of the Orinda Area

Between the time of its original deposition (6 to 10 million years ago) and the present, the block of hills between the Hayward and Calaveras faults has been subjected to enormous lateral, or tectonic pressures, which have caused marked crustal shortening. Graham et al. (1984) presented a cross section of the Berkeley Hills (Figure 65) that helps readers to appreciate how ancillary uplift along the Hayward Fault has progressively displaced proto-highlands composed of crystalline basement rocks. Crustal shortening between the Hayward rift and the Moraga Thrust is likely several kilometers (Graham et al., 1984).

Most of this shortening has been accommodated by over-thrusting, where one "plate" of material overrides another, typically leaving older rocks lying above younger strata (representing one key piece of field evidence, among others). Crustal shortening is also evidenced in the form of tight folding, recorded in the anticlines and synclines that underlie the Lamorinda area.

Recognition of Blind Thrusts

Until the early 1990s, most of the thrust faults had been overlooked, as these structures can be hard to discern when they parallel the structural grain (strike and dip) of the sedimentary strata. Regional correlations that included "balanced" and "semi-balanced cross sections" were undertaken by Crane (1988), Jones and Brabb (1992), and Wakabayashi et al. (1992).

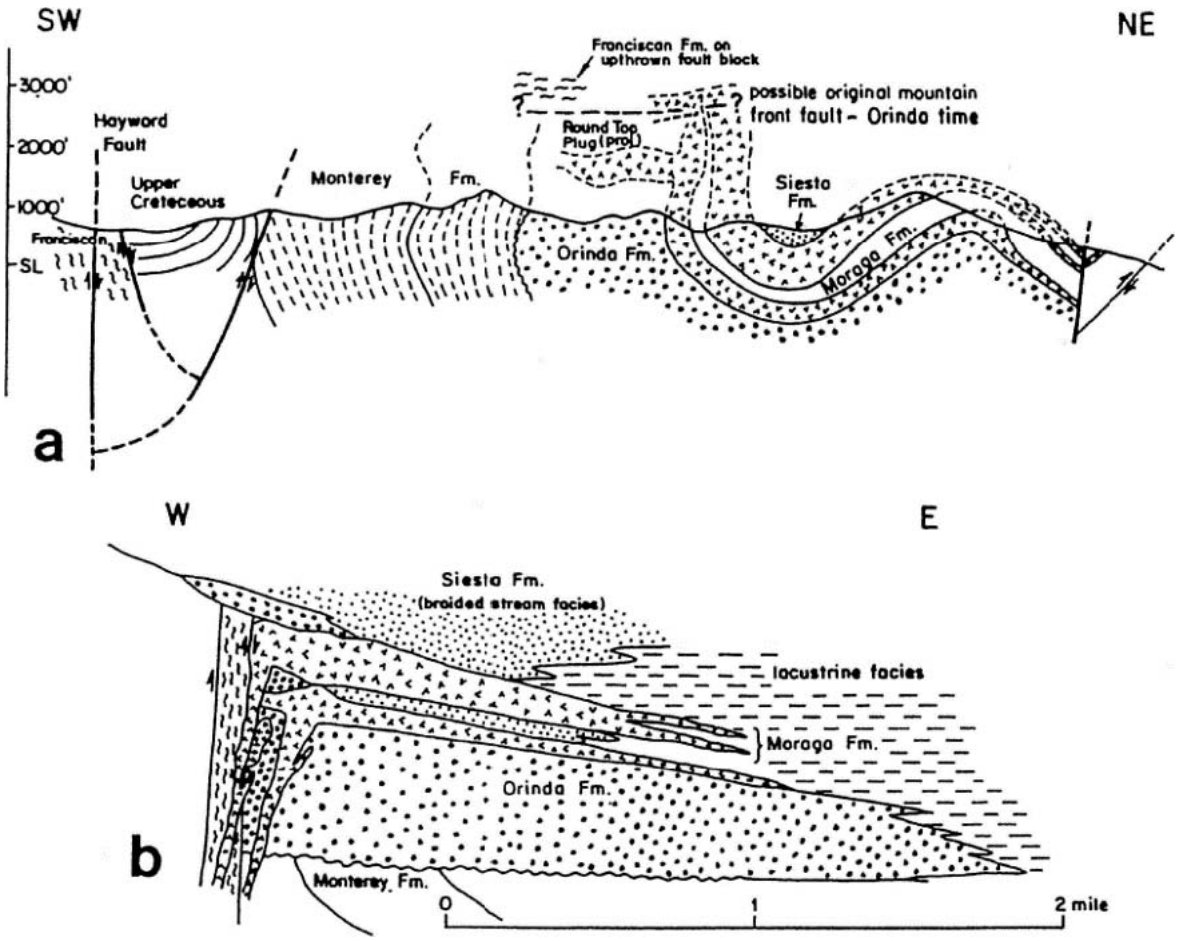

Figure 65. Cross sections illustrating spatial relations of westward thickening of the Moraga Volcanics west of the Siesta Valley Syncline (from Graham et al., 1984).

Downloaded from http://pubs.geoscienceworld.org/aeg/eeg/article-pdf/31/1/i/6130855/i1558-9161-31-1-i.pdf
by AEG RBAC user

These interpretations demonstrated that thrusting is necessary to kinematically explain observed structural and stratigraphic relationships (such as the overturned beds west of Moraga Way and through the Campolindo Homes area of Moraga, and into eastern Orinda).

Crustal shortening and thrust faulting of the Mulholland and Contra Costa sediments in the region have engendered a consistent northwest-southeast strike with steep southwest or northwest dips. Bedrock strata exposed within the Orinda area strikes approximately N. 45° W. and dips either to the southwest or northeast. These structural relationships can be most readily appreciated in the cross sections presented earlier.

GEOMORPHOLOGY AND LANDSLIDING

Introduction

There exists an abundance of data and historical experience that suggests most of Orinda is covered by relict landslides and colluvium (Nilsen and Turner, 1975). The most common type of landslides are coalescing earthflows (Radbruch and Weiler, 1963) and complex earth slide-earthflows (Varnes, 1978). The earthflows generally occupy natural swales developed on the higher ridges (Figure 66). More deep-seated rotational slump features generally occur along the lower slopes, often within deeper accumulations of colluvium, and adjacent to incised stream channels (Figure 67). Large bedrock slumps are, for the most part, relict slides that move episodically, usually adjacent to steep-sided ravines excavated by channel downcutting. In most instances, the more geologically recent slides are superposed upon relict slide masses that are largely dormant, as presented in "Channel Downcutting Causes Local Over-Steepening".

An independent assessment of landslides and surficial deposits thought to blanket the hillslopes in the Orinda area was the central premise of this study, and our interpretations are presented on 12 separate map sheets at two different scales. This slide mapping was accomplished on orthophoto topographic maps prepared by Hammon, Jensen & Wallen of Oakland, CA, at a scale of 1:3,600 (1 in. = 300 ft [1 cm = 36.0 m]), with a contour interval of 10 vertical feet (3.1 m) (assumed to be accurate to within 5 ft [1.5 m] of actual elevations).

Figure 66. Active earthflow complexes in the Contra Costa Hills east of El Sobrante. These slides were partially reactivated during the 7-day storm sequence of mid-February 1986 (J. David Rogers).

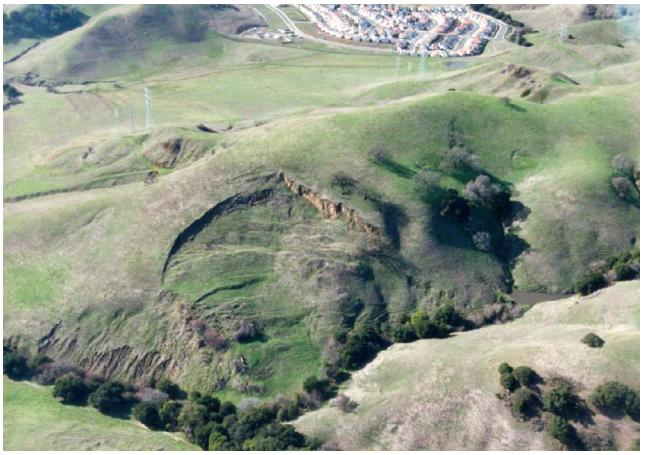

Figure 67. Evolving bedrock landslide in the upper Briones Creek watershed in 1986. Note linearity of en-echelon joints controlling the right side of the mass and the arcuate tensile scarp bounding the opposing margins of the slide. The slide is effectively damming both tributaries in the near foreground (J. David Rogers).

The density of landsliding is typical for the Lamorinda area and exhibits no greater density than nearby areas mapped on a similar scale for the towns of Danville, Martinez, Moraga, and Pleasant Hill (Rogers/Pacific, Inc., 1985, 1989; Rogers, 1997.

Past landslide mapping efforts by state and federal agencies have been on a much larger but far less detailed scale, usually at scales between 1:24,000 (1 in. = 2,000 ft [1 cm = 240.0 m]) and 1:62,500 (1 in. = 5208 ft [1 cm = 625.0 m]). These maps generally identify 30 percent to 65 percent of the largest landslides but delineate a lower percentage of the smaller slides revealed in more detailed assessments (Rogers/Pacific, Inc., 1989).

Geometry of Landslides

The landslides most commonly observed across Orinda are coalescing earthflows, as well as larger rotational and translational failures that are floored within the jointed bedrock of the Siesta, Mulholland, undifferentiated Contra Costa, and Orinda formations. Many of the slides appear to be earthflows approximately 20 (6.1 m) to 50 ft (15.2 m) deep. Deep-seated bedrock landslides also exist, but they typically would require further exploration if development were contemplated on such features to characterize their geometry. Most of these "ancient slide masses" appear to be older than a few thousand years and

Downloaded from http://pubs.geoscienceworld.org/aeg/eeg/article-pdf/31/1/i/6130855/i1558-9161-31-1-i.pdf
by AEG RBAC user

may have been triggered by wetter climates than presently exist. Most of these relict bedrock slide complexes have been dissected by smaller, near-surface erosional processes, such as retrogressive slumps, coalescing earthflows, and runoff-induced erosion, producing colluvial slope wash (which tends to subdue irregularities in slope morphology).

Influence of Systematic Jointing

The sedimentary units are regularly perturbed by recurring sets of regional systematic joints that are more-or-less orthogonal to bedding (often discernible in recent road cuts). Being at mutual right angles to one another, one of the joint sets is usually subparallel to the hillslope's azimuth or trend. The presence of tensile joints under low confining pressure serves to reduce bedrock cohesion and provides ample conduits for seepage infiltration and migration.

After mapping landslides across Orinda in 1962–63, Radbruch and Weiler (1963) reported that 70 percent of active slope failures in this area (between May 1961 and January 1963) occurred on "anti-dip" slopes in tilted, regularly jointed sedimentary rocks. This mechanism of failure is sketched in Figure 68. It is easily observed along the East Bay Regional Park District's hiking and biking trail along the old Sacramento Northern Railroad right-of-way through Moraga and Lafayette.

Back-Analyzed Strengths of Landslides

The slump-earthflow landslides are common in Orinda where the slopes are mantled with colluvium and/or the detritus of recent debris flows. Their physical properties are degraded to figures representative of a residual soil cover and are capable of periodically mobilizing on slopes as gentle as 6 degrees (Figure 69) in Moraga (Rogers, 1986).

Duncan (1971) utilized back-analyses to show that landslides involving sediments from the Contra Costa Group differ little from those of the residual soils developed upon them, e.g., $\Phi = 20$ degrees and $c = 20$ psf (0.96 kPa) for soil and $\Phi = 20$ degrees and $c = 54$ psf (2.6 kPa) in the underlying "bedrock." This was a significant finding that surprised many geo-professionals familiar with the Contra Costa Basin.

More back-analyses were subsequently performed by Duncan and Stark (1992). These later analyses suggested that for large, naturally occurring landslides in the Contra Costa Group bedrock, an "average" strength of $\Phi' = 25$ degrees and $c = 40$ psf (19 kPa) should probably be assumed. These values would appear to apply to rotational and translational slides, and not to debris flows or earthflows, for which the triggering mechanisms appear to be most strongly influenced by seepage pressures.

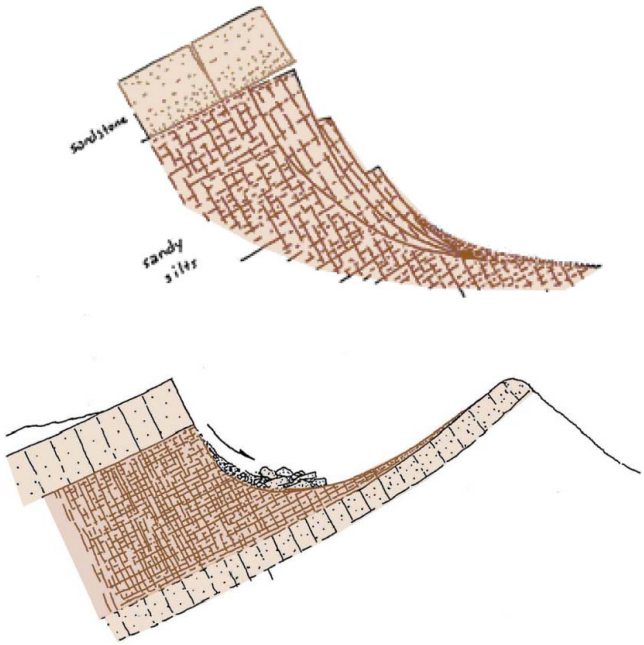

Figure 68a. The geometry of retrogressive slump blocks usually controlled by jointing. The sliver wedges tend to initiate in the toe mass. These failures are common in cases of toe undercutting by watercourses or through removal of smaller, joint-bordered blocks (Rogers, 1986).

Figure 68b. As the more massive beds are displaced, they serve to armor and buttress the toe of the eroding slope (Rogers, 1986).

Figure 69. A virgin earthflow at the base of a natural slope at St. Mary's College in Moraga in 1981. The average grade of the failed slope was only 6 degrees, which suggests that the mass became saturated when it mobilized (J. David Rogers).

Duncan and Stark's 1992 analyses could not incorporate the less-definable roles of emergent seepage pressure, drainage and infiltration concentrations, erosion/creep, and the progressive removal of material following erosive cycles. Area experience gleaned from measuring excavated slopes of known age (Rogers, 1988b) suggests that over time, slopes greater than 15 ft (4.6 m) high cut into the Mulholland and Contra Costa Group

Downloaded from http://pubs.geoscienceworld.org/aeg/eeg/article-pdf/31/1/i/6130855/i1558-9161-31-1-i.pdf
by AEG RBAC user

sediments steeper than 3:1 (horizontal to vertical) will likely erode and slough until they reach equilibrium grade at somewhere between 2.5:1 (22 degree) and 3:1 (18 degree) inclined slopes. These concepts are shown schematically in Figures 70 and 71.

Recurrence Intervals for Landsliding

Aerial photographs of the Campolindo Ridge area of southeast Orinda taken in 1946 by the USGS suggest that the bedrock ravines on the anti-dip or obsequent slope were actively sliding around the same time the images were taken (likely during the winters of 1940 through 1943). Twenty years later, the slides within these same swales appear to be dormant. The slides did not reactivate until March 1983, after 41 in. (104.1 cm) of cumulative seasonal rainfall (Rogers, 1986). They continued to move through the remainder of that winter (1982–83). Curiously, the 7-day deluge that brought 18.8 in. (47.7 cm)

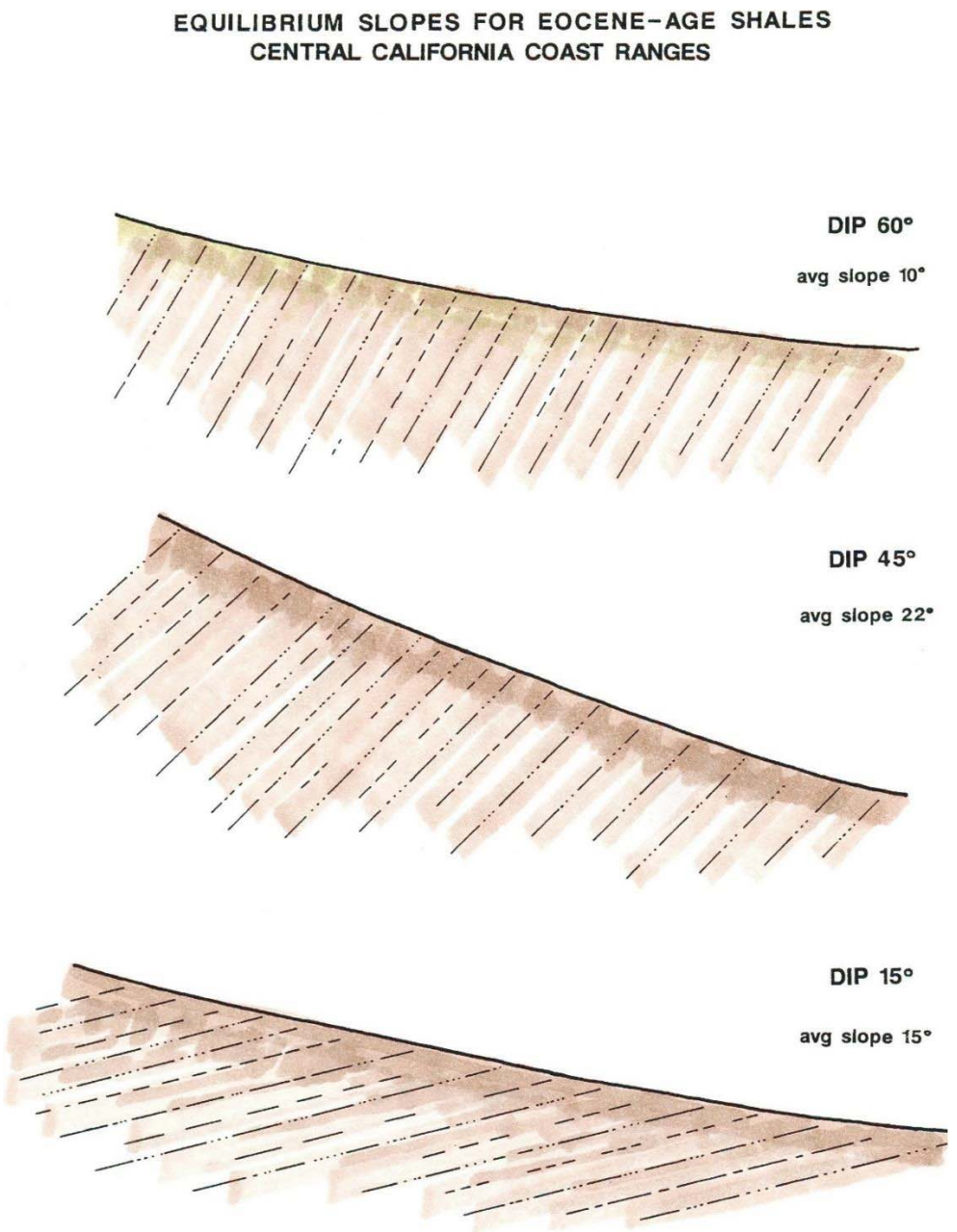

Figure 70. Schematic representation of the influence of shear test data on slope morphology in the Nortonville Shale Member of the Krayenhagen Formation, from Rogers (1986). These over-consolidated shales outcrop across Contra Costa, Alameda, Solano, and Napa Counties. Note how the steepest slopes are underlain by strata inclined at 45 degrees, while the gentlest slopes can be expected when the same beds are inclined at 60 degrees from horizontal.

Downloaded from http://pubs.geoscienceworld.org/aeg/eeg/article-pdf/31/1/i/6130855/i1558-9161-31-1-i.pdf
by AEG RBAC user

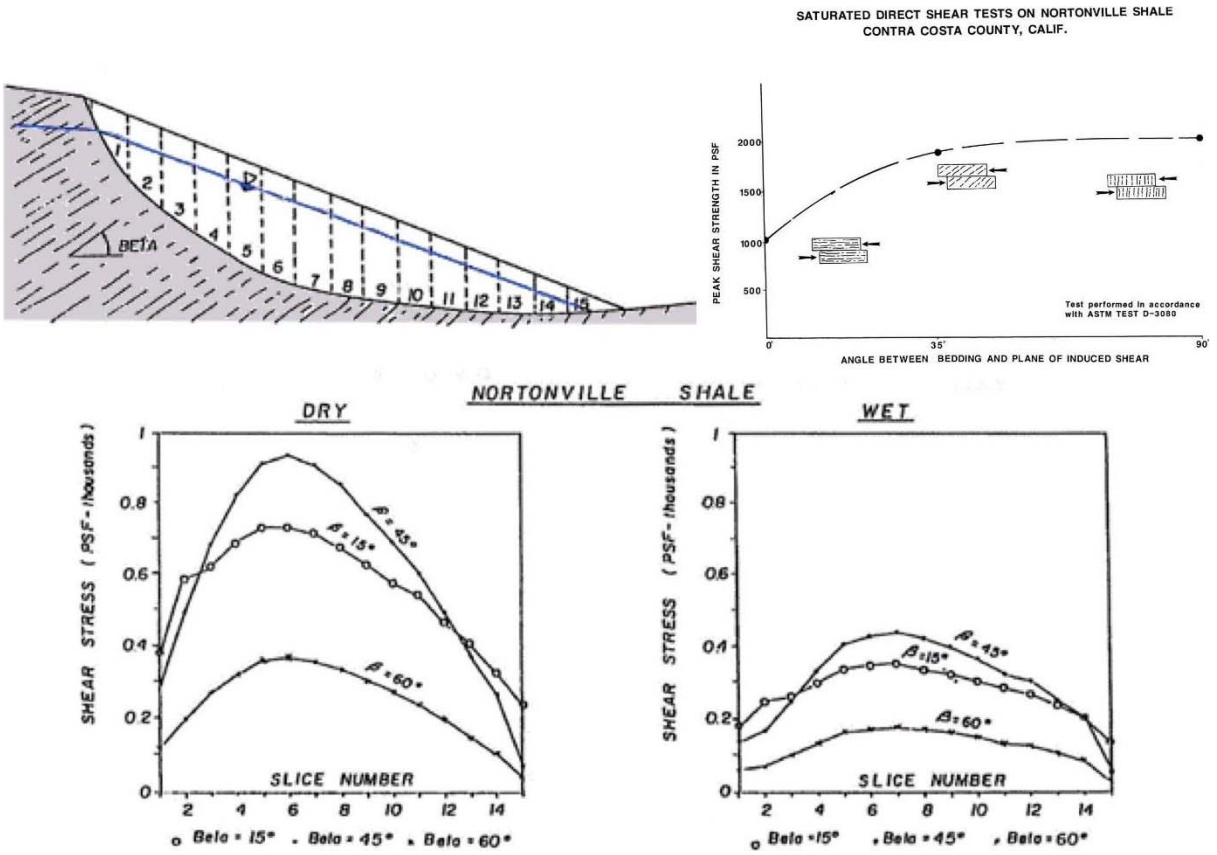

Figure 71. Variation in mobilized shear strength with position in the slope and dip of bedding for the Domengine, Nortonville, and Markley Members of the Krayenhagen Formation (Rogers, 1986). Note how a 15-degree change in dip lowered the mobilized strength by 60 percent, between dips of 45 and 60 degrees from horizontal.

of rain during February 14–20, 1986, failed to reactivate these earthflow slides (Rogers, 1986).

Debris Flows

During the El Niño storms of January 3–5, 1982, several prominent debris flows occurred, emanating from colluvial-filled bedrock ravines along the northeastern side of South Campolindo Ridge, Gateway Valley, and several other parts of Orinda. These debris flows mobilized under extremely high fluid pressures, promoted by the percolation of near-surface groundwater. Reviews of historic aerial photography showed that no similar events had occurred in these same ravines over the previous 55 years. Debris accumulates below these bedrock ravines, and this material, which has been recurrently mobilized, appears to be sensitive to cumulative precipitation. These lower deposits, or "lobes" of clayey debris, did not mobilize in any of the significant El Niño storm events of 1955, 1962, 1967, 1973, and 1982, but they did reactivate in early March 1983, after 3 consecutive years of above-average precipitation (El Niño cycles also occurred in 1997–98, 2009–10, and 2015–16).

Sensitivity of Slide Types to Weather Patterns

These observations would suggest that dormant landslide deposits are sensitive to various types of weather patterns. It would appear that shallow debris flows emanating from steep slopes are triggered by sudden intense storms, especially those which occur on the heels of drought, or early in the wet season. Two such events were the storms of December 14, 1918 (4.5 in. [11.4 cm] in 48 hours) and November 1925, which recorded 9 in. (23 cm) of precipitation in a single week. Shallow debris flows likely generated by the 1925 storms are clearly visible on the February 1928 photos, but they do not appear to have been reactivated again until 2005, despite higher levels of cumulative precipitation. Other drought-ending events have also triggered landslides, in December 1950, February 1978, February 1986, and January 1993.

In the post–World War II period, a series of intense short-duration storms known as "atmospheric rivers" struck the Orinda area. These included the rains of December 1955, October 1962, December 1964, January 1967, January 1973, January 1982, March 1993, January 1997, and January 1998. Deep-seated earthflows floored

Downloaded from http://pubs.geoscienceworld.org/aeg/eeg/article-pdf/31/1/i/6130855/i1558-9161-31-1-i.pdf
by AEG RBAC user

on upland slopes and earthflow lobes deposited on relatively gentle slopes appear to have been most sensitive to cumulative accumulations of moisture, such as those recorded in the winters of 1888–89, 1940–43, 1962–65, 1980–83, 1996–97, 2004–05, and 2017. The consecutive years 1981–83 recorded the highest 3-year running accumulation of rainfall since San Francisco Bay area records began in 1849 in San Francisco and 1895 in Orinda (see Appendix 4).

FUNDAMENTALS OF TERRAIN ANALYSIS

Introduction

Recognition and identification of landslides can be complicated by the inherent heterogeneities of component materials and the physical processes responsible for triggering landslides. Quasi-unique series of factors generally combine to foster landslides, many of which are set in motion hundreds or thousands of years earlier (unique because weather patterns, taken as a whole, are seldom duplicative). Although a large storm can capture newspaper headlines with stories of destructive mudslides, the sudden mass movement of hillsides is only one step in a process of mass wasting that was likely initiated sometime within the past 11,000 years, that period of time geologists term the "Holocene Epoch," the most recent age (Lamb, 1985).

What follows are individual factors that appear to have influenced landsliding in the Lamorinda area over the last 180 years (Joaquin Moraga built his rancho near the future site of Miramonte High School in 1841).

Geologic Factors

The present-day landscape of Orinda is the result of thousands of years of climatic variations, adjustments, and modifications. The topography we see today is just the latest geologic feature, carved during the wetter climates of the ice ages (over the past 1.2 million years). In Lamorinda, the nearby presence of the Hayward Fault Zone has been instrumental in accommodating regional crustal shortening, leading to intensely folded strata that have been perturbed by localized faulting. Ancillary uplift of this folded strata has also been intense, with the greatest uplift likely occurring between the Hayward Fault and Moraga Thrust fault, creating the steep highlands that rise west of Camino Pablo/Moraga Way (Buwalda, 1929; Graham et al., 1983, 1984).

Coincident with the high rate of uplift adjacent to the Hayward Fault, active downcutting of the Berkeley Hills has occurred. The factor controlling base level during most of the Pleistocene (90 percent of the last 1.2 million years) has been a proto–Pacific Ocean surface that lay approximately 350 ft (106.7 m) lower than sea level today (Atwater et al., 1977). The latest Pleistocene shoreline was situated slightly west of the Farallon Islands.

In the gross development of landforms, ridgelines have been exposed to subaerial exposure and weathering/soil development longer than adjoining lowlands. The discovery of highly indurated colluvium atop Orinda Hill in 1983 and above Briones Dam in 1967 (Curtis, 1984) suggests that these pockets of colluvium developed *in situ* in excess of 100,000 years ago, making them some of the oldest surficial soil deposits identified in Orinda.

Environmental Factors

The development of landforms in the Orinda area has been largely controlled by the weather patterns of the past. Most of the landscape we see today was shaped during the Pleistocene Epoch, over roughly the last 1.2 million years. Commonly referred to as the "ice ages," this interim of time was characterized by long periods of cool weather interspersed with short, "interglacial periods" comprised of warmer weather (Lamb, 1985; Bull, 1991). Each of the glacial periods lasted approximately 100,000 years and witnessed sea levels 250 (76.2 m) to 400 ft (121.9 m) lower than present, because a portion of the world's ocean water was locked up in large polar ice caps.

In the most recent glacial age, known in North America as the "Wisconsin glacial stage," ice sheets stretched as far south as the present courses of the Missouri and Ohio River systems, but they did not extend as far as the San Francisco Bay (Lamb, 1985). However, alpine glaciation did dominate much of the Sierra Nevada Mountains, carving most of the higher elevations in such areas as present-day Yosemite National Park.

The cooler climes of the glacial stages persisted for approximately 90 percent of the last 1.2 million years, while warmer interglacial cycles were much shorter, approximately 10 percent of the same interim. At the latitude of Orinda (around 38° N), most scientists feel that average annual precipitation was about 40 percent greater than that recorded over the past 150 years.

Given the long duration of cool glacial stages as opposed to the relatively short interglacial stages (commonly 10,000 to 20,000 years each), 40 percent greater precipitation was likely the operable climate over 90 percent of the past million or so years. These conditions were likely a prominent factor in shaping the morphology of Orinda's hillsides.

Between 14,000 and 11,000 years ago, the present warming trend began, ending the Wisconsin glacial stage. This change in weather brought about a sharp increase in sea level, rising from −300 ft (91.4 m) below sea level to −65 ft (19.8 m) in just 2,700 years, with a

Downloaded from http://pubs.geoscienceworld.org/aeg/eeg/article-pdf/31/1/i/6130855/i1558-9161-31-1-i.pdf
by AEG RBAC user

much slower rise over the last 8,300 years (Atwater, 1979). During the last 6,800 years, there has been a generally steady warming trend, with the exception of three "Little Ice Ages" (Grove, 1988), the last of which stretched from the mid-15th century into the late 19th century. The principal change ushered out with the end of the last Little Ice Age has been in the apparent concentration of precipitation during the winter months with virtual droughts occurring during a 7- to 8-month interim (Leopold et al., 1964; Cooke and Reeves, 1976).

Annual Rainfall Variability (1951–2008)

According to Elissa Lynn, chief of the Climate Change Program Section of the California Department of Water Resources in Sacramento, scientists now believe that about half of California's water supply comes from atmospheric river (AR) precipitation events. ARs are powerful subtropical storms that can strike coastal California in rapid succession. However, the trend California has witnessed since about 1950 has been a diminishing number of ARs and more droughts. In a 2020 online lecture, Lynn noted that seven of the last 12 drought cycles in California concluded with dramatic AR precipitation events.

It turns out that over the past 70 years, the southern half of California has recorded the most rainfall variability of any geographic sector in the United States (Figure 72). In fact, 2 out of 3 years are technically droughts if you employ the proper definitions. These issues were succinctly summarized in a 2011 article by Dettinger et al. (2011) titled "Atmospheric rivers, floods and the water resources of California." This realization has triggered deeper evaluations of the infrastructure sustainability of California's water resources and called into question the wisdom of using average rainfall figures for realistic urban planning because the actual figures can be expected to fall noticeably "below average" two out of three times.

Contra Costa County Rainfall Patterns

A brief review of County rainfall records (Appendix 4) revealed that intense storm sequences fell on the Orinda area in 1904–05, 1913–14, September 1924, October 1936, March 1938, December 1955, April 1958, February 1962, October 1962, January 1963, December 1964, January 1967, February 1969, January 1973, January 1982, February 1986, January 1993, and January 2000.

It can be appreciated from Table 1 that peak rainfall occurrences vary, depending on the time period considered.

Nilsen and Turner (1975) suggested that when seasonal precipitation exceeds 40 annual in. (101.6 cm), less additional precipitation is necessary to trigger damaging landslides. For Orinda, the most destructive cycles of landsliding occurred in 1904, 1909, 1940 through January 1941, January–February 1943, December 1950, December 1955, April 1958, January 1963, January 1967, February–March 1969, October 1969–January 1970, January 1973, February 1978, January–March 1981, January 1982, February–March 1983, February 1986, December 1996–January 1997, January–April 1998, December 2004–January 2005, and January 2017. These dates correlate well with those presented in Table 1.

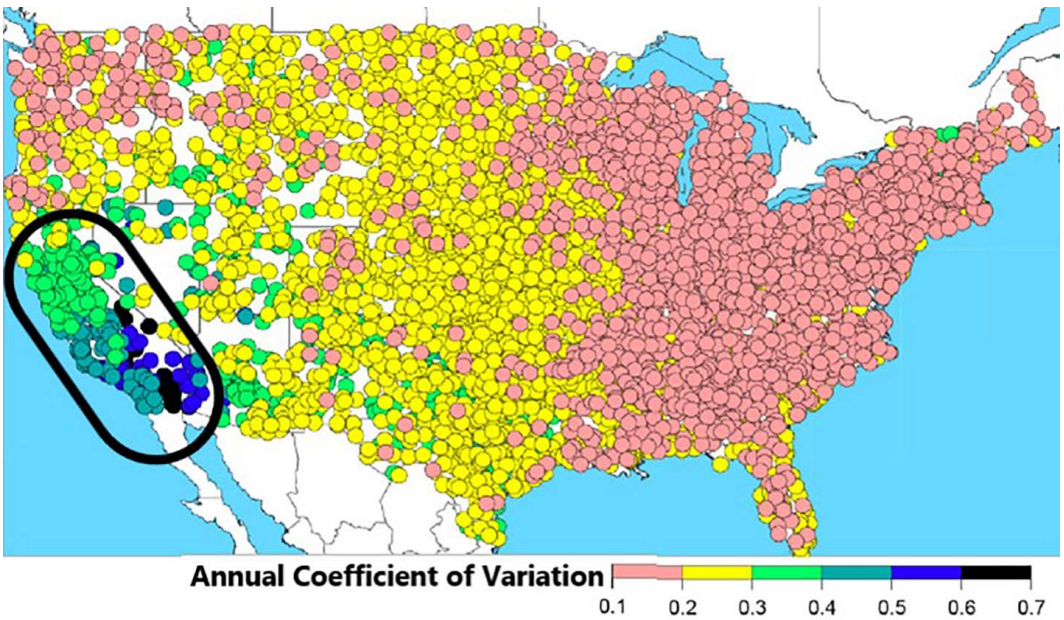

Figure 72. Plot of annual rainfall variability for U.S. Weather Bureau Stations 1951–2008. Note severe variations that pervade central and southern California (Dettinger et al., 2011).

Downloaded from http://pubs.geoscienceworld.org/aeg/eeg/article-pdf/31/1/i/6130855/i1558-9161-31-1-i.pdf
by AEG RBAC user

The sustained storms of February 15–21, 1986, caused the greatest number of debris flows documented in the East Bay since the mid-1920s and triggered record flows along San Pablo Creek. Although no single day's storms exceeded a 9-year recurrence interval in central Contra Costa County, the combined effect of 15 in. (38.1 cm) of rain in 6.5 days spawned record levels of flooding, including involuntary spilling at San Pablo Dam and innumerable shallow debris flow slides across the Lamorinda area (Rogers, 1986).

Effects of Runoff

Just as simple rainfall recorded in a single storm cannot, in and of itself, necessarily trigger landslides, so also is the case with runoff. The amount of runoff induced by any given storm is strongly influenced by antecedent ground moisture (due to past storm activity), as well as other factors, such as short-term intensity (Harden et al., 1978).

A considerable body of geomorphic evidence and historical accounts suggests that Orinda's streams have incised themselves over the past 170 years (Pape, 1978; Rogers, 1988a; and Reid, 1989). For example, historical records suggest that both Lauterwasser and Bear Creek channels have incised as much as 6 vertical ft (1.8 m) over the past 180 years. However, this downcutting of local streams appears to be a regional phenomenon and not necessarily tied to anthropogenic modifications, such as urbanization. Massive vegetation changes exerted by agrarian land practices may have played a significant role as well (see following discussion).

The incision, or downcutting, of the local stream network has given cause for increased landslippage of adjoining steam banks over the past 180 years. Don Pape (1978) reported stark evidence that channel downcutting exists along all the branches of Lauterwasser, upper San Pablo, and upper west branch of Moraga creeks.

Effects of Earthquakes

During the 1906 moment magnitude (M_w) 7.9 San Francisco earthquake, numerous landslides were triggered in the East Bay Hills (Lawson, 1908; Youd and Hoose, 1978). Many of these failures were observed along the flanks of San Pablo Ridge, above what is now El Sobrante, San Pablo, Richmond, and El Cerrito. There is some evidence that a large slide above Lake Cascade may also have been reactivated, based on photos of fresh-looking scarps viewed in 1925 and 1948 (Figures 73 and 74).

The effects of earthquakes on slope stability have received much attention from geotechnical engineers since the March 1964 Great Alaska Earthquake (Seed, 1967; Youd and Hoose, 1978). Many geotechnical engineers agree that the principal factors controlling the seismic response of hillsides include (in decreasing importance): pre-earthquake stability; duration of strong shaking; antecedent soil moisture levels; steepness of slope; and peak ground acceleration (Rogers, 1992). In this context, duration is equated to the number of equivalent cycles of loading (Borcherdt, 1970).

Figure 73. 1926 view of Orinda Country Club, showing the newly completed clubhouse overlooking Lake Cascade, at far left. The arcuate scarp at far right may have served as a quarry for borrow material or the lateral scarp of a recent translational landslide (Orinda Historical Society).

The April 1906 San Francisco earthquake occurred towards the close of what had been the wettest winter in the previous 10 years. As a consequence of the wet conditions, and shaking duration of up to 43 seconds, several landslides were reactivated, including some significant movements along San Pablo Ridge in what is now Richmond and El Sobrante (Youd and Hoose, 1978). Anderson (1908) described earthflow slides and sudden springs triggered by the 1906 earthquake. Although no landslides were reported in Orinda, Kimball (1987) reported that the Bernal Adobe in lower Happy Valley of Lafayette (0.5 mi [0.8 km] north of downtown) was "damaged beyond repair" by the 1906 earthquake.

Other significant earthquakes have recently struck the Orinda area (See Table 3). Theoretically, the greatest of these other earthquakes might have been the June 10, 1836, M_w 6 to 7 earthquake on the northern half of the Hayward Fault, epicentered 4 to 5 mi (6.4 to 8 km) west of Orinda. Unfortunately, the area was just becoming inhabited at that time, so little record of damage exists (Borchardt and Rogers, 1991). Some accounts assert that the area's first home on the Moraga Rancho was built in the late summer of 1835, but Kimball (1987) asserted that the Moraga Adobe was not constructed until 1841.

We note that there was considerable seismic activity in the latter half of the 19th century, preceding the 1906

Downloaded from http://pubs.geoscienceworld.org/aeg/eeg/article-pdf/31/1/i/6130855/i1558-9161-31-1-i.pdf
by AEG RBAC user

Figure 74. Aerial oblique view of the Orinda Country Club area and Lake Cascade taken in March 1948. The dam, clubhouse, and the city's only golf course were constructed in 1924–25 (Pacific Aerial Surveys).

Table 3. *Notable East Bay earthquakes with greater than modified Mercalli intensity V that could have affected Orinda slopes since 1800.**

Date of Occurrence	Likely Richter Magnitude	Fault Likely Responsible for Earthquake (City Nearest Epicenter)
June 10, 1836	M. 6.8–7.2	San Andreas (Santa Cruz Mountains)
November 26, 1858	M. 6.1	Calaveras? (near Calaveras Reservoir)
July 3, 1861	M. 6.9	North Calaveras (Dublin)
May 21, 1864	M. 5.3	South Hayward (Union City)
July 22, 1864	M. 4.7	Mission Hills? (Sunol)
March 5, 1864	M. 5.7	North Calaveras (Dublin area)
October 21, 1868	M. 6.8	South Hayward (Hayward)
April 2, 1870	M. 5.3	North Hayward (Albany)
November 18, 1888	M. 4.3	North Hayward (Albany)
July 31, 1889	M. 5.2	North Hayward (Montclair)
June 30, 1893	M. 4.6	North Hayward step-over (San Pablo Bay)
March 31, 1898	M. 6.2	Rodgers Creek (Sears Point)
December 14, 1904	M. 4.0	Hayward (El Cerrito)
April 18, 1906	M. 8.3	San Andreas (off Golden Gate)
October 8, 1915	M. 4.5	Hayward (East Oakland)
March 8, 1937	M. 4.5	Hayward (Holy Names College)
December 29, 1942	M. 4.3	Hayward (Lake Chabot)
October 13, 1952	M. 4.2	Hayward system (near Oakland Coliseum)
October 22, 1952	M. 4.0	Hayward (Skyline High School)
October 24, 1955	M. 5.4	Concord (Walnut Creek)
May–July 1970	M. 1–4.0	Danville swarm #1 (Blackhawk area)

continued

Downloaded from http://pubs.geoscienceworld.org/aeg/eeg/article-pdf/31/1/i/6130855/i1558-9161-31-1-i.pdf
by AEG RBAC user

Table 3. *Continued.*

Date of Occurrence	Likely Richter Magnitude	Fault Likely Responsible for Earthquake (City Nearest Epicenter)
August 1976	M. 1–4.1	Danville swarm #2 beneath Sherborne Hills
January 8, 1977	M. 4.3	Briones Reservoir (Orinda)
January 1980	M. 5.5/5.3	Greenville & associated faults (NE Livermore Valley)
March 27, 1984	M. 4.1	Hayward/reverse (San Leandro)
April 24, 1984	M. 6.2	South Calaveras (Morgan Hill)
March 31, 1986	M. 5.7	Mt. Lewis (Lake del Valle)
June 13, 1988	M. 5.3	South Calaveras (Alum Rock)
October 17, 1989	M. 7.1	San Andreas strand (Santa Cruz Mountains)
April 1990	M 1–4.5	Alamo swarm (Livorna Road/Walnut Creek)

* Other significant earthquakes that have likely impacted the Orinda area include: the July 1861 M 6.3–6.9 earthquake on the northern Calaveras Fault, the October 1868 M 6.8–7.1 earthquake on the southern Hayward Fault, and the March 1898 M 6.2 Mare Island earthquake, now ascribed to the Rodgers Creek Fault (Toppozada et al., 1981).

San Francisco earthquake. This was also true of the Hayward Fault Zone, and its related splays. The two greatest events in historic time have been the October 1868 earthquake on the southern Hayward Fault in Fremont and the April 1906 San Francisco earthquake on the San Andreas Fault, epicentered west of the Golden Gate.

Following the 1906 earthquake, there was a long period of relative seismic quiescence in the San Francisco Bay area, interrupted briefly by smaller earthquakes on the Hayward Fault, including a M 5.4 earthquake in October 1955 in Walnut Creek and the M 5.3 Lake Merced earthquake in March 1957, which caused slight accelerations in Orinda.

Between 1979 and 1984, the southern strand of the Calaveras Fault spawned three moderate-sized earthquakes, with another on the Greenville Fault, bordering the east side of Livermore Valley (January 1980). The January 1980 M 5.4 event was followed a few days later by a M 5.2 earthquake on an unnamed splay, trending N. 10° W. off of the Greenville Fault. A similar left-lateral compressional release earthquake was recorded during the March 1986 M_w 5.7 Mt. Lewis earthquake, thought to be in response to the previous three earthquakes on the south Calaveras Fault (Oppenheimer and Macgregor-Scott, 1992).

The October 1989 M_w 6.9 Loma Prieta earthquake, centered in the Santa Cruz Mountains, was of abnormally short duration for a magnitude 6.9 event, and it was sufficiently distant to cause little damage to Orinda (strong motion recorders inside the Caldecott Tunnels recorded semi-free-field bedrock accelerations of approximately 0.04*g*).

Localized Earthquake Swarms (1970–90)

Several sets of earthquake swarms have also been recorded in central Contra Costa County. The first of these swarms consisted of several thousand small-magnitude earthquakes recorded in the hills east of Danville during May, June, and July 1970 (Lee et al., 1971). These varied in magnitude between 1 and 4. Another swarm of small earthquakes occurred slightly west of the 1970 group in August 1976 (M 4.1), occurring in a previously aseismic area beneath the Sherburne and Hemme Hills (along either side of Camino Tassajara). These earthquakes recorded northwest-southeast–aligned compression. By the early 1990s, seismologists believed that these swarms were tied to stress redistributions within the step-over region between the right-lateral Calaveras Fault and Concord Fault systems (Oppenheimer and Macgregor-Scott, 1992).

Another curious swarm of small earthquakes emanated from the Briones Reservoir area on January 8, 1977, rupturing along north-northwest–trending geologic structures (Ellsworth et al., 1982). The largest of these quakes registered M 4.3 and caused slight damage to some homes in Orinda.

In late March and early April 1990, another earthquake swarm was recorded in central Contra Costa County beneath Livorna Road on the Alamo/Walnut Creek border. The earthquakes recorded magnitudes up to 4.5 on Friday, April 6. These epicenters were aligned in an east-west direction, suggestive of compressional release in the step-over region between the Calaveras and Concord faults. Crane (1988) had predicted such swarms in this area, attributing them to the continued uplift of Mt. Diablo in a direction west-southwest of the main peak.

Some of the most likely earthquakes to impact the East Bay Hills in the foreseeable future include events sourced in the northern Calaveras Fault in the vicinity of the Calaveras Reservoir. A M_w 6 earthquake emanating from this area could be expected to send shock waves up the San Ramon segment of the Calaveras Fault and onto the south Hayward Fault via the Mission Fault cross-over (Oppenheimer and Macgregor-Scott 1992). Schwartz et al. (1992) also predicted that the southern strand of the Rodgers Creek Fault, parallel to and across San Pablo Bay from the Hayward Fault, can be expected

Downloaded from http://pubs.geoscienceworld.org/aeg/eeg/article-pdf/31/1/i/6130855/i1558-9161-31-1-i.pdf
by AEG RBAC user

to rupture in the next 35 to 100 years. A magnitude 7 event on the Rodgers Creek Fault could severely impact Orinda hillslopes, depending on the antecedent soil moisture levels.

Human Factors

Nilsen and Turner (1975) estimated that approximately 80 percent of the active landslides in Contra Costa County are related to human activity in one way or another. These activities include construction for highways or structures, which can disturb adjacent slopes or alter seepage sufficiently to trigger slope failures that might otherwise not have occurred. In most instances, the primary cause of cut-slope failures within the Orinda area has been due to the over-steepening of slopes, which removes lateral support and engenders stress relaxation due to unloading (which typically leads to dilatancy).

As discussed previously, numerous cut slopes excavated in the Orinda area have subsequently failed. The most notable of these cut-slope failures were associated with the present alignment of State Highway 24 and its predecessor routes, dating back to 1913. In a synthesis of Radbruch and Weiler's (1963) work, Duncan (1971) found that all but one landslide that occurred in Orinda between 1960 and 1963 occurred on slopes steeper than 3:1 (horizontal to vertical).

Temporal Factors

Time is a factor common to all of the physical processes profiled above. Landsliding is simply one form of mass wasting by which slopes are brought to the limits of natural equilibrium, given the environmental extrema to which they are subjected.

Slope shape and form, or morphology, are sculpted by those processes that predominate over a longer time span. Comparative photographs and topographic surveys performed over the past 250 years suggest that the landscape has changed very little over that interim, except where the efforts of humans have altered the existing ecosystems. Much of that impact has been in the realm of introduced non-native vegetation, cattle grazing, and weather patterns (McBride, 1964, 1974; McBride and Heady, 1968).

Sharpe (1938b) stated that landslides are most prevalent in youthful topographic evolution, or within those areas subjected to high uplift and channel downcutting rates. Virtually all of coastal California in the proximity of the San Andreas Fault and its associated structures would fall into this context. Uplift rates adjacent to the Hayward Fault are not precisely known (Graham et al., 1984), but they appear to hover around 0.05 mm/yr, based on observed down-dropping and uplift over the past 13 million years (Buwalda, 1929; Wagner, 1978; and Graham et al., 1984). Ancillary uplift along the San Andreas Fault within the San Francisco Peninsula averages 0.02 to 0.04 in./yr (0.50 to 1.03 mm/yr) (Atwater, 1979; Rogers, 2001b).

Rib and Liang (1978) presented models of hillslope evolution that are recounted here: Geologically youthful hillslopes are typified by steep side slopes and relatively few stream channels, such as the erosional escarpments viewed in "badlands." Youthful erosion gullies typically exhibit V-shaped cross sections (Figure 75a).

Geologically immature slopes are those beginning to develop an integrated system of drainage. Topography consists mainly of hillsides and valley sides. Drainage divides are sharp, allowing the maximum possible relief. Vertical downcutting has ceased, and lateral destruction of the adjacent hillslopes by landslides persists as the predominant mode of erosion (Figure 75b).

In geologically mature slopes, valleys are extremely broad and gently sloping, both laterally and longitudinally. Floodplains are well developed, and streams meander on low gradients. Stream divides are not sharp, and hilltops are broadly rounded (Figure 75c).

KEY INDICATORS OF LANDSLIDING

Once the various forms of landsliding are identified, "key indicators" aiding in their identification can be formulated based upon the principle that similar topographic patterns and styles of mass wasting tend to occur under similar environmental and climatological conditions. The existence of such key indicators will generally vary slightly, according to different stages of the mass-wasting cycles. For example, recent landslides will exhibit sharp, definable boundaries (like those shown in Figure 67). As slides lie dormant for periods of time, their physical boundaries become increasingly subdued, making identification more difficult.

Typical examples of "topographic healing" of landslide crown scarps are included in Figures 76a–d and Figures 77–78. These images feature an obvious bedrock landslide that occurred in March 1983 near the intersection of State Highway 4 and Christie Road, just east of the BNSF rail line and Rodeo Creek, close to the Hercules city limits. The most-striking changes occurred between 2001 and 2016, because that time period witnessed abandonment of cattle grazing and some significant wet-and-dry weather cycles. It appears that the annual grasses growing on the slide were overtaken by coyote brush (*Baccharis pilularis* DC), which forms a dense mat of vegetation that obscures surface anomalies typical of old landslides (McBride, 1964).

Downloaded from http://pubs.geoscienceworld.org/aeg/eeg/article-pdf/31/1/i/6130855/i1558-9161-31-1-i.pdf
by AEG RBAC user

Figure 75a. A hydraulic mining operation in Alaska, which is the epitome of an active erosional escarpment.

Figure 75b. An example of an immature drainage system that is developing in Alamo, CA.

Figure 75c. A geologically mature landscape in present-day Moraga Country Club.

Figure 75d. An example of geologically old terrain underlain by relict bedrock landslides in Orinda's Gateway Valley (J. David Rogers).

Figure 76a. The Christie slide shortly after it occurred in March 1983.

Figure 76b. The Christie slide in March 1986, when the lateral scarps were beginning to crumble.

Figure 76c. The Christie slide in May 1992, when the headscarp was being modified by raveling erosion.

Figure 76d. The Christie slide imaged in April 2001, 18 years after initial movement. Note the smoothed but clearly defined breaks in slope along the lateral margins of the headscarp (J. David Rogers images).

Downloaded from http://pubs.geoscienceworld.org/aeg/eeg/article-pdf/31/1/i/6130855/i1558-9161-31-1-i.pdf
by AEG RBAC user

Figure 77. After 33 years, the Christie slide no longer exhibits physical evidence of its recent movement. This is because the slope is no longer being grazed by cattle, and coyote brush has overtaken the site, concealing any tell-tale anomalies in slope morphology along the headscarp (J. David Rogers).

Key indicators of landsliding were identified for the Orinda area by assessing the following characteristics:

(1) compilation of historic landslide data over the past 100 years within the Orinda area, including subsurface exploration data;
(2) detailed on-site evaluations of recent landslides at a number of locations within and around Orinda (subsurface structure is best revealed in excavations made for landslide repairs);
(3) differences in topographic patterns exhibited by different types of landslides (irrespective of volume);
(4) physical characteristics (topographic expression) associated with different types of landslides in mature stages of erosion, when recognition is most difficult (younger slides often lie upon less-expressed, but deeper-seated ancient landslides);
(5) detailed assessments of the physical and topographic expression exhibited on slopes *before* historic slides moved (like the Camino Ricardo cul-de-sac in Moraga), including evaluations of tonal variations, scale, parallax, vegetation, soil tones, and microfeatures that might be indicative of past landslippage;
(6) orthophoto topographic map coverage with a suitably fine contour interval (preferably between 3 and 10 ft [0.9 to 3.1 m]) to enable the identification of slides as small as 30 by 100 ft (9.1 to 30.5 m), with at least 30 ft (9.1 m) of vertical differential;
(7) criteria for the identification of coalescing landslides (generally earthflows) within larger hillslope complexes exhibiting obvious signs of instability, such as hummocky topography; and
(8) field checks of those localities that presented puzzling characteristics that did not initially appear to fit "key indicator" models.

Compiling Basic Data for Landform Identification and Mapping

The procedure described below is a general process for compiling the basic data required for landform identification and mapping, and it was used in the aerial photo-interpretive portion of this study:

(1) All existing information pertaining to the area of study is assembled. This includes historic topographic maps, ground photos, historical accounts, records of slope instability, geologic hazards identified by others, university studies, published sources of information, etc. A good place to begin is by accessing http://historicalmaps.arcgis.com/usgs/ and local historical archives, such as the Orinda Historical Society and the Contra Costa County Historical Society. Two other sources for historical information used in this study included the East Bay Regional Park District and the EBMUD in Oakland.
(2) All available information on bedrock geology and structural geology (faults and folds) is standardized with the most accepted stratigraphic nomenclature

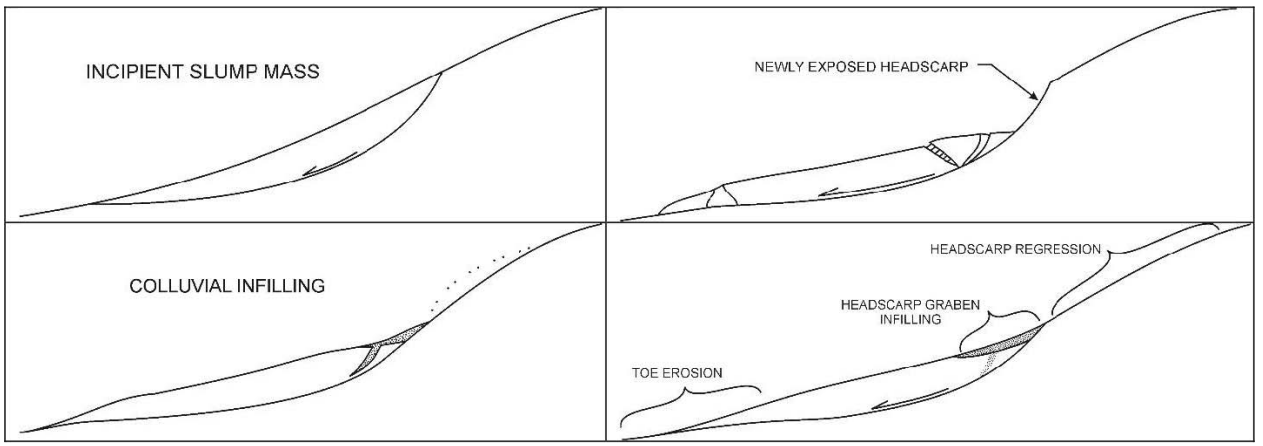

Figure 78. Schematic cross sections through the Christie slide-earthflow, showing how progressive infilling and erosion of the slide's crown scarp and lateral scarps make identification more difficult with the passage of time.

Downloaded from http://pubs.geoscienceworld.org/aeg/eeg/article-pdf/31/1/i/6130855/i1558-9161-31-1-i.pdf
by AEG RBAC user

and overlain on a master map of the study area (Figure 48). It is often useful to identify the spatial extent of similar parent materials, which can weather into residual soils, alluvium, or colluvium (slope wash).

(3) All first-order and higher natural watercourses (both ephemeral and perennial) should be identified and plotted. The texture of the drainage patterns should be identified (Figure 79). These patterns are then compared to the bedrock geologic compilation to

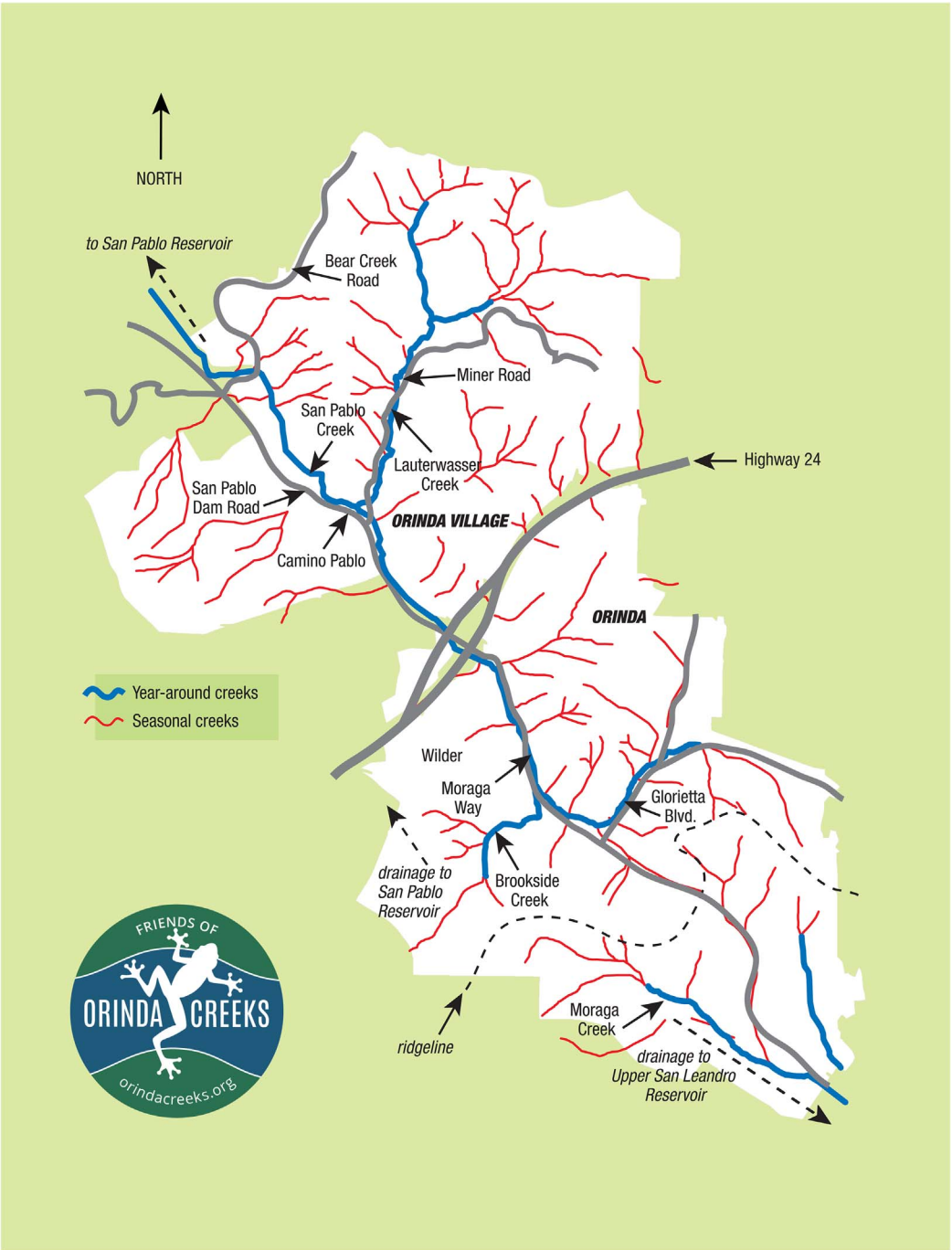

Figure 79. Map of ephemeral and perennial watercourses in Orinda, along with the principal vehicular corridors. Retrieved from https://orindacreeks.org/.

Downloaded from http://pubs.geoscienceworld.org/aeg/eeg/article-pdf/31/1/i/6130855/i1558-9161-31-1-i.pdf
by AEG RBAC user

ascertain where underlying structural control is likely exerted on the watercourses.

(4) U.S. Department of Agriculture–Natural Resources Conservation Service soil survey maps are also compiled, and relationships among soil types, underlying bedrock, drainage courses, salient geologic structures, and slopes are delineated.

(5) The National Flood Insurance Program—Flood Insurance Rate Maps (flood inundation probability maps produced by the Federal Emergency Management Agency [FEMA]) are consulted, verifying that the posted map is the most current. In many instances, it is desirable to construct a few representative thalweg stream profiles. Profiles are one of the best indicators of massive system perturbation by such features as paleo-landslides, mega-landslides, or, depending on the scale of the topographic data, geologically recent landslides.

This list forms the "basic data" from which to begin a photo-geologic assessment. The basic parent materials are usually identified from the most recent geologic maps. Within these zones, subunits may be identified based on surficial soils information. Soils will exhibit various textures depending on their slope, thickness (sometimes called stoniness), and water content at the time of imaging, sun angle/incidence, vegetation, and degree of erosion. Common surface textures are sought out and identified in those discrete areas within which the photo-interpreter has first-hand experience or reliable data upon which to "ground truth" textural inferences.

In this study, several sites within and adjacent to Orinda were studied in considerable detail over the past 45 years in the course of engineering geologic studies associated with research, landslide studies and repairs, and earthwork for engineered facilities.

IDENTIFICATION OF LANDFORMS SUSCEPTIBLE TO LANDSLIDES

Introduction

Landslides can occur in almost any landform, provided that conditions exist that are adverse to long-term stability. A slope's sensitivity to destabilizing factors varies as a function of the geologic structure, slope steepness, slope height (scale), moisture content, vegetative cover, and anthropogenic disturbance. Experience with slides in the Lamorinda area has shown that landslides are common in some landforms but relatively rare elsewhere.

Geomorphologists (Way, 1978; Selby, 1993) tend to classify landforms according to their topographic expression and drainage patterns. For slopes in the East Bay Hills, Rogers (1987a) has suggested that hillslope profile is a key factor in assessing past landslippage. In Tertiary-age sedimentary strata like those deposited in the Contra Costa Basin, hillslope profile is largely shaped by hydrologic requirements, such as slope, roughness, and runoff quantity, and mass-movement processes, such as soil creep, colluvium production, and mass-wasting events.

Factors Controlling Hillslope Profile

Geomorphologists and engineering geologists can gain insight as to prehistoric slope instabilities by comparing two basic slope forms: those typical of quasi-equilibrium conditions (Figure 80) and those of a slope with varying profile, which may not be in equilibrium (Figure 81). In the Lamorinda area, the hillslope profile is slightly more complicated than the models shown in Figures 80 and 81, mimicking, more often, the stepped profile presented in Figures 82 and 83 (Campolindo Ridge).

Around the turn of the 20th century, Davis (1899) formulated the accepted premise of a mature slope in

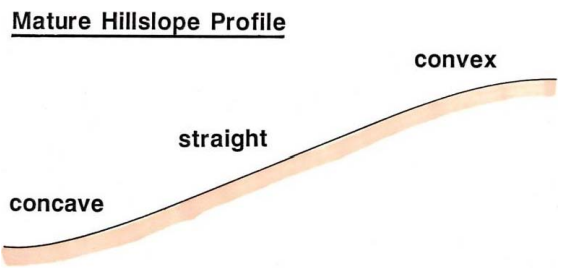

Figure 80. Postulate for mature hillslope profile, presented by William Morris Davis in 1899. Davis suggested that slopes composed of homogeneous materials will develop concave-straight convex profiles, when in equilibrium.

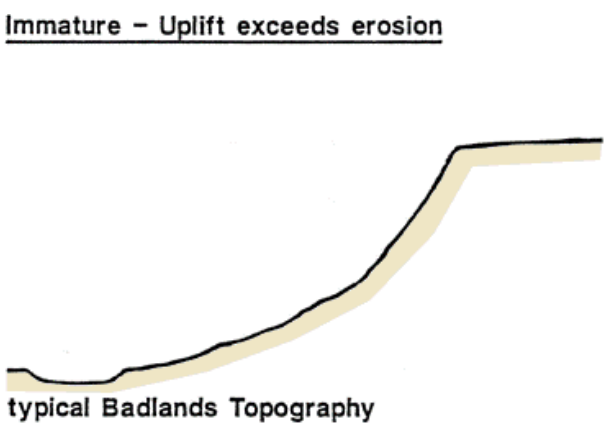

Figure 81. Slopes that erode at extremely rapid rates, or are uplifted suddenly, are generally believed to be in a state of disequilibrium. In this case, the concave slope section dominates the profile, with a short straight section and with no recognizable convex form at the crown-of-slope. This form can take shape in areas where uplift exceeds erosion, or in the case of badlands, where erosion of the uplifted highland is occurring at a rapid pace.

Downloaded from http://pubs.geoscienceworld.org/aeg/eeg/article-pdf/31/1/i/6130855/i1558-9161-31-1-i.pdf
by AEG RBAC user

Figure 82. Stepped hillslope profile observed on the northeast-facing slope of Campolindo Ridge near the Orinda-Moraga border. The bumps in the profile are formed by resistant sandstone and conglomerate dipping to the southwest towards Rheem Boulevard (J. David Rogers).

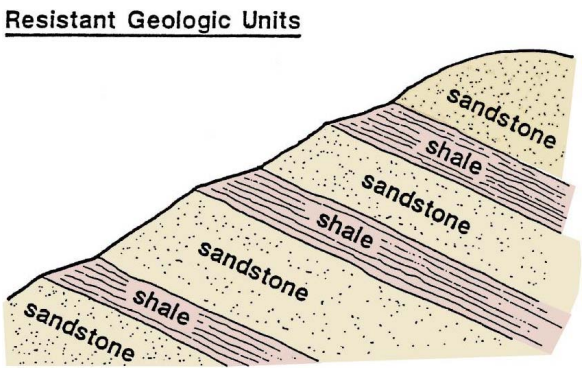

Figure 83. Contra Costa slopes are typified by inclined series or alternating soft and hard strata, as depicted above. Although shale units lose strength upon saturation, the intervening beds of sandstone are just as important in shaping slopes because they can selectively concentrate groundwater to near-surface areas (depending upon structure and catchment area).

equilibrium spawning a concave-straight-convex profile, as presented in Figure 80. Slopes form in response to geologic uplift, which in the Orinda area has been tied to regional tectonic forces. Slope form is also influenced by localized downcutting of streams, due to changes in erosive base level (sea or lake levels) and climatic changes (Bull, 1991).

Absent landsliding, slope form in the relatively soft sedimentary strata of the Contra Costa Hills is largely influenced by hydrologic criteria, such as lithology (underlying rock type), height of slope, and tributary watershed area (Figure 84). A series of slopes in quasi-equilibrium may exhibit differing slopes due to proximity of the controlling base level (trunk stream position). An example of variance of slope profile with stream position is presented below.

Figure 84 illustrates explain how the slope profile is influenced by hydrology in softer materials, like the Contra Costa Group of sediments. In softer materials, hillslope profile is influenced by slope height, flow distance, and controlling base level. The slope's hydraulic grade must be sufficient to convey the imposed sheet flow or channelized runoff. As runoff volume and velocity drop, suspended sediment and bed load (shown in yellow) will typically be deposited immediately downstream of a hydraulic flow transition (or "hydraulic jump"). Note how the eroded material tends to infill the transition between ascending slope and flat alluvial valley. This fill maintains a progressively diminishing slope to maintain the sheet flow of imposed runoff.

More-resistant materials can exhibit steeper faces, as shown on Figure 84. H_c equates to Terzaghi's concept of critical height for cohesive materials (Terzaghi, 1943):

$$H_c = 3.85 \text{ to } 4\,(c/g),$$

where H_c is the critical height, c is the unit cohesion of the slope material, and g is the unit density of the material.

In Figure 84, note how the profiles become more mature with increasing watershed area and flow distance. These parameters likely increase stream power, which increases the rate of erosional adjustments to variances in flow. In this case, the most influential parameter appears to be flow distance to the controlling base level (the trunk stream).

Figures 84 and 85 illustrate how the shape of the hillslope profile is tied to the location of the controlling base level, which is usually the next lower watercourse receiving the slope's runoff, the level of a standing body of water, or sea level.

A typical erosion cycle triggered by sea-level drop or by tectonic uplift hastened by crustal compression is common within central Contra Costa County, as sketched in Figures 86 through 90. Figure 86 presents a mature slope with concave toe, straight mid-slope, and rounded, convex crest. The underlying lithologies are relatively homogeneous, and only a slight break in slope exists over the more-resistant beds of sandstone. This mature slope is suggestive of geologic quiescence, where little change in climate or vegetation patterns has occurred for some time.

If the hills are tectonically uplifted, or a lower base level is exerted (due to lowering of sea level), trunk streams in valley bottoms can be expected to begin downcutting, which can lead to over-steepening of channel banks and increased bank height. The combination of these physical changes serves to upset hillslope equilibrium. The early stages of this condition are shown diagrammatically in Figure 86. The slope profile will generally exhibit marked changes in slope gradient.

Downloaded from http://pubs.geoscienceworld.org/aeg/eeg/article-pdf/31/1/i/6130855/i1558-9161-31-1-i.pdf
by AEG RBAC user

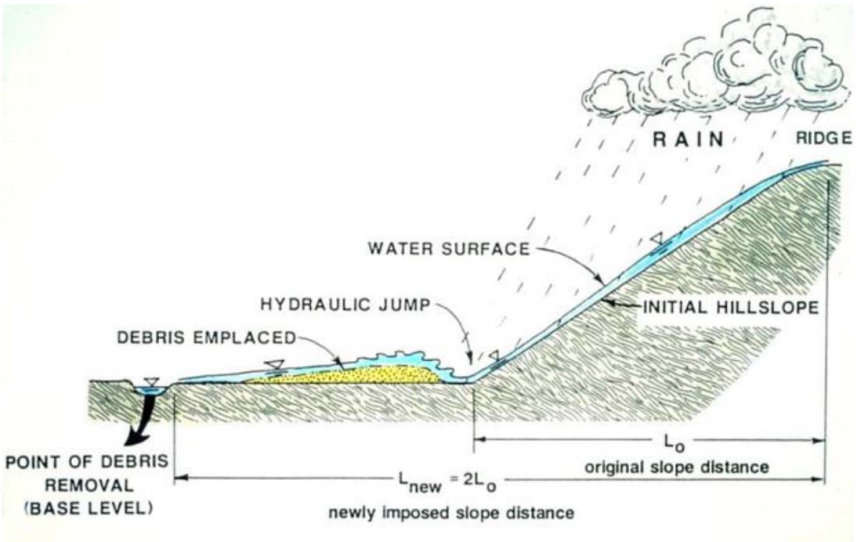

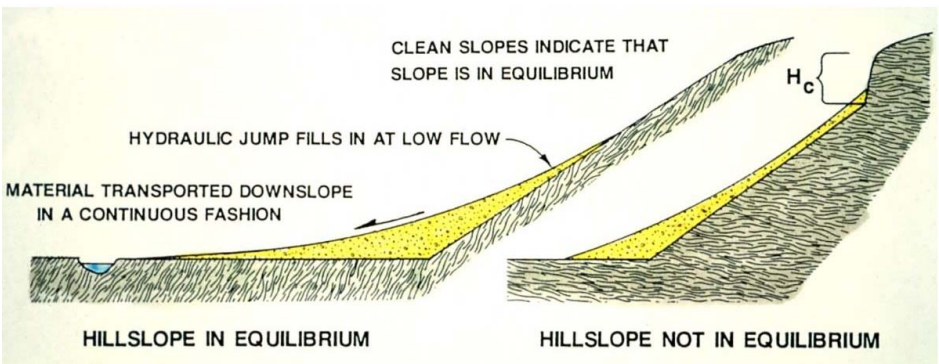

Figure 84. Concepts of equilibrium for a slope underlain by semi-homogeneous material (Rogers, 1980).

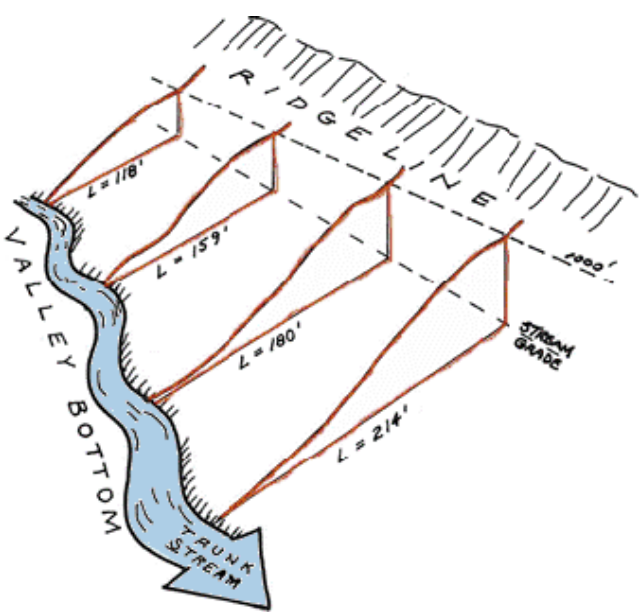

Figure 85. Successive hillslope profiles surveyed near Pinedale, WY. Note how the profiles vary with the position of the trunk stream, which influences the local base level (Rogers, 1980).

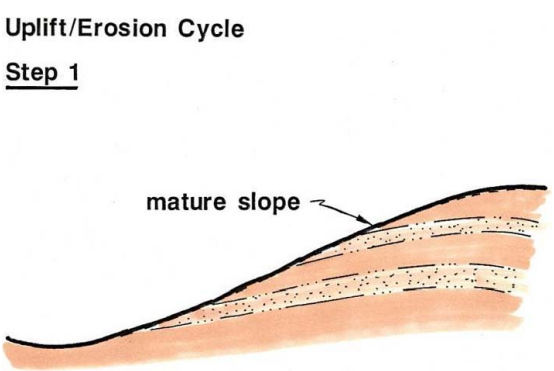

Figure 86. A mature slope develops in response to equilibrium conditions being achieved after some period of time.

Most Orinda hillslopes exhibit these features, on small and large scales. These features attest to repeated episodes of stream-channel entrenchment, infilling, and re-trenchment, which is supported by the records of late Quaternary sea-level rise and fall over the last 27,000 years (Atwater et al., 1977).

As erosive downcutting continues, a steeper slope often develops at the toe of the slope or along the creek

Downloaded from http://pubs.geoscienceworld.org/aeg/eeg/article-pdf/31/1/i/6130855/i1558-9161-31-1-i.pdf
by AEG RBAC user

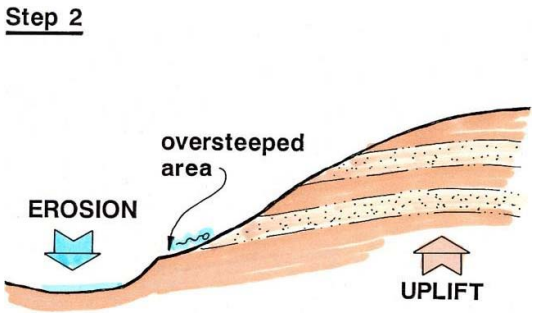

Figure 87. This equilibrium is disturbed when the local base level is adjusted by regional channel downcutting or regional tectonic uplift.

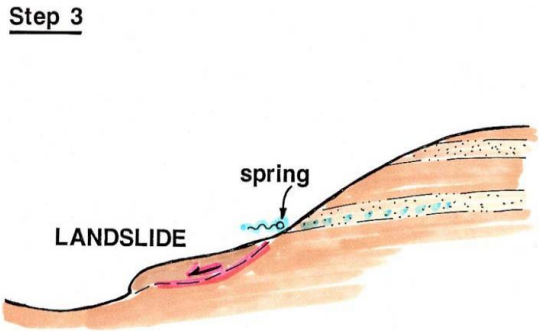

Figure 88. The first landslides of a disequilibrated system usually occur as a rotational slump of surficial soils or colluvium adjacent to a locally over-steepened stream bank. The presence of ephemeral springs is a frequent trigger factor.

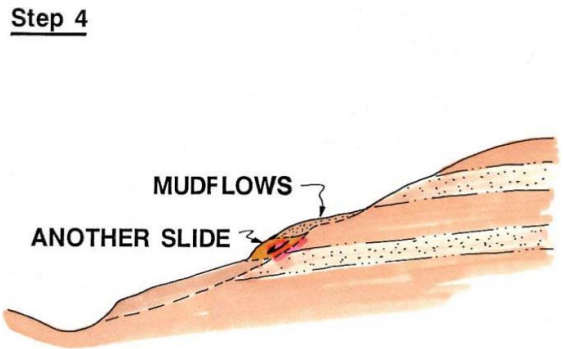

Figure 89. Minor sliding often occurs in response to over-steepening of the evacuation scar of the previous slope movement. Shallow earthflows may emanate from areas underlain by stratigraphically controlled layers of increased conductivity, such as sandstone, conglomerate, and even intensely fractured porcelaneous siltstone.

bank. Shallow groundwater flow patterns can be expected to emerge from the slope in this newly excavated area (Dietrich et al., 1987). Emergent seepage, which used to be drawn to the old valley bottom, can be re-directed, seeping out of the newly excavated zone. These "emergent seepage pressures" play a significant role in destabilizing over-steepened slopes during wet

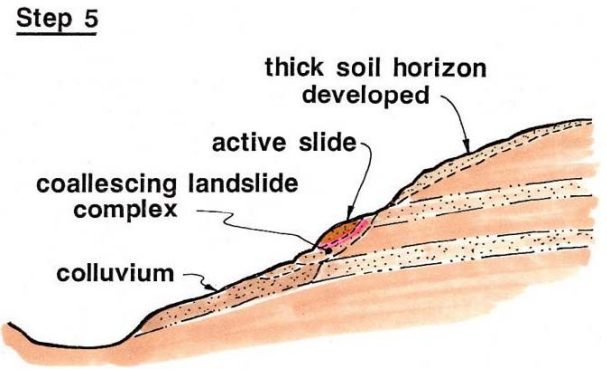

Figure 90. In a coalescing landslide complex, innumerable forms of mass wasting can occur simultaneously within a given watershed. These include debris and earthflows of crown and toe/areas, rotational slumping of headward-retreating scarps, rill erosion of unconsolidated colluvium and landslide debris, and structurally controlled translational sliding (block glides).

cycles that rise within ~10 ft (3.1 m) of the natural ground surface (Cedergren, 1989).

In their independent studies of shallow debris-flow initiation, Wilson and Dietrich (1987) and Johnson and Sitar (1989) were able to demonstrate that storm runoff infiltrates most easily into the weathered rock regolith bordering colluvial-filled bedrock ravines. The weathered rock horizon has been subjected to eons of downslope creep and dilation, creating a more permeable zone (Sharpe, 1938 a&b). Storm runoff can percolate into such a system and move significant distances in short periods of time. The weathered bedrock regolith is easily seen in Orinda as a discrete zone of oxidation, most commonly a reddish or yellow ocher color, while that of the unweathered bedrock is usually gray (Figure 91).

It is inevitable that, within such a system, preferentially directed percolation "conduits" will form, conducting water to a point of controlling base level, commonly nearby streams. If these streams begin a cycle of downcutting, then this near-surface seepage may begin to seep from the slope *above* the lowered position of the streambed. When seepage pressures become emergent, or springing from the slope, they can act to destabilize the soil covering or weathered bedrock regolith. According to Cedergren (1989), emergent seepage exerts 25 percent greater destabilizing force than an equal volume of seepage directed *downward*. Given such conditions, it is likely that a net buildup of hydrostatic pressure will accumulate if additional moisture percolates into the weathered regolith, particularly if the water is not allowed to seep out of the slope as interflow. In such instances, a slide may initiate as nature's mechanism of reducing the accumulated pore-water pressure of the transient near-surface groundwater table (Dietrich and Rogers, 1988). These situations are sketched in Figures 88 through 92.

Downloaded from http://pubs.geoscienceworld.org/aeg/eeg/article-pdf/31/1/i/6130855/i1558-9161-31-1-i.pdf
by AEG RBAC user

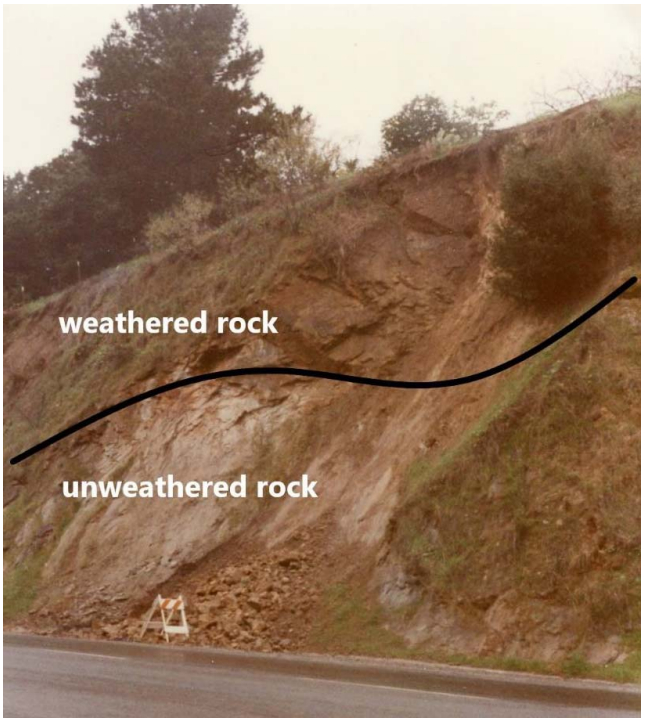

Figure 91. Wedge failure of a cut slope in the Neroly Sandstone along Pleasant Hill Road in January 1997. The demarcation between the oxidized (weathered) horizon and the less weathered zone is shown by the dark line (J. David Rogers).

The translation of a soil/rock mass as a semi-coherent landslide serves to remove lateral support from the remaining (unfailed) slope, immediately above the headscarp. In such situations, a series of retrogressive headscarps may begin to climb upslope (Figure 89). With each landslide, a new cap of material often buries what previously had been free-flowing ephemeral (intermittent) springs. Seepage from near-surface springs often seeps into newly displaced material, destabilizing such a mass. In this manner, landslides will tend to reoccur at the same locations.

As smaller slides move to new positions on the hillside, they will also be subjected to the effects of surface runoff–induced erosion that shaped the hillside (described above). Headscarp areas forming closed depressions are usually filled rather quickly (Figures 76–78), and runoff is often diverted into gapping tensile fissures, reducing effective stresses in the surrounding earth mass and promoting mass wasting (Rogers and Chung, 2016).

While locally over-steepened headscarp areas erode upslope, the toe areas of old slides are often mobilized as slow-moving earthflows, creeping downslope episodically when sufficient moisture is entrapped. In this manner, slide debris continues translating downslope at an imperceptible rate (referred to as "slope creep" by Sharpe, 1938a, 1938b). This slide debris often mixes with native soils, and is often misidentified as colluvium or gravity-borne "slope wash."

A hillslope profile that is out of equilibrium is presented schematically in Figure 90. The slope profile is irregular and hummocky. The slope may be mantled by deposits of varying genesis and age. A crenulated, or "bumpy" surface profile is a key indicator that the slope is out of equilibrium, although details of the underlying structure must also be considered (as shown in Figure 83).

MAP TECHNIQUES FOR LANDSLIDE DETECTION

Introduction

Once the interpreter is sufficiently knowledgeable about the bedrock geology, underlying structure, and landslide mechanisms commonly recognized in the area

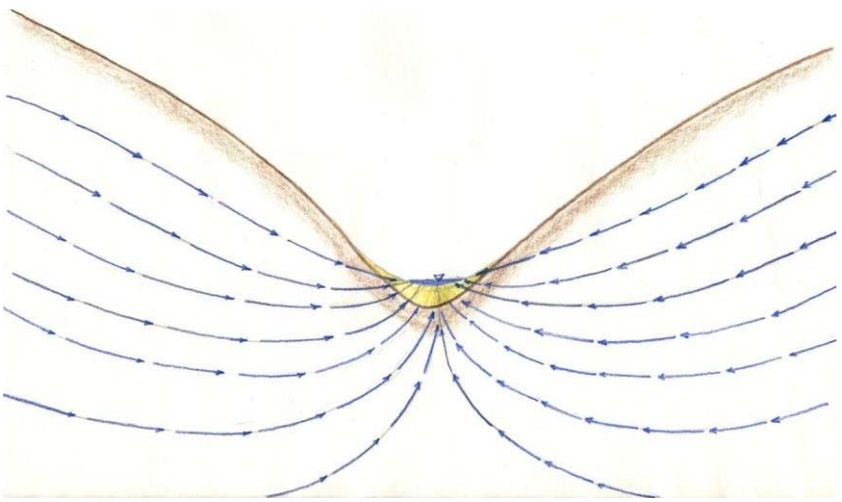

Figure 92. Preferential subterranean flow paths tend to develop in the slopes, becoming tributaries to natural watercourses over eons of time. Excavation and grading can change the surface topography but will not change the preexistence of these preferential flow paths. The youngest seepage is usually the shortest and most shallow flow path, while deeper flow paths are typically older, longer, and curvilinear, as shown above.

Downloaded from http://pubs.geoscienceworld.org/aeg/eeg/article-pdf/31/1/i/6130855/i1558-9161-31-1-i.pdf
by AEG RBAC user

of study, they can begin to isolate and evaluate topographic anomalies in stereo-pair aerial imagery or on topographic maps. Orthophoto-derived or light detection and ranging (LiDAR) bare Earth–derived topographic maps are the most suitable for landslide mapping. All landslides exhibit varying degrees of topographic expression, which can usually be detected by a seasoned engineering geologist with local experience.

A key factor in exploiting topographic information is the density and quality of the topographic data. Large-scale maps (>1:24,000 scale) or areas covered with heavy vegetation will tend to mask out details of smaller slides. In general, more precise mapping can be accomplished using larger map scales, and small slides may be delineated with some degree of precision (Ahmed and Rogers, 2014).

What follows are examples of landslide-prone topography that are typical of the Orinda area. With sufficient area experience, a map interpreter should be able to delineate many slide features that may not be readily apparent through the use of published landslide geometric ratios (Cruden, 1990, 1991a, 1991b; Cruden and Varnes, 1996; and Rogers and Chung, 2017). Examples of landslide length-to-depth and length-to-width ratios in Contra Costa County are presented in the section titled "Limiting Geometry of Active Landslides." Map-scale factors and masking effects of vegetation (Figure 77) and development will also be discussed, with examples from the Orinda area.

Colluvium, Debris Flows, and Alluvium

Topographic Expression of Colluvium

Colluvium is locally derived soil and rock debris that has been transported short distances downslope, principally by gravity-borne means. The principal processes by which colluvium is generated are normal surficial weathering processes, such as root action, displacement of root balls when dead trees topple over, animal and rodent burrows, gravity displacement by either of the above, and the erosive action of flowing water. The colluvial infilling cycle is presented in Figure 93.

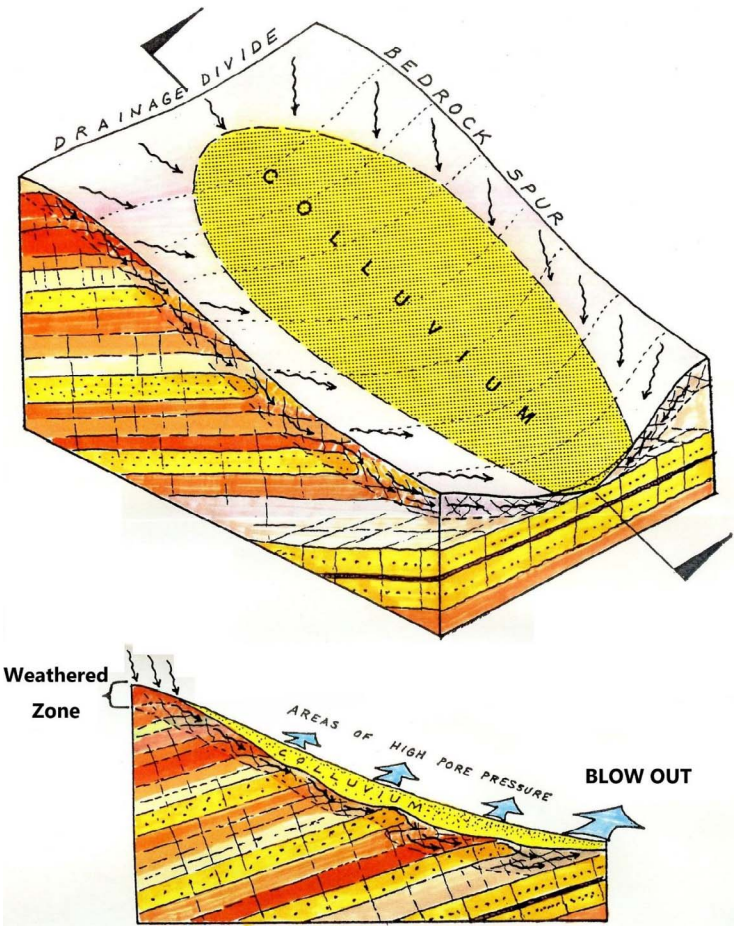

Figure 93a. Block diagram illustrating a typical spoon-shaped colluvial-filled bedrock ravine.

Figure 93b. Slope profile highlighting bedrock undulations that tend to promote flow convergence and elevate transient pore-water pressures. Slope failures tend to initiate in shallow spots that experience higher differential pore pressure (shown by the blue arrows).

Downloaded from http://pubs.geoscienceworld.org/aeg/eeg/article-pdf/31/1/i/6130855/i1558-9161-31-1-i.pdf
by AEG RBAC user

Colluvium production is favored upon intensely jointed, layered, fissile, or fractured strata like chert, as opposed to more massive and/or less intensely jointed strata like marble. Outcrops of intensely jointed material develop innumerable individual blocks of material that are easily displaced when exposed to surficial weathering processes (Figure 94).

Colluvial particles are typically angular and appear virtually identical to side-cast fill when encountered in excavations. Most colluvium collects in bedrock ravines, or "hollows," within zero- and first-order drainages (Kirkby, 1988). Colluvium is typically stratified in a manner semi-parallel to the hillslope, with a coarse basal layer forming a sort of natural subdrain (Figure 95).

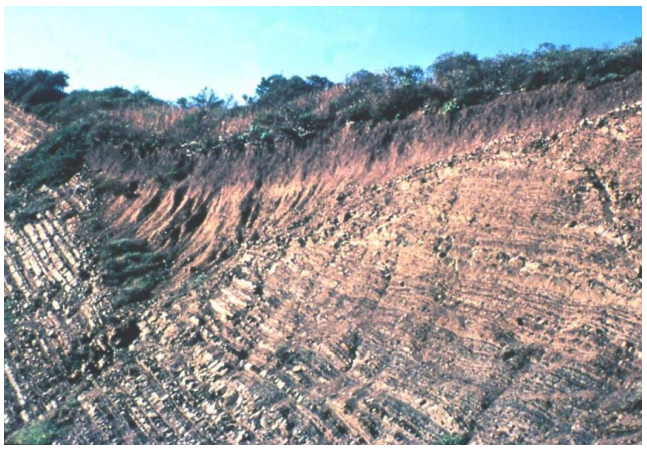

Figure 94. Colluvial-filled bedrock ravine exposed in a cut along CA State Route 1 in Monterey County. The bedrock is intensely fractured chert of the Monterey Formation. The colluvial cover varies in thickness from 2 to 17 ft (0.6 to 5.2 m) (Donald H. Gray).

Most "hollows" form naturally, as spoon-shaped depressions. Humphrey (1982) demonstrated that the buildup of entrapped moisture within a spoon-shaped bedrock depression can easily cause slope instability (Figure 96). Utilizing effective stress theory, Rogers/Pacific, Inc. (1984) was able to demonstrate that 2 ft (0.6 m) of hydrostatic head could "lift" up to 5 ft (1.5 m) of saturated unconsolidated colluvium.

Wilson and Dietrich (1987) presented field data to suggest that colluvial-filled ravines are recharged through the weathered bedrock horizon, a mechanism sketched in Figures 92 and 93 and Figures 96 and 97. Others who monitored continuously recording piezometers installed adjacent to colluvial pockets reached the same conclusions in the late 1980s (Rogers, 1987b; Johnson and Sitar, 1989).

The geometry of (colluvial-filled) spoon-shaped depressions is usually structurally controlled (Figures 98 and 99), with massive or resistant strata bounding the lower limits of the bedrock depression (Figure 95). Colluvial-filled ravines are often repeated within a zero-order watershed (Reneau et al., 1984; Dengler et al., 1987; and Shlemon et al., 1987).

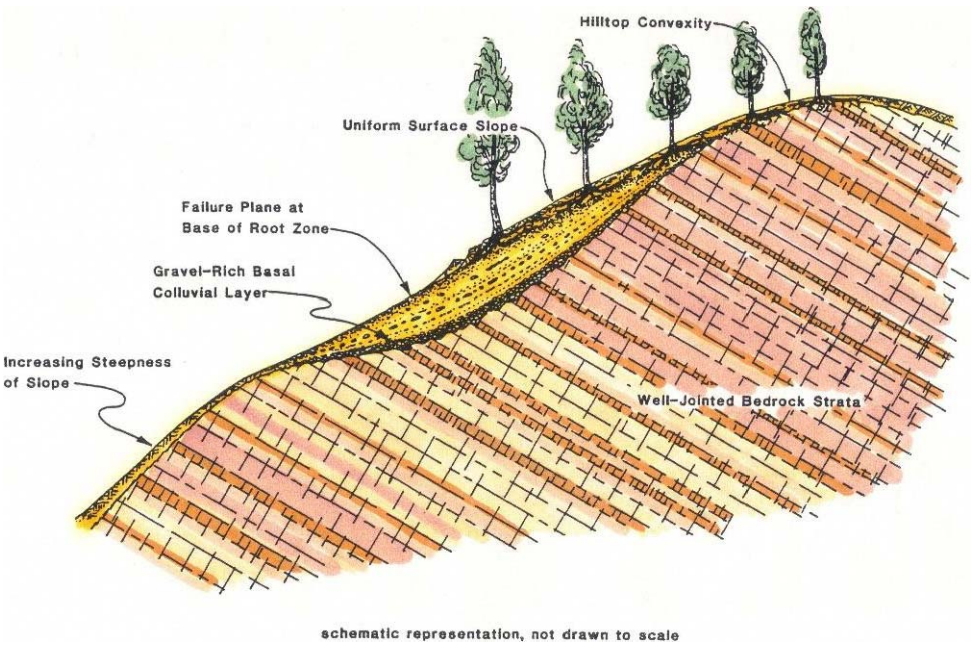

Figure 95. Colluvial-filled ravines in coastal California typically exhibit a coarse cobble basal layer, rough stratification within the main mass, and an oxidized root zone that may include an argillic horizon 1.5 to 3 ft (0.5 to 0.9 m) thick mantling the ground surface. Depending on its age, this surficial layer is often more resistant to erosion because of its clay content (a weathering product).

Downloaded from http://pubs.geoscienceworld.org/aeg/eeg/article-pdf/31/1/i/6130855/i1558-9161-31-1-i.pdf
by AEG RBAC user

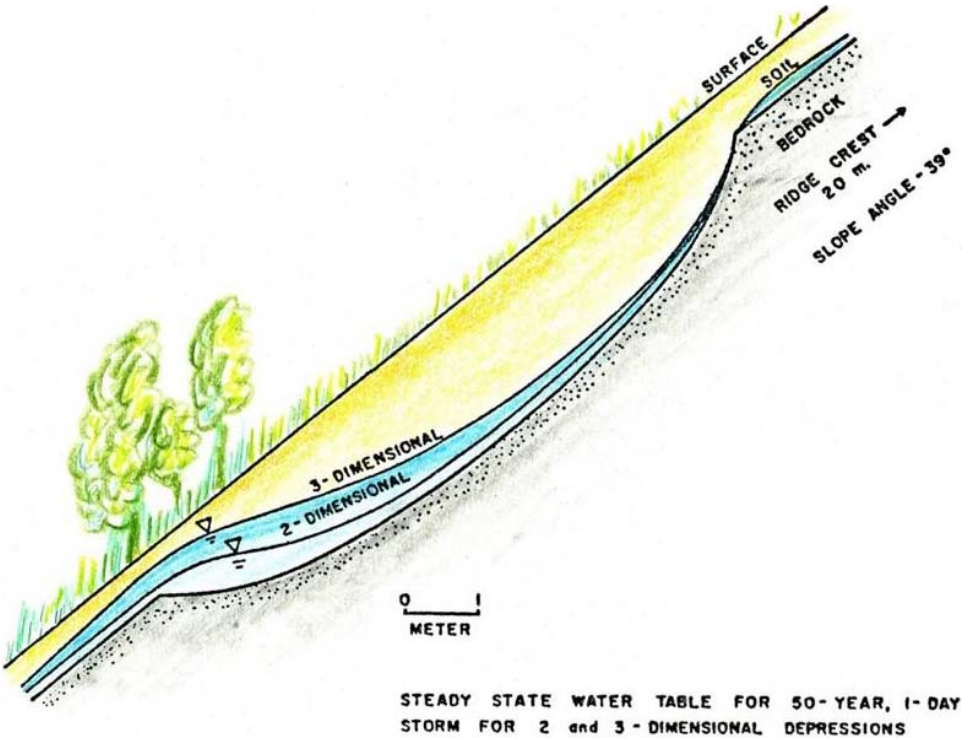

Figure 96. Effects of a spoon-shaped colluvial-filled bedrock depression on development of transient pore-water pressures that trigger debris flows. A two-dimensional depression is bereft of lateral convergence, while a three-dimensional depression produces a more realistic appraisal (Humphrey, 1982).

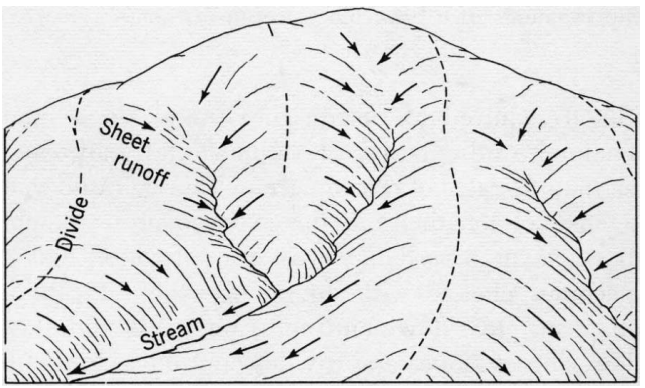

Figure 97. Three-dimensional evaluations of runoff are essential where overland sheet flow from headwater areas of zero-, first-, and second-order streams accumulate within each sub-watershed (Strahler, 1965).

Key Topographic Indicators of Colluvial-Filled Ravines

As presented schematically in Figures 93 and 94, colluvium is collected within ravines during aggradational periods and removed from these same ravines during erosional episodes (Reneau, 1988). Erosion cycles may suddenly occur without any systematic warning (Lehre, 1982). On some occasions, the colluvial-filled depression may be of immense scale, leading to catastrophic results (Shlemon et al., 1987). Reneau and Dietrich (1987) discovered that colluvium in the San Francisco Bay area tends to occupy bedrock depressions for periods of between 1,000 and 7,000 years. Erosive cycles are likely triggered by climatological changes that promote variances in rainfall, vegetation, and runoff (Rodine, 1974; Lehre, 1982). Reneau (1988) suggested that local variations in rainfall intensity can serve to spawn sudden and often catastrophic erosion of unconsolidated colluvium from ravines that may have withstood climatic effects for thousands of years.

There are few topographic indicators of dormant colluvial-filled bedrock ravines. The presence of ravines must be field checked, usually by inspection of road cuts. An example of successive ravines stacked one above another is shown in Figure 100. Figure 101 presents examples of colluvial-filled bedrock depressions in differing stages of erosion. Occasionally, sharp topographic breaks will reveal recent erosion of colluvium, as presented in case 1 of Figure 101. Case 2 represents a dormant ravine infilled with colluvium. Such deposits may remain undisturbed for several thousand years, or they might experience partial excavations during intense precipitation events, often infilling the scarred areas. Case 3 presents a ravine where the erosive cycle is essentially completed, revealing the topographic expression of the ravine.

Downloaded from http://pubs.geoscienceworld.org/aeg/eeg/article-pdf/31/1/i/6130855/i1558-9161-31-1-i.pdf
by AEG RBAC user

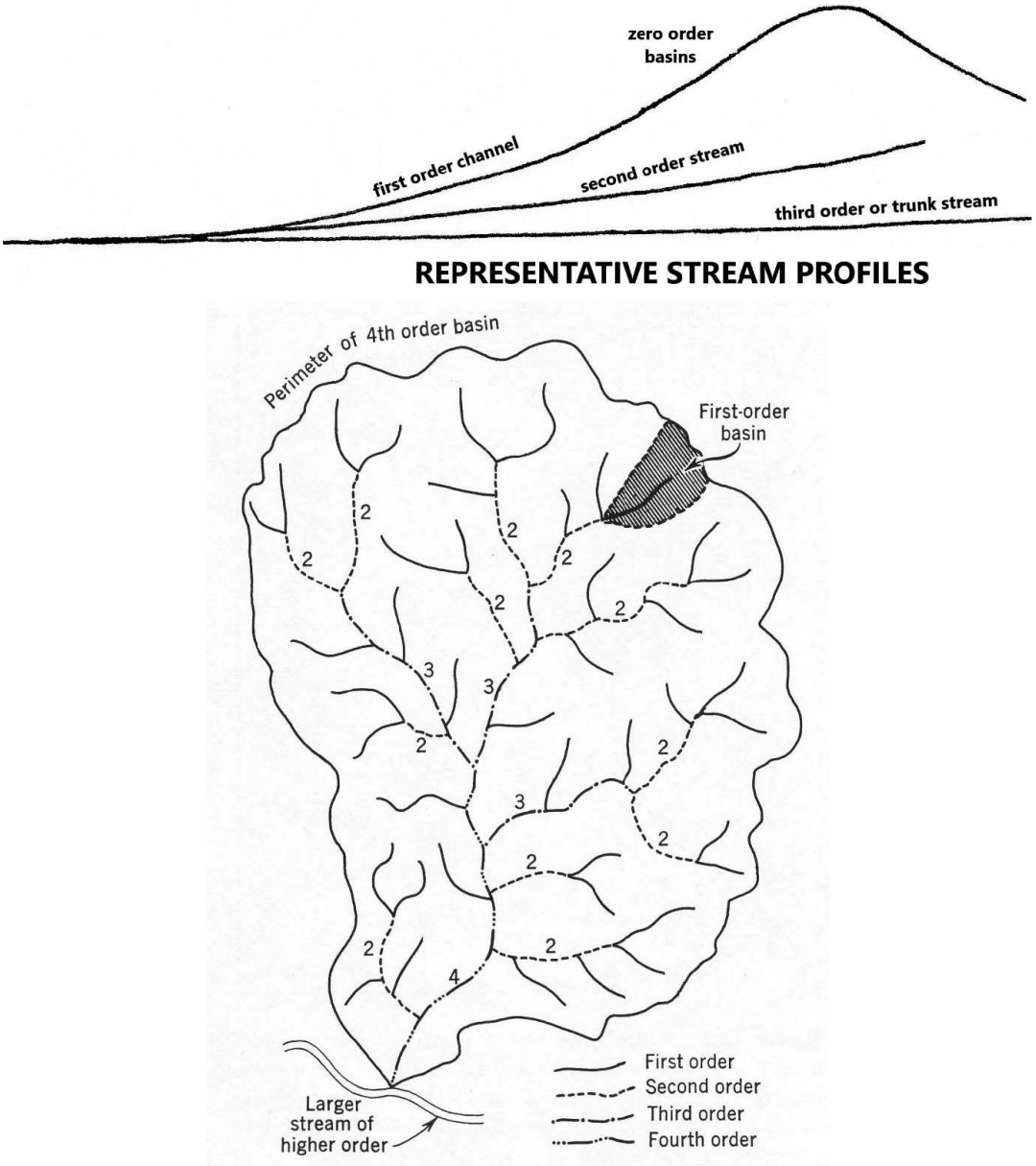

Figure 98. Orders of magnitude are routinely assigned to channel segments comprising a normal dendritic pattern, as shown in the lower figure from Strahler (1952). Each increasing stream order exhibits a flatter profile, as sketched in "representative stream profiles."

Key Topographic Indicators of Debris Flows

The key topographic indicator of past debris-flow activity is opposing contours within unchannelized (zero-order) basins, usually situated upon steep side slopes. Horton (1945) and Strahler (1952) presented evidence that natural fluvial systems are logically organized and exhibit considerable regularity. They pioneered the numbering of tributary watersheds, with the smallest watercourses denoted as "first-order" channels, corresponding to first-order watersheds or basins, which are assumed to occupy the highest position within a given sub-basin (Figures 98 and 99).

Thirty years later, Warntz (1975) defined "zero-order basins" as those bereft of a recognizable channel (exhibiting noticeable troughs, channel beds, or opposing banks), normally comprising the highest watershed catchment. When runoff from zero-order basins coalesces to increase streampower, at some point, the concentration of flow will begin excavating a trough, which would be the demarcation of a first-order channel. An example of successive ravines stacked one above another is shown in Figure 100.

Two examples of simple debris-flow complexes are shown in Figure 102. Whenever inward-shaped contours

Downloaded from http://pubs.geoscienceworld.org/aeg/eeg/article-pdf/31/1/i/6130855/i1558-9161-31-1-i.pdf
by AEG RBAC user

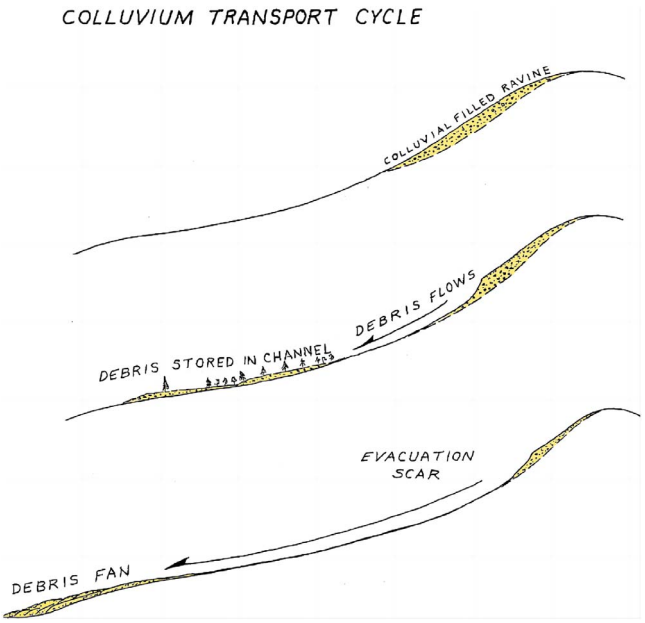

Figure 99. Three stages of colluvial-filled bedrock ravines: The upper profile is colluvial storage in quasi-equilibrium. The middle profile illustrates an erosion cycle, and the lower profile is typical of the close of an erosion cycle, as the ravine begins filling with more colluvium. It is generally believed that these cycles are triggered by changes in prevailing climate, vegetation, and/or base level.

oppose outward-shaped contours along the same fall line, a repeating series of flow slides is often indicated. Each debris-flow lobe truncates the next oldest flow, creating a series of overlapping debris packages that can be difficult to sort out, depending on the bounding features at the time of the flows (trees, boulders, other debris lobes, landslide debris, trash, etc.). On some occasions, parallel first-order channels will form below the head-scarp evacuation scar.

In some cases, flow debris does not accumulate in coalescing fans but is temporarily stored within a ravine, some distance downslope of its source (Rodine, 1974). Such a case is sketched in Figure 103. In this example, the natural slope is sufficiently long and steep so as to prevent the buildup of a debris fan.

In some cases, rejuvenation of the trunk-stream network (at the base of the slope) will excavate debris accumulation (such as cones or lobes) near the toe of the slope. In other cases, debris will simply be held within confined bedrock channels until such a time when sufficient tractive effort is expended to flush the debris out of its confines (Rodine, 1974; Reneau, 1988).

Some common forms of debris-flow lobes, fans, cones, and channel storage are sketched in Figure 104. In most cases, colluvium tends to accumulate in zero-order basins, close to the watershed divide, where there is less concentrated overland flow (Figure 105b). As portions of this colluvium are mobilized, it is transported as debris flows or torrents, usually excavating older flow material stored in the channel confines or within its parent basin (Figure 105b).

Debris can be stored within flow lobes, caught in the bedrock channels for dozens of years or centuries (Rodine, 1974; Reneau, 1988). When low-frequency storms unleash intense precipitation over an extended period of time, excessive runoff may trigger mobilization of the debris stored within the bedrock channel during higher-frequency flow events (Rodine, 1974). When this happens, a large amount of colluvial debris may be actively mobilized, beginning with an initial detachment within the zero-order basin and building like a snowball as this debris torrent scours the steep, bedrock channel. This snowball accumulation was described in the various accounts of the deadly 1976 Big Thompson Flood in Colorado (Gruntfest, 1987, 1997).

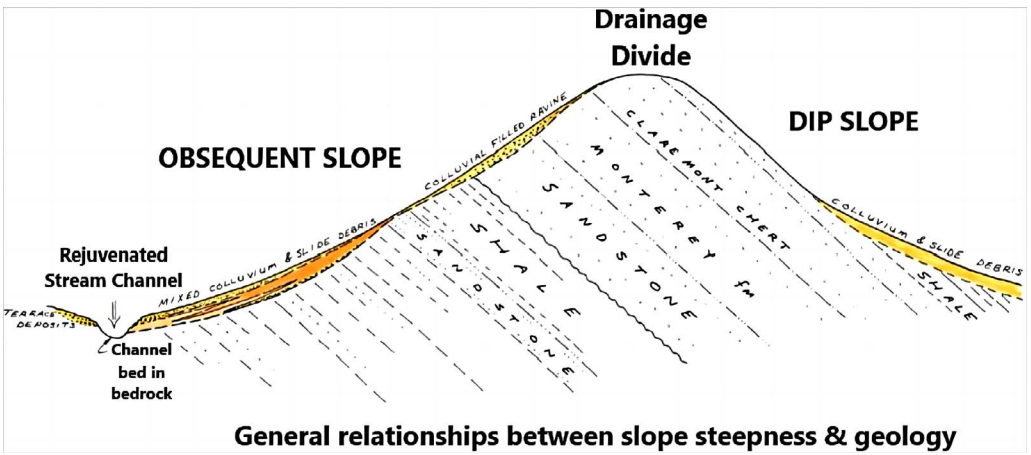

Figure 100. Geologic section through Grizzly Peak Ridge above the Caldecott Tunnels. Note how the ridge is mantled with deep accumulations of gravel colluvium derived from the Claremont chert and the Sobrante sandstone of the Monterey Group.

Downloaded from http://pubs.geoscienceworld.org/aeg/eeg/article-pdf/31/1/i/6130855/i1558-9161-31-1-i.pdf
by AEG RBAC user

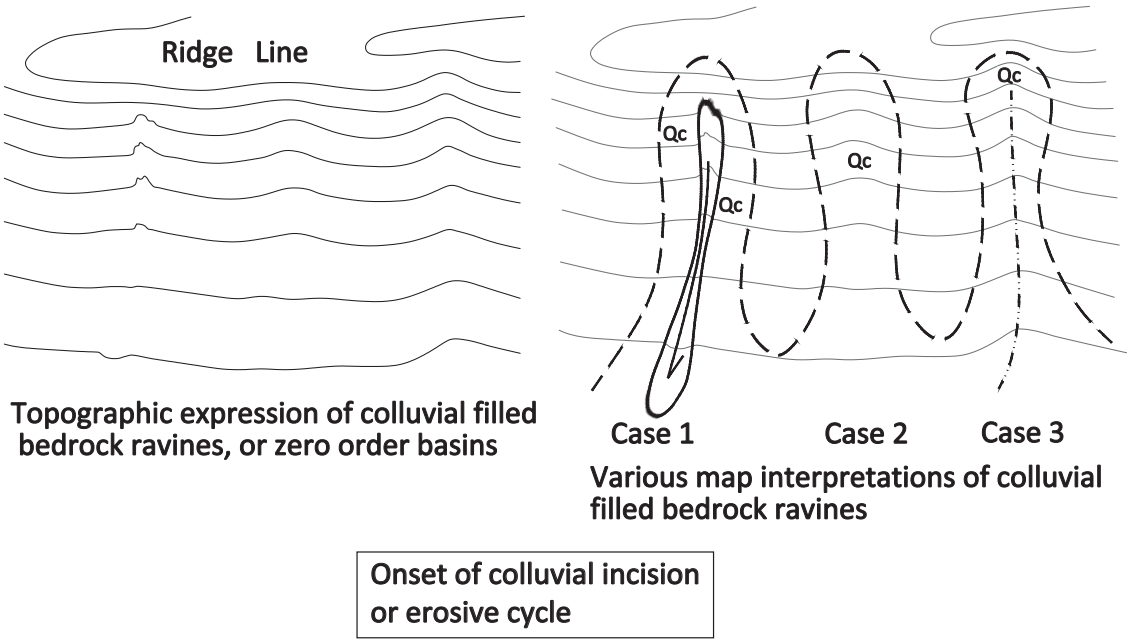

Figure 101a. Topographic patterns at top-left are typical of colluvial-filled bedrock ravines in various stages of activity.

Figure 101b. The three adjacent ravines at top-right represent interpretive mapping of these same features, after reviewing stereo-pair aerial photos. Case 1 was a recently active debris flow, while case 3 had emptied itself of most of its stored colluvium, leaving a barely discernible first-order channel.

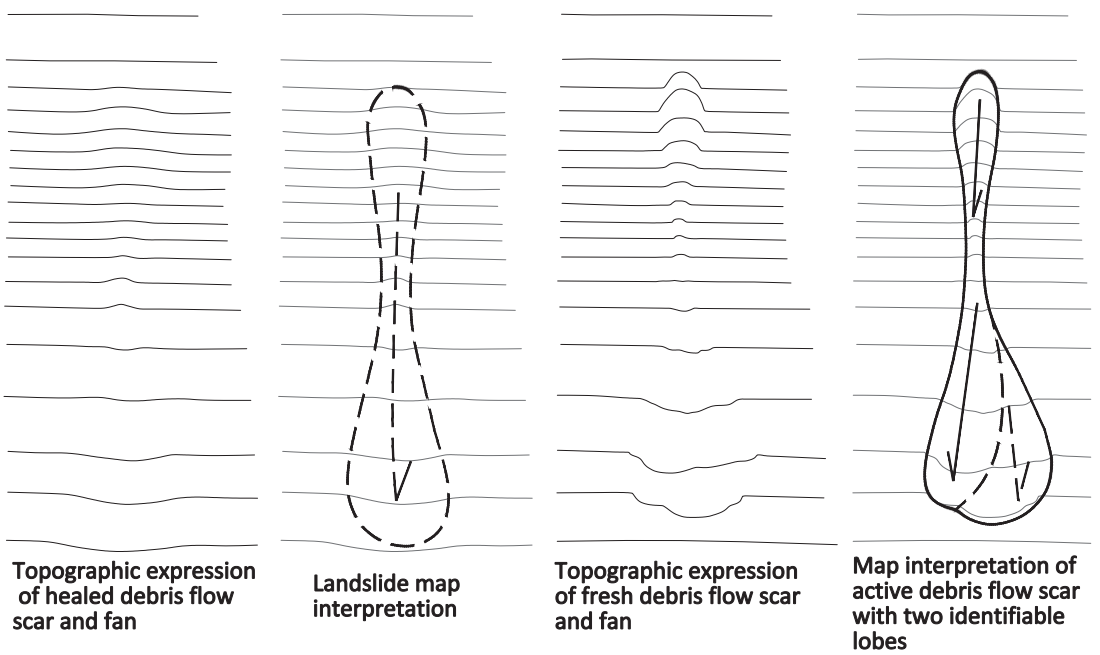

Figure 102. Examples of simple debris-flow complexes with their respective map interpretations.

Reneau (1988) described several such occurrences on the northeast side of San Pedro Ridge in San Rafael during the January 3–5, 1982, storms. Some of these flows began with as little as 380 cubic yards (290 m^3) of material, which later swelled to as much as 12,000 cubic yards (9,168 m^3) by the time the material reached the bottom of the first-order ravines. In this manner, the mobilized debris will tend to be deposited in the alluvial transition where the hydraulic grade dips below 1.5 percent (sketched in Figure 105b).

Downloaded from http://pubs.geoscienceworld.org/aeg/eeg/article-pdf/31/1/i/6130855/i1558-9161-31-1-i.pdf
by AEG RBAC user

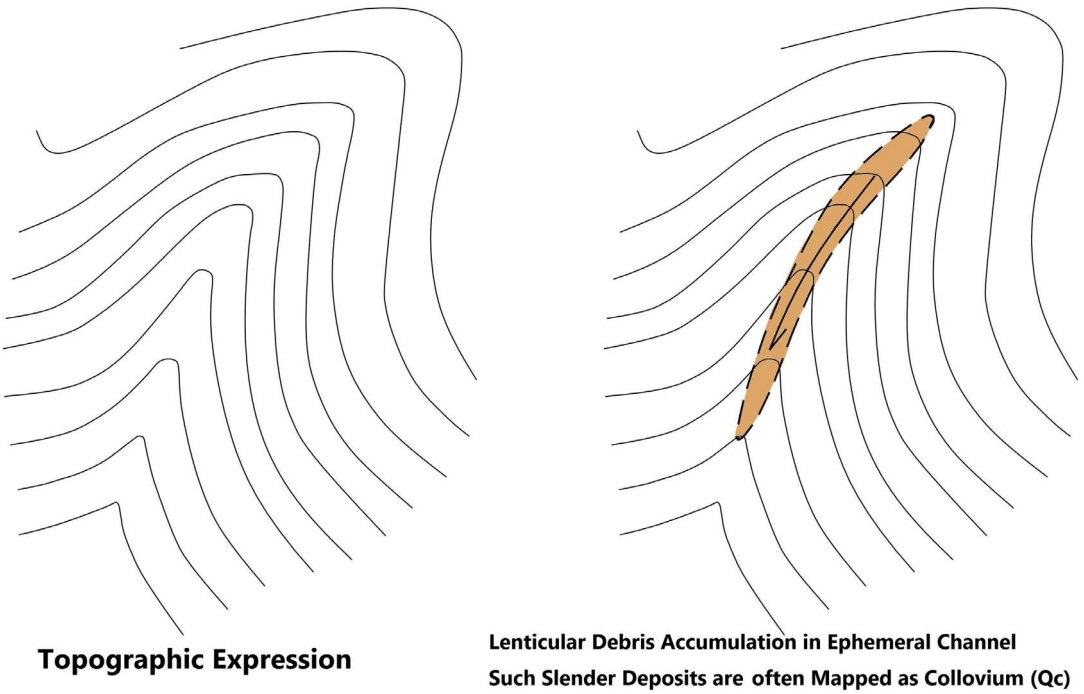

Figure 103. The depth of channel fill within a confined ravine or canyon influences the curvature and sharpness of succeeding contours defining a watercourse. In the case shown here, the contours with sharp V's depicted on the left are bereft of much channel fill. The contours with rounded V's upstream of the sharp contour are typical channel fill from past flow events, which has been stored, as shown in the interpretation at right.

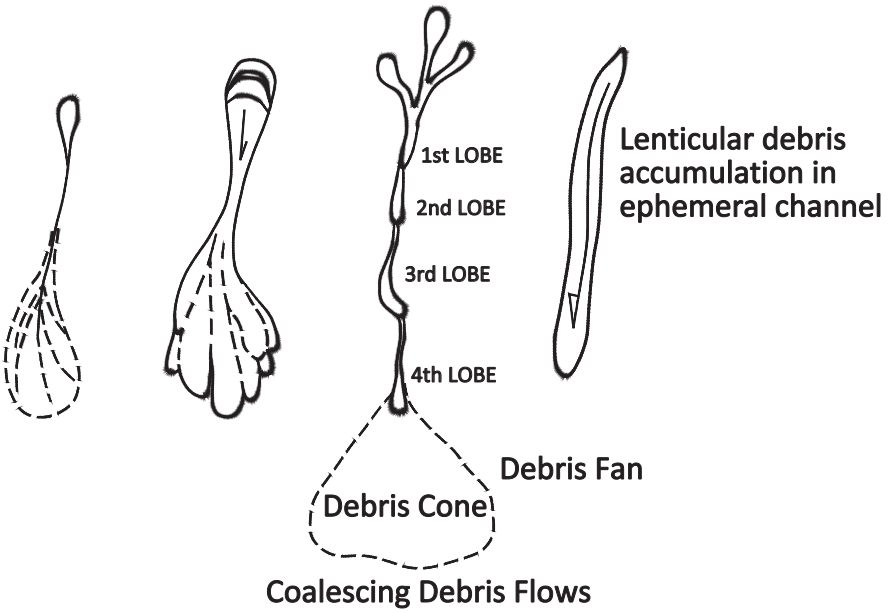

Figure 104. Common morphologies of debris-flow lobes, fans, debris cones, and channel storage of debris. Accumulated debris stored in confined bedrock channels can be swept out of the system in an instant during extreme flow events.

Colluvium and Debris-Flow Fans

Colluvium is commonly commingled with debris-flow fans and immature alluvium (mature alluvium is rounded, while colluvium contains subangular particles). In terms of mechanical consistency, these materials appear to be similar, causing some degree of subjectivity when delineating their respective boundaries. In reconnaissance-level mapping accomplished without field inspection, the demarcation between any of these

Downloaded from http://pubs.geoscienceworld.org/aeg/eeg/article-pdf/31/1/i/6130855/i1558-9161-31-1-i.pdf
by AEG RBAC user

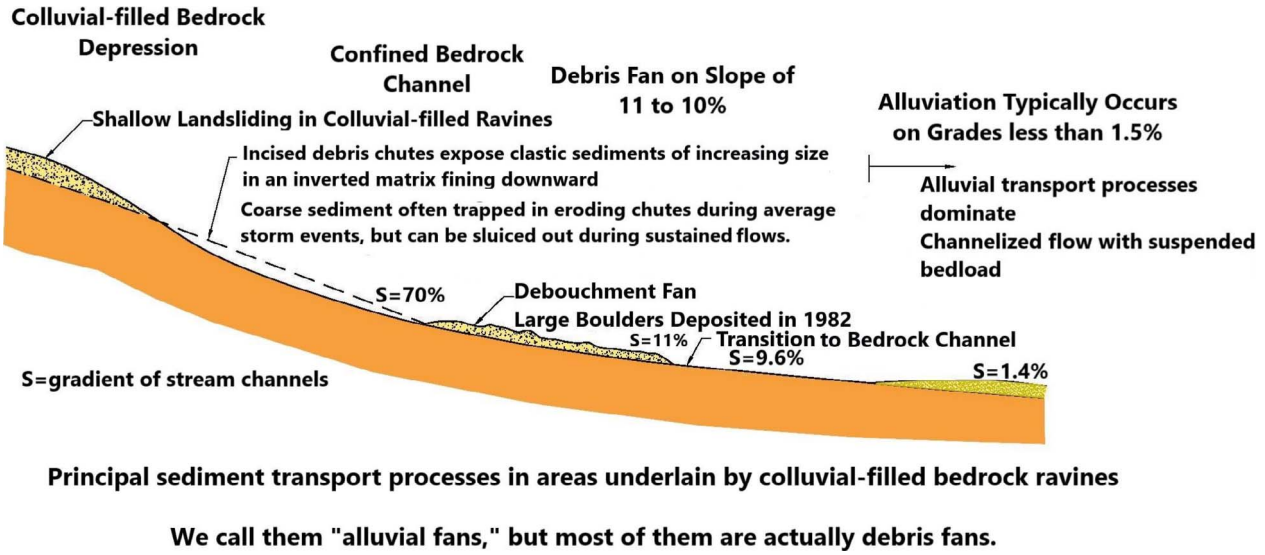

Figure 105a. Thalweg profile along a first-order channel that spawned deadly debris flows during the storm of January 3–5, 1982, in San Rafael, CA. This upper section contains physical descriptions of the debris sources and the materials deposited downstream (Rogers/Pacific, Inc., 1985).

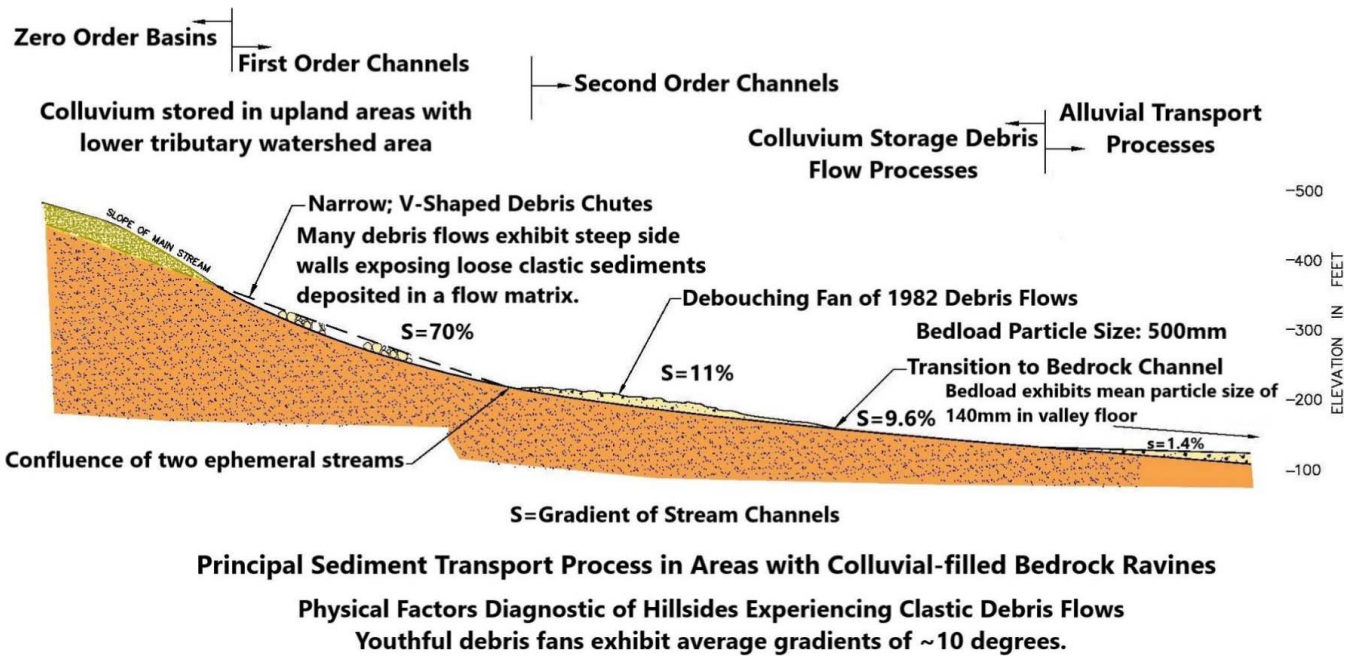

Figure 105b. Description of downcutting that occurred in the first-order channels during the January 3–5, 1982, precipitation event and the physical characteristics of the new debris fan (Rogers/Pacific, Inc., 1985).

units is largely a matter of experience. Local experience with similar deposits will generally influence the interpreter's choices. As shown in Figure 105b, a slope-based demarcation (e.g., $s = 1.5$ percent) would appear to be appropriate for delineating alluvium from debris cones, debris fans, and colluvium.

In the coastal hills of California, colluvium is stored high on the slopes, close to the watershed divides (Montgomery and Dietrich, 1988). When these deposits are unchannelized, they are loosely referred to as "zero-order basins" (as opposed to "first-order streams," which refer to the highest definable channel within a watershed). In the East Bay Hills, zero-order basins generally occupy the upper slopes (Warntz, 1975), where ridge-top convexity allows slopes inclined between 10 and 35 degrees. Occasionally, portions of the stored colluvium high on the slope or buried in bedrock ravines mobilize into debris flows and move rapidly downslope. In most instances,

Downloaded from http://pubs.geoscienceworld.org/aeg/eeg/article-pdf/31/1/i/6130855/i1558-9161-31-1-i.pdf
by AEG RBAC user

this debris train expends energy overcoming frictional and organic obstacles within the channel, such as boulders, tree trunks, root balls, and dead logs. In these situations, colluvial debris can be caught and temporarily stored in narrow V-shaped channels or debris chutes.

In the field example presented in Figure 105b, the gradients of this reach (a first-order channel) hover between 0.20 and 0.70 (20 percent to 70 percent slope). During large storm events, sufficient debris or runoff may sluice the stored debris from the V-shaped channel/chute. When this occurs, a large volume of debris can be sluiced and carried downstream, where it is commonly deposited on debris fans, which are often mistaken for "alluvial fans." In the East Bay Hills, the slope of these debris fans ranges between 1.5 percent and 20 percent slope. Alluvium generally infills slope gradients less than 1.5 percent.

Debris fans appear topographically similar to alluvial fans. Subsurface exploration of debris fans reveals that the sediments were deposited by debris flows, torrents, avalanches, and earthflows, rather than by channelized flow. In fact, on fans exhibiting slopes greater than 2 percent to 5 percent, debris flow–related processes are likely responsible for the deposits (Rogers/Pacific, Inc., 1985).

The topography of a typical debris fan is presented in Figure 106. In this example, Holocene-age debris lobes can be traced emanating from youthful ravines carved from a steep bedrock escarpment. Each of these fans is composed of countless flow lobes juxtaposed one over another. Towards the lower third of these fans, the debris has been slowly reworked by occasional sheet flow and redeposited as hydraulically sorted sediment of fine texture, lower on the same fan. Eventually, finer-grained alluvium infills anastomosing branch channels carved upon older debris channels, out to the distal margins of the fan. As a consequence, debris is intermingled with colluvium (decreasing down gradient) and alluvium (increasing down gradient).

The approximate limits of discrete-source debris fans emanating from the principal ravines are shown with a single arrow, indicative of an earthflow/debris flow. However, the reader should appreciate that this material was NOT likely deposited as a single semi-coherent mass, but as an innumerable series of small flows building upon one another.

Figure 107 presents an example taken from mapping the Amber Valley Drive–Singingwood Lane neighborhood of northeast Orinda. This area is typified by structurally controlled ridges, underlain by the Neroly Sandstone member of the San Pablo Group. On large-scale maps, like that presented here, many individual features can be delineated. In this example, colluvial-filled zero-order swales are indicated on the upper slopes as "Qc." Some of these appear to have spawned debris fans or debris cones, commingling with alluvium as the slope gradient decreases. Note the larger expanse of alluvial fans, labeled "Qal." This example is typical of the method of mapping employed in the Orinda study of 1993–94.

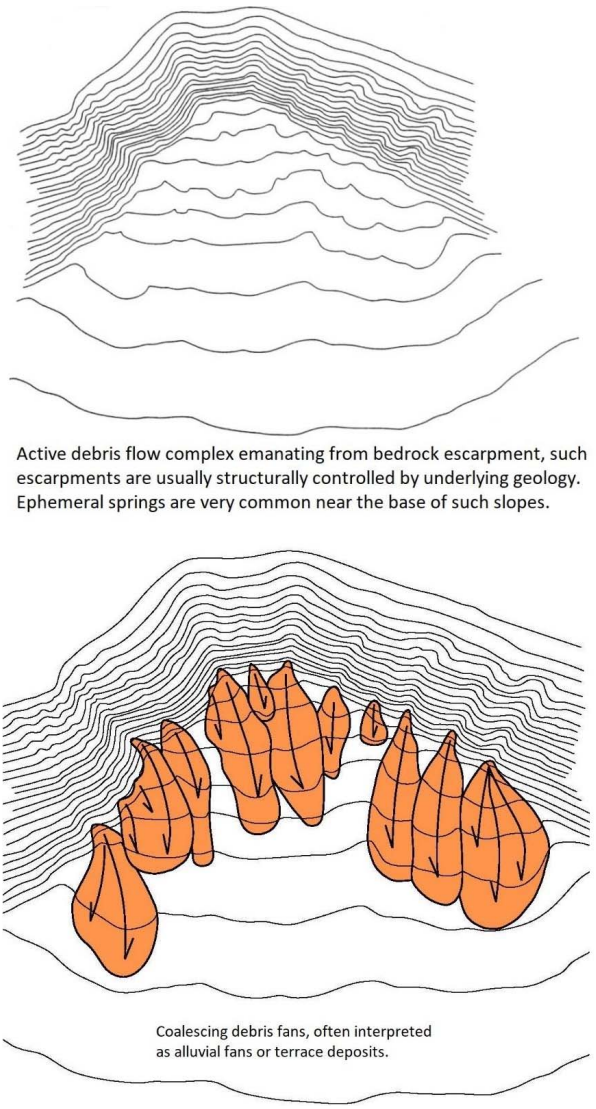

Figure 106. Upper image presents topography of an erosional escarpment in bedrock with an active debris fan covered by fanglomerate and rocky debris trains. The lower pane shows active coalescing debris fans highlighted in brown. The gradients of these youthful lobes were between 10 and 13 degrees, which are typical of clastic materials that drain quickly.

Earthflows

Mechanics of Earthflows

The dominant style of mass wasting within the Orinda Hills is shallow earthflows, which are colloquially referred to as "mudslides," "mud flows," or "earth

Downloaded from http://pubs.geoscienceworld.org/aeg/eeg/article-pdf/31/1/i/6130855/i1558-9161-31-1-i.pdf
by AEG RBAC user

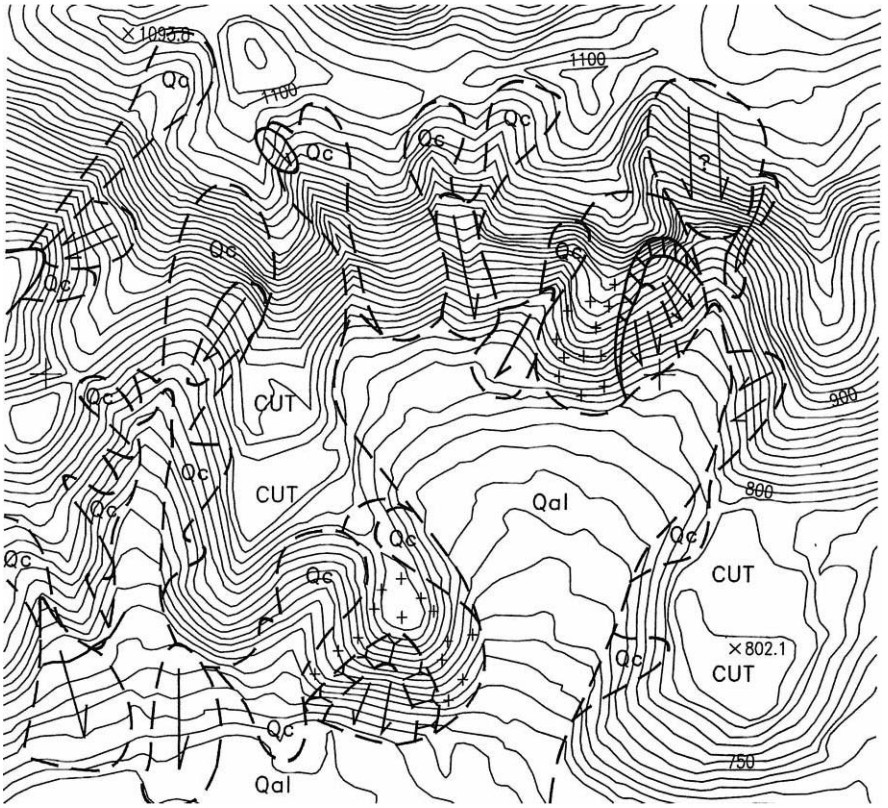

Figure 107. Coincident delineation of colluvial-filled ravines mantling upland slopes and large alluvial fans in Orinda that have developed on a much lower gradient. Note how artificial cuts for house pads are also identified because they truncate the natural slope morphology.

slides." In this book, we have chosen to retain the generally accepted terminology posed by Varnes (1958) of the USGS and expanded by Varnes (1978) and Cruden and Varnes (1996). Varnes introduced the term "earthflow" to describe soil-like material that exhibits behavior akin to the rheological model of a low-viscosity fluid (Bruckl and Scheidegger, 1973; Selby, 1993).

Earthflows tend to concentrate in natural swales, as shown in Figure 66 and presented conceptually in Figure 108. Slump-flows and earthflows can also exist without any outward topographic pattern (Figure 69). Slump-flows commonly begin as small rotational slumps, failing along log-spiral–shaped rupture surfaces (Rendulic, 1936a&b; Terzaghi, 1950). When these materials begin to translate downslope, moisture is trapped within the cohesive debris, causing excess pore-water pressures, which significantly degrade interparticle friction to levels approximating a viscous fluid (Hutchinson and Bhandari, 1971).

As the material runs further downslope, the accompanying particle disintegration allows for rapid drainage of trapped pore water, and the mass becomes increasingly viscous as it drains. Eventually, sufficient drainage occurs so that the mass regains interparticle friction/cohesion and comes to a rest (Campbell, 1966).

Radbruch and Weiler (1963) were the first to recognize that earthflows in the East Bay Hills formed in "coalescing complexes," composed of multiple flow lobes. These complexes tend to reactivate only one or two individual lobes about once in every 8 to 15 years on average, dating back to the late 1920s (the oldest aerial imagery reviewed for this study dated back to February 1928).

Topographic Expression of Earthflows

Shallow earthflows like those profiled in Figure 108 are the easiest of the various types of slides to identify within the East Bay Hills of Alameda and Contra Costa Counties (Radbruch and Weiler, 1963; Waltz, 1967; and Keefer and Johnson, 1983). As with debris flows, divergent contours within a natural swale or hillslope are one of the best indicators of earthflows (Figure 109). Earthflows and debris flows tend to spawn broad, circular-shaped headscarp evacuation areas, which neck down at the deflation/inflation zone transition (Varnes, 1978). The character of the depositional lobe, or toe, is dependent on several factors: (1) the cohesion of the parent material; (2) the fluidity/motion/inertia of the failed mass; (3) the slope gradient/channel constriction; and

Downloaded from http://pubs.geoscienceworld.org/aeg/eeg/article-pdf/31/1/i/6130855/i1558-9161-31-1-i.pdf
by AEG RBAC user

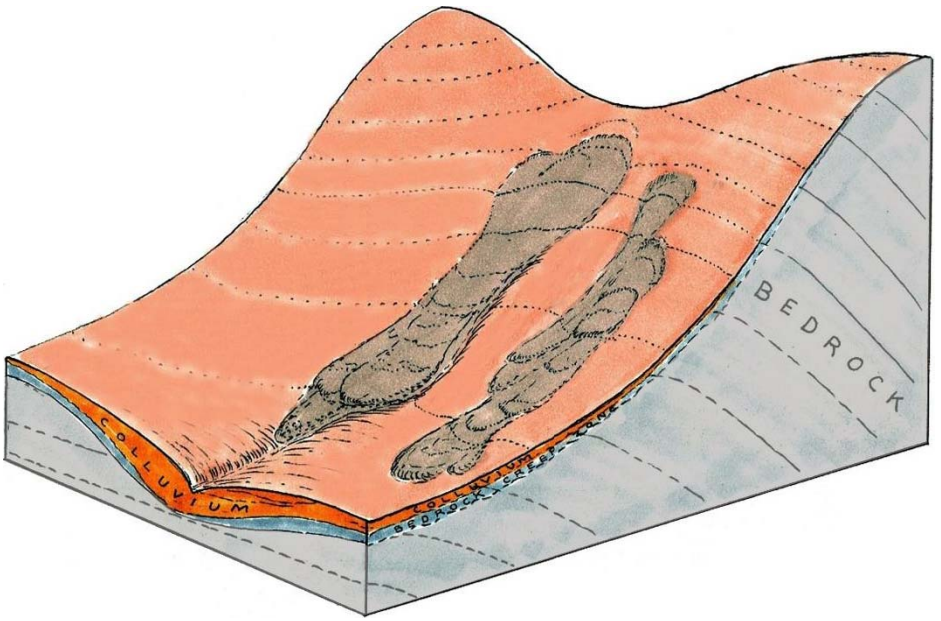

Figure 108. Earthflows are largest when centered on ephemeral watercourses within small watersheds that tend to concentrate surface and subsurface flowage along a path that is often coincident with the thickest accumulations of colluvium and older slide debris.

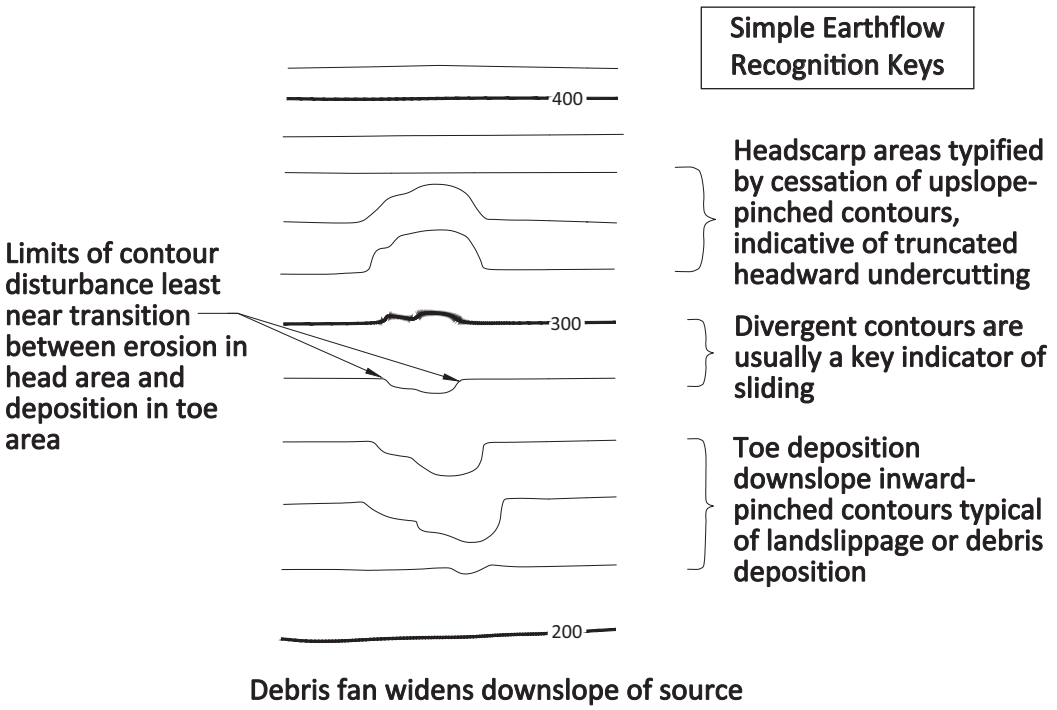

Figure 109. Recognition keys for shallow earthflows include arcuate headscarp evacuation scars, divergent contours, and crenulated contours from multiple debris lobes along the same fall line.

(4) the degree of dissection effected by subsequent weathering processes.

Figure 110a–d presents a series of topographic models of the same coalescing earthflow in various stages of development. In general terms, the topographic expression is often pretty clear for the first 8 to 15 years (Figure 110a). Between 15 and 50 years, the slide can still be clearly delineated, provided that the contour lines are of sufficient density (Figure 100b). Beyond 50 to 100 years, the topographic expression becomes increasingly

Downloaded from http://pubs.geoscienceworld.org/aeg/eeg/article-pdf/31/1/i/6130855/i1558-9161-31-1-i.pdf
by AEG RBAC user

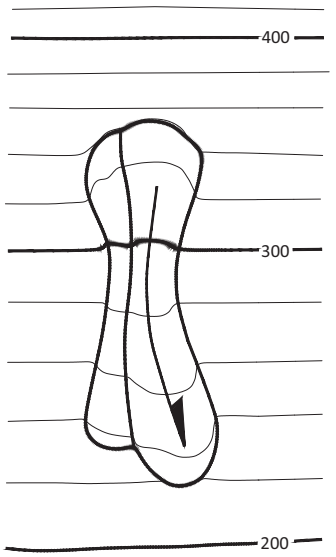

Landslide Map Interpretation

Figure 110a. Interpretation of a recently active earthflow with two discernible lobes, with the younger lobe truncating the older lobe.

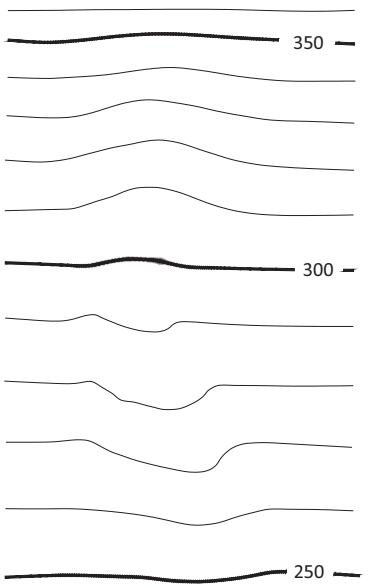

Combination earth/debris flow 10 to 100 years old

Figure 110b. Combination earth- and debris-flow feature between 10 and 50 years old.

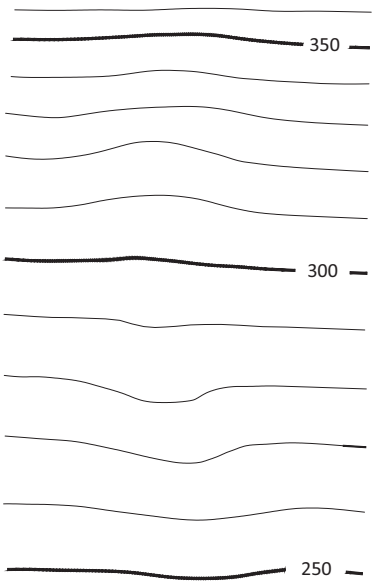

Combination earth/debris flow 100 to 500 years old

Figure 110c. Combination earth- and debris-flow feature between 50 and 150 years old.

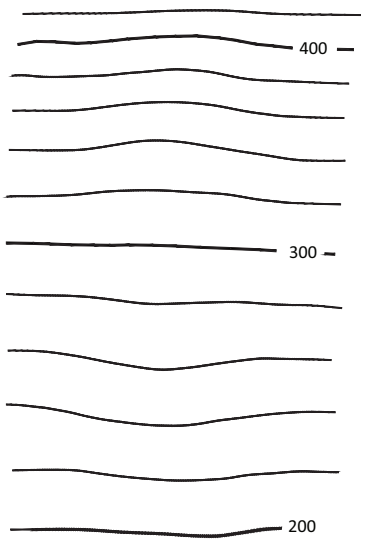

Combination earth/debris flow more than 500 years old

Figure 110d. Combination earth- and debris-flow feature more than 150 to 500 years old.

moderated as the headscarp evacuation scar infills with colluvium and brushy vegetation (Figure 110c). Beyond 150 years, the topography may become so subdued that only the largest slide masses might be noticeable (Figure 110d).

In instances where greater tributary watershed exists upslope of the earthflow, the debris will be more noticeably dissected, as presented in Figure 111. In this instance, an older slide will have more crenulated flow-lobe contours, providing excellent textural identification,

Downloaded from http://pubs.geoscienceworld.org/aeg/eeg/article-pdf/31/1/i/6130855/i1558-9161-31-1-i.pdf
by AEG RBAC user

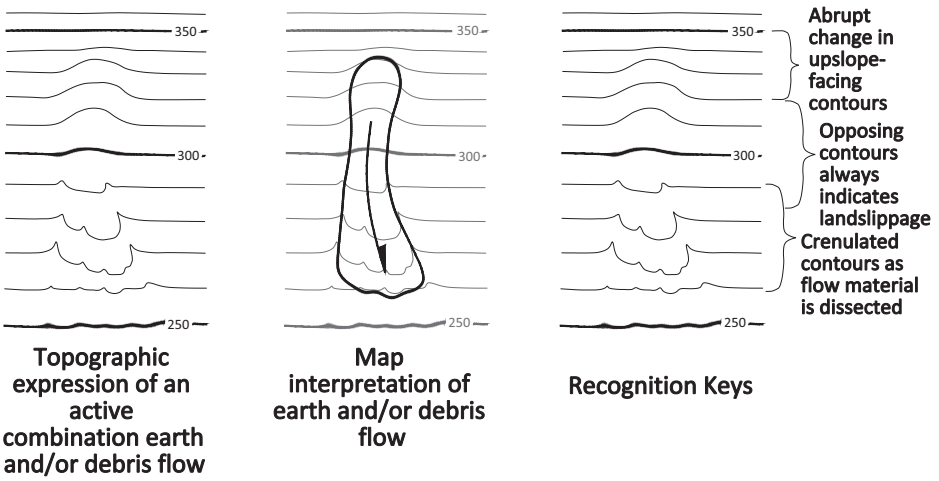

Figure 111. Older flow slides subjected to surficial runoff tend to develop rill erosion, which often results in more crenulated contours of the lower-density flow lobes, as shown in this example.

provided the topography is sufficiently detailed. Figures 106 through 108 present the most common form of earthflows observed in the Orinda area, that of a coalescing earthflow complex occupying a broad natural drainage. Coalescing complexes are typified by "distracted" slope contours and a general absence of V-shaped contours in natural swales/ravines, such as that shown on the left side of Figure 106. In active complexes, concave-inward contours will be noted positioned above convex-outward contours. Repeated crenulation of individual contours often indicates boundaries of individual lobes, one superposed upon another.

Figure 112 & 113 present an example of a coalescing earthflow complex dormant for more than 10 years. At this juncture, individual contours exhibit less crenulation, as the individual flow lobes are "melted" together by erosion, settlement, and biogenic activity. In this instance, aerial photo interpretation may be a superior method of evaluation because the flow lobes generally support more lush vegetation than the undisturbed margins of the slide complex. If mapping simply from the topographic expression, the resulting landslide map might appear as presented on the right-hand side of Figure 113. Note how this varies with the same area mapped in Figure 112.

Figure 114 presents the same example, but the earthflow complex has laid dormant for 50 to 100 years. In an advanced stage of healing, the toe lobes become increasingly subdued, but they can also be masked by increased vegetation fed by near-surface seepage within the old slide complex. At this stage, significant portions of the coalescing complex might easily be mapped as colluvium (slope wash), with a few older flows and slumps delineated about the margins of the colluvial-filled ravine (right side of Figure 114).

From the preceding examples, we may conclude that in the case of shallow earthflows and debris flows, the density of mapped landslides is influenced by how recently any slides have occurred in the study area. In developed areas, the physical evidence of recent slide activity is often masked by cursory earthwork intended to restore drainage or other facets of functionality.

Other examples of earthflows and debris flows are presented in Figures 115 and 116. In Figure 115, crenulated contours within first-order drainage swales should serve as key indicators of recent earthflows.

As in the discussion of colluvial mobilization in the preceding section, one of the most common failure modes for earthflows is for the material to flow a short distance downslope until it dilates sufficiently to drain itself, lose inertia, and stop. This accumulation of debris in the ephemeral channels creates the crenulated topography that is characteristic of debris-flow complexes. At some point in the future, the aggregate sum of this displaced material could be swept downslope, sometimes with catastrophic results.

Figure 116 presents another example from the Dublin Grade along Interstate 580 west of Dublin, Cal. These slopes are underlain by sediments of the Great Valley Sequence of Cretaceous age. The site might appear benign to an inexperienced interpreter. Subsurface exploration revealed a dense pattern of landslide types and sizes, shown on the interpretive (right) side of Figure 116. The most compelling evidence of past sliding was the opposing contours below a slight bedrock swale. These divergent contours identify a relatively recent earthflow. Note how first-order channels are beginning to incise along the lateral margins of the earthflow. Parallel drainages are almost always indicative of recent landsliding in the East Bay Hills.

Downloaded from http://pubs.geoscienceworld.org/aeg/eeg/article-pdf/31/1/i/6130855/i1558-9161-31-1-i.pdf
by AEG RBAC user

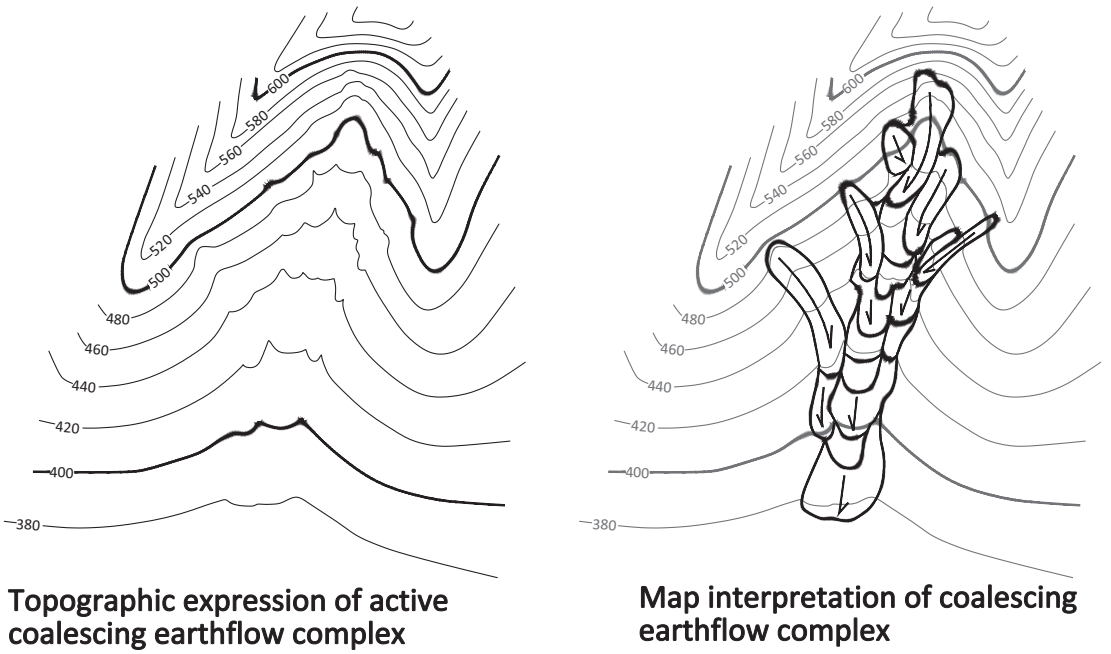

Figure 112a. Aerial oblique view of a coalescing earthflow complex at the south end of Mulholland Ridge in Moraga in 1986 (J. David Rogers).

Figure 112b. Topographic expression of an active coalescing earthflow complex with multiple lobes on the left and the interpretation of the active lobes on the right.

Rotational Slumps

Concept of Rotational Failures

An example cross section through a simple rotational slump is presented in Figure 117. This figure shows that through simple rotation, a soil mass increases its own stability by lowering the relative position of the water table. Slumps generally occur after periods of sustained precipitation, when the inflow of water exceeds the outflow, and a net buildup of moisture and pore-water pressure occurs (shown in upper pane of Figure 117). In this manner, semi-homogeneous soil masses tend to move and dilate to a more stable configuration, shown in the lower pane of Figure 117.

Downloaded from http://pubs.geoscienceworld.org/aeg/eeg/article-pdf/31/1/i/6130855/i1558-9161-31-1-i.pdf
by AEG RBAC user

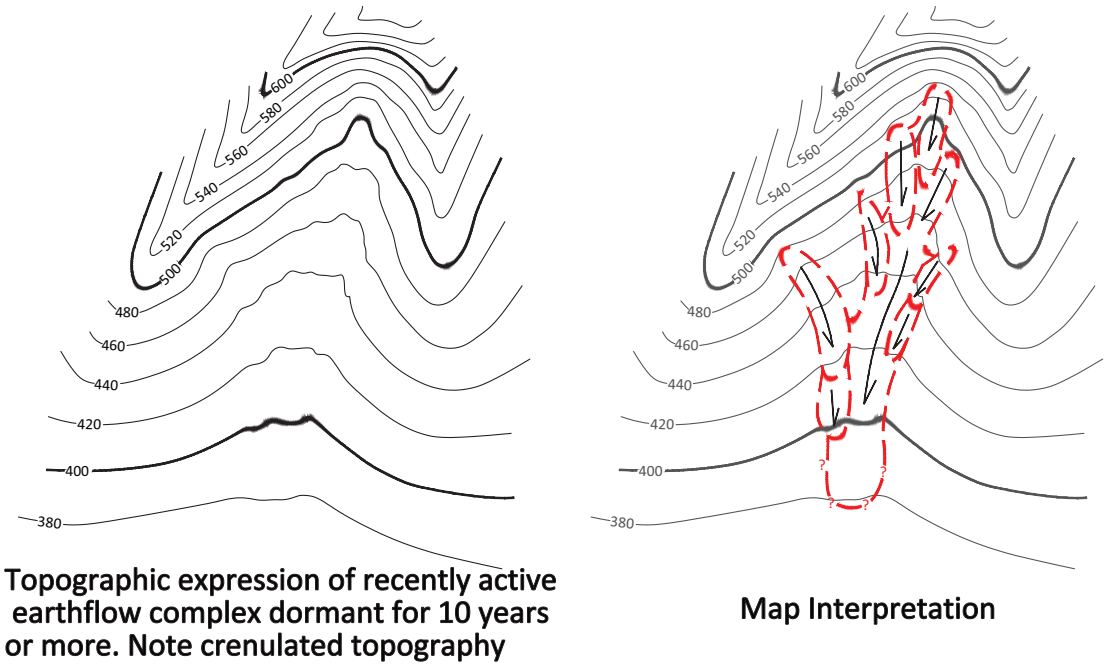

Figure 113. Topographic expression of a coalescing earthflow complex on the left with multiple lobes that has been dormant for more than 10 years. The right pane shows the interpretation of flow lobes, which are more abstract and approximate.

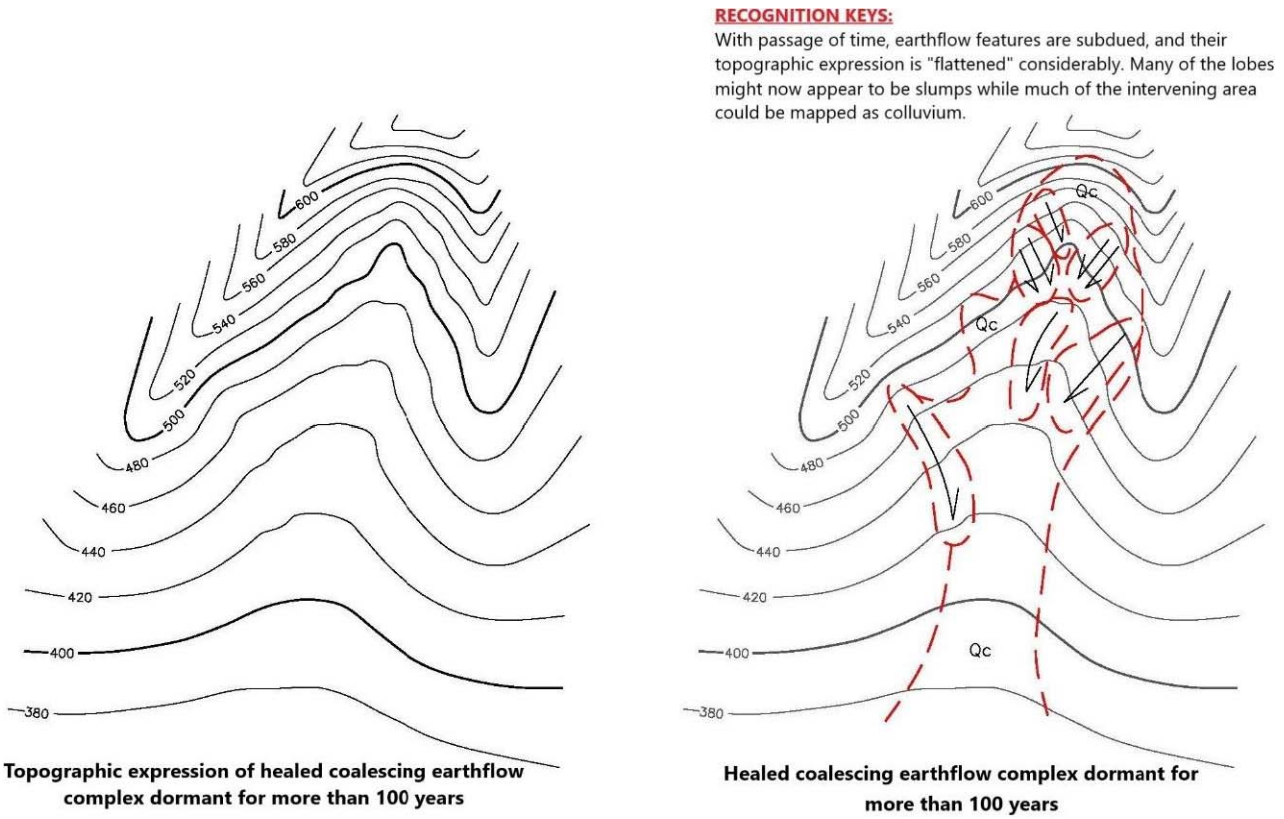

Figure 114. The left pane shows the topographic expression of a coalescing earthflow complex that has been dormant for more than 50 to 100 years. In such cases, it is very difficult to recognize the most active flow lobes, as shown at right, where material may be interpreted as colluvium if it was deposited over vegetation without forming a shearing surface.

Downloaded from http://pubs.geoscienceworld.org/aeg/eeg/article-pdf/31/1/i/6130855/i1558-9161-31-1-i.pdf
by AEG RBAC user

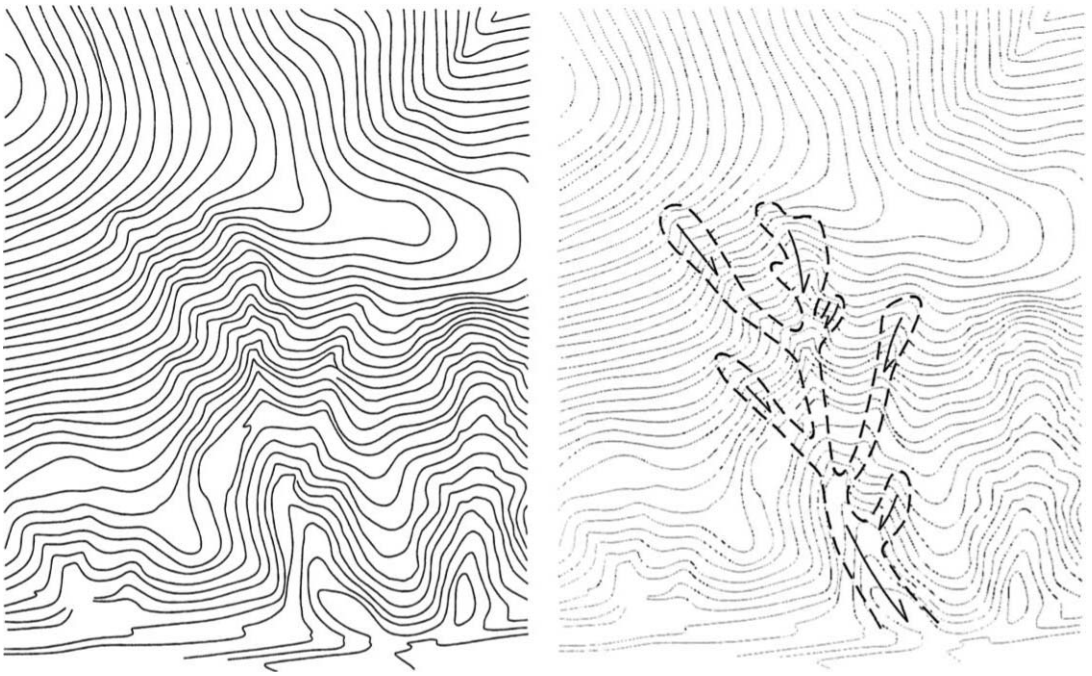

Figure 115. Topography of colluvial-filled bedrock ravines that are actively raveling.

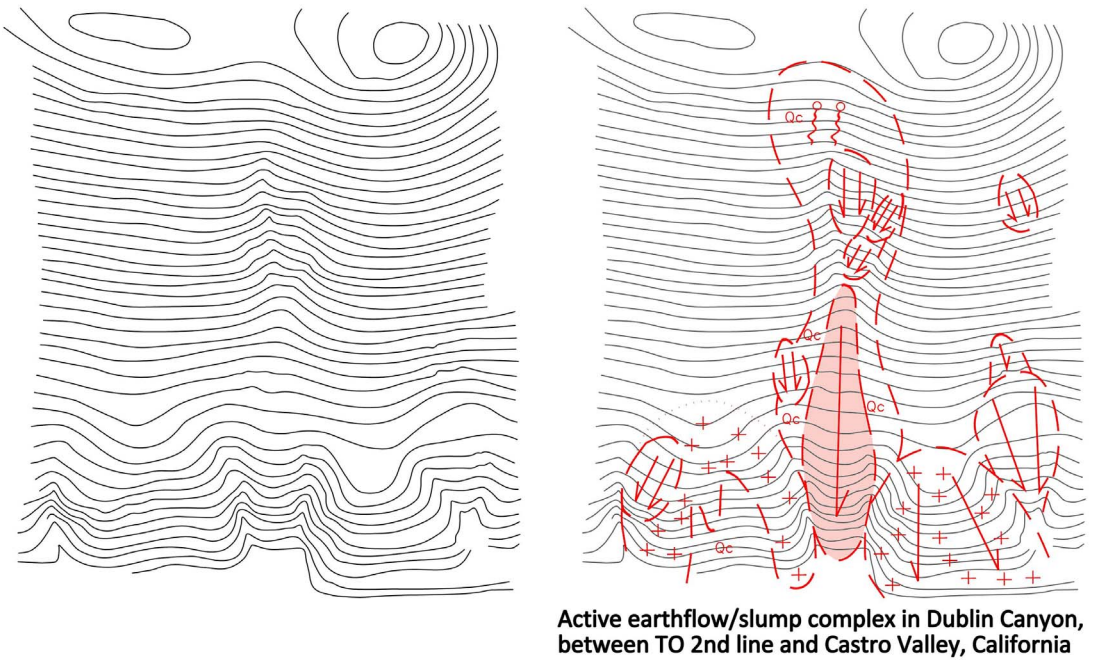

Figure 116. The left pane shows an orthophoto-derived topographic map along Interstate 580 near Dublin, CA. Thee right pane is the interpreted landslide features, dominated by a single earthflow surrounded by colluvium (Qc) and relicts of prehistoric slumps (cross overlays).

The geometry of rotational failures, often termed "slumps," depends on the thickness and consistency of the affected soil or rock mass. Slumps are one of the most common types of slides, often confined to the soil regolith developed upon weathered bedrock. Thick zones of soil, colluvium, and detritus from the bedrock creep zone can also foster spoon-shaped slumps (Varnes, 1958), like the examples shown in Figure 118a–c. Thin

Downloaded from http://pubs.geoscienceworld.org/aeg/eeg/article-pdf/31/1/i/6130855/i1558-9161-31-1-i.pdf
by AEG RBAC user

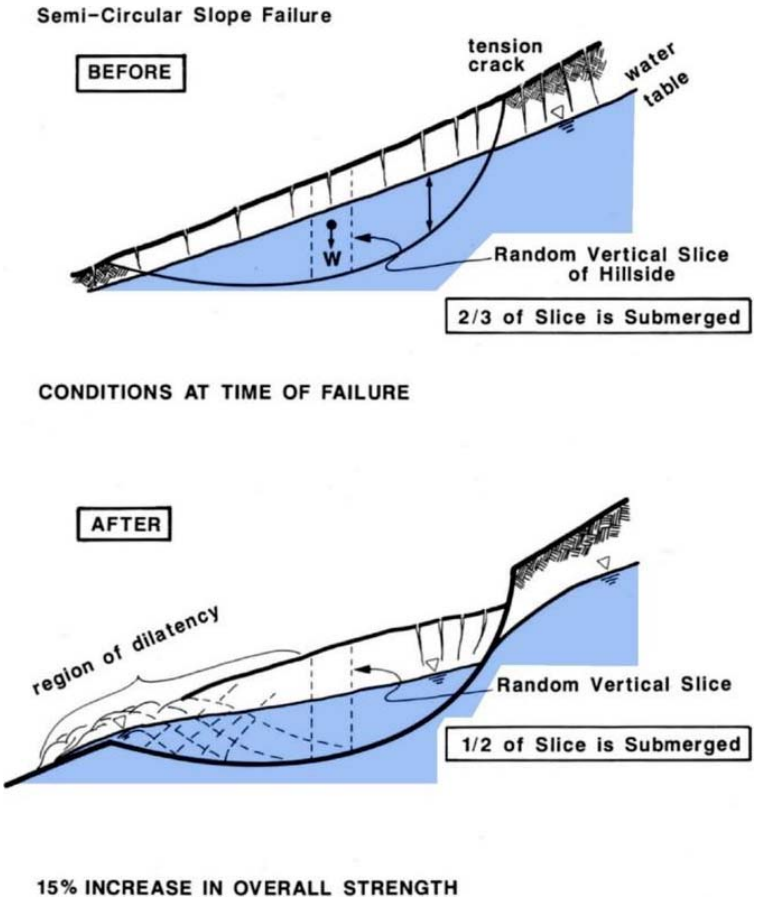

Figure 117. Mechanics of rotational slump failure. Note how the relative proportion of saturated soil in a random vertical slice is lessened by simple rotation to a more stable condition (Dietrich and Rogers, 1988).

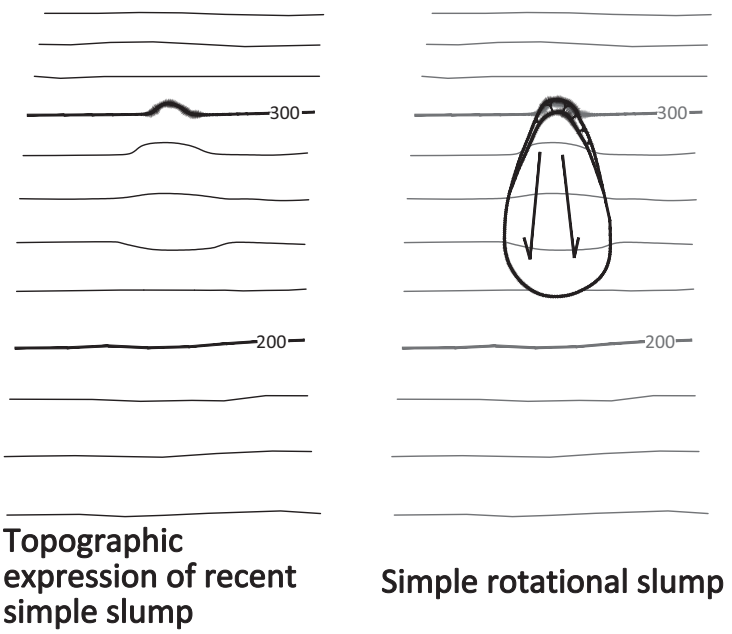

Figure 118a. Topographic expression of a recent soil slump landslide.

Figure 118b. Resulting interpretation of a spoon-shaped soil slump.

Downloaded from http://pubs.geoscienceworld.org/aeg/eeg/article-pdf/31/1/i/6130855/i1558-9161-31-1-i.pdf
by AEG RBAC user

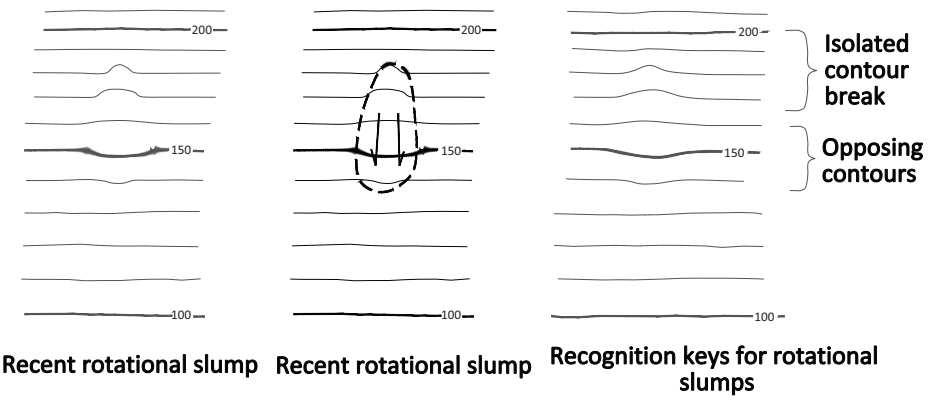

Figure 118c. Topographic expression of recent soil slump failure.

Figure 118d. Interpretation of slump feature.

Figure 118e. Recognition keys for simple slump landslides.

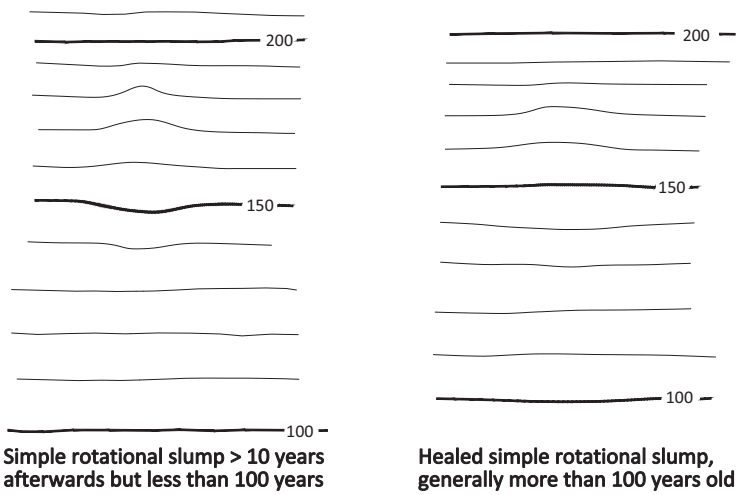

Figure 118f. Topographic expression of rotational soil slump between 10 and 100 years old.

Figure 118g. Subdued topography of soil slump more than 100 years old.

regoliths of soil tend to foster broad, shallow slumps, like that in Figure 119.

Analysis of Rotational Slumps

Rotational slides have been described and evaluated by civil engineers more than any other slide type (Baltzer, 1880). For almost 250 years, engineers and scientists have recognized two components of soil strength: friction and cohesion (Coulomb, 1776). Friction is generated in a soil/rock mixture through interparticle contact, while cohesion is fostered by physiochemical forces of attraction between individual clay particles (Mitchell, 1993). Clays derive their soil shear strength principally from cohesion. The addition of moisture has the greatest effect on the frictional component, but it can affect cohesion as well.

Petterson (1916) and Fellenius (1919, 1936) were among the earliest researchers to apply the analytical concept of a circular failure surface varying as a function of soil friction, formulating what became known as the "Swedish circle method" of analysis, which served as the primary method of analyzing rotational failures until computerized limit equilibrium analyses began appearing in the mid-1950s (Bishop, 1955). Fellinius' theory predicted that soils possessing low values of interparticle friction would spawn progressively deeper and more circular slip surfaces. In 1936, Terzaghi's doctoral student Leo Rendulic demonstrated that landslide virgin rupture (failure) surfaces in rotational slides are log-spiral shaped, a tenet that has gained universal acceptance (Rendulic, 1936 a&b; Terzaghi, 1950; and Skempton, 1964).

Bishop (1953, 1954, 1959) presented the concept of effective soil stress, which explained how the frictional

Downloaded from http://pubs.geoscienceworld.org/aeg/eeg/article-pdf/31/1/i/6130855/i1558-9161-31-1-i.pdf
by AEG RBAC user

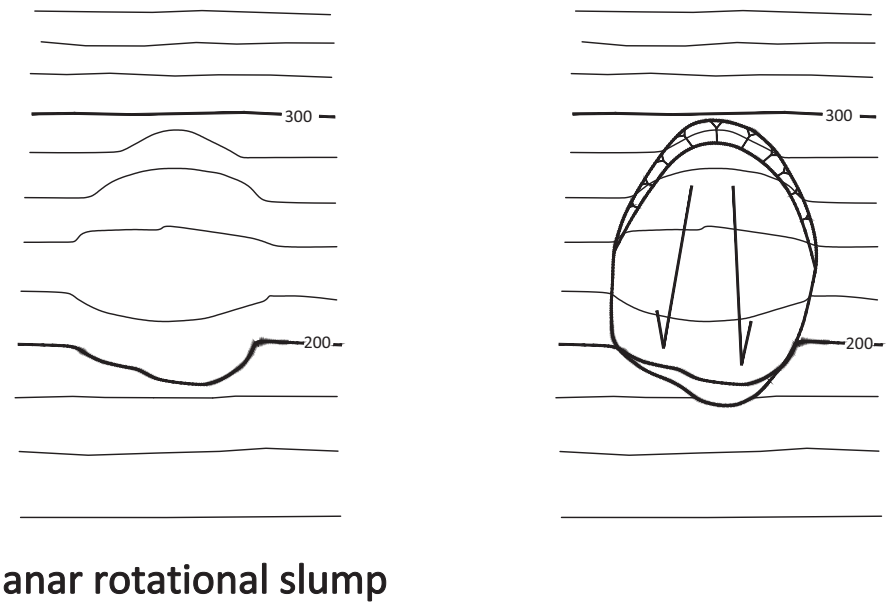

Figure 119. The left pane presents the topographic expression of a planar rotational slump feature, which tends to form on materials of higher friction, like weathered bedrock. The right pane shows the interpretation of a shallow slump landslide developed in higher-strength material. Note the pancake-like shape and form.

component of soil strength is degraded through buoyancy (saturation). Simons and Menzies (1974) demonstrated that the state of effective stress within a soil mass also varies with deformation. Up until the late 1980s, most geotechnical engineers felt that soil cohesion was an intrinsic component of strength, unaffected by other environmental factors. Morganstern and Eigenbrod (1974) showed that the cohesion measured in clays was subject to variations associated with saturation and pore pressure. Rogers and Pyles (1980) demonstrated that an over-consolidated clay shale lost two thirds of its intrinsic cohesion with long-term saturation.

Skempton (1964) showed that circular analyses did not approximate actual field conditions, but they were the best tool engineers had to work with at the time. Skempton also showed that the depth of the predicted failure circle depended on the assumed properties of the soil, which were themselves functions of the loading criteria (such as long-term drained creep versus short-term undrained responses).

Morganstem and Price (1965) devised more sophisticated analyses, which could analyze any shape of the failure surface. This method utilized a pattern of interslice force inclinations, iterating to solve for the change in inclination with each location. The method allowed for close approximation of field examples for the first time. Their work suggested that the log-spiral shape is engendered in nature as the loci of "pure shear" beneath the slope, because the position of effective horizontal thrust is very steeply inclined in the upslope portion of the slide mass, but it is nearly horizontal in the downslope toe.

By failing along a log-spiral–shaped surface, there is a minimal amount of interslice bending (or moment-induced rotation) to be overcome in forming a shear rupture surface to accommodate downslope movement. This is because the sum of bending moments about the base of sliding is nearly equal to zero. In this manner, the slope fails in the most energy-efficient manner.

Topographic Examples of Rotational Slumps

Shallow rotational slumps within the soil mass can be difficult to identify, depending on contour fineness, map scale, vegetative cover, and age since occurrence. A simple example is presented in Figure 118. Figure 118a presents the topographic expression of a recent slump, while Figure 118b shows the map interpretation of the slide. Figure 118c presents typical recognition keys, such as asymmetric opposing contours absent any ravine above or below and isolated contour breaks (pinching of contours) in the headscarp evacuation zone.

Figure 118d shows topographic healing typical of the first 100 years. Beyond 100 years, topographic recognition becomes much less obvious in a humid climate (Figure 118e). Opposing contours within an otherwise uniform contour field are one of the best indicators that rotational sliding has occurred sometime in the past.

Figure 119 presents a topographic example of a planar slump, such as commonly occurs within soil regoliths developed upon sandstone and conglomerate beds within the Orinda area. In this instance, the failure surface is generally shallow (3 to 10 ft [0.9 to 3.1 m]) with

Downloaded from http://pubs.geoscienceworld.org/aeg/eeg/article-pdf/31/1/i/6130855/i1558-9161-31-1-i.pdf
by AEG RBAC user

respect to the slide overall dimensions. Planar rotational slumps tend to become subdued more quickly than other types of slides, depending on their depth.

A classic feature of rotational slumps within bedrock is the topographic expression of back-rotated grabens, which often form prominent curvilinear benches of slight depressions. Figure 120a and 120b shows photos of the same slump-flow complex taken about 73 years after its activation during the M 7.9 San Francisco earthquake in 1906.

Figure 121 presents cross sections through this slump feature, illustrating the character of the headscarp graben that formed coincidently with the slope movement. Depositional infilling of the graben feature often serves to mask its presence (Rogers and Chung, 2016). Geologists mapping landslides should be suspicious of isolated topographic benches. Few of these features are structurally controlled in the Lamorinda area.

Figure 120a. Back-rotated bedrock slump-flow complex in the Berkeley-Contra Costa Hills almost a century after it was was initially recognized by USGS geologist G. K. Gilbert following the 1906 San Francisco Earthquake. Image taken by J. David Rogers in 1979.

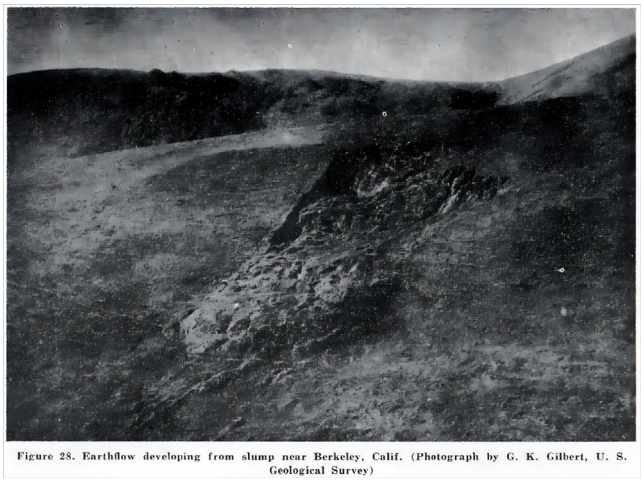

Figure 120b. Same view of the slump-flow complex taken by Gilbert in 1906, while he was stationed at the University of California at Berkeley. It was included as Figure 28 in Varnes' 1958 article on "Landslides Types and Processes" for the Highway Research Board's Special Report 29 on *Landslides and Engineering Practice* (Varnes, 1958).

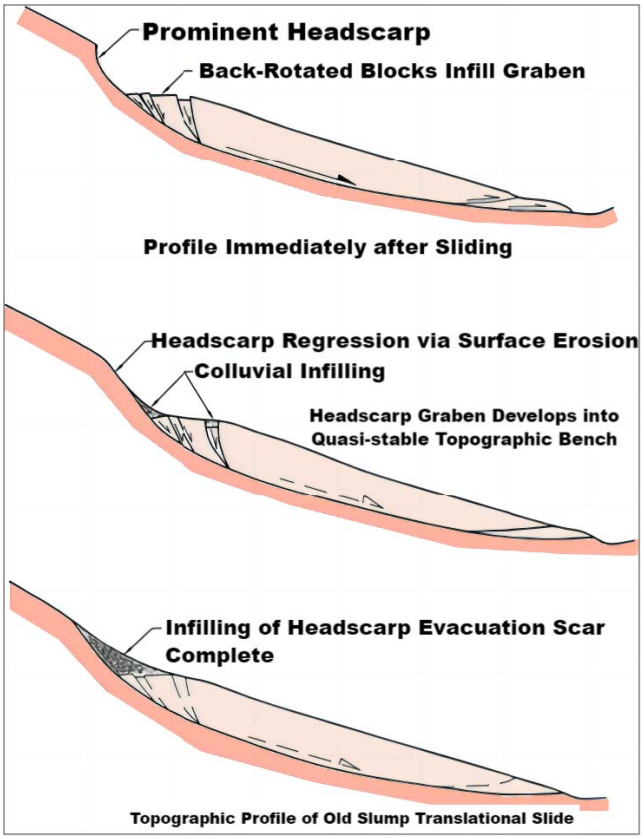

Figure 121. Progressive sections cut through a tranlational bedrock slump, illustrating how rapidly the slide's headscarp area is infilled and healed. On many occasions, only a slight topographic bench gives any hint of past instability.

Retrogressive Rotational Slumps

Another common failure is progressive or retrogressive sliding (Bjerrum, 1966; Goodman, 1976; and Zaruba and Mencl, 1982). A typical example is presented in Figure 122a. When one mass of material rotates downslope, the void generated in the headscarp separation removes lateral support from the next adjacent mass. Simple limit equilibrium slope stability analyses can be used to demonstrate the destabilizing effect of the loss of lateral support. Such a situation is portrayed in Figure 122b, where the two-dimensional safety factor has been calculated for the various positions represented.

It can be appreciated that when a block translates downslope, the stability of the next-adjacent block upslope becomes more precarious. In such a manner, block rotation can simply migrate upslope. This mechanism of progressive failure is most troublesome in

Downloaded from http://pubs.geoscienceworld.org/aeg/eeg/article-pdf/31/1/i/6130855/i1558-9161-31-1-i.pdf
by AEG RBAC user

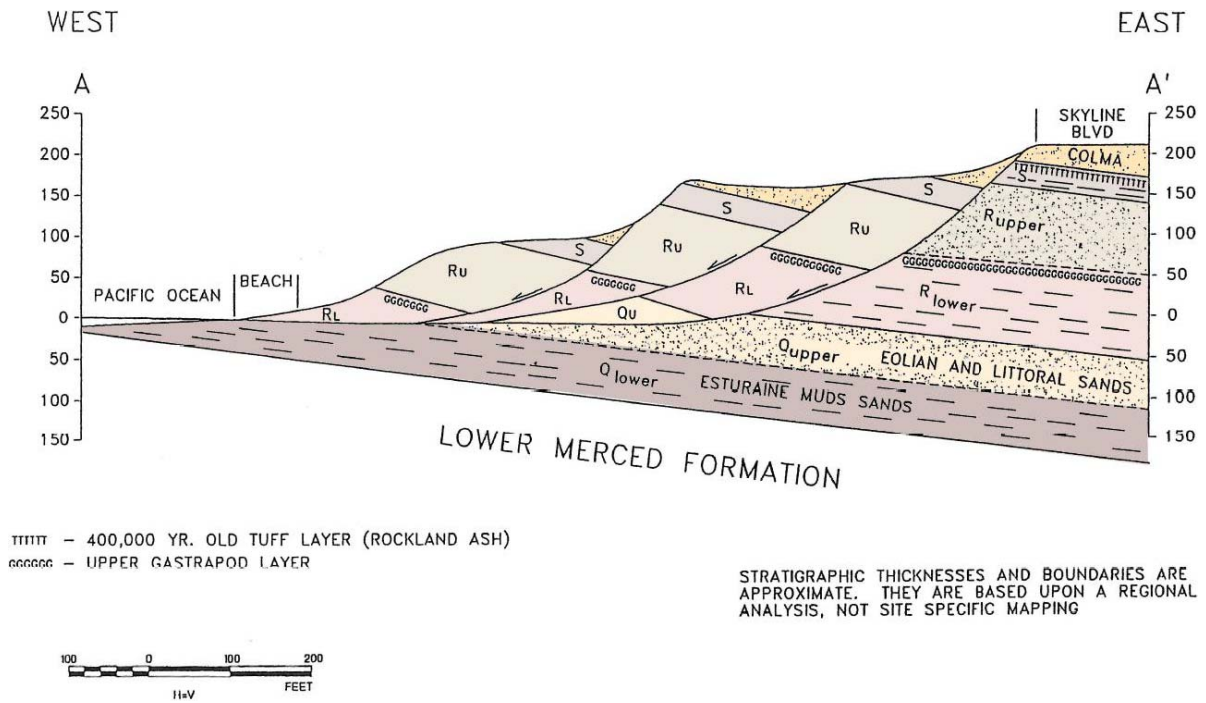

Figure 122a. Retrogressive slump blocks in the Merced Formation along the Pacific Ocean bluffs on the western shore of San Francisco (Rogers/Pacific, Inc., 1993).

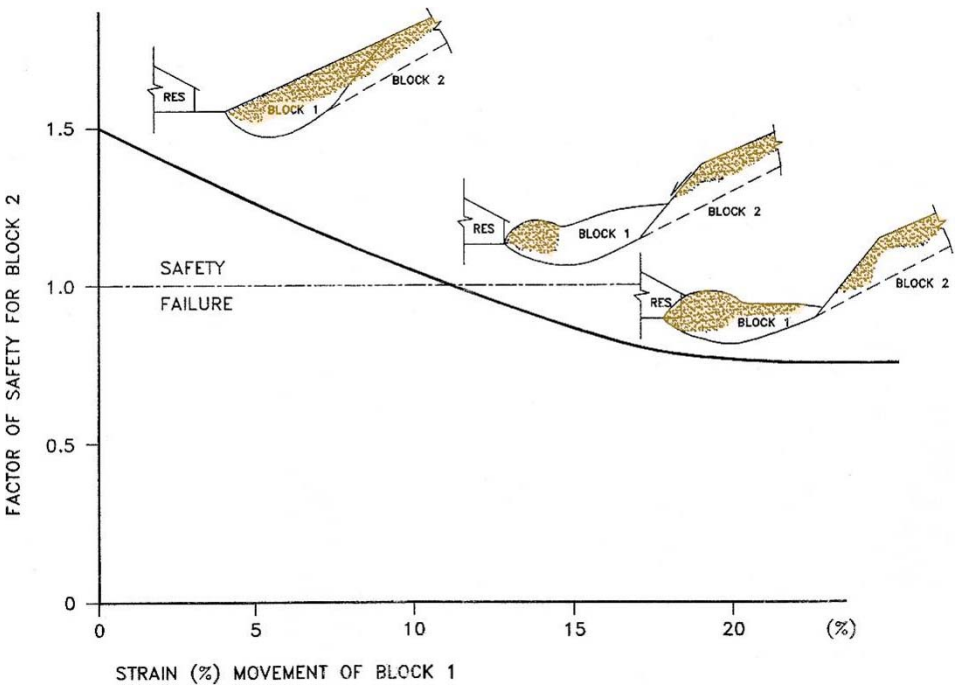

Figure 122b. Degradation of the safety factor with retrogressive slumping due to loss of lateral support each time block 1 slumps and moves downslope.

situations where an underlying zone of weakness exists (Hutchinson, 1969).

Headscarp retrogression, characterized by progressively smaller headward slumping, is common in situations involving bedrock slumps, as sketched in Figure 121, extending the topographic expression of the sliding upslope of its original position, as shown in the examples presented in Figures 120 through 125.

Downloaded from http://pubs.geoscienceworld.org/aeg/eeg/article-pdf/31/1/i/6130855/i1558-9161-31-1-i.pdf
by AEG RBAC user

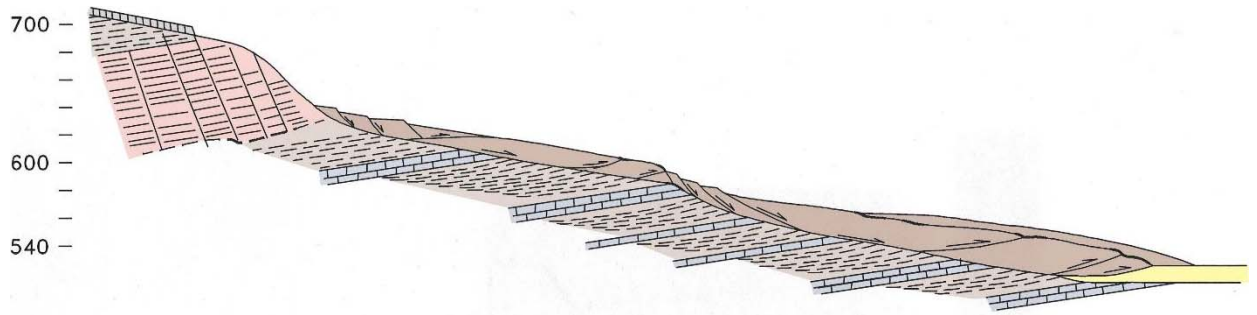

Figure 123. Retrogressive slide complex on right abutment of Mora Dam, in Czech, Slovakia, taken from Malgot and Boliak (1993). Extensive slide complexes often develop in overconsolidated shales when strain softening hastens their loss of shear strength.

Topographic Expression of Retrogressive Blocks

The one indicator of repeated retrogressive slumping is multiple topographic benches, such as those shown in section in Figure 122a. In plan, these types of features often appear as series of small terraces (Sharpe 1938a and Sharpe 1938b), often infilling established channels. In other instances, retrogressive blocks simply nurture the enlargement of a landslide complex.

Identifying retrogressive blocks is largely a function of topographic fineness, or contour interval. In suitably fine scales with 1 to 5 ft (0.3 to 1.5 m) contour intervals, such features can be identified, depending on the volume of colluvial infilling (Figure 121). In this study, no attempt was made to identify individual scarps, only the areal limits of sliding.

Translational Failures

Concept of Translational Failures

Sharpe (1938a&b) formulated the first basic classification of landslides, which became the basis for most accepted classification schemes developed since that time (Eckel, 1958; Schuster and Krizek, 1978; Cruden and Varnes, 1996; and Hungr et al., 2014). Sharpe (1938a) and Sharpe (1938b) chose to make a fundamental distinction between "flow-related" and "slip-related" landslides. He termed "true landslides" as those that exhibit slippage or detachment of a semi-coherent mass (which included slumps, debris slides, debris falls, rockslides, and rockfalls).

Varnes (1958) appears to have accepted the term "block glide" to describe translational landslides that moved as a semi-coherent block upon a discrete failure surface, usually a preexisting geologic discontinuity or formational contact (Miller, 1931; Leighton, 1966; Appendix 1). Zaruba and Mencl (1969) and Varnes (1978) expanded the descriptor "translational slide" to encompass sliding on planar surfaces as a semi-coherent mass. Such classification would not include debris avalanches like the 1903 Turtle Mountain, Alberta, Canada, or 1925 Gros Ventre, WY, events, where the material becomes disaggregated and flows like a giant mass with reduced viscosity (Voight and Pariseau, 1979; Melosh, 1987; Legros, 2002; and Iverson, 2003).

Examples of translational failure would include décollement, or detachment-style failures, such as the Vaiont Reservoir slide (Mencl, 1966), translation along liquefied layers (Casagrande, 1952; Green and Ferguson, 1971), or seismically induced lateral spreads (Hansen, 1965).

Analysis of Translational Slides

Translational slides occur along non-circular slip surfaces. Penck (1894) was the first to offer rational analytical techniques to describe rock mass strength along discrete boundaries and, thus, quantitatively explain translational failures. Much later, Janbu (1957) introduced the first generalized method of slices, which could analyze non-circular failure surfaces. Not long afterward, Morganstern and Price (1965) and Spencer (1967) introduced limit equilibrium techniques to evaluate non-circular slip surfaces. Spencer's procedure is the simplest because it assumes interslice forces to be equal. This method yields fair results provided that additional slices are utilized to model sharp turns, bends, or transitional portions of a translating mass (Duncan and Wright, 1980). Wright's (1969) force equilibrium method can also accommodate non-circular failure surfaces by making assumptions about the inclination of interslice thrust.

Topographic Examples of Translational Slides

Figure 124a–c presents schematic sections through the 1967 Tahos Road landslide, which destroyed two homes (Figures 27–28). Kachadoorian (1956, 1959) had mapped a dormant bedrock slide in the lower half of this same draw. Figure 124a presents key identifying elements of a dormant translational bedrock landslide, typical of the Lamorinda area. Figure 124b shows how most of these dormant slides were reactivated: (1) by adding

Downloaded from http://pubs.geoscienceworld.org/aeg/eeg/article-pdf/31/1/i/6130855/i1558-9161-31-1-i.pdf
by AEG RBAC user

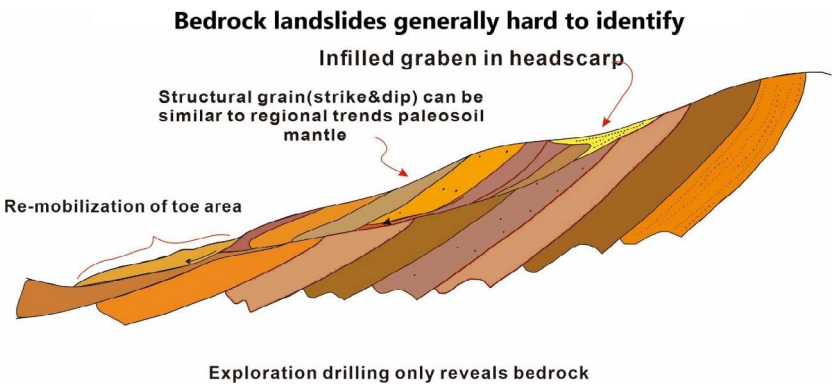

Figure 124a. Cross section through the dormant Tahos Road landslide prior to development in the late 1950s. Kachadoorian (1956) of the USGS recognized the remobilized toe area as an earthflow slide mass, but not the dormant bedrock slide.

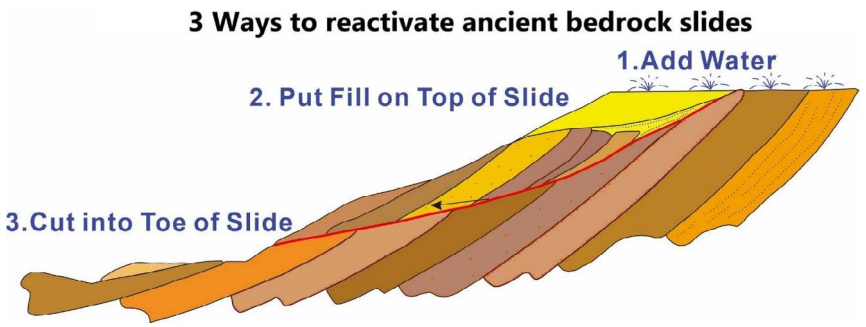

Figure 124b. Common mistakes associated with hillside development that ignores engineering geologic characterization of landslide hazards.

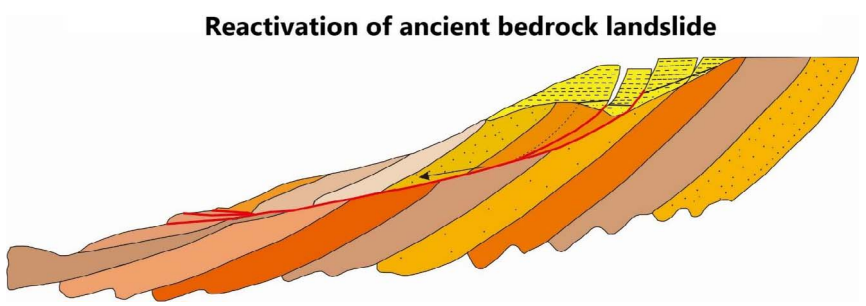

Figure 124c. Within just a few years of construction, two homes along Tahos Road were undermined by a massive landslide along a preexisting slip surface, shown in red.

water to the slide mass through landscape watering, operation of leach fields, or disturbing the natural runoff and infiltration regime; (2) by surcharging of the dormant slide mass by adding compacted fill; and (3) by removing lateral support of the slope toe through excavation. After studying landslides in Contra Costa County during the period 1950–73, Nilsen and Turner (1975) estimated that approximately 80 percent of the slides were triggered by or related to some slort of human activity. Figure 124c presents the style of slippage that began in January 1967 due to surcharging of the dormant slide mass with engineered fill. Figure 125 presents a perspective view of the Tahos Road slide, which was partially activated in January 1967 and fully reactivated in 1983 and 1986.

Translational failures like those shown in Figures 124 and 125 are often difficult to detect because the displaced strata exhibit similar structure to the parent material underneath or on either side of the dormant prehistoric slide. The only difference is that the material that has slid usually dilates and absorbes more pore water, so it tends to exhibit higher water contents with lower bulk densities.

Smaller translational slides can be even harder to discern unless they are geologically active, as shown in

Downloaded from http://pubs.geoscienceworld.org/aeg/eeg/article-pdf/31/1/i/6130855/i1558-9161-31-1-i.pdf
by AEG RBAC user

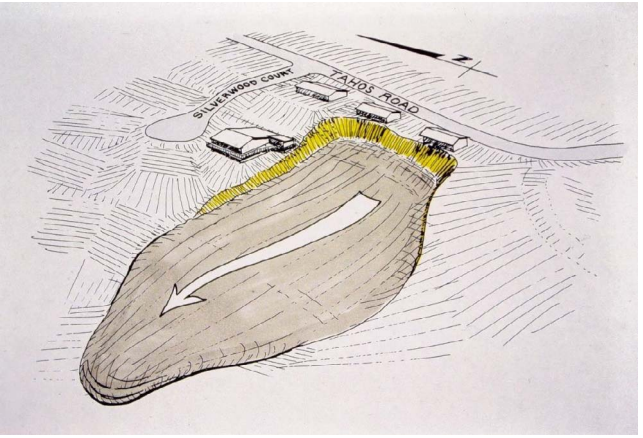

Figure 125. Conceptual sketch of the Tahos Road Landslide, which was reactivated by the simultaneous placement of fill surcharge and excavation of the slope's toe to construct building pads.

Figures 126 to 132 (Stages 1–6). These figures illustrate the typical genesis of a modest translational slide along Cayetano Creek, blocking southward flow adjacent to Tassajara Creek Regional Park in July 1983. This slide appears to have been intermittently active for an unknown period of time.

Figure 126a presents the likely pre-failure topography of a mature bedrock slope where a third-order watercourse is gradually lowering its bed and undercutting a channel bank on the outside of a turn.

Figure 126b presents this same situation, as it would appear in a reconnaissance engineering geologic map of the site. Holocene-age alluvium (Qal) infills the low-flow channel, while older, elevated terrace deposits (Qt) infill portions of the main channel. Colluvium (Qc) is shown occupying what appear to be broad bedrock depressions within the first-order and second-order channel complex. The topographic expression is sufficiently sharp to preclude additional mapping of colluvium in other first-order basins, although field checking might confirm such a presumption.

Figure 127a–b shows the topographic expression typical of stage 2 conditions. Interpretive keys suggest the onset of translational sliding towards the undercut stream bank. A photograph of this site is included in Figure 128.

The disturbed topography of a bedrock slump like that shown in Figure 128 will remain less degraded than a soft soil slump, which is much more erodible. Bedrock slumps of varying ages are widespread across the East Bay Hills.

In translational slides, the length-to-width (L/W) ratio can be much lower than that for virgin rotational slump-style failures, although not without exceptions. Planar slip surfaces are more common in bedrock slides where

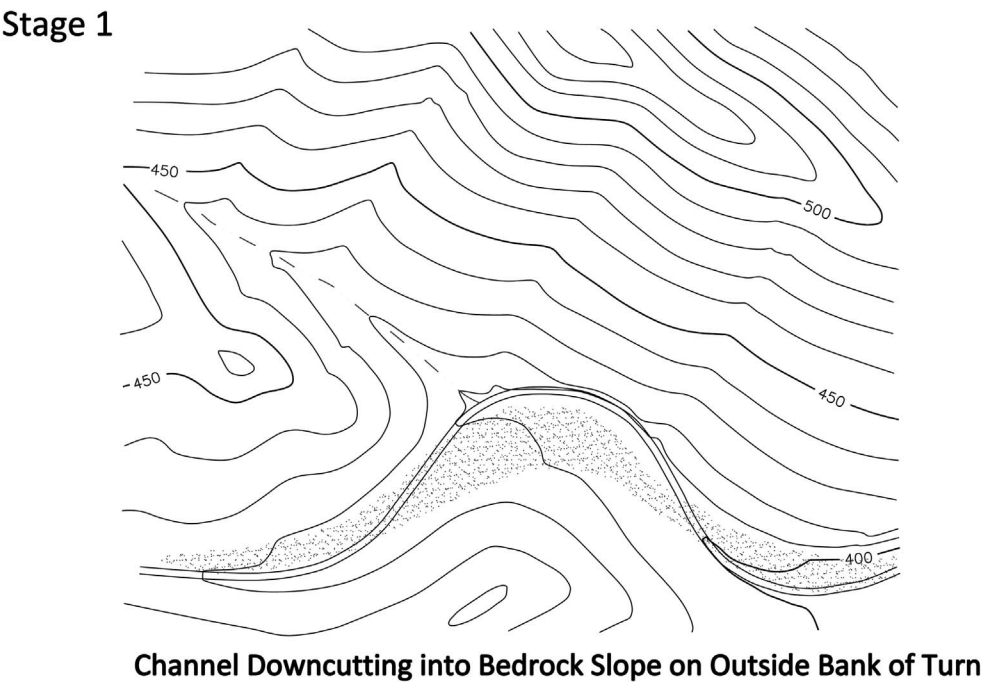

Figure 126a. Stage 1 of an undercut creek bank, which can eventually trigger a landslide along the outer margins of a curving cut bank in the channel (flow is from left to right).

Downloaded from http://pubs.geoscienceworld.org/aeg/eeg/article-pdf/31/1/i/6130855/i1558-9161-31-1-i.pdf
by AEG RBAC user

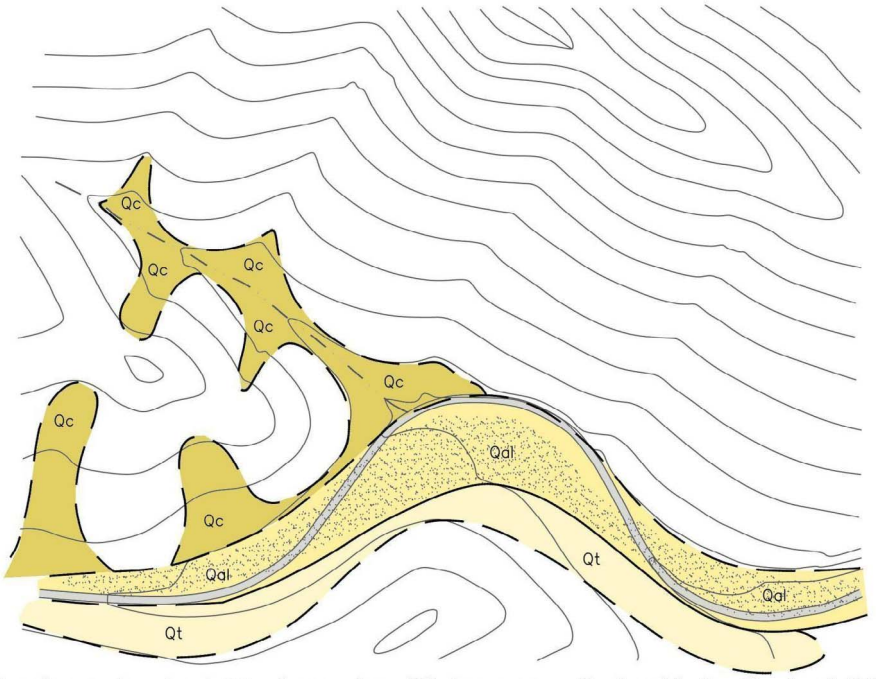

Mapping mature landslide in quasi-equilibrium, generally devoid of active landsliding. However, channel exhibits of slow, but persistent downcutting.

Figure 126b. Interpretation of stage 1 conditions often include spatial distributions of channel alluvium (Qal), inset terrace deposits (Qt), and colluvium (Qc). The areal distrubutions of these materials record the channel's geomorphic responses to environmental factors, such as climate and vegetation cycles.

Figure 127a. Topographic expression developed during stage 2. Note pinching of contours in the headscarp area and divergent contours in the body of the slide mass.

Downloaded from http://pubs.geoscienceworld.org/aeg/eeg/article-pdf/31/1/i/6130855/i1558-9161-31-1-i.pdf
by AEG RBAC user

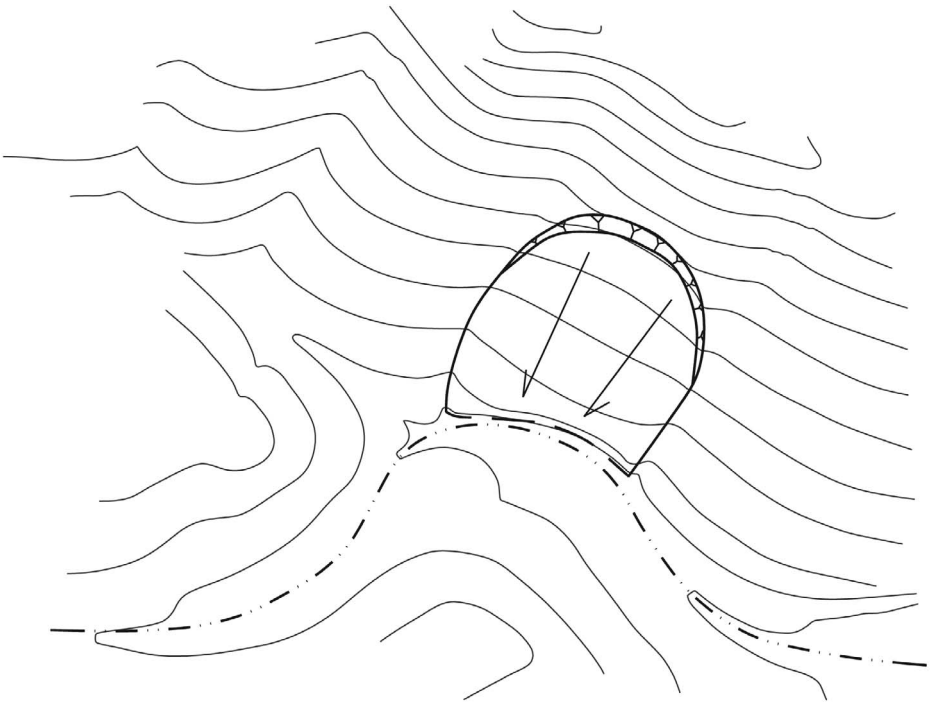

Large Bedrock Slump Begins to Translate towards Undercut Toe

Figure 127b. Map interpretation of stage 2 slope morphology, where a large bedrock slump has formed and begun moving toward the deepest portion of the undercut creek bank.

Figure 128. Landslide dam across Cayetano Creek in the Tassajara Hills in 1983. Note green slime floating on several feet (~0.6 m) of water ponded by a recent landslide dam (J. David Rogers).

underlying discontinuities often exert a controlling role. These same structural features can promote periodic reactivation of sliding if pore water becomes perched on rupture surfaces (Rogers, 1986; Cronin, 1992).

Figure 129a–b presents the topographic expression of the same translational slide at stage 3, following enlargement of the headscarp (Figure 129a). The longer the displaced mass remains dormant, the more obvious becomes the incision and erosion of its lateral scarps, which appear to be immature first-order rills or ephemeral flow paths. Secondary slumps along the oversteepened cutbank are quite common, as shown in the map interpretation (Figure 129b).

When the slide initiates movement, it usually blocks the active stream channel, creating a landslide dam like that shown in Figure 128. Channels impacted by slide debris usually excavate short-lived bypasses within 24 hours, which displace the channel thalweg and perturbing the longitudinal gradient of the watercourse. Pinching of the channel width usually triggers an increased flow gradient, normally evidenced by shallow riffles or rapids (Bull, 1991).

Some of the most common manefestations of natural landslide dams are presented in Figure 129b. These include: (1) perturbed geometry of a channel turn; (2) presence of riffles at the base of a bank; (3) flat stream gradient upstream of riffles; (4) channel aggradation with terrace deposits upstream of landslide dam site; (5) narrowness of active channel across slide area (blockage); (6) relative lack of recent terrace deposits downstream of the landslide (blockage); and

Downloaded from http://pubs.geoscienceworld.org/aeg/eeg/article-pdf/31/1/i/6130855/i1558-9161-31-1-i.pdf
by AEG RBAC user

Figure 129a. Stage 3: Development of linear first-order channels that appear to be converging with increasing elevation. The slide appears to have periodically impinged upon the creek channel, pinching it. This narrowing increases flow velocities, promoting downcutting of the channel bed.

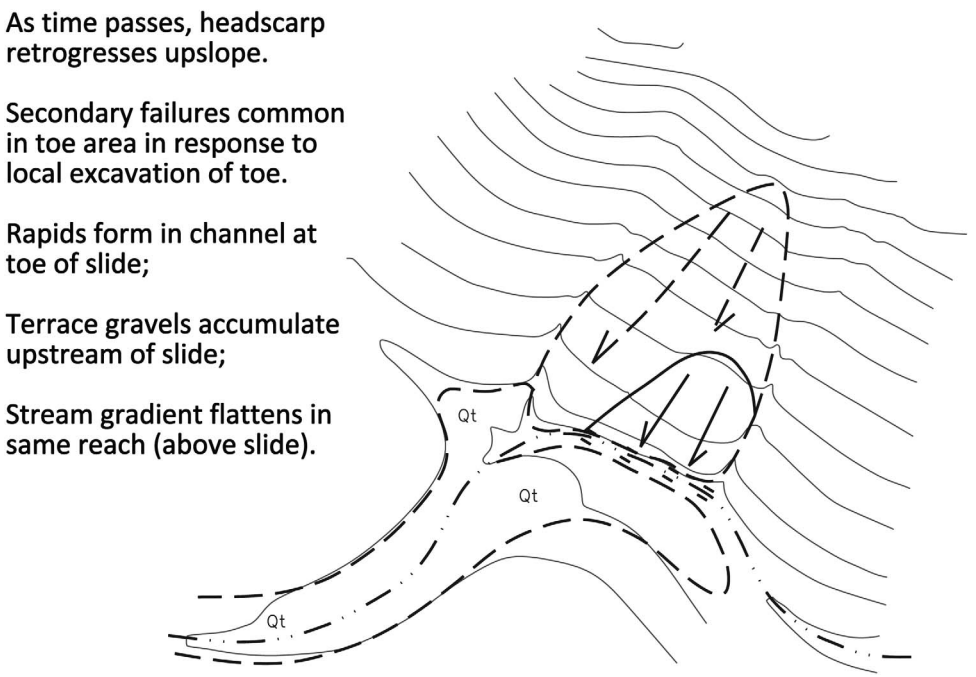

Figure 129b. Interpretation of morphologic features in stage 3. Headscarp of parent mass is drifting upslope. Secondary slumps are common along the undercut stream bank. Inset terraces line either side of the channel upstream of the slide.

Downloaded from http://pubs.geoscienceworld.org/aeg/eeg/article-pdf/31/1/i/6130855/i1558-9161-31-1-i.pdf
by AEG RBAC user

(7) topographic expression of sliding on the slope above the observed riffles.

Figure 130 shows an example of the topographic expression typical of dormant bedrock slides as the slide remains dormant. First-order streams begin to incise more noticeably and generally form convergent diagonals, diverging slightly from the natural fall-line of the ridge and contrasting with adjacent first-order streams.

At some time in the weathering process, the trunk stream will resume downcutting, likely in response to climate changes, absent other factors (Bull, 1991). Figure 131a is an example of long-term dormancy, for 2,000 to 11,000 years. In this case, the old lateral scarps will have exerted structural control on first-order watercourses, but without any evidence of geologically recent activity near the slide's toe, like that shown in the previous stages.

Figure 131b presents a typical example of how this topography would be mapped in a reconnaissance-level mapping of landslides and surficial deposits, like that accomplished for this project. The translational slide has been identified, but its relative lack of youthful geomorphic indicators has caused it to be classified as "relict," shown with cross hachures.

In such situations, which are common along the southwest side of Orinda, the slide's toe is likely buttressed by alluvium and terrace deposits. Such slides could remain dormant provided that no destabilizing activities are performed (such as those discussed with respect to Figure 124b).

Figure 132 presents some of the recognition keys for dormant translational slides, regardless of scale. With increased dormancy, the rapids, or riffles, disappear, and terrace deposits are often masked from view. The stream channel returns to smooth, sweeping turns, and there is little evidence of active channel downcutting.

The first-order gullies are convergent and short-lived or truncated, with obvious "knick points." However, in this example, topographic contours adjacent to the channel are suggestive of recent movement. In this case, the translational slide mass would be mapped as "potentially active," usually with dashed lines delineating the approximate boundaries.

Shallow Compound Slides

The term "compound slides" was originated by Albert Heim (1882) to describe those slides that involve more than one of the simpler mechanisms of sliding. The term was first applied in American geologic literature by Howe (1909). In the early 1900s, G. K. Gilbert recorded and photographed "slump-earthflow" slides in the hills between Berkeley and Orinda, shown in Figure 120b (from Varnes, 1958).

In the mid-1930s, Sharpe (1938 a&b) reproduced a cross section created by Dr. James K. Rogers of typical

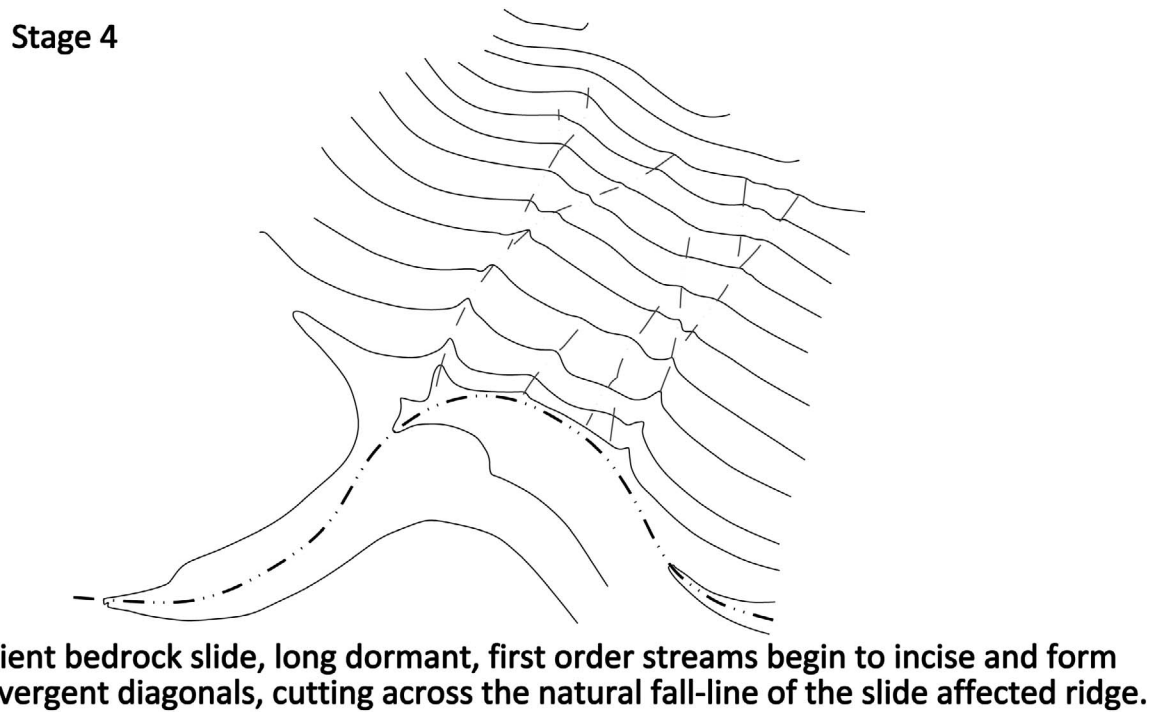

Figure 130. Stage 4: After sitting dormant for centuries, the first-order streams begin to incise on convergent diagonals, often cutting across the slope's original fall line. Note the increased channel width caused by aggradation of coarse debris (skeleton blocks).

Downloaded from http://pubs.geoscienceworld.org/aeg/eeg/article-pdf/31/1/i/6130855/i1558-9161-31-1-i.pdf
by AEG RBAC user

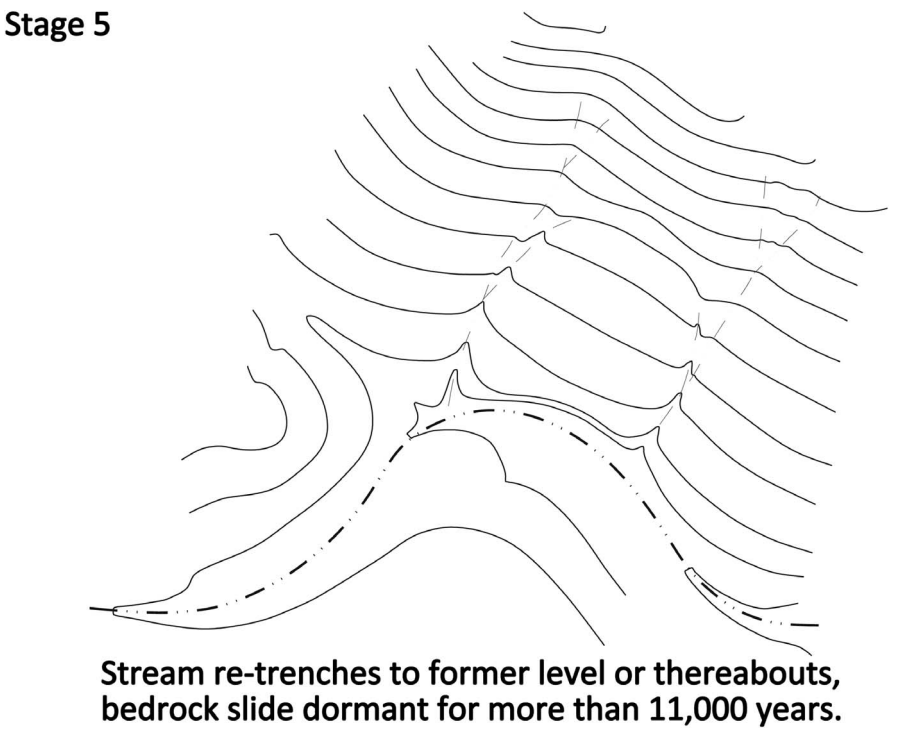

Figure 131a. In stage 5, the stream has succeeded in re-excavating its bed to its pre-slide elevation after lying dormant for an extended period of time.

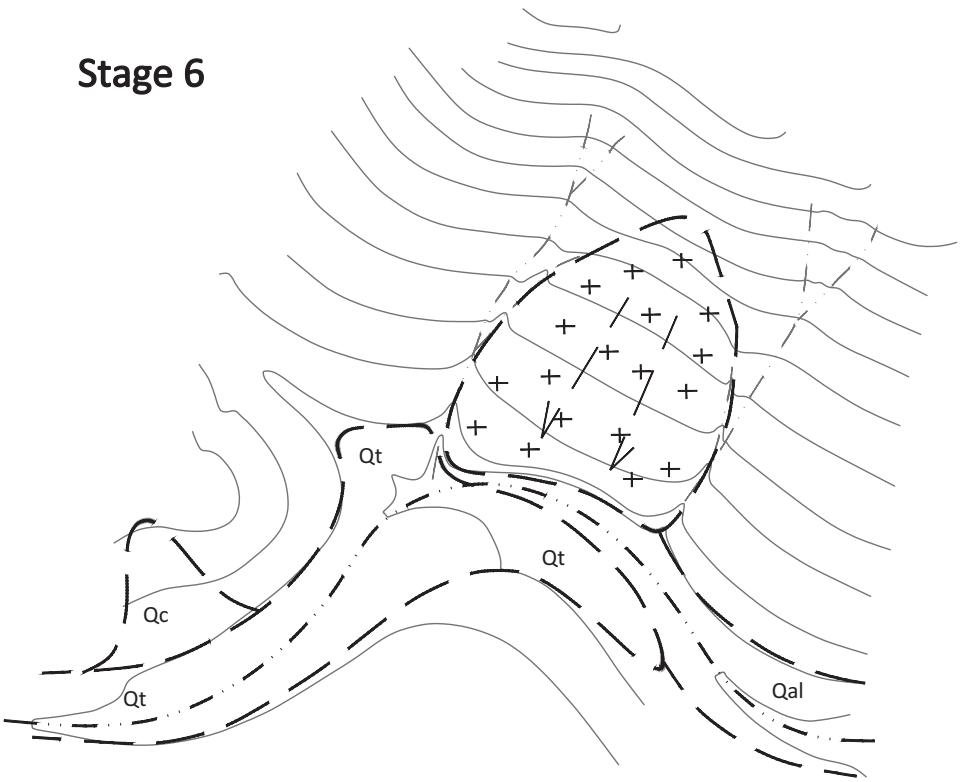

Figure 131b. Stage 6: The dormant landslide dam can become stabilized by maintaining drainage through a system of fissures along the lateral scarps and within the toe mass, which tend to form during downslope movement.

Downloaded from http://pubs.geoscienceworld.org/aeg/eeg/article-pdf/31/1/i/6130855/i1558-9161-31-1-i.pdf
by AEG RBAC user

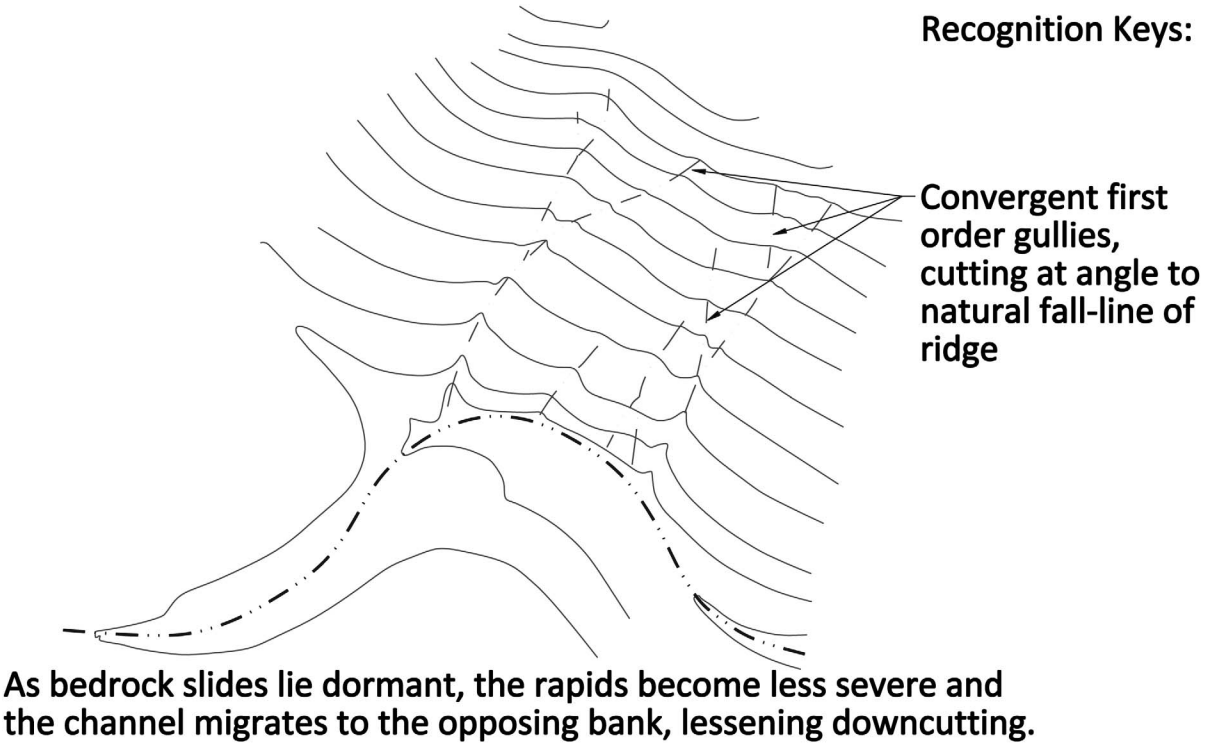

Figure 132. Recognition keys for dormant bedrock slides often include convergent first-order gullies at angles cutting across the slope's old fall lines, as sketched here. The erratic nature of the small first-order gullies is a key indicator of past disturbance.

"slump-earthflows" he had observed in clay terraces of the Licking River in Ohio, reproduced here in Figure 133a (Rogers, 1929). Several decades later Radbruch and Weiler (1963) asserted that slump-earthflows were the most common type of landslide in the Lamorinda area.

The topographic form of a slump-earthflow slide is presented in Figure 133b. In this example, the uppermost portion of the slide mass has slumped, or experienced rotational failure. The middle section has translated downslope more-or-less as a semi-coherent mass, while the toe is disintegrating into an earthflow. Thus, it is often easy to observe earthflows, rotational slumps, and translational sliding within the parent slide mass. As a consequence of their compound lineage, shallow compound slides will tend to exhibit recognition keys associated with three types of slides:

(1) The rotational slump portion will generally leave a deep headscarp, which forms a topographic bench, such as the situation shown in Figure 133b.
(2) The translational portion will tend to foster a stable displaced block, bordered by youthful gullies or incised first-order channels.
(3) The earthflow portion is usually the most difficult to detect years later, as this material is easily assimilated into the underlying slope. If covered with vegetation, it may be very difficult to detect, unless working with contour intervals of less than 10 ft (3.1 m). With a 2-ft (0.6-m) contour map, most earthflow debris lobes can be identified.

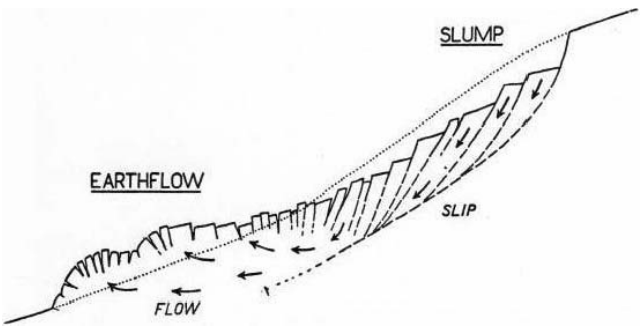

Figure 133a. One of the first sections drawn through a rotational slump-earthflow slide, as viewed in the failure of clay terraces along the Licking River in Ohio (Rogers, 1929).

The term "compound slides" was used to describe retrogressive slides by Cronin (1992), as well as "multiple slumping," which is also very common in the Orinda area. The United Nations Educational, Scientific and

Downloaded from http://pubs.geoscienceworld.org/aeg/eeg/article-pdf/31/1/i/6130855/i1558-9161-31-1-i.pdf
by AEG RBAC user

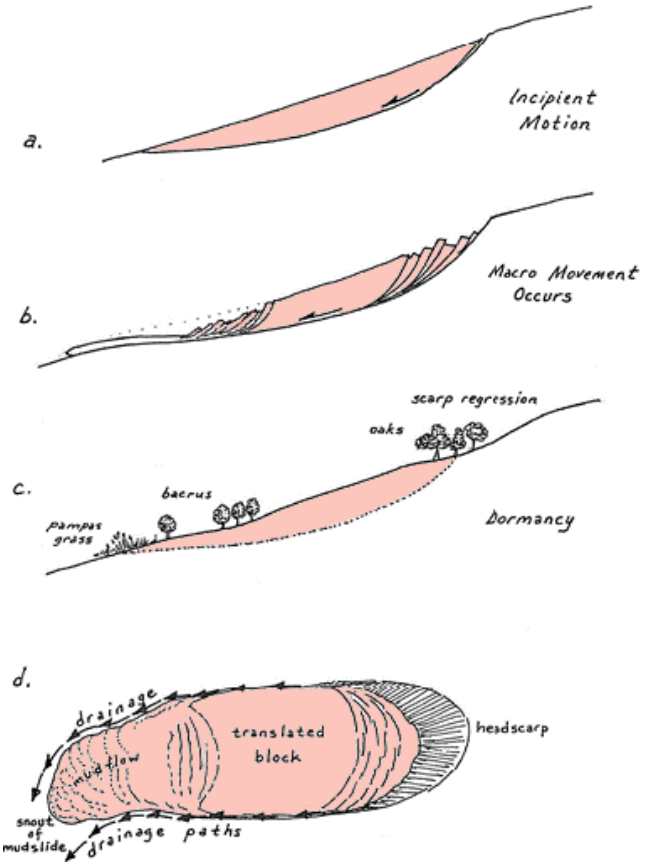

Figure 133b. As a landslide mass translates downslope, preferential "flow conduits" are created along the lateral margins of a slide, and dilation occurs in the flowing toe area. Decades later, the geomorphology of an old slide area becomes less obvious but will retain key physical characteristics common to slide-prone terrain.

Cultural Organization (UNESCO) *Multilingual Landslide Glossary* (IGS UNESCO WP/WLI, 1994b) refers to these as "multiple landslides" or "multiple rotational slides."

Figure 134a presents a section view of multiple translational slides, and Figure 134b illustrates an example of multiple slump-earthflow slides. In the United States, the most cited nomenclature emanates from Cruden and Varnes (1996), who would term these "retrogressive, multiple rotational slides."

Analysis of Shallow Composite Earth Slides–Earthflows

Analytical modeling of composite earth slide–earthflows can be difficult, due to the complex curvature of the rupture surfaces and the water table. Transient pore pressures, emergent seepage pressures, and wetting fronts are key facets in triggering earthflow regression. These physical factors can prove troublesome to measure, analyze, or model with limit equilibrium analyses (Iverson, 1992).

Modeling of shallow composite slides that include rotational rockslides, downslope translation, and eventual transition to disaggregated soil flows has not been profiled with much precision in the literature, although methods of modeling complex slide geometry have been presented. The most common approach is to lessen slice thicknesses in areas where slip surfaces or transient water tables suddenly shift or change. The strategy employed in such a technique is to lessen the variance between interslice forces and thereby more easily achieve mathematical closure in a balance of forces analysis. An effective stress analysis is the usual starting point to evaluate rotational slides in soil or weak rock, foregoing analysis of the earthflows that typically dominate the toe area (Skempton, 1964).

An example of the conventional strategy is presented in Figure 135a–b. Some practitioners have evaluated earth- and debris-flow runout by modeling the flow as a slurry, usually characterized as a Bingham fluid (Johnson, 1970). This method has some limitations, depending on the mineralogy of the suspended matter. For instance, flows composed of micaceous material will

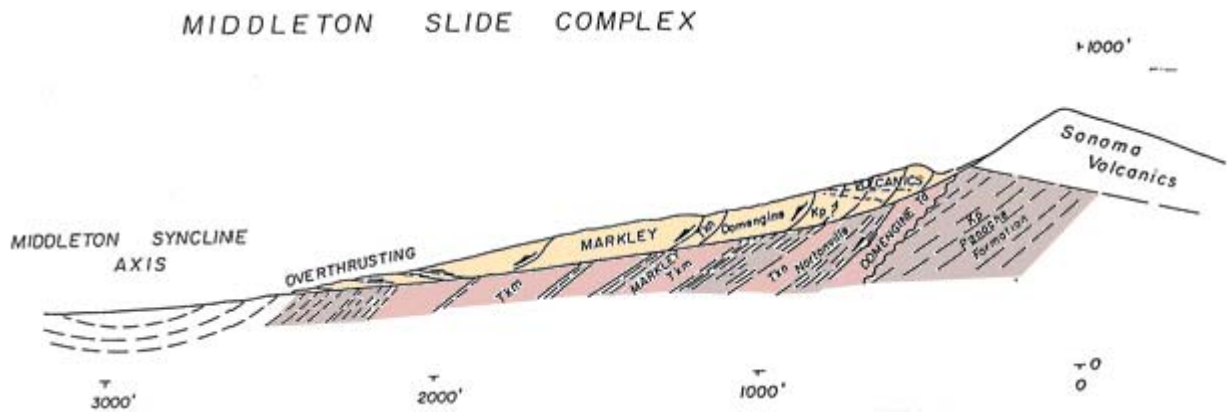

Figure 134a. Schematic section view through series of retrogressive bedrock landslides that mantle the Middleton escarpment, north of Highway 12 in Jameson Canyon in southern Napa County (Rogers, 1991).

Downloaded from http://pubs.geoscienceworld.org/aeg/eeg/article-pdf/31/1/i/6130855/i1558-9161-31-1-i.pdf
by AEG RBAC user

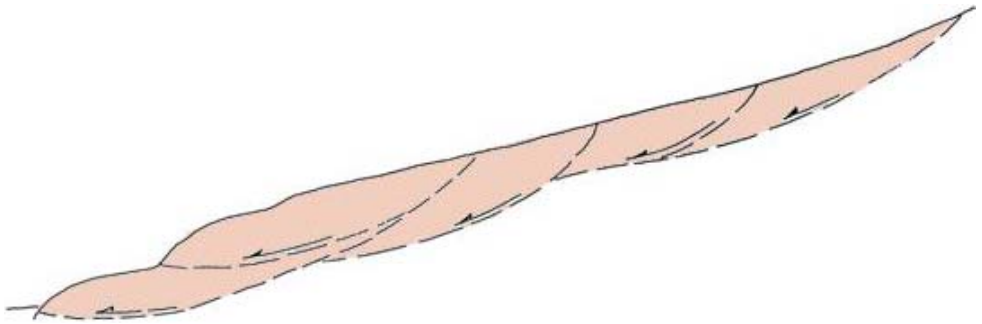

Figure 134b. Example of retrogressive rotational/translational slide complexes, taken from Molgotand Boliak et al. (1993).

tend to maintain pore pressure and behave more like a laminar fluid (Sharp and Nobles, 1953; Johnson, 1970; Morton and Campbell, 1974; Costa and Fleisher, 1984; and Pierson and Costa, 1987).

The upper half of Figure 135 shows the basic method of slices employed using the principles of limit equilibrium to analyze rotational failures in semi-coherent soils, where the soil's physical properties are averaged. The lower half presents a limit equilibrium analysis where slices of varying widths are employed to lessen the differences in interslice forces due to geometry or changes in pore-water pressure.

In attempting two-dimensional modeling of multiple earthflows, a staged analysis is necessary, in which various factors are progressively modeled and analyzed. The results of each analysis must then be applied to each succeeding step in the analytical process, controlling strain by forceful input, and adjusting depletions or accretions of transient pore-water pressures on the basis of experience. Internal pore pressures may vary with time and entrapment, as well as the rate of strain. The inclusion of static and dynamic pore-water pressures can be both tedious and expensive, necessitating a considerable deal of expertise, judgement, and experience. Free water can become trapped in the passive pressure zone of a clayey landslide mass through open fissures. This approach has been most successfully employed as a back-analysis technique.

Deep-Seated Complex and Composite Rockslides

"Deep-seated complex slide" refers to cases where various movements occur in a sequence. These often involve previously unfailed bedrock materials. Composite slides are those where different types of movements

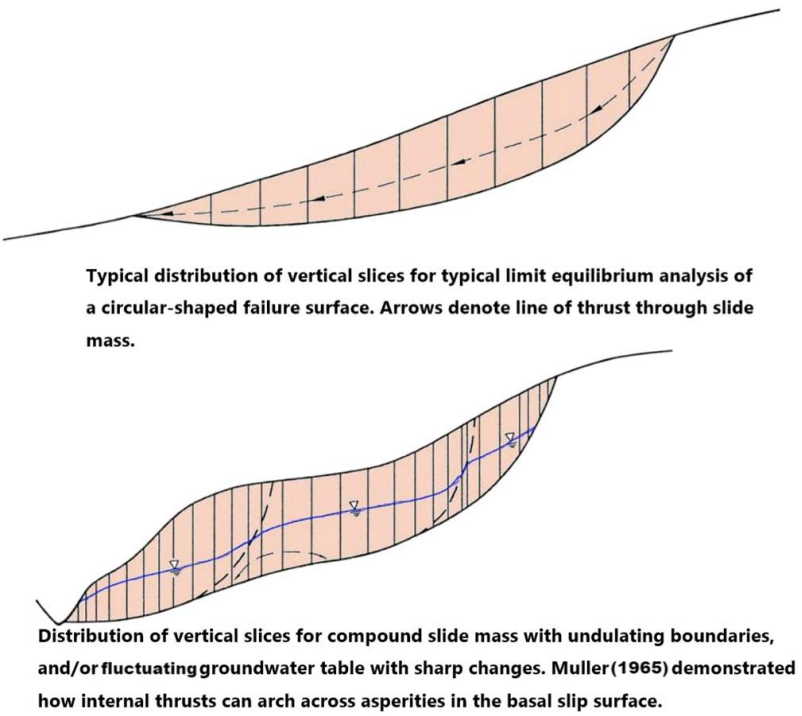

Figure 135a–b. Method of slices limit equilibrium analyses of virgin soil slumps.

Downloaded from http://pubs.geoscienceworld.org/aeg/eeg/article-pdf/31/1/i/6130855/i1558-9161-31-1-i.pdf
by AEG RBAC user

occur in different areas of the landslide mass. These tend to be deeper because they are often influenced by preexisting discontinuities and underlying geologic structure. As a consequence, most bedrock landslides fall within either of these categories.

Complex bedrock landslides can be difficult to explore or analyze. Composite landslides are not unusual when landslides extend into the underlying rock, where its stratigraphy and structure exert control on the operative failure modes, which "compete" with one another simultaneously (Vaughan and Isenberg, 1991; Cruden et al., 1991; Cruden and Varnes, 1996; and Rogers et al., 2008).

Cronin (1992) was one of the first researchers to attempt an explanation of the mechanisms likely working in complex slides. When such masses move, the hydrologic regimen is forever altered, causing perching of groundwater within discrete, slide-bounded "compartments" (Rogers, 1986). As a consequence of altered seepage flow paths and truncation boundaries, new slides will generally emerge from the underlying "parent mass" (Cronin, 1992). In this manner, complex slides generally spawn many smaller slides mantling an older, less-visible "parent slide mass." This form of superposed sliding is common to the Orinda area.

Analysis of Complex and Composite Slides

Trollope (1973, 1977) performed pioneering studies of the role played by block kinematics in the geometry of rockslides, evaluating variances in strain hardening, strain softening, pore pressure, and volume change with increasing strain. He proposed five basic failure mechanism groups with increasing complexity. These were based on the number of active failure surfaces, as shown in Figure 136.

Trollope's fifth-order mechanism is similar to the Monte Toc mega-landslide that slid into Vaiont Reservoir in September 1963, displacing the lake water over the world's highest concrete dam (at that time). This mass then swept down a narrow canyon, killing more than 1,400 people (Muller, 1964; Mencl, 1966). Mencl's analysis was unique in that he explored the concept of arching of shear stresses across asperities along the detachment boundary, illustrating that large slides can translate along fairly broad zones of shear-induced deformation.

Rogers and Pyles (1980) presented examples of some of the largest complex landslides documented in North America. They identified a fifth-order complex slide as a "block glide with rotated graben," shown in Figure 137. Unlike the cases cited by Mencl (1966), Rogers and Pyles were able to examine the detachment boundary first-hand because it was excavated by a stream. They observed a mega-breccia zone approximately 100 ft (30.5 m) thick. Catastrophic mega-landslides (slides with volumes >10 million m^3) that move rapidly seldom develop thick brecciated zones (Shreeve, 1968; Melosh, 1987).

Topographic Examples of Complex and Composite Bedrock Slides

The topographic expression of complex and composite bedrock landslides is a function of both their gross

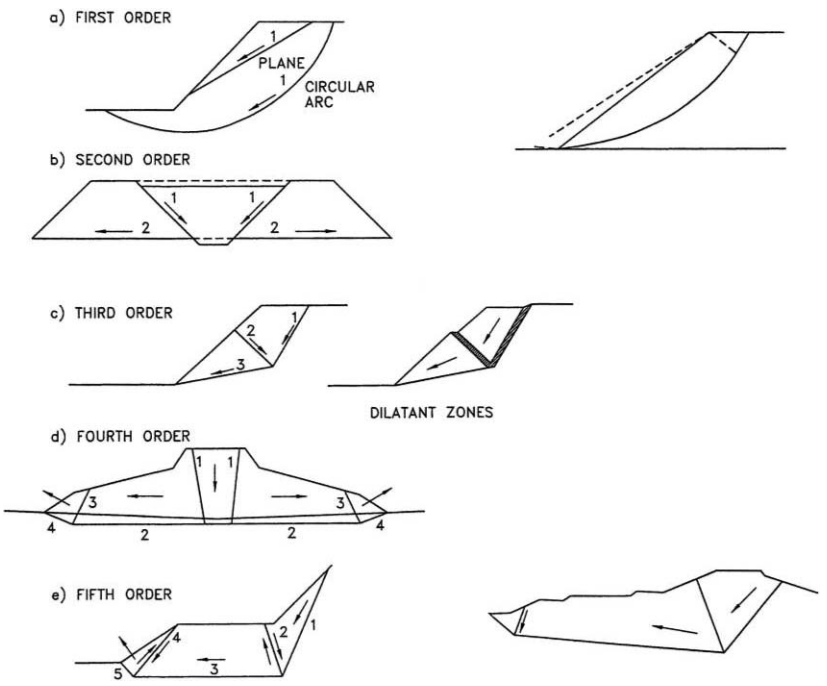

Figure 136. Complex and composite mechanisms for sliding in discontinuous rock (Trollope, 1977).

Downloaded from http://pubs.geoscienceworld.org/aeg/eeg/article-pdf/31/1/i/6130855/i1558-9161-31-1-i.pdf
by AEG RBAC user

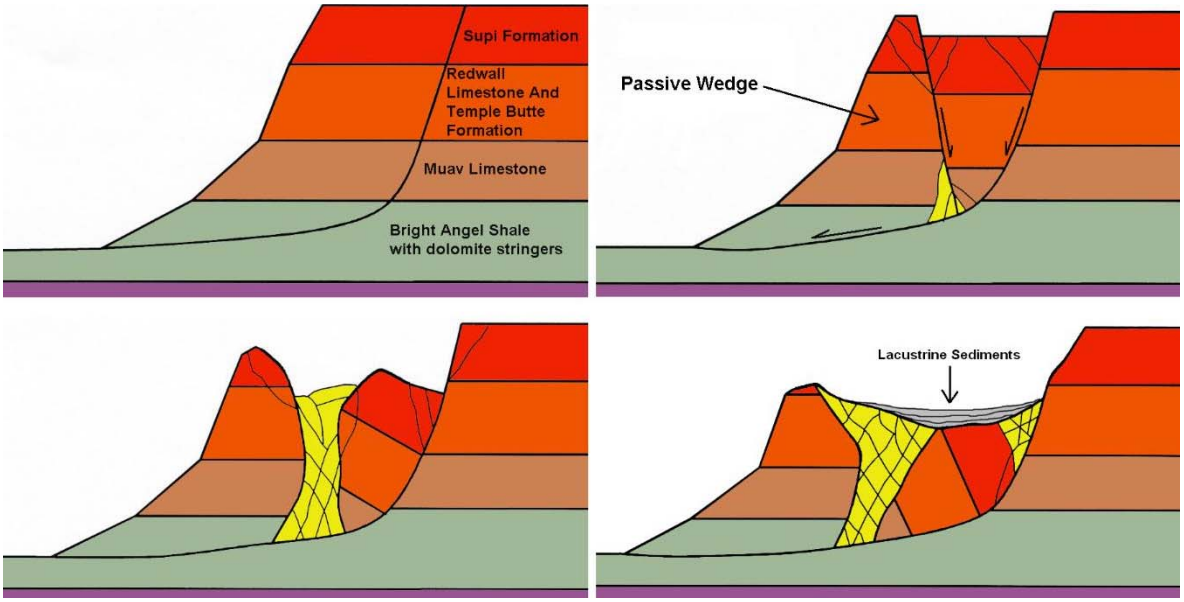

Figure 137. Hypothesized genesis of Thunder River slide, a block glide with rotational graben 2,200 ft (670.6 m) high in the western Grand Canyon (modified from Rogers and Pyles, 1980).

size and the fineness of the contour interval. Figure 138 illustrates why many of the smallest compound landslides are sufficiently large to escape notice by inexperienced interpreters. Only after sufficient familiarization with an area may interpreters be able to sift out the key indicators of compound movements. Several examples are described below.

Figure 138 presents a pair of diagrams with typical depictions of the minimum dimensions of likely bedrock landslide features as a function of map scale and topographic contour interval. Most complex or composite landslides extending into rock require a minimum of five consecutive contours to decide if the slope under analysis exhibits an anomalous morphology, suggestive of past landsliding (Ahmed and Rogers, 2014).

For a 2:1 slope inclined at 26.7 degrees from horizontal (Profile A in Figure 138), the map length of the suspected landslide would need to be >1,640 ft (499.9 m) if the contour interval is 131 feet (19.9 m). If the average slope is 3:1 (18.1 degrees from horizontal), then the minimum map length for five contour intervals would be >2,000 ft (609.6 m).

In the Orinda study, the contour interval of the orthophoto topographic map sheets was 10 ft (3.1 m). For a 2:1 slope, the minimum slope length for five contours would be >100 ft (30.5 m). For a 3:1 slope, the minimum length would be >153 ft (46.6 m).

Figure 139a presents an undeveloped area of complex sliding in the upper Pinole Creek watershed of Briones

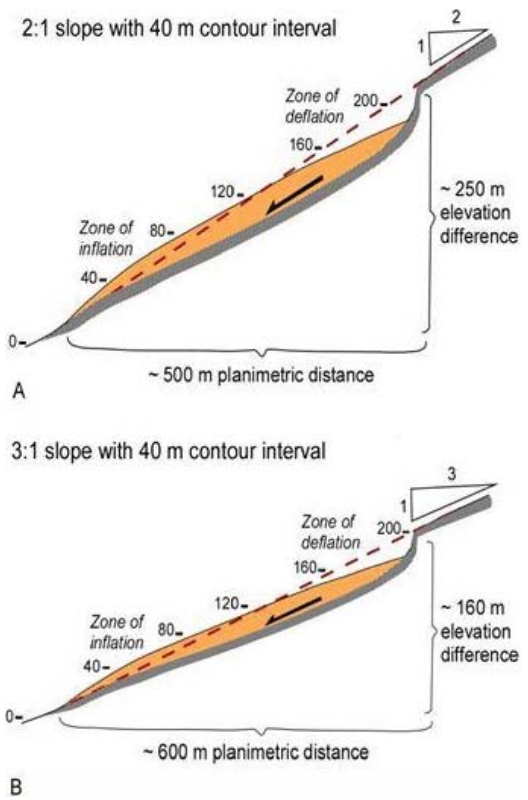

Figure 138. Illustration of how the minimum size of a mappable landslide is tied to map scale and the resolution of the contour intervals, if five consecutive contours are required to identify a potential slide feature (from Ahmed and Rogers, 2014).

Downloaded from http://pubs.geoscienceworld.org/aeg/eeg/article-pdf/31/1/i/6130855/i1558-9161-31-1-i.pdf
by AEG RBAC user

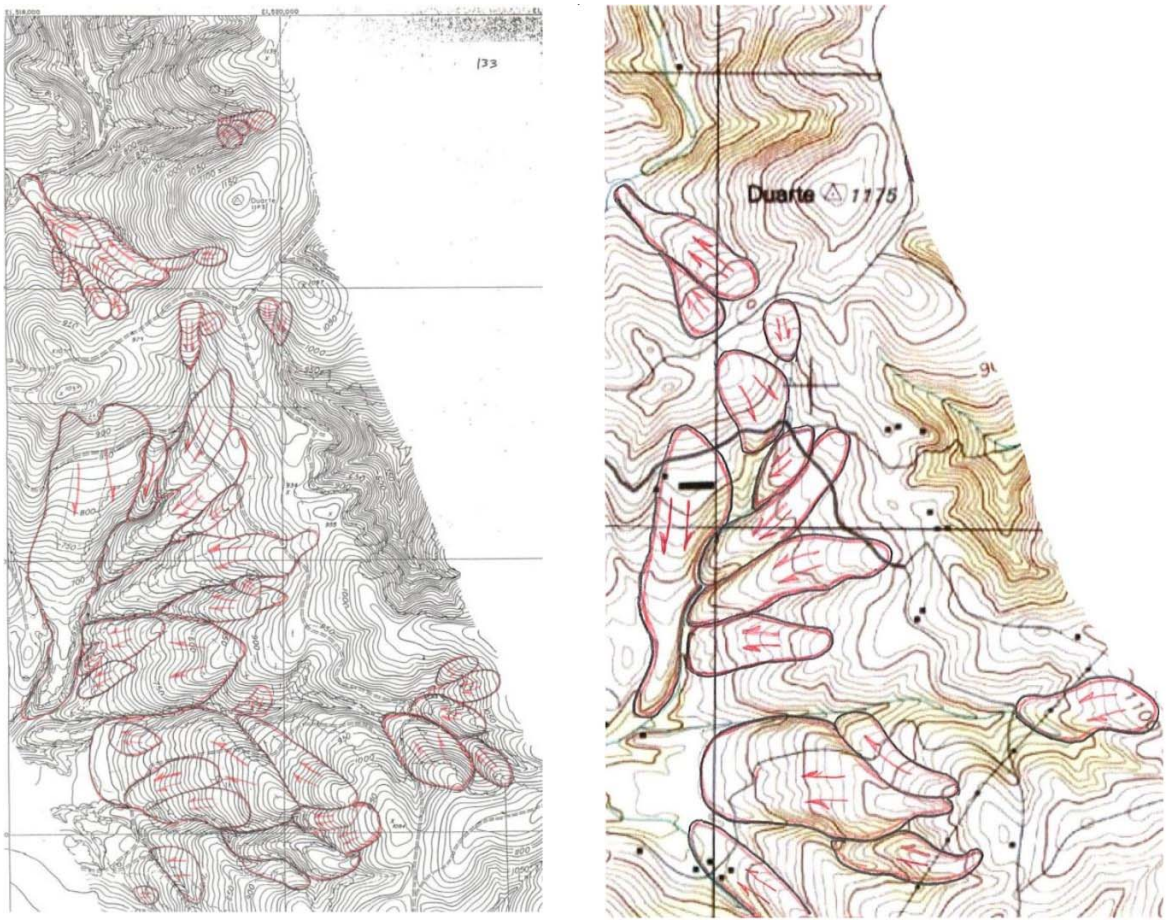

Figure 139a. Landslide map based on topographic expression, with a contour interval of 10 ft (3.1 m) at a scale of 1:4,800 (1 in. = 400 ft [1 cm = 48.0 m]).

Figure 139b. Landslide map of the same area on a USGS 7.5-minute quadrangle with a contour interval of 20 ft (6.1 m) at a scale of 1:24,000 (1 in. = 2,000 ft [1 cm = 240.0 m]).

Regional Park, northeast of Orinda. The two panels compare landslide maps prepared on a topographic base map with a scale of 1:4,800 (1 in. = 400 ft [1 cm = 48.0 m]) with a contour interval of 10 ft (3.1 m). This map is a photo-interpretation of landslides based solely on topographic expression. This area contains some of the largest landslides in Contra Costa County, with younger, smaller slides superposed upon older, and generally larger, bedrock slide masses.

Figure 139b shows a standard USGS 7.5-minute topographic map of the same area, compiled at an original scale of 1:24,000 with a contour interval of 20 ft (6.1 m). Note how the topographic expression of most of the smaller slides is noticeably obscured by the 20 ft (6.1 m) topographic contours. This contrast in scale and resolution is why landslide maps prepared by government agencies at scales of 1:24,000 or larger are compiled from of interpretation of aerial photos before being overlain on the USGS quadrangle maps as GIS "shape files."

PHOTO-GEOLOGIC ASSESSMENT OF LANDFORMS

Understanding the Geologic Framework

The first step in any photo-geologic assessment of a study area should be to identify landform units. To do this, the geologist examines visual patterns exposed in stereo-pair aerial photos or remotely sensed images that can be examined with a digital stereographic viewer or using virtual reality software and headset. The interpretive technique utilizes deductive reasoning to sort out what might underlie the ground surface to account for the observed patterns. The key factor is to recognize anomalous topographic features, which are usually discontinuous. Geomorphologists often employ "multiple working hypotheses" to sort out characteristic features of the slope morphology and begin grouping their observations.

The process is enhanced by researching and reviewing available geologic information regarding the area of

Downloaded from http://pubs.geoscienceworld.org/aeg/eeg/article-pdf/31/1/i/6130855/i1558-9161-31-1-i.pdf
by AEG RBAC user

interest. For instance, information on underlying rock formations, previous interpretations of geologic structure, soil science information, any site-specific data on depth of soil cover at discrete, identifiable locations, within or immediately adjacent to the study area, the hydrologic regimen (rainfall, seasonal intensities, mass permeability, water well information, or active pumping efforts), and an historic sense of previous physical processes. This was a methodology pioneered by Dr. Karl Terzaghi (1883–1963), recognized as the father of modern soil mechanics and geotechnics (Bjerrum, 1960; Goodman, 1999; and Rogers and Chung, 2016).

Irreproducibility of Landslides within the Human Timescale

In assessing landslide-prone terrain, a thorough knowledge of past weather patterns and the manner, scale, and distribution of slope-stability problems are of great importance. Within any given environmental extrema (such as a tropical storm), there exists a finite number of preexisting landslides or colluvial-filled ravines that possess low safety factors and are, by definition, "ripe for failure" (Terzaghi, 1950; Duncan, 1971; and Duncan and Stark, 1992). In engineering terms, these are those slopes that presently exist on the verge of failure. One great storm may be enough to trigger failure of such slopes, but it is insufficient, in and of itself, to trigger many more. Some people would feel a sense of security if no landsliding had ever been observed or appreciated, but creep and the passage of time usually combine to bring a slope closer and closer to its point of limiting stability. It is through such episodic processes that granite sea cliffs regress along portions of the California coastline.

AERIAL PHOTOGRAPHIC ANALYSIS OF LANDSLIDES

By using aerial photographic interpretation, engineering geologists can obtain a unique overview of slope morphology, or geologic form, which can be almost impossible to appreciate during casual field surveys. Ta Liang at Cornell University was the first scientist/engineer to demonstrate how aerial photos allowed geologists to peer into the past and judge how a particular slope has fared, take note of where other slides have recently occurred, and then identify those areas that might require more detailed assessment (Liang, 1952; Liang and Belcher, 1958). Universal aerial photo interpretation and mensuration techniques were established during the 1920s, 1930s, and 1940s and more widely applied to landscape and scientific studies after World War II because the predominant USGS quadrangle scale dropped from 1:62,500 to 1:24,000 (Colwell, 1960; Way, 1978).

Principle of Landslide Interpretation

In order to effectively identify various types of landslides, possibly as old as 11,000 years, it is necessary to formulate precise models of the various landslide components to be identified in the terrain analysis. Identification of landslides and landslide-prone terrain is largely a matter of scale and precision of the base map. In this study, we employed digitized topographic maps at a scale of 1:3,600 (1 in. to 300 ft [1 cm = 36.0 m]), an aerial photo base map at the same scale, and 65 years of stereo-pair imagery with scales between 1:1,200 and 1:36,000.

Key Steps when Beginning Aerial Photo Interpretation

A key step when beginning aerial photo interpretation of landslides and landslide-prone slopes is learning how to identify surficial landforms most commonly associated with past landsliding. Where soil cover exists, its presence must be identifiable. This can usually be accomplished if the underlying geology has been studied in considerable detail, and the interpreter is familiar with the respective units. For example, a clay shale, like those found in the Contra Costa Group of sediments, will have a predictable appearance on aerial photographs, as well as measurable accumulations of fine-grained colluvium, if the aerial photographs were imaged at the ends of a rainy season (commonly in late April or early May for the best tonal variations in the Lamorinda area). An example of variances in vegetation with underlying geology and slope aspect is presented in Figure 140. The lines of dry grass along the right side of the ridge are lenses of pebble conglomerate, which are the first units to dry out after the spring rains.

Before the photo-interpreter can effectively identify tonal variations and geomorphic patterns indicative of past landslippage, they must first learn to recognize key indicators of the various types of slides. This is best accomplished by evaluating case examples of landslides in the form of both ground photos and stereo-pair aerial photos. The balance of this chapter will seek to present representative examples from the Lamorinda area. Due to the difficulty in reproducing stereo-pair aerial photographs of sufficiently keen resolution, no examples will be presented in this report.

Photos of Colluvial-Filled Ravines

Colluvial-filled bedrock ravines represent the statistically most common form of landslide-related feature mapped across the Orinda area. Colluvial-filled ravines take several forms, depending on the character of the underlying bedrock. In the Lamorinda area, colluvium can be most easily seen on the undeveloped, grass-covered, southwest-facing bedrock slopes (Figure 141).

Downloaded from http://pubs.geoscienceworld.org/aeg/eeg/article-pdf/31/1/i/6130855/i1558-9161-31-1-i.pdf
by AEG RBAC user

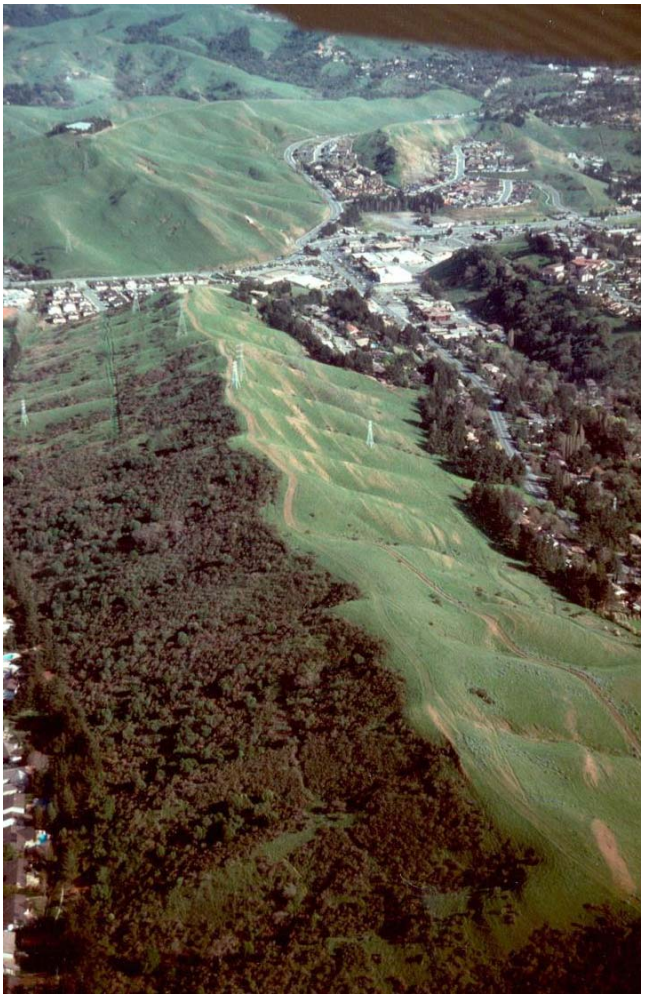

Figure 140. Aerial oblique view of Campolindo Ridge looking southeast from the Orinda-Moraga border. Note the stark contrast in vegetation between the sunny side of the ridge (at right) facing southwest and the shady side (at left) looking northeast (image by J. David Rogers in spring 1986).

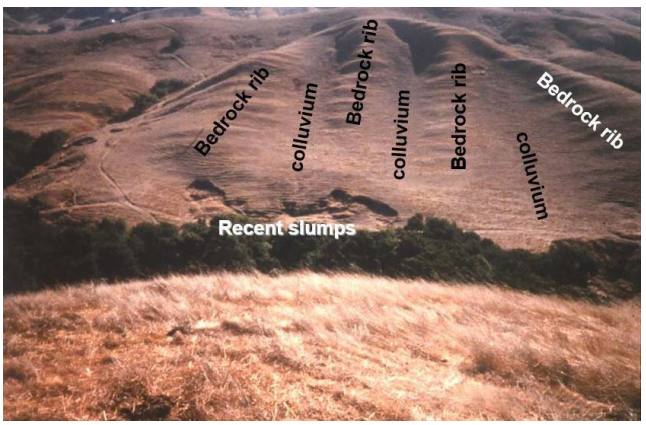

Figure 141. Alternating series of bedrock ribs with intervening colluvial-filled bedrock ravines. This was taken at Sanders Ranch in Moraga before the site was developed via mass-grading techniques espoused by Scullin (1983). Image of Sanders Ranch area in 1985 by J. David Rogers.

In other areas underlain by more homogeneous strata, rounded zero-order (slopes devoid of any discernible runoff channels) basins generally contain substantial deposits of colluvium (Figure 142). In the Briones Hills, much of the colluvium has been eroded from the bedrock basins, presumably from headward erosion of first-order streams (Montgomery and Dietrich, 1988).

These basins often appear to be pear-shaped, as seen in Figure 143. The steep-sided slopes of these basins do not allow for significant storage of colluvium, but that which is loosened by severe storm events (Cannon and Ellen, 1985) can accumulate sufficient velocity to flow with some destructive mass and velocity, depending on the watershed size and the hydraulic grades.

Figure 142. Grass-covered zero-order basins along the northeast side of Redwood Canyon in Redwood Regional Park. The faint curving trail on the ridgeline dates from the mid-1880s, when the coast redwoods in this area were initially harvested (Donald H. Gray).

Figure 143. Oblique aerial view of a classic first-order watershed in the Sunol Regional Wilderness, shortly after an intense storm triggered debris flows in January 1993. Note the streaks of muddy debris flowing into the axial first-order channel, clogging the channel (J. David Rogers).

Downloaded from http://pubs.geoscienceworld.org/aeg/eeg/article-pdf/31/1/i/6130855/i1558-9161-31-1-i.pdf
by AEG RBAC user

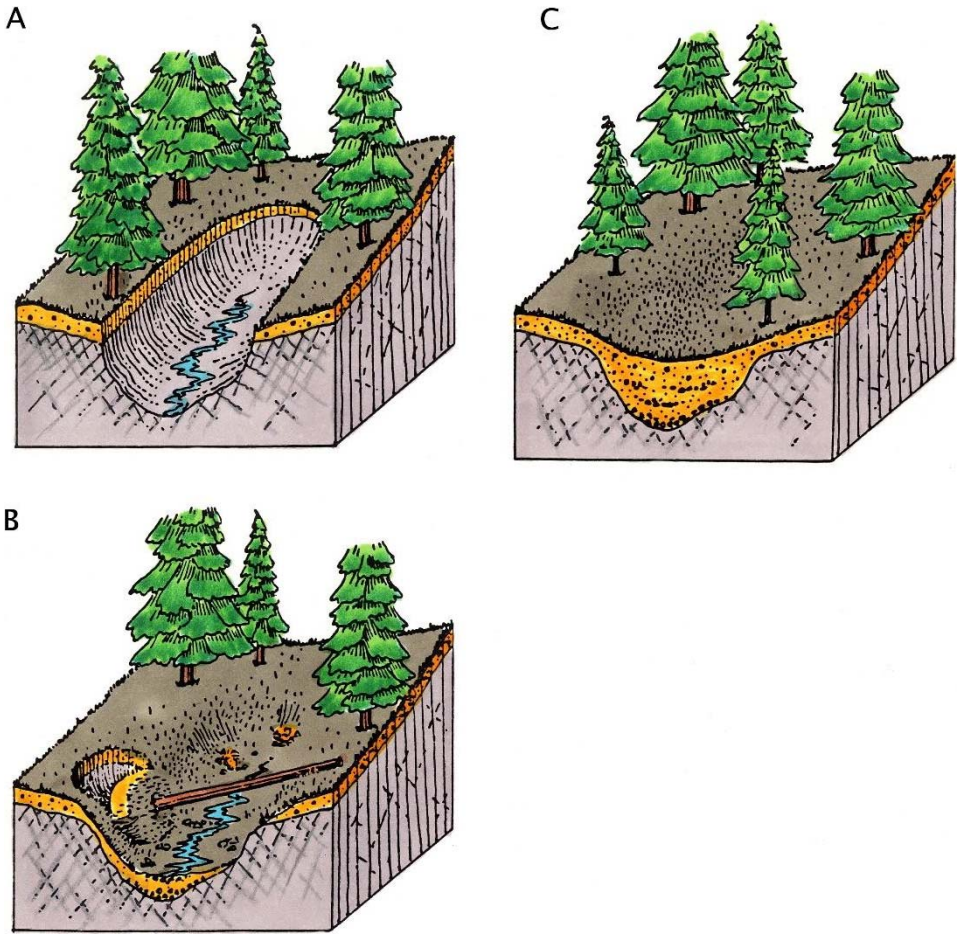

Figure 144. Successive block diagrams illustrating: (a) the end of the erosional cycle; (b) the beginning of the depositional cycle; and (c) infilling of the ravine under quasi-equilibrium conditions (modified from Dietrich et al., 1982).

The three stages of colluvial accumulation, storage, and erosion are presented schematically in Figure 144. The most common form of colluvial erosion is partial loosening of the upper 3 to 6 ft (0.9 to 1.8 m) of material, confined to the A and B soil horizons, or rooted zone closest to the ground surface.

Examples of this shallow sliding are presented in Figures 145 and 146. The photo in Figure 145 was taken from a southwest-facing grass-covered slope, while that in Figure 146 was taken on a shaded, northeast-facing slope. Note how the failure on the northeast-facing slope is about twice as deep and involved overcoming the shear strength engendered by hundreds of deep roots (Gray and Leiser, 1982).

The upper pane of Figure 147 shows how the girth and heights of the blue gum eucalyptus (*Eucalyptus globulus*) trees tend to decrease with thinning of the colluvium approaching the crest of slope. The lower pane illustrates the planar character of the A-B soil horizon that has developed on the gravelly colluvium. This horizon averages about 0.9 ft (0.3 m) thick, but increases to almost 6.6 feet (2 m) approaching the toe of the slope.

Figure 145. Shallow erosional scar in granular colluvium on an upland slope facing southwest in Marin County, CA, following intense precipitation in November 1986 (J. David Rogers).

This horizon is very porous and was noticeably compressible during exploration with hammer-driven soil samplers. The tree's root systems spread radially upon the soil-colluvium interface without meaningful

Downloaded from http://pubs.geoscienceworld.org/aeg/eeg/article-pdf/31/1/i/6130855/i1558-9161-31-1-i.pdf
by AEG RBAC user

Figure 146. Blow-out failure of a colluvial-filled ravine caused by excess seepage pressures built up behind a tear fault crossing east Glorietta Boulevard at this location in March 1983. The additional shear strength engendered by hundreds of woody roots seemed to have little impact on preventing the failure. The material was surprisingly fine grained, sourced from the Contra Costa (undivided) Formation (J. David Rogers).

penetration of the latter. The rootballs appear asymmetrical, possibly because of perennial onshore winds. Oils from the blue gum eucalyptus also tend to accumulate in the forest litter, which can volatilize during a brush fire.

Figure 147 presents a detailed cross section of the rooted zone, which is coincident with the A and B soil horizons. Reneau (1988) found this zone to have a markedly lower bulk density (due to root action and rodent activity) than the underlying zone, which accounts for its statistically frequent mobilization. Colluvium stored on rooted northeast-facing slopes would appear to have increased shear strength, due to root action. However, Radbruch and Weiler (1963) found that 70 percent of the active landslides identified between 1960 and 1963 occurred on the shaded, northeast-facing slopes of Lamorinda, which tend to support higher antecedent soil moisture levels.

According to Reneau (1988), colluvium of the San Francisco Bay region is commonly stored in bedrock ravines for 1,000 to 8,000 years, on average. The upper portions of the accumulated colluvium are often eroded

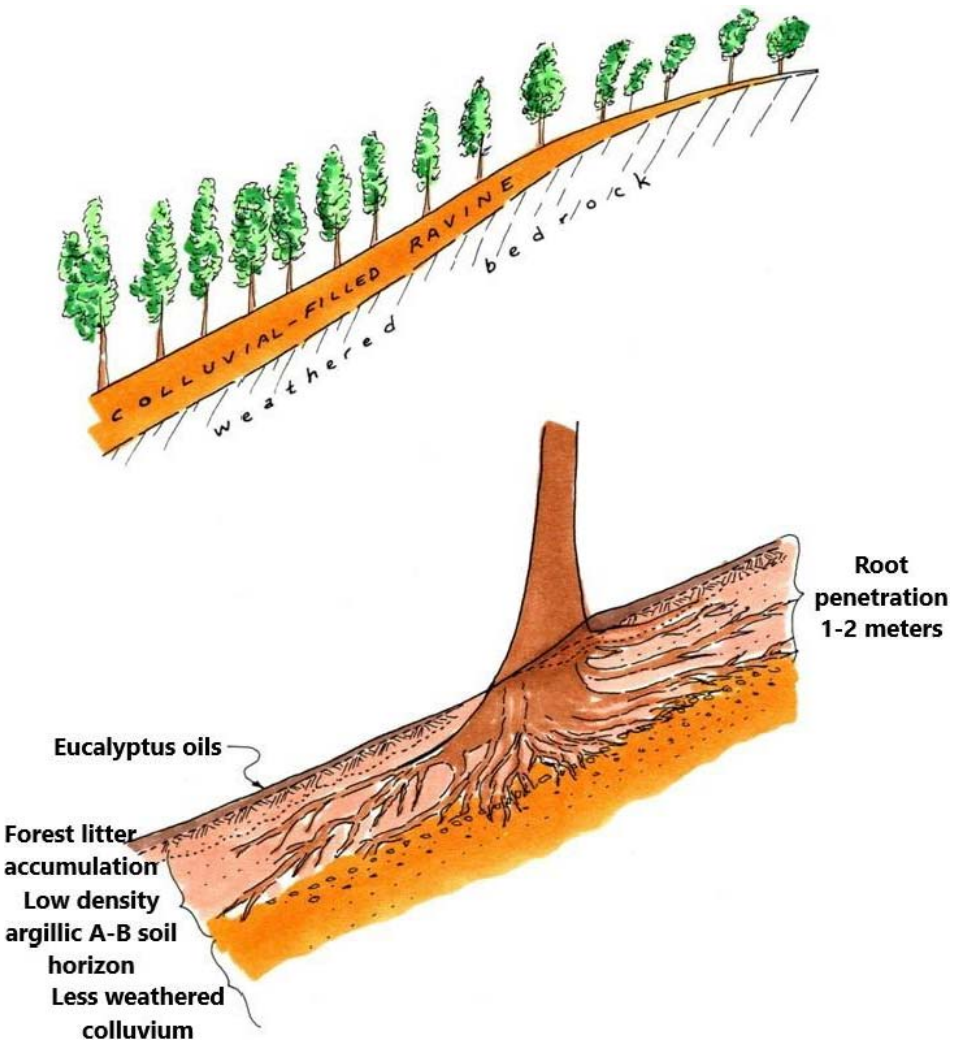

Figure 147. Sketches of weathered rooted horizon observed in a colluvial-filled ravine in upper Claremont Canyon. This southwest-facing slope recieves more precipitation than its northeastern side because of orographic (effects of hill shape on air flow) lifting and effective rainfall.

Downloaded from http://pubs.geoscienceworld.org/aeg/eeg/article-pdf/31/1/i/6130855/i1558-9161-31-1-i.pdf
by AEG RBAC user

during intense storms of extra-normal duration. Changes in prevailing weather patterns often accompany geomorphic responses, although the time necessary to invoke such responses varies according to any number of environmental factors, such as vegetation, animal habitat changes, watershed area, stream power, or global warming (Bull, 1991).

When the accumulation of environmental changes is sufficient to induce erosion of the colluvium, we often observe an active erosive cycle suddenly emerging in adjacent ravines, as shown in Figure 143. This sequence of allied erosion is colloquially referred to as an "erosive cycle," and it has been identified at other San Francisco Bay area locations between 1962 and 1988 (Lehre, 1982; Reneau, 1988). The storms of 1962, 1982, and 1986 caused countless colluvial debris flows, but many ravines were not adversely affected, probably because of effective rainfall and natural perturbations in subdrainage. Many of these could be activated during severe storm conditions, such as those that often bring extended droughts to a close when the slopes are covered by desiccation cracks that allow the maximum infiltration.

Field Examples of Earthflows

Photographic interpretation of earthflows is largely a matter of slide size, age, and vegetative cover. Recent earthflows are some of the easiest of all landslides to identify because they appear as a covering of fluid-like material, frozen in time on a smooth hillside, which is frequently referred to as "melted ice cream" flowing over the slope.

Figures 148 through 151 present examples of active earthflows common to the Orinda area. Figure 148 shows colluvial hollows undergoing an erosive cycle. In this case, the materials stored high on the slopes in bedrock depressions are too fine grained and cohesive to liquefy and become 100 percent fluidized. Instead, they just turn to sticky muck that manages to experience partial flowage (less than 300 ft [91.4 m] flow distance in episodes of maybe once every 8 to 15 years). Figure 149 presents a ground view of a large active earthflow confined to the weathered regolith and colluvium on a barren, grass-covered slope. This is perhaps the easiest form of landsliding to recognize.

Figure 150 is a low-level aerial oblique view of a dormant earthflow complex. The low sun angle allows for easy recognition of the evacuation scars and the downslope limits of the most recent flow lobe, but it does not

Figure 148. Reactivation of stored debris within colluvial hollows in the upper Tassajara Creek watershed, east of Blackhawk, in the summer of 1983, following one of the wettest 4-year periods on record. The infill is so cohesive such that the accumulated debris becomes a series of slow-moving earthflows that only travel a few tens to few hundred feet (meters to tens of meters) during a reactivation cycle (J. David Rogers).

Figure 149. Lenticular coalescing earthflow more than 2,000 ft (609.6 m) long that reactivated in March 1983 in the Tassajara Hills east of Blackhawk, blocking the channel. Note the absence of woody vegetation because of grazing and a mean annual precipitation of just 15 in./yr (38.1 cm/yr), about 58 percent of that normally recorded in Orinda (J. David Rogers).

Figure 150. Active earthflow lobes viewed in January 1993 near Carriage Hills, off Alhambra Valley Road, southeast of Pinole. The large, rounded mound in the lower center accumulated a fine-grained slide and colluvial debris up to 60 ft (18.3 m) deep (J. David Rogers).

Downloaded from http://pubs.geoscienceworld.org/aeg/eeg/article-pdf/31/1/i/6130855/i1558-9161-31-1-i.pdf
by AEG RBAC user

enhance the older, dormant lobe that extends some fair distance downslope. An experienced interpreter would map the entire lobe, down to the dirt road, as a slide, but a less-experienced person might stop at the active lobe, about 225 ft (68.5 m) upslope of the ranch road.

Figure 151 is a ground view of two blow-out failures that occurred in January 1982 along the northeastern slope of Campolindo Ridge, not far from the Rheem Valley Shopping Center in Moraga. Earthflows that fluidize and move quickly like debris flows are relatively rare in Lamorinda because of the cohesive soils. These were triggered by 8+ in. (20 cm) of rainfall recorded in 31 hours between January 3 and 5, 1982. These debris flows in clayey and silty materials flowing on a 6 degree slope are very unusual.

In most instances, the morphologic expression of earthflows is more subdued than those presented in the foregoing examples. After the passage of several years, the depositional lobes are usually dissected into chaotic microforms, giving the appearance of crenulated topography, like that seen in Figure 152. On a topographic map, this crenulated topography is a strong indicator of recent and surficial erosion (shown in Figure 120).

In the 1940s, engineering geologists colloquially referred to features like those shown in Figure 152 as "tension crack sloughs." This was because the desiccation cracks were assumed to extend only 3 (0.9 m) to 6 ft (1.8 m) beneath the ground surface during the dry summer and fall months.

In coastal California, debris-flow and earthflow events tend to re-occur every 8 to 15 years. They gradually transport soil debris to the natural drainage outlet shown above. Soil probes at that location encountered a plug of debris more than 20 ft (6.1 m) thick!

Debris flows are more likely to occur at the end of a sustained drought, when desiccation (shrinkage) cracks are deepest and most developed. The surficial desiccation allows massive infiltration of surface runoff.

Figure 151. Explosive blow-out failures of two colluvial-filled hollows on the northeastern side of Campolindo Ridge, as seen from Moraga Road in January 1982. Note fluidized silt and clay deposited on the grassy slope below the failures (J. David Rogers).

Figure 152. A coalescing earthflow complex developed within a relatively small zero-order basin off Camino Tassajara in Danville, before mass grading for residential development in the 1980s (J. David Rogers).

Figure 153 presents a low-level aerial oblique view of a dormant coalescing earthflow complex, developed upon older bedrock landslides. The hummocky nature of the surface topography is a key indicator of youthful landsliding. In addition to hummocks, the drainage pattern is deranged or without repeatable pattern or consistent form. In addition, there are many parallel-order gullies and sag ponds. Most of these features can become masked if the slopes are covered by heavy stands of vegetation. The topographic expression of the same area would be in the form of continuously crenulated surface contours. Some undeveloped areas of Lamorinda exhibit slopes that appear to be similar to this, but that are presently much drier.

Figure 153. Mature landslide terrain, like that shown here in the Klamath National Forest, is typified by hummocky topography, deranged drainage networks, often isolated sag ponds, and a surface texture that looks like a layer of "melted ice cream flowing over the hillsides" (Donald H. Gray).

Downloaded from http://pubs.geoscienceworld.org/aeg/eeg/article-pdf/31/1/i/6130855/i1558-9161-31-1-i.pdf
by AEG RBAC user

Examples of Rotational Slumps

Rotational slumps generally occur within semi-homogeneous deposits of soil and colluvium. Occasionally, rotational failures can also occur in weathered rock. A key recognition factor in slumps is their distinctively sharp headscarp, usually in a semi-circular shape. The integral accumulation of strain in an upslope direction (along the landslide slip surface) results in the sum of all downslope strain accumulating at the headscarp.

From the headscarp downward, the shear strain decreases with each increment of distance, diminishing to zero at the toe of incipient rupture (Bishop, 1971; Rogers, 1986). The distribution of shear strain engendered by incremental creep along a plane of rupture is presented schematically in Figure 154a. Figure 154b shows the various states of activity observed in creeping slopes. Creep refers to "the measured strain under sustained load" normally experienced by slopes with fine-grained materials like silt and clay. Figure 155 shows the lateral displacements that would be measured in slope inclinometers for the situation posed in Figure 154.

The shear strength mobilized within the slide plane is a function of strain. As the slide begins to creep, the strain due to slope creep retrogresses upslope (Rogers, 1979), towards the headscarp. In cohesive materials like those typical of Orinda, peak shear strengths are not usually reached until the accumulated strain along the plane of rupture exceeds between 1.5 percent and 3.5 percent, depending on clay content, plasticity, and length of the rupture surface (under "soaked conditions," but not evaluated for percent saturation). By such a mechanism, cumulative strain and mobilized shear strength are initially unique for each location along the potential slip surface, as sketched hypothetically in Figure 154a.

After examining slope creep data recorded in the weeks preceding the reactivation of the Monte Toc landslide into Vaiont Reservoir in October 1963 (Muller, 1964), most earth scientists became more respectful of the destabilization contributed by toe saturation and slope creep in triggering catastrophic landslides (Rossi and Semenza, 1967). The generalized model for creep displacement of landslides during different states of activity is presented in Figure 154b.

Many workers, such as Karl Terzaghi and David J. Varnes, believed that landslides can literally "creep themselves to rupture" because peak shear strengths are only mobilized in a single location along the rupture surface at any given time (Terzaghi, 1950; Lutton et al., 1979; and Varnes, 1997). When shearing proceeds beyond peak strength, the shear strength can drop to residual values if the materials are subject to strain softening (e.g., most common in over-consolidated shales).

The morphological form generated by rotational slumping is one of sharp, tensile headscarps or crown scarps, with much less topographic expression of the toe. An example typical of the Lamorinda area is shown in Figure 156, which is a classic log-spiral–shaped failure confined to colluvium and soil mantling a bedrock slope.

In classic back-rotation, the former slope surface becomes flattened, and over time, a topographic bench forms, as presented in Figure 120. An excellent example of a back-rotated bench is presented in Figure 157. It shows a large rotational failure that re-occurred between Warford Terrace and Muth Drive in February 1969 (it had previously failed in December 1964). Years later, the topographic bench formed by this slump appeared to the unwary as a favorable building site! The headscarps of soil/colluvium slumps can degrade rapidly (Nash, 1980), as demonstrated in Figure 75a–d and Figure 76.

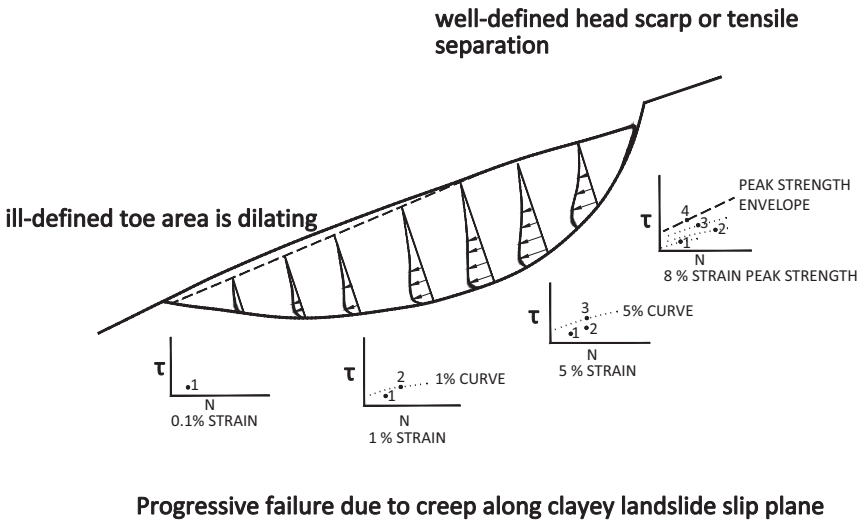

Figure 154a. Conceptual model of the progressive failure of a natural hillside triggered by recurring episodes of seasonal slope creep, exacerbated by swelling and shrinkage cycles that normally accompany wet and dry seasons (Rogers, 1986).

Downloaded from http://pubs.geoscienceworld.org/aeg/eeg/article-pdf/31/1/i/6130855/i1558-9161-31-1-i.pdf
by AEG RBAC user

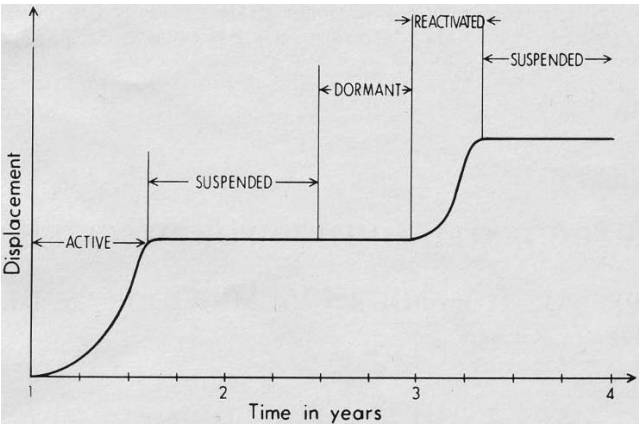

Figure 154b. Displacement of a landslide during different states of activity (IGS UNESCO WP/WLI, 1993).

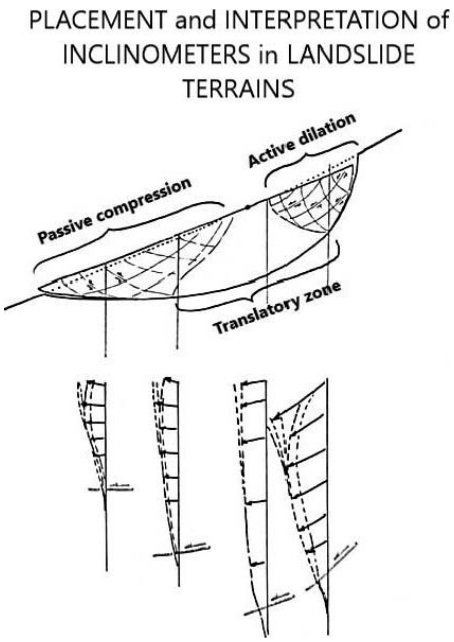

Figure 155. Representative slope inclinometer readings from the Lamorinda area. Note how the recorded movement increases upslope as an integral function of cumulative displacement, a common trait of grouted inclinometer measurements (Machan and Bennett, 2008).

Rotational slumps within weathered bedrock strata are statistically less frequent, but they occur nonetheless. Figure 152 presents a shallow coalescing earthflow complex along Camino Tassajara in 1983. The disturbed topography of a bedrock slump will remain less degraded than a similar slump in soil, which is softer and more erodible. Bedrock slumps of varying ages are widespread across the Contra Costa Hills, as shown in Figure 67.

Photographic Examples of Translational Landslides

Translational slides tend to be larger features, generally involving weathered bedrock, which usually possesses

Figure 156. Rotational slump-earthflow landslides with log-spiral–shaped failure surfaces. These examples were observed along the shady northeast-facing slope of Campolindo Ridge east of Moraga Road in March 1986 (J. David Rogers).

Figure 157. Large rotational slump block that reactivated between Muth Drive and Warford Terrace in February 1969. It had previously slid in December 1964 (Dorothy H. Radbruch, USGS).

greater shear strength than soil or colluvium slides (see Figure 158). Translational failures occur less frequently and tend to be driven by long-term accumulation of moisture (Nilsen and Turner, 1975 a&b; Rogers, 1986.

The winter of 1982–83 witnessed the reactivation of some of the largest landslides ever observed in the San Francisco East Bay Hills (Rogers, 1986). Two of these are shown in Figures 159 and 160. Figure 159 presents a low-level aerial oblique view of the Rancho La Boca slide. This slide is almost wholly composed of sandstone of the Briones Formation.

The slide reactivated in March 1983 and involved more than 1 million cubic yards (764,000 m^3) of material, being about 500 ft (152.4 m) wide and a little over 2,000 ft (609.6 m) long. The headscarp grew to about 30 ft (9.1 m) high before the downslope translation was

Downloaded from http://pubs.geoscienceworld.org/aeg/eeg/article-pdf/31/1/i/6130855/i1558-9161-31-1-i.pdf
by AEG RBAC user

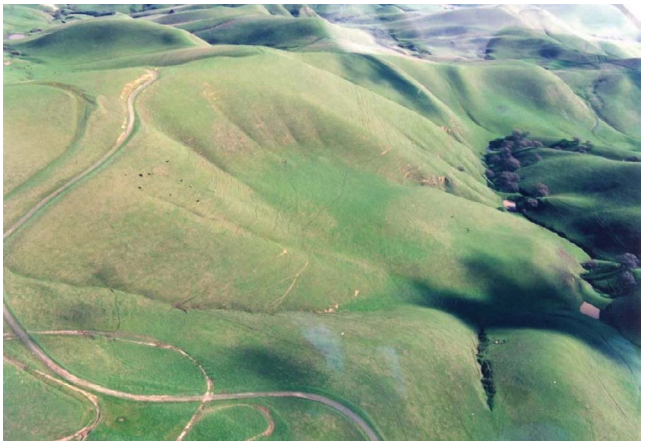

Figure 158. Aerial oblique view of a prehistoric landslide dam in the North Livermore Hills, which has quasi-stabilized itself. The movement was from left to right, with the new channel situated about 1,000 ft (304.8 m) southwest of its original location (J. David Rogers).

Figure 159. Head-on aerial oblique view of the Rancho La Boca landslide, which was reactivated in 1983. Note the plethora of open fissures in the lower half of the slide mass. It lies in the upper Pinole Creek watershed in the Briones Hills, a few miles (kilometers) northeast of Orinda (J. David Rogers).

arrested naturally. The slide reactivated in February–March 1986, but it has not been active since that time.

Figure 160 is an aerial oblique view of an unnamed bedrock slide also floored in the Briones sandstone with a headscarp 20 to 30 ft (6.1 to 9.1 m) high, similar to the La Boca slide. Note the immature parallel first-order drainages. These are often a key indicator of recent sliding. Also note the outward deflection of the gravel road crossing the upper third of the slide mass, likely attesting to greater movement in the center of the slide mass. This slide exhibits geomorphic expression typical of dormant bedrock slides in the Lamorinda area.

Other Examples of Bedrock Slides

Dormant bedrock landslides are often overlooked by geotechnical practitioners who are bereft of any previous experience with such features. To the experienced interpreter, however, many of these features exhibit key indicators that can be readily recognizable, once they have been appreciated. One of the best indicators of relict bedrock sliding is perturbed first-order drainages, especially parallel gullies that terminate short of a drainage divide.

Figure 161 presents a low-level aerial oblique view of a dormant bedrock landslide in the Contra Costa Hills between Pittsburg and Concord. Key indicators of past slippage include: (1) parallel drainages that terminate just short of the drainage divide (ridgeline); (2) anomalous pear-shape of the mass between resistant bedrock ridges; (3) anomalous topographic bench at the crown of the slide mass that is not continuous with adjacent bedrock ridges (not stratigraphically connected); and (4) anomalous outward-directed contours at the head of a second-order ravine valley.

Figure 162a presents a block diagram of this dormant bedrock slide, illustrating the outward deflection of slope contours and the parallel drainage gullies, which

Figure 160. Another aerial oblique view of a similar bedrock slide within the Briones Formation, about 1 mi (1.6 km) south of the Rancho La Boca slide (J. David Rogers).

Downloaded from http://pubs.geoscienceworld.org/aeg/eeg/article-pdf/31/1/i/6130855/i1558-9161-31-1-i.pdf
by AEG RBAC user

Figure 161. Aerial oblique view of a dormant slide mass that slid off a high point in the Los Medanos Hills between Concord and Bay Point, CA (J. David Rogers).

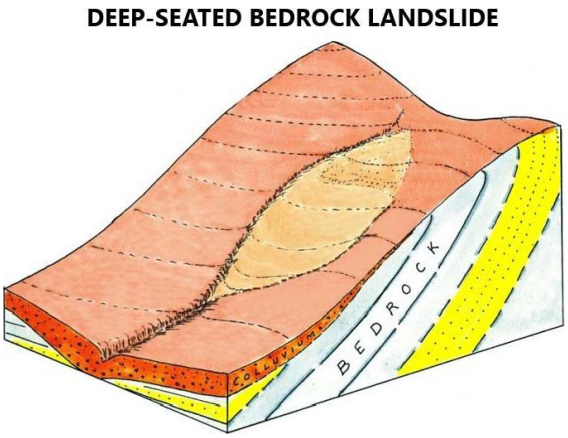

Figure 162a. Block diagram of a dormant bedrock slide mass in the East Bay Hills. These masses often slide along old bedding planes, which are inclined by local tectonic distortions, such as the uplifting of Mt. Diablo or Gudde Ridge in the crest of the Berkeley Hills.

terminate near the headscarp. Figure 162b shows a cut-away drawn through the slide mass. If an exploratory trench were to be excavated across the old headscarp of a dormant bedrock slide, this is one of the best methods to verify if underlying features have been formed by mass wasting (Rogers and Chung, 2016).

Geotechnical explorations of such features without subsurface trenches or down-hole logging of bucket-auger (large-diameter) borings often miss key structural details like those shown here. This is often because the bedrock stratigraphy tends to mimic the regional structure beneath translational block glide landslides (Varnes, 1958).

Careful evaluation of bulk density values of "weathered rock" often reveals that the materials exhibit markedly lower density values than one would expect from

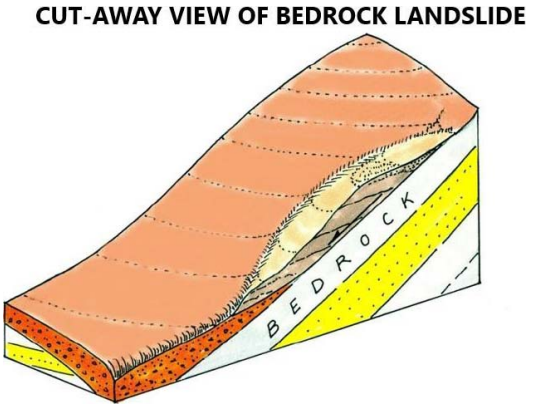

Figure 162b. Cut-away view of a relict bedrock slide (shown in light brown). Such features can usually be confirmed by trenching the bench beneath the summit of the slope and/or another trench parallel to the slope's toe. If it is an ancient feature, portions of the old slide block are often found lying above younger colluvium, shown in dark orange. Down-hole logging of 2- to 3-ft-diameter (0.6- to 0.9-m-diameter) shafts can also be employed to characterize the three-dimensional geometry of such features.

normally consolidated materials. This is usually due to dilation during downslope translation. Bedrock bulk density values of less than 120 pounds per cubic foot (pcf) (1,922 kg/m^3) should always be suspect, while values less than 100 pcf (1,601 kg/m^3) more-or-less confirm past landsliding (if the parent material is not diatomaceous or pyroclastic).

Field Examples of Dormant Bedrock Slides

Dormant bedrock slides litter the Contra Costa Hills in all shapes, sizes, and ages. Figure 163 presents a low-level aerial oblique view of the Eli Wilson landslide, the largest bedrock translational failure to occur in 1983, one of the worst years for landslide damage ever recorded. Note the blue sag ponds that have formed in the arcuate headscarp near the crest of the active slide mass. This slide is a retrogressive translational flow slide, like the infamous Slumgullion landslide in Colorado's Rocky Mountains. The Eli Wilson slide was over 1 mi (1.6 km) long and up to about 2000 ft (609.6 m) wide, with a total volume of just under 10 million cubic yards (7.64 million m^3).

The toe of the slide was regraded, and a new highway with subdrainage was installed. The slide has not reactivated significantly, and the toe is now covered with vegetation. Note that gullies have not developed upon either lateral scarp, a feature that is common in more mature bedrock slides. This may be because there is insufficient tributary watershed to sustain the volume of discharge required to excavate gullies. In either case, the accumulated runoff has been insufficient to excavate first-order channels (Bull, 1991).

Downloaded from http://pubs.geoscienceworld.org/aeg/eeg/article-pdf/31/1/i/6130855/i1558-9161-31-1-i.pdf
by AEG RBAC user

Figure 163. Aerial oblique view of the Eli Wilson landslide along Wildcat Canyon Parkway (crossing the bottom of the image) in Wildcat Canyon Regional Park during the late spring of 1983 (J. David Rogers).

Key Landslide Recognition Factors Ascribable to Weathering

Whenever bedrock masses are displaced by mass wasting, they are subject to an appreciable degree of dilation, unless the rupture surface is a perfect circle. The volumetric dilation causes a net decrease in bulk unit density of the displaced materials, such as fractured or weathered rock, saprolite, soil, and/or colluvium. Dilation and loss of bulk density generally foster advanced weathering, due to increased specific surface area of the disaggregated rock mass and proximity to surface infiltration. This infiltration of oxygenated groundwater, often containing weak carbonic acid derived from decaying organic matter, tends to promote rapid oxidation of the dilated mass. In near-surface excavations, this weathering is typified by a mottled coloration, usually reddish, brownish, or ocher- to yellow-colored hues.

As the rock weathers chemically, it becomes increasingly susceptible to mechanical weathering and runoff-induced erosion. Figure 164 presents a textbook case of selective weathering. Several intensely weathered landslide masses are being eroded by runoff in a second-order channel. A location within the natural watercourse increases the volume of concentrated flow, far exceeding that shown in Figure 161 (the two slides lie just a few miles [kilometers] from one another). Here, the topographic expression of active raveling and earthflows is dramatic, and few interpreters would overlook such a feature. On the other hand, features like that shown in Figure 161 are seldom identified in reconnaissance engineering geologic studies unless they are scrutinized by individuals with considerable experience evaluating similar features.

Figure 164. Aerial oblique view of almond-shape landslides being actively eroded by runoff in a second-order watercourse just west of Bailey Canyon in the Los Medanos Hills above Bay Point, CA.

Slope Morphologies Associated with Extended Dormancy

If hillslope profiles are shaped by innumerable series of mass-wasting events, one atop another, discontinuous remnants of relict slide masses may offer some protection from further disintegration by insulation. The example shown in Figure 164 is representative of the case where rapid breakdown would be expected due to the size of the tributary watershed upstream of the displaced masses.

In other instances, mass transport of a displaced mass is capable of moving it to a more stable orientation, usually on a much slighter grade. In such a position, reactivation may be unlikely, due to the lessened gradient and partial excavation of the slide mass. When slopes fail naturally, they initially assume a more stable geometry, aided by increased fracture porosity that enhances subdrainage. A 15 percent increase in their factor of safety is quite common, as shown in Figure 117.

Figure 165 presents a ground view of an ancient bedrock landslide in the Tassajara Hills south of Mt. Diablo.

Downloaded from http://pubs.geoscienceworld.org/aeg/eeg/article-pdf/31/1/i/6130855/i1558-9161-31-1-i.pdf
by AEG RBAC user

Figure 165. Accumulation of translated slide debris that appears to have lain dormant for thousands of years, with a high factor of safety. Note the black oak trees growing out of the displaced mass. Taken near Riggs Canyon in the Tassajara Hills south of Mt. Diablo (J. David Rogers).

The anomalous "mound" in the center of the photo are the remains of a relict landslide. Note the presence of well-developed first-order gullies along both sides of this mound. Mature valley oaks sprouting from the mass attest to an age of least 50 years, and up to 175 years in some cases (Coate, 1990). Some geologists have gone on record as stating that the presence of mature oak trees obviates any possibility of recent landsliding, but this assertion does not appear to be substantiated by tree-ring analyses.

The larger bedrock slide complexes appear to have translated about as far as they can reasonably be expected to displace before achieving long-term stability. It is also possible that some of these slides occurred in response to paleo-environmental extrema, such as sustained wet weather cycles or paleo-seismic events (Rogers and Halliday, 1992a&b).

Many of these mega-slide features blanket the Lamorinda area, though few of them pose an obvious threat, so long as large amounts of moisture are not diverted onto them.

Figures 166a–b and 167a–b are aerial oblique views of what may be a relict translational slide beneath the old county library in Orinda Village. Note the arcuate shape of the bedrock ridges above the mass and the well-developed parallel drainages. This feature might not exhibit any conclusive evidence of Holocene activity (within the past 11,000 years), but it would still require detailed subsurface sampling and mapping to enable any sort of meaningful hazard evaluation.

Figure 166a. Aerial oblique view of Orinda Village looking southeast. This was taken by Pacific Aerial Surveys on March 4, 1948. Note how few homes have been constructed on the adjacent hillsides. The horse-collar–shaped feature in the right foreground appears to be a dormant translational landslide upon which the public library is being constructed (Pacific Aerial Surveys).

Downloaded from http://pubs.geoscienceworld.org/aeg/eeg/article-pdf/31/1/i/6130855/i1558-9161-31-1-i.pdf
by AEG RBAC user

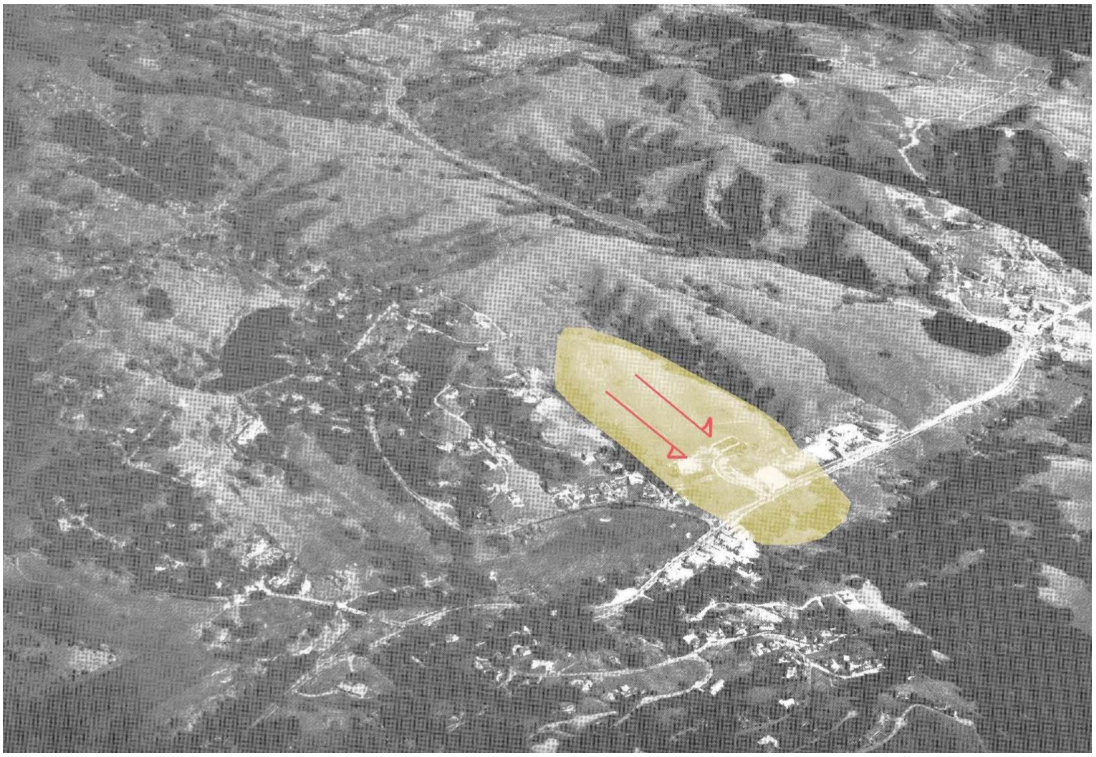

Figure 166b. On the same 1948 image, we are highlighting what appears to be a dormant prehistoric landslide feature beneath the library and the original city offices. The red arrows indicate the original direction of movement, towards the southwest (Sorrick, 1986).

Figure 167a. Aerial oblique image of the Orinda Village, Country Club, and Sleepy Hollow area by Pacific Aerial Surveys on March 12, 1954.

Downloaded from http://pubs.geoscienceworld.org/aeg/eeg/article-pdf/31/1/i/6130855/i1558-9161-31-1-i.pdf
by AEG RBAC user

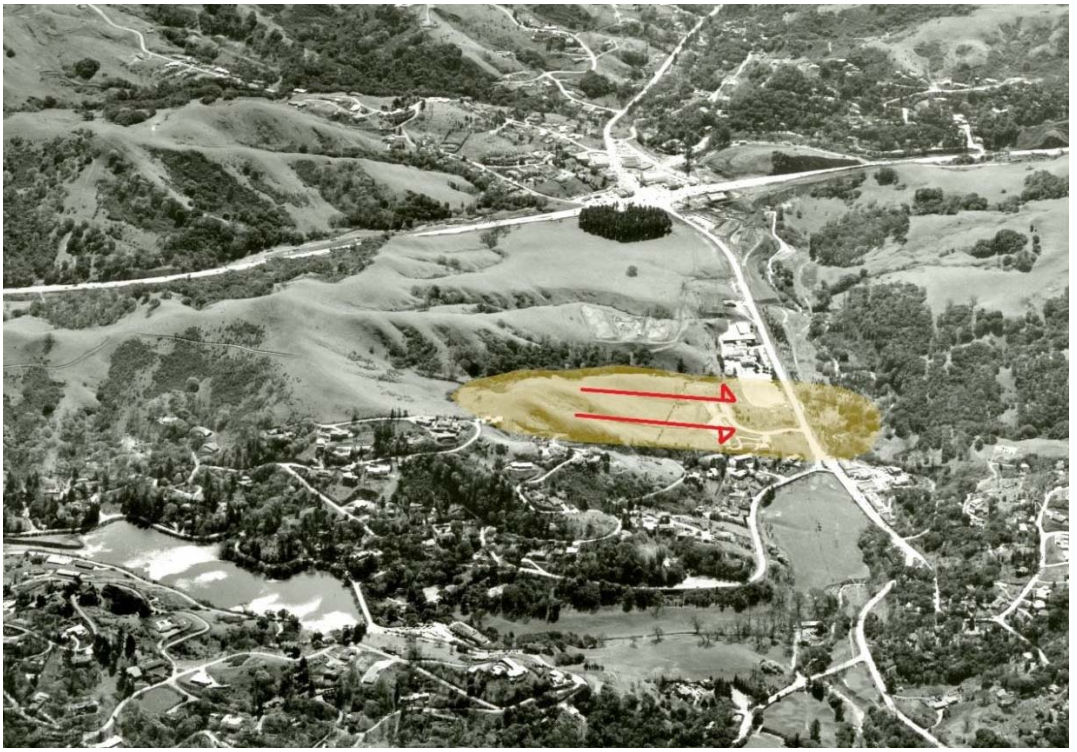

Figure 167b. Aerial oblique image highlighting the location of the dormant landslide feature beneath the library and future city offices.

Photos of Compound Landslides

No discussion of landslide morphology would be complete without including examples of compound slides, which are the most common bedrock landslide type in the East Bay Hills. Figure 168 presents an example from the Black Diamond Mines Regional Preserve south of Pittsburg and Antioch. This bedrock landslide reactivated in 1983 within a shale member of the Markley Formation. The head of the slide is a classic rotational failure, with a crown scarp ~60 ft (18.3 m) high.

Figure 168. Aerial oblique view of the "Slug slide" of December 1983, a classic slump-earthflow that was structurally controlled by a shale member of the Markley Formation at Black Diamond Mines Regional Preserve (J. David Rogers).

The central portion of the slide is a translational failure, where a semi-coherent block of bedrock and colluvium moved about 100 ft (30.5 m) downslope. The lower half of the slide is a series of shallow coalescing earthflows, which spread over unfailed side slopes and plucked additional debris by traction. In several locations along the upper flanks of the slide, there are series of retrogressive slumps, which likely occurred in response to the loss of lateral constraint and emergent seepage pressures.

LIMITING GEOMETRY OF ACTIVE LANDSLIDING

Introduction

In mapping landslides on topographic maps or aerial images, the approximate boundaries must be estimated in situations where finite boundaries may not be readily discernible, for a variety of reasons (shadows, vegetation, gaps in data, man-made alterations such as grading, etc.). In such situations, a degree of error must be expected, even in the most detailed mapping efforts. When a slide mass activates, it generally represents only a portion of the prehistoric mass wasting within the immediate area. Prediction of the precise limits of future landslippage is

Downloaded from http://pubs.geoscienceworld.org/aeg/eeg/article-pdf/31/1/i/6130855/i1558-9161-31-1-i.pdf
by AEG RBAC user

very difficult unless subsurface instrumentation, such as slope inclinometers, is available, and monitored and maintained for 6+ months.

Morphometric Analysis of Landslide Geometry (Worldwide)

The idea of evaluating landslide geometry in terms of maximum depth and length was introduced by Sir Alec Skempton in 1953, while he was studying landslides in West Durham, England. Skempton used morphometric ratios to differentiate between "surficial slips," "deep rotational slips," and "slumps."

This work was followed by that of Janbu et al. (1956) at the Norwegian Geotechnical Institute in Oslo. They measured landslide length and depth below the hypotenuse (Figure 169a) to describe variances in the depth of slide surfaces (relative to length), depending on the strength characteristics of the groundmass.

By simply ascertaining slope geometry, these relationships became an integral part of what came to be known as Janbu's simplified analysis when it was published in English (Janbu, 1969, 1973). The Janbu depth-over-length (D/L) charts allow for estimation of the calculated factor of safety with varying slip surface geometry for three differing soil types by their respective strength parameters: (1) all cohesion; (2) all friction; and (3) combination cohesion-and-friction materials.

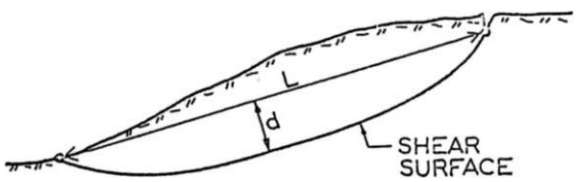

Figure 169a. Landslide length, L, and depth, d, as defined by Janbu et al. (1956).

In the geologic literature, Jones et al. (1961) selected the ratio of horizontal to vertical components of landslide length-to-depth as the significant quantitative descriptor of landsliding. Their work centered upon rotational slumps exposed along the Columbia River Valley in northeastern Washington, where first- and second-order channels have bisected older slump-style slides. These exposures had been photographed by some of the landslide studies pioneers like Sharpe (1938a&b) and Varnes (1958), which allowed for direct measurement of the maximum depth of sliding.

A few years later, Davidson (1965) made similar measurements for his master's degree research on landslides in New Zealand. This and subsequent measurements were presented by McLean and Davidson (1968). They assembled a compelling case for landslide depth-to-length ratios as constants for various types of landslides that they evaluated on the Gisborne Coast of New Zealand. Selby (1967) made similar comparisons in his graduate studies in the Waikato Hills of New Zealand.

Beginning in 1968, Crozier (1973) carried the idea a step further by presenting pioneering data on the shape and planimetric form of various types of landslides. He defined landslide length as the entire distance over which movement could be traced upon a map or photograph (Figure 169b). Crozier differentiated between

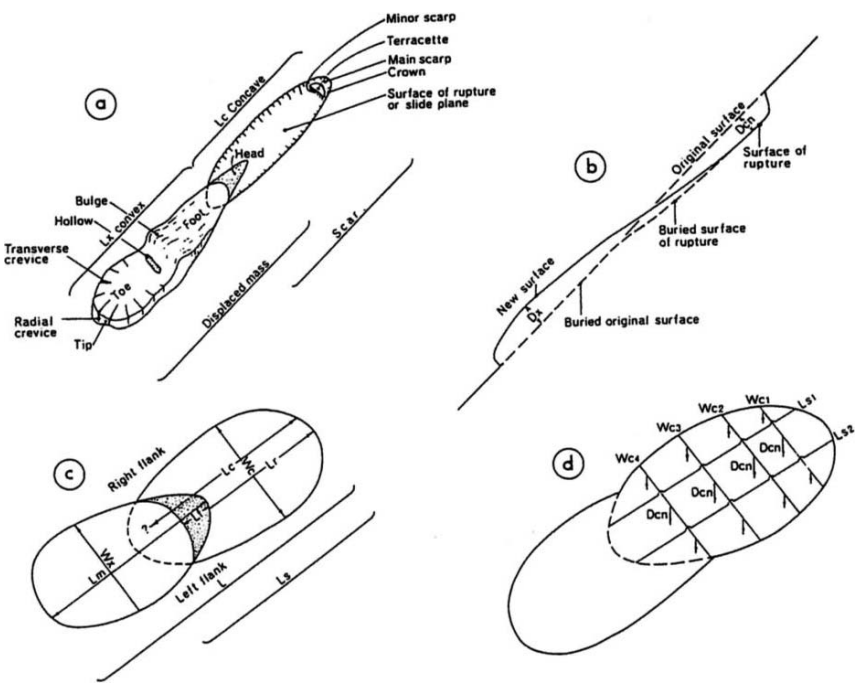

Figure 169b. Landslide terminology and indices proposed by Crozier (1973) and used by many other workers since, like Selby (1993).

Downloaded from http://pubs.geoscienceworld.org/aeg/eeg/article-pdf/31/1/i/6130855/i1558-9161-31-1-i.pdf
by AEG RBAC user

landslide width in the evacuation scar (W_c) and width of the displaced mass (W_x). This schema was subsequently adopted by other geographers and geomorphologists, including Selby (1982, 1993).

In the geotechnical engineering literature, Skempton and Hutchinson (1969) suggested a standardized system by which landslide dimensions could be compared (Figure 169c). This information could then be applied as a limiting bound for estimating the depth and shape of landslide slip surfaces to construct more accurate analyses of slope stability. In analyzing the Eau Brink cut-slope failure, Skempton (1964) demonstrated that circular failure surfaces predicted in soil mechanics analyses did not match the positions of rupture surfaces measured in the field.

In the early 1990s, Baum and Fleming (1991) presented a pioneering effort that evaluated the accretion of tension and compression within active slide masses. They demonstrated that the maximum displacement within large landslides occurs within a relatively undeformed zone, between the zones of stretching (headscarp) and shortening (toe). Their work also suggested that the boundary between driving and resisting elements of any slide is very close to the thickest (deepest) area of the active slide mass.

Macdonald et al. (1993) presented relationships among slide width, thickness (depth), and cross-sectional area in describing paleo-megaslides and slide sheets on Alexander Island in Antarctica. They also included similar geometric data on other mega-landslides from around the globe.

Morphometric Analysis of Landslide Geometry (Northern California)

In studying the limiting geometry of landslides of the Orinda area, Dorothy Radbruch and Louise Weiler (1963) were the first USGS scientists to attempt comparative measurement of slide features. In their 1960–63 study of 229 active landslides in the Lamorinda area, Radbruch and Weiler measured lengths and widths of the virgin ground displacements, as defined in Figure 169d.

Waltz (1967) also measured length and width values for the virgin failure area on shallow landslides in Alameda and Contra Costa Counties in the mid-1960s. He assumed the failure surfaces of the slides to be log-spiral shaped. The log-spiral shape of a virgin rupture surface was introduced in 1936 by Leo Rendulic, a doctoral student of Karl Terzaghi at the Vienna University of Applied Sciences. He approximated log-spiral–shaped failure surfaces as primary ellipsoids, a technique that produced a more realistic approximation of the failure surface geometry than semi-circles of constant radius describing the zone of rupture, especially for shallow earthflows (Rendulic, 1936a&b; Goodman, 1999).

In his master's degree research at Humboldt State University, Rex Upp (1977) attempted to estimate slip surface geometry from initial landslide width and overall slope length on relatively small landslides in the Rio Dell Formation of Humboldt County (Figure 169e). He also measured the cross-sectional area of these slides. Upp found that the shape of the failure surface depended on the underlying geology and the physical properties controlling shear strength, a similar conclusion to that of Skempton (1953). Upp concluded that the maximum depth of sliding could be described by the relationship $D = 0.17W \pm 0.09W$, where D = maximum depth, and W = maximum width, with the proviso that the relationship only applied to active surficial slides within the Rio Dell Formation.

In 1983, Greta Orris of the USGS began measuring the maximum lengths and widths of active landslides within the Santa Clara Formation in the vicinity of Palo Alto for her master's degree research at San Jose State University (Orris, 1983). Her test sample grew to include 157 slides in Santa Clara County as far south as

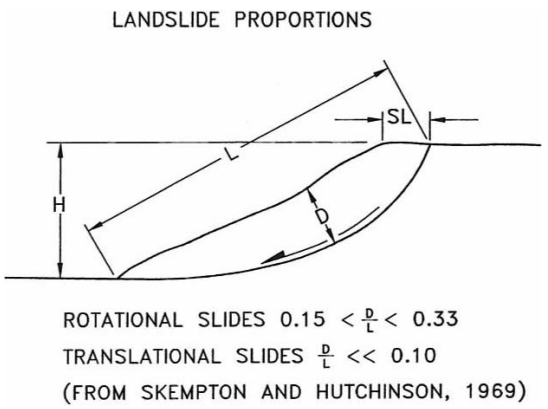

Figure 169c. Definitions of landslide proportions, length (L), depth (D), height (H), and scarp length (SL), from Skempton and Hutchinson (1969).

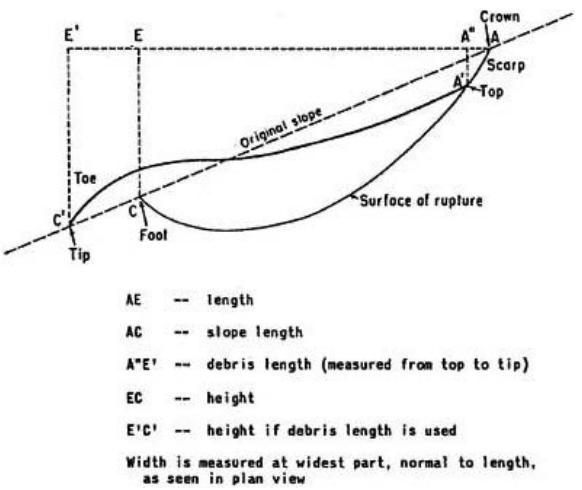

Figure 169d. Definitions of landslide indices proposed by Radbruch and Weiler (1963) while mapping landslides in the Orinda area.

Downloaded from http://pubs.geoscienceworld.org/aeg/eeg/article-pdf/31/1/i/6130855/i1558-9161-31-1-i.pdf
by AEG RBAC user

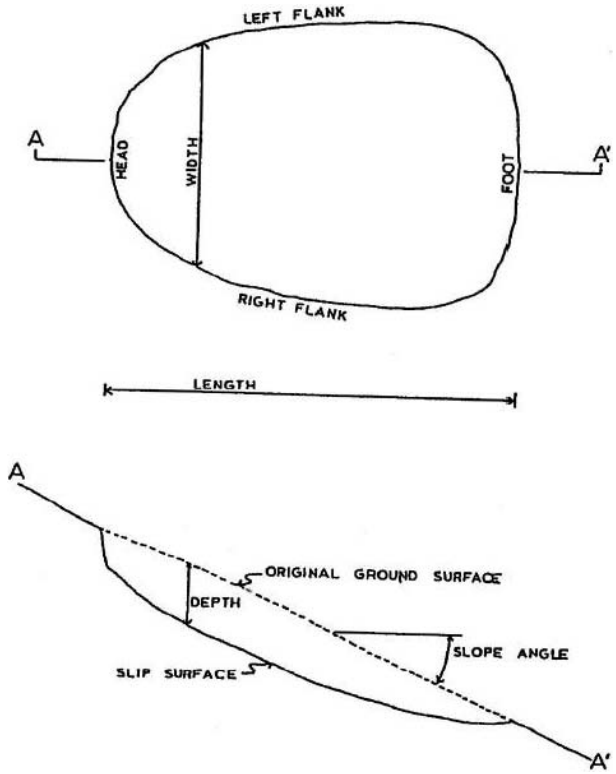

Figure 169e. Landslide dimension schema proposed by Upp (1977) in his study of slump-earthflow slides in Humboldt County, CA.

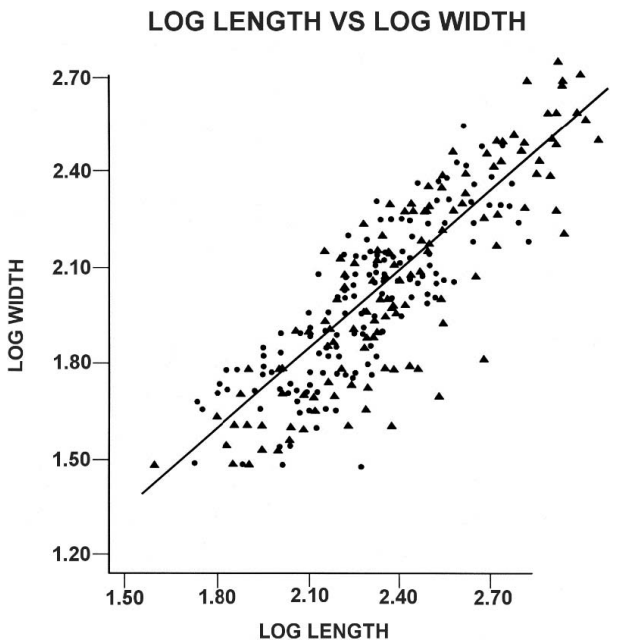

Figure 170. Relationship between logarithmic values of landslide width versus length for recently active slides. The solid circles represent 157 slides in Santa Clara County, and 89 triangles denote additional data measured by Rogers and Chung (2017) in Alameda and Contra Costa Counties (modified from Orris and Williams, 1984).

Gilroy (Orris and Williams, 1984). The data exhibited a great deal of scale variability using the maximum length and width measurements across recently active slides (and not the virgin rupture surfaces hidden below the ground surface). The plot created by Oris and Williams is reproduced in Figures 170 & 171, along with 89 additional measurements gleaned from Alameda and Contra Costa Counties by Rogers and Chung (2017).

In 1977, Rogers (1986) began tabulating landslide length-to-depth measurements in Alameda and Contra Costa Counties. This work continued through 2016. Rogers and Chung's charts were published in 2017; these charts were limited to virgin rupture surface dimensions, the schema suggested by Skempton and Hutchinson (1969). They found that *L*:*D* ratios tend to rise with increasing length to as much as 30, but they noted that some of the non-linearity is likely influenced by the structural and stratigraphic controls on deep-seated rupture surfaces and the presence of low-strength discontinuities (Rogers and Chung, 2017).

PHYSICAL FEATURES OF LANDSLIDES

Inclusive Definition of a Landslide

From 1932 to 1937, C. F. Stewart Sharpe studied mass wasting and landslides in North America for his doctoral dissertation at Columbia University titled *Landslides and Related Phenomena*. In 1935, he moved to Washington, D.C., to work for the newly established Soil Conservation Service (SCS) as an assistant soil conservationist. In 1941, he was promoted to acting head of the Physiographic Section of the Climatic and Physiographic Division of SCS, where he remained until 1943.

In his Ph.D. dissertation, Sharpe outlined the first formal classification of landslides in a tabular form that recognized different types of mass movements, as well as their respective mass-transport mechanisms, such as slippage, flow, glacial transport, and fluvial transport. This effort is described in more detail in Appendix 1.

Sharpe's classification schema is reproduced in Figure 172a. He attempted to mix the various types of mass movements and the modes of material transport. These distinctions included the kind of movement and the speed of movement, and whether it was transported by glacial (ice) material or water. The types of slides were "earth or rock plus ice, earth or rock dry or small amounts of water, and earth or rock plus water."

The categories of mass wasting included subsidence, rockfalls and rockslides, debris slides/debris falls, debris avalanches, mudflows, earthflows, solifluction, soil creep, talus creep, and rock creep. These subdivisions influenced several generations of earth scientists and physical geographers and led indirectly to the sponsorship of a more in-depth volume on the same

Downloaded from http://pubs.geoscienceworld.org/aeg/eeg/article-pdf/31/1/i/6130855/i1558-9161-31-1-i.pdf
by AEG RBAC user

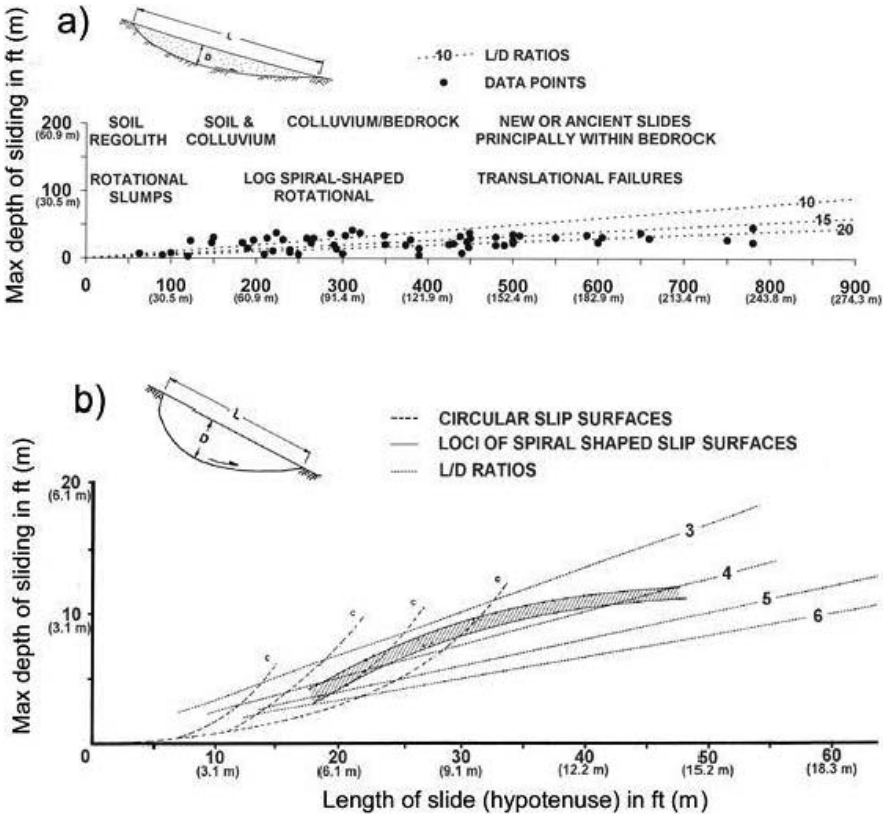

Figure 171. Length to depth ratios reported by Rogers and Chung (2017) for a wide range of studies in Contra Costa and Alameda Counties between 1976 and 2016.

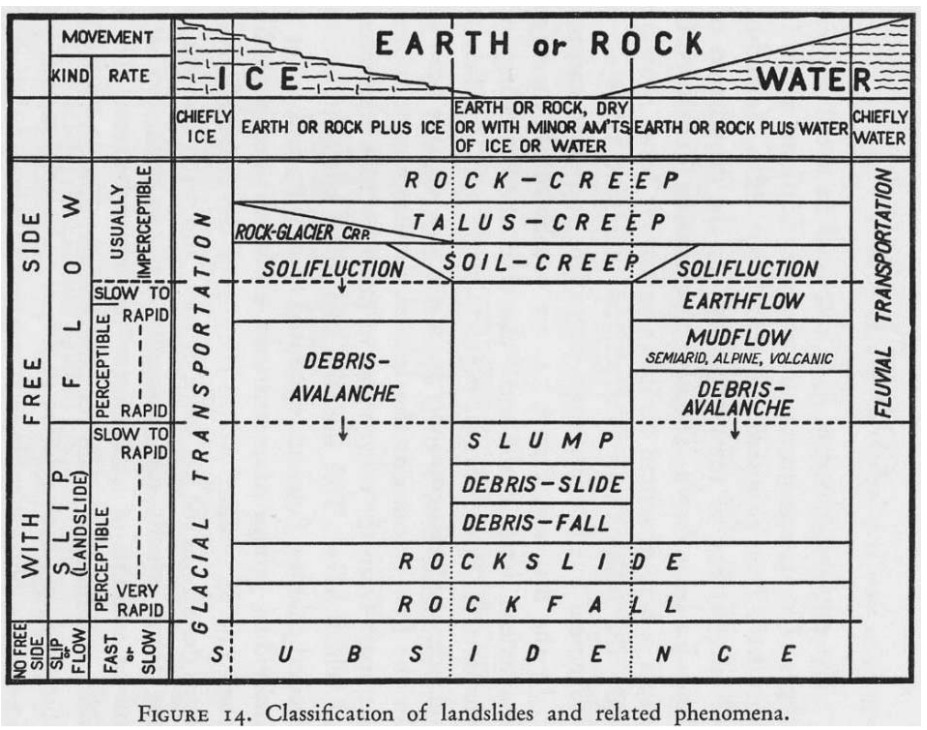

Figure 172a. The first formal classification of landslides and related phenomena was prepared by C.F. Stewart Sharpe (1938b) of the new U.S. Soil Conservation Service in 1938.

Downloaded from http://pubs.geoscienceworld.org/aeg/eeg/article-pdf/31/1/i/6130855/i1558-9161-31-1-i.pdf
by AEG RBAC user

TYPE OF MOVEMENT	TYPE OF MATERIAL			
	BEDROCK		SOILS	
FALLS	ROCKFALL		SOILFALL	
SLIDES — FEW UNITS	ROTATIONAL SLUMP	PLANAR BLOCK GLIDE	PLANAR BLOCK GLIDE	ROTATIONAL BLOCK SLUMP
SLIDES — MANY UNITS		ROCKSLIDE	DEBRIS SLIDE	FAILURE BY LATERAL SPREADING
FLOWS	ALL UNCONSOLIDATED			
	ROCK FRAGMENTS	SAND OR SILT	MIXED	MOSTLY PLASTIC
DRY	ROCK FRAGMENT FLOW	SAND RUN	LOESS FLOW	
		RAPID EARTHFLOW	DEBRIS AVALANCHE	SLOW EARTHFLOW
WET		SAND OR SILT FLOW	DEBRIS FLOW	MUDFLOW
COMPLEX	COMBINATIONS OF MATERIALS OR TYPE OF MOVEMENT			

Figure 172b. Abbreviated version of David J. Varnes' initial classification of landslides presented in HRB SR 29 in 1958 (Varnes, 1958).

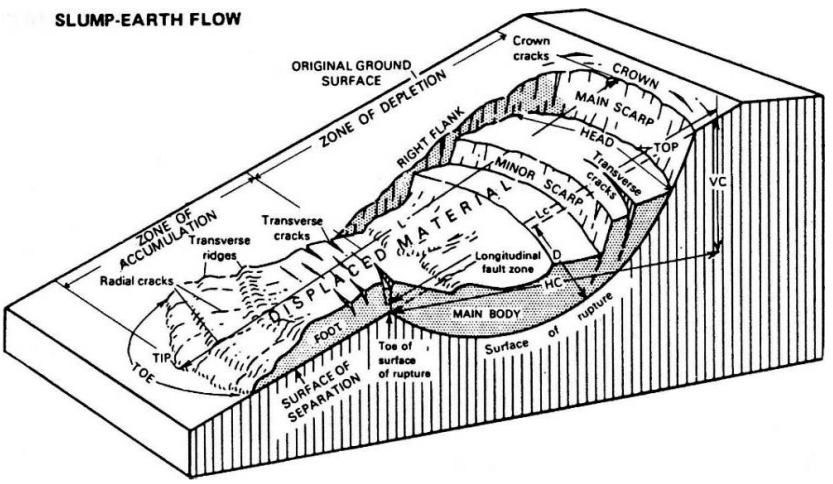

Figure 172c. Suggested nomenclature for physical characteristics of a landslide, using a slump-earthflow slide as the generic surficial landslide (Varnes, 1958).

subject for highway engineers and engineering geologists, described below.

Highway Research Board Special Report 29 (1958)

In the early 1950s, the U.S. Highway Research Board (HRB) set up the landslide committee to evaluate the various kinds of slides common to North America that often impact highways. The committee's 15 members were composed primarily of engineering geologists employed by state and federal agencies, along with the three professors and two consultants that comprised HRB's Department of Soils, Geology, and Foundations.

The key personnel assigned to the effort were from the Engineering Geology Branch of the USGS, established in 1945 and led by Edwin B. Eckel until 1961. Eckel chaired HRB's Committee on Landslide Investigations, which spent 3 years preparing a 232-page monograph titled *Landslides and Engineering Practice*, released in 1958 as Highway Research Board Special Report 29 (HRB SR 29; Eckel, 1958).

HRB's point man for characterizing the various types of landslides and their physical processes was Eckel's principal subordinate, David J. Varnes of the USGS Engineering Geology Branch in Denver. A 1940 graduate of the California Institute of Technology (Caltech) in geology, Varnes was a legendary figure in the USGS because of his insights into the interplay of associated scientific theories that allowed him to work on the periphery of many related fields, including reconnaissance field mapping, earthquakes and seismo-tectonics, economic and structural geology, and even rock

Downloaded from http://pubs.geoscienceworld.org/aeg/eeg/article-pdf/31/1/i/6130855/i1558-9161-31-1-i.pdf
by AEG RBAC user

mechanics. His interest in landslides emanated from his first wife Helen Dowling, a fellow USGS scientist who had studied complex and composite bedrock landslides in southwestern Colorado in the late 1940s.

Varnes was a self-starter. He loved studying new problems that had surprising consequences or to be entrusted with solving some new problem. Whenever he received a new assignment to investigate a particular phenomenon, he would expend considerable effort to understand what everyone preceding him had tried and what their respective conclusions had been. He was undoubtedly motivated by scientific curiosity. When placed in the framework of a disciplined work ethic, he willingly accepted multi-disciplinary challenges during his 53-year career with the USGS.

For HRB SR 29 (Eckel, 1958), Varnes began with a thorough review of Stewart Sharpe's text, which led to a correspondence between the two men. David Varnes decided to classify landslide movements according to the physical factors that would be relevant to their prevention or control, because those aspects were the central theme of HRB's project. Briefly summarized, state highway engineers wanted technical guidance in their operations and maintenance decisions, not a compendium of scientific studies.

As a consequence, Varnes (1958) defined landslides in very basic terms that most engineers could understand on Page 2:

> "Landslide" denotes downward and outward movement of slope-forming materials composed of natural rock, soils, artificial fills, or combinations of these materials. The moving mass may proceed by any of three principal types of movement: falling, sliding, or flowing, or by their combinations.

Perhaps the most important contribution was the committee's oversized "Classification of Landslides," which included 20 examples of various types of mass movements with a simple descriptive nomenclature (included in Appendix 1). Figure 172c shows the most cited of the example landslide types. This nomenclature has appeared in many publications since 1958. Some of the technical terms are colloquial, such as "crown scarp," "main scarp," and "headscarp," any of which could be describing the same feature/aspect. Most of these descriptive terms remain in use today, although more comprehensive schemata have been advanced from time to time, such as that presented by Hungr et al. (2014).

The First "Gold Standard": HRB SR 29 (1958–78)

HRB Special Report 29 (Eckel, 1958) soon became the "gold standard" for landslide studies for public and private entities/organizations. It was not superseded until 1978, when HRB's successor agency, the Transportation Research Board (TRB), released Special Report 176 *Landslides: Analysis and Control*, edited by Robert Schuster and Raymond Krizek (1978). This volume became the most-cited publication on landslides until 1996, when the TRB released Special Report 247, *Landslides: Investigation and Mitigation*, edited by Keith Turner and Robert Schuster (1996). Both of these monographs were published by the National Academy of Sciences of the United States of America and quickly established themselves as "benchmark contributions."

In 1961, Varnes succeeded Ed Eckel as chief of the Engineering Geology Branch of the USGS. In 1964, he was among the star performers at USGS who were dispatched to Alaska to document the effects of the second-largest earthquake ever measured on the planet up to that time.

In the 1970s, Varnes guided the UNESCO publication on engineering geologic mapping and landslide hazard zonation, which netted several international awards. After these globe-trotting assignments, he began working with Dorothy Radbruch-Hall on rock creep to failure and sackungen spreading phenomena, beginning in the late 1970s (Varnes et al., 1976, 1989).

Varnes was keenly aware of the early research activities conducted by the USGS in the Orinda area, which led to a dramatic expansion in urban and engineering geology in the 1970s. Much of this work focused on performance research in Alameda and Contra Costa Counties, and series of planning documents that were without precedent at that time, using San Mateo County as the example government entity, and then enlarging these efforts through significant collaboration with the Association of Bay Area Governments to reach the 10 counties comprising the San Francisco Bay Delta region, which supports a population of 7.75 million people.

The definition of landslides has continued to evolve with time, and the International Association of Engineering Geology and the Environment (IAEG) Congress in Paris adopted the present definition in 1991 (Cruden, 1991b). Varnes (1958) also prepared a simple classification scheme for landslides based on four types of movement: falls, slides, flows, and complex (Figure 172b). The two fundamental material types were "soils" and "bedrock."

In 2014, Oldrich Hungr, Serge Leroueil, and Luciano Picarelli (Hungr et al., 2014) published "The Varnes classification of landslide types, an update." It suggested 29 classes of landslides based on seven types of movement: fall, topple, rotational sliding, rock sliding, translational sliding, lateral spreading, and flows, and three types of materials: rock, debris, and earthen. It provides a succinct executive summary of the variety, volume, and complexity of landslides, especially those emanating from crystalline bedrock terrain in mountainous locales. Hungr, Leroueil, and Picarelli's scheme for landslide classification is described in more detail in Appendix 1.

Downloaded from http://pubs.geoscienceworld.org/aeg/eeg/article-pdf/31/1/i/6130855/i1558-9161-31-1-i.pdf
by AEG RBAC user

Attempts to Formulate Standardized Methods for Measurement of Landslides

In 1990, the UNESCO Working Party on World Landslide Inventory and IAEG suggested a standardized methodology for reporting the position, date, type, geometry, volume, and damage of significant landslides (Cruden, 1990). They suggested features and dimensions for reporting landslide geometry reproduced herein as Figure 173. Cruden (1991a, 1991b) reported on the UNESCO group's recommendations within both international and American engineering geologic literature. Cruden (1991b) also presented simple definitions for the term "landslide," which have come into widespread acceptance.

Landslide Features

Definitions of various landslide features (Figure 173) and measurement of landslide dimensions (Figure 174) were adopted by IAEG in 1990–93 (Cruden et al., 1990) and published in *Landslides: Investigation and Mitigation*, by the Transportation Research Board and the National Academy of Sciences of the United States of America (Turner and Schuster, 1996), for use in the United States and Canada.

In 1990, the IAEG Commission on Landslides established a nomenclature for the observable features of an active landslide (IAEG Commission on Landslides, 1990). In reference to Figure 173, showing a plan and section of a complex earth-slide earthflow, the features were defined as:

(1) Crown: The practically undisplaced material adjacent to the highest parts of the main scarp.

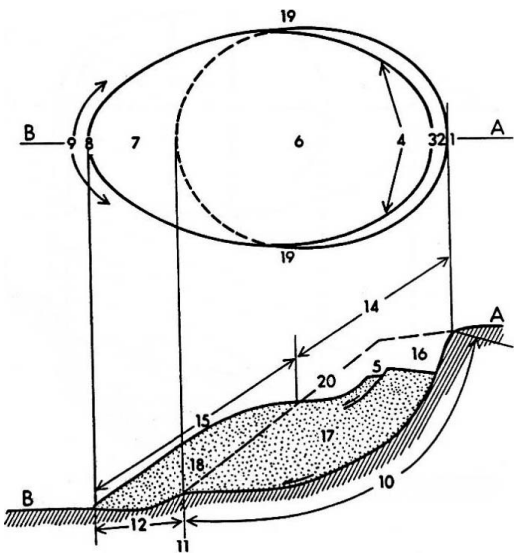

Figure 173. Schema for reporting physical features common to active landslides, recommended by Cruden et al. (1990) and included in Cruden and Varnes (1996).

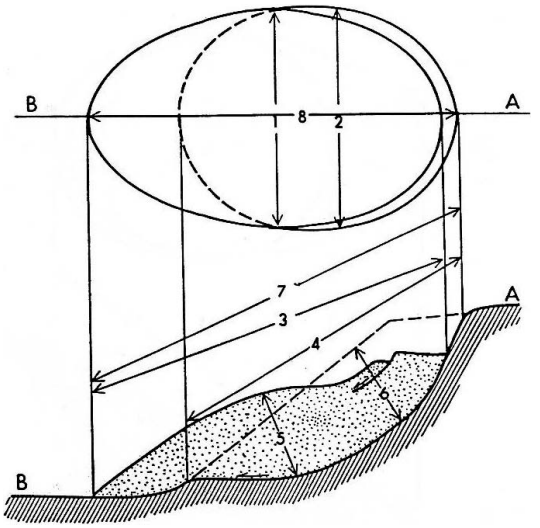

Figure 174. Recommended schema for recording the dimensions of a typical landslide, recommended by Cruden et al. (1990) and included in Cruden and Varnes (1996). The hachure pattern indicates undisturbed ground.

(2) Main scarp: A steep surface on the undisturbed ground at the upper edge of the landslide caused by movement of the displaced material (13, all the stippled part) away from the undisturbed ground. It is the visible part of the surface of rupture (10).
(3) Top: The highest point of contact between the displaced material (13) and the main scarp (2).
(4) Head: The upper parts of the landslide along the contact between the displaced material and the main scarp (2).
(5) Minor scarp: A steep surface on the displaced material of the landslide produced by differential movements within the displaced material.
(6) Main body: The part of the displaced material of the landslide that overlies the surface of rupture between the main scarp (2) and the toe of the surface of rupture (11).
(7) Foot: The portion of the landslide that has moved beyond the toe of the surface of rupture (11) and overlies the original ground surface (20).
(8) Tip: The portion on the toe (9) farthest from the top (3) of the landslide.
(9) Toe: The lower, usually curved margin of the displaced material of a landslide, which is the most distant from the main scarp (2).
(10) Surface of rupture: The surface that forms (or that has formed) the lower boundary of the displaced material (13) below the original ground surface (20). The mechanical idealization of the surface of rupture is called a slip surface in Chapter 12 and 13 (IAEG Commission on Landslides, 1990).
(11) Toe of surface of rupture: The intersection (usually buried) between the lower part of the surface of

Downloaded from http://pubs.geoscienceworld.org/aeg/eeg/article-pdf/31/1/i/6130855/i1558-9161-31-1-i.pdf
by AEG RBAC user

rupture (10) of a landslide and the original ground surface (20).

(12) Surface of separation: The part of the original ground surface (20) now overlain by the foot (7) of the landslide.

(13) Displaced material: Material displaced from its original position on the slope by movement in the landslide. It forms both the depleted mass (17) and the accumulation (18). It is stippled in Figure 3.1 (IAEG Commission on Landslides, 1990).

(14) Zone of depletion: The area of the landslide within which the displaced material (13) lies below the original ground surface (20).

(15) Zone of accumulation: The area of the landslide within which the displaced material lies above the original ground surface (20).

(16) Depletion: The volume bounded by the main scarp (2), the depleted mass (17), and the original ground surface (20).

(17) Depleted mass: The volume of the displaced material that overlies the surface of rupture (10) but underlies the original ground surface (20).

(18) Accumulation: The volume of the displaced material (13) that lies above the original ground surface (20).

(19) Flank: The undisplaced material adjacent to the sides of the surface of rupture. Compass directions are preferable in describing the flanks, but if left and right are used, then they refer to the flanks as viewed from the crown.

(20) Original ground surface: The surface of the slope that existed before the landslide took place.

Measuring and Appreciating the Limiting Geometry of Landslides

Tracking geometric parameters of landslides within any given area is a valuable tool to incorporate in reconnaissance mapping of landslides. Limiting ratios on expected length-to-width or length-to-depth values can help to delineate likely boundaries when such features become obscured. In addition, a simple check of the area's L/D ratio will usually aid in any subsurface exploration or slope-stability analysis.

(1) Width of the displaced mass, W_d: the maximum breadth of the displaced (d) mass perpendicular to the length, L_d.

(2) Width of the surface of rupture, W_r: the maximum width between the flanks of the landslide, perpendicular to the length, L_r.

(3) Length of the displaced mass, L_d: the minimum distance from the tip to the top.

(4) Length of the surface of rupture, L_r: the minimum distance from the toe of the surface of rupture (r) to the crown.

(5) Depth of the displaced mass, D_d: the maximum depth of the displaced mass, measured perpendicular to the plane containing W_d and L_d.

(6) Depth of the surface of rupture, D_r: the maximum depth of the surface of rupture below the original ground surface measured perpendicular to the plane containing W_r and L_r.

(7) Total length, L: the minimum distance from the tip of the landslide to its crown.

(8) Length of the center line, L_{cl}: the distance from the crown to the tip of the landslide through points on the original ground surface equidistant from the lateral margins of the surface of rupture and the displaced material.

Methods Employed in the Orinda Study

In this study, geometric controls were often applied to areas that appeared to have fostered past landslippage. These controls consisted of applying appropriate landslide length-to-depth and length-to-width ratios for single slide events, based on measurements in the East Bay Hills in the 1980s (Rogers, 1986) and included in the data shown in Figures 170 and 171.

FIELD CHECKING TECHNIQUES

Appreciating Local Experience with Landslides

For engineering geologists studying landslides, a longer window of observance will increase the chance that various styles and manners of landslides will be revealed. Having a "window" of site-performance experience of 25 years or more to draw upon might seem like a lot to an engineer, but it is a mere blink of time for the geologist (Terzaghi, 1945). This is because geologists are trained to think in terms of thousands and millions of years, while most people tend to view age in terms of a normal lifetime (e.g., ~84 years).

Engineers tend to assume that all of the slopes with low factors of safety could be expected to fail in a 100-year recurrence event. Engineering geologists tend to be more aware of geologic time, but they seldom collect sufficient data to substantiate the relative ages of various elements, like terrace deposits. Engineers and geologists should appreciate that a significant storm lasting several days in duration does not necessarily trigger mass wasting on every slope, even statistically significant storms (i.e., 1 in 100 chance of occurrence). This is because we do not know what a 100-year recurrence event is until we have ~1,000 years of hydrologic records (Chow and Takase, 1977).

Terzaghi (1950) opined that natural slopes experience a diminution in safety factor with each significant load cycle (wet-dry season), and that we should expect every

Downloaded from http://pubs.geoscienceworld.org/aeg/eeg/article-pdf/31/1/i/6130855/i1558-9161-31-1-i.pdf
by AEG RBAC user

slope's intrinsic factor of safety to degrade with time. He also suggested that slope failures are generally limited to those slopes that were on the verge of failing when the storms began.

This premise is supported by field evidence gathered during the 20th century. In a detailed evaluation of landslide reactivation in Moraga during the period 1925 to 1988, Rogers/Pacific, Inc. (1989) found that very few landslides recurred during that 60-year interval, despite a series of extreme weather events between the mid-1920s and the late 1980s.

Some measure of this is likely due to significant variability in weather patterns. When considering patterns of succeeding months or years, Dettinger et al. (2011) found that very few atmospheric river events are statistically repeatable. In 1950, Terzaghi opined that natural slopes or embankments exist at their own unique factors of safety, which tend to degrade slightly with each load cycle (such as freeze-thaw, wet versus drained, or moisture accumulations over periods of decades or centuries, etc.).

In the Orinda study, we were fortunate to have gathered aerial photos dating back 65 years (1928 to 1993) with weather records dating back to the mid-19th century (the oldest beginning in 1849, while another data set stretched back to 1895). Added to this raw data, we drew on the tremendous body of experience with slides accumulated over the previous century.

Field Exploration Techniques

Down-hole logging of large-diameter bucket-auger borings has been in continuous use in southern California since the mid-1930s (Lebarre, 1936; Scullin, 1994; and Johnson and Cole, 2001). This method is one of a few that allows an engineering geologist to descend into the ground to observe and record three-dimensional geologic structures, a key aspect in most assessments of bedrock landslides, which are usually structurally controlled by discontinuities such as bedding and jointing.

The down-hole logging technique also allows for the acquisition of oriented samples of discrete geologic discontinuities, such as ancient landslide slip surfaces. If budgets allow, there is no better method of subsurface exploration in complex landslide-prone terrain. Only experienced drilling contractors and consultants are allowed to perform down-hole geologic logging, and these individuals must observe applicable California Division of Occupational Safety and Health safety criteria (Scullin, 1994).

Shallow exploratory trenches lie at the opposite end of the exploration budget spectrum. They are usually the least expensive option available for shallow subsurface exploration. Backhoe trenches can yield valuable information, if employed in strategic locations on the hillsides. Often, the most critical location is across anomalous bedrock saddles or benches, which are often underlain by unconsolidated colluvium within detachment zones (Figure 175). In many instances, these soil-filled tension cracks can be quite narrow, requiring delicate probing with hand tools in the exposed walls of an exploratory trench.

Subsurface flight auger borings are the most common tool utilized in geotechnical investigations across the Lamorinda area. Flight augers range in diameter from around 3.5 in. (8.9 cm) for a Mobile Drill Minuteman portable drill rig up to 8.5 in. (21.6 cm) for hollow flight auger drill rigs. The idea employed in completing shallow flight auger borings is to recover subsurface soil or rock samples with a "drive sampler." This sampling is forced downward by repeatedly dropping a 140-lb (63.5-kg) weight over a 30-in. (0.76-m) run and pounding the sampler through approximately 18 in. (45.7 cm) of soil. Geo-practitioners record the number of 30-in. (76.2-cm) weight drops (termed "blows") for each 6-in. (15.2-cm) "round." The number of weight drops is only recorded for the last two rounds (12 in. [30.5 cm]) of any sampling cycle. Depending on the diameter of the sample barrel, these recorded values can then be correlated with other values recorded in various types of soils, and qualitative assessments can be made.

This method came to be known as the Standard Penetration Test, or SPT (ASTM Test Designation D 1586). The method is meant to be applied to sands and gravels and is not as meaningful in clays, because their penetration resistance is a function of water content at the time of testing and the rate of penetration (Rogers, 2006).

Larger-diameter borings are occasionally advanced by utilizing rotary wash drilling techniques, usually using tricone drill bits, like those commonly employed in water-well drilling. Rotary wash borings become necessary if the flight auger drill rig has insufficient power to drill through hard strata or to depths in excess of 50 to 65 ft (15.2 to 19.8 m).

The Cone Penetrometer Test (CPT) has gained considerable acceptance since its introduction in the late 1930s (Hogentogler, 193 C.A., 1937, Engineering Properties of Soil, McGraw-Hill Book Co, New York, 434 p. Utilizing ASTM Test Designation D-3441, the CPT method employs *in situ* (in-place) continuous testing of soil and soft rock strata by pushing a 1.75-in.-diameter (4.45-cm-diameter) stainless-steel cone through the ground at a penetration rate of ~0.8 in./s (~2 cm/s). Strain gauges embedded within the cone tip and along the sides of the cylindrical shaft just above the tip allow for continuous recording of tip resistance and shaft skin friction, in tons per square foot (or kPa). Most modern CPT apparatus can also incorporate measurement of transient pore-water pressures and ground temperature.

Downloaded from http://pubs.geoscienceworld.org/aeg/eeg/article-pdf/31/1/i/6130855/i1558-9161-31-1-i.pdf
by AEG RBAC user

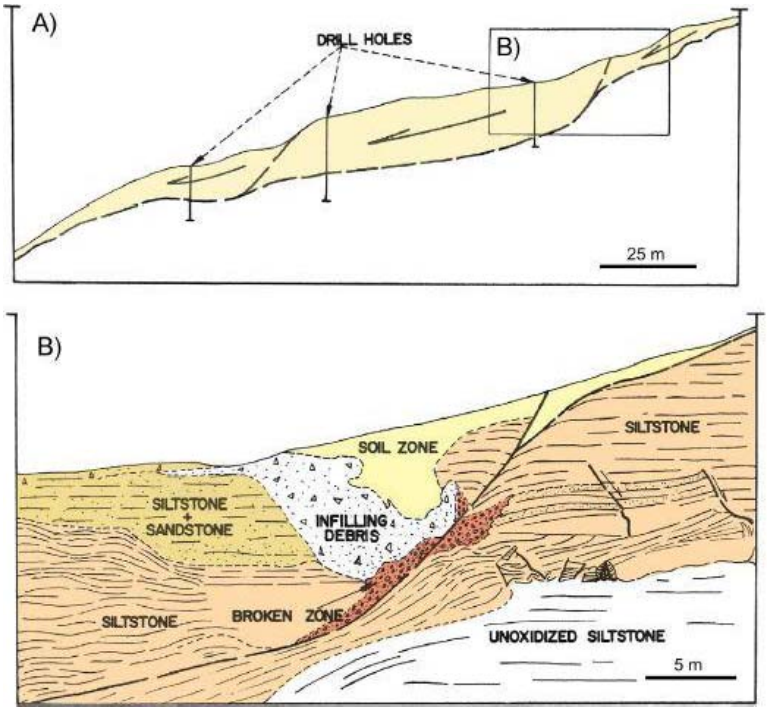

Figure 175a. A longitudinal section through a bedrock landslide in southern California described by Leighton (1966).

Figure 175b. The log of an exploratory trench through the break in slope caused by an old landslide headscarp (Rogers and Chung, 2016).

Rogers (1986) promoted the CPT apparatus as a valuable tool in assessing bedrock landslides, as well as embankment fills and colluvium (Rogers, 1992, 2006). The CPT method requires additional experience and expertise in the interpretation of raw data, because the cone head "senses" material 6 to 8 in. (15 to 20 cm) in front of the tip. If the cone tip cuts through a soft lens of clay only 3 in. (7.6 cm) thick, then the "average" tip resistance within this thin horizon includes the stiff material lying beneath it (Rogers, 2006).

As with the SPT test discussed above, CPT results are biased within muds, clays, and shales, the behavior of which is influenced by water content, stress state, and accumulated strain. Pore-water pressure measurements are also subject to inflated values, depending on the clogging of the porous stone and the low hydraulic conductivity of isolated clay layers. Anomalously high pore pressures can be generated by forcing the cone through saturated muds and clays. In these instances, the cone head may be held in horizons of interest and the pressure dissipation observed over time.

Geophysical techniques, such as shallow refraction seismic exploration, have been employed in the exploration of landslides (Cummings and Clark, 1988) and of colluvial-filled bedrock ravines (Rogers/Pacific, Inc., 1992 a&b). Geophysical techniques have proven to be extremely valuable in assessing the position of perched groundwater tables within the weathered rock horizon. Reflection or refraction seismic programs generally work best when "ground-truthed" by the soil samples or drill cuttings recovered from a conventional boring (Rogers, 2006).

One problem that has been recognized when comparing conventional subsurface exploration with geophysically generated profiles is that of characterizing weathered rock horizons. In conventional geophysical surveys, the boundary between hard, unweathered rock and its weathered covering can be very gradual or uneven, especially in saprolite. The geophysical profile will tend to enhance this boundary, especially if there are anomalies in water content. In such cases, the geophysical profiles often mask the lithologic boundary between weathered rock and the soil regolith developed in place. If the geophysical survey is performed in combination with "ground truthing" using conventional borings or auger probes with cuttings, it can reflect subsurface conditions, but this also depends on the experience of the person directing the drilling and sampling.

Bedrock mapping is the simplest of all exploration techniques, but the one that requires the most local experience. Most rock exposures in the Lamorinda area are covered by residual soils, alluvium, terrace deposits, colluvium, or landslide-derived debris. Stereo-pair aerial photographs taken prior to hillside development can yield a wealth of information about the subsurface structure and highlight outcrop locations with the potential for direct field examination.

Downloaded from http://pubs.geoscienceworld.org/aeg/eeg/article-pdf/31/1/i/6130855/i1558-9161-31-1-i.pdf
by AEG RBAC user

Bedrock mapping has not proven to be a reliable indicator of bedrock landslippage in the Lamorinda area. This is because most of the larger slides are translational and tend to displace the bedrock *en masse*, often without appreciable rotation of the parent groundmass.

EXAMPLES OF LANDFORM DEVELOPMENT IN ORINDA

Introduction

As mentioned previously, the slopes of the East Bay Hills have developed over the last 11,000 to 14,000 years, with one type of landslide superjacent to another type. In this manner, slides of varying age become mixed with an array of soil and rock types that are dominated by debris of older landslides. When reconnaissance-level landslide maps are prepared, they usually recognize the most recent, near-surface slides. In this style of mapping, less visible or dormant features are easily overlooked.

This complexity can be appreciated in Figure 176a, a block diagram of the lower slopes of Gateway Valley. Shallow earthflows were generated by concentrated runoff emanating from the old Kaiser Sand & Gravel Quarry haul roads in 1982, 1983, and 1986, shown in Figure 176b. These recent erosional scars were the area's most visible physical elements. The hummocky nature of these slopes and the active erosion cusps attest to recent surficial erosion and sliding, which tend to mask much larger hazards lying beneath the ground surface.

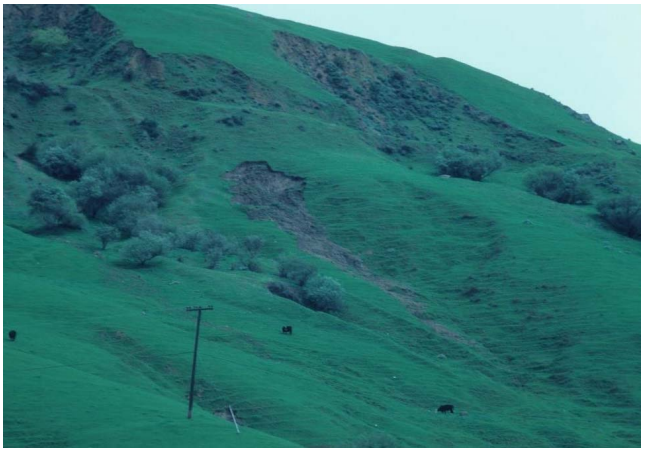

Figure 176b. Shallow earthflows and retrogressive slumps-flow slides emanating from abandoned haul roads of the old Kaiser Sand & Gravel Quarry in lower Gateway Valley, after a series of storms in mid-February 1986 (J. David Rogers).

The easiest way of understanding the successive and overlapping nature of landslides across long spans of time is to view hillslope morphology sequentially through time, noting each slide as a member in a series of discrete, but discernible events. Figures 177 through 189 present a series of mass-wasting events typical of the Lost Valley, Gateway, and Siesta Valley areas of Orinda, CA.

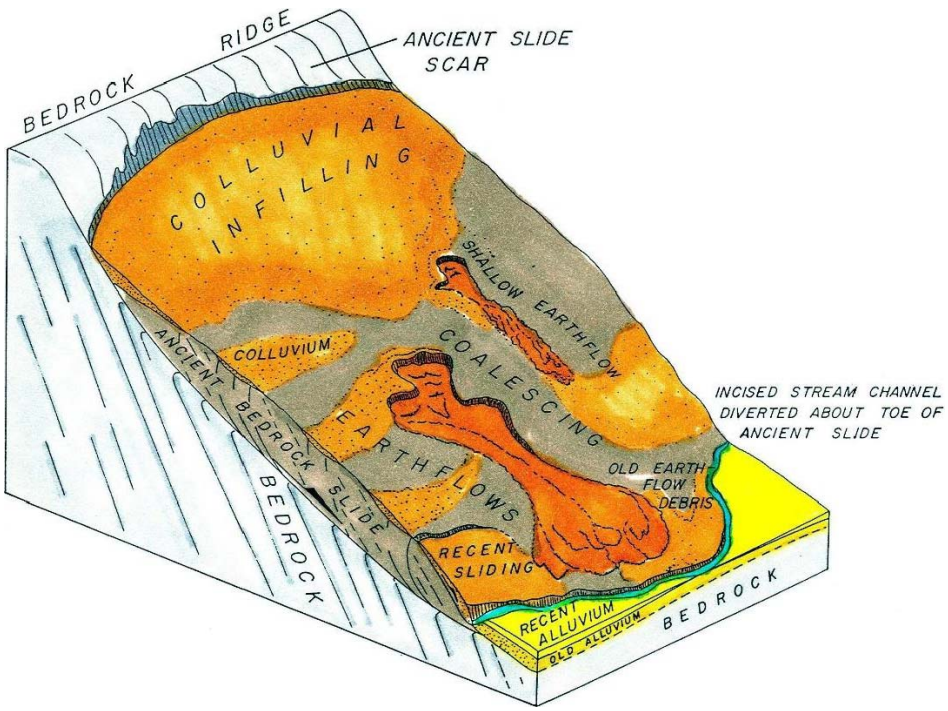

Figure 176a. Schematic block diagram illustrating how various "layers" of landslides tend to develop one upon another, often masking a more ominous bedrock landslide that underlies the entire complex, such as the Gateway Valley, shown above.

Downloaded from http://pubs.geoscienceworld.org/aeg/eeg/article-pdf/31/1/i/6130855/i1558-9161-31-1-i.pdf
by AEG RBAC user

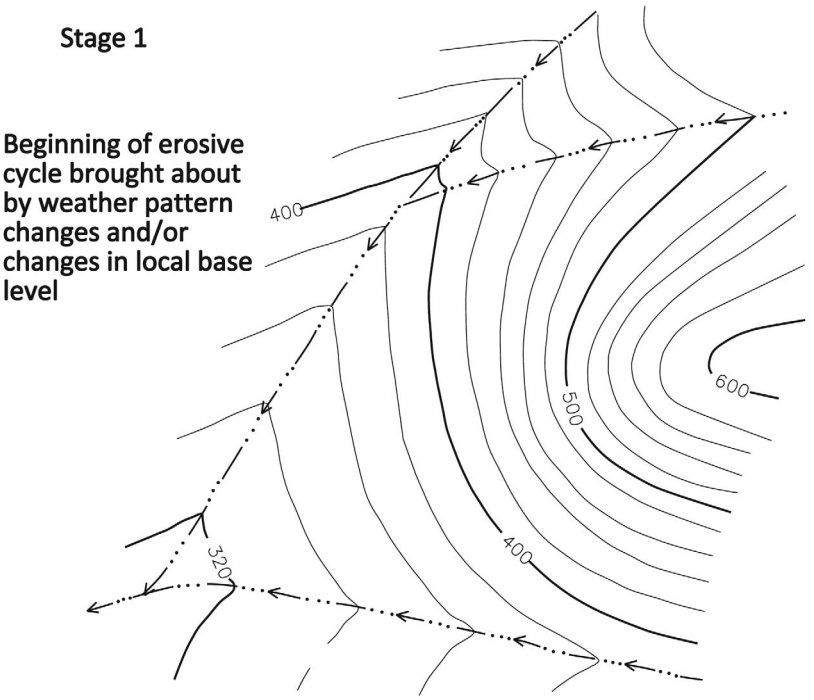

Figure 177a. Map view portraying the physical conditions of a hillside at the beginning of an erosive cycle, which we will refer to as stage 1. These cycles might be triggered by changing weather patterns or local changes in base level (lake or ocean levels).

Channel Downcutting Often Accompanied by Local Over-Steepening

Figure 177 is a topographic map of a hypothetical Orinda hillside exhibiting features typical of a slope in quasi-equilibrium (Davis, 1899; Gilbert, 1909). The distinguishing features include smooth slopes with increasing steepness, which terminate in a broad, rounded crest at the ridgelines. The topographic pattern is clean and undisturbed by active erosion or mass wasting. The early stages of an erosive cycle are suggested by shallow entrenchment of established first- and second-order watercourses delineating the lower slopes.

Figure 178 presents the same topography during a sequence of channel rejuvenation. This renewed downcutting may be ascribable to weather pattern changes (Grove, 1988), changes in vegetation (Reid, 1989), or changes in erosive base levels (Bull, 1991). In the San Francisco Bay area, base-level changes have occurred with the rise and fall of sea level, which controls the base level of all the area's trunk channels.

Figure 179 depicts the continuing process of downcutting. Tributaries issuing from the largest watersheds are the first to respond to base-level adjustments, because of their increased stream power (Bull, 1991). In this manner, higher-order channels will tend to lower their channel beds more quickly than the channels emanating from smaller watersheds (Horton, 1945; Bull, 1991). In this example, the opposing sides of a ridge are beginning to be undercut by first-order channels, while the nose of the ridge is gradually truncated by a second-order channel from a larger watershed area (upper-right portion of Figure 179a).

Local Over-Steepening of Slopes Along Water CoursesastingEventually, downcutting on three sides of the ridge progresses sufficiently to locally undermine the stability of the highest slopes. This can result in an almost imperceptible mobilization of a larger bedrock slide mass, pinching off the youthful channels. An example of such a situation is depicted in Figure 180a. The key topographic indicators of recent movement include : (1) A natural bench often forms at the end of linear ridgelines; (2) slope contours may be extended in tension along the lateral slide scarps; (3) the trends of the linear stream channels tend to be pushed outward by the creeping/ slide mass; and (4) increased channel gradients develop at the "pinch points," constricting the channel. Figure 180b presents the map interpretation of such a landslide feature.

Translational landslides generally move in a series of discrete translate in episodes, typified by slow "stick-slip" movement episodes (Schaeffer and Iverson, 2008). Through this translation, alleviates its local pore water-water table position through simple rotation (as shown in Figure 117) and fracture-induced drainage along the margins of the slide mass (depicted in Figure 133b).

Figure 181a, depicts the renewed translation of the translational bedrock slide after some period of time.

Downloaded from http://pubs.geoscienceworld.org/aeg/eeg/article-pdf/31/1/i/6130855/i1558-9161-31-1-i.pdf
by AEG RBAC user

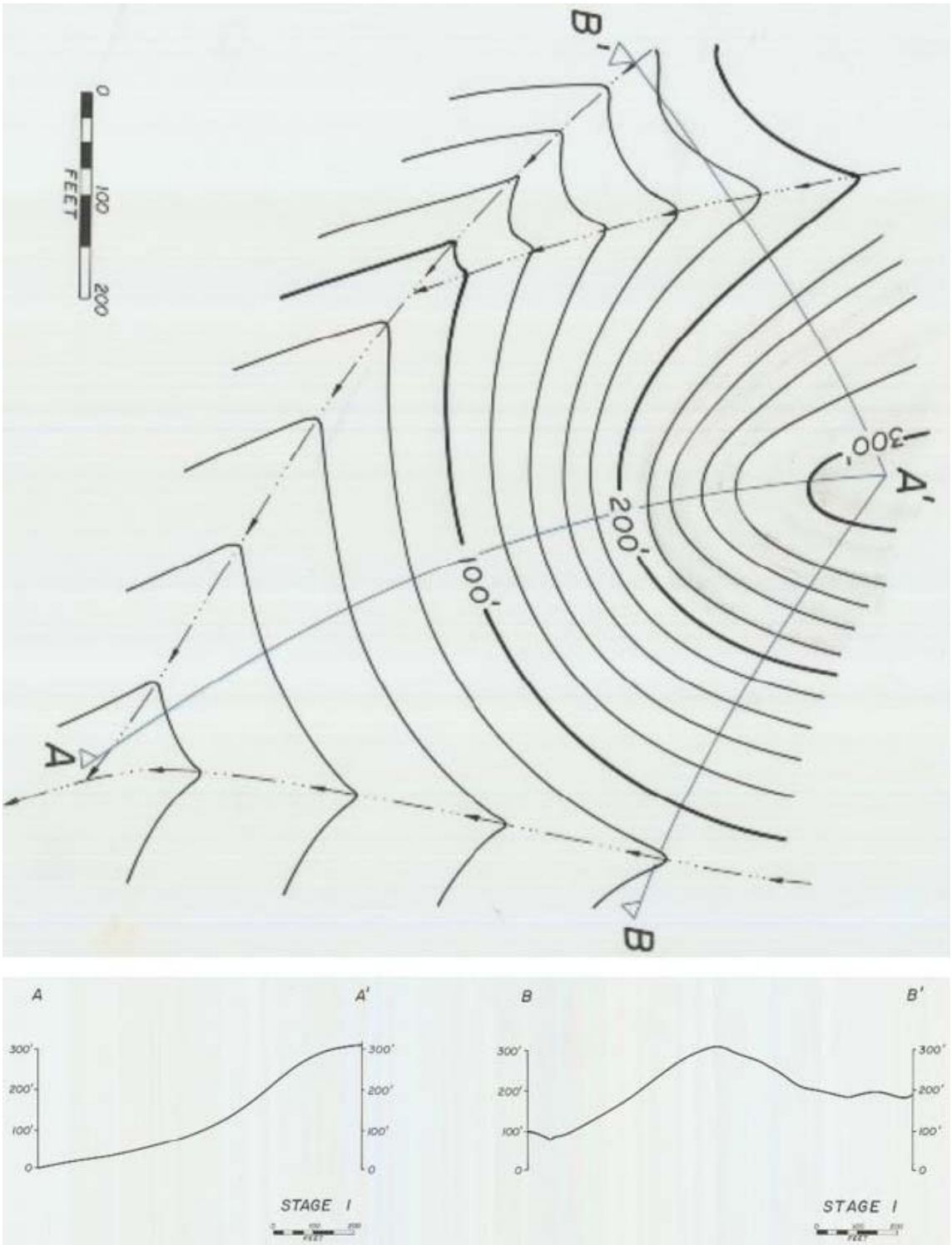

Figure 177b. Initial slope profiles A-A′ along the nose of a natural ridge, and along an axis transverse to the ridge in profile B-B′.

This interval might be a few hundred to a few thousand years, depending on the stream's efficiency in re-excavating its locally pinched channels (which further undermines the creeping slide mass). Figure 181b presents an interpretive landslide map of the slopes and watercourse features shown in in Figure 181a.

Large translational bedrock slides generally buttress themselves by mechanical contact with opposing slopes

Downloaded from http://pubs.geoscienceworld.org/aeg/eeg/article-pdf/31/1/i/6130855/i1558-9161-31-1-i.pdf
by AEG RBAC user

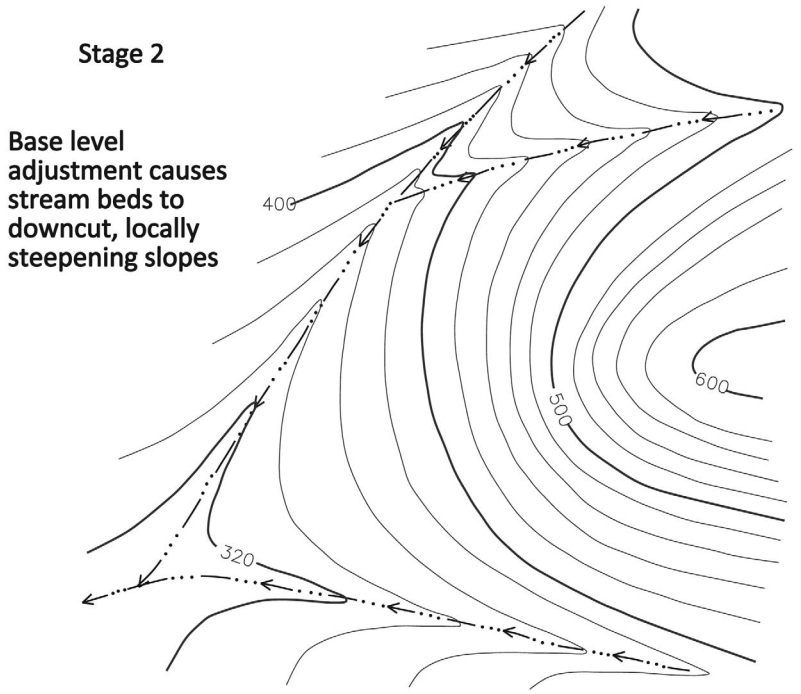

Figure 178. In stage 2, base-level adjustment is causing the first- and second-order channels stream channels to begin excavating their beds. Downcutting will gradually sculpt over-steepened channel banks.

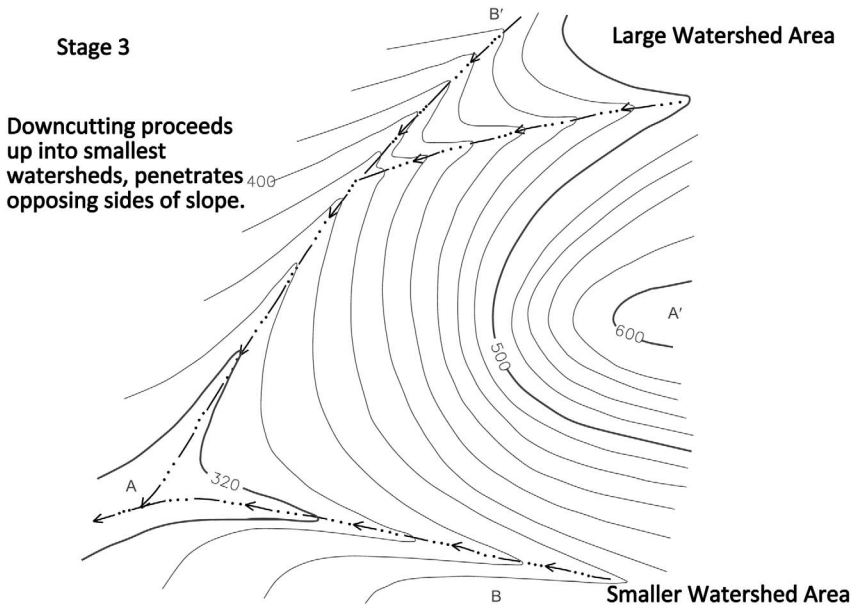

Figure 179a. This map depicts stage 3, when the channel downcutting proceeds upstream into a smaller watershed and begins to penetrate the far side of the local first-order channels.

(Hungr et al., 2014). In some instances, this contact is only partial due to the stream's ability to quickly re-excavate its channels (Schuster, 1986).

Partial toe buttresses fashioned by mechanical obstruction(s) may trigger dormancy for thousands of years, depending on the climate and available stream power (Rogers et al., 1992). As the parent slide mass remains dormant, a string of smaller, secondary slope failures often occurs about the toe and flanks of the parent mass.

Downloaded from http://pubs.geoscienceworld.org/aeg/eeg/article-pdf/31/1/i/6130855/i1558-9161-31-1-i.pdf
by AEG RBAC user

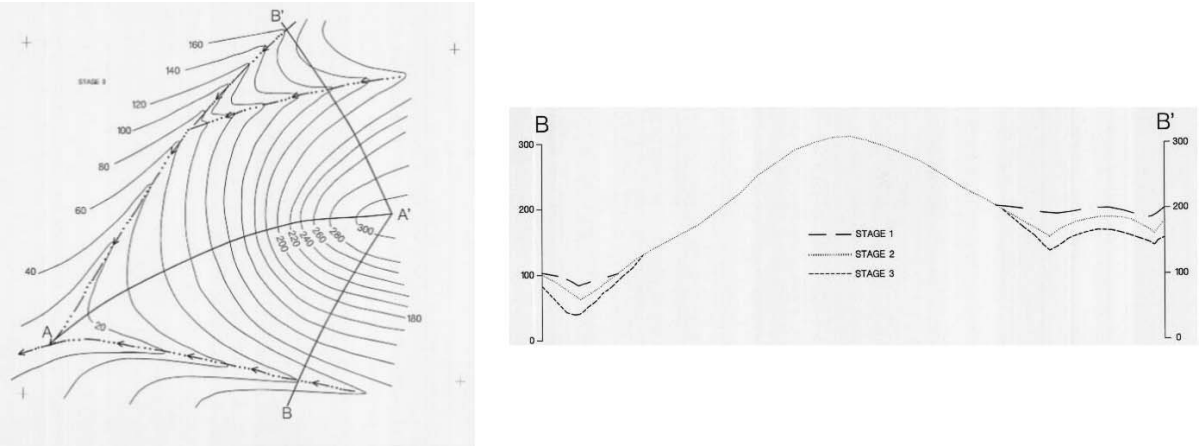

Figure 179b. Changes in the transverse profile B-B′ after the first-order channels dropped their beds by 2 to 20 ft (0.6 to 6.1 m) during stage 3 in response to a change in base level (Horton, 1945; Strahler, 1952). (b) This downcutting steepens the channel side slopes and decreases the intervening slope's factor of safety against landsliding.

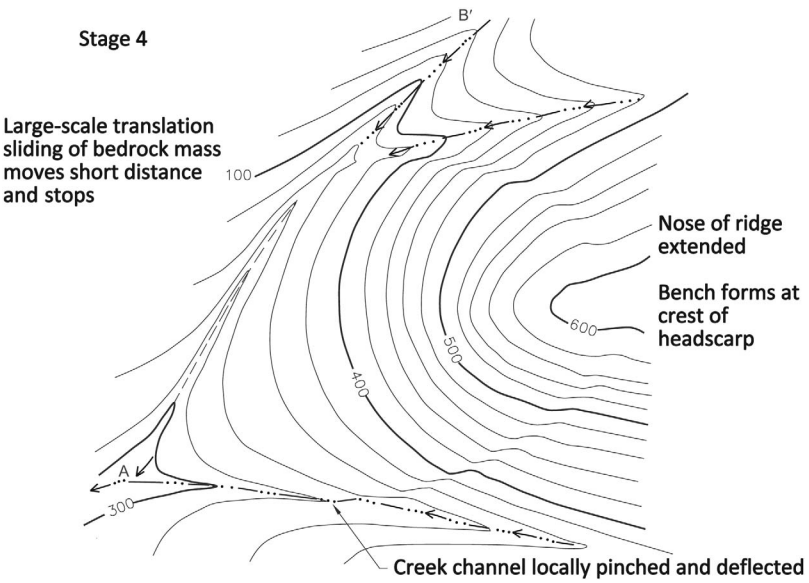

Figure 180a. Map of stage 4 conditions, when large-scale translation of the ridge nose begins. Note kinked contours along the lateral margins of this massive slide block, and the locally pinched and deflected channel.

Secondary Landslides Often Develop upon Older Parent Slide Masses

Figure 182a is the topographic expression we would expect after a long period of dormancy. The following features typify this expression: (1) excavation of youthful gullies or ravines along the lateral margins of the dormant slide mass; (2) development of colluvial-filled pockets along the lateral margins and headscarp separation zones; (3) development of these colluvial pockets into active earthflows and debris flows (depending on the cohesion of the colluvial materials); (4) erosion of toe areas, with zones of active raveling and hummocky micro-topography (often observed on maps employing 5 ft [1.5 m] contour intervals); (5) localized sinuosity of first- and second-order channels about the toes of active slumps, and (6) earthflows beginning to occur in the lower third of the dormant (parent) slide mass due to increased seepage from fracture dilation.

These reactions are accompanied by the deposition of terrace deposits choking first- and second-order channels upstream of the dormant slide mass and substantive alluvial infilling of the toe area. Occasionally, braided

Downloaded from http://pubs.geoscienceworld.org/aeg/eeg/article-pdf/31/1/i/6130855/i1558-9161-31-1-i.pdf
by AEG RBAC user

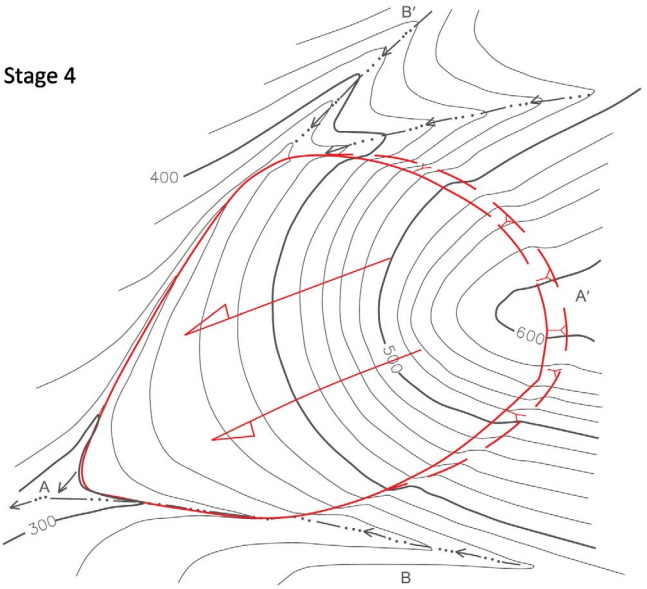

Figure 180b. This would be the map interpretation of a deep-seated transitional landslide in stage 4. Natural materials with higher friction tend to exhibit more pancake-shaped sections with low *L*:*D* and high *L*:*W* ratios, like the planar slide mass depicted here.

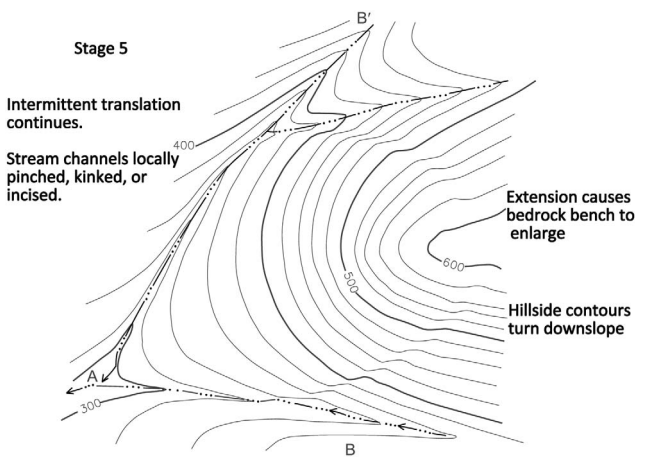

Figure 181a. Map of stage 5 conditions, when extension of the ridgeline causes an anomalous elongated bench, with increasingly kinked contours along the lateral margins of the slide block, beginning to offset the pinched channels.

channel forms will be observed immediately downstream of the parent mass, due to an overwhelming volume of sediment that has accumulated during periodic breaching of landslide dams across the tributaries. Figure 182b presents the landslide map interpretation of the stage 6 geomorphic response.

With the passage of more time, perturbations that emanate from the undercut toe of the dormant parent slide eventually retrogress, as depicted in stage 7 in Figure 183a. rogression is usually accompanied by a progressive

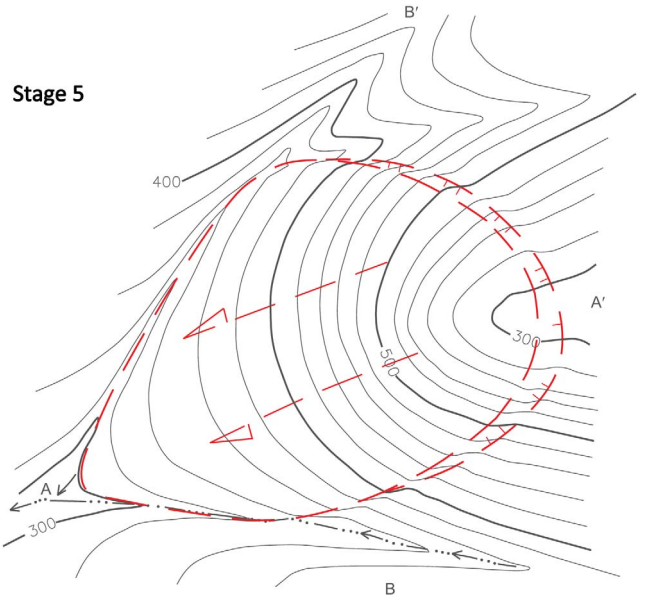

Figure 181b. Map interpretation of a deep-seated transitional landslide in stage 5 of geomorphic alteration.

enlargement of slumps and earthflows, often in response to continued channel downcutting. First- and second-order stream channels bounding such features are often displaced, or banks are undercut in pinched reaches.

If erosion persists, hillside contours will begin to exhibit crenulated textures. Incision of the lateral scarp separations may also lead to the development of an isolated bedrock knob at the crest of the displaced mass. The landslide map interpretation of this situation is shown in the accompanying Figure 183b.

The new slumps and earthflows tend to coalesce with time into larger translational slides developed upon and within the parent slide mass (Figure 184a; Stage 8). Weathering of the parent slide mass increases fabric porosity and decreases shear strength, making the dormant mass more susceptible to sliding with increased age and weathering.

These new translational slides and retrogressive slumps will tend to move episodically in small increments, which seldom produce dramatic scarps or grabens. This makes delineation of their physical boundaries more difficult. The topographic expression may not be suggestive of recent movement. The lateral margins of the parent slide mass are often masked by younger landslides and/or colluvial infilling.

Renewal of Deeper Landsliding

If weather patterns were to change sufficiently, new episodes of deeper-seated bedrock landsliding could recur. This renewed sliding could be triggered by additional downcutting stimulated by tectonic uplift, changes

Downloaded from http://pubs.geoscienceworld.org/aeg/eeg/article-pdf/31/1/i/6130855/i1558-9161-31-1-i.pdf
by AEG RBAC user

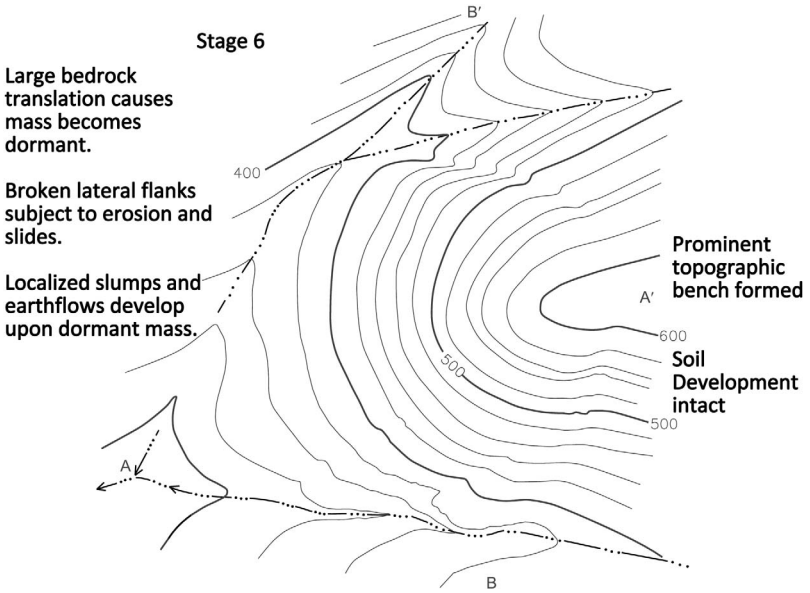

Figure 182a. After a sustained period of dormancy, downcutting is rejuvenated during stage 6. The parent mass remains dormant, but smaller slides develop along the lateral margins of the relict block glide slide, where fracture porosity is highest. On one side of the old block glide, this increased porosity triggers erosional downcutting, while on the other side, it triggers slump-earthflows.

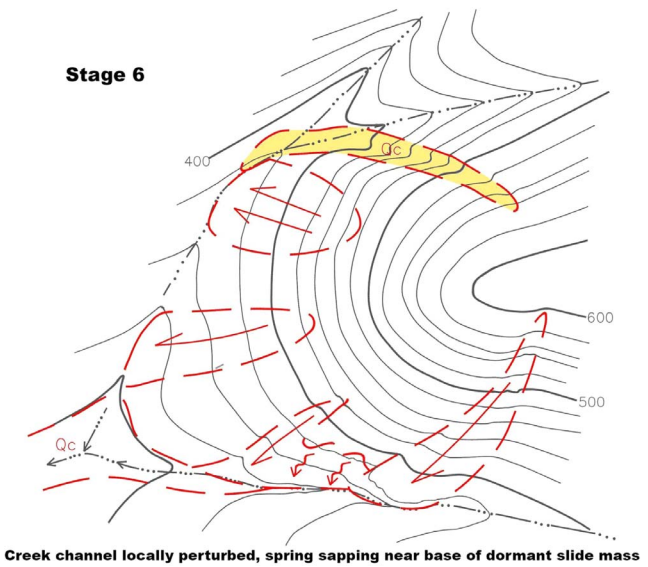

Figure 182b. This is the interpretation of secondary slides and colluvial infilling developed on the dormant slide mass underlying these semi-active features during stage 6 alterations.

in local base level, or increased stream power due to sustained shifts in patterns of precipitation.

Figure 185a presents the situation that can occur when dormant bedrock slide masses reactivate. Periods of reactivation might last 1,000 to 20,000 years, depending on the prevailing climatic cycles. The reactivated mass might move several hundred feet (tens of meters) until it bumps into a formidable obstruction, like the opposing bank of the toe depression. The landslide map interpretation of these stage 9 topographic features is presented in Figure 185b.

Triangular headscarp facets tend to be preserved over longer periods of time than other headscarps. They can serve as key indicators of recent or prehistoric landsliding. In this situation, the displaced bedrock knob, or bench, is an obvious anomaly, which serves as another

Downloaded from http://pubs.geoscienceworld.org/aeg/eeg/article-pdf/31/1/i/6130855/i1558-9161-31-1-i.pdf
by AEG RBAC user

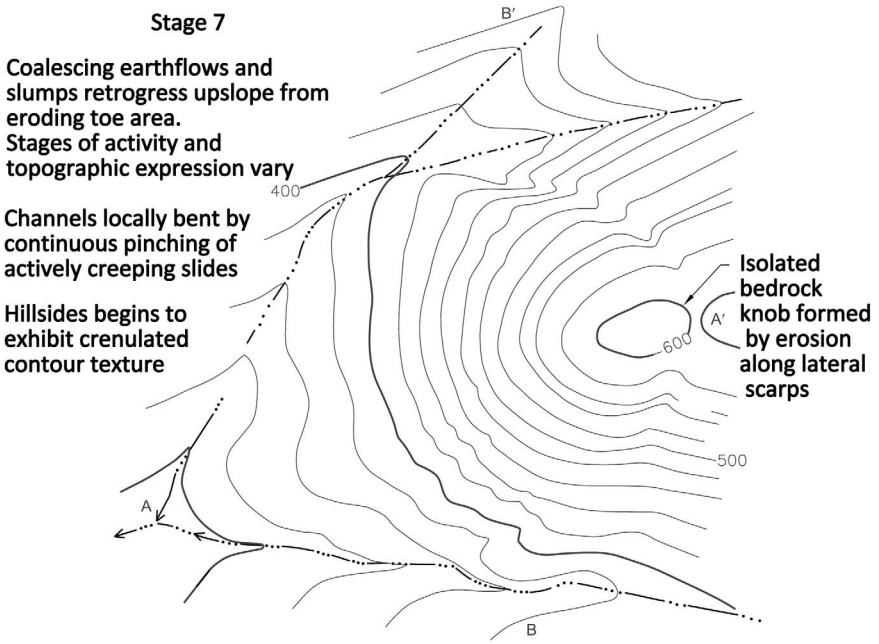

Figure 183a. During stage 7, weathering and mass wasting trigger coalescing earthflows and rotational slumps that tend to retrogress upslope of eroding toe areas. Note the bounding first- and second-order channels, which are intermittently blocked, bent, or pinched by creeping surficial slides. These slopes begin to exhibit a crenulated texture.

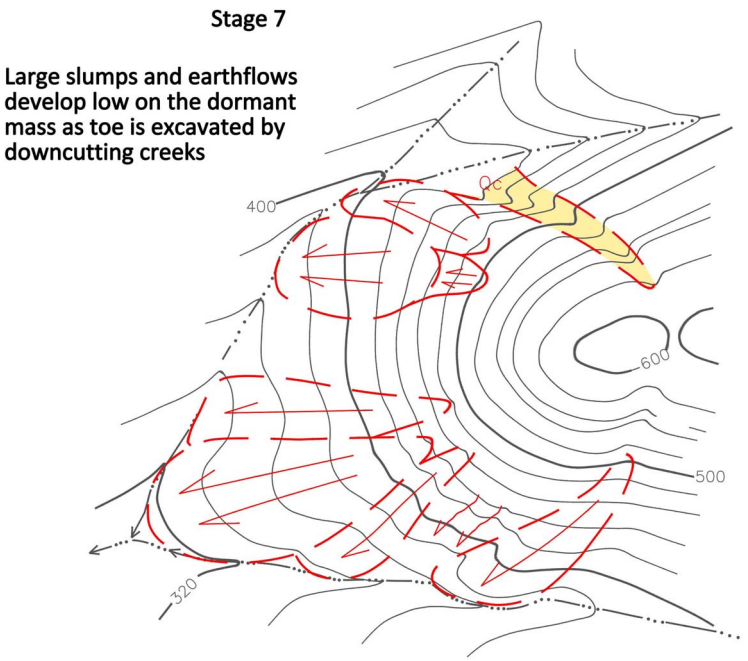

Figure 183b. Map interpretation of locally crenulated elevation contours and pockets of colluvium. Note the almond shapes and bulbous toes of the secondary slump-earthflows.

key indicator of a bedrock landslide feature. Lateral translation can also trigger the formation of triangular facets across the nose of the parent ridgeline (sketched in Figure 185c).

Due to the same factors described in Figures 181 and 182, translational bedrock slides often lie dormant if they did not move considerable distances. This is because translation usually increases dilation and breakup of the

Downloaded from http://pubs.geoscienceworld.org/aeg/eeg/article-pdf/31/1/i/6130855/i1558-9161-31-1-i.pdf
by AEG RBAC user

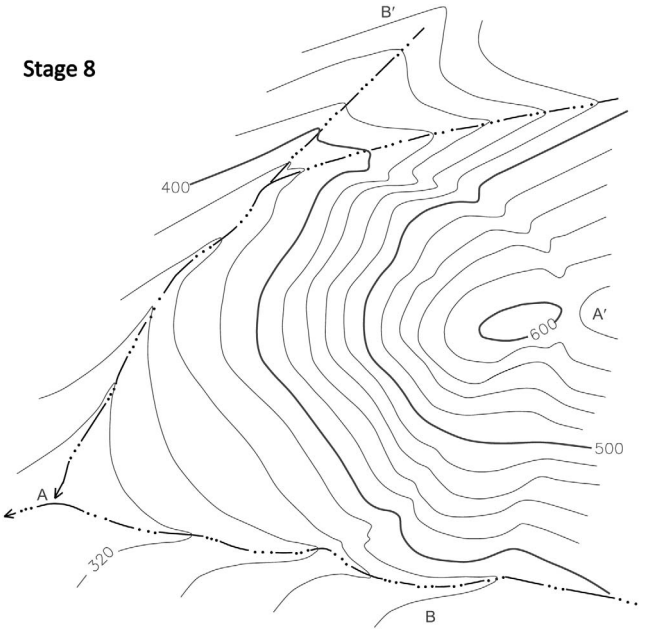

Figure 184a. Map illustrating topographic recognition keys for stage 8 conditions. The multiple slumps emanating from the toe of slope may coalesce into a larger translational slide developed in the parent slide mass, which continues to weather.

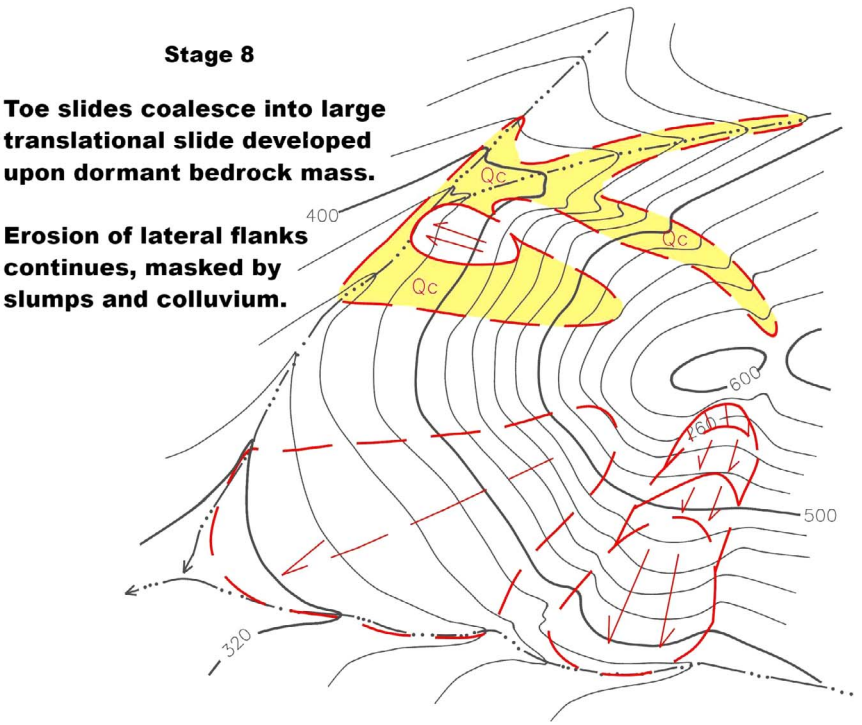

Figure 184b. Interpretation of topographic expression revealed in stage 8. Erosion of the parent slide's lateral flanks is likely exacerbated by fracture porosity along old detachment surfaces and/or shallow burial beneath colluvial infilling (shown in yellow).

bedrock fabric and structure, especially adjacent to the plane of rupture.

In confined ravines or incised canyons, movement of the slide mass can be abruptly halted by topographic obstructions, such as the opposing face of the ravine or channel depression. The thrust of the bedrock slide can also be transferred by arching, which precludes dilation.

If the bedrock units remain confined, then they are less likely to dilate through bending-induced tension. Where the slide mass is less confined, its lateral margins

Downloaded from http://pubs.geoscienceworld.org/aeg/eeg/article-pdf/31/1/i/6130855/i1558-9161-31-1-i.pdf
by AEG RBAC user

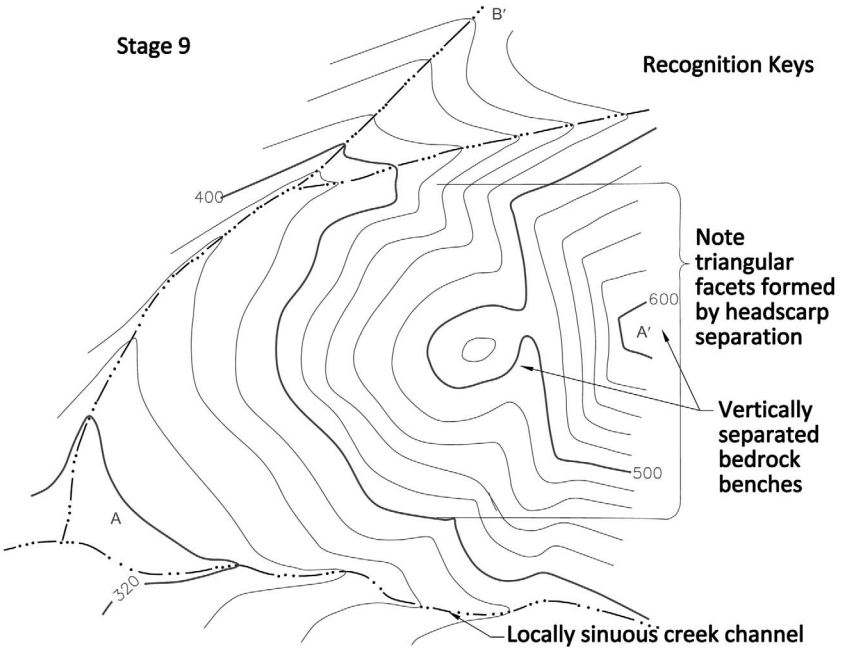

Figure 185a. Topographic recognition keys for stage 9 of geomorphic progression. Note the pronounced triangular facets formed by reactivation of the underlying bedrock slide. Facets can also form from steeply inclined fault offset in an active tectonic environment, like the Hayward, Mission Peak, or Calaveras Faults.

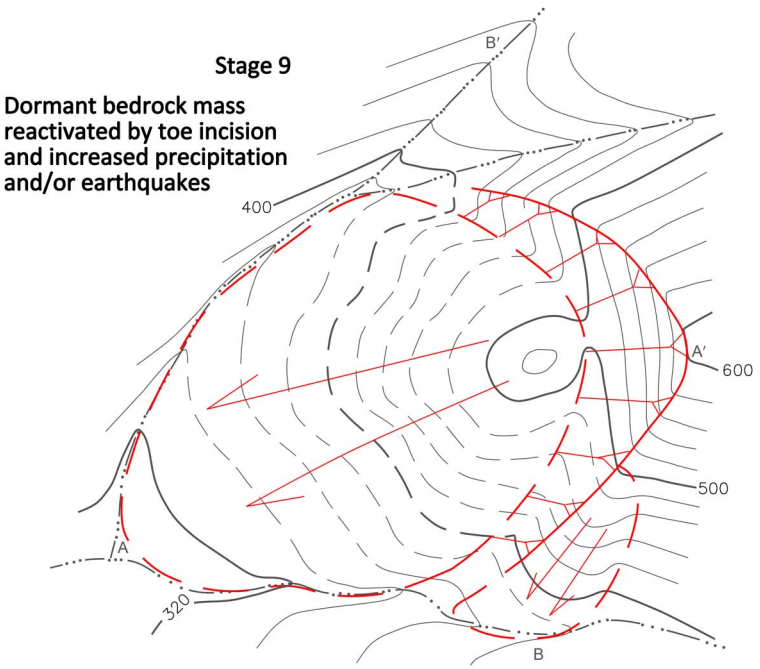

Figure 185b. Map interpretation of a dormant bedrock landslide complex that has suddenly reactivated, forming triangular facets in the headscarp evacuation area, which looks like a near-vertical cliff.

tend to relax and dilate, making them more susceptible to future episodes of sliding. This situation is presented in topographic plan as Figure 186a, the formation of an isolated knob in Figure 186b, a typical geologic section in Figure 186c, and the map interpretations in Figure 186d.

Bedrock slides that translate hundreds of feet (tens of meters) will tend to form distinctive first-order gullies

Downloaded from http://pubs.geoscienceworld.org/aeg/eeg/article-pdf/31/1/i/6130855/i1558-9161-31-1-i.pdf
by AEG RBAC user

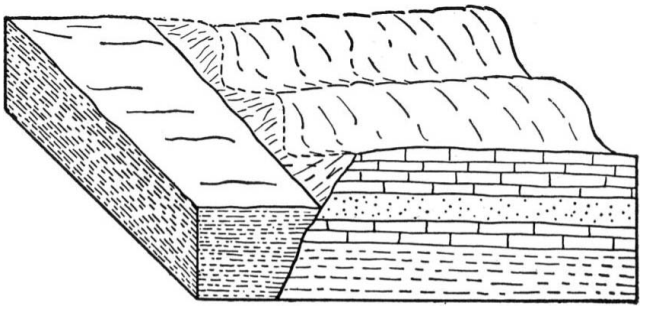

Figure 185c. Triangular facets are erosional escarpments sculpted by fault offset or mass wasting (Cotton, 1950). Mass wasting usually involves more isolated and discontinuous occurrences.

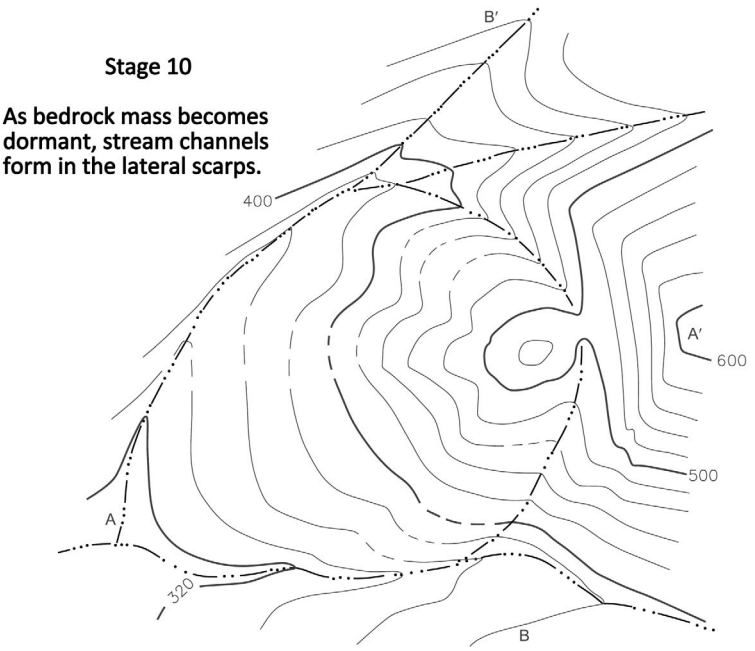

Figure 186a. Recognition keys for stage 10 in the geomorphic progression. As the reactivated translational slide is somewhat stabilized by mechanical obstructions and subdrainage through open fissures, first-order ephemeral channels often develop along fractured lateral scarps, and colluvial materials begin to accumulate in immature ravines.

along their lateral margins. In this case, those gullies curve towards one another, a key indicator that they are slide-related (as suggested in Figure 133). As dormancy is sustained, the same suite of secondary slides (earthflows, slumps, and translational slides) will begin to form in the lower third of the displaced slide mass.

The toe area is closest to the downcutting channels, which are attempting to readjust their perturbed gradients. This adjustment usually fosters local oversteepening of the channel side slopes, which, in turn, promotes the secondary failures. Figure 186b presents the landslide map interpretation of this stage of geomorphic development. Accumulations of colluvium will increase with longer periods of dormancy.

Colluvium Production as the Dominant Slope-Forming Mechanism

In instances where the parent bedrock type is massive yet fissile or intensely jointed, the principal erosional agent may become colluvial infilling, an erosional cycle, and ravine downcutting instead of landslides.

Colluvial infilling is the dominant form of hillslope evolution observed within the Claremont chert member of the Monterey Formation, comprising Grizzly Peak Ridge and the canyons west of this drainage divide between Alameda and Contra Costa Counties (Figure 58). In some cases, these deep accumulations of colluvium can become sufficiently unstable under unnatural concentrations of runoff as to promote debris flows or

Downloaded from http://pubs.geoscienceworld.org/aeg/eeg/article-pdf/31/1/i/6130855/i1558-9161-31-1-i.pdf
by AEG RBAC user

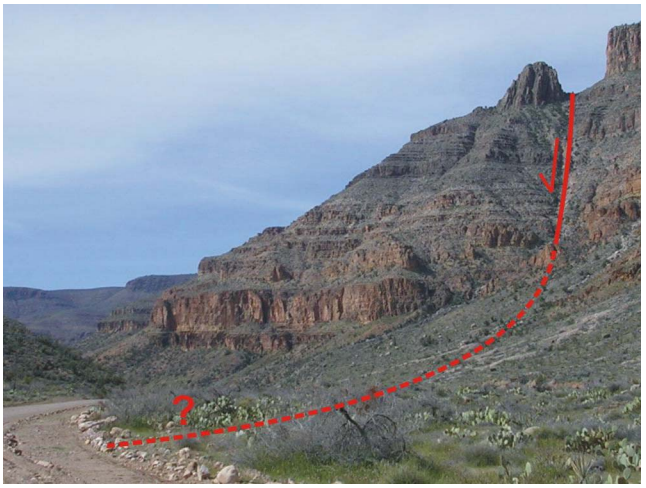

Figure 186b. Physical characteristics of a dormant translational bedrock slide that has dropped about 213 ft (64.9 m), detaching itself along curving shear surfaces and leaving an isolated knob. This view is looking up Peach Springs Canyon, AZ (Watkins et al., 2007).

earthflows (Reneau et al., 1984). This mechanism is common in the Briones (Figure 150) and Panoche Formations blanketing much of north-central Contra Costa County.

If weather patterns shift to a wetter, more humid climate, increased volumes of vegetation and animal forms may also foster increased production of colluvium. In this situation, stream channels become over-taxed or incapable of transporting the volume of colluvial sediment generated on the slopes. Such a situation would tend to favor the accumulation of large volumes of colluvium, which can also serve to buttress adjacent bedrock slopes.

If colluvial production were the dominant slope-forming process, a situation might emerge like that sketched in Figures 187a and 187b. Colluvium tends to collect in zero- and first-order watershed basins. As shown in Figure 187a, these ravines, or bedrock "hollows," tend to be regularly spaced, one adjacent to another. The intervening bedrock ridges are termed "ribs," as shown in Figure 187b. Colluvial detritus is generated from the ribs and the tributary outcrops comprising bounding ridges.

Accumulations of colluvium are periodically eroded in response to weather pattern changes or changes in local or regional base levels. Colluvial accumulation and periodic removal generally promote an intertwined system of colluvial-filled bedrock ravines. The topographic expression of such features may be very slight, depending on the age of the infilling, and whether retained colluvium has survived periods of partial erosion (Lehre, 1982; Dengler et al., 1987).

Figure 188a presents the topographic expression of colluvial-filled bedrock ravines developed upon a dormant bedrock landslide. If the landslide map interpreter is aware of localized colluvial-filled ravines, then they can assume that such features likely exist on fairly regular intervals, and their size is likely limited by that of the parent watershed.

Given such tenets, slight expressions of channels present telltale clues of underlying bedrock ravines, masked by the colluvium. In these situations, the resulting landslide interpretation map might appear as presented in Figure 188b. The sequential changes in slope profile between stages 1 and 13 are presented in Figures 188c–d.

The Finished Product

In the Lamorinda area, all of the various slide and colluvium-production mechanisms discussed previously apply. Active landsliding extended well into the Pleistocene Epoch, and many dormant bedrock slides might even date from >100,000 years before present (Rogers and Halliday, 1992a, 1992b).

The juxtaposed remnants of older bedrock slides are typical of many of the uplifted hillslopes west of the

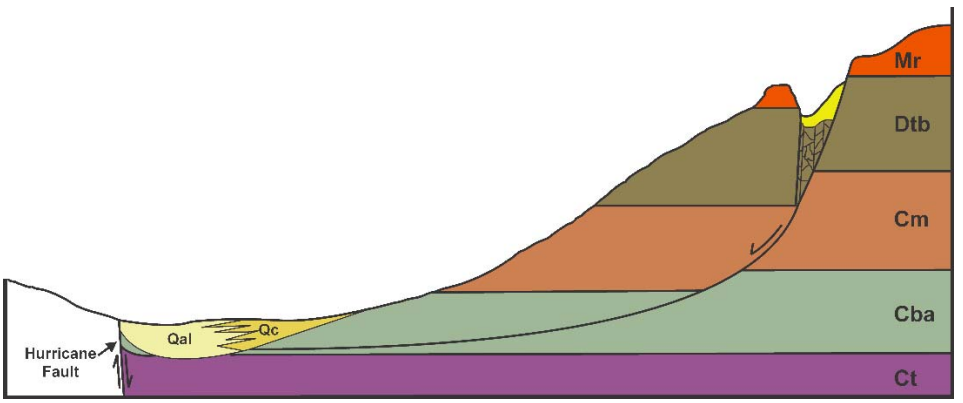

Figure 186c. Profile view through the landslide feature shown above (modified from Watkins et al., 2007). 57 percent of the rupture plane lies within the Bright Angel Shale (Cba).

Downloaded from http://pubs.geoscienceworld.org/aeg/eeg/article-pdf/31/1/i/6130855/i1558-9161-31-1-i.pdf
by AEG RBAC user

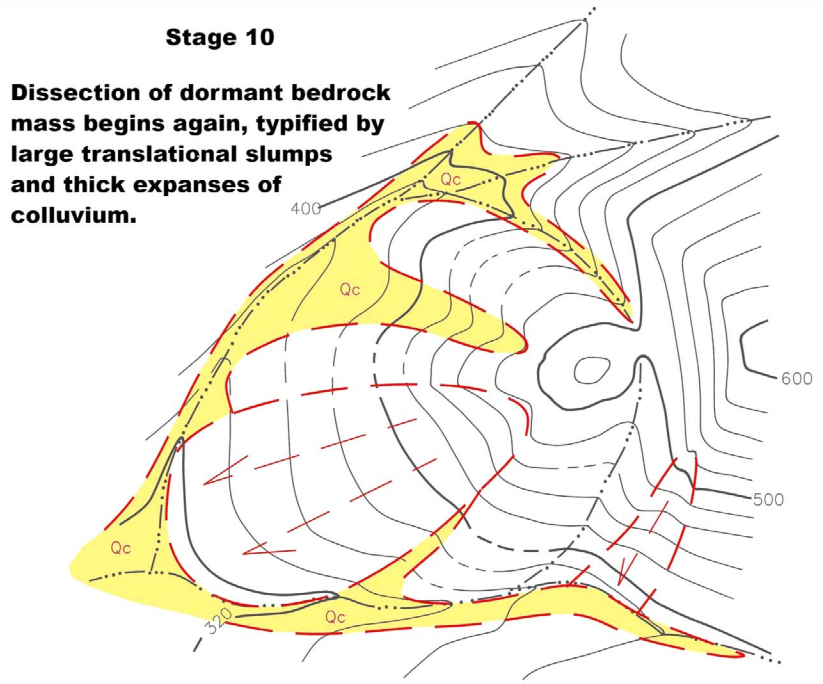

Figure 186d. Map interpretation of a dormant bedrock landslide complex with a triangular facet coincident with the crown scarp evacuation scar. Note rapid colluvial infilling (shown in yellow).

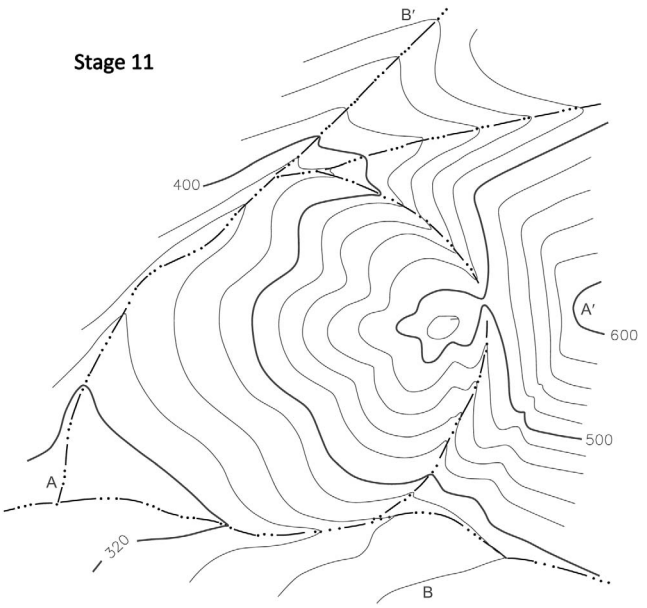

Figure 187a. Recognition keys for stage 11 in the geomorphic progression. As the displaced mass lies in dormancy for >11,000 years, it is subject to multiple colluvial-filling and erosion cycles. During wet periods, more colluvium is produced and stored in shallow bedrock depressions, and during perennial drought periods followed by intense long-duration storms, an erosive cycle can be triggered, which empties the colluvium from storage in the shallow bedrock depressions.

Moraga Thrust fault. These were among the most complicated of any landslides investigated in this study. Figure 189a presents a topographic map illustrating the rejuvenation of an erosive cycle and how this would be increasingly reflected in the slope profiles when mass wasting ensued. We identified this as stage 13, and the new map interpretations are presented in Figure 189b.

In this example, the triangular facets and bedrock knob are key indicators of relict bedrock landsliding (Codilean et al., 2006). However, the advanced

Downloaded from http://pubs.geoscienceworld.org/aeg/eeg/article-pdf/31/1/i/6130855/i1558-9161-31-1-i.pdf
by AEG RBAC user

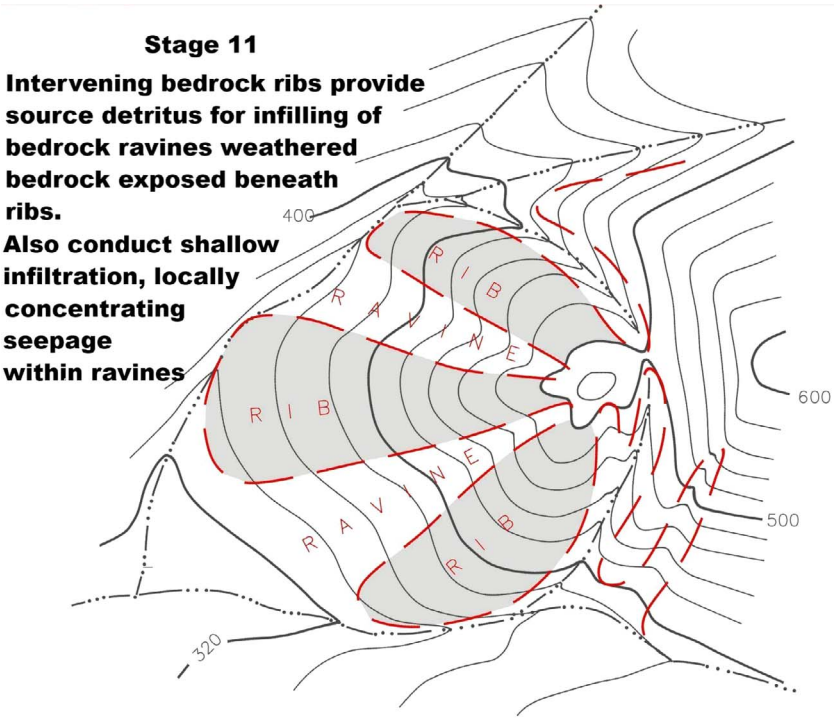

Figure 187b. Map interpretation of a dormant bedrock landslide complex with triangular facets above its headscarp evacuation scar and rapid colluvial infilling of natural bedrock ravines between adjacent bedrock ribs (shown in light gray).

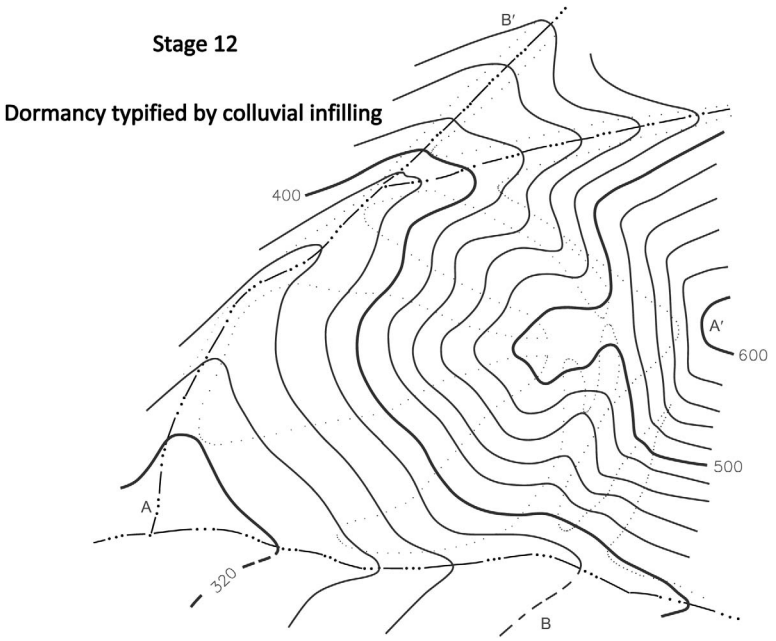

Figure 188a. Stage 12 might be typified by colluvial infilling if the average precipitation levels diminish and a drier climate prevails.

dissection of this mass suggests that the feature has been dormant well beyond the Holocene Epoch (>11,000 years).

Large bedrock slumps developed upon the parent slide mass may not exhibit sharpness and are, therefore, mapped with approximate (dashed or queried) boundaries. Several shallow earthflows did express topographic expression of recent movement or dissection, and these are delineated by continuous red lines. The paleo-slide features are denoted by hachures, making it an "ancient" or relict landslide feature, not necessarily likely or capable of future movement.

Downloaded from http://pubs.geoscienceworld.org/aeg/eeg/article-pdf/31/1/i/6130855/i1558-9161-31-1-i.pdf
by AEG RBAC user

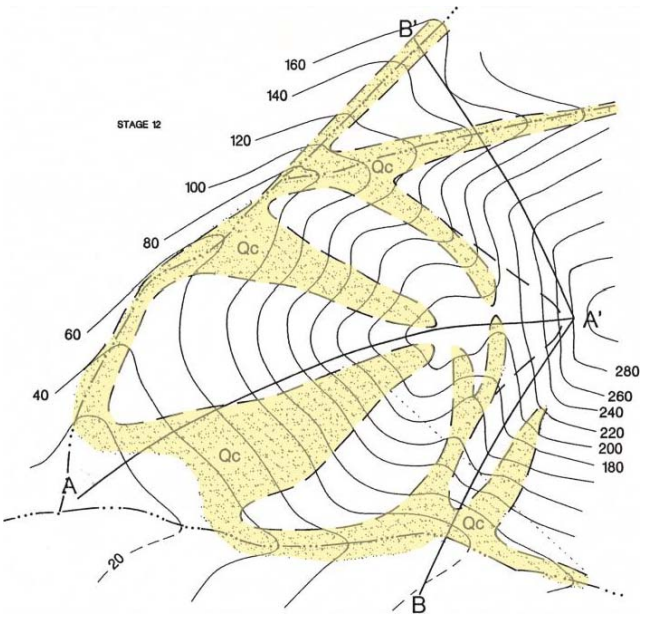

Figure 188b. Map interpretation of stage 12, which is relatively quiescent. Note extensive network of unconsolidated colluvium accumulating in shallow bedrock depressions.

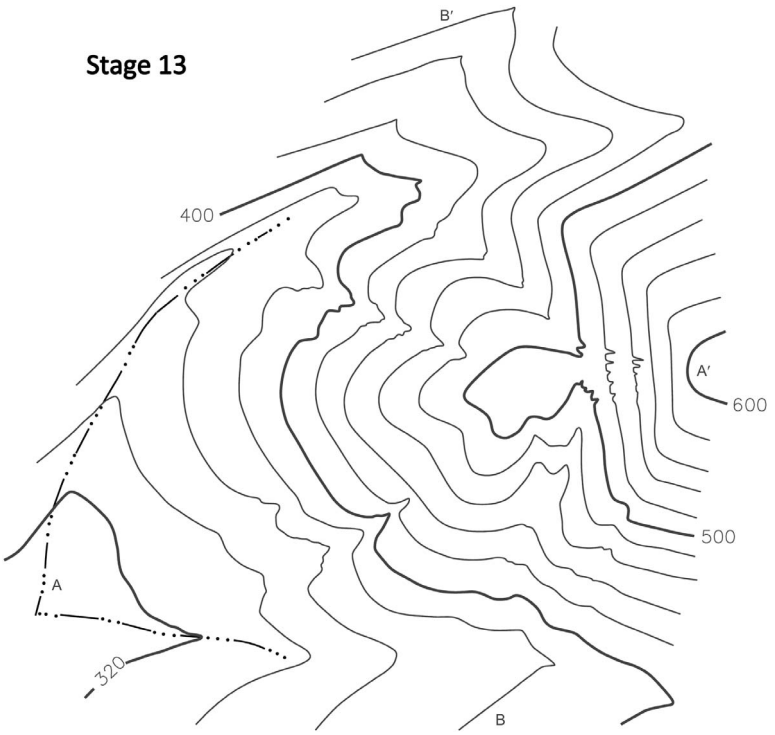

Figure 189a. Topographic expression of colluvial erosion accompanying stage 13.

Colluvial infilling of the headscarp face helps to mask this distinctive feature (Figure 189a). The juncture between colluvium and the bedrock bench/knob would be a good location to conduct subsurface exploration using backhoe trenches to quickly confirm or refute the presence of prehistoric sliding. Other patches of colluvium have eroded and mobilized into earthflows and debris flows, with movement directions indicted by single or parallel arrows. In this final view (Figure 189b), the slight sinuosity of the adjacent streams also points to the paleo-slide as a controlling factor on their bowed orientations around the distal margins of the parent landslide's toe.

Downloaded from http://pubs.geoscienceworld.org/aeg/eeg/article-pdf/31/1/i/6130855/i1558-9161-31-1-i.pdf
by AEG RBAC user

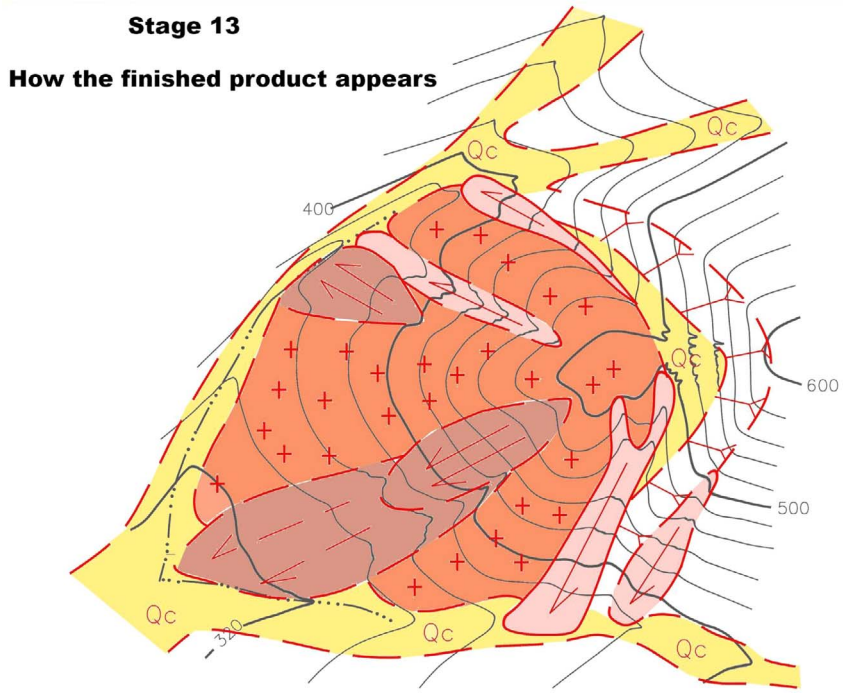

Figure 189b. Map interpretation of stage 13, which represents the rejuvenation of an erosive cycle.

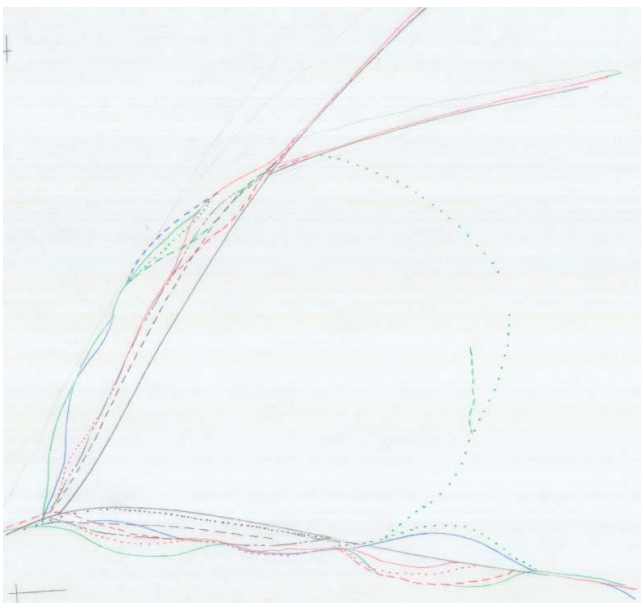

Figure 189c. Plane view of *x-y* migration of first-order channel thalwegs during the hypothetical interval between geomorphic stages 1 and 13. Note how the bounding channels are periodically pushed outward by gross translational movements as well as localized slumps that temporarily pinch or block the channels.

Summary and Conclusions

By reviewing the examples presented in Figures 177 through 189, the reader will hopefully be equipped to more readily appreciate the overlapping and complex nature of landslide mapping in most areas. Different types of landslides of vastly different ages are commonly superposed one upon another. The slide maps prepared for the City of Orinda are rough approximations of the most geologically recent, or topographically prominent, landslides, in some areas likely dating back thousands of years.

SOURCES OF INFORMATION EMPLOYED IN THIS STUDY

Sources of Topographic Maps

U.S. Coast and Geodetic Survey 15-Minute Topographic Maps

Historical USGS topographic maps have recently been overlaid on ArcGIS for public access at http://historicalmaps.arcgis.com/usgs/. The earliest topographic map of Orinda was that compiled by the U.S. Coast and Geodetic Survey (USCGS) as part of the Concord 15-minute quadrangle that was released in November 1897. This map was at a scale of approximately 1 in. = 1 mi (1 cm = 625.0 m) (1:62,500) with a contour interval of 25 ft (7.6 m). This sheet was reprinted in September 1910.

Most of the early geologic mapping of the Lamorinda area was accomplished on these maps (Clark, 1914; Lawson and Merriam, 1914), with the exception of Lawson and Palanche (1902), which was prepared in 1900

Downloaded from http://pubs.geoscienceworld.org/aeg/eeg/article-pdf/31/1/i/6130855/i1558-9161-31-1-i.pdf
by AEG RBAC user

by the University of California at a scale of 1:12,000 (1-in. = 1,000 ft [1 cm = 120.0 m]) with a contour interval of 10 ft (3.1 m) (the university produced other topographic maps of the Berkeley Hills area behind the campus into the mid-1930s).

A second edition of the 15-minute topographic sheet was subsequently prepared by the USCGS in June 1915, whereupon the expanding culture of the San Francisco East Bay was added to the older topographic base (which had originally been surveyed by plane table in 1893–94). This map was reprinted in 1939. It retained the same contour interval of 25 ft (7.6 m).

A third 15-minute series map was produced in 1943, during World War II. This map contains additional information on paved highways and as well as mudflats and sloughs along the San Francisco and Suisun Bay margins. This map was intended for the utilization of transportation for the war effort, especially the San Francisco Port of Embarkation and associated subordinate facilities, like the Oakland Army Base.

1948/1959 East Bay Municipal Utility District Maps

In mid-1948, the EBMUD commissioned a series of orthophoto[1] topographic maps of their facilities and utility corridors utilizing post-war aerial photos. These maps were prepared at a scale of 1 in. = 200 ft (1 cm = 24.0 m) with a contour interval of 5 ft (1.5 m). The USGS utilized one of these sheets as the base map for their early studies in Warford Mesa (Kachadoorian, 1956, 1959).

In the late 1950s, EBMUD updated their maps to include all of their watershed areas. Publications of importance to Orinda is a series of orthophoto-derived topographic sheets covering the tributary watershed of Briones Reservoir, which includes northeast "Orinda Briones Sheet 3." These maps were compiled from aerial photos taken in June 1959. The maps were produced at a scale of 1 in. = 400 ft (122 cm = 48.0 m) with a contour interval of 10 ft (3.1 m).

For many years blueline prints of these sheets were available over the counter from Contra Costa County Public Works in Martinez. A portion of one of these maps is presented here in Figure 133.

USGS 7.5-Minute Topographic Maps

In 1946, the USGS hired several photogrammetry firms to overfly the Orinda area taking stereo-pair aerial photos with a 60 percent overlap suitable for the production of a new generation of stereo-derived topographic maps. The first 7.5-minute USGS series quadrangles covering the Orinda area were the Briones Valley and Oakland East Quadrangles, which appeared in 1946 and 1949. These replaced the western half of the old Concord 15-minute quadrangle. The new maps were prepared at a scale of 1:24,000, or 1 in. equals 2,000 ft (1 cm = 240. m), with a contour interval of 20 ft (6.1 m).

Most of the 7.5-minute quadrangles located in areas of noticeable growth were updated in 1959, based on USGS imagery collected in 1958. In 1968, the Briones Valley Quadrangle was photo-revised (overlaid) using the 1968 aerial photos. A portion of this map is here reproduced in Figure 139. The Oakland East quadrangle was photo-revised in 1980, based on imagery taken that same year. These were the USGS quadrangles available to the public for the following 30+ years.

USGS quadrangles may be purchased online as inexpensive portable document format (pdf) files from the USGS Online Store online at https://www.usgs.gov/products/maps/topo-maps.

1959 Contra Costa County Maps

In 1959, Contra Costa County Public Works Department engaged Hammon, Jensen & Wallen of Oakland, CA, to prepare a series of topographic maps for the Bollinger Canyon Project. These maps were prepared at a scale of 1 in. = 200 ft (1 cm = 24.0 m) with a 10 ft (3.1 m) contour interval. Several of these maps reached into the south and east portions of Orinda, south of Highway 24. These included Contra Costa County Map Sheets 1518, C504, and C509. Blueline prints of these topographic maps were available in digital format from County Public Works in Martinez. These maps were utilized in delineating relict bedrock landslides in the Tahos Road area, as they pre-dated grading that took place in the early 1960s.

1966 Caltrans Maps

In 1966, the State Division of Highways (now within the California Department of Transportation) commissioned Sholtz Associates of Los Angeles to prepare orthophoto topographic maps of the Orinda area, stretching from San Pablo Dam south to Moraga. These maps were based on aerial imagery shot in March 1966 and produced at a scale of 1 in. = 200 ft (1 cm = 24.0 m) (1:2,400) with a 10 ft (3.1 m) contour interval. Contra Costa County still sells digital copies of these maps over the counter in Martinez. The County has designated these sheets T-563 through T-567.

[1] An orthophoto is a photo image that has been corrected so that its scale is uniform across the image. A topographic map is made from photographs but the photos themselves are not rectified. These are two distinct products and orthophotos are not used to produce topographic maps. When topographic maps are produced from aerial photographs, it is implied or could be described as being photogrammetrically derived.

Downloaded from http://pubs.geoscienceworld.org/aeg/eeg/article-pdf/31/1/i/6130855/i1558-9161-31-1-i.pdf
by AEG RBAC user

Topographic Maps for the Orinda Landslide Mapping Project (1992)

Hammon, Jensen & Wallen, Inc., of Oakland was retained by the City of Orinda through Rogers/Pacific, Inc., to prepare digitized topographic maps of all Orinda, including the undeveloped areas, such as Gateway Valley and the Wagner Ranch. These maps were prepared from imagery flown in June 1992 and prepared at an original scale of 1 in. = 300 ft (1 cm = 36.0 m) on photographic prints with a contour interval of 5 ft (1.5 m). These topographic maps were intended to be scale compatible with the County tax assessor parcel maps, in original hardcopy format. The topography data were digitized on a DXF file compatible with AutoCad 11, which was compatible with Contra Costa County's Intergraph GIS software. Separate DXF soft-copy files of Orinda's topography were presented to City staff as a part of Rogers/Pacific's 1992–94 landslide hazard mapping study (Rogers/Pacific, Inc., 1992a, 1992b, 1993, 1994).

Sources of Aerial Photographs

Introduction

The landslide and surficial deposits maps prepared for the City of Orinda were compiled after reviewing series of stereo-pair aerial photographs, aerial oblique photos, ground photos, topographic maps, bedrock geology maps, previous landslide mapping, review of published literature, and past reports by consultants in the Orinda area.

The features identified in this mapping were common surficial deposits often associated with various types of landslides. Since approximately 75 percent of the natural hillslope area within Orinda is blanketed by slides or unconsolidated colluvium of varying age, some attempt was also made to delineate the "relative recency of movement," as judged from the clarity of surface character exposed in historic stereo-pair aerial photographs and the site's "bare earth" topographic expression.

In many cases, slides were of sufficient age (>11,000 years old) to be classified as "relict" and are therein annotated on the maps, either with the word "relict" or with a series of "X" hachures. Explanation of the map symbols employed in the 1994 study was provided on each map sheet and is described in greater detail below.

Overview of Orinda Aerial Photo Sources

The earliest source of stereo-pair aerial photographs of Orinda was those taken by Fairchild Aerial Surveys of Los Angeles in February 1928. William Irvine of the Irvine Company retained Fairchild to photograph his newly acquired Moraga Rancho as a form of inventory. This collection includes most of the Oakland Hills, Moraga, Orinda, Lafayette, and portions of Walnut Creek. The original photos appear to have been taken with a Fairchild K-5 camera (Erickson, 1930) utilizing 100-ft-long (30.5-m-long) rolled film with 7 × 9-in. (17.8 × 22.9 cm) negatives. Overlap on the photos is approximately 60 percent along the flight lines and 40 percent on the side-lap. Two original sets of prints are maintained; one in the Bancroft Library at Cal Berkeley (donated from the Fairchild Collection at Whittier College) and the other by the Moraga Historical Society at the Moraga Library (donated by the Moraga Ranch Company). Duplicate prints may be purchased through Pacific Aerial Surveys in Novato, CA.

The earliest East Bay aerial surveyor appears to have been George S. Young Aerial Photographic Mapping of Oakland. Young photographed the proposed alignment of the Caldecott Tunnels (between Orinda Crossroads and Lake Temescal) for Joint Highway District 13 in August 1928. These stereo-pair photos include portions of Orinda and the freshly graded Brookwood, Underhill, and Barbara Roads in Oak Springs Units 1 and 2 near Orinda Crossroads. These images came from the Pacific Aerial Surveys collection.

In September 1928, Young photographed the rapid slumping of the downstream face of Lafayette Dam for the EBMUD. These images are included in the J. D. Galloway and W. L. Huber collections of the Water Resources Center Archives at the University of California at Riverside.

Young's most extensive collection was imaged in 1930, covering most of the East Bay plain, from San Leandro to El Cerrito. This collection consists of 120 photos and is kept in the History Room of the Oakland Public Library. Copies of these photos are also included in the Pacific Aerial Surveys collection.

In June 1937, Harrison C. Ryker of Standard Aerial Surveys in Oakland shot a series of vertical stereo-pair photos of the East Bay area that are part of the holdings reserved in the Oakland Library's History Room.

U.S. Department of Agriculture Photos

Soon after its establishment in 1935, the SCS of the U.S. Department of Interior initiated an aerial photo inventory of the United States and its territories. In the San Francisco Bay area, the first aerial photo inventory was flown in June 1939. The original photos were taken at an approximate scale of 1:20,000 and printed on 30-in. (76 cm) square sheets (from 9-in. [23 cm] square negatives). Soil scientists then used the photos in combination with their field studies to delineate the various soil deposits across the county, introduced after World War II. The original Soil Survey of Contra Costa County

Downloaded from http://pubs.geoscienceworld.org/aeg/eeg/article-pdf/31/1/i/6130855/i1558-9161-31-1-i.pdf
by AEG RBAC user

was completed in 1933 without benefit of aerial photos. In 1988, the Contra Costa County field office of the SCS (which became the Natural Resources Conservation Service, or NRCS, in 1994) donated their collection of oversize images to the Contra Costa County Historical Society. These are archived at their History Center in Martinez. Most of these were photographed and printed in 1950.

USGS Photos

Prior to 1946, USGS maps were compiled utilizing hand-acquired data with ground-controlled triangulation (producing maps at a scale of 1:62,500, or approximately 1 in. = 1 mile [1 cm = 625.0 m]). During World War II, the military engaged in widespread mapping of foreign shores and territories through the use of aerial reconnaissance photography. Topographic mapping techniques quickly surpassed the older methods, and a new, larger scale of map resulted (1:24,000, or 1 in. = 2,000 ft [1 cm = 240.0 m]).

During the summer of 1946, the USGS photographed most of the San Francisco Bay area, covering Orinda in July. These photos were made at an original (negative) scale of 1:23,600, just a bit larger than the 1:24,000-scale topographic map sheets that were produced from these images over the next decade.

The USGS took succeeding sets of photography at approximately 10-year intervals, covering Orinda again in 1958, 1968, 1980, and 1982 (due to the January 1982 storm). These photos were all taken at scales of between 1:20,000 and 1:24,000, and at $5 apiece (for a 9-in. [23 cm] square photo), they are the least expensive of all commercially available imagery.

The USGS used to maintain over 500,000 aerial photographs at their library located in Menlo Park, CA. The photos are cataloged according to their respective fiducial (photo) centers, which are plotted on USGS 7.5-minute quadrangle sheets. Hard copies of the photos are stored in the library according to the USGS quadrangle containing the photo centers. These images are now archived by the USGS Earth Resources Observation and Science (EROS) Center in Sioux Falls, SD, at https://www.usgs.gov/centers/eros.

The EROS Data Center in Sioux Falls includes all USGS imagery ever collected, dating back to World War II, and all National Aeronautics and Space Administration (NASA)–generated imagery, taken from high-altitude U-2 spy planes, as well as manned spacecraft, dating to the mid-1960s. Either duplicate negatives (film) or hard-copy prints may be ordered, up to 36 in. (91.4 cm) square (color negatives are not offered). When ordering aerial photos, it is usually necessary to first obtain or check the available photo indexes (which can also be purchased).

EROS Data Center also periodically releases special publications, such as *California and Landsat* (U.S. Geological Survey, 2021).

Pacific Aerial Surveys Collection

For almost nine decades, the largest collection of aerial imagery in the San Francisco Bay area has been the Pacific Aerial Surveys (PAS) collection. Pacific Aerial's historic collection emanated from aerial photo pioneer Clyde Sunderland (1900–91), who founded an aerial photography company at the old Oakland municipal airport in 1927. In the pre-war years, Sunderland shot aerial oblique photos, including the first ever photo of Yosemite Park in the winter of 1937–38. After serving as an aerial photo instructor for the U.S. Navy at Naval Air Station Pensacola (Florida) during World War II, Sunderland began amassing vertical stereo-pair imagery suitable for compiling accurate maps. In 1947, he began shooting "library coverage" of the inhabited portions of Alameda and Contra Costa Counties, initially at a scale of 1 in. = 1,666 ft (1 cm = 199.9 m), similar to the USGS imagery of that era.

In 1953, Sunderland photographed much of Orinda at a scale of 1 in. = 750 ft (1 cm = 90.0 m), the best library imagery up to that time. Sunderland's big break came in 1957, when PG&E contracted for 4,000 stereo-pair photos of Alameda and Contra Costa Counties. These were shot at a scale of 1 in. = 1,000 ft (1 cm = 120.0 m), and they exhibited excellent parallax characteristics for stereographic viewing. The 1 in. = 1,000 ft (1 cm = 120.0 m) scale was then adopted as Pacific Aerial's "standard" scale for "library stereo-pair imagery," flown with an aerial camera having an 8.25-in. (21.0-cm) focal length.[2]

In 1964, Sunderland sold his company, cameras, aircraft, and most of his negatives to Hammon, Jensen & Wallen, an Oakland-based surveying and photogrammetry firm. The new aerial survey arm, incorporating Sunderland's old company, was called Pacific Resources. This name was modified to Pacific Aerial Surveys in 1972.

The lack of mid-1960s 1:12,000-scale images in the PAS collection stems from the fact that the 1963 "library coverage" over Orinda was flown by Sunderland under contract to Hammon, Jensen & Wallen (prior to this, Sunderland had been forced to fly "library coverage" at his own expense, hoping to make up for the investment in succeeding years by sales of the photos). However, Hammon, Jensen & Wallen cut a deal with Aeroservices of Los Angeles (who had just purchased Fairchild Aerial Surveys) to provide the film with the agreement that

[2] PAS found that using a camera with an 8.25-in. (21-cm) focal length produced a better-scaled photo image than other configurations.

Downloaded from http://pubs.geoscienceworld.org/aeg/eeg/article-pdf/31/1/i/6130855/i1558-9161-31-1-i.pdf
by AEG RBAC user

Table 4. *Stereo-pair aerial photo sources (1994).*

Year	Agency That Took Photos	Source for This Study
1928	Fairchild Aerial Surveys (for the Irvine Company)	Bancroft Library, Moraga Historical Society & Pacific Aerial Surveys
1928	George S. Young (for Highway 24)	Caltrans and Pacific Aerial Surveys
1939	USDA Soil Conservation Service	Contra Costa History Center & USGS EROS Data Center
1945	Fairchild Aerial Surveys for State Division of Highways	Pacific Aerial Surveys
1946	U.S. Geological Survey	USGS Library Menlo Park & USGS EROS Data Center
1947	Clyde Sunderland Aerial Photography	Pacific Aerial Surveys (AV-11-1/13)
1950	USDA Soil Conservation Service (series BUU-12G)	Oakland Public Library & ASCS Salt Lake City
1953	Clyde Sunderland	Pacific Aerial Surveys (A V-119-1/13)
1957	Clyde Sunderland	Pacific Aerial Surveys (A V-253-12-1/20)
1959	Clyde Sunderland	Pacific Aerial Surveys (AV-334-14/15/19)
1963	Aeroservice	Intera-Aeroservices & Aerial Viewpoint (in Houston, TX)
1965	Cartwright Aerial Surveys	Geonex-Cartwright
1968	U.S. Geological Survey	USGS Library Menlo Park & EROS Data Center
1968	Pacific Resources	Pacific Aerial Surveys (AV-844 & 858)
1969	Pacific Resources	Pacific Aerial Surveys (A V-902 & 905)
1971	Pacific Resources	Pacific Aerial Surveys (A V-995 & 996)
1973	Cartwright Aerial Surveys	Geonex-Cartwright
1974	Pacific Aerial Surveys	Pacific Aerial Surveys (AV-1102)
1976	Pacific Aerial Surveys	Pacific Aerial Surveys (AV-1235 & 1251)
1978	Pacific Aerial Surveys	Pacific Aerial Surveys (AV-1515)
1982	Pacific Aerial Surveys	Pacific Aerial Surveys (AV-2145)
1983	Pacific Aerial Surveys	Pacific Aerial Surveys (AV-2300)
1986	Pacific Aerial Surveys	Pacific Aerial Surveys (AV-2861)
1991	Hammon Jensen & Wallen (for City of Orinda)	Pacific Aerial Surveys
1992	Pacific Aerial Surveys	Pacific Aerial Surveys (AV-4230)

they would then retain the negatives. Aeroservices was subsequently acquired by Litton Industries in the late 1960s, who moved all operations to Houston. In 1989, Litton Aeroservices was acquired by Intera Corporation. For several decades, stereo-pair images from the 1963 Orinda overflight could be obtained from Intera Aeroservices.

From 1964 to 2001, PAS was a subsidiary company of Hammon, Jensen & Wallen, located on Edgewater Drive near Oakland Airport. In July 2001,[3] Hammon, Jensen & Wallen was purchased by a private investor and became HJW Geospatial, Inc./Pacific Aerial Surveys. The PAS collection consisted of more than two million aerial image negatives, including those taken by Clyde Sunderland Aerial Photography, dating back to 1928.

In October 2009, HJW Geospatial/Pacific Aerial Surveys was purchased by Photo Science, and in 2013, they merged with two other aerial imagery firms to become Quantum Spatial, Inc. (QSI).[4] In 2014, QSI/Pacific Aerial Surveys purchased the aerial photo collection of Air Flight Services, increasing its library collection to approximately 3.5 million negatives. In June 2019, Alan Kropp & Associates, geotechnical consultants of Berkeley, CA, purchased the collection from QSI to keep the negatives in the San Francisco Bay area.

The PAS collection is presently (2021) stored in Novato and maintained by photo archivist David Ruiz. They maintain additional coverage in relation to the collections indicated above, having flown surveys over Orinda on approximately 1- to 2-year intervals from 1957 to 2000, with a gap of 1:12,000 coverage in the mid-1960s. The PAS collection includes 1:36,000-scale coverage imaged in 1963, 1966, and 1969. The years shown in the above table are only those utilized in this study.

Other Suppliers of Vertical Stereo-Pair Aerial Photos

One of Pacific Aerial Survey's competitors was Cartwright Aerial Surveys of Sacramento, CA, founded in 1946, until 1989, when it was acquired by Geonex. Cartwright flew library coverage of Orinda and all of Contra Costa County in 1965 and 1973 at a scale of 1 in. = 1,000 ft (1 cm = 120.0 m) (1:12,000 scale) and in 1987 at a scale of 1 in. = 2,000 ft (1 cm = 240.0 m) (1:24,000). Their 1965 and 1973 photos of Orinda were exceptional, taken with a camera having an 8.25-in. (21.0-cm) focal length at an original scale of 1:12,000.

The Geonex-Cartwright Aerial Surveys (CAS) collection was gifted to the University of California at Santa

[3] In 1999, Hammon, Jensen, Wallen & Associates and Pacific Aerial Surveys were acquired by The Map Factory and rebranded HJW GeoSpatial. Subsequent mergers with other aerial survey firms, culminating with Quantum Spatial, eliminated the HJW name but brought an additional 4.5 million images into the PAS collection.

[4] See press release of September 6, 2013: https://www.sco.wisc/2013/09/06/quantum-spatial-formed-through-merger-of-aerometric-photo-science-wsi/

Downloaded from http://pubs.geoscienceworld.org/aeg/eeg/article-pdf/31/1/i/6130855/i1558-9161-31-1-i.pdf
by AEG RBAC user

Barbara Library by the California State Library, after it was donated to the state when Cartwright was sold to Geonex in 1989. This collection includes material from >100 flights from the late 1950s to early 1980s, when there were few competitors photographing central and northern California municipalities. The scale of CAS imagery is usually 1:20,000 or larger, and the majority of the collection is available in digital format. The CAS flight line codes typically include an acronym for the city or county covered by the flight, while others have a four-digit number, e.g., CAS-SAC, CAS-3266. For this material, see https://www.library.ucsb.edu/geospatial/airphotos/cartwright-aerial-surveys-cas.

Another Sacramento-based aerial mapping firm that occasionally photographed Contra Costa County was Radman Aerial Surveys. Their clients included the U.S. Army Corps of Engineers, the State Department of Water Resources, and local municipalities, such as Pleasant Hill. Some of the library coverage of creek systems has been photographed in color.

Aerial Photo Collections Archived by the State of California

Other stereo-pair aerial photography covering much of the Orinda area is also maintained by the California Geological Survey at their Bay Area Regional Office in San Francisco. This collection includes many specialty photos taken along known fault lines in the early 1970s.

Caltrans has taken stereo-pair aerial photos of their major highway alignments about every 10 years since 1927. These photos include the series taken in July 1945 (by Fairchild Aerial Surveys) mentioned in the accompanying table, as well as sets taken in the late 1950s, mid- and late 1960s for Highway 24 widening (1967), for BART construction, the third bore of the Caldecott Tunnels (1960–62), and the proposed Gateway Boulevard extension (1969).

All of these images were accessed by Rogers/Pacific, Inc., during the Orinda landslide mapping study of 1992–94. Though incomplete in their coverage of the Orinda city limits, the Caltrans photos were generally taken at much larger scales than was commercially available from other sources, and they were some of the highest-definition images we viewed (e.g., Figure 34) for this study. Photo indexes are available for 1927 to 1956 and 1957 to 2021.

Imagery can be purchased from the Caltrans Office of Photogrammetry (OoP) and Office of Land Surveys in Sacramento. Guidance is offered in the *Caltrans Photogrammetry Surveys Manual* (https://dot.ca.gov/-/media/dot-media/programs/right-of-way/documents/ls-manual/13-surveys-a11y.pdf) and *Caltrans User's Guide to Photogrammetric Products and Services*. The third source is OoP's internet web site at: http://onramp.dot.ca.gov/hq/esc/sdsee/photogrammetry/index.shtml. The OoP also has a web site accessible via the internet at: http://www.dot.ca.gov/hq/esc /PHOTOGRAMMETRY. The OoP has a high-resolution, high-accuracy aerial film scanner suited for large-volume scanning of roll film.

All orders are normally coordinated with a Caltrans District photogrammetry coordinator (DPC), surveys section representative, and/or a Caltrans contract manager.

Caltrans Photogrammetry Surveys also offer the following products:

(1) Digital ortho-photography: High-accuracy digital images produced from stereo-photography and digital terrain information that can be used with reliability approaching that of conventional photogrammetric mapping.
(2) Digital Highway Inventory Photogrammetry Program (DHIPP): Intranet-accessible geo-referenced ortho-rectified digital color aerial images of the California highway system for non-engineering applications.
(3) Satellite imagery: High-altitude, low-resolution images available from remote-sensing satellite operators, which are appropriate for public displays and other non-engineering functions.
(4) Light detecting and ranging (LIDAR): LIDAR imaging that provides a high-density digital elevation model of a site by using an airborne laser to scan the terrain, producing a large number of geo-referenced points.

Aerial Oblique Photography

Several collections of aerial oblique photography were also utilized as part of the Orinda landslide study. These included photos taken by the U.S. Army Air Corps in 1935, by Les Sipe of the *Oakland Tribune* (1950–73), by Clyde Sunderland (1927–63), by Jack Logan of Sunderland (1945–63) and Pacific Aerial (1963–84), by Herington-Olsen (1946–96), by the California Department of Transportation, and by private individuals.

The finest set of pre–World War II imagery is that taken of the Oakland Hills by the U.S. Army Air Corps for the National Park Service in January 1935. Flying out of Crissy Field in the Presidio of San Francisco in an Army biplane, the air crew shot 93 stereo-pair images that comprise the 1935 collection. These images were made using a 7.5 × 9-in. (19.1 × 22.9-cm) hand-held Keystone aerial camera.

The U.S. Army was requested by the National Park Service/Forest Service Experimental Station in Berkeley to document conditions in the Berkeley–Oakland Hills, where Dr. Charles J. Kraebel of the U.S. Forest Service

Downloaded from http://pubs.geoscienceworld.org/aeg/eeg/article-pdf/31/1/i/6130855/i1558-9161-31-1-i.pdf
by AEG RBAC user

had recently designed a program to study biotechnical erosion control of fill slopes along Grizzly Peak Boulevard and other roads in the Tilden Park area. These pioneering efforts are archived in a collection of 7,500 photographs in the Charles J. Kraebel Collection of the Bancroft Library at Cal Berkeley: https://oac.cdlib.org/search?style=oac4;titlesAZ=c;idT=UCb162344326.

In January 1935, the twin Caldecott Tunnel bores were under construction, as well as State Routes 24 and 13, making these a key set of images from which to gleen details about the pre-development topography. The hills west of Camino Pablo and Moraga Way in Orinda are vividly displayed (Figure 7), and ancient landslides are much more easily identified than in subsequent photos because residents began planting abundant foliage to provide shade and windbreaks.

Copies of the January 1935 oblique photos may be obtained from Pacific Aerial Surveys. Pacific Aerial Surveys maintained a photo index map showing the coverage of each of the 63 frames prepared by Rogers/Pacific, Inc., on a 1935 series USGS 15-minute quadrangle mosaic.

Around 1936, other local aerial photographers started photographing Orinda. Some of these photos are presented in Figures 11b and 166–167. Prints from original negatives of these views are still available commercially from Pacific Aerial Surveys in Novato. Some of these photos give an excellent accounting of development activities in Orinda in the 1950s. Many of the pre-1941 PAS oblique photos are also located on the same 1935 USGS 15-minute map mosaic compiled by Rogers/Pacific, Inc., and passed onto Pacific Aerial Surveys.

Between 1927 and 1964, Clyde Sunderland maintained one of the finest aerial photography services in the San Francisco Bay area. Sunderland was bought out by Hammon, Jensen & Wallen in 1964. Many of his prewar photos were maintained by himself until his death in 1990, whereupon his widow donated them to the Bancroft Library at Cal Berkeley, where they are presently archived.

In the years following World War II, local newspapers began to utilize aerial oblique photography to cover newsworthy events that could be photographed from the air, such as fires, airplane crashes, flood damage, landslides, and development changes. Les Sipe worked as an independent press photographer for the *Oakland Tribune* between 1946 and 1973. His collection of both aerial and ground photos includes those presented in Figures 9 and 10. The Les Sipe collection is cataloged and maintained by the Contra Costa County Historical Society at their History Center in Martinez.

Another important source of post–World War Il aerial oblique photos was Herrington-Olsen of Oakland, who began photographing the East Bay in 1946. For that collection, 99 percent of the Herrington-Olsen images consisted of low-level aerial oblique photos shot for commercial clients, such as EBMUD, East Bay Regional Parks, oil companies, and the like. Herrington-Olsen maintained a collection of negatives and notebooks containing contact prints of the various subjects. Many of these covered the East Bay and subjects in Orinda, such as the EBMUD filtration plant along Camino Pablo.

Ground Photos

Many sources of ground photos were utilized in this study. These included photos taken from the Orinda Historical Society, from the Contra Costa County Historical Society (especially the Louis Stein and Les Sipe collections), from the USGS Library in Menlo Park, from local history books (*Hanson, 1988*), from *California Highways and Public Works* magazine (published by the State Division of Highways between 1925 and 1967), from university geology dissertations, from collections of prominent civil engineers maintained by the University of California Water Resources Center Archives, from the Frank Draeger civil engineering collection of the Moraga Historical Society, from the Contra Costa County Department of Disaster Services, from the State Office of Emergency Services, from the Contra Costa Consolidated Fire District, and from residents, surveyors, engineers, and geologists who have lived or worked in the Orinda area.

LANDSLIDE AND SURFICIAL DEPOSITS MAPPED IN THIS STUDY

Introduction

Many different types of landslides have been observed in the Lamorinda area. In mapping slides for the City of Orinda, we have attempted to combine all recognized slides into three basic groups: earthflows, slumps, and translational slides. Within these distinctions, there are several subgroups, such as debris flows, coalescing earthflow complexes, compound slides, and ancient slide complexes, which often underlie more recent but smaller slides. Other surficial deposits, several of which are prone to landsliding, were also mapped. These included colluvium, alluvium, and stream terrace deposits. Simplified explanations and examples of these slide types follow.

Alluvium is a general term for unconsolidated clay, silt, sand, or gravel that has been deposited by waterborne transport, such as in a floodplain, delta, valley bottom, etc. The texture of alluvium can be hydraulically sorted, with progressively coarser grained materials lying near the source or point of origin, such as on an

Downloaded from http://pubs.geoscienceworld.org/aeg/eeg/article-pdf/31/1/i/6130855/i1558-9161-31-1-i.pdf
by AEG RBAC user

alluvial fan below a mountain front. Alluvium is easily recognized by the rounded nature of entrained clasts and hydraulic sorting (clasts of similar size within a given stratum). In the Briones Regional Park northeast of Orinda's city limits, alluvium up to 100 ft (30.5 m) thick infills small upland valleys. Within Orinda, alluvium is most pronounced in the valley bordering San Pablo Creek, upon which the City's central business districts are constructed.

Saturated unconsolidated alluvium is particularly susceptible to earthquake shaking–induced liquefaction if it exhibits low cohesion (low clay content) and is subject to more than four or five equivalent cycles of loading (Cloud, 1959). For these reasons, most of the Holocene-age alluvium has been carefully mapped across the developed margins and tributaries of the San Francisco Bay, including central Contra Costa County within and surrounding Orinda (Witter et al., 2006).

Terrace deposits are typically remnants of a river's former floodplain or channel that were deposited before the stream cut down to its current position. Terraces are much more locally restricted as opposed to alluvium. Most of Orinda's stream channels contain noticeable inset terraces (Pape, 1978; Rogers, 1988a), and most of these features were too small to be included in this study. Terraces also form in channels subjected to landslide damming of creek channels, a common occurrence in Orinda's geologic past (Figures 128, 129b, and 158).

Colluvium, or "slope wash," is angular detritus that has been transported downslope through gravitational means, such as biogenic activity (root action or displacement by animals), sheet runoff by rainfall over a short distance, or soil creep into natural depressions. In outcrop, colluvium is roughly stratified parallel to the slope fall line, and it commonly lies upon a basal layer of larger-diameter material that serves as a "natural subdrain." In outcrop, colluvium can appear identical to man-made fill, in that it is generally composed of subangular to angular clasts of local parent material. Sequential cartoons depicting the depositional phases of colluvium production, infilling, and evacuation are shown in Figure 144.

Colluvium is preferentially generated upon intensely jointed bedrock strata or strata of fissile character or thinly bedded strata. Soil horizons commonly form within 6 ft (1.8 m) of the ground surface, with immature argillic B-horizons overlain by calcium-rich A-horizons. This upper mantle of soil-like material also generally has a lower bulk density, due to rooting, and, therefore, it is more subject to landslippage (Reneau, 1988).

Colluvial-filled bedrock ravines are very prone to erosion by overland flow. This is because once the protective covering of soil (the upper 1 to 6 ft [0.3 to 1.8 m]) is broken, the underlying colluvium derives most of its strength from interparticle friction (Reneau et al., 1984). As a consequence, colluvium often disintegrates into destructive debris flows, capable of causing great harm (Reneau and Dietrich, 1987; Shlemon et al., 1987).

Earthflows are the most common type of landslide in the East Bay Hills of San Francisco Bay. Earthflow denotes a style of landsliding in which the parent material has disintegrated to the point of becoming a semi-homogeneous mixture of slide debris that moves *en masse* as a semi-viscous fluid. Earthflows tend to be composed of coalescing masses, containing many lobes, each attesting to individual sequences of separation and flowage within a larger, semi-coherent mass. In the context used in the Orinda landslide mapping, debris flows and debris avalanches are included within earthflows as a style of landslippage.

In studying landslides of the Lamorinda area, Radbruch and Weiler (1963) coined the term "coalescing earthflows" to describe the multiplicity of flow lobes exposed in the area's earthflows. Only portions of the earthflow typically mobilize during any single winter, and then, on about a 10-year recurrence average.

Earthflows are the easiest of all landslide forms to detect, because they are easily identified by the following factors: They generally occupy natural drainage swales (where they are most subject to groundwater recharge); they are typified by a melted, hummocky appearance (Figures 151–153); and their topographic expression is generally crenulated (Figures 112, 115, and 116). A block diagram representative of typical earthflows in the Lamorinda area is presented in Figure 108.

Earth slumps are a form of landslippage wherein a coherent mass of either soil or bedrock has experienced backward rotation along a semi-circular failure surface and translated *en masse* downslope. Slumps are more difficult to distinguish, especially depending on their relative age. If the ground moves a sufficient distance, then the toe materials may disintegrate into an earthflow or debris-flow cone, merging smoothly with the underlying slope.

Large ancient bedrock slumps, long dormant, may be very difficult to ascertain with insufficient area experience. The cartoon presented in Figure 156 presents an example typical of the Contra Costa Hills. Slides of this type were reactivated after fill was surcharged upon them during residential construction in the early 1960s, at Muth Drive and Austin Court on upper Tahos Road, and above Silverwood Court (Figures 190 and 191).

Translational slides, block glides, and other large landslide types were included within this distinction. The largest active slide complexes, like that below Zander Drive, are composed of rotational movement in the headscarp region, translational movement in the middle section, and flowage in the toe areas. Arguments over

Downloaded from http://pubs.geoscienceworld.org/aeg/eeg/article-pdf/31/1/i/6130855/i1558-9161-31-1-i.pdf
by AEG RBAC user

the proper nomenclature, therefore, are somewhat redundant, depending on the portion of the landslide being described.

Ancient or relict translational and compound slides are delineated by crossed "x" patterns on a field in the landslide maps. These overlays delineate large ancient slides that are thought to be >11,000 years old. As a consequence of their age, these slides are not thought to be susceptible to potential reactivation. In many instances, these slides are large compound slide masses, or they are slides composed of many components within a single semi-continuous zone.

Examples of compound slides are presented in Figures 134–137, as well as some enormous complex bedrock slides mantling the slopes of San Pablo Ridge north and south of El Toyonal. Descriptive cross sections of this area are presented in Figures 60–63.

Figure 190. Aerial oblique view of the Silverwood Court landslide area below Tahos Road in 1986. These slides were intermittently active between 1967 and 1986, when cumulative rainfall levels reached record levels (J. David Rogers).

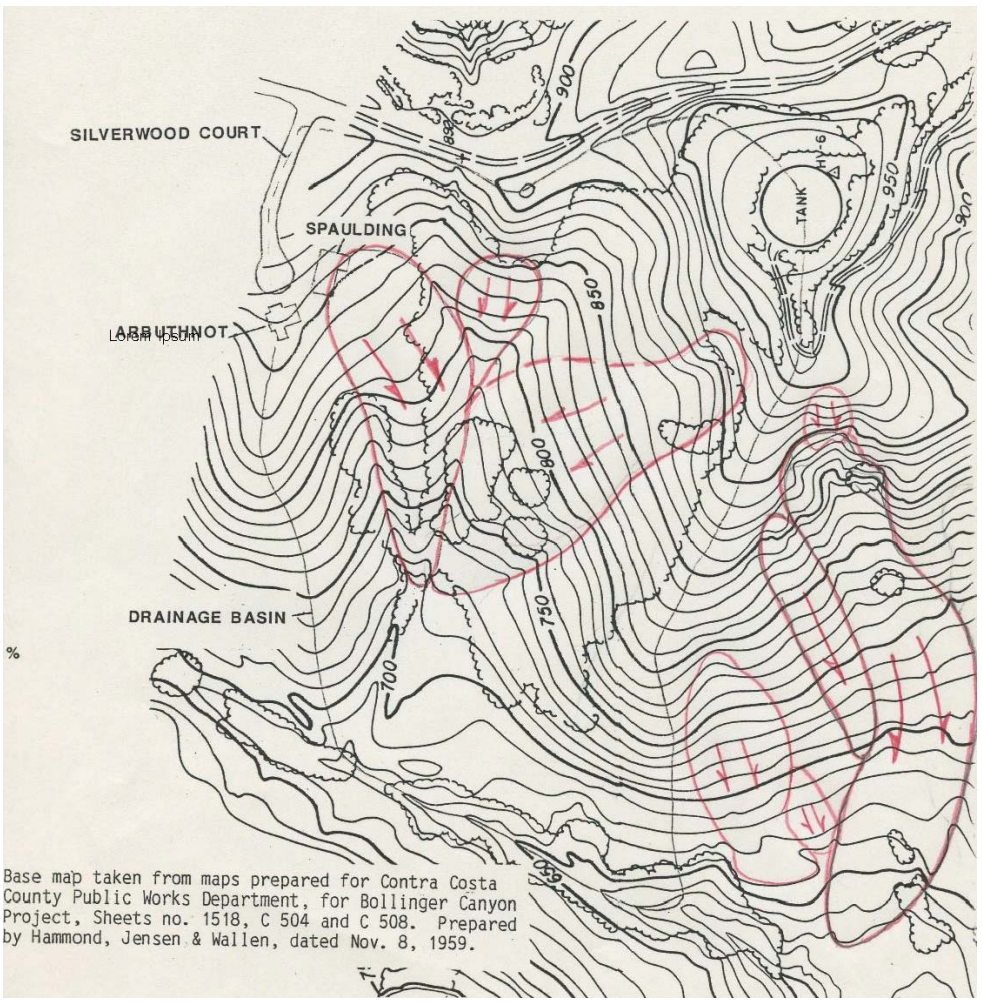

Figure 191. Dormant bedrock landslides mapped in the vicinity of Tahos Road and Silverwood Court for settlement conferences for litigation in the early 1990s. The slide mass coming off the Spaulding and Arbuthnot residences reactivated in 1983 and 1986. The topographic map represents pre-grading conditions surveyed in 1959.

Downloaded from http://pubs.geoscienceworld.org/aeg/eeg/article-pdf/31/1/i/6130855/i1558-9161-31-1-i.pdf
by AEG RBAC user

Vagueness Inherent in Delineating Boundaries of Dormant Landslides

As mentioned at the outset of this book, the boundaries delineated in this landslide mapping project are completely subjective. In those instances where development has occurred, anthropogenic activities often mask past geomorphic or topographic evidence of landslippage, inhibiting any definitive identification of landslide margins. In other instances, the age of landslippage precludes definitive expression of landslide boundaries. Last, vegetation and subsequent landsliding may also serve to mask older slide features. In such instances, the interpreter is forced to rely upon their area experience and the geometric limitations imposed by the kinematics inherent in various forms of landsliding (discussed in section on "Limiting Geometry of Active Landsliding"). Despite these shortcomings, few other photo-interpretive landslide analyses have been preceded by so many years of field work within a particular outcrop area.

Localities within Orinda that Were Field Checked

In this study, the following locations were field checked with benefit of subsurface exploration and mapping to confirm the physical processes of past landslippage that had controlled subsequent slope instability: Toledo Drive (Lafayette), Moraga Road (Lafayette), Campolindo Ridge (Moraga), St. Stephen's Road, Via Floreado, Gardiner Lane, Lucy Lane, Zander Drive, Alice Lane, Donald Drive, Hall Drive, upper Tahos Road, Austin Court, Muth Drive, Warford Terrace, Tara Road, Stein Way, Barbara Road, Knickerbocker Lane, Ironwood Circle, El Toyonal, La Encinal, Cañon Road, Ardilla Road, Camino Sobrante, Mira Loma, Camino Pablo, the Orinda BART Station slide, Monte Vista Road, Charles Hill Circle, Tiger Tail Court, Tappan Lane/Bear Ridge Road, Wanda Lane, Orchard Road, Parklane Drive, Las Palomas, Altarinda Drive, Don Gabriel Way, Valencia Road, and area studies in Siesta Valley, Gateway Valley, above Miramonte High School/Moraga Adobe, in the Bear Creek watershed, and in the upper Pinole Creek watershed.

ACKNOWLEDGMENTS

The authors are indebted to all those people whose tutelage, exposure, or exchange of ideas have fostered a greater understanding of landslide processes. Foremost among these was Rogers' professional mentor Alan L. Kropp, P.E., G.E., in Berkeley. During graduate school at Cal Berkeley (1976–82), the many hours spent by the senior author with the U.S. Geological Survey's Engineering Geology Branch in Menlo Park provided the formative basis upon which these scientific studies of landslides were pursued. Their key individuals included David Keefer, Gerry Wieczorek, Ed Harp, Ray Wilson, Steve Ellen, Les Youd, Dorothy Radbruch-Hall, and Earl Brabb. Alan Kropp and Earl Brabb always challenged the senior author to focus on doing something valuable for mankind, and to serve peers in whatever way possible.

Conversations with the senior author's principal advisor, Richard E. Goodman, led to many lasting and valuable contacts, including Mike Duncan, Hugh Trollope, Nilmar Janbu, and Alec Skempton. Contacts with the geology department also proved especially valuable in formulating an appreciation of physical processes responsible for landsliding. These individuals included Garniss Curtis, Clyde Wahrhaftig, and Luna Leopold from Cal Berkeley and Dick Jahns at Stanford University.

Upon leaving graduate school, the senior author mixed frequently with a number of individuals who exerted considerable influence on his thinking. These included Professors Bill Dietrich, David Cruden, Bill Bull, Rob Olshansky, Ron Shreeve, Don Gray, Ralph Peck, Tom Dunne, Arvid Johnson, Marty Stout, Perry Ehlig, Nick Sitar, and Vince Cronin. It also included USGS geologists David J. Varnes, Robert L. Schuster, Earl Brabb, Bill Brown, David Keefer, Tom Pierson, Mark Reid, and Manuel (Doc) Bonilla; U.S. Army Corps of Engineers scientists Ellis Krinitzky, Don Banks, and Mary Ellen Hynes; U.S. Park Service at Yosemite N.P. geologists Bill Weaver; California Geological Survey scientists Earl Hart, Bob Sydnor, Chris Wills, Tim McCrink, Cliff Davenport, Salem Rice, Ted Smith, and Mike Mansfield; and fellow consultants Bill Cotton, Jon Bray, Mike Scullin, Alan Kropp, P. Erik Mikkelsen, Darwin Myers, Laurel Collins, Cathy Wilson, Steve Reneau, Marc Seeley, Earl Buckingham, Bob Wright, Rex Upp, Richard Proctor, Leo Devito, George Reid, David Snyder, Jim Baker, Sandy Figuers, John Walkinshaw, Chris Alger, Joel Baldwin, Bob Tepel, Dick Meehan, Bruce Clark, and Jim Slosson.

Of these people, David Varnes, Bob Schuster, Bill Cotton, Bill Dietrich, Earl Brabb, Dave Keefer, Dick Goodman, and Hugh Trollope exerted the most considerable influence on current thinking. Correspondence with others, such as Dave Cruden, Barry Voight, Beach Leighton, Perry Rahn, K. O. Emery, and Finn Jorstad, provided many valuable references. Last, the writings of such individuals as C. F. S. Sharp, David J. Varnes, Harry Cedergren, Bob Schuster, Rex Baum, John Costa, George F. Sowers, Dave Montgomery, George Kiersch, Stanislav Novosad and Ludek Novosad, M. J. Selby, Jack Mollard, Mike Kirkby, Mike Crozier, Pierre Londe, Douglas Way, USFS geologists Bob Davis and Allen Hatheway have been instrumental in completing this work.

Downloaded from http://pubs.geoscienceworld.org/aeg/eeg/article-pdf/31/1/i/6130855/i1558-9161-31-1-i.pdf
by AEG RBAC user

Older works that left a lasting impression include the writings of C.F.S. Sharpe, Karl Terzaghi, Quido Zaruba, Vojtech Mencl, Hyde Forbes, Bailey Willis, Kirk Bryan, G.K. Gilbert, Donald F. MacDonald, A. W. Root, Edwin B. Eckel, and George Edgar Ladd.

Between 1984-1997 the staff at Rogers/Pacific, Inc., provided an immense level of help, without which this publication would not have been possible. We are especially indebted to Gary Ham and Dan Wang, who utilized their skills as AutoCad operators to electronically draft most of the principal figures. Dan Wang upgraded and colored all of the files included in this special publication. We would also like to thank David Ruiz of Pacific Aerial Surveys for his review of the "Sources of Information Employed in this Study," particularly the aerial photography section.

REFERENCES

Ahmed, M. F. and Rogers, J. D., 2014, First-approximation landslide inventory maps for northern Pakistan, using ASTER DEM data and geomorphic indicators: *Environmental and Engineering Geoscience*, Vol. 20, No. 1, pp. 67–83.

Anderson, R., 1908, Earth flows at the time of the San Francisco earthquake: *Geological Society of America Bulletin*, Vol. 18, p. 643.

Atwater, B. F., 1979, Ancient processes at the site of southern San Francisco Bay: Movement of the crust and changes in sea level. In Conomos, T. J., (Editor) *[The] San Francisco Bay, Urbanized Estuary: 58th Annual Meeting of the Pacific Division*: American Association for the Advancement of Science, San Francisco, CA, pp. 31–46.

American Society for Testing and Materials (ASTM), 1955, Laboratory Compaction Characteristics of Soil Using Standard Effort (12,400 ft-lbf/ft^3). ASTM Test Designation D 698, *Annual Book of ASTM Standards, Section 4-Construction, Volume 04.08 Soil and Rock*. West Conshohocken, PA.

American Society for Testing and Materials (ASTM), 1957, Laboratory Compaction Characteristics of Soil Using Modified Effort (56,000 ft-lbf/ft^3). ASTM Test Designation D 1557, *Annual Book of ASTM Standards, Section 4-Construction, Volume 04.08 Soil and Rock*. West Conshohocken, PA.

American Society for Testing and Materials (ASTM), 1958, Standard Test Method for Penetration Test and Split-Barrel Sampling of Soils. ASTM Test Designation D 1586. ASTM *Annual Book of ASTM Standards, Section 4-Construction, Volume 04.08 Soil and Rock*. West Conshohocken, PA.

American Society for Testing and Materials (ASTM), 1975, Standard Test Method for Quasi-Static, Cone, and Friction-Cone Penetration Test of Soil. ASTM Test Designation D 3441. *Annual Book of ASTM Standards, Section 4-Construction, Volume 04.08 Soil and Rock*. West Conshohocken, PA.

Atwater, B. F.; Hedel, C. W.; and Helley, E. J., 1977, *Late Quaternary Depositional History, Holocene Sea-Level Changes, and Vertical Crustal Movement, Southern San Francisco Bay, California*: U.S. Geological Survey Professional Paper 1014, 15 p., 1 plate.

Baker, R. F. and Marshall, H. C., 1958, Control and correction. In Eckel, E. B. (Editor), *Landslides and Engineering Practice*: Highway Research Board (HRB) Special Report 29, pp. 150–188.

Baltzer, A., 1880, Uber Bergsturze: *Neues Jahrbuch für Mineralogie, Geognosie, Geologie und Petrefaktenkunde*, Vol. 2, pp. 197–199.

Baum, R. L. and Fleming, R. W., 1991, Use of longitudinal strain in identifying driving and resisting elements of landslides: *Geological Society of America Bulletin*, Vol. 103, No. 8, pp. 1121–1132.

Beaty, C. B., 1956, Landslides and slope exposure: *Journal of Geology*, Vol. 64, pp. 70–74.

Bechtel Corporation, 1965, *Engineering Geology of the Berkeley Hills Tunnel–Contra Costa Line* (consultant's report to San Francisco Bay Area Rapid Transit District): Bechtel Corporation, San Francisco, CA, 27 p., 6 plates.

Betz, C., 1993, personal communication. Clarence Betz was Secretary Treasurer of the local Chamber of Commerce in 1953–54 when the suggestion was offered.

Bishop, A. W., 1955, The use of the slip circle in the stability analysis of slopes: *Geotechnique*: Vol. 5, No. 1, pp. 7–17.

Bishop, A. W., 1959, The principle of effective stress: Text of lecture delivered to the Norwegian Geotechnical Society, in 1955: *Teknisk Ukeblad*, Vol. 106, No. 39, pp. 859–863.

Bishop, A. W., 1971. The influence of progressive failure on the choice of the method of stability analysis. Geotechnique, 21(2), pp. 168–172.

Bjerrum, L., 1960, Some notes on Terzaghi's method of working. In Terzaghi, K., *From Theory to Practice in Soil Mechanics*: John Wiley and Sons, London, pp. 22–25.

Bjerrum, L., 1966, Mechanisms of progressive failure in slopes of overconsolidated plastic clays and shales: Third Terzaghi lecture: *Journal Soil Mechanics and Foundation Engineering Division: American Society of Civil Engineers*, Vol. 93 (1967), No. SM-5, pp. 1–49.

Black, I. W. and Degenkolb, O. H., 1964, The Caldecott Tunnels: *California Highways and Public Works*, Vol. 44, No. 7–8, pp. 12–18.

Bonilla, M. G., 1960, *Landslides in the San Francisco South Quadrangle*, California: U.S. Geological Survey Open-File Report 60-15, 44 p.

Borchardt, G. and Rogers, J. D., 1991, Earthquake potential along the Hayward Fault, California. In *Proceedings of the Second International Conference on Recent Advances in Geotechnical Earthquake Engineering and Soil Dynamics*, Vol. 3: University of Missouri-Rolla, St. Louis, MO, pp. 2295–2308.

Borcherdt, R. D., 1970, Effects of local geology on ground motion near San Francisco Bay: *Bulletin of the Seismological Society of America*, Vol. 60, No. 1, pp. 29–61.

Bowen, O. E., 1951, Highways and byways of particular geologic interest: Oakland to Byron via Broadway Tunnel and Marsh Creek Roads. In Jenkins, O. P. (Compiler), *Geologic Guidebook of the San Francisco Bay Counties*: California Division of Mines Bulletin 154, pp. 344–357.

Bowen, O. E., 1951, Highways and byways of particular geologic interest: Oakland to Byron via Broadway Tunnel and Marsh Creek Roads. In Jenkins, O. P. (Compiler), *Geologic Guidebook of the San Francisco Bay Counties*: California Division of Mines Bulletin 154, pp. 344–357.

Bowers, N. A., 1928, Uncompleted Lafayette Rolled-fFill Earth Dam Dmaged by Movement: *Engineering News Record*, September 27, 1928, pp. 483–485.

Brabb, E. E.; Pampeyan, E. H.; and Bonilla, M. G., 1972, *Landslide Susceptibility in San Mateo County, CA*: U.S. Geological Survey Miscellaneous Field Studies Map MF-360, scale 1:24,000.

Brabb, E. E.; Sonneman, H. S.; and Switzer, J. R., 1971, *Preliminary Geologic Map of the Mt. Diablo–Byron Area, Contra Costa, Alameda, and San Joaquin Counties, California*: U.S. Geological Survey Open-File Map 71-53, scale 1:62,500.

Brown, I. R.; Brekke, T. L.; and Korbin, G. E., 1981, *Behavior of the Bay Area Rapid Transit Tunnels through the Hayward Fault*: Final report to the U.S. Department of Transportation, Urban Mass Transit Administration, Washington, D.C., 208 p.

Brown, W. M., 1982, *Debris Flows, Landslides, and Floods in the San Francisco Bay Region January 1982: Overview and Summary of a Conference Held at Stanford University, August 23–26, 1982*:

Downloaded from http://pubs.geoscienceworld.org/aeg/eeg/article-pdf/31/1/i/6130855/i1558-9161-31-1-i.pdf
by AEG RBAC user

National Research Council/U.S. Geological Survey/National Academy Press, Washington, D.C., 83 p.

Bruckl, E. and Scheidegger, A. E., 1973, Application of the theory of plasticity to slow mudflows: *Geotechnique*, Vol. 23, No. 1, pp. 101–107.

Bruggers, J., 1989, Buying a hillside home? First ask the experts: *Contra Costa Times*, Vol. 78, No. 272 (Monday, February 27, 1989), p. 6A.

Buckingham, E. M., 1947, Landslide repairs in Oakland: *Transactions American Society of Civil Engineers*: Vol. 112, pp. 419–424.

Buckingham, E. M., 1962, Investigation and correction of landslides. In Brown, P. and Shockley, W. (Editors), *Field Testing of Soils*: ASTM Special Technical Publication 322, International, West Conshohocken, PA, pp. 159–165.

Bull, W. B., 1991, *Geomorphic Responses to Climatic Change*: Oxford University Press, New York, 326 p.

Buwalda, J. P., 1929, Nature of the late movements on the Haywards Rift, central California: *Bulletin Seismological Society of America*, Vol. 19, No. 4, pp. 187–199.

California Division of Highways, 1967, *Slope Stability and Foundation Investigation*: University of California, Institute of Transportation and Traffic Engineering, pp. 41–75.

California Division of Mines & Geology, 1992, *Landslide Hazard Identification Program, Annual Report*: [California] Department of Conservation, Sacramento, CA, 12 p.

California State Legislature. California Code of Regulations, Title 21. Public Works. 1950.

Campbell, A. P., 1966, Measurement of movement of an earthflow: *Soil and Water*, Vol. 2, No. 3, pp. 23–24.

Cannon, S. H. and Ellen, S., 1985, Abundant debris avalanches, San Francisco Bay region, California: *California Geology*, Vol. 38, No. 12, pp. 267–272.

Case, J. E., 1963, *Geology of Parts of the Berkeley and San Leandro Hills, California*: Ph.D. dissertation, Department of Geology & Geophysics, University of California, Berkeley, CA, 216 p., 3 plates, scale 1:24,000.

Casagrande, A., 1952, Notes on the design of earth dams. In *Contributions to Soil Mechanics*, Vol. II: Boston Society of Civil Engineers, Boston, MA, 497 p.

Cedergren, H. R., 1989, Slope stabilization with drainage. In Cedergren, H. R., *Seepage, Drainage and Flow Nets*, 3rd ed.: John Wiley & Sons, New York, 465 p.

Chow, V. T. and Takase, N., 1977, Design criteria for hydrologic extremes: *Journal of the Hydraulics Division*, Vol. 103, No. 4, pp. 425–436.

Clark, B. L., 1914, *Geology and Paleontology of the Concord 15-Minute Quadrangle*: unpublished map, Paleontology Museum, University of California, Berkeley, CA, 1 sheet.

Clark, B. L., 1921, The marine Tertiary of the west coast of the United States; its sequence, paleogeography, and the problems of correlation: *Journal of Geology*, v. 29, no. 7, p. 583–614.

Clark, B. L., 1930, Tectonics of the Coast Ranges of middle California: Geological Society of America Bulletin, v. 41, no. 4, p. 747–828.

Cloud, W. K., 1959, Intensity and ground motion of the San Francisco earthquake of March 22, 1957. In Oakeshott, G. B. (Editor), *San Francisco Earthquakes of March 1957*: California Division of Mines Special Report 57, pp. 49–57.

Coate, B. D., 1990, *Water-Conserving Plants & Landscapes for the Bay Area*: East Bay Municipal Utility District, Oakland, CA.

Codilean, A. T.; Bishop, P.; and Hoey, T. B., 2006, Surface process models and the links between tectonics and topography: *Progress in Physical Geography*, Vol. 30, pp. 307–333.

Colwell, R. N. (Editor), 1960, *Manual of Photographic Interpretation*: American Society of Photogrammetry, Falls Church, VA, 888 p.

Content, C., 1967, Berkeley Hills Tunnel holes through: *The Engineering Geologist: Quarterly Newsletter, Engineering Geology Division, Geological Society of America*, Vol. 2, No. 3, pp. 8–9.

Contra Costa County, 1960, *County Ordinance 1491 (Grading)*: November 30, 1960 (incorporated as Article 716-4 of the Contra Costa County Code) Department of Building and Inspection, Contra Costa County, Martinez, CA.

Contra Costa County, 1977, *Contra Costa County Mean Seasonal Isohyets (B-166) and Precipitation Duration-Frequency-Depth Curves (B-152 thru B-162), Compiled from Precipitation Records 1879–1973*: Public Works Department, County Flood Control and Water Conservation District, Contra Costa County, Martinez, CA.

Contra Costa Standard, 1943, Moving mountain stops; County road rerouted: *Contra Costa Standard* (newspaper), June 4, 1943 [Contra Costa History Center, Martinez, CA].

Cooke, R. U. and Reeves, R. W., 1976, *Arroyos and Environmental Change in the American Southwest*: Clarendon Press, Oxford, U.K., 213 p.

Costa, J. E. and Fleisher, P. J. (Editors), 1984, *Developments and Applications of Geomorphology*: Springer-Verlag, New York, 372 p.

Cotton, C. A., 1950, Tectonic scarps and fault valleys: *Geological Society America Bulletin*, Vol. 61, No. 7, pp. 717–758.

Coulomb, C. A., 1776, *Essai sur une Applicationdes Regles des Maximis et Minimis a quelques Problemes de Statique Relatifsa l'Architecture*: Memoires de la Mathematique et de Physique 7, Academie Royale des Sciences, France, Paris.

Crane, R. C., 1988, Geologic map of the Las Trampas Ridge quadrangle. In Crane, R. C., *Field Trip Guide to the Geology of the San Ramon Valley and Environs*: Northern California Geological Society, Hercules, CA.

Creely, S.; Savage, D. E.; and Ogle, B. A., 1982, Stratigraphy of Upper Tertiary nonmarine rocks of central Contra Costa Basin, California. In Ingersoll, R. V. and Woodburne, M. O. (Editors), *Cenozoic Nonmarine Deposits of California and Arizona*: Society of Economic Paleontologists and Mineralogists, Pacific Section, Los Angeles, CA, pp. 11–22.

Cronin, V. S., 1992, Compound landslides: Nature and hazard potential of secondary landslides within host landslides. In Slosson, J. E.; Keene, A. G.; and Johnson, J. A. (Editors), *Landslides/Landslide Mitigation*: *Geological Society of America Reviews in Engineering Geology*, Vol. IX, pp. 1–10.

Crozier, M. J., 1973, Techniques for the morphometric analysis of landslips: *Zeitschrift für Geomorphologie*, Vol. 17, No. 1, pp. 78–101.

Cruden, D. M. (Compiler), 1990, A suggested method for reporting a landslide: *Bulletin of the International Association of Engineering Geologists* (Paris), Vol. 41, pp. 5–12.

Cruden, D. M., 1991a, A suggested method for a landslide summary: *Bulletin of the International Association of Engineering Geologists* (Paris), Vol. 43, pp. 101–110.

Cruden, D. M., 1991b, A simple definition of a landslide: *Bulletin of the International Association of Engineering Geologists* (Paris), Vol. 43, pp. 27–29.

Cruden, D. M., Thomson, S. and Hoffman, B. A., 1991. Observation of graben geometry in landslides. In Slope stability engineering developments and applications: Proceedings of the international conference on slope stability organized by the Institution of Civil Engineers and held on the Isle of Wight on 15–18 April 1991 (pp. 33–35). Thomas Telford Publishing.

Cruden, D. M.; Novograd, S.; Pilot, G. A.; Krauter, E.; Bhandari, R. K.; Cotecchia, V.; Nakamura, H.; Okagbue, C. O.; Zhuoyuan, Z.; Hutchinson, J. N.; and Varnes, D. J., 1990, Suggested nomenclature for landslides: *Bulletin of the International Association of Engineering Geology* (Paris), Vol. 41, No. 1, pp. 13–16.

Cruden, D. M., and Varnes, D. J., 1996, Landslide types and processes. In Turner, A. K. and Schuster, R. L. (Editors), *Landslides: Investigation and Mitigation*: Transportation Research Board Special Report 247, National Academy of Sciences, Washington, D.C., pp. 36–75.

Downloaded from http://pubs.geoscienceworld.org/aeg/eeg/article-pdf/31/1/i/6130855/i1558-9161-31-1-i.pdf
by AEG RBAC user

Cummings, D. and Clark, B. R., 1988, Seismic refraction and electric resistivity surveys in landslide investigations: *Bulletin of the Association of Engineering Geologists*, Vol. XXV, No. 4, pp. 459–464.

Curtis, G., 1978, personal communication. Department of Geology & Geophysics at the University of California at Berkeley. Dr. Garniss Curtis visited the Orinda BART Station landslide and collected samples for evaluation at the X-ray fluorescence laboratory at the University of California at Berkeley.

Curtis, G., 1984, personal communication. Department of Geology & Geophysics at the University of California at Berkeley.

Dalton, W. C., 1954, Road bond issue: Contra Costa makes big strides with FAS program: *California Highways and Public Works*, Vol. 33, No. 11–12, pp. 27–29 & 63.

Danehy, E. A., 1969, Tunnels of the Bay Area. In Danehy, E. A. (Editor), *Urban Environmental Geology in the San Francisco Bay Region*: Special Publication, San Francisco Section, Association of Engineering Geologists, San Francisco, CA, pp. 93–104.

Davis, W. M., 1899, The geographical cycle: *Geographical Journal*, Vol. 14, pp. 481–504.

Davidson, C. F., 1965. Mass-movement on the Gisborne Coastline (Doctoral dissertation, University of Canterbury) Degenkolb, O. H., 1960, Third Tunnel, new parallel bore through Berkeley Hills is planned: *California Highways and Public Works*, Vol. 39, No. 7–8, pp. 31–34.

Demoro, H. W., 1967, BART at mid-point: Interurbans Magazine, Vol. 25, No. 3. Reprinted by Interurban Associates, Los Angeles, CA, 1968, 117 p.

Dengler, L.; Lehre, A. K.; and Wilson, C. J., 1987, Bedrock geometry of unchannelized valleys: In *Proceedings of the Symposium on Erosion and Sedimentation on the Pacific Rim*, 3–7 August 1987, Corvallis, Oregon: Publication 165, International Association of Hydrological Sciences, Vienna, Austria, pp. 81–90.

Dettinger, M. D.; Ralph, F. M.; Das, T.; Neiman, P. J.; and Cayan, D. R., 2011, Atmospheric rivers, floods and the water resources of California: *Water*, Vol. 3, No. 2, pp. 445–478.

Dibblee, T. W., Jr., 1980, *Preliminary Geologic Map of the Briones Valley Quadrangle, Contra Costa, California*: U.S. Geological Survey Open-File Report 80-536.

Dibblee, T. W., Jr., and Darrow, R. L., 1981, Guidebook to the regional geology of the East Bay Hills and the northern Diablo Range–Livermore Valley area. In Frizzell, V. (Editor), *Geology of the Central and Northern Diablo Range, California*: Annual Meeting Guidebook, SEPM Fieldtrips 2 and 5, Pacific Section, Society of Economic Geologists and Paleontologists, Los Angeles, CA, pp. 65–76.

Dietrich, W. E.; Dunne, T.; Humphrey, N. F.; and Reid, L. M., 1982, Construction of sediment budgets for drainage basin catchments. In Swanson, F.; Janda, R. J.; Dunne, T.; and Swanston, D. N. (Editors), *Sediment Budgets and Routing in Forested Drainage Basins*: General Technical Report PNW-141, U.S. Forest Service Pacific Northwest Forest and Range Experiment Station, Portland, OR, pp. 5–24.

Dietrich, W. E., and Rogers, J. D., 1988, Mass wasting and slope failure: Landform development. Back, W.; Rosenshein, J. S.; and Seaber, P. R. (Editors), *Hydrogeology*: Geology of North America, Vol. O-2, Geological Society of America, Boulder, CO, pp. 383–400.

Dietrich, W. E.; Wilson, C. J.; and Reneau, S. L., 1987, Hollows, colluvium and landslides in soil-mantled landscapes. In Abraham, A. D. (Editor), *Hillslope Processes*: Allen and Unwin, Boston, MA, pp. 371–397.

Duncan, J. M., 1971, Prevention and correction of landslides. In *Sixth Annual Nevada Street and Highway Conference*, Section II (April 7, 1971), pp. 1–42.

Duncan, J. M., and Stark, T. D., 1992, *Soil Strengths from Back Analysis of Slope Failures: Stability and Performance of Slopes and Embankments—II*: Geotechnical Special Publication 31, American Society of Civil Engineers, New York, pp. 890–904.

Duncan, J. M. and Wright, S. G., 1980, The accuracy of equilibrium methods of slope stability analysis. In Koh, S. L. (Editor), *Mechanics of Landslides and Slope Stability*: Engineering Geology, Vol. 16, pp. 5–17.

Eckel, E. B. (Editor), 1958, *Landslides and Engineering Practice*: Highway Research Board Special Report 29, National Academy of Sciences/National Research Council, Washington, D.C., 232 p.

Ellen, S. D. and Wieczorek, G. F. (Editors), 1988, *Landslides, Floods, and Marine Effects of the Storm of January 3–5, 1982, in the San Francisco Bay Region, California*: U.S. Geological Survey Professional Paper 1434, 310 p., 11 plates.

Ellsworth, W. L.; Olson, J. A.; Shijo, L. N.; and Marks, S. M., 1982, Seismicity and active faults in the eastern San Francisco Bay region. In Hart, E. W.; Hirschfeld, S. E.; and Schwartz, S. S. (Editors), *Proceedings [First] Conference on Earthquake Hazards in the Eastern San Francisco Bay Area*: Special Publication 62, California Division of Mines and Geology, Sacramento, CA, pp. 83–91.

Engineering News Record, 1928, Committee named to report on slump in Lafayette Dam: *Engineering News Record*, October 25, 1928, p. 634.

Engineering News Record, 1929a, Modified completion of Lafayette Dam recommended: *Engineering News Record*, January 17, 1929, p. 116.

Engineering News Record, 1929b, Reconstruction of Lafayette Dam Advised: *Engineering News Record*, January 31, 1929, pp. 190–192.

ENGEO, 2008. *Application Management for Sea Level Rise – Geologic Hazard Abatement Districts*, Prepared for the California Association of Geologic Hazard Abatement Districts. Available from: https://ghad.org/wp-content/uploads/2019/01/Application-Management-for-Sea-Level-Rise_11-2008.pdf.

Erickson, H. A., 1930, Making aerial mapping pay: *Aviation*, June 7, 1930, pp. 1125–1127.

Federal Housing Administration. (FHA). (1956). Neighborhood standards for California: San Francisco jurisdiction (Land Planning Bulletin; no.3-5B).Washington, DC: U.S.Government Printing Office

Fellenius, W., 1919, Utredning betraffande kajbyggnaden for Trondbeims hamn (Design considerations for a quay in Trondheim Harbor): Teknisk Tidskrift, Vol. 49, No. I, pp. 1–19.

Fellenius, W., 1936, Calculation of the stability of earth dams. In *Second International Congress on Large Dams, Transactions*, Vol. 4: U.S. Government Printing Office, Washington, D.C., pp. 445–465.

Fleming, R. W. and Taylor, F. A., 1980, *Estimating the Costs of Landslide Damage in the United States*: U.S. Geological Survey Circular 832, 21 p.

Forbes, J. H., 1947, Landslide investigation and correction: *Transactions of the American Society of Civil Engineers*, Vol. 112, pp. 377–442.

Gerwick, B. C., Jr., and Woolery, J. C., 1983, *Construction and Engineering Marketing for Major Project Services*: John Wiley & Sons, New York, pp. 282–283 ("Walking off the Job").

Gilbert, G. K., 1877, LandDelete reference from listSculpture. In *Report on the Geology of the Henry Mountains: U. S. Geographical and Geological Survey of the Rocky Mountain Region*: U.S. Department of the Interior, Washington, D.C., pp. 99–150.

Gilbert, G. K., 1909, The convexity of hilltops: *Journal of Geology*, Vol. 17, No. 4, pp. 344–350.

Gilbert, G. K., 1917, *Hydraulic Mining Debris in the Sierra Nevada [Mountains]*: U.S. Geological Survey Professional Paper 105, 154 p.

Goodman, R. E., 1976. Toppling of rock slopes. In Proc. Specialty Conf. on Rock Engineering for Foundations and Slopes (Vol. 2, pp. 201–234). Amer. Soc. Civil Eng.

Goodman, R. E., 1999, *Karl Terzaghi: The Engineer as Artist*: American Society of Civil Engineers Press, New York, 327 p.

Downloaded from http://pubs.geoscienceworld.org/aeg/eeg/article-pdf/31/1/i/6130855/i1558-9161-31-1-i.pdf
by AEG RBAC user

Goodman, R. E.; Rogers, J. D.; and Chan, L. Y., 1981, *Development of Techniques for Evaluating Seismic Hazards of Creeping Landslides and Old Dams*: Final Report for USGS-NEHRP Grant, U.S. Geological Survey Open-File Report 81-50.

Graham, S. A.; Gavigan, C.; McCloy, C.; Hitzman, M.; Ward, R.; and Turner, R., 1983, Basin evolution during the change from convergent to transform continental margin: An example from the Neogene of central California. In Cherven, V. B. and Graham, S. A. (Editors), *Geology and Sedimentology of the Southwestern Sacramento Basin and East Bay Hills*: Field Trip Guidebook, Pacific Section, Society Economic Paleontologists and Mineralogists, Los Angeles, CA, pp. 101–117.

Graham, S. A.; McCloy, C.; Ritzman, M.; Ward, R.; and Turner, R., 1984, Basin evolution during change from convergent to transform continental margin in central California: *of the American Association of Petroleum Geologists Bulletin*, Vol. 68, No. 3, pp. 233–249.

Gray, D. H. and Leiser, A. T., 1982, *Biotechnical Slope Protection and Erosion Control*: Van Nostrand Reinhold, New York, 271 p.

Graymer, R. W.; Jones, D. L.; and Brabb, E. E., 1994, *Preliminary Geologic Map Emphasizing Bedrock Formations in Contra Costa County, California: A Digital Database*: U.S. Geological Survey Open-File Report 94-622.

Graymer, R. W., Jones, D. L., Brabb, E. E., and Helley, E. J., 1994, *Preliminary Geologic Map of the Niles 7.5-Minute Quadrangle*. U.S. Geological Survey Open-File Report 94-132.

Green, P. A. and Ferguson, P. A. S., 1971, On liquefaction phenomena, by Professor A. Casagrande: Report of lecture: *Geotechnique*, Vol. XXI, No. 3, pp. 197–202.

Grim, R. E., 1968, *Clay Mineralogy*, 2nd ed.: McGraw-Hill, New York, 596 p.

Grove, J. M., 1988, *The Little Ice Age*: Methuen & Company, New York, 498 p.

Gruntfest, E. C., 1987, *What We Have Learned Since the Big Thompson Flood*: Special Publication 16, Natural Hazards Research and Applications Information Center, University of Colorado, Boulder, CO, 271 p.

Gruntfest, E. C., 1997, *Twenty Years Later: What We Have Learned Since the Big Thompson Flood*: Special Publication 33, Natural Hazards Research and Applications Information Center, University of Colorado, Boulder, CO, 205 p.

Hansen, W. R., 1965, *Effects of the Earthquake of March 27, 1964, at Anchorage, Alaska*: U.S. Geological Survey Professional Paper 542-A, 68 p.

Hanson, E. C., 1988, *California and Nevada Railroad*: R & S Printers, Northampton, PA, 65 p.

Harden, D. R.; Janda, R. J.; and Nolan, K. M., 1978, *Mass Movement and Storms in the Drainage Basin of Redwood Creek, Humboldt County, California—A Progress Report*: U.S. Geological Survey Open File Report 78-486, 161 p., 1 plate.

Harding, R. C., 1969, Landslides—A continuing problem for Bay Area development. In Danehy, E. A. (Editor), *Urban Environmental Geology in the San Francisco Bay Region*: Special Publication, San Francisco Section, Association of Engineering Geologists, Sacramento, CA, pp. 65–74.

Heim, A., 1882, Der Bergsturtz von Ehn: *Zeitschrift der Deutschen geologischen Gesellschaft*, Vol. 34, pp. 7 4–115.

Herlinger, E. W. and Stafford, G. F., 1952, Orinda slide: Installation of 95 horizontal drains was monumental project: *California Highways & Public Works*, Vol. 31, No. 1–2, pp. 45–60.

Hersey Inspection Bureau, 1955, *Preliminary Soils Investigation, Warford Mesa Unit 1*: Consultant's report to A.B. Muth & Sons, Orinda, CA, Job 386-55, October 31, 1955.

Hersey Inspection Bureau, 1958, *Investigation of Slipout on Lots 84, 85, 80 and 81, Warford Mesa Unit 1, Orinda, CA*: Consultant's report to A.B. Muth & Sons, Orinda, CA, Job 339-55, February 21, 1958.

Hoffmann, W. and Rantz, S. A., 1963, *Floods of December 1955 and January 1956 in the Far Western States*: U.S. Geological Survey Water Supply Paper 1650-A and 1650-B, 156 p. and 580 p.

Hogentogler, C. A., 1937, Engineering Properties of Soil, McGraw-Hill Book Co, New York, NY, 434 p.

Horton, R. E., 1945, Erosional development of streams and their drainage basins; hydrophysical approach to quantitative morphology: *Geological Society of America Bulletin*, Vol. 56, pp. 275–370.

Howe, E., 1909, *Landslides in the San Juan Mountains, Colorado*: U.S. Geological Survey Professional Paper 67, 58 p.

Humphrey, N. F., 1982, *Pore Pressures in Debris Failure Initiation*: Master's thesis, Department of Geological Sciences, University of Washington, Seattle, WA, 169 p.

Hungr, O.; Leroueil, S.; and Picarelli, L., 2014, The Varnes classification of landslide types, an update: *Landslides*, Vol. 11, No. 2, pp. 167–194.

Huntting, M. T., 1945, Geology in highway engineering: *Transactions of the American Society of Civil Engineers*, Vol. 112, Paper 2238, pp. 271–344.

Hutchinson, J. N., 1969, A reconsideration of the coastal landslides at Folkstone Warren, Kent: *Geotechnique*, Vol. 19, No. 1, pp. 6–38.

Hutchinson, J. N. and Bhandari, R. K., 1971, Undrained loading, a fundamental mechanism of mudflows and other mass movements: *Geotechnique*, Vol. 21, No. 4, pp. 353–358.

IAEG (International Association of Engineering Geology) Commission on Landslides, 1990, Suggested nomenclature for landslides: *Bulletin International Association of Engineering Geology*, Vol. 41, pp. 13–16.

IGS UNESCO WP/WLI (International Geotechnical Societies' UNESCO Working Party on World Landslide Inventory), 1993, A suggested method for describing the activity of a landslide: *Bulletin of the International Association of Engineering Geology*, Vol. 47, pp. 53–57.

IGS UNESCO WP/WLI (International Geotechnical Societies' UNESCO Working Party on World Landslide Inventory), 1994, A suggested method for reporting landslide causes: *Bulletin of the International Association of Engineering Geology*, Vol. 50, pp. 71–74.

IGS UNESCO WP/WLI (International Geotechnical Societies' UNESCO Working Party on World Landslide Inventory), 1994, *Multilingual Landslide Glossary*: BiTech Publishers Ltd., Richmond, British Columbia, Canada, 32 p.

International Society for Soil Mechanics and Foundation Engineering, Technical Committee 11, 1993, *Landslide Illustrations: A Collection of 26 Slides*: Department of Engineering, Cambridge University, Cambridge, U.K.

Iverson, R. M., 1992, Sensitivity of stability analyses to groundwater data. In *Proceedings of the Sixth International Symposium on Landslides*: Christchurch, New Zealand, 7 p.

Iverson, R. M., 2003, How should mathematical models of geomorphic processes be judged? In Wilcock, P. R. and Iverson, R. M. (Editors), *Prediction in Geomorphology*: Geophysical Monograph 135, American Geophysical Union, Washington, D.C., 256 p.

Janbu, N., 1957. Earth pressures and bearing capacity calculations. In Proc., 4th ICSMFE (Vol. 2, pp. 207–212).

Janbu, N., 1969, *An Advanced Method of Slope Stability Analysis*: lecture manuscript (in English), University of California, Los Angeles and Berkeley, CA, spring quarter 1969, 56 p. (prepared by Nilmar Janbu while he was a visiting scholar at the University of California at Berkeley in 1969).

Janbu, N., 1973, Slope stability computations. In Hirschfeld, R. C. and Poulos, S. J. (Editors), *Embankment Dam Engineering*: John Wiley & Sons, New York, pp. 47–86.

Janbu, N.; Bjerrum, L.; and Kjaernsli, B., 1956, Veiledning ved losning av fundamenteringsoppgaver (Soil mechanics applied to some

Downloaded from http://pubs.geoscienceworld.org/aeg/eeg/article-pdf/31/1/i/6130855/i1558-9161-31-1-i.pdf
by AEG RBAC user

engineering problems): Publication 16, Norwegian Geotechnical Institute, Oslo, Norway, Chapters 1 and 2, pp. 5–26.

Johnson, A. M., 1970, *Physical Processes in Geology*: Freeman, Cooper & Co., San Francisco, CA, 577 p.

Johnson, K. A., and Sitar, N., 1989, Significance of transient pore pressure and local slope conditions in debris flow initiation. In *Proceedings 12th International Conference on Soil Mechanics and Foundation Engineering*: Rio de Janeiro, Brazil, pp. 1619–1622.

Johnson, P. L. and Cole, W. F., 2001, The use of large-diameter boreholes and downhole logging methods in landslide investigations. In Ferriz, H. and Anderson, R. (Editors), *Engineering Geology Practice in Northern California*: Special Publication 12, Association of Engineering Geologists, Los Angeles, CA, California Geological Survey Bulletin 210, pp. 95–106.

Jones, D. L., 1992, *Tectonics of Transgressive Plate Boundary: A New Paradigm for the Central California Coast Ranges: Proceedings of Second Conference on Earthquake Hazards in the Eastern San Francisco Bay Area*: Special Publication 113, California Division of Mines and Geology, p. 28.

Jones, D. L. and Brabb, E. E., 1992, *Tectonic Significance of the Neogene Berkeley Hills Fold and Thrust Belt: Proceedings of the Second Conference Earthquake Hazards in the Eastern San Francisco Bay Area*: Special Publication 113, California Division of Mines and Geology, p. 17.

Jones, D. L. and Curtis, G., 1991, *Guide to the Geology of the Berkeley Hills, Central Coast Ranges, California: Geologic Excursions in Northern California, San Francisco to Sierra Nevada*: Special Publication 109, California Division of Mines and Geology, pp. 63–73.

Jones, F. O., Embody, D. R. and Peterson, W. L., 1961. Landslides along the Columbia river valley, Northeastern Washington (Vol. 367). US Government Printing Office.

Kachadoorian, R., 1956, *Engineering Geology of the Warford Mesa Subdivision, Orinda, California*: U.S. Geological Survey Open File Report, 13 p., 1 plate, scale 1:6,000.

Kachadoorian, R., 1959, *Engineering Geology of the Orinda Crossroads Area, Orinda, California*: Master's thesis, School of Mineral Sciences, Stanford University, Stanford, CA, 24 p., 9 plates.

Keefer, D. K. and Johnson, A. M., 1983, *Earth Flows—Morphology, Mobilization, and Movement*: U.S. Geological Survey Professional Paper 1264, 56 p., 3 plates.

Kleinpell, R. M., 1938. Miocene stratigraphy of California: tulsa, Oklahoma. American Association of Petroleum Geologists, 22.

Kessell, J. E., 1943, Disintegrating soil slips of the Coast Ranges of central California: *Journal of Geology*, Vol. 51, pp. 342–352.

Kiersch, G. A., 1969, *Pfeiffer versus General Insurance Corporation—Landslide Damage to Insured Dwelling, Orinda, California: Engineering Geology Case Histories No. 7: Legal Aspects of Geology in Engineering Practice*: Engineering Geology Division, Geological Society of America, New York, pp. 81–93.

Kiersch, G. A. and Waggoner, E. B., 1991, The geologist and legal responsibilities. In Kiersch, G. A. (Editor), *The Heritage of Engineering Geology: The First Hundred Years*: Centennial Special Volume 3, Decade of North American Geology series, Geological Society of America, Boulder, CO, pp. 559–573.

Kimball, S., 1987, *Moraga's Pride*: Moraga Historical Society, Moraga, CA, 225 p.

Kirkby, M., 1988, Hill slopes and hollows: *Nature*, Vol. 336, p. 201.

Ladd, G. E., 1935, Landslides, Subsidence and Rock-falls: Proceedings of the 36th Annual Convention: American Railway Engineering Association: Chicago: Vol 36, pp. 1091–1162.

Lamb, H. H., 1985, Climatic History and the Future: Princeton University Press: 835 p.

Lawson, A. C. (Editor), 1908, Minor geological effects of the earthquake [landslides]. In *The California Earthquake of April 18, 1906*: Report of the State Earthquake Investigation Commission, Carnegie Institution of Washington, Washington, D.C., pp. 384–409.

Lawson, A. C., 1914, *Description of the San Francisco District; Tamalpais, San Francisco, Concord, San Mateo, and Hayward (15-Minute) Quadrangles*: U.S. Geological Survey Geologic Atlas, Folio 193, 24 pp., 5 plates.

Lawson, A. C. and Palanche, C., 1902, The Berkeley Hills: A detail of Coast Range geology: *Bulletin of the Department of Geology, University of California* (Berkeley), Vol. 2, No. 12, pp. 349–450, 1 plate.

Lawson, Andrew C.; Merriam, John C.; Haywards Quadrangle. Structure Sections. Edition of Jan. 1914.; 6384.033; Color. Surveyed 1896-1910

Lebarre, R. V., 1936, Test Pit Exploration Kit for Foundation Study: Engineering News Record, Vol. 117, pp. 194–197.

Lee, W. H. K.; Eaton, M. S.; and Brabb, E. E., 1971, The Earthquake Sequence near Danville, California, 1970: Bulletin of the Seismological Society of America: vol. 61, no. 6, pp. 1771–1794.

Legros, F., 2002, The mobility of long-runout landslides, Engineering Geology, Vol. 63, pp. 301–331.

Lehre, A. K., 1982, Sediment mobilization and production from a small mountain catchment: Lone Tree Creek, Marin County, California: Ph.D. dissertation: Department of Geology & Geophysics: University of California, Berkeley: 320 p.

Leighton, F. B., 1966, Landslides and Hillside Development: in Engineering Geology in Southern California: R.V. Proctor and R. Lung, eds.: Special Publication of the Los Angeles Section of the Association of Engineering Geologists: pp. 149–190.

Leopold, L. B.; Wolman, M. G.; and Miller, J. P., 1964, Fluvial Processes in Geomorphology: W.H. Freeman & Co., San Francisco, 522 p.

Liang, T., 1952, Landslides: An Aerial Photographic Study, Ph.D. dissertation, Cornell University, Ithaca, NY 274 p.

Liang, T. and Belcher, D. J., 1958, Airphoto Interpretation, in E.B. Eckel, (Editor), Landslides and Engineering Practice, Highway Research Board Special Report 29, pp. 69–92.

Liniecki, M., 1982, Lacustrine Facies of the Mulholland Formation (Upper Miocene, Upper Contra Costa Group), Moraga, Central California. In Cherven, V. B. and Graham, S. A. (Editors) *Geology and Sedimentology of the Southwestern Sacramento Basis and East Bay Hills*: Field Trip Guidebook: Pacific Section, Society of Economic Paleontologists and Mineralogists, Los Angeles, CA, pp. 93–99.

Liniecki, M., 1986, *Late Miocene Paleoenvironments of the Lower Mulholland Formation, West-Central California*: Master's thesis, San Jose State University, San Jose, CA, 88 p.

Liniecki-Laporte, M. and Andersen, D. W., 1988, Possible new constraints on late Miocene depositional patterns in west-central California: *Geology*, Vol. 16, pp. 216–220.

Louderback, G. D., 1930, *Preliminary Report on the Geological Conditions along the Line of the Proposed Highway Tunnel between Alameda and Contra Costa Counties*: Consultant's report to Joint Highway District 13, July 7, 1930, 7 p., 1 plate.

Lutton, R. J.; Banks, D. C.; and Strohm, W. E., 1979, Slides in Gaillard Cut, Panama Canal Zone. In Voight, B. (Editor), *Rockslides and Avalanches, 2*: Elsevier Scientific Publishing, New York, pp. 151–224.

Macdonald, D. I. M.; Moncrieff, A. C. M.; and Butterworth, P. J., 1993, Giant slide deposits from a Mesozoic fore-arc basin, Alexander Island, Antarctica: *Geology*, Vol. 21, No. 11, pp. 1047–1050.

Machan, G. and Bennett, V. G., 2008, *Use of Inclinometers for Geotechnical Instrumentation on Transportation Projects: State of the Practice*: Transportation Research Circular E-C129.

Malgot, J. and Baliak, F., 1993. Engineering-geological maps with respect to slope stability in Slovakia. In International conference and field workshop on landslides (pp. 97–101).

McBride, J. R., 1964, *Invasion of East Bay Regional Parks Grassland by Baccharis pilularis DC*: Master's thesis in Forestry, University of California, Berkeley, CA.

McBride, J. R., 1974, Plant succession in the Berkeley Hills, California: *Madrono*, Vol. 22, No. 7, pp. 317–329.

Downloaded from http://pubs.geoscienceworld.org/aeg/eeg/article-pdf/31/1/i/6130855/i1558-9161-31-1-i.pdf
by AEG RBAC user

McBride, J. R. and Heady, H. F., 1968, Invasion of grassland by *Baccharis pilularis* DC: *Rangeland Ecology & Management/Journal of Range Management Archives*, Vol. 21, No. 2, pp. 106–108.

McCarty, J. E. and Bryant, C. W., 1962, *The October 1962 Storm Report of the Street and Engineering Department*: unpublished report, Office of the City Engineer, City of Oakland, Oakland, CA, 21 p.

McGlashan, H. D., and Briggs, R. C., 1939, *Floods of December 1937 in Northern California*: U.S. Geological Survey Water Supply Paper 843, 497 p.

McLean, R. F. and Davidson, C. F., 1968. The role of mass-movement in shore platform development along the Gisborne coastline, New Zealand.

Melosh, H. J., 1987, The mechanics of large rock avalanches. In Costa, J. E. and Wieczorek, G. F. (Editors), *Debris Flows/Avalanches: Process, Recognition, and Mitigation*: *Geological Society of America Reviews in Engineering Geology*, Vol. VII, pp. 41–50.

Mencl, V., 1966. Mechanics of landslides with non-circular slip surfaces with special reference to the Vaiont slide. Géotechnique, 16(4), pp. 329–337.

Miller, W. J., 1931, The landslide at Point Fermin, California: *Science Monthly*, Vol. 32, pp. 464–469.

Merriam, J. C., 1898, The distribution of the Neocene sea urchins of middle California and its bearing on the classification of the Neocene formations: University of California Publications in Geological Sciences, v. 2, no. 4, p. 109–118.

Mitchell, J. K., 1993, *Fundamentals of Soil Behavior*, 2nd ed.: John Wiley & Sons, New York, 577 p.

Montgomery, D. M. and Dietrich, W. E., 1988, Where do channels begin?: *Nature*, Vol. 336, pp. 232–234.

Morganstern, N. R. and Eigenbrod, K. D., 1974, Classification of argillaceous soils and rocks: *Journal of the Geotechnical Engineering Division, American Society of Civil Engineers*, Vol. 100, No. 10, pp. 1137–1158.

Morganstern, N. R. and Price, V. E., 1965, The analysis and stability of general slip surfaces: *Geotechnique*, Vol. 15, No. I, pp. 79–93.

Morton, D. M. and Campbell, R. H., 1974, Spring mudflows at Wrightwood, southern California: *Quarterly Journal of Engineering Geology*, Vol. 7, pp. 377–384.

Muller, L., 1964, The rock slide in the Vaiont Valley: *Rock Mechanics and Engineering Geology*, Vol. 2, pp. 148–212.

Nash, D. B., 1980, Morphologic dating of degraded normal fault scarps: *Journal of Geology*, Vol. 88, pp. 353–360.

Nilsen, T. H., 1975a, *Preliminary Photointerpretation Map of Landslide and Other Surficial Deposits of the Briones Valley 7.5-Minute Quadrangle, Contra Costa County, California*: U.S. Geological Survey Open-File Map 75-277, plate 8.

Nilsen, T. H., 1975b, *Preliminary Photo-interpretive Map of Landslides and Other Surficial Deposits of the Oakland East 7.5-Minute Quadrangle, Alameda and Contra Costa Counties, California*: U.S. Geological Survey Open-File Map 75-277, plate 41.

Nilsen, T. H. and Brabb, E. E., 1977, Slope stability studies in the S. F. Bay Region, CA. In Coates, D. R. (Editor), *Landslides*: *Geological Society of America Reviews in Engineering Geology*, Vol. III, p. 235–243.

Nilsen, T. H. and Turner, B. L., 1975, *Influence of Rainfall and Ancient Landslide Deposits on Recent Landslides (1951–71) in Urban Areas of Contra Costa County, California*: U.S. Geological Survey Bulletin 1388, 18 p., 1 plate.

Olshansky, R. B., 1986, Geological Hazard Abatement Districts: *California Geology*, Vol. 39, No. 7, pp. 158–159.

Olshansky, R. B., 1989, Landslide hazard reduction: A need for greater government involvement: *Zoning and Planning Law Report*, Vol. 12, No. 13, pp. 104–112.

Olshansky, R. B. and Rogers, J. D., 1987, Unstable ground: Landslide policy in the United States: *Ecology Law Quarterly*, Vol. 13, No. 4, pp. 201–267.

Oppenheimer, D. H. and Macgregor-Scott, N., 1992, The seismotectonics of the eastern San Francisco Bay region. In Borchardt, G. (Editor), *Proceedings of the Second Conference on Earthquake Hazards in the Eastern San Francisco Bay Area*: Special Publication 113, California Division of Mines and Geology, Sacramento, CA, pp. 11–16.

Orris, G. J., 1983, *A Quantitative Investigation of Landslides in a Portion of the Santa Clara Formation, Santa Clara County, California (1979): Master's thesis*, Department of Geology, San Jose State University, San Jose, CA, 80 p., 1 plate.

Orris, G. J. and Williams, J. W., 1984, Landslide length-width ratios as an aid in landslide identification and verification: *Bulletin of the Association of Engineering Geologists*, Vol. 21, No. 3, pp. 371–375.

Page, B. M., 1950, Geology of the Broadway Tunnel, Berkeley Hills, California: *Economic Geology*, Vol. 45, No. 2, pp. 142–166.

Pape, D. A., 1978, *Terraced Alluvial Fills in Contra Costa County, California*: Master's thesis, Department of Geology & Geophysics, University of California, Berkeley, CA, 44 p.

Penck, A., 1894, *Morphologie der Erdoberflache*, Vol. I: Engelhorn, Stuttgart, Germany, pp. 222–231.

Petterson, K. E., 1916, Kajraset i Goteborg den 5 mars, 1916 (The quay slide in Gothenburg on 5 March 1916): *Teknisk Tidskrift*, Vol. 46, No. 30, pp. 281–287 and No. 30, pp. 289, 291.

Phelps, G. A.; Graymer, R. W.; Jachens, R. C.; Ponce, D. A.; Simpson, R. W.; and Wentworth, C. M., 2008, *Three-Dimensional Geologic Map of the Hayward Fault Zone, San Francisco Bay Region, California*: U.S. Geological Survey Scientific Investigations Map 3045.

Pierson, T. C. and Costa, J. E., 1987, A rheologic classification of subaerial and sediment-water flows. In Costa, J. E. and Wieczorek, G. F. (Editors), *Debris Flows/Avalanches: Process, Recognition, and Mitigation*: *Geological Society of America Reviews in Engineering Geology*, Vol. VII, pp. 1–12.

Provenzano, J. M., 1965, *Report to Theodore Matley on Soils Investigation for 4 Warford Terace and 28 Muth Drive, Orinda, CA*: Consultant's report by Gribaldo, Jacobs and Jones, Oakland, CA, File No. E2990-01, June 23, 1965, 45 p.

Provenzano, J. M., 1983, *Earth Slide at 4 Warford Terrace, Orinda, CA*: Consultant's report by Provenzano & Associates, Emeryville, CA, Job #1298, August 22, 1983, 9 p.

Purcell, M. F., 1940, *History of Contra Costa County*, 1st ed.: Gilleck Press, Berkeley, CA, 742 p.

Radbruch, D. H., 1957, *Areal and Engineering Geology of the Oakland West Quadrangle, California*: U.S. Geological Survey Miscellaneous Geologic Investigations Map I-239, scale 1:24,000.

Radbruch, D. H., 1969, *Areal and Engineering Geology of the Oakland East Quadrangle, Alameda and Contra Costa Counties, California*: U.S. Geological Survey Map GQ-769, scale 1:24,000.

Radbruch, D. H. and Case, J. E., 1967, *Preliminary Geologic Map and Engineering Geologic Information, Oakland and Vicinity, California*: U.S. Geological Survey Open File Report 67-183, 3 sheets, scale 1:24,000.

Radbruch, D. H. and Weiler, L. M., 1963, *Preliminary Report on Landslides in a Part of the Orinda Formation, Contra Costa County, California*: U.S. Geological Survey Open-File Report 63-112, 34 p.

Rantz, S. E., 1971, *Precipitation Depth-Duration-Frequency Relations for the San Francisco Bay Region, California*: U.S. Geological Survey Professional Paper 750-C, pp. C237–C241 (also published as ABAG Basic Data Contribution 25 and as a U.S. Geological Survey Open-File Report).

Rantz, S. E. and Harris, E. E., 1963, *Floods of January–February 1963 in California and Nevada*: U.S. Geological Survey Water Resources Division Open-File Report, March 1963, 74 p.

Reid, L. M., 1989, *Channel Incision by Surface Runoff in Grassland Catchments*: Ph.D. dissertation, Department of Geological Sciences, University of Washington, Seattle, WA, 135 p.

Downloaded from http://pubs.geoscienceworld.org/aeg/eeg/article-pdf/31/1/i/6130855/i1558-9161-31-1-i.pdf
by AEG RBAC user

Rendulic, L., 1936a, Porenziffer und porenwasserdruck in Tonen: *Der Bauingenieur*, Vol. 17, pp. 559–564.

Rendulic, L., 1936b, Relation between void ratio and effective principal stress for a remolded silty clay. In *Proceedings of the 1st International Conference on Soil Mechanics and Foundation Engineering*: Harvard University, Cambridge, MA, pp. 48–51.

Reneau, S. L., 1988, *Depositional and Erosional History of Hollows: Application to Landslide Location and Frequency, Long-Term Erosion Rates, and the Effects of Climatic Change:* Ph.D. dissertation in geology, University of California, Berkeley, CA, 328 p.

Reneau, S. L. and Dietrich, W. E., 1987, The importance of hollows in debris flow studies: Examples from Marin County, California. In Costa, J. F. and Wieczorek, G. F. (Editors), *Debris Flows/Avalanches: Process, Recognition, and Mitigation: Geological Society of America Reviews in Engineering Geology*, Vol. VII, pp. 165–180.

Reneau, S. L.; Dietrich, W. E.; Wilson, C. J.; and Rogers, J. D., 1984, Colluvial deposits and associated landslides in the northern San Francisco Bay area, California, U.S.A. In *Proceedings of the 4th International Conference on Landslides*: Canadian Geotechnical Society, Toronto, Ontario, Canada, pp. 425–430.

Rib, H. T. and Liang, T., 1978, Recognition and identification [of landslides]. In Schuster, R. L. and Krizek, R. J. (Editors), *Landslide Analysis and Control*: Special Report 176, Transportation Research Board, National Academy of Sciences, pp. 34–80.

Robinson, J., 1965, Christmas floods 1964: *California Highways and Public Works*, Vol. 44, No. 1–2, pp. 2–17.

Rodine, J. M., 1974, *Analysis of Mobilization of Debris Flows:* Ph.D. dissertation, School of Earth Sciences, Stanford University, Stanford, CA, 137 p.

Rogers, J. D., 1979, *Shallow Creep Measurements in Landslides*: M. S. thesis, Department of Civil Engineering, University of California, Berkeley, CA, 133 p.

Rogers, J. D., 1980, *Geologic Factors Affecting Hillslope Profile*: Current Topics in Geomorphology, unpublished manuscript, Water Resources Archives, University of California, Riverside, CA, 65 p.

Rogers, J. D., 1986, *Landslide Processes of the East Bay Hills*: Field Trip Guidebook, 29th Annual Meeting, October 5–10, 1986, Association of Engineering Geologists, San Francisco, CA.

Rogers, J. D., 1987a, Topographic expression of landslide-prone terrain. In *Notes from 6th National Short Course on Slope Stability and Landslides*: University of Wisconsin Extension, Madison, WI, pp. 1–16.

Rogers, J. D., 1987b, Evolution of colluvial-filled ravines In *Notes from the 6th National Short Course on Slope Stability and Landslides*: University of Wisconsin, Madison, WI 11 p.

Rogers, J. D., 1988a, Pleistocene to Holocene transition in Contra Costa County. In Crane, R. C. (Editor), *Geology of the San Ramon Valley and Environs*: Field Trip Guidebook, Northern California Geological Society, San Francisco, CA, pp. 29–52.

Rogers, J. D., 1988b, Grading practices in the development of Contra Costa County, California. In Crane, R. C. (Editor), *Geology of the San Ramon Valley and Environs*: Field Trip Guidebook, Northern California Geological Society, San Francisco, CA, pp. 99–162.

Rogers, J. D., 1991, Landslides of the Cordelia-Vallejo area, Napa and Solano Counties, California. In *Field Trip Guide to the Geology of Western Solano County*: October 12, 1991, Northern California Geological Society and Association of Engineering Geologists, San Francisco, CA, pp. 128–159.

Rogers, J. D., 1992, *Seismic Response of Highway Embankments*: Transportation Research Record No. 1343, Transportation Research Board/National Research Council, National Academy Press, Washington, D.C., pp. 52–62.

Rogers, J. D., 1997, Spatial geologic hazard analysis in practice. In Frost, J. D. (Editor), *Spatial Analysis in Soil Dynamics and Earthquake Engineering*: Geotechnical Special Publication 67, American Society of Civil Engineers, New York, pp. 15–28.

Rogers, J. D., 2001a, Influence of geology on BART's Orinda Station landslide and the Berkeley Hills tunnels. In Ferriz, H. and Anderson, R. (Editors), *Engineering Geology Practice in Northern California*: Special Publication 12, Association of Engineering Geologists, San Francisco, CA, and California Geological Survey Bulletin 210, pp. 475–486.

Rogers, J. D., 2001b, Influence of geology on BART's San Francisco subways. In Ferriz, H. and Anderson, R. (Editors), *Engineering Geology Practice in Northern California*: Special Publication 12, Association of Engineering Geologists, San Francisco, CA, and California Geological Survey Bulletin 210, pp. 501–517.

Rogers, J. D. (2006). Subsurface exploration using the standard penetration test and the cone penetrometer test. Environmental & Engineering Geoscience, 12(2), 161–179.

Rogers, J. D.; Boutwell, G. P.; Schmitz, D. W.; Karadeniz, D.; Watkins, C. M.; Athanasopoulos, A. G.; and Cobos-Roa, D., 2008, Geologic conditions underlying the 2005 17th Street Canal levee failure in New Orleans: *Journal of Geotechnical and Geoenvironmental Engineering*, Vol. 134, No. 5, pp. 583–601.

Rogers, J. D. and Chung, J. W., 2016, Applying Terzaghi's method of slope characterization to the recognition of Holocene land slippage: *Geomorphology*, Vol. 265, pp. 24–44.

Rogers, J. D. and Chung, J., 2017, A review of conventional techniques for subsurface characterization of landslides: *Environmental Earth Sciences*, Vol. 76, No. 3, p. 120.

Rogers, J. D. and Halliday, J. M., 1992a, Exploring the Calaveras–Las Trampas Fault junction in the Danville–San Ramon area. In Borchardt, G.; Hirschfeld, S. E.; Lienkaemper, J. J.; McClellan, P.; Williams, P. L.; and Wong, I. G. (Editors), *Proceedings of the Second Conference on Earthquake Hazards in the Eastern San Francisco Bay*: Special Publication 113, California Division of Mines and Geology, Sacramento, CA, pp. 271–280.

Rogers, J. D. and Halliday, J. M., 1992b, Tracking the Elusive Calaveras Fault from Sunol to Danville. In Borchardt, G.; Hirschfeld, S. E.; Lienkaemper, J. J.; McClellan, P.; Williams, P. L.; and Wong, I. G. (Editors), *Proceedings of the Second Conference on Earthquake Hazards in the Eastern San Francisco Bay*: Special Publication 113, California Division of Mines and Geology, Sacramento, CA, pp. 261–270.

Rogers, J. D.; Herber, L. J.; and Hibner, T., 1992, Paleolandslides in San Antonio Canyon, California. In Pipkin, B. W. and Proctor, R. J. (Editors), *Engineering Geology Practice in Southern California*: Special Publication 4, Association of Engineering Geologists, San Francisco, CA, pp. 579–594.

Rogers, J. D.; Olshansky, R. B.; and Alger, C. A., 1989, Geology, geomorphology and landslide processes of the East Bay Hills, San Francisco Bay region, California. In Brown, W. M. (Editor), *Landslides of Central California: San Francisco and Central California*: 28th International Geological Congress Field Trip Guidebook T381, American Geophysical Union, Washington, D.C., pp. 90–97.

Rogers, J. D. and Pyles, M. R., 1980, Evidence of cataclysmic erosional events in the Grand Canyon of the Colorado River, Arizona. In *Proceedings of the Second Conference on Scientific Research in the National Parks, San Francisco, California*: National Park Service, Washington, D.C., pp. 392–454.

Rogers, J. K., 1929, A type of landslide common in clay terraces: *Proceedings of the Ohio Academy Science*, Vol. 8, p. 304.

Rogers/Pacific, Inc., 1984, *Geotechnical Investigation, Monte Vista Ridge, Subdivision 6522, Orinda, California*: Consultant's report, Rogers/Pacific, Inc., Project 101–1 (May 26, 1984), 27 p., 4 plates.

Rogers/Pacific, Inc., 1985, *Geotechnical/Hydrologic Review of Proposed Loch Lomand Unit 10, San Rafael, CA*: Consultant's report to City of San Rafael, Department of Public Works, by Rogers/Pacific, Inc., Job No. 168-1, L 1445, 28 October 1985, 9 p., 2 plates.

Downloaded from http://pubs.geoscienceworld.org/aeg/eeg/article-pdf/31/1/i/6130855/i1558-9161-31-1-i.pdf
by AEG RBAC user

Rogers/Pacific, Inc., 1989, *Moraga Development Capability Map*: Consultant's report to Town of Moraga by Rogers/Pacific, Inc., Project PE0477T, September 5, 1989, 47 p., 3 appendices.

Rogers/Pacific, Inc., 1992a, *Geological and Geotechnical Portions, Gateway Valley 90/10 Plan Draft Environmental Impact Report*: Consultant's report by Rogers/Pacific, Project Pll 124T, June 4, 1992, 27 p.

Rogers/Pacific, Inc., 1992b, *855 Bridgeway, Sausalito*: Consultant's report by Rogers/Pacific, Inc., on proposed restaurant and hotel.

Rogers/Pacific, Inc., 1993, *Geotechnical Review, Proposed Grading Operations at Lakeside Facility, Olympic Club Golf Course Renovation, San Francisco/Daly City, CA*: Consultant's Report by Rogers/Pacific, Inc., to The Olympic Club of San Francisco, October 5, 1993.

Rogers/Pacific, Inc., 1994, *Draft Report Accompanying Map of Landslides and Other Surficial Deposits of the City of Orinda, California*: Consultant's report by Rogers/Pacific, Inc., for City of Orinda Public Works Department, 162 p., 12 oversize (1:3,600) and 12 county assessor map (1:7,200) plates.

Root, A. W., 1938, Problem of slipouts studied by state highway engineers: *California Highways & Public Works*, Vol. 17, No. 3, pp. 18–19.

Root, A. W., 1955a, Correction of landslides and slipouts: *Transactions of the American Society of Civil Engineers*, Vol. 120, Paper 2738, pp. 281–289.

Root, A. W., 1955b, Horizontal drill: New California approach in landslide control: *California Highways & Public Works*, Vol. 33, No. 2, pp. 26–29.

Root, A. W., 1958, Prevention of landslides. In Eckel, E. B. (Editor), *Landslides and Engineering Practice*: Highway Research Board Special Report 29, and Publication 544, National Academy of Sciences–National Research Council Washington, D.C., pp. 113–149.

Rossi, D. and Semenza, E., 1967, La bassa Valle del Vajont e lo scovolamento dep 9 octtobre 1963. In Leonardi, P. (Editor), *Le Dolomiti*, Vol. 2: Manfrini, Rovereto, Italy, pp. 937–944.

Saul, R. B., 1973, *Geology and Slope Stability of the S.W. 1/4 Walnut Creek Quadrangle, Contra Costa County, California*: California Division of Mines & Geology Map Sheet 16, scale 1:12,000.

Savage, D. E.; Ogle, B. A.; and Creely, R. S., 1951, Subdivision of vertebrate-bearing nonmarine Pliocene rocks in west-central Contra Costa County, California: *Geological Society of America Bulletin*, Vol. 62, p. 1511 (abstract).

Schaeffer, D. G. and Iverson, R. M., 2008, Steady and intermittent slipping in a model of landslide motion regulated by pore-pressure feedback: *SIAM Journal on Applied Mathematics*, Vol. 69, No. 3, pp. 769–786.

Schuster, R. L. (Editor), 1986, *Landslide Dams: Processes, Risk, and Mitigation*: Geotechnical Special Publication 3, American Society of Civil Engineers, New York, 162 p.

Schuster, R. L. and Krizek, R. J. (Editors), 1978, *Landslides: Analysis and Control*: Transportation Research Board/National Research Council Special Report 176, National Academy of Sciences, Washington, D.C., 234 p.

Schwartz, D. P., Pantosti, D., Hecker, S., Okumura, K., Budding, K. E., Powers, T., Borchardt, G., Hirschfeld, S. E., Lienkaemper, J. J., McClellan, P. and Wong, I. G., 1992. Late Holocene behavior and seismogenic potential of the Rodgers Creek fault zone, Sonoma County, California. In Proceedings of the second conference on earthquake hazards in the eastern San Francisco Bay Area: California Department of Conservation, Division of Mines and Geology Special Publication (Vol. 113, pp. 393–398).

Scullin, C. M., 1966, History, development, and administration of excavation and grading codes. In Lung, R. L. and Proctor, R. J. (Editors), *Engineering Geology in Southern California*: Association of Engineering Geologists, Los Angeles, CA, pp. 227–236.

Scullin, C. M., 1983, *Excavation Grading Code Administration, Inspection and Enforcement*: Prentice Hall, Englewood Cliffs, NJ, 189 p.

Scullin, C. M., 1993, Changes to U.B.C. Chapter 70, Grading: Building standards. In *International Conference of Building Officials*, Whittier, July/August 1993, pp. 10–13.

Scullin, C. M., 1994, Subsurface exploration using bucket auger borings and down-hole geologic inspection: *Environmental & Engineering Geoscience*, Vol. 31, No. 1, pp. 91–105.

Seed, H. B., 1967, Slope stability during earthquakes: *Journal of the Soil Mechanics and Foundations Division: American Society of Civil Engineers*, Vol. 93, No. SM4, pp. 299–323.

Seeley, M. W., 1984, *Engineering Geology of the Mulholland Formation Moraga, California*: Master's Thesis, California State University, Hayward, CA.

Seidelman & Associates, 1983, *Geotechnical Investigation of the Landslide on the Property of Mr. and Mrs. James Bufton, #6 Warford Terrace, Orinda, CA*: Consultant's report by Seidelman & Associates for R. M. Abend, Attorney at Law, Job 83406, September 30, 1983, 37 p.

Selby, M. J., 1967. Erosion by high intensity rainfalls in the Lower Waikato.

Selby, M. J., 1982. Hillslope materials and processes. Hillslope materials and processes.

Selby, M. J., 1993, *Hillslope Materials and Processes*, 2nd ed.: Oxford University Press, Oxford, U.K., 451 p.

Sharp, R. P. and Nobles, L. H., 1953, Mudflow of 1941 at Wrightwood, Southern California: *Geological Society of America Bulletin*, Vol. 64, No. 5, pp. 547–560.

Sharpe, C. F. S., 1938a, *What Is Soil Erosion*: Miscellaneous Publication 286, U.S. Department of Agriculture Washington, D.C., 84 p.

Sharpe, C. F. S., 1938b, *Landslides and Related Phenomena*: Columbia University Press, New York, 137 p.

Shlemon, R. J.; Wright, R. H.; and Montgomery, D. R., 1987, Anatomy of a debris flow, Pacifica, California. In Costa, J. E. and Wieczorek, G. F. (Editors), *Debris Flows/Avalanches: Process, Recognition and Mitigation*: *Geological Society of America Reviews in Engineering Geology*, Vol. VII, pp. 181–200.

Shreve, R. L., 1968, *The Blackhawk Landslide*: Special Paper 108, Geological Society of America, New York, 47 p.

Simons, N. E. and Menzies, B. K., 1974, A note on the principle of effective stress: *Geotechnique*, Vol. 24, No. 2, pp. 259–260.

Skempton, A. W. (1953). Soil mechanics in relation to geology. Proceedings of the Yorkshire Geological Society, 29(1), 33–62.

Skempton, A. W., 1964, Long-term stability of clay slopes (Fourth Rankine Lecture, Institute of Civil Engineers, London): *Geotechnique*, Vol. 14, No. 2, pp. 75–102.

Skempton, A. W., & Hutchinson, J. (1969). Stability of natural slopes and embankment foundations. In Soil Mech & Fdn Eng Conf Proc/Mexico/.

Smith, T. C. and Hart, E. W., 1982, Landslides and related damage, January 1982, San Francisco Bay region: *California Geology*, Vol. 35, No. 7, pp. 139–151.

Smith, T. W. and Cedergren, H. R., 1962, *Cut Slope Design and Landslides*: Special Technical Publication 322, ASTM, West Conshohocken, PA, pp. 135–158.

Smith, T. W. and Stafford, G. V., 1957, Horizontal Drains on California Highways: *Journal Soil Mechanics and Foundations Division, American Society of Civil Engineers*, Vol. 83, No. 3, pp. 1–26.

Sorrick, M., 1986, *The History of Orinda*: Gateway to Contra Costa County: Orinda Library Board, Orinda, CA, 204 p.

Spencer, E., 1967, A method of analysis of the stability of embankments assuming parallel inter-slice forces: *Geotechnique*, Vol. 17, No. 1, pp. 11–26.

Downloaded from http://pubs.geoscienceworld.org/aeg/eeg/article-pdf/31/1/i/6130855/i1558-9161-31-1-i.pdf
by AEG RBAC user

Stanton, T. E., 1948, Hydrauger method: *California Highways & Public Works*, Vol. 26, No. 1, pp. 6–10.

State of California, 1956, *Floods of December 1955 in California*, revised ed.: Department of Public Works, Division of Water Resources, Sacramento, CA, March 1956, 97 p., 7 plates.

Strahler, A. N., 1952, Hypsometric (area-altitude) analysis of erosional topology: *Geological Society of America Bulletin*, Vol. 63, No. 11, pp. 1117–1142.

Strahler, A. N., 1965, *Physical Geography*, 2nd ed.: John Wiley & Sons, New York, 534 p.

Taylor, P. A. and Brabb, E. E., 1972, *Maps Showing Distribution and Cost by Counties of Structurally Damaging Landslides in the San Francisco Bay Region, California, Winter of 1968–69*: U.S. Geological Survey Miscellaneous Field Studies Map MF-327.

Tembe, S.; Lockner, D. A.; and Wong, T.-F., 2010, Effect of clay content and mineralogy on frictional sliding behavior of simulated gouges: Binary and ternary mixtures of quartz, illite, and montmorillonite: *Journal of Geophysical Research: Solid Earth*, Vol. 115, No. B3, B03416.

Terzaghi, K., 1943, *Theoretical Soil Mechanics*: John Wiley & Sons, New York, 510 p.

Terzaghi, K., 1945, Discussion of geology in highway engineering, by M. T. Hunting: *Transactions of the American Society of Civil Engineers*, Vol. 112, Paper 2238, pp. 324–328.

Terzaghi, K., 1950, Mechanism of Landslides. In Berkey, C. (Editor), *Applications of Geology to Engineering Practice (Berkey Volume)*: Geological Society of America, Boulder, CO, pp. 83–123.

Thomas, E. H., 1939, *Landslide Forms and Their Origin in Middle Coast Ranges*: Master's thesis, Department of Geology, University of California, Berkeley, CA, 69 p.

Toppozada, T. R.; Real, C. R.; and Parke, D. L., 1981, *Preparation of Isoseismal Maps and Summaries of Reported Effects for Pre–1900 California Earthquakes*: California Division of Mines & Geology Open-File Report 81-11, 182 p.

Trask, P. D., 1922, The Briones formation of middle California: University of California, Bulletin of the Department of Geology, v. 13, no. 5, p.

Trollope, D. H. (1973): Sequential Failure in Strain-Softening Soils. Proc. 8th Int. Conf. SM and FE, Moscow4 38.

Trollope, D. H., 1977, *Landslip Mechanisms: 5th International Congress on Rock Mechanics*, Montreux, Switzerland: unpublished lecture notes, International Society for Rock Mechanics, Salzburg, Austria, 18 p.

Turner, A. K. and Schuster, R. L., 1996, *Landslides: Investigation and Mitigation*: Transportation Research Board Special Report 247, National Academy of Sciences, Washington, D.C., 678 p.

Upp, R. R., 1977, *Prediction of Slip-Surface Geometry from Landslide Width*: Master's thesis, Department of Geological Sciences, Humboldt State University, Arcata, CA, 65 p.

U.S. Department of Agriculture, 1977, *Soil Survey of Contra Costa County*: U.S. Department of Agriculture, Washington, D.C., in cooperation with University of California, Agricultural Experiment Station.

U. S. Geological Survey, 2021, *California and Landsat*: U.S. Geological Survey Fact Sheet 2021–3034, 2 p.

Varnes, D. J., 1958, Landslide types and processes. In Eckel, E. B. (Editor), *Landslides and Engineering Practice*: Highway Research Board Special Report 29, pp. 20–47.

Varnes, D. J., 1978, Slope movement types and processes. In Schuster, R. L. and Krizek, R. J. (Editors), *Landslide Analysis and Control*: Transportation Research Board Special Report 176, National Academy of Sciences, Washington, D.C., pp. 12–33.

Varnes, D. J., 1997, personal communication, October 3, 1997.

Varnes, D. J.; Radbruch-Hall, D. H.; and Savage, W. Z., 1976, Gravitational spreading of steep-sided ridges ("sackung") in western United States: *International Association of Engineering Geology Bulletin*, Vol. 14, pp. 23–35.

Varnes, D. J.; Radbruch-Hall, D. H.; and Savage, W. Z., 1989, *Topographic and Structural Conditions in Areas of Gravitational Spreading of Ridges in the Western United States*: U.S. Geological Survey Professional Paper 1496, 26 p.

Vaughan, D. K. and Isenberg, J., 1991. Stability of openings in jointed rock. International journal for numerical and analytical methods in geomechanics, 15(6), pp. 433–442.

Voight, B. and Pariseau, W. G., 1979, Rockslides and avalanches: An introduction. In Voight, B. (Editor), *Rockslides and Avalanches, 1: Natural Phenomena*: Elsevier Scientific Publishing Co., New York, pp. 1–67.

Waananen, A. O.; Harris, D. D.; and Williams, R. C., 1971, *Floods of December 1964 and January 1965 in the Far Western States*: U.S. Geological Survey Water Supply Paper 1866-A, 265 p.

Wagner, J. R., 1978, *Late Cenozoic History of the Coast Ranges East of San Francisco Bay*: Unpublished Ph.D. dissertation, University of California, Berkeley, CA.

Wakabayashi, J.; Smith, D. L.; and Hamilton, D. H., 1992, Miller Creek and related faults: A potentially active fold and thrust belt, eastern San Francisco Bay area. In Borchardt, G. (Editor), *Proceedings of the Second Conference on Earthquake Hazards in the Eastern San Francisco Bay Area*: Special Report 113, California Division of Mines and Geology, Sacramento, CA, pp. 345–354.

Walkinshaw, J. L., 1978, *Route 24 Orinda Slide Review*: Federal Highway Administration, Region 9, San Francisco, CA, March 10, 1978, 2 p.

Walkinshaw, J. L., 1979, *Route 24 Orinda Slide Review*: Federal Highway Administration, Region 9, San Francisco, CA, April 5, 1979, 3 p.

Waltz, J. P., 1967, *An Analysis of Selected Landslides in Alameda and Contra Costa Counties, California*: Ph.D. Dissertation, School of Earth Sciences, Stanford University, Stanford, CA, 197 p.

Warntz, W., 1975, Stream ordering and contour making: *Journal of Hydrology*, Vol. 25, pp. 209–227.

Watkins, C. M.; Rogers, J. D.; and Warme, J. E., 2007, Reconstruction of composite landslides in flat-lying sedimentary strata using graphical methods. In Turner, A. K. and Schuster, R. L. (Editors), *Landslides and Society: First North American Conference on Landslides*: Special Publication 23, Association of Environmental and Engineering Geologists, Denver, CO, pp. 488–501.

Way, D. S., 1978, *Terrain Analysis: A Guide to Site Selection Using Aerial Photographic Interpretation*: Van Nostrand Reinhold, New York, pp. 31–57.

Wieczorek, G. F.; Harp, B. L.; Mark, R. K.; and Bhattacharyya, A. K., 1988, Debris flows and other landslides in San Mateo, Santa Cruz, Contra Costa, Alameda, Napa, Solano, Sonoma, Lake and Yolo Counties, and factors influencing debris-flow initiation. In Ellen, S. D. and Wieczorek, G. F. (Editors), *Landslides, Floods, and Marine Effects of the Storm of January 3–5, 1982, in the San Francisco Bay Region, California*: U.S. Geological Survey Professional Paper 1434, pp. 133–161.

Wieczorek, G. F.; Wilson, R. C.; Ellen, S. D.; Reid, M. E.; and Jayko, A. S., 2007, Thirty-one years of debris-flow observation and monitoring near La Honda, California, USA. In Chen, C. L. and Major, J. J. (Editors), *Proceedings of the 4th International Conference on Debris-Flow Hazards Mitigation: Mechanics, Prediction, and Assessment*: Millpress Science Publishers, Rotterdam, Netherlands, pp. 55–63.

Willes, B., 1966, *Orinda, A Pictorial History of a Suburb*: Self-published, 73 p.

Wills, C. J.; Roth, N. E.; McCrink, T. P.; and Short, W. R., 2017, The California Landslide Inventory Database. In *3rd North American Symposium on Landslides*, pp. 666–674.

Downloaded from http://pubs.geoscienceworld.org/aeg/eeg/article-pdf/31/1/i/6130855/i1558-9161-31-1-i.pdf
by AEG RBAC user

Wilson, C. J. and Dietrich, W. E., 1987, The contribution of bedrock groundwater flow to storm runoff and high pore pressure development in hollows. In *Proceedings of the Symposium on Erosion and Sedimentation in the Pacific Rim*, 3–7 August 1987: Publication 165, International Association of Hydrological Sciences, Washington, D.C., pp. 49–59.

Witter, R. C.; Knudsen, K. L.; Sowers, J. M.; Wentworth, C. M.; Koehler, R. D.; Randolph, C. E.; Brooks, S. K.; and Gans, K. D., 2006, *Maps of Quaternary Deposits and Liquefaction Susceptibility in the Central San Francisco Bay Region, California*: U.S. Geological Survey Open-File Report 2006-1037.

Wright, S. G., 1969, *A Study of Slope Stability and the Undrained Shear Strength of Clay Shales*: Ph.D. dissertation, Department of Civil Engineering, University of California, Berkeley, CA.

Youd, T. L. and Hoose, S. N., 1978, *Historic Ground Failures in Northern California Triggered by Earthquakes*: U.S. Geological Survey Professional Paper 993, 176 p., 3 plates.

Young, D. M., 1954, Orinda Crossroads: First link of Oakland–Walnut Creek job for traffic relief: *California Highways and Public Works*, Vol. 32, No. 5–6, pp. 46–48.

Zaruba, Q. and Mencl, V., 1969, *Engineering Geology*: Elsevier Scientific Publishing Co., New York, 503 p.

Zaruba, Q. and Mencl, V., 1982, *Landslides and Their Control*, 2nd ed.: Elsevier Scientific Publishing Co., New York, 324 p.

APPENDIX 1—CLASSIFICATION OF LANDSLIDES (1935–2014)

Appendix 1 provides examples of the classification of landslides that evolved between 1935 and 2014.

- Classification of Landslides by Sharpe (1938)
- Physical Classification and Suggested Nomenclature of Landslides by Varnes from HRB SR 29 in 1958
- Classification of Landslides in Bedrock, Debris, and Soils from TRB SR 176 in 1978
- Establishment of UNESCO Standards for Landslide Types and Processes during the International Decade for Natural Hazards Reduction (1990–2000)
- Folder Containing Copies of 10 Most Cited Articles on Recommended Standards for Landslide Classification Released between 1990 and 1996
- Standard Nomenclature and Methods of Reporting Introduced in the United States by Release of TRB Special Report 247 by Cruden and Varnes (1996)
- Review of the Classification of Flowing Landslides by Hungr, Evans, Bovis, and Hutchinson in 2001
- Summary of "The Varnes classification of landslide types, an update," by Hungr et al. (2014)

Stewart Sharpe's Landslide Classification Scheme (1938)

Charles Farquharson Stewart Sharpe (Figure A1-1) was a native of Canada born in Winnipeg, Manitoba, Canada, on October 21, 1907. He grew up in New York and attended Columbia University in Manhattan, completing his A.B. degree in English and economics in 1928. Sharpe became interested in landslides in 1922 while climbing the White Mountains of New Hampshire. On other trips to the White Mountains, he began noticing outward manifestations of frost heave above the timberline. These outdoor trips piqued his interest in the study of landforms, so he enrolled in Columbia University's master's program in geology.

In the summer of 1929, he began recognizing examples of similar creep features in the mountains of western Virginia. In 1930, he ventured westward to the Rocky Mountains of Colorado and Wyoming, where he began to discern the telltale signs of several recent landslide movements that had similar physical characteristics, but varying scale.

After completing his M.S. degree in 1931, he began exploring options for a doctoral research topic. He spent the summer of 1932 engaged in a geologic reconnaissance of the mountainous portions of upstate New York, Pennsylvania, and New England. In the fall of 1932, Professor Douglas W. Johnson, one of the faculty advisors of Columbia's Graduate Seminar in Geomorphology, encouraged Sharpe to begin an extensive study of the existing literature on mass movements, which is the topic he chose and then pursued for the next 5 years!

Sharpe continued his summer-long field reconnaissance trips in 1933 and 1934. In 1935, he was offered a position with the newly established U.S. Soil Conservation Service (SCS), and he moved to Washington, D.C. His new duties included the preparation of a well-illustrated and informational publication on soil erosion, and

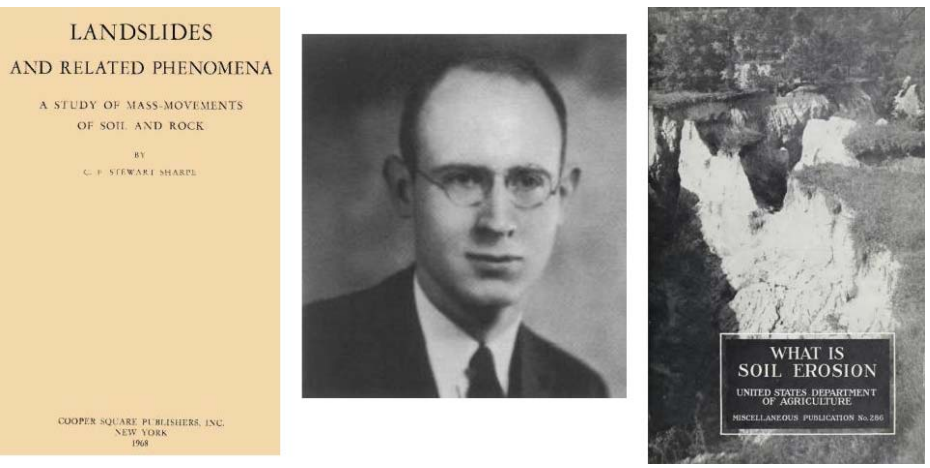

Figure A1-1. Dr. C. F. Stewart Sharpe in 1935 when he joined the Soil Conservation Service as an assistant soil conservationist while working on his Ph.D. in geology at Columbia University. In 1938, he received his Ph.D. degree from Columbia, published a monograph for the new Soil Conservation Service, and issued the first textbook on landslides in English.

Downloaded from http://pubs.geoscienceworld.org/aeg/eeg/article-pdf/31/1/i/6130855/i1558-9161-31-1-i.pdf
by AEG RBAC user

the agricultural practices that were likely exacerbating surficial erosion, which included all forms of mass movements, including landslides. These were responsibilities that dove-tailed nicely with Sharpe's doctoral research, especially the sites he had documented with high-quality photographs (Figure A1-2).

During the summer of 1935, he organized an ambitious tour of "the most important mass-movement localities in the United States and southern Canada" (Sharpe, 1938b). This effort involved 16,000 miles (25,750 km) of travel across 28 states and three Canadian provinces. This massive reconnaissance was part of his new duties as an assistant soil conservationist in the Climatic and Physiographic Division of the SCS, which had just been established within the U.S. Department of Agriculture (Sharpe, 1938a). From 1933 to 2935, the same body of scientists had staffed the short-lived Soil Erosion Service (SES) within the U.S. Department of the Interior.

In January 1936, Sharpe married Lois Kremer, who had completed her B.A. degree at Milwaukee-Downer College in 1927 and her M.S. degree in geology at the University of Rochester in 1932. She went onto complete her Ph.D. in geology at Northwestern University in 1942 (where her dissertation was titled "The Paragenesis of Southern Jackson and Macon Counties, North Carolina"). She was credited by Sharpe as having aided him in the bibliographic research and gathering of materials in preparing the landslides manuscript for publication, and for preparing most of the field sketches (Sharpe, 1938a).

Sharpe's SCS assignment was to reconnoiter examples of slope creep, mudslides, earthflows, slumps, and catastrophic erosional features, such as the breached Gros Ventre landslide dam of 1925–27 in Wyoming. Significant historical slides were sought out, and several new slides were documented. In the summer of 1936, Sharpe studied erosion-impacted sites in Oklahoma, Mississippi, and South Carolina, examining the agricultural importance of creep, slumps, and other forms of mass movements. The sites in Mississippi and South Carolina were part of a series of sites that SCS researchers had selected within different geographic sectors of the continental United States (Effland and Effland, 1994).

The stated purpose of Sharpe's physiographic research was to discover the processes that were likely responsible for accelerating erosion versus those that did not. The density of vegetation cover was an obvious trigger that could increase velocities of concentrated runoff, and most workers of that era assumed that accelerated erosion occurred in areas where large tracts of forested lands were cleared to accommodate the planting of orchards and row crops.

In 1938, Sharpe published two significant works: *What is Soil Erosion*? released by the SCS (Sharpe, 1938a), and *Landslides and Related Phenomena* published by Columbia University Press (Sharpe, 1938b). The former included more than 100 photos in 84 pages, which the U.S. Department of Agriculture (USDA) released in February 1938 (Figures A1-2 and A1-3). It was published as U.S. Department of Agriculture (USDA) Miscellaneous Publication No. 286 (Sharpe, 1938a). Unlike most government manuals, it was profusely illustrated with photos taken by Sharpe during his summer trips, which were impressive (Figures A1-2 and A1-3).

His doctoral dissertation on "Landslides and Related Phenomena" was completed in the fall of 1937 but not published until the following summer, shortly after receiving his Ph.D. degree from Columbia University in June 1938. The hard-cover textbook was Number II of the Columbia Geomorphic Studies series, edited by his major field advisor Douglas W. Johnson and published by Columbia University Press (Sharpe, 1938b). It was the first textbook in English focused solely on mass-wasting processes (Collin, 1846, 1956). It was so popular with physical geographers and geomorphologists that it was reprinted in 1960 and 1968.

Sharpe's Landslide Classification Schema (1938)

In 1938, Sharpe's stated purpose in the Page xii was "to review the present state of our knowledge of mass-movements and to bring together under one cover a discussion of all the major types."

Figure A1-2. Photos of and by Stewart Sharpe that appeared in *What Is Soil Erosion?* (Sharpe, 1938a). These are typical of the images collected during the summer field seasons. A few of the images even show Sharpe (upper and lower left) and his trusty SCS vehicle (lower right).

Downloaded from http://pubs.geoscienceworld.org/aeg/eeg/article-pdf/31/1/i/6130855/i1558-9161-31-1-i.pdf
by AEG RBAC user

Slump landslide near Bath, New York (Sharpe, 1938a)

Slump of spillway excavation in Clark County, Kansas

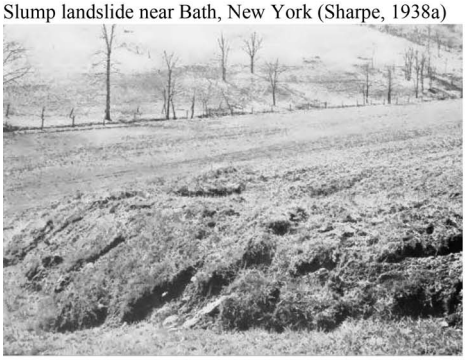

Flowing toe of the same slide in Tuscarawas County, Ohio

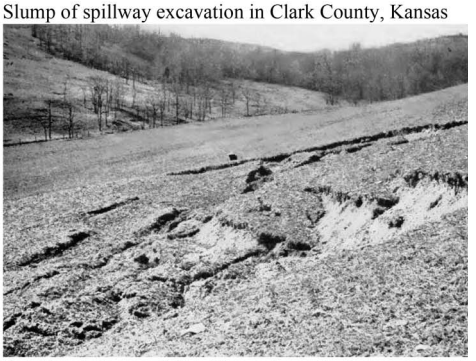

Rotational slumps defined by main and minor scarps of active slide in Tuscarawas County, Ohio

Figure A1-3. A few examples of the images taken by Stewart Sharpe that appeared in *What Is Soil Erosion?* (Sharpe, 1938a) and *Landslides and Related Phenomena* (Sharpe, 1938b). Rotational slump-earthflows were the most common type of slide he encountered.

Sharpe began his studies with a thorough literature review, collecting >1,200 references in English on soil creep and erosion, debris flows, landslides, catastrophic rockslides, talus slopes, landslide dams, etc. Instead of listing all of these in his bibliography, he gathered the best articles for his "Selected Bibliography" of 237 references, which were included in *Landslides and Related Phenomena* (Sharpe, 1938b).

Sharpe began with a fundamental premise taught to him in his geology courses at Columbia University:

> The uniformitarian concept of geology emphasized the continuous action of four erosional processes: running water, winds, waves, and moving ice.

In his synthesis of the collected information Sharpe attempted to address the physical processes responsible for various forms of mass wasting. In the end, he decided to classify mass wasting based on the kind of movement and the relative velocity of motion as the two most fundamental factors, with water or ice content as secondary factors, and the overall composition of the impacted mass as the third factor. So, he chose four principal headings for his classification scheme: slow flowage, rapid flowage, sliding, and subsidence (Figure A1-4).

The engineering definition of creep is "strain under sustained load." In the 1930s, soil scientists, geomorphologists, and physical geographers were very cognizant of the cumulative effects of slope creep, even when the velocities were unmeasurable. Their awareness came from direct observations of displaced monuments, poles, retaining walls, posts, curved tree trunks, and foundation elements.

The same could not be said for soil and foundation engineers of that same era, who rarely recognized nor paid much attention to slope creep in their evaluations. This dichotomy was likely influenced by the lifestyles of their instruction and daily routine. In the late 1930s, engineering students wore suits and ties, took all of their courses in lecture halls and indoor laboratories, and worked at spacious drafting tables indoors. Physical geographers and geologists of that same era dressed in field khakis and were trained to observe natural settings and take detailed notes of everything they stopped to observe or study. The exceptions to these boundaries were military engineers, who received two summers of surveying and cartography training, which enabled them to quickly make maps that were remarkably accurate.

Sharpe decided to group rock creep, talus creep, soil creep, rock glacier creep, and solifluction under the banner of "imperceptible" slow flowage (Figure A1-4). Sharpe noted that the rate of soil creep depends on the clay and silt content. Slope creep occurred at minimum rates in highly porous loess (due to drainage) and was "pronounced" in loose soils, depending on the degree of saturation (wetness and wet-dry/swell-shrink load cycles). He was correct in pointing out that most soils are partially saturated and that the transition to full saturation generally triggers the greatest slope creep (downslope movement) or rate of erosion.

Sharpe also grouped earthflows, mudflows, and debris avalanches as examples of "rapid flowage," and "the causes of rapid flowage" were addressed in Chapter 4 (Figure A1-4). In his travels back and forth across North America, Sharpe (1938b) noticed that "earthflows tended to occur on gentle slopes with slippery clay beds," while "mudflows are more rapid because of higher water contents and steeper slopes, usually following stream courses." Sharpe also made observations about the nuances of mudflows in various geomorphic terranes, like semiarid lands bereft of protective vegetation, and alpine, volcanic, or boggy terrain.

Sharpe also classified debris avalanches as flow slides for which the "initial movement is caused by slippage." He asserted that these examples were "almost always" preceded by intense

Downloaded from http://pubs.geoscienceworld.org/aeg/eeg/article-pdf/31/1/i/6130855/i1558-9161-31-1-i.pdf
by AEG RBAC user

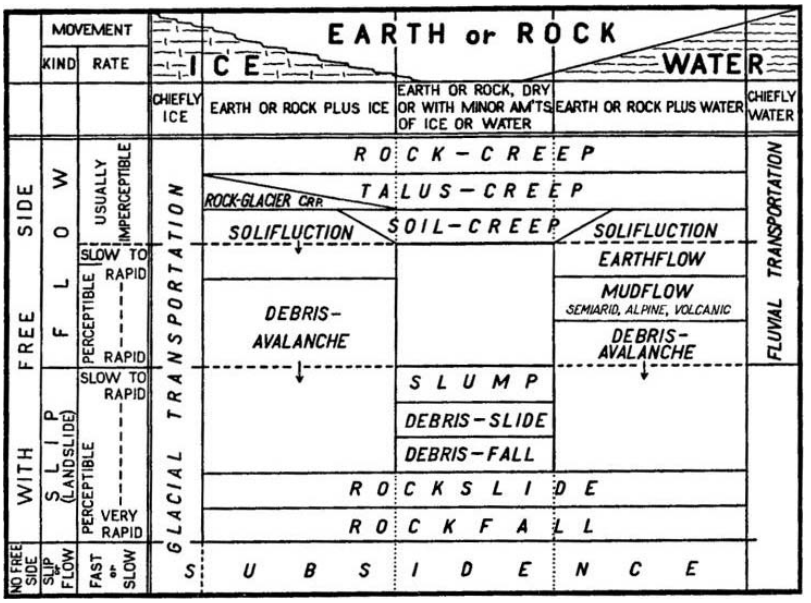

Figure A1-4. Sharpe's 1938 classification of landslides and related phenomena. It was intended to communicate the premise that various forms of mass movement tend to form "continuous series, grading from mass-movement of dry earth or rock into mass transport by fluvial and glacial processes."

precipitation, which increased the unit weight of the slope materials and lubrication induced by the additional pore water, which tend to be more common in humid climes.

Sharpe ended up defining a landslide as "the perceptible downward sliding or falling of a relatively dry mass of earth, rock, or mixture of the two." He observed that landslides tend to move slowly to very rapidly, noting that slump blocks (with higher clay content) tended to be the slowest slides, followed by debris slides, debris falls, rockslides, and rockfalls.

He also provided descriptive details of soil slumps and soil creep in agricultural areas and potential mitigation measures that could be employed to repair landslide-induced damage. One of his most useful descriptions was the analogy he drew between a shallow earth-slump plane of rupture and the shape of a spoon, shown in Figure A1-5b.

In 1938, Dr. Sharpe was promoted to associate soil conservationist within the same SCS research group, and he became its acting head in 1941. In 1943, he joined the Office of Strategic Services and became chief of the Joint Army-Navy Intelligence Summary. He remained affiliated with the Central Intelligence Agency (CIA) when it was formed in 1947 and edited basic geological and petroleum studies for the CIA before retiring from government service in 1989. He and his wife Lois used to attend many of the annual meetings of the Association of Engineering Geologists, including the meeting in San Francisco in 1986, where the senior author met and conversed with him about his unusual career path.

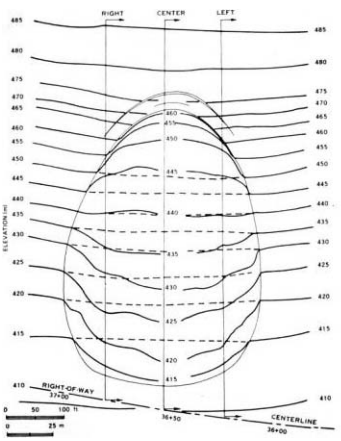

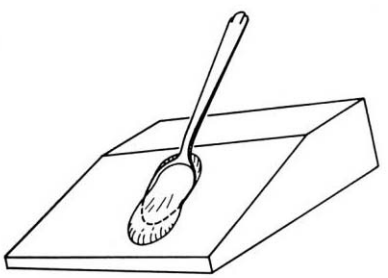

Figure 8. Spoon-shaped slope failure. Slope failures are often spoon-shaped, as in this sketch, or cylindrical as shown in Figure 9.

Figure A1-5a. Sharpe observed that rotational movement of soil slumps is accompanied by dilation of the upper portion of the mass, which Varnes (1978, Fig. 2.1t) later termed the "zone of depletion," and a corresponding "zone of accumulation," which comprises the lower portion of the displaced mass, as shown in the left panel. These offsets result in divergent contours along the fall line of a slope, as shown in the contours at left.

Figure A1-5b. Note the almond shape typical of a shallow soil slump. The sketch in the right panel illustrates Sharpe's observation that the basal rupture surface of an earth slump is "spoon-shaped" (images from Varnes, 1958).

Downloaded from http://pubs.geoscienceworld.org/aeg/eeg/article-pdf/31/1/i/6130855/i1558-9161-31-1-i.pdf
by AEG RBAC user

Background on David J. Varnes, P.E., R.G., C.E.G.

David J. Varnes possessed a unique set of skills that began with the fundamentals of field work, geologic mapping (Varnes, 1974), and quantitative analyses in a wide array of applied geology problems. He was one of the most respected American engineering geologists affiliated with the International Association of Engineering Geology and UNESCO while working for the USGS Engineering Geology Branch between 1948 and 1992 (Fig. A1-6). A 1940 graduate of Caltech, he was cross registered as a professional engineer (P.E.) in Colorado and certified engineering geologist (C.E.G.) in California.

Varnes was born in Howe, IN, in 1919, where his father David J. Varnes, Sr., was the registrar of Howe Military Academy. In 1934, the family moved to Los Angeles, CA, where David's father accepted the position of registrar at the Black-Foxe Military Institute in Hollywood. In July 1937, Mr. Varnes Sr. suddenly died of a heart attack at age 51, leaving his widow Florence (50) and their three sons: John (25), Robert (21), and David, Jr. (18).

David, Jr., had attended Los Angeles High School and graduated a year early (1936) when he received a scholarship from Caltech in Pasadena.

Four years later, he graduated with honors in Caltech's Class of 1940 with a major in geology. He spent the following year as a graduate student at Northwestern University in Evanston, IL. It was common during the Great Depression to enroll for a year of graduate study with the hope of securing some sort of funding for post-graduate research, which normally required 2 or more years to complete because advanced degrees in the earth sciences and geography usually required a year of additional field work. During the Great Depression (1929–41), there was a significant drop in the number of graduate students because of the expense (only 6 percent of America's high school graduates completed their bachelor's degrees during the 1930s).

In mid-1940, World War II was just getting under way, and the Germans were in the process of over-running Belgium, Holland, Norway, and France. During the fall of 1940, the United States instituted mandatory registration for the Selective Service, which included all male college students. After filling out his selective service information card in October 1940, Varnes wrote to the USGS inquiring about full- or part-time positions. The USGS considered his professional training and asked him to sit for their civil service exam in Chicago (Varnes, 1997). He must have scored very high on the exam because a few months later he received an offer to serve as a recorder in the Areal Geology Section of the Geologic Division of the USGS. Varnes did not know what a recorder's duties were or that it was an entry-level position with the lowest pay the USGS could offer to a degreed scientist.

Figure A1-6. (Right) David J. Varnes (1919–2002) worked for the USGS from 1941 to 1995 (USGS). (Left) In 2003, the International Program on Landslides began awarding the Varnes Medal for professional excellence in landslide research.

In June 1941, Varnes began his professional career assisting USGS geologist Charles Deiss in his preparation of a geologic reconnaissance of the Saypo quadrangle in northwestern Montana. The summer of 1941 was the fifth of six summers Deiss spent mapping the Saypo quadrangle (which is just south of the Flathead Mountains near Glacier National Park). Varnes served as his "geologic sherpa," hauling the camp and field equipment, preparing the meals, and getting in some field mapping here and there, as directed by Deiss (Varnes, 1997).

The following winter of 1941–42, Varnes was dispatched to the Caribbean to support economic geology evaluations of nickel, gold, copper, and laterites in the Dominican Republic. From 1942 to 1948, he was assigned to the Mineral Deposits Branch of the USGS, where he learned the techniques employed in underground mapping of exposed ore bodies in a handful of gold–silver–base metal mining operations in the San Juan Mountains of Colorado. Most of this early work was incorporated into *Geology and Ore Deposits of the South Silverton Mining Area* (Professional Paper 378-A), which was not released until 1963 (Varnes, 1963).

In 1943, David married fellow USGS geologist Helen Dowling, who spent 3 years studying active landslides in southwestern Colorado. These included the Cedar Creek landslide near Montrose, the Knife Edge landslide in Mesa Verde National Park, and the Ames landslide near Telluride (H. D. Varnes, 1949). Each of these was a formidable bedrock slide that had caused considerable damage to transportation links (highways and railroads). Helen's 1949 report was issued as USGS Circular 31, and it began with a recitation on landslide terminology, citing Sharpe (1938a&b) as the only definitive work then existing in the United States. She described the landslides she had studied using Sharpe's proposed terminology and concluded that most of the slides that blanket the San Juan and La Plata Mountains were "spectacular agents of erosion." All of the slides she studied were originally comprised of bedrock, which often included the Mancos Shale of Cretaceous age, which was subject to slumping and then transitioning to earthflows of considerable runout (see Figure A1-7 of the Cedar Creek slide and Figure A1-8 of the Ames slide). She found that the three principal slides had experienced reactivations in close proximity to recent excavations for highways and railroad right-of-ways or as a consequence of agricultural irrigation.

In her conclusions stated on Page 13 in USGS Circular 31, Helen noted some significant challenges with mitigating landslide hazards that still ring true today:

> The corrective measures noted above for the three [active] landslide areas illustrate the general inadequacy of many common methods of landslide control and show the urgent need for more knowledge concerning landslides and for finding new methods of dealing with them.
>
> In addition to aiding the search for new remedial measures, an understanding of the geology is needed in planning what can be done to stop such landslides before they start, as well as the planning stages of any major construction project, so that areas in which conditions favor earth movement can be avoided, if at all possible. If construction in such areas cannot be avoided, a complete understanding of the geologic conditions may help in controlling the activating causes before slides occur or become serious.

Downloaded from http://pubs.geoscienceworld.org/aeg/eeg/article-pdf/31/1/i/6130855/i1558-9161-31-1-i.pdf
by AEG RBAC user

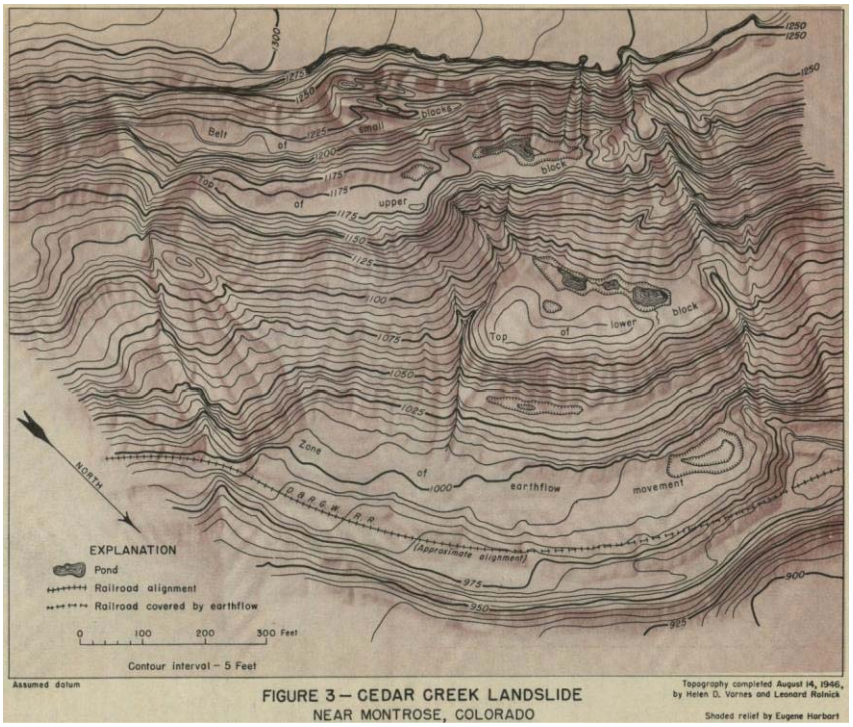

Figure A1-7. Topography of the Cedar Creek landslide east of Montrose, CO, surveyed by Helen Varnes and Leonard Rolnick in the summer of 1946 from USGS Circular 31.

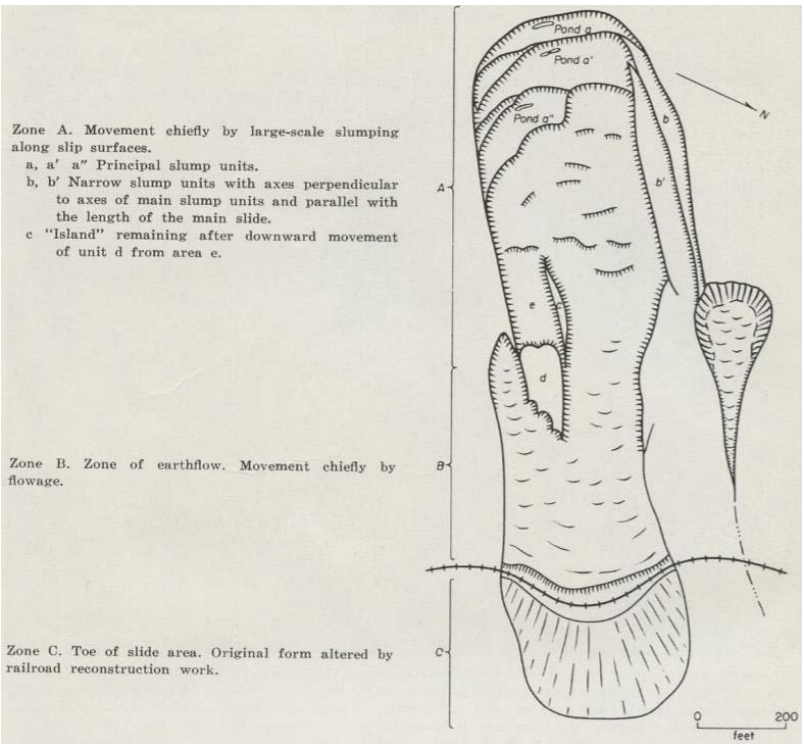

Figure A1-8. Dave Varnes included this sketch of the Ames slide near Telluride, CO, in Chapter 3 of HRB SR 29 (Varnes, 1958). It was taken from USGS Circular 31 by Helen Varnes in 1949. He included it as a representative example of a slump-earthflow.

Downloaded from http://pubs.geoscienceworld.org/aeg/eeg/article-pdf/31/1/i/6130855/i1558-9161-31-1-i.pdf
by AEG RBAC user

The Cedar Creek landslide is a slump-earthflow slide floored in the Mancos Shale and capped by pervious boulder gravels. Periodic reactivation of earthflows along the slide's lower margins forced repeated closures and re-alignment of the Rio Grande Railroad line (H. D. Varnes, 1949). The railroad eventually moved their tracks onto an embankment fill constructed beyond the reach of the offending earthflows.

The Ames landslide was developed in glacial till lying on the Mancos Shale, with a series of retrogressive main scarps and parallel lateral scarps b and b′ along the left shoulder of the slide (from H. D. Varnes, 1949).

USGS Circular 31 (H. D. Varnes, 1949) was a popular publication on landslides and was reprinted in 1959. In 1950, Helen joined a new team guided by famed geomorphologist Charley Hunt to evaluate the Quaternary geology of glacial Lake Bonneville in northern Utah Valley (along with H. E. Thomas) until 1953. This was followed in 1960–64 by a study of the geology of the Fort Peck area of Montana, which was already recognized by the poor foundation behavior where the Cretaceous-age Bearpaw Shale was exposed in outcrop or close by, such as exposed surfaces in excavations.

It appears that Dave Varnes' unofficial inspections of Quaternary landforms and measurements of active and dormant landslides in Colorado likely played an important role in his shifting career path with the Engineering Geology Branch in the succeeding decades. In the spring of 1964, Helen suddenly passed away while Dave was in Anchorage, AK, evaluating the Government Hill slide, one of the largest mass movements in the Great Alaska Earthquake of 1964 (Varnes, 1969). Later that year, Dave Varnes married USGS geologist Katherine Lutz Buck, who was the widow of USGS engineering geologist Larry Buck, who had died in July 1957.

Role of USGS Engineering Geology Branch in Supporting HRB SR 29 (1951–58)

When the HRB convened its first Landslide Committee meeting, Ed Eckel was selected to serve as chairman. Later, he decided to shoulder the responsibility of serving as the lead editor, whose principal challenge was to craft compromises whenever members of the committee disagreed on something.

The more mountainous areas of the western United States experienced significant interruptions to traffic flow caused by landslides and floods because they tended to occur in constricted bedrock canyons, which offered few options for the construction of temporary bypasses while enabling a nearby slope repair.

In a post-war reorganization in the fall of 1945, the Geologic Branch of the USGS was divided into two groups or sections, economic geology and the other basic and engineering sciences. This reorganization included sections for new specialties in foreign geology, engineering geology, military geology, and geophysics. The name and function of the engineering sciences group were altered to establish an Engineering Geology Branch (EGB), and Edwin B. Eckel (Figure A1-9) was selected as its first chief, a responsibility he held for 16 years.

In his December 1950 Presidential Address to the Colorado Scientific Society, Eckel summarized the "obstacles in communication between engineers and geologists":

> This is the essentially human problem of how to present geologic facts to engineers so that they will understand and use them to maximum advantage. This is a subject within itself, yet one that must be solved. It ranges from the discovery and training of potential engineering geologists, through methods of presenting our data, to research on the psychology of salesmanship. Suffice it to say now that the essence of the problem is the need for *conviction by demonstration*. The geologist and engineer think differently and work differently. The engineer thinks concrete facts and figures, he reasons from *cause to effect*, and he depends very largely on what he can see and measure. The geologist normally reasons from effect to cause and is perhaps all too conscious that his is an inexact science. If he is as skillful and brave as he should be, however, and if he has observed and understood enough facts, he should be willing and able to predict the geologic conditions and their meaning to the engineer. If he continues to make such predictions accurately, he will, by *demonstration*, bridge whatever gaps there are between himself and the engineer. (from Varnes, 1990, Page 90).

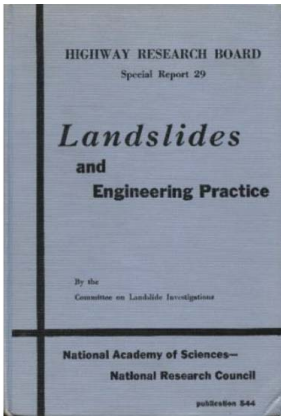

Figure A1-9a. Edwin B. Eckel (1906–89) was the founder and first chief of the Engineering Geology Branch (EGB) of the USGS between 1945 and 1961 (photo courtesy of the Geological Society of America).

Figure A1-9b. Eckel selected the lead authors for each chapter of HRB SR 29 (Eckel, 1958), but every member of the HRB committee was encouraged to read and edit as many of the chapter drafts as they had time to review.

The new "engineering branch" was intended to help bridge the gap separating engineers and geologists, who needed to respect each other's abilities and understand what the limitations were in terms of actually predicting site conditions when less than one millionth of the soil or rock materials are probed in most site investigations.

There was also a lack of knowledge—geological as well as engineering—of the mechanics, recognition, and control of landslides. There was little understanding on the part of geologists about facts and observations needed on maps for use by engineers, and engineers did not appreciate how geologic maps could provide background data for their work (Varnes, 1974). Eckel brought the two disciplines closer together.

Among the landslide investigations undertaken while Eckel was chief of the EGB were those in reservoir areas (Lake Roosevelt and Fort Randall Reservoir), coastal areas (Pacific Palisades, Martha's Vineyard), urban settings (La Paz, Anchorage, Los Angeles, San Francisco Bay area, several Chilean cities, Rapid City, SD), and in a variety of mountainous areas (east-central Utah, Jackson Hole, and the Colorado Front Range). These

Downloaded from http://pubs.geoscienceworld.org/aeg/eeg/article-pdf/31/1/i/6130855/i1558-9161-31-1-i.pdf
by AEG RBAC user

studies added to the body of knowledge of potentially destructive geohazards that were becoming economically important as constructed facilities began to blanket hilly areas that had been perceived as "unbuildable" in the decades predating the introduction of massive earth-moving equipment.

Highway Research Board Committee on Landslides (1951)

Seward Horner died of a sudden heart attack on July 8, 1954, and the HRB Landslide Committee recognized his spirited support of HRB SR 29 by dedicating the volume to him when it appeared in 1958. Their necrology read:

> As Chief Geologist, State Highway Commission of Kansas, he did more than any other to develop the application of all the disciplines of geology to a single and practical end—better road building. As a member of this Committee, he was a tower of strength. As an advisor, to us and to many other engineers and geologists, he was without equal. As a friend, he can never be forgotten or replaced. (Committee on Landslide Investigations)

In May 1949, Edwin B. Eckel was asked by Harold Allen, chairman of the Department of Soils Investigations of the HRB, to convene a committee that would be focused solely on the investigation of landslides. The proposal was accepted by Eckel, but nothing significant occurred until the annual HRB meetings of January 1951, when the HRB set up the Committee on Landslides under the leadership of Eckel, who was then serving as chief of the Engineering Geology Branch of the USGS.

The new committee's initial charge was to evaluate the various types of landslides common to the continental United States (Alaska and Hawaii were not yet states) that often impacted developed infrastructure. The members of the committee included Chairman Ed Eckel of the USGS, R. F. Baker of the State Road Commission of West Virginia, Arthur B. Cleaves of Washington University in St. Louis, Seward E. Horner of the State Highway Commission in Kansas, Ta Liang of Cornell University, Henry Marshall of the Ohio Department of Highways, Shailer S. Philbrick of the U.S. Army Corps of Engineers, Arthur M. Ritchie of the Washington Department of Highways, A. W. Root of the California Division of Highways, Rockwell Smith of the Association of American Railroads, David J. Varnes of the USGS, W. A. Warrick of the Pennsylvania Highway Department, and Eldon J. Yoder of Purdue University's Joint Highway Research Project. Sometime during the next year and a half, the group's name became "The Committee on Landslide Investigations—Highway Research Board."

At that time, Seward Horner (Figure A1-10) was serving as chief geologist of the State Highway Commission of Kansas in Topeka, KS. A native of Abilene, KS, he was the first graduate of Kansas State University to receive a bachelor's degree in geology in 1933. Years later, he became the first geological engineer licensed in the state of Kansas. In 1943, he was appointed chief geologist of the Department of Design of the Kansas State Highway Commission just before taking a leave of absence to serve as chief geologist for the U.S. Public Roads Administration on the wartime construction of the 1,543-mi-long (2,483-km-long) Alcan Highway between Dawson Creek, Canada, and Fairbanks, AK.

In the fall of 1945, he returned to resume his duties with the Kansas State Highway Commission. In the post-war expansion of highways, he emerged as one of the most visible engineering geologists/geological engineers, contributing several very practical articles between 1942 and 1953 in 8 years. In 1949, Horner developed a questionnaire on the role geology played in each of the nation's state highway departments. He received detailed responses from 47 of the 48 states. In 1950, he co-authored an article titled "Application of Geology to Highway Engineering" (Horner and McNeal, 1950), which addressed many of the problems with subdrainage for years thereafter. Horner gained vast experience in overcoming problematic site conditions while working on the Alaska Highway, which set him apart from most

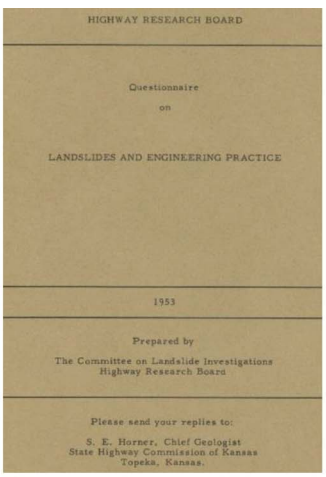
HIGHWAY RESEARCH BOARD

Questionnaire
on

LANDSLIDES AND ENGINEERING PRACTICE

1953

Prepared by
The Committee on Landslide Investigations
Highway Research Board

Please send your replies to:
S. E. Horner, Chief Geologist
State Highway Commission of Kansas
Topeka, Kansas.

Cover of HRB Committee on Landslides questionnaire of 1953. It contained the first oversize plate depicting four types of movement and 19 types of landslides (Figures A1-11 through A1-15).

Special Report 29 was dedicated to Seward Ellis Horner (1906-54), who oversaw the preparation and evaluations of the 250 landslide questionnaires the HRB Landslide Committee distributed in 1953.

Figure A1-10a. Cover of the "Questionnaire on Landslides and Engineering Practice" sent to state highway departments, government agencies involved in heavy construction, and major railroads in 1953.

Figure A1-10b. Seward E. Horner, oversaw the production of the questionnaires and supervised processing of the data on landslides that were returned to his office in Topeka, KS.

Downloaded from http://pubs.geoscienceworld.org/aeg/eeg/article-pdf/31/1/i/6130855/i1558-9161-31-1-i.pdf
by AEG RBAC user

highway geologists, who had not battled with as many sorts of problems (Rogers, 2022). This made Horner a highly respected figure in the HRB when the Landslide Committee was established in 1951. At that time, Horner was serving on the HRB Committee on Highway Subdrains, which was editing HRB Bulletin 45 on subsurface drainage (Keene and Horner, 1951).

As one might expect from someone who had previously prepared a detailed questionnaire for distribution to all 48 states, Horner volunteered to oversee the preparation of what became a 16-page "Questionnaire on Landslides and Engineering Practice" that was dispatched far and wide to gain a sense of how landslides were impacting engineered works, especially linear infrastructure like highways and railroads (Figs. A1-11 to A1-15). The 1953 questionnaire was deemed sufficiently valuable to have been reproduced as an Appendix of HRB SR 29 when it was released in 1958 (Eckel, 1958, pp. 224–232).

Up until the advent of computer-driven geographic information systems (GIS) in the 1990s, many state transportation agencies used portions of the 1953 questionnaire for internal recordation of key aspects of landslides such as weather leading up to failure, physical dimensions, rate of movement, observed dilation, fissure-induced subdrainage, and so forth. It remains a very thorough checklist that is not outdated.

On the document's first page, the report's purpose was summarized:

> The Committee on Landslides of the Highway Research Board requests your help in preparing a monograph, LANDSLIDES AND ENGINEERING PRACTICE. Emphasis will be on highways and railroads. The Committee has been working on this project for nearly 2 years. This book, which we hope will be useful as a manual for the practicing engineer as well as a worthwhile text and reference work, is now about half complete. If it is to come up to our expectations, however, we need help in assembling fresh and authoritative data. To this end we would greatly appreciate your completing the enclosed questionnaire and information sheets. (Eckel, 1958)

The HRB questionnaires were sent to a total of 250 entities. These included all of the state highway departments, state geologists, the nations' largest railroads, Canadian railroads, and federal agencies associated with major engineering construction work (like Federal Lands, the Bureau of Land Management, etc.). Other recipients included turnpike authorities, the U.S. Army Corps of Engineers, Naval Facilities Engineering Command, U.S. Air Force, Bureau of Reclamation, private sector companies and engineers and geologists, and civil engineering and geology departments at major universities.

The 16-page survey was divided into three principal parts. The first section was composed of questions of a general nature intended to provide background information for the proposed specialty chapters addressing the following subjects:

I. Introduction
II. Landslide Types and Processes
III. Criteria for Recognition
IV. Analysis of Landslides
V. Prevention of Landslides
VI. Control and Correction of Landslides
VII. Economics and Legal Aspects
VIII. Discussion of Further Research Needed
IX. Bibliography

For the second part of the questionnaire, representatives of each state were asked to mark the locations of all known or

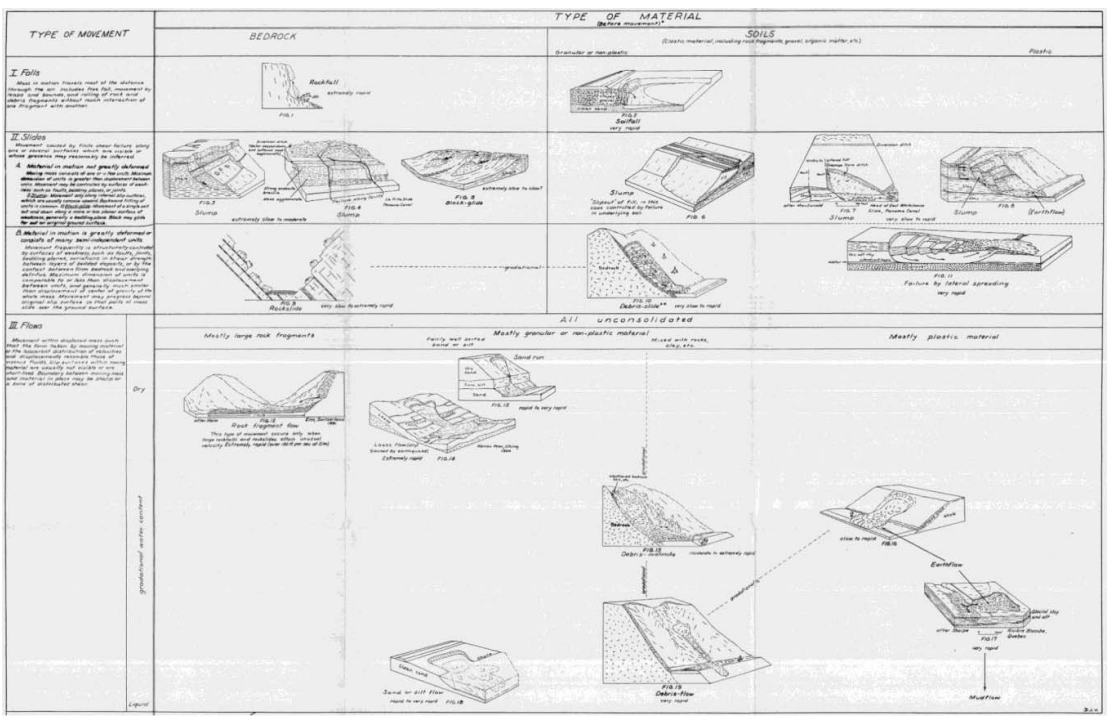

Figure A1-11. The first American Classification of Landslides by the HRB's Landslide Committee in 1953, which was included in the 250 questionnaires sent to state highway departments, geological surveys, and major railroads.

Downloaded from http://pubs.geoscienceworld.org/aeg/eeg/article-pdf/31/1/i/6130855/i1558-9161-31-1-i.pdf
by AEG RBAC user

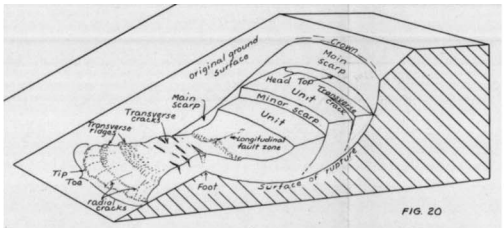

The original pen-in-ink sketch of a typical slump-earthflow landslide by John R. Stacy, with labels on the principal physical features. The pencil sketch was prepared by Dave and Helen Varnes.

PLATE I

CLASSIFICATION OF LANDSLIDES

Highway Research Board Landslide Committee

Recommended nomenclature of the parts of a landslide were described along the lower 4 in (10cm) of the 17 x 22 inch (43 x 56 cm) of Plate 1 (note hand drafting).

Nomenclature of the parts of a landslide
(see drawing at right)

Main scarp – A steep surface on the undisturbed ground along the periphery of the slide, caused by movement of slide material away from the undisturbed ground. The projection of the scarp surface under the disturbed material becomes the surface of rupture.

Minor scarp – A steep surface on the disturbed material produced by differential movements within the sliding mass.

Head – The upper parts of the slide material along the contact between the disturbed material and the main scarp.

Top – The highest point of contact between the disturbed material and the main scarp.

Foot – The line of intersection (sometimes buried) between the lower part of the surface of rupture and the original ground surface.

Toe – The margin of disturbed material most

Suggested Nomenclature of the parts of a landslide.

Tip – The point on the toe most distant from the top of the slide.

Flank – The side of the landslide, usually referring to the disturbed material.

Crown – The undisturbed material adjacent to the highest parts of the main scarp.

Original ground surface – The slope that existed before the movement which is being considered took place. If this is the surface of an older landslide, that fact should be stated.

Left and right – Compass directions are preferable in describing a slide, but if right and left are used they refer to the slide as viewed from the toe.

Notes on the principal physical elements of a typical slump-earthflow landslide, as portrayed in the block diagram.

For the purpose of the Committee's symposium, now in preparation, the following definition of a landslide has been adopted:

Landslide – The term landslide denotes downward and outward movement of slope forming materials composed of natural rock, soils, artificial fills, or combinations thereof.

Landslides move along surfaces of separation by falling, sliding, and by flowing. Parts of a landslide may move upward while other parts move downward. The lower limit of the rate of movement of landslide material is restricted in this book by the economic aspect to that rate of movement which provokes correction or maintenance.

The official "definition of a landslide" adopted by the HRB Landslide Committee in 1953.

* The type of material involved is classified according to its state prior to initial movement or, if the type of movement changes, according to its state at the time of the change in movement. Thus, the Elm slide (Fig. 12) began as a rock-slide and rock-fall in bedrock, but at the time a flowing type of movement started the material was an "unconsolidated" mass of extremely rapidly moving rock fragments.

* * By debris is meant natural soil and rock detritus.

Explanation of the material type classes for landslides adopted by the HRB Landslide Committee in 1953.

Figure A1-12. Notes on suggested nomenclature for landslides that the HRB Landslide Committee agreed upon before sending out 250 questionnaires in 1953. These were listed across the lower margins of oversize Plate 1—Classification of Landslides. Most of these suggestions were included in HRB SR 29 when it appeared in 1958 (Eckel, 1958).

suspected landslides of which they had any knowledge on maps of 1:500,000 scale or smaller (e.g., 1:250,000).

Then, there was a battery of 32 general questions, numbered using Roman numerals. These included a string of details that, when combined, could trigger mass wasting, especially in response to human-controlled activities like blasting or grading and excavating. It appears that the geologists on Horner's subcommittee were hoping to demonstrate how the underlying geology, geomorphology, and climatic conditions of various areas might influence the frequency of mass wasting and landslides.

The concluding portion of the 1953 questionnaire was a series of four-page questionnaires that requested recordation of a long list of physical characteristics and geologic and hydrologic variables that might allow the HRB to categorize the sensitivities of recent historic landslides of consequence (for instance, they mention the destabilizing tendency of the Mancos Shale where it is capped by the more brittle Mesa Verde Sandstone). In descending order, these fill-in-the-blanks questionnaires requested detailed information on the following topics:

(1) Descriptions of Individual Slides (physical locations, volume of materials involved, physical dimensions, velocity of movement, precipitation previous to failure, and whether concentrations of subsurface seepage were noted).
(2) Type or Types of Material Involved in the Slide (types of soils, depth of weathering, surficial deposits, bedrock geology, and stratigraphy, etc.).
(3) Likely Cause or Causes of the Slide (which included a checklist of 28 destabilizing attributes, such as hydrologic changes, clay mineralogy, sudden shifts in loads associated with earth moving, etc.).
(4) Types of Treatment (such as off-haul of excess materials, use of various types of retention structures, cast-in-ground structures, rockbolts, lightweight backfill, chemical treatment subdrainage, sealing of open fissures, etc.).

Only 75 of the 250 questionnaires were returned for review and compilation by Horner's subcommittee, but these included every state and all the major railroads in the United States and Canada. So, it became a valuable document nonetheless because it recognized slump flows as the predominant type of slide, with soil plasticity having the greatest impact on fracture-induced drainage and viscosity/plasticity having the greatest impact on the speed of movement.

After 6.5 years of intense effort, HRB SR 29 ended up being 232 pages (Eckel, 1958), which was right about what they were aiming for when they began the project (175 to 200 pages). The hardback volume was published by the National Academy of

Downloaded from http://pubs.geoscienceworld.org/aeg/eeg/article-pdf/31/1/i/6130855/i1558-9161-31-1-i.pdf
by AEG RBAC user

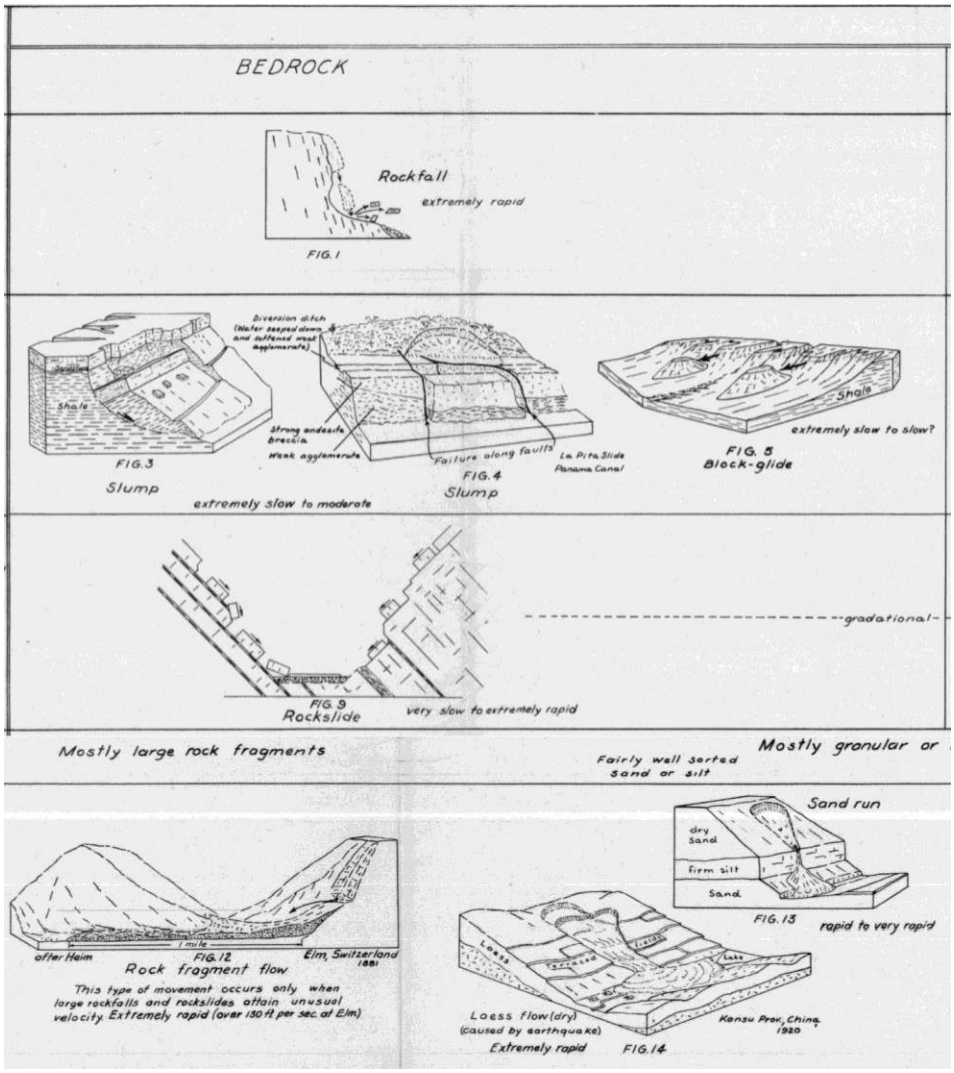

Figure A1-13. Sketches and block diagrams of bedrock falls, slides, and flows from the first HRB Classification of Landslides oversize plate circulated for comment in 1953.

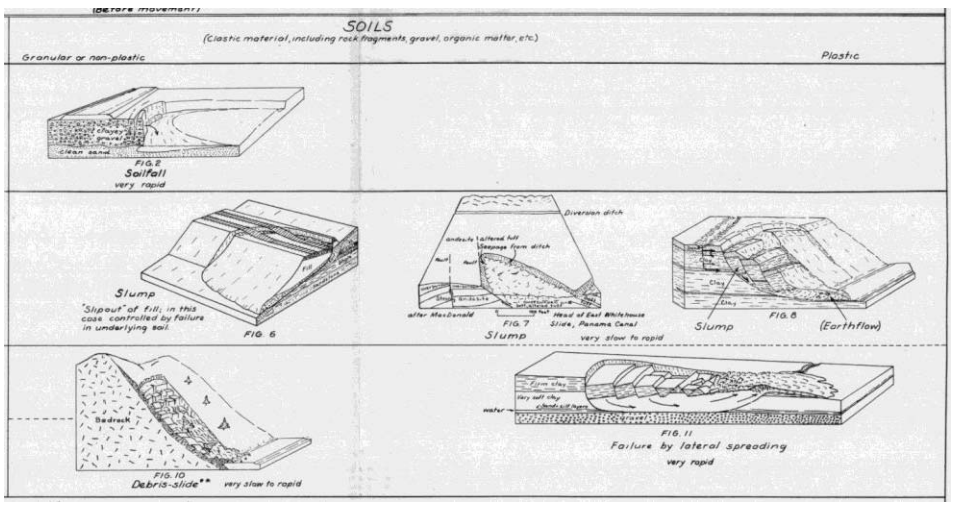

Figure A1-14. Block diagrams portraying falls and slides in soils and clastic materials, including rock fragments, from the first HRB Classification of Landslides plate in 1953.

Downloaded from http://pubs.geoscienceworld.org/aeg/eeg/article-pdf/31/1/i/6130855/i1558-9161-31-1-i.pdf
by AEG RBAC user

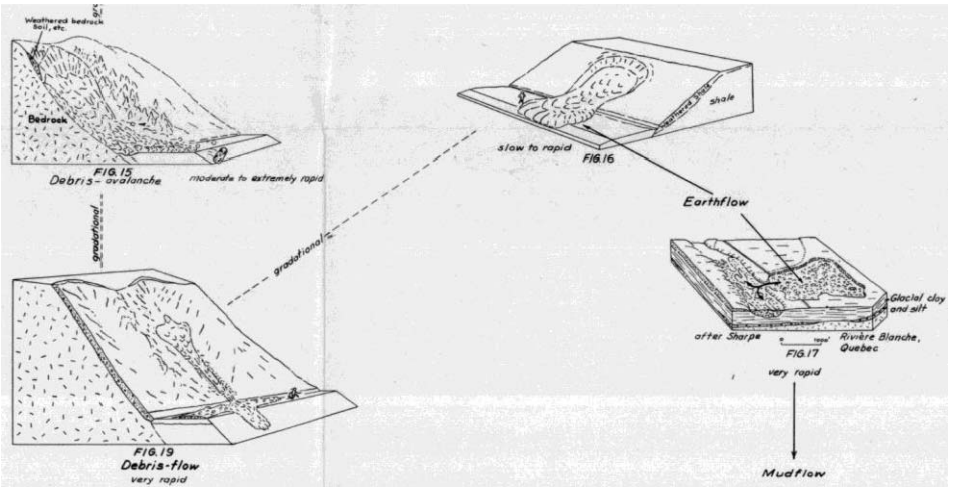

Figure A1-15. Block diagrams portraying flows in unconsolidated materials. The style of movement for non-plastic materials is shown at left, while that for mostly plastic materials is shown at right. These are a portion of the 20 examples sketched in the first HRB Classification of Landslides oversize plate in 1953.

Sciences and the National Research Council as HRB Special Report 29 in 1958 by the U.S. Government Printing Office in Washington, D.C. It sold for $2 apiece. The book was so popular and practical that it and was sold out by 1964–65.

Efforts to Standardize Terminology and Classification of Landslides (1951–58)

The first official accomplishment of the new Committee on Landslides was to sponsor the gathering of citations to construct a current bibliography on landslides (Tompkin and Britt, 1951). The second was to prepare insightful profiles and block diagrams of various types of landslides that would illustrate key identifiers, so that the slides could be arranged into categories based on physical attributes and common behaviors.

At this juncture, one of the key figures was John R. Stacy of the USGS Engineering Geology Branch. He was a draftsman and technical illustrator who was experienced in drawing block diagrams and cut-away views of geological structures. Ed Eckel arranged for Stacy to work with Dave Varnes and Seward Horner to begin illustrating the most common forms of landslides in a manner that allowed end users to recognize the key identifying features of the various types of slides. Stacey also received unofficial guidance from Helen Varnes because she illustrated her own reports, including USGS Circular 31 on *Landslide Problems of Southwestern Colorado* in 1949. Dave Varnes suggested borrowing Stewart Sharpe's fundamental drivers: "type of movement" and "type of material."

A parallel track was to encourage standard nomenclature for describing the key physical characteristics of a landslide. That created three fundamental descriptor "bins." From the very outset, Varnes chose to use block diagrams of the various types of landslides based on the type of movement and the type of materials because those factors were easily observed in the field.

This process began with a thorough review of Stewart Sharpe's 1938 a&b text and his common attribute/common mode of transport model. The committee members were also encouraged to contribute examples of terminology and nomenclature that had been used in the published literature. One of the most confusing terms was "mud slide," which the media and the public overused to describe any sediment-charged mass moving at a speed that appeared to be destructive.

The key elements of their first "Landslide Identification Chart," or oversize plate (43 × 56 cm; 17 × 22 in.), was identifying four types of movement, cited along the left margin of the chart in a vertical column (with I at the top and IV at the bottom):

I. Falls
II. IIa. Slides little deformed by movement
IIb. Slides greatly deformed by movement
III. Flows
IV. Complex Landslides

The types of materials were:

Bedrock transported by falls or slides
Soils moved by falls or slides
Bedrock transported by flows
Soil transported by flows (with soil plasticity high-medium-low)

Getting a Handle on the Costs of Landslides to Society

While interviewing Dave Varnes in 1997 about his service on the HRB and TRB committees, he summarized the experience as follows:

> In the early days (mid-1950s), the committee was stymied in their attempt to get some idea of the financial losses attributable to landslides. At that time, the nation's highway system was growing at a quick pace, and there were no historical case studies one could study to ascertain what a reasonable figure should be in the state highway budgets to fix and repair slip-outs.

One of the few multi-lane highways with a record spanning more than 10 years of operation was the Pennsylvania Turnpike, which had been constructed with engineering geologic input in 1937–40. However, highways generally take more operational maintenance as they grow older, especially asphalt pavements.

The other vexing problem was that most landslides occurred when there had been extra-normal levels of precipitation or runoff, which varied considerably from year-to-year. The operation and

Downloaded from http://pubs.geoscienceworld.org/aeg/eeg/article-pdf/31/1/i/6130855/i1558-9161-31-1-i.pdf
by AEG RBAC user

maintenance budgets of most states were fixed from year to year, based on past experience. When a natural disaster was declared by the president, FEMA could supply funds to restore public improvements to their prior condition, but not to repair preexisting landslides. So, landslide losses tended to be dispersed and "spotty," which reduced political support from unaffected jurisdictions or neighboring states.

In some of the early meetings, the members of the Landslide Committee were briefed on a series of case studies by committee member Rockwell Smith, who worked for the Association for American Railroads in Chicago. They soon learned that the railroads occasionally spent millions of dollars to repair their right-of-way at places like the Cameo slide along the upper Colorado River in De Beque Canyon (between Grand Junction and Rifle, CO). The slide occurs in the Mesa Verde Sandstone where it overlies the Mancos Shale at an old landslide dam site (where the slide had pushed the river channel ~300 ft [91.4 m] easterly, deflecting the river to run around the toe of the slide).

The original rail line was constructed along the river's banks until a portion of the dormant slide reactivated. The failure extended 350 ft (106.7 m) above the channel. After repeated attempts to re-establish their right-of-way, the railroad excavated an expensive tunnel beneath the slide mass. When the slide reactivated, drag features damaged the tunnel and hastened the need to look at a longer, deeper tunnel around the massive landslide or a grading solution by removing about 75 ft (22.9 m) of sandstone off the upper margins of the slide mass, thereby reducing the driving force by 30 percent. The costs of combating the Cameo slide included an option to construct a longer and deeper bypass tunnel, the cost of which was nearly as much as what most state highway departments allotted for annual maintenance!

After figuring the resources necessary to combat such challenging problems, most members of the committee adopted the proviso that "the best way to fight a bedrock landslide would be to avoid it altogether." Of course, simple avoidance was easier to accomplish in the plains of Kansas than in the Colorado Rockies.

By the time that TRB SR 247 was released in 1996, there was a much wider recognition within government circles about the hazard that landslides present, as well as greater recognition within the general population because of increased media coverage. Robert L. Schuster described and summarized many of these issues in his chapter on "Socioeconomic Significance of Landslides in Landslides Investigation and Mitigation," Chapter 2 of TRB SR 247 (Schuster, 1978b, pp. 12–31).

Varnes Assigned Chapter 3 on "Landslide Types and Processes" (1954–58)

Ed Eckel selected Dave Varnes to prepare Chapter 3 on "Landslide Types and Processes," providing information about the most common forms of landslides and the physical processes governing their behavior. From his daily interactions with combat engineers during World War II and highway engineers in the postwar era, Eckel recognized that Varnes' practical insights and his quantitative skills would likely be respected by highway engineers, whose biggest concerns were how to recognize landslide features so they could avoid them altogether. Eckel understood that compromises only occur when both sides of an issue respect each other's technical abilities.

When Varnes accepted new assignments, he would usually begin with a thorough literature review. He would also enroll himself in challenging graduate courses to familiarize himself with the latest technical tools and analytical techniques. He also opened up technical discussions by soliciting commentaries from the leading experts in their respective specialties. A typical example would be his collaboration with USGS vulcanologist Dwight "Rocky" Crandell on studying the kinematics of the perennially active Slumgullion landslide dam in the Colorado Rockies.

Sometimes, these discussions were in letters, and other times, they occurred via phone or meeting at technical society conventions, like those held by the American Geophysical Union. Varnes multi-faceted approach allowed him to advance balanced evaluations that were usually met with universal acceptance, and many of his publications received international recognition.

When Ed Eckel retired in 1961, he asked Dave Varnes to take over the reins of the EGB. One of the surprising things that Varnes did as branch chief was passing the various examinations to become a professional engineer (P.E.) in Colorado at age 45 in August 1964. It was his hope that the engineers would have an increased level of respect for someone with dual registration in engineering and geology, like he had witnessed with the geological engineering students matriculating through the Colorado School of Mines. Not long after geology registration laws were enacted in California in June 1969, Varnes became a registered geologist (R.G.) and a certified engineering geologist (C.E.G.) in December 1970. Most of the ECB chiefs that followed were either registered as geologists and engineering geologists (Jack McGill 1969–74) or as professional engineers (Bob Schuster 1974–79).

For the HRB project in 1956–58, Varnes began with a thorough review of Stewart Sharpe's textbook, which Helen had found valuable in the late 1940s when she was studying three significant bedrock landslides in southwestern Colorado (H. D. Varnes, 1949). This led to a polite correspondence between the two men on the nuances of slope creep and why engineers did not seem to have any rational theories for how to estimate its long-term impacts, because there was so little credible data available for review.

Varnes decided to classify landslide movements according to the physical factors that would be relevant to their prevention or control, because those aspects were the central theme of the HRB project. He appreciated that the state highway engineers sought technical guidance in their operations and maintenance decisions, not a compendium of scientific studies. Because of its almost imperceptible rate of movement, creep was excluded from consideration as a mass movement injurious to most paved highways, which were all less than 20 years old when HRB SR 29 appeared in 1958.

He assembled a simple chart that recognized the type of movement, which was of primary importance, and the type of material, which was assumed to have somewhat lesser importance. Another common variable was the relative moisture observed during failure (wet or dry), as shown in Figure A1-16. The oversize plate containing block diagrams of the various types of landslides is shown in Figure A1-17. The original image in Figure A1-16 did not show a block diagram of a "complex landslide," but it defined the type of movement category as:

> Movement is by a combination of one or more of the three principal types of movement described above [on Plate 1]. Many landslides are complex, although, as illustrated in Plates 1-k and 1-l, one type of movement generally dominates over the others at certain areas within a slide or at a particular time in the evolution of a slide.

Figure A1-18 lists the common technical terms, such as "crown scarp," "main scarp," and "headscarp," any of which could be dbedrock escribing the same feature/aspect. Most of these descriptive

Downloaded from http://pubs.geoscienceworld.org/aeg/eeg/article-pdf/31/1/i/6130855/i1558-9161-31-1-i.pdf
by AEG RBAC user

TYPE OF MOVEMENT	TYPE OF MATERIAL			
	BEDROCK		SOILS	
FALLS	ROCKFALL		SOILFALL	
SLIDES — FEW UNITS	ROTATIONAL SLUMP	PLANAR BLOCK GLIDE	PLANAR BLOCK GLIDE	ROTATIONAL BLOCK SLUMP
SLIDES — MANY UNITS		ROCKSLIDE	DEBRIS SLIDE	FAILURE BY LATERAL SPREADING
FLOWS	ALL UNCONSOLIDATED			
	ROCK FRAGMENTS	SAND OR SILT	MIXED	MOSTLY PLASTIC
DRY	ROCK FRAGMENT FLOW	SAND RUN	LOESS FLOW	
WET		SAND OR SILT FLOW	RAPID EARTHFLOW DEBRIS FLOW	DEBRIS AVALANCHE MUDFLOW SLOW EARTHFLOW
COMPLEX	COMBINATIONS OF MATERIALS OR TYPE OF MOVEMENT			

Figure A1-16. Abbreviated version of Varnes' Classification of Landslides in 1958. The left column identifies the type of movement (falls, slides, flows, or complex), while the remainder of the chart denotes the type of material (bedrock or soils), and whether it was wet or dry when displaced.

terms remain in use today, although more comprehensive schemata have been introduced in the literature by Varnes (1978), Cruden and Varnes (1996), and Hungr et al. (2014).

The most cited contribution was the Committee on Landslide Investigation's oversize plate "Classification of Landslides," which included 20 examples with simple descriptive nomenclature (Figure A1-17). This plate was intended to present representative examples of the most common types of landslides generally recognized in the late 1950s. Its suggested nomenclature became the operative terminology for scientific and engineering reports in the United States, and many of the descriptive terms were even adopted for work in other parts of the world.

TRB Task Force on Review of Special Report 29—Landslides (1972–78)

In 1972, the National Research Council (NRC) formed a Task Force on Review of Special Report 29–Landslides because HRB

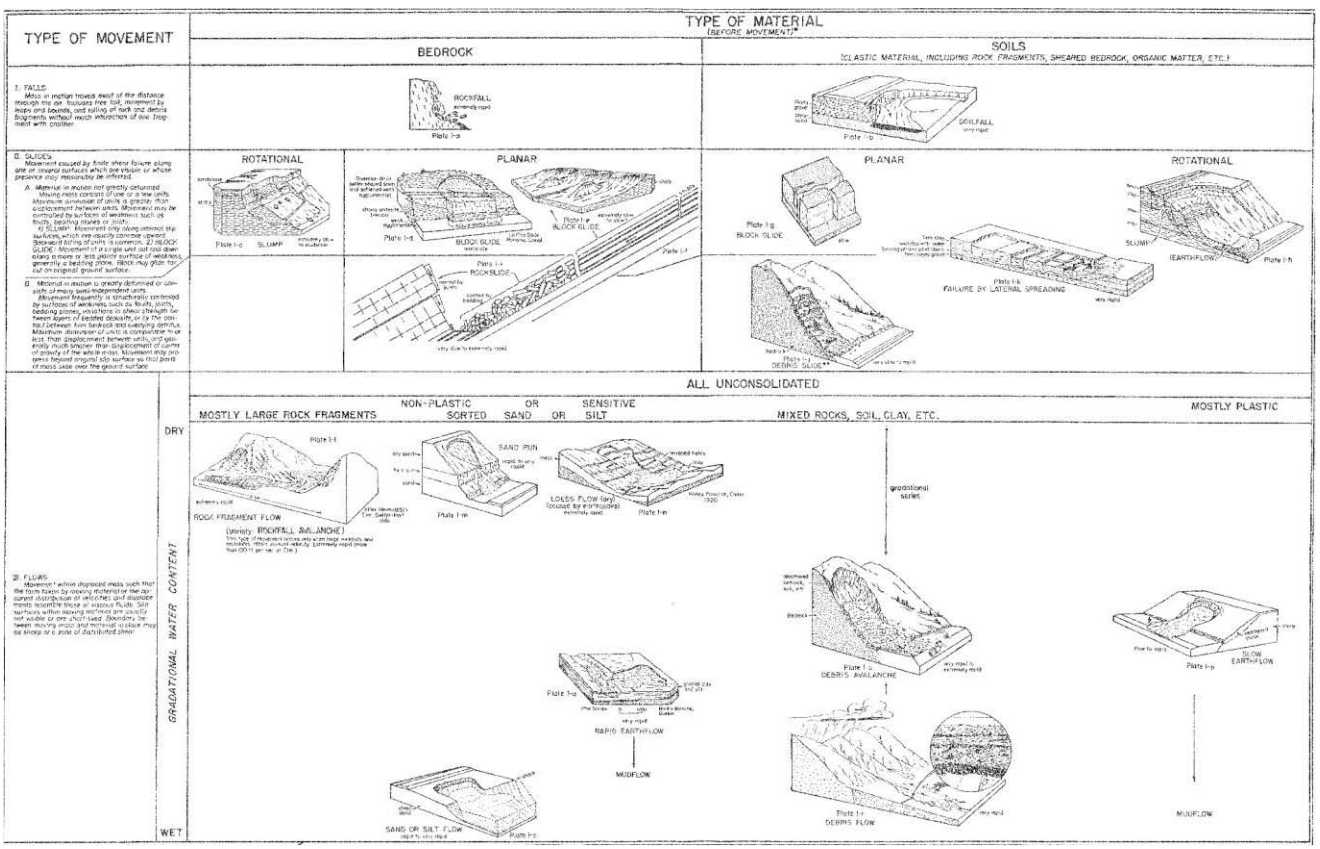

Figure A1-17. The oversize Classification of Landslides included in the end pocket of HRB SR 29 released in 1958 (Eckel, 1958).

Downloaded from http://pubs.geoscienceworld.org/aeg/eeg/article-pdf/31/1/i/6130855/i1558-9161-31-1-i.pdf
by AEG RBAC user

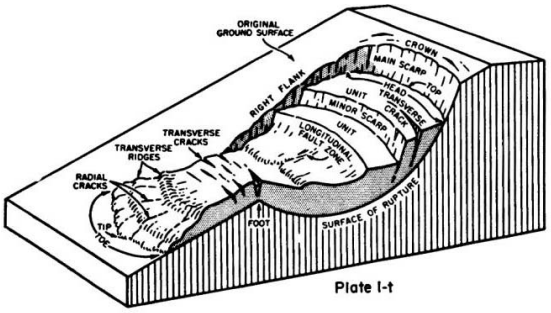

TIP– The point on the toe most distant from the top of the slide.
FLANK– The side of the landslide.
CROWN– The material that is still in place, practically undisturbed, and adjacent to the highest parts of the main scarp.
ORIGINAL GROUND SURFACE– The slope that existed before the movement which is being considered took place. If this is the surface of an older landslide, that fact should be stated.
LEFT AND RIGHT– Compass directions are preferable in describing a slide, but if right and left are used they refer to the slide as viewed from the crown.

Nomenclature of the parts of a landslide
(see drawing at right)

MAIN SCARP– A steep surface on the undisturbed ground around the periphery of the slide, caused by movement of slide material away from the undisturbed ground. The projection of the scarp surface under the disturbed material becomes the surface of rupture.
MINOR SCARP– A steep surface on the disturbed material produced by differential movements within the sliding mass.
HEAD– The upper parts of the slide material along the contact between the disturbed material and the main scarp.
TOP– The highest point of contact between the disturbed material and the main scarp.
FOOT– The line of intersection (sometimes buried) between the lower part of the surface of rupture and the original ground surface.
TOE– The margin of disturbed material most distant from the main scarp.

Figure A1-18. Suggested nomenclature of the parts of a landslide from HRB SR 29 (Varnes, 1958). At that time, the terms "main scarp" and "crown scarp" were often used interchangeably to describe the scarp of greatest exposure or the highest-tensile-strength scarp.

SR 29 (1958) was out of print, and there was a pressing need for something to fill the gap as a standard reference on the subject. Most of the committee's 16 members were drawn from HRB's Soils and Geology Group. Their charge was to recommend what action could be taken in response to the interest of HRB members requesting an updated volume that might include new concepts and methods of slope restoration that had come into practice since 1958.

At their first meeting in 1972, the new committee chose to retain the scope of HRB SR 29 while searching for information that might prove "useful to those who must recognize, avoid, control, design for, or correct landslide movement" (Schuster, 1978a). Another conscious decision was made to equip users with guidance on analysis and control of soil and rock slopes and an awareness of their differences and similarities. These included new computerized techniques for slope-stability analyses and the selection of shear strength parameters for rock slope stability evaluations, which were not available in 1958.

The new book was to be divided into two parts. The first was the definition and assessment of the landslide problem, which had increased significantly in the past 14 to 21 years (TRB SR 176 was not printed until 1979 [imprinted 1978, published 1979]). This included overviews of slope movement types and processes, recognition of landslide features in field investigations, options for instrumentation, and evaluation of strength parameters. The second half of the new volume was intended to deal specifically with landslide mitigation. This included slope-stability analyses, design methodologies, and case histories of remedial measures.

In 1973–74, the Highway Research Board (HRB) was reorganized into the Transportation Research Board (TRB) and became one of seven major divisions of the National Academies of Sciences, Engineering, and Medicine, formerly known as the National Research Council. Today, the TRB hosts 200 standing committees and task forces that deal with various aspects of transportation and attracts 14,000 transportation professionals from the United States at their annual conferences each January in Washington, D.C.

Varnes appreciated that the state highway engineers sought technical guidance in their operations and maintenance decisions, not a compendium of scientific studies. He agreed to modify the classification of landslide movements according to the physical factors that would be relevant to their prevention or control, because those aspects were the central theme of the project. In addition, now that the task force was under the guidance of the TRB, they would be subject to an umbrella fact-checking, editing, and peer-review process from members of the National Academies of Sciences, which was assumed to encourage a state-of-the-practice report. In the end, it took 6 years to produce TRB SR 176, and although it was dated 1978, its first printing was not until 1979. Examples of these types of bedrock landslides can be found in Figs. A1-19 o A1-22.

Downloaded from http://pubs.geoscienceworld.org/aeg/eeg/article-pdf/31/1/i/6130855/i1558-9161-31-1-i.pdf
by AEG RBAC user

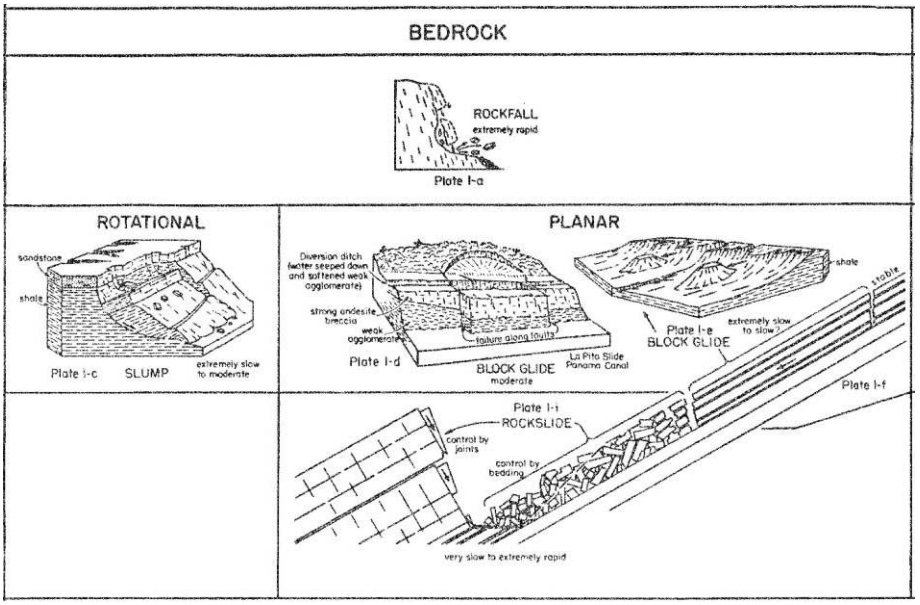

Figure A1-19. Examples of bedrock landslides with planar rupture surfaces usually controlled by bedding, foliation, or pervasive jointing. Block glide failures are representative of planar slides, while rotational slumps are typical of bedrock slides floored in over-consolidated shales.

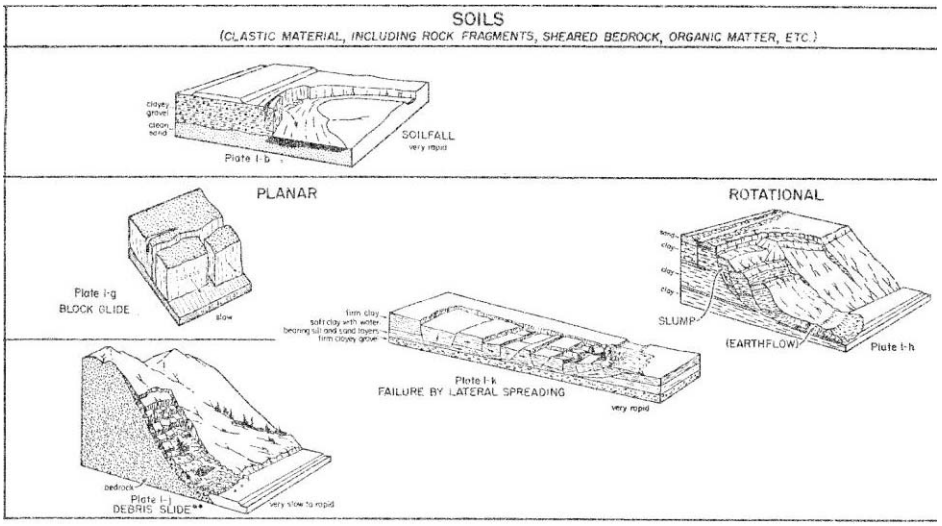

Figure A1-20. Examples of planar and rotational slides developed in clastic materials, including slump-earthflows, block glides, debris slides, and lateral spreads.

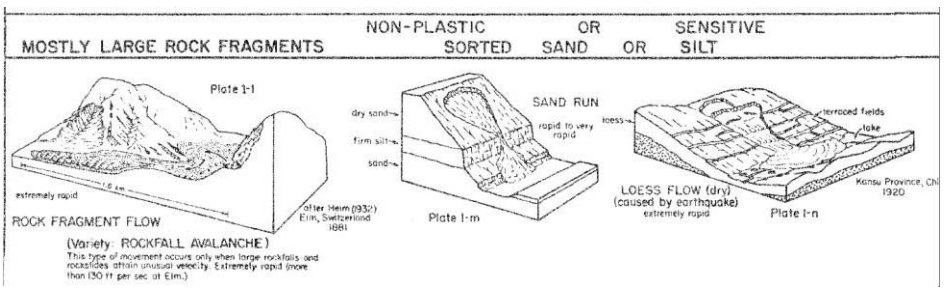

Figure A1-21. Examples of relatively dry rock fragment flows, non-plastic sorted sands, and sensitive silts often associated with rockfall avalanches, sand runs, and flowage of dry loess.

Downloaded from http://pubs.geoscienceworld.org/aeg/eeg/article-pdf/31/1/i/6130855/i1558-9161-31-1-i.pdf
by AEG RBAC user

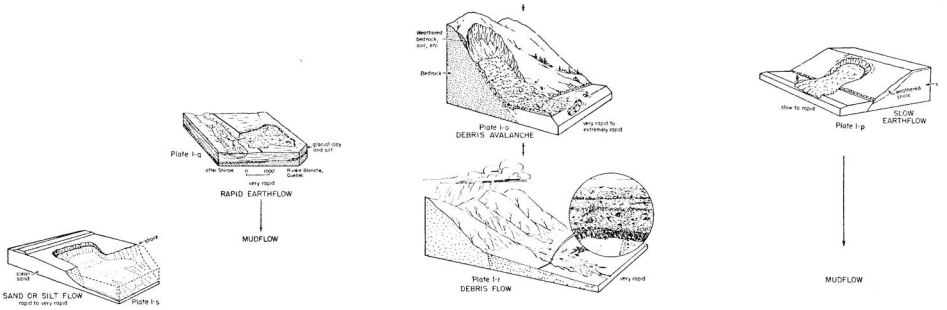

Figure A1-22. Representative mixtures of wet semi-cohesive materials often associated with rapid flow failures, debris avalanches, debris flows, and creeping earthflows. Debris flows seldom exhibit significant cohesion and often include subangular to subrounded clasts within a granular matrix.

Landslide Types and Processes for TRB SR 176 (1978)

Dave Varnes and the majority of his fellow committee members felt that slope movements should be divided into five main groups: falls, topples, slides, spreads, and flows. An additional caveat was that a landslide was defined as constituting those slope movements wherein some sort of shearing failure occurred along a specific surface or combination of surfaces.

The members also agreed that of the five groups of mass movements, only slides were susceptible to quantitative stability analyses by use of "conventional sliding-wedge or circular-arc techniques." This was an obvious change from 1958, when there was no mention of limit equilibrium analytical techniques to evaluate factors of safety for slope stability, exclusive of the "method of slices" introduced in 1955, which was very conservative.

Varnes principal assignment on the 1978 TRB effort was preparing Chapter 2, "Slope Movement Types and Processes" and the oversize plate illustrating the various types of slope movements, similar to his effort in 1952–58 (Fig. A1-23). In 1978, he prepared a similar abbreviated slope movement table with similar key traits for classification, but with 33 graphic examples in lieu of the 20 examples presented in 1958 (Figure A1-24). This table listed seven types of movement (falls, topples, rotational, translational, lateral spreads, flows, and complex) and two types of materials (bedrock and engineering soils). Flow slides, rockfall avalanches, and lateral spreads were vividly displayed in Alaska after the Great Alaska Earthquake of March 27, 1964. The USGS dispatched all of the engineering geologists that they could spare, including Varnes, to participate in the reconnaissance of the largest natural disaster in American history (which it remains).

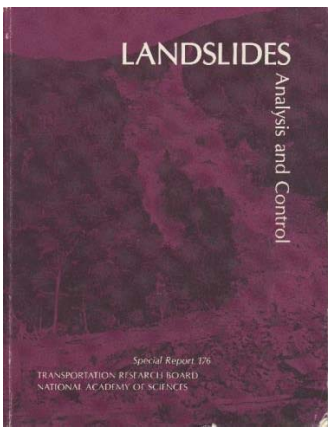

Figure A1-23. TRB SR 176 (Schuster and Krizek, 1978) was completed in 1978 but was not printed until 1979 because of run-away inflation at that time causing annual budgets to be exceeded. It was reprinted four times, in March 1979, November 1979, October 1981, and October 1985. The soft cover option sold for just $8. One of the fundamental changes incorporated in TRB SR 176 was a broader definition of the term "landslide."

TYPE OF MOVEMENT		TYPE OF MATERIAL		
		BEDROCK	ENGINEERING SOILS	
			Predominantly coarse	Predominantly fine
FALLS		Rock fall	Debris fall	Earth fall
TOPPLES		Rock topple	Debris topple	Earth topple
SLIDES	ROTATIONAL	Rock slide	Debris slide	Earth slide
	TRANSLATIONAL			
LATERAL SPREADS		Rock spread	Debris spread	Earth spread
FLOWS		Rock flow (deep creep)	Debris flow (soil creep)	Earth flow
COMPLEX		Combination of two or more principal types of movement		

Figure A1-24. Varnes' (1978) simplified classification of slope movements that appeared in TRB SR 176 (Schuster and Krizek, 1978). Between 1958 and 1978, the number of descriptive block diagrams increased from 20 to 29 types of slides.

Downloaded from http://pubs.geoscienceworld.org/aeg/eeg/article-pdf/31/1/i/6130855/i1558-9161-31-1-i.pdf
by AEG RBAC user

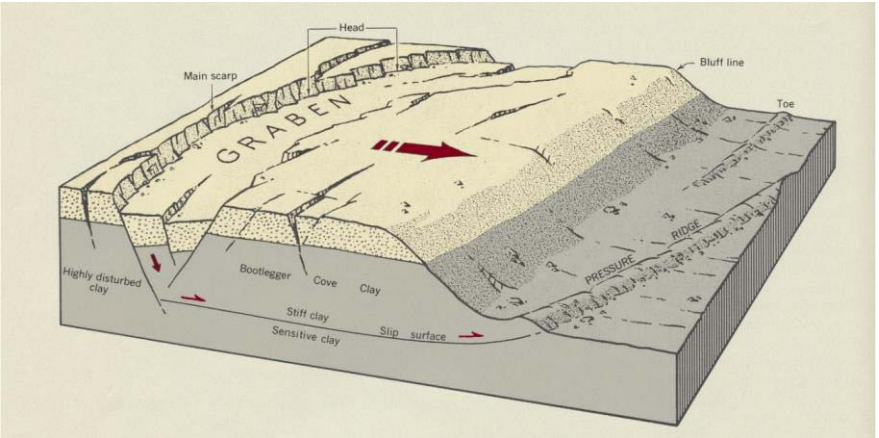

Figure A1-25. Schematic block diagram of a subaqueous "earth block slide" on Government Hill in Anchorage, AK, after the 1964 earthquake (modified from Hansen, 1965). It was included as an oversize Figure 2.1 in TRB SR 176 (Schuster and Krizek, 1978) Figure 3-22 in TRB SR 247 (Cruden and Varnes, 1996). Most geoengineers consider this to be a seismically induced lateral spread.

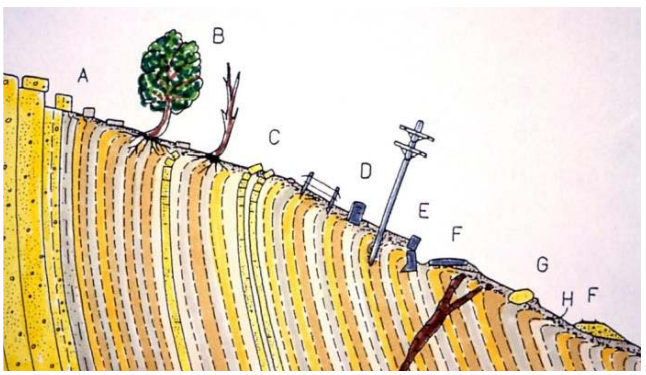

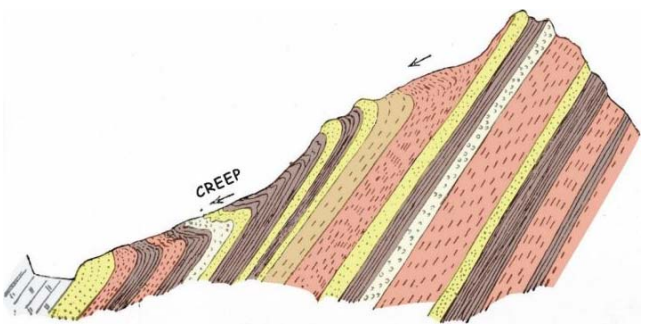

Varnes was assigned to document much of the liquefaction damage and lateral spread features that damaged the Government Hill Port Area of Anchorage (Fig. A1-25), where two thirds of the port's infrastructure had been destroyed (Varnes, 1969). There was so much to do in the unspoiled expanse of Alaska that several of his engineering geology colleagues never left Alaska, choosing to affiliate with the Alaskan Geology Branch for the balance of their careers.

Another new category of mass wasting emanating from the post-earthquake studies in Alaska was the recognition of solifluction, as shown in panel B-q, and catastrophic rockfall avalanche streams (sturzstroms), shown at far-left end of the Type VI complex landslides. Nearly 400 of these enormous dry flow slides were triggered in the Great Alaska Earthquake of March 1964. Most of these occurred in the glacial highlands of the Brooks Range, but several also occurred along the Alaskan coastline.

Soil creep and toppling also made the cut this time around because they were beginning to attract the attention of highway operations and maintenance personnel (Fig. A1-26). Creep loads were also beginning to cause noticeable tilting of retaining walls, usually along the toes of highway cuts and fill slopes.

Establishing International Standards for Landslide Types and Processes (1990s)

In 1989, a study committee was organized by the TRB to review TRB SR 176 to ascertain if it was still relevant because it was then 12 years old. The consensus was that an even better document could be produced that considered more modern analytical techniques and the introduction of geomembranes, soil reinforcement, and the like, which had impacted the heavy construction industry.

←

Figure A1-26a. Common expressions of slope creep (colored sketch from Sharpe, 1938a&b).

Figure A1-26b. Plastic deformation triggered by slope creep tends to be most noticeable in over-consolidated clay shales, like those shown in this colored sketch from Fox (1935).

Figure A1-26c. Slope creep exerting a sustained lateral load on the foundation of a garage wall on Brook Street in Lafayette, CA, in July 1971 (Fred Taylor, USGS).

Downloaded from http://pubs.geoscienceworld.org/aeg/eeg/article-pdf/31/1/i/6130855/i1558-9161-31-1-i.pdf
by AEG RBAC user

Several of the people who had served on the task force that prepared TRB SR 176 agreed to serve on this new committee chaired by Professor A. Keith Turner at the Colorado School of Mines and Robert L. Schuster of the USGS in Golden, CO, who jointly served as the volume's editors.

The committee's first meeting was in Washington, D.C., during the annual TRB meeting in January 1990. Volunteers were selected to develop chapters on their expertise areas, utilizing previous authors whenever possible to trim down people's workloads. After this, the committee held three additional meetings where a number of concerns were expressed face-to-face in order to avoid excessive overlap in each subject area. In the end, they committed to the preparation of 25 different chapters written by 30 authors.

This time, the chapter on "Landslide Types and Processes" would be prepared by Professor David M. Cruden of the University of Alberta in Edmonton and David J. Varnes of the USGS. Cruden was cross trained in geology and civil engineering and for several decades held a dual faculty appointment in both departments at the University of Alberta in Edmonton. He was also recognized as the moving force behind the activities of IAEG's Commission on Landslides and Other Mass Movements and the Working Party on the World Landslide Inventory, which was working to establish internationally accepted classification of landslide types, technical terms, and kinematic understanding of the physical processes involved in all types of mass wasting during the UNESCO-sponsored International Decade for Natural Hazard Reduction in 1990–2000. David Varnes was the only author of TRB SR 247 who had previously prepared chapters for HRB SR 29 (1958) or TRB SR 176 (1979).

Working Party on the World Landslide Inventory and the International Decade for Natural Hazard Reduction

In 1989, the announcement was made by the United Nations that 1990–2000 would be designated as the International Decade for Natural Hazard Reduction. At that time, the IAEG had a Commission on Landslides and Other Mass Movements formed in 1978 that was already working on a program to standardize the technical terminology associated with mass wasting and landslides.

In 1990, the IAEG commission led the way by releasing for publication their *Suggested Nomenclature for Landslides* (IAEG Commission on Landslides, 1990), and the Working Party on the World Landslide Inventory (WP/WLI) was established (IGS UNESCO WP/WLI, 1993).

The WP/WLI was staffed by a number of agencies, including the IAEG Commission on Landslides, the Technical Committee on Landslides of the International Society for Soil Mechanics and Foundation Engineering, the International Society for Rock Mechanics, the International Geotechnical Societies (IGS), and the United Nations Educational, Scientific, and Cultural Organization (UNESCO). One of their first collaborations was to publish a *Directory of the World Landslide Inventory* (Brown et al., 1992). The working party also wrote the *Multilingual Landslide Glossary* (IGS UNESCO WP/WLI, 1994b).

The overarching goal of these collaborations was to develop common terminology for descriptions of physical aspects of landslides as well as analytic and scientific aspects (Cruden and Lefebvre (1994). Historically, workers had used the type of movement physical mechanisms, appearance, common triggers, and velocity, at the expense of the much more complicated question of how to mitigate the destructive capabilities of such catastrophes. The TRB volumes consistently sought out that compromise, seeking to intertwine scientific aspects with practical problem solving.

The rest of 1990 TRB committee members wanted "to stick to the Varnes (1978) model," which emphasized the type of landslide/rockfall movement and the parent material (rock debris and earth). They also decided to retain the five primary types of movement: falls, topples, slides, spreads, and flows, dropping complex landslides (Fig. A1-27), the sixth type that had been introduced in 1978.

In 1996, the TRB released *Landslides: Investigation and Mitigation* as Special Report 247 (673 p.), ISBN 0-309-06151-2 (Fig. A1-31). The new terminology used in TRB SR 247 was consistent with the glossary of the UNESCO working party (IGS UNESCO WP/WLI, 1990, 1991, 1993, 1994a, 1994b, 1995; produced by WP/WLI with input from the Canadian Geotechnical Society). This was a significant achievement, and the new terminology soon appeared in published articles, papers, and textbooks emanating from scientists and researchers in the field. It has taken American engineers a bit longer to convert to terms like "complex" and "composite" landslides, but consistent peer review has introduced the terms into the engineering literature without too much grumbling. A tabular summary of the key papers introducing these new international standards is listed in Appendix Table A1-1. The types of slope movements predominatedly coarse debris and predominately fine-grained soils are illustrated in Fig. A1-28. Wet sand and silt, loess, and earthflows and mud flows from 1978 can be found in Fig. A1-29.The concepts of "zone of depletion" and "zone of accumulation" are illustrated in Fig. A1-30.

Cognizance of Landslide State of Activity

The general state of activity of any landslide should be investigated and noted during its initial reconnaissance. This usually requires some detailed evaluations of potentially displaced debris that might provide a general idea of the age of exposure to the elements, like precipitation and drought. In TRB SR 247 (Fig. A1-31), Cruden and Varnes (1996) recommended using the terms suggested in Appendix Table A1-1 (Table 3.2 in TRB SR 247). These terms are intended to define a single sequence of movement or a repetition of said movement. These modifiers are grouped under three headings: (1) state of activity (what is known about the movements); (2) distribution of activity (where the landslide is moving); and (3) style of activity (the manner in which such movements contribute to the landslide).

Visual examples of the various topographic cues to help interpret and report a landslide's state of activity were developed by the International Society for Soil Mechanics and Foundation Engineering's Technical Committee 11 on Landslides in 1989–94, chaired by David M. Cruden and assisted by Professor Guy Lefebvre at the University of Sherbrooke (Cruden and Lefebvre, 1994). One of their examples is reproduced here in Figure A1-32.

In the series of sections shown in Figure A1-32, note the hummocky debris field that results from gradual disintegration of the displaced materials (ISSMFE, 1993; Cruden and Varnes, 1996). The rates of terrain mollification depend on prevailing weather patterns, especially precipitation and shrink-swell cycles (which influence slope creep).

Landslide Distribution of Activity

There are a number of modifying terms used to describe the distribution of activity in a landslide, more so in larger landslide complexes as compared to compact or isolated masses. Some of

Downloaded from http://pubs.geoscienceworld.org/aeg/eeg/article-pdf/31/1/i/6130855/i1558-9161-31-1-i.pdf
by AEG RBAC user

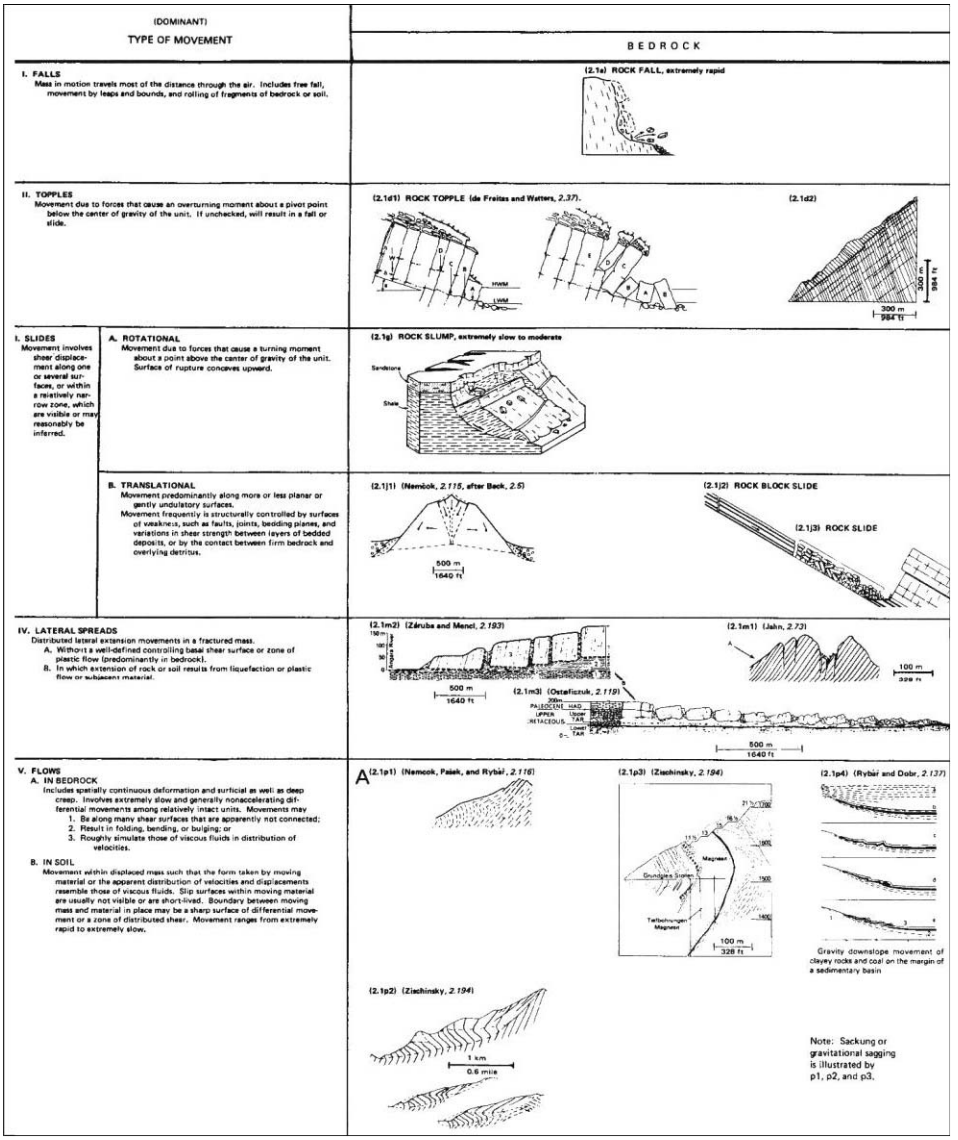

Figure A1-27. Five principal types of mass wasting were listed along the left margin of the oversize plate titled "Types of slope movement." Examples of bedrock landslide features corresponding to the five types of movement are shown on the right half of this portion of the oversize plate. Note the inclusion of a sackungen ridge splitting in panel 2.1j1. Also note line of increasing back-rotated rocks in panel 2.1m2. The geological engineers called these "bearing-capacity failures," while geologists labeled them "floaters" or "knockers" within the "slope creep zone."

Table A1-1. *International standards proposed by UNESCO's Working Party on the World Landslide Inventory during the Decade of Natural Hazards Reduction (1990–2000).*

Brown, W. M.; Cruden, D. M.; and Dennison, J. C., 1992, *The Directory of the World Landslide Inventory*: U.S. Geological Survey Open-File 92-427, 216 p.

International Association of Engineering Geology Commission on Landslides, 1990, Suggested Nomenclature for Landslides: *Bulletin of the International Association of Engineering Geology*, Vol. 41, pp. 13–16.

International Geotechnical Society's UNESCO Working Party on World Landslide Inventory (IGS UNESCO WP/WLI), 1990, A suggested method for reporting a landslide: *Bulletin of the International Association of Engineering Geology*, Vol. 41, pp. 5–12.

International Geotechnical Society's UNESCO Working Party on World Landslide Inventory (IGS UNESCO WP/WLI), 1991, A suggested method for a landslide summary: *Bulletin of the International Association of Engineering Geology*, Vol. 43, pp. 101–110.

International Geotechnical Society's UNESCO Working Party on World Landslide Inventory (IGS UNESCO WP/WLI), 1993, A suggested method for describing the activity of a landslide: *Bulletin of the International Association of Engineering Geology*, Vol. 47, pp. 53–57.

continued

Downloaded from http://pubs.geoscienceworld.org/aeg/eeg/article-pdf/31/1/i/6130855/i1558-9161-31-1-i.pdf
by AEG RBAC user

Table A1-1. *Continued.*

International Geotechnical Society's UNESCO Working Party on World Landslide Inventory (IGS UNESCO WP/WLI), 1995, A suggested method for describing the rate of movement of a landslide: *Bulletin of the International Association of Engineering Geology*, Vol. 52, pp. 75–78.

International Geotechnical Society's UNESCO Working Party on World Landslide Inventory (IGS UNESCO WP/WLI), 1994, A suggested method for reporting landslide causes: *Bulletin of the International Association of Engineering Geology*, Vol. 50, pp. 71–74.

International Geotechnical Society's UNESCO Working Party on World Landslide Inventory (IGS UNESCO WP/WLI), 1994, *Multilingual Landslide Glossary*: BiTech Publishers Ltd., Richmond, British Columbia, Canada, 32 p.

International Society for Soil Mechanics and Foundation Engineering, Technical Committee 11, 1993, *Landslide Illustrations: A Collection of 26 Slides*: Department of Engineering, Cambridge University, Cambridge, England, U.K.

Cruden, D. M. and Varnes, D. J., 1996, Landslide types and processes, Chapter 3. In Turner, A. K. and Schuster, R. L. (Editors), *Landslides: Investigation and Mitigation*: Transportation Research Board Special Report 247, National Academy of Sciences, Washington, D.C., pp. 36–75.

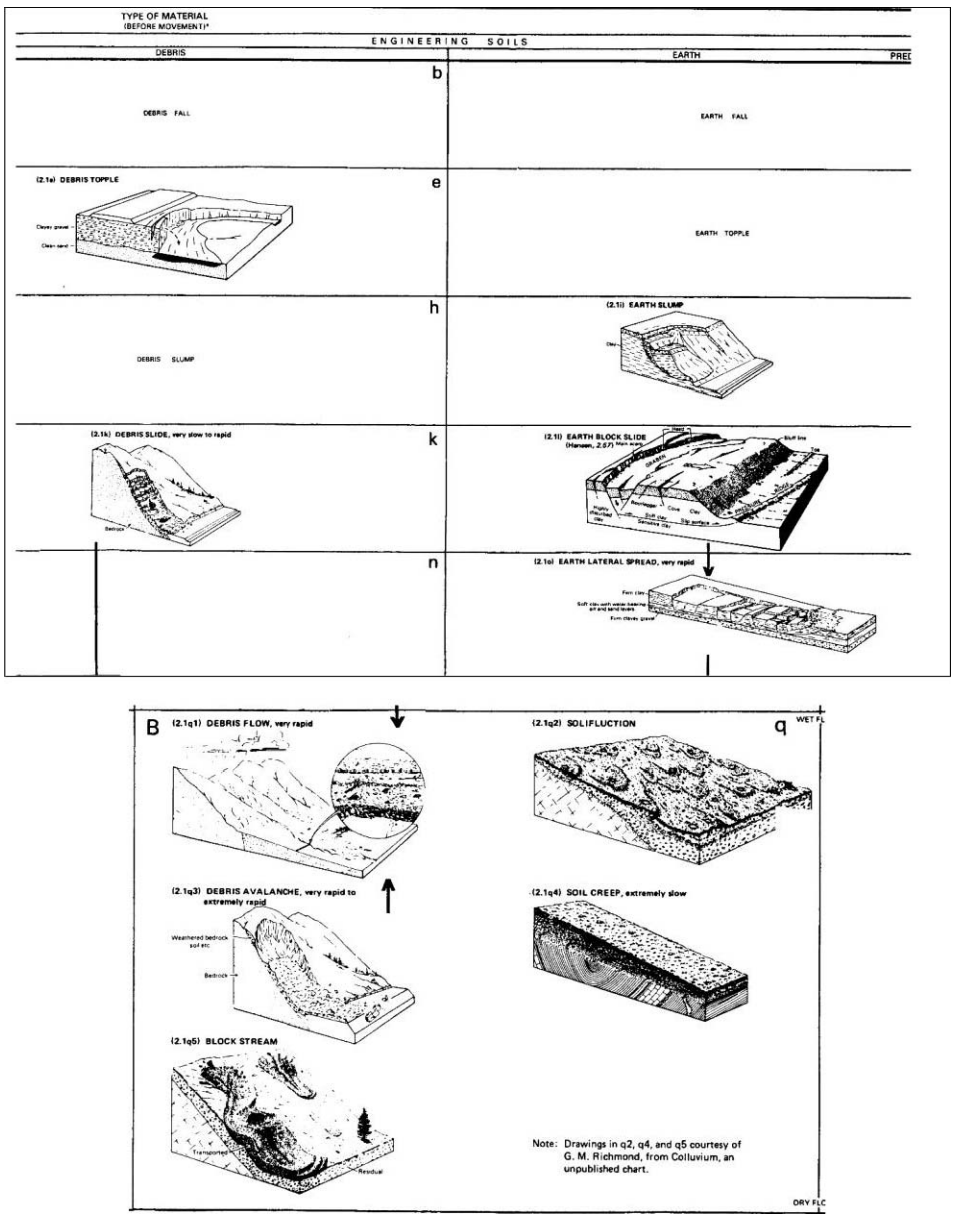

Figure A1-28. Types of slope movements, predominately coarse debris on the left and predominately fine-grained soils on the right half of the upper pane. The diagrams right of k and n are lateral spread features, while those below include solifluction and slope creep.

Downloaded from http://pubs.geoscienceworld.org/aeg/eeg/article-pdf/31/1/i/6130855/i1558-9161-31-1-i.pdf
by AEG RBAC user

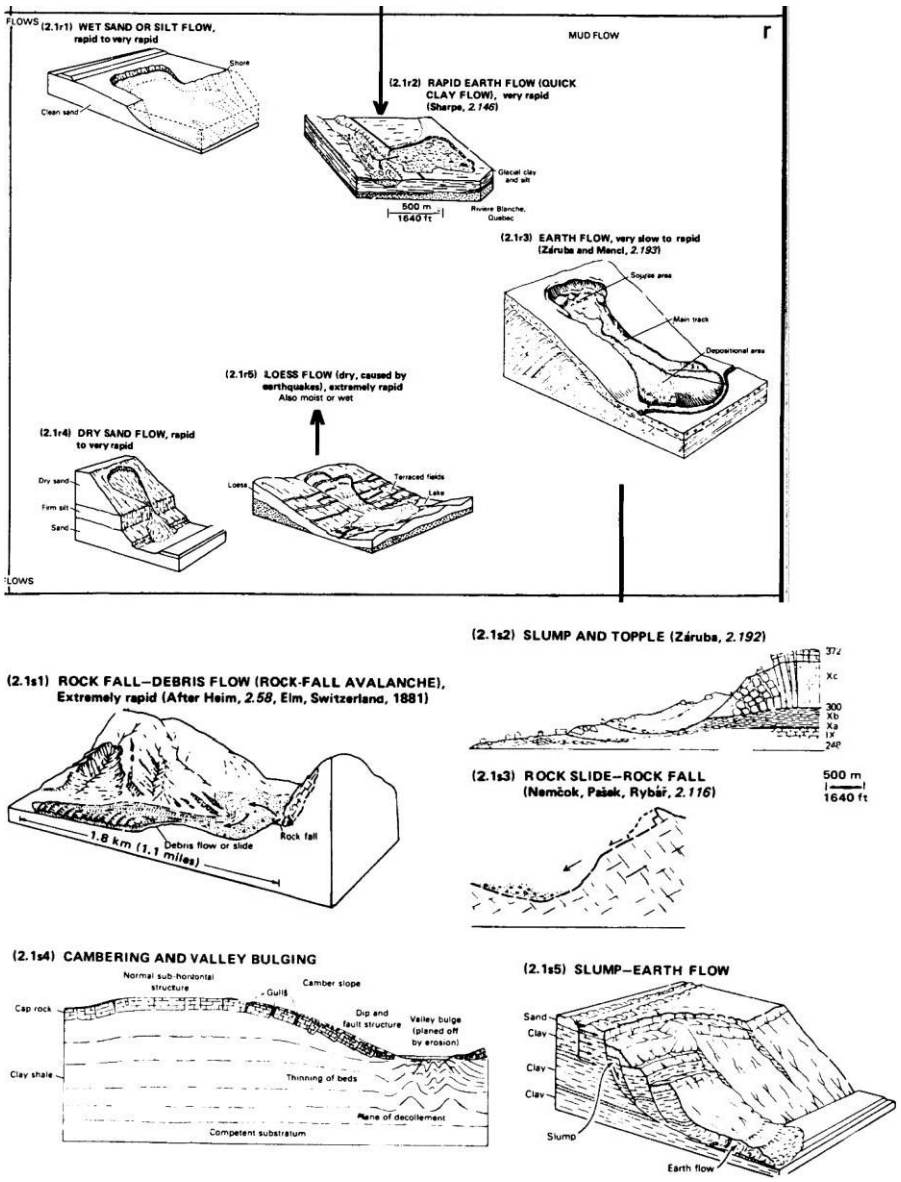

Figure A1-29. Top panels show wet sand and silt, loess, and earthflows and mud flows from 1978. Bottom panels are examples of complex landslides taken from then-recent literature.

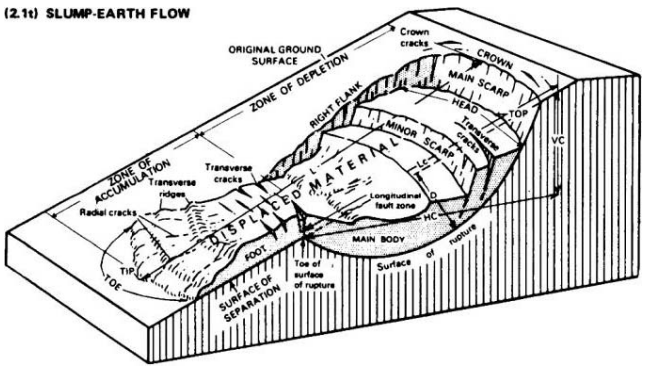

Figure A1-30. In Fig. 2.1t (above) of TRB SR 176, Varnes (1978) selected the descriptive terms "zone of depletion" to denote the area of a landslide within which the displaced material lies below the original ground surface and a corresponding "zone of accumulation" to denote the area of a landslide within which the displaced material lies above the original ground surface. These terms have been in general use since 1978.

Downloaded from http://pubs.geoscienceworld.org/aeg/eeg/article-pdf/31/1/i/6130855/i1558-9161-31-1-i.pdf
by AEG RBAC user

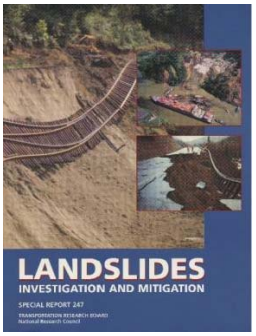


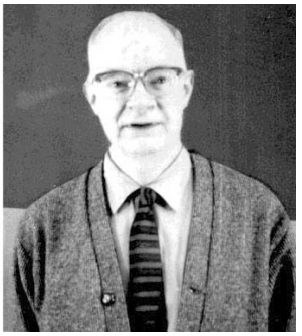

Figure A1-31a. Cover of TRB Special Report 247 (Cruden and Varnes, 1978) released in mid-1996 at a cost of $65.

Figure A1-31b. Professor David M. Cruden of the University of Alberta was a respected advocate for the adoption of international standards for classification, nomenclature for landslide descriptions, standardized reporting, and physical measurements of landslides as some of the established standards that resulted from the International Decade for Natural Hazard Reduction in the 1990s.

Figure A1-31c. David J. Varnes of the USGS was the only contributor to TRB SR 247 (Cruden and Varnes, 1978) who had previously contributed to HRB SR 29 (Varnes, 1958) or TRB SR 176 (Varnes, 1978).

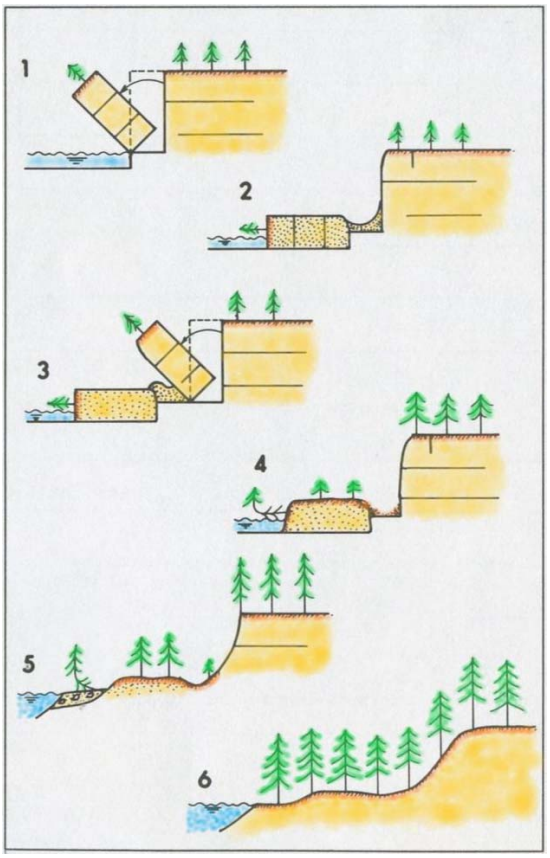

Figure A1-32. Examples of landslide state of activity, in this case, for simple toppling failures (modified from ISSMFE, 1993): (1) an active slope failure, triggered by toe erosion; (2) suspended activity, with local cracking near crown of topple; (3) reactivated, where another block topples over; (4) dormant, where the displaced mass begins to regain tree cover with weathering of exposed scarps; (5) stabilized, where fluvial deposition tends to stabilize the slope toe, and this area starts to recover tree growth; (6) relict activity, reached when the entire area regains a more uniform tree canopy. (7) At each of these stages, there is usually increased weathering of displaced and/or newly exposed materials, depending on the hydrologic regimen.

the most common activity terms are shown in Figure A1-33 and defined below:

(1) advancing landslides are those that are extending their rupture surface in the direction of movement;
(2) if the landslide is extending its rupture surface in the direction opposite of the movement of displaced material, its activity is assumed to be retrogressive; and
(3) if the surface of rupture is widening itself at its lateral margins, its activity is widening.

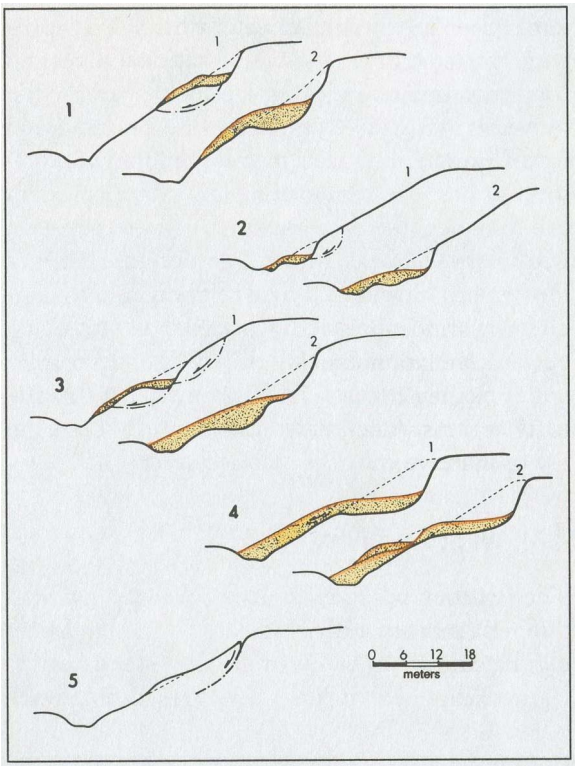

Figure A1-33. Different distributions of landslide activity: (1) advancing, (2) retrogressing, (3) enlarging, (4) diminishing, and (5) confined (modified from ISSMFE, 1993; Cruden and Varnes, 1996).

Downloaded from http://pubs.geoscienceworld.org/aeg/eeg/article-pdf/31/1/i/6130855/i1558-9161-31-1-i.pdf
by AEG RBAC user

Different Styles of Landslide Activity

The style of landslide activity refers to the different kinematic mechanisms that contribute to the landsliding. In 1978, Varnes defined complex landslides as those exhibiting at least two types of movement (e.g., sliding and toppling or slumping and flowage). Figure A1-34 presents examples of complex, composite, and successive landslides, and Figure A-35 shows a typical retrogressive slide.

Single Landslides

Single landslides are those that exhibit only a single sequence of movement of displaced material, often as a semi-intact mass or rotated block of material. For instance, a single block can topple, or there can be multiple toppling events, as sketched in Figure A1-36. Single landslides are unique from other landslide styles because they do not require disruption of the displaced mass or accommodation of independent portions of the slide mass (Cruden and Varnes, 1996).

The kinematics of any landslide is how movement is distributed through the translating mass. It is the most recognized criteria for classification of landslides because it describes the physical processes triggering and then driving mass wasting of earth and rock materials.

The five kinematically distinct types of landslide motion is the sequence fall, topple, slide, spread, and flow (Figure A1-37). Each type of mass wasting event has one or more of these modes of translation providing the input energy to nature's dynamic system of propulsion. Any of these modes can work in unison with another or can recur after long periods of dormancy.

Complex (Rock) Falls

Sturzstroms are dry-flow rockfall avalanche streams that typically exhibit gross volumes >500,000 m^3, and these events are triggered by sudden rockfalls typically >150 m high (Keefer, 1984). This combination of forces appears to reduce interparticle friction through intense vibration of the angular particles against one another (exercising conservation of momentum). This temporary loss of interparticle friction causes the mass to behave like a fluid bereft of any shear strength until the forward velocity drops sufficiently to recover interparticle friction (Van Gassen and Cruden, 1989; Legros, 2002; and Iverson, 2003, 2006). In HRB SR 29 in 1958 and TRB SR 176 in 1978, Varnes called these rockfall avalanches, citing the pioneering work of Albert Heim on the catastrophic 1881 Elm slide in Austria, which Heim published in 1932 (translated by Skermer, 1989).

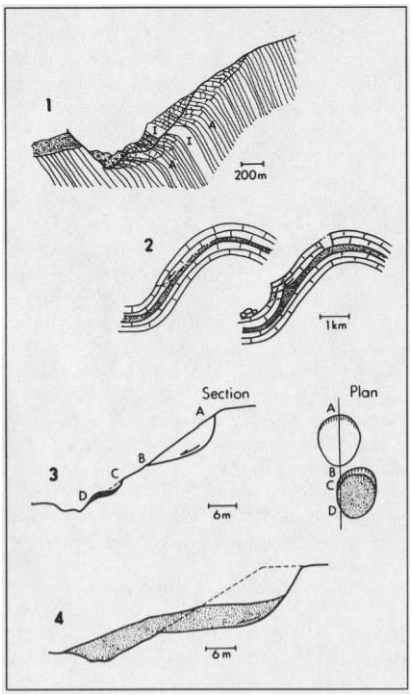

Figure A1-34. More kinematically complicated landslides expressing different styles of activity: (1) A complex slide composed of gneiss (A) and migmatites (I) exhibits a flexural toppling failure triggered by channel incision that was in turn triggered by the topple blocking the channel. As the older alluvium fills the constricted channel, secondary sliding initiates in the toe of the topple by sliding (Giraud et al., 1990). (2) A composite slide has developed on limestone folds sandwiching a shale interbed. When the upper limestone unit slides off the shale bed, it triggers a toppling failure below the toe of the slide (Harrison and Falcon, 1936). (3) A successive landslide (AB) is one triggered by the same mechanism as landslide CD, but it does not share displaced material or rupture surface. (4) An example of a single slide. These are usually characterized by a single sequence of movement without being influenced by adjacent mass wasting or unnatural concentrations of bedrock slide debris.

Only the lowest portion of the slide detached itself and became a fast-moving rockslide avalanche that dammed the Lost Trail Creek channel for more than 1.7 km (Figure A1-38). The profile section in the lower pane suggests that only 20 to 25 percent of the displaced material actually fluidized and achieved an average velocity of approximately 35 m/s. The fluidized portion of the

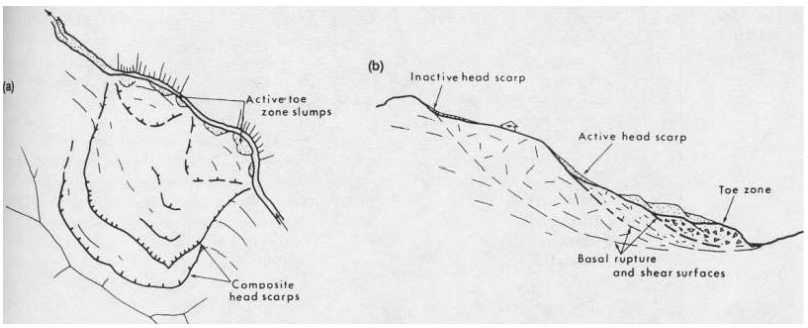

Figure A1-35. Map view and section through a retrogressive multiple rotational slide. Note successive failure surfaces enlarge as they progress upslope (Eisbacher and Clague, 1984).

Downloaded from http://pubs.geoscienceworld.org/aeg/eeg/article-pdf/31/1/i/6130855/i1558-9161-31-1-i.pdf
by AEG RBAC user

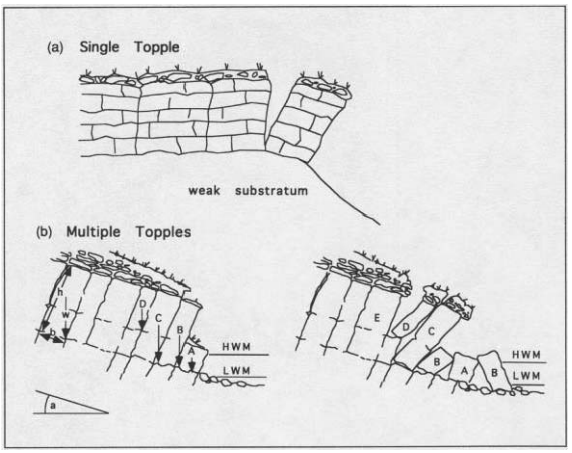

Figure A1-36. Contrast between single topples (a) and multiple topples (b) modified from Varnes (1978) and presented together in Cruden and Varnes (1996).

slide dropped about 427 m and ran approximately 61 m up the opposing slope before coming to a halt.

Modes of Toppling

Modes of toppling are illustrated in Figure A-39 as flexural toppling, complex rock topple-rock slide, and block flexure topple.

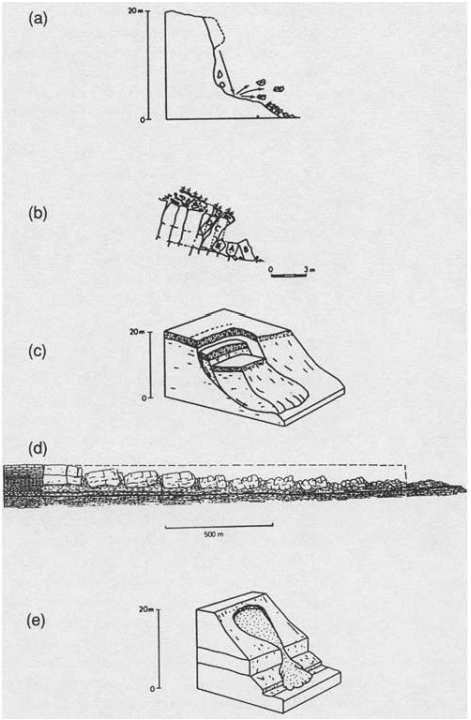

Figure A1-37. Type of movement: (a) a fall; (b) a topple; (c) a slide; (d) a lateral spread; (e) a fluid-like flow.

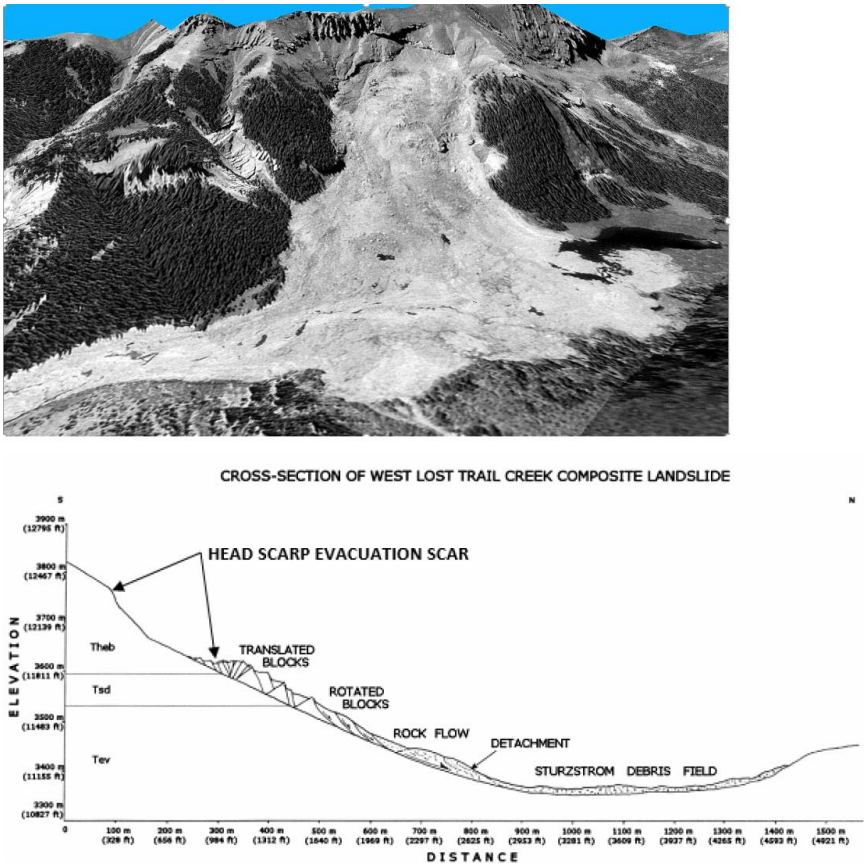

Figure A1-38. A digital image wrap on 10-m-resolution digital elevation model of the July 30, 1991, West Lost Trail Creek composite landslide in the San Juan Mountains, CO (Rogers and Beckmann, 2003).

Downloaded from http://pubs.geoscienceworld.org/aeg/eeg/article-pdf/31/1/i/6130855/i1558-9161-31-1-i.pdf
by AEG RBAC user

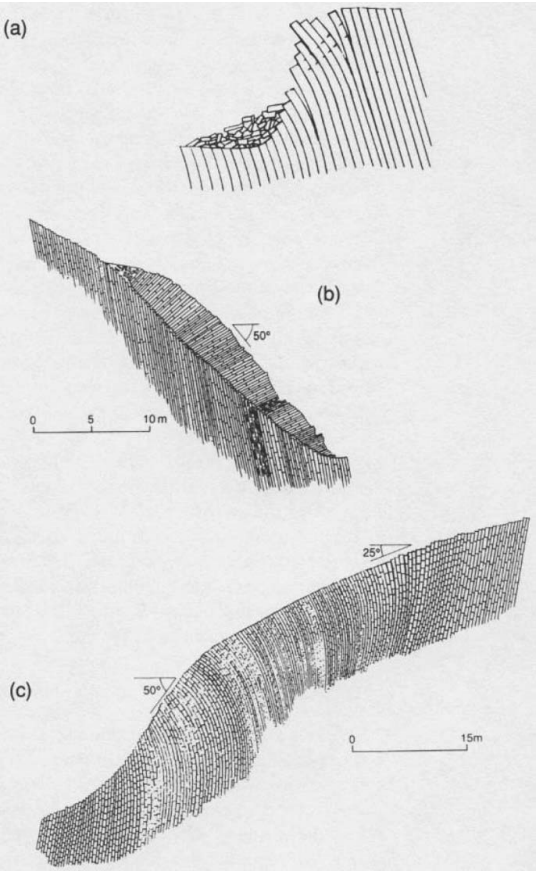

←

Figure A1-39a. Flexural toppling is common in rocks that exhibit a preferred system of discontinuities that are steeply dipping and possess low interface friction between adjacent columns of rock. Flexural toppling occurs most frequently in slates, phyllites, and schist, usually exhibiting back-facing scarps. This is an example of a retrogressive, complex rock topple–rockfall.

Figure A1-39b. An example of a complex rock topple–rockslide that is becoming a translational slide along a "hinge line" forming in response to the accumulated overturning dilation of the cross joints, which will gradually form a basal detachment surface. At some future date, this seam will allow the entire mass to be swept off the mountainside in a catastrophic rockslide.

Figure A1-39c. A typical block flexure topple, common in interbedded sandstones and shales and thin-bedded limestones. As the upper slope begins flexing to the left, it places more lateral load on the lower slope, forcing toppling towards the slope's toe by bending the inclined strata to the left.

Modes of Sliding

In TRB SR 176, David Varnes (1978) made a definite distinction between rotational and translational slides when it came to analyzing their stability and methods of mitigation. Rotational slides are analyzed in two dimensions, typically using the deepest plane of rupture. However, the actual plane of rupture is usually spoon-shaped for a virgin slope failure (Figure A1-5), but this discrepancy is typically overlooked because it is assumed to be conservative. Translational slides usually move along preexisting planar discontinuities with plane strain conditions that often require more sophisticated three-dimensional analyses. Common examples would be linear structures like embankment dams and levees or slot keyways in slide repairs employing mass-grading techniques (Figure A1-40).

Rotational slides typically move along curved rupture surfaces that are concave. If the plane of rupture is a perfect circle (assumes 100 percent of strength derived from clay cohesion and no friction), then the displaced material can be transported without much dilation.

Most planes of basal rupture are log-spiral shaped, with decreasing slope of the slip surfaces (Rendulic, 1936), and the transport mechanism shifts from simple rotation to translation and spreading (with considerable dilation) below the toe of the surface of rupture, as shown in Figure A1-41. For these reasons, most rotational slides are short-lived and remain laterally restricted before being swallowed up in some sort of translational movement or flowage, or other combinations, making it a complex landslide.

The zone of accumulation is usually characterized by obvious disintegration and dilation and fracture porosity that can promote drainage along transverse ridges. The basic observations made by Varnes (1978) of the block kinematics exhibited by rotational slides were reprinted in 1996 and are included here as Figures A1-42 and A1-43. More examples of rotational and translational slides can be found in Figure A1-44.A

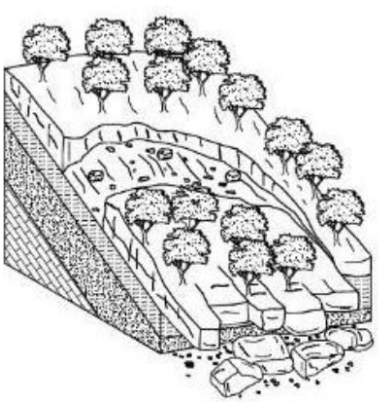

Figure A1-40. Translational failures are usually structurally influenced by preexisting discontinuities such as faults, bedding, foliation, joints, or lithologic contacts. Diagram at left is from Suarez (1998), while photo at right shows the basal rupture surface of the Spillway rockslide of May 1967 on the right abutment of Ruedi Dam in Colorado (J. David Rogers).

Downloaded from http://pubs.geoscienceworld.org/aeg/eeg/article-pdf/31/1/i/6130855/i1558-9161-31-1-i.pdf
by AEG RBAC user

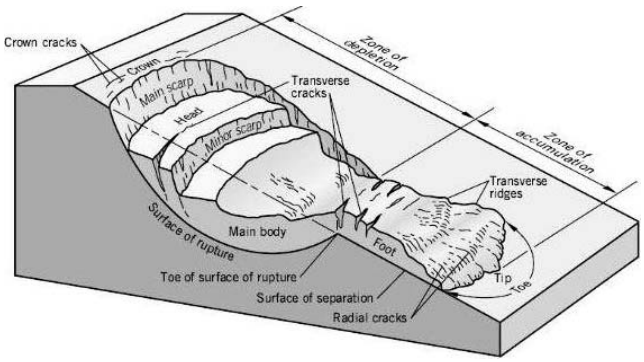

Figure A1-41. Block diagram of a complex earth slide-earthflow (Cornforth, 2005). Note the position of the "toe of surface of rupture" between the zone of depletion and the zone of accumulation (Varnes, 1978). This is where the operative mechanism shifts from rotational slumping to earth-flowage. This shift from rotational slumping to translational sliding makes it a complex landslide.

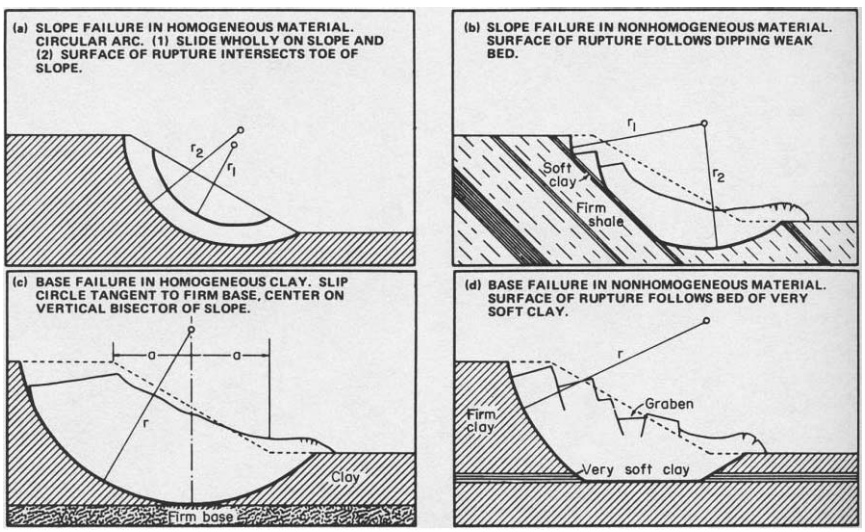

Figure A1-42. Varnes' observations about rotational slumps are valuable in analyzing the operative failure modes and design of mitigation measures.

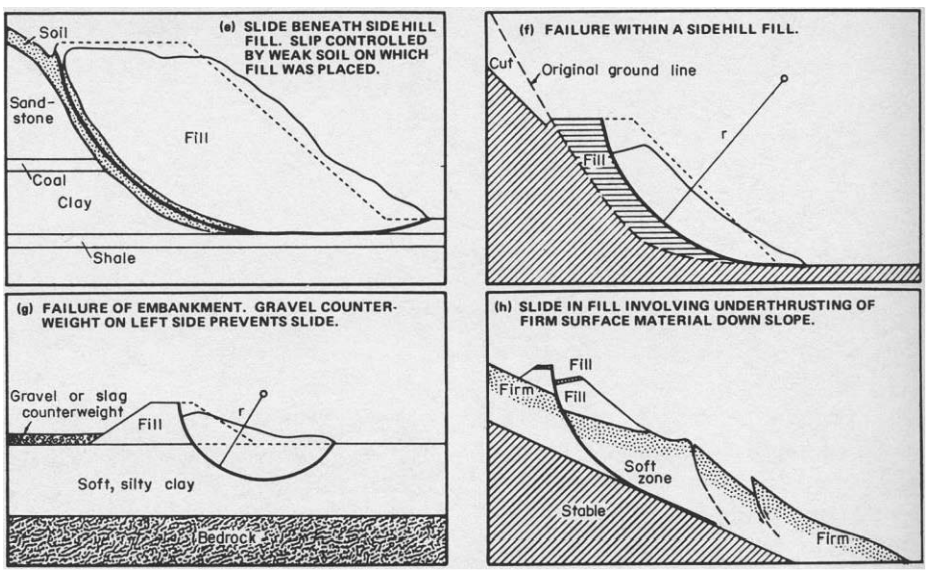

Figure A1-43. Rotational slides most commonly occur in homogeneous materials, so they are most common in engineered fill embankments. Natural materials are seldom uniform, and most rotational slumps are slightly to noticeably asymmetric due to inhomogeneities and discontinuities in the slopes.

Downloaded from http://pubs.geoscienceworld.org/aeg/eeg/article-pdf/31/1/i/6130855/i1558-9161-31-1-i.pdf
by AEG RBAC user

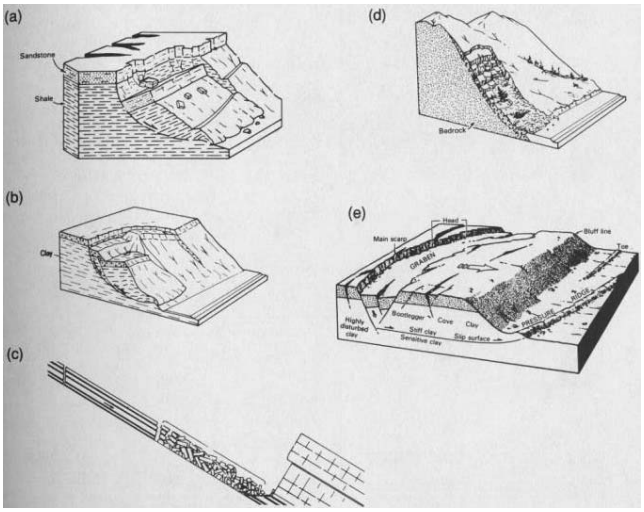

Figure A1-44. More examples of rotational and translational slides: (a) rotational rockslide, (b) rotational earth slides, (c) translational rockslide (upper portion is a block slide), (d) debris slide, (e) translational earth block slide.

Modes of Spreading

There are many modes of spreading or lateral extension without well-defined basal shear surfaces. Most of these features occur where a thick layer of consolidated/cemented material overlies materials subject to plastic deformation, such as silt or clay with access to moisture. Argillaceous materials possess physiochemical attractions to moisture and are subject to seasonal shrinkage and swelling. In outcrops, the shale- or clay-rich beds often exhibit a messy zone of plastic deformation, in large measure because the swelling of clay depends on effective confinement, and the section modulus (stiffness) of shale is usually one or two orders of magnitude lower than the consolidated cap or base formed by clastic units retaining their cementation (usually carbonate). Some typical examples of "strain incompatibility" between wetted shales and clastic horizons are presented in Figure A1-45:

Profile (a) is a creeping block slide on the bank of the Angara River near the Bratsk Dam in Siberia (from Zaruba and Mencl, 1969). The rate of movement in such features is usually very small.

Profile (b) is representative of rock spreads that exhibit obvious lateral extension, but without a well-defined shear surface or zone of plastic flow (from Ostaficzuk, 1973).

Profile (c) is a typical lateral spread triggered by liquefaction or plastic flow within a layer of soft clay in proximity to water-bearing silt and sand layers (from Varnes, 1978).

Various Modes of Flow Slides

Cruden and Varnes (1996) defined a flow as a "spatially continuous movement" in which shear surfaces are "short-lived, closely spaced, and not usually preserved." The distribution of operative velocities in the displaced debris field resembles the features one would expect in a viscous liquid, almost like concrete that suddenly "set up" when the mass came to a halt. The lower boundary (floor) of the debris field may be a thin shear surface that accommodated differential movement or a thick zone of distributed shear. The block diagrams illustrating the examples of flow slides can be found in Fig. A1-47.

Layers of volcanic ash or floods can appear similar. The speed of their deposition has to be inferred. The spongy nature and contrasting soil types and the clods of organic silty peat over clean channel sands shown in Figure A1-46 suggest rapid placement during a short-lived flood event because of the lack of soil mixing and the apparent eddy turbulence.

Debris flows are generally clastic masses devoid of large quantities of cohesive clay fines, and their matrix-supported deposits often show an inverse particle sorting (larger clasts lying over smaller clasts), absence of imbricated layers, and indications of high flow velocities (Fig. A1-48).

Earthflows are much slower because they are usually composed of substantial mixtures of silt and clay. In general, the higher

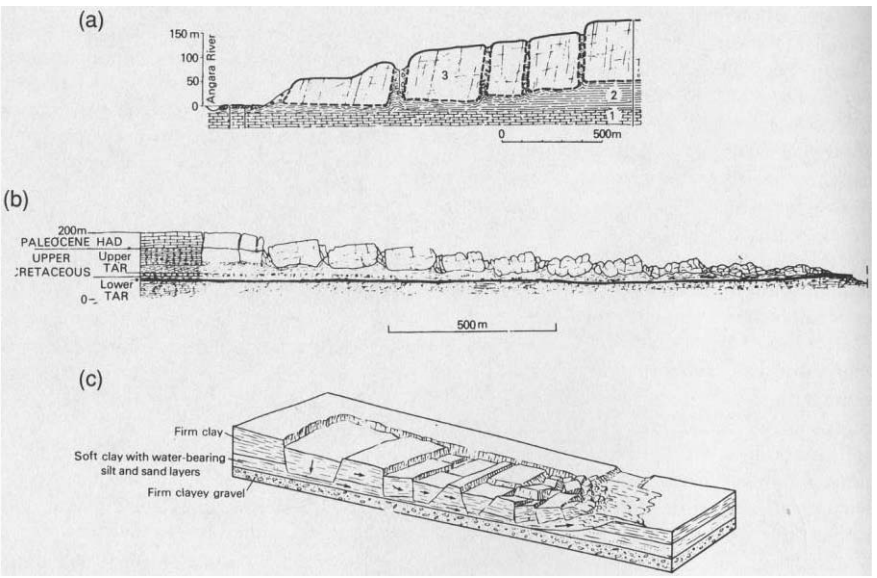

Figure A1-45. (a–c) Profiles and block diagram of rock and earth spreads from Cruden and Varnes (1996).

Downloaded from http://pubs.geoscienceworld.org/aeg/eeg/article-pdf/31/1/i/6130855/i1558-9161-31-1-i.pdf
by AEG RBAC user

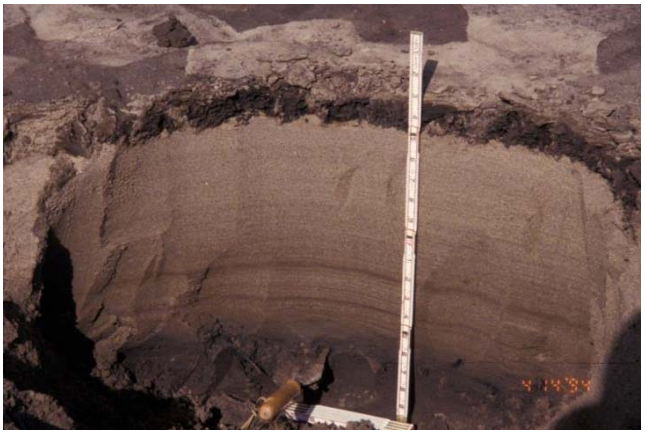

Figure A1-46. Spongy crenulated layer of silty organic clods deposited in a few seconds on a sandy floodplain near Orrick, MO, when an earthen levee collapsed during the Missouri River flood of 1993 (Robert Holmes, USGS).

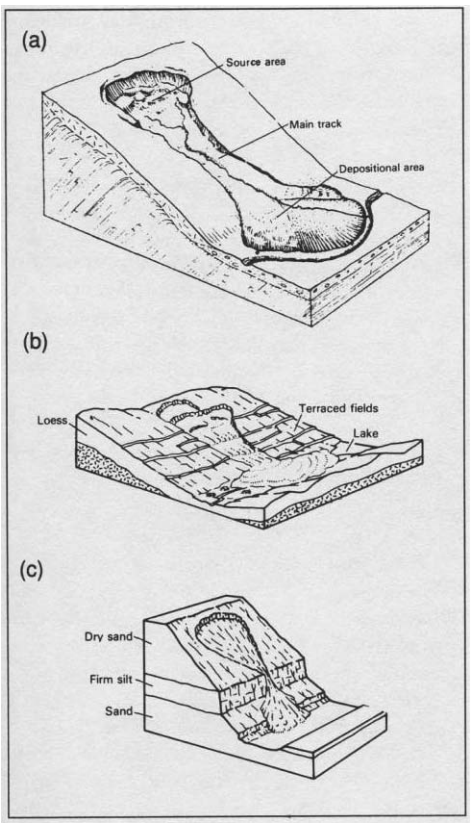

Figure A1-47. Block diagrams illustrating examples of flow slides: (a) slow earth flow, (b) wet loess flow, (c) dry sand flow.

clay content results in slower movement, and the higher soil plasticity creates more resistance to static or earthquake shaking–induced liquefaction.

A block stream is an accumulation of boulders or angular blocks with no fine sizes in the upper part, which is deposited over solid or weathered bedrock, colluvium, or alluvium. Block streams usually occur at the heads of ravines, as narrow bodies, which are more extensive downslope than along the slope (Neuendorf et al., 2005).

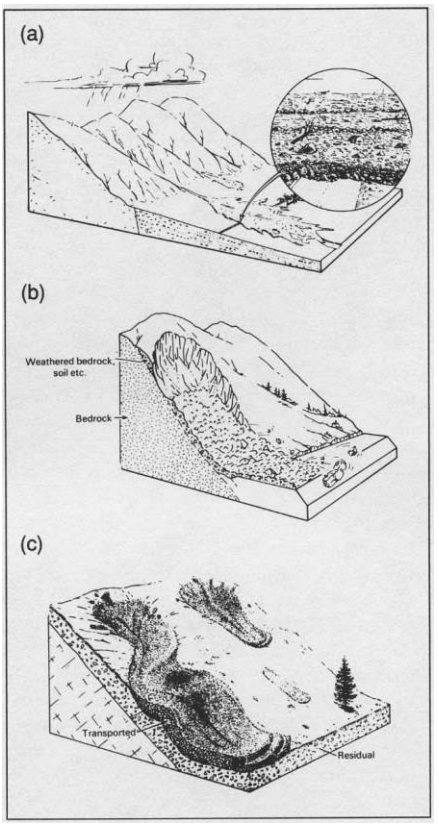

Figure A1-48. Block diagrams illustrating examples of channelized debris flows: (a) classic debris flow, (b) debris avalanche, (c) block stream.

Review of the Classification of Landslides of the Flow Type (2001)

In the August 2001 issue of *Environmental & Engineering Geoscience*, Oldrich Hungr and Michael J. Bovis of the University of British Columbia, Stephen G. Evans of the Geological Survey of Canada, and John N. Hutchinson of Imperial College in London (Figure A1-49) co-authored a very practical article titled "A Review of the Classification of Landslides of the Flow Type," which won the 2001 Association of Environmental & Engineering Geologists Publication Award.

John Hutchinson had previously written influential articles on allied subjects, such as "General Report: Morphological and Geotechnical Parameters of Landslides in Relation to Geology and Hydrogeology" for the Fifth International Symposium on Landslides in Lausanne, Switzerland, in 1988. This was a significant contribution in understanding how the physical processes of mass wasting can be influenced by an array of factors that can shift and change with time, causing a slope to become less or more stable. It also demonstrated that significant professional judgement was involved, especially in estimating operative pore-water pressure values at the time of failure.

The authors pointed out that engineering geologists had grown used to using an array of colloquial terms such as "debris flow," "debris avalanche," and "mudslide." They proposed that more precision should be exercised in the selection of terms that would be less arbitrary, such as threshold values presented by Varnes (1978) of >1.5 m/d for "rapid flow" and <1.5 m/d for "less than rapid" flow,

Downloaded from http://pubs.geoscienceworld.org/aeg/eeg/article-pdf/31/1/i/6130855/i1558-9161-31-1-i.pdf
by AEG RBAC user

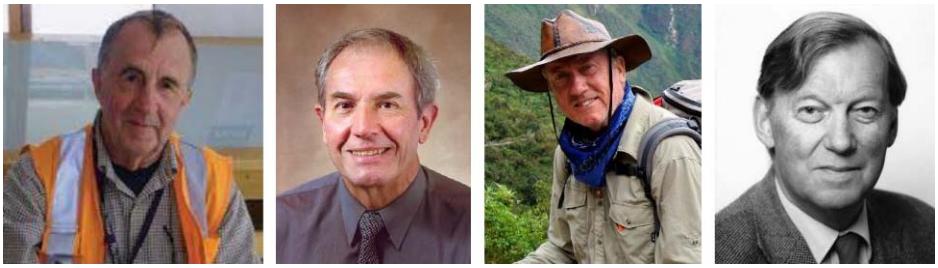

Figure A1-49. Oldrich Hungr (https://give.ubc.ca/memorial/oldrich-hungr/), Michael J. Bovis (https://geog.ubc.ca/profile/michael-bovis/), Stephen G. Evans (https://uwaterloo.ca/earth-environmental-sciences/profile/sgevans), and John N. Hutchinson (https://www.geolsoc.org.uk/en/About/History/Obituaries%202001%20onwards/Obituaries%202011/John%20Neville%20Hutchinson%201926%202011).

Table 1. *Key terms for mass movement in the "flows" category according to Varnes (1978).*

Rate of Movement	Bedrock	Debris (<80% Sand and Finer)	Earth (>80% Sand and Finer)
rapid and higher (>1.5 m/day)	rock flow (creep, slope sagging)	debris flow debris avalanche	wet sand and silt flow rapid earth flow loess flow dry sand flow
less then rapid (<1.5 m/day)		solifluction soil creep block stream	earth flow

Table 2. *Landslide velocity scale (Cruden and Varnes, 1996).*

Velocity class	Description	Velocity (m/sec)	Typical velocity
7	Extremely Rapid	5	5 m/sec
6	Very Rapid	0.05	3 m/min
5	Rapid	5×10^{-4}	1.8 m/hr
4	Moderate	5×10^{-6}	13 m/month
3	Slow	5×10^{-8}	1.6 m/year
2	Very Slow	5×10^{-10}	16 mm/year
1	Extremely Slow		

Figure A1-50. More precise key terms for flows.

summarized in the article's Table 1 (above) and Table 2 (below) (see Figure A1-50 for reproductions of these tables).

For descriptions of earthflows, debris flows, and mudflows, Hungr et al. (2001) cited this ternary diagram (Figure A1-51), which charts the respective percentages of silt and clay, sand, and gravel of three kinds of matrix source areas: (1) non-volcanic debris, (2) volcanic debris flows, and (3) earthflows.

Figure A1-52 from Pierson (1986) illustrates how different physical processes occur simultaneously within most flow slides. Geoscientists and geoengineers tend to focus on the boulder front and head of a debris flow in a confined bedrock channel because this feature is the most destructive and often leads to debris avulsion when encountering flow obstructions at culverts or bridges.

In Table 3 of the 2001 article (reproduced here in Figure A1-53), the authors proposed a new division of landslides of the flow type based on genetic and morphological aspects rather than the grain-size thresholds proposed by Varnes (1978). Their new basic material groups included the sorted materials gravel, sand, silt, and clay, and the unsorted materials composed of debris, earth and mud, peat, and rock.

In Table 4 of the 2001 article (reproduced here in Figure A1-54), the authors recommended input descriptions of six variables:

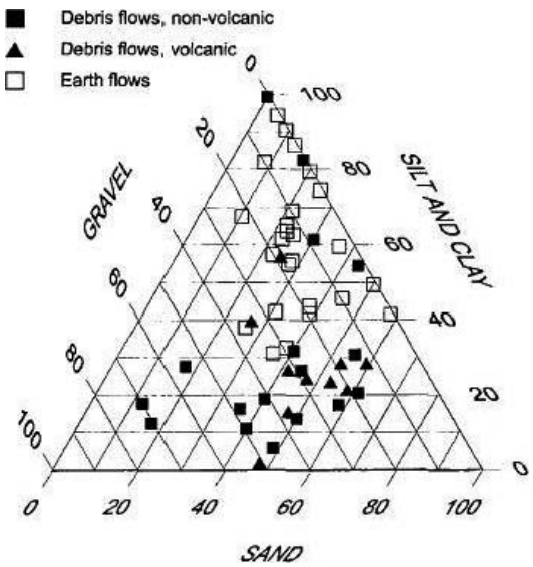

Figure A1-51. Ternary diagram.

Downloaded from http://pubs.geoscienceworld.org/aeg/eeg/article-pdf/31/1/i/6130855/i1558-9161-31-1-i.pdf
by AEG RBAC user

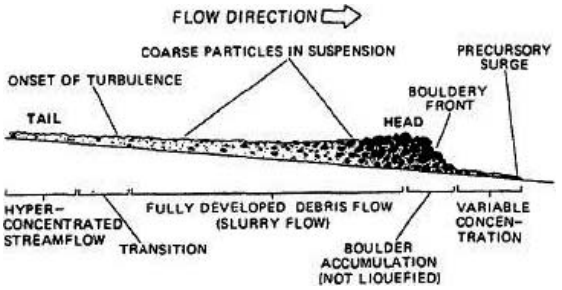

Figure A1-52. Simultaneous physical processes within flow slides.

material, water content, special conditions, velocity, and name. Hungr et al. (2001) also proposed definitions for relatively slow-moving flow mixtures, such as non-liquefied sand or gravel flows; extremely rapid sand, silt, or debris-flow slides accompanied by liquefaction; clay-flow slides involving sensitive clay and peat flows; slow to rapid earthflows in non-sensitive plastic clays; debris flows that occur in steep established channels or gullies; cohesive mudflows that should be re-branded as cohesive debris flows; debris floods capable of transporting massive volumes of sediment in slurries; massive sediment transport with limited discharge (as often occur in one watershed, but not in subjacent watersheds); and debris avalanches and rock avalanches resulting from large volumes of rock being disaggregated by traumatic

Table 3. *Material involved in landslides of the flow type.*

Origin	Character	Condition[1]	Name
SORTED (marine, lacustrine, fluvial, eolian, volcanic, anthropogenic)	Non-cohesive (Plastic Limit < 5%)	Dry or Saturated	- Gravel - Sand - Silt
	Cohesive (Plastic Limit > 5%)	- Plastic (I_L< 0.5) - Liquid (I_L> 0.5)	- Clay - Sensitive Clay
UNSORTED (residual, colluvial, glacial, volcanic, anthropogenic)	Non-cohesive (Plastic Limit < 5%)	Dry or Saturated	- Debris[2]
	Cohesive (Plastic Limit < 5%)	- Plastic (I_L< 0.5) - Liquid (I_L> 0.5)	- Earth - Mud
PEAT	Organic	Saturated	- Peat
ROCK	Fragmented	Dry or Saturated	- Rock

Figure A1-53. New division of flow-type landslides.

Table 4. *Classification of landslides of the flow type.*

Material	Water Content[1]	Special Condition	Velocity	Name
Silt, Sand, Gravel, Debris (talus)	dry, moist or saturated	- no excess pore-pressure, - limited volume	various	Non-liquefied sand (silt, gravel, debris) flow
Silt, Sand, Debris, Weak rock[2]	saturated at rupture surface content	- liquefiable material[3], - constant water	Ex. Rapid	Sand (silt, debris, rock) flow slide
Sensitive clay	at or above liquid limit	- liquefaction *in situ*,[3] - constant water content[4]	Ex. Rapid	Clay flow slide
Peat	saturated	- excess pore-pressure	Slow to very rapid	Peat flow
Clay or Earth	near plastic limit	- slow movements, - plug flow (sliding)	< Rapid	Earth flow
Debris	saturated	- established channel[5], - increased water content[4]	Ex. Rapid	Debris flow
Mud	at or above liquid limit	-fine-grained debris flow	> Very rapid	Mud flow
Debris	free water present	- flood[6]	Ex. Rapid	Debris flood
Debris	partly or fully saturated	- no established channel[5], - relatively shallow, steep source	Ex. Rapid	Debris avalanche
Fragmented Rock	various, mainly dry	- intact rock at source, - large volume[7]	Ex. Rapid	Rock avalanche

Figure A1-54. Descriptions of the six variables.

Downloaded from http://pubs.geoscienceworld.org/aeg/eeg/article-pdf/31/1/i/6130855/i1558-9161-31-1-i.pdf
by AEG RBAC user

impact and helical mixing at the snout of a large mass moving at a relatively high velocity.

Proposed Update of the Varnes Classification of Landslide Types (2014)

In 2014, landslide researchers and respected Professors Oldrich Hungr of the Department of Earth & Ocean Sciences at the University of British Columbia, Professor Serge Leroueil of the Department of Civil and Water Engineering at Université Laval in Quebec, Canada, and Professor Luciano Picarelli in the Department of Civil Engineering, Design, Construction, and Environment at the Università della Campania in Naples, Italy, published a recommendation in the journal *Landslides* (Figure A1-55) to modify the engineering geologic definition of landslide-forming materials to be more in step with accepted geotechnical and geological terminology. In 2015, it was recognized as the best paper published in the journal *Landslides* for the previous year.

Several important suggestions were described, which had resulted from advances in understanding of the transitions to which landslide debris is normally subjected as it is transported over significant distances. Many of these changes in rheology are a result of behavioral changes in cohesion and cementation, absorption of moisture, volumetric dilation, etc., as the materials are transported and deposited elsewhere.

Table 1 from Hungr et al. (2014) (reproduced here in Figure A1-56) summarizes Varnes' classification system established in 1978 for TRB SR 176. This assumed six fundamental types of movement: fall, topple, slumps, rotational sliding, lateral spreading, and flows.

Note the tradition of acknowledging three fundamental materials: rock, debris, and earth. The relative proportions of these materials can shift and change dramatically as the natural materials are disaggregated by tortuous dynamic forces, such as helical mixing going around channel bends or blunt trauma accompanying sudden detachments from weathered escarpments or slamming into the opposing slope of an incised canyon.

A few examples of complete disintegration are shown in Figure A1-57 (coastal bluff failure in Santa Monica, CA, in 1951 and a recent collapse of the White Cliffs near Dover, England, in March 2012). Rock cleaves and initially fractures under induced tension, when blocks crash into one another or become unconstrained in a particular axis due to sudden removal of lateral and subjacent support.

It only takes a few minutes of turbulent mixing to disaggregate a large volume of material, such as the 200 rockslide avalanches triggered during the Great Alaskan Earthquake of 1964. We must conclude that the operative mechanisms to change seemingly intact bedrock to a neat gravel pile are not unusual happenstance. So, we could expect to see an initial rockfall quickly transition into a rock topple or a debris slump, followed by a debris slide, all during the "same mass-wasting event."

When one observes these movements, it is easier to visualize how most bedrock slides are complex and/or composite slides, depending on when and where we are observing them. Like in rotational slump-earthflows, there is usually more than one type of movement if we observe the failure sequence in its entirety. This

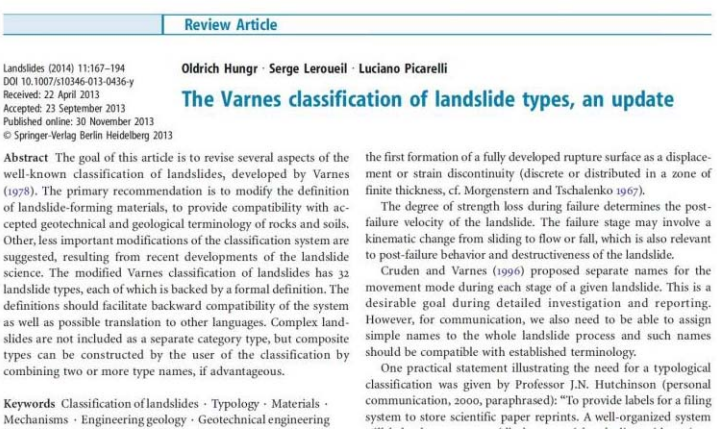

Review Article

Landslides (2014) 11:167–194
DOI 10.1007/s10346-013-0436-y
Received: 22 April 2013
Accepted: 23 September 2013
Published online: 30 November 2013
© Springer-Verlag Berlin Heidelberg 2013

Oldrich Hungr · Serge Leroueil · Luciano Picarelli

The Varnes classification of landslide types, an update

Abstract The goal of this article is to revise several aspects of the well-known classification of landslides, developed by Varnes (1978). The primary recommendation is to modify the definition of landslide-forming materials, to provide compatibility with accepted geotechnical and geological terminology of rocks and soils. Other, less important modifications of the classification system are suggested, resulting from recent developments of the landslide science. The modified Varnes classification of landslides has 32 landslide types, each of which is backed by a formal definition. The definitions should facilitate backward compatibility of the system as well as possible translation to other languages. Complex landslides are not included as a separate category type, but composite types can be constructed by the user of the classification by combining two or more type names, if advantageous.

Keywords Classification of landslides · Typology · Materials · Mechanisms · Engineering geology · Geotechnical engineering

the first formation of a fully developed rupture surface as a displacement or strain discontinuity (discrete or distributed in a zone of finite thickness, cf. Morgenstern and Tschalenko 1967).

The degree of strength loss during failure determines the post-failure velocity of the landslide. The failure stage may involve a kinematic change from sliding to flow or fall, which is also relevant to post-failure behavior and destructiveness of the landslide.

Cruden and Varnes (1996) proposed separate names for the movement mode during each stage of a given landslide. This is a desirable goal during detailed investigation and reporting. However, for communication, we also need to be able to assign simple names to the whole landslide process and such names should be compatible with established terminology.

One practical statement illustrating the need for a typological classification was given by Professor J.N. Hutchinson (personal communication, 2000, paraphrased): "To provide labels for a filing system to store scientific paper reprints. A well-organized system

Figure A1-55. (above) Oldrich Hungr, Serge Leroueil, and Luciano Picarelli and (below) excerpt from the first page of their 2014 article (Hungr et al., 2014).

Downloaded from http://pubs.geoscienceworld.org/aeg/eeg/article-pdf/31/1/i/6130855/i1558-9161-31-1-i.pdf
by AEG RBAC user

Movement type	Rock	Debris	Earth
Fall	1. Rock fall	2. Debris fall	3. Earth fall
Topple	4. Rock topple	5. Debris topple	6. Earth topple
Rotational sliding	7. Rock slump	8. Debris slump	9. Earth slump
Translational sliding	10. Block slide	11. Debris slide	12. Earth slide
Lateral spreading	13. Rock spread	–	14. Earth spread
Flow	15. Rock creep	16. Talus flow	21. Dry sand flow
		17. Debris flow	22. Wet sand flow
		18. Debris avalanche	23. Quick clay flow
		19. Solifluction	24. Earth flow
		20. Soil creep	25. Rapid earth flow
			26. Loess flow
Complex	27. Rock slide-debris avalanche	28. Cambering, valley bulging	29. Earth slump-earth flow

Figure A1-56. Table 1 from Hungr et al. (2014) summarizes Varnes' classification system established in 1978 for TRB SR 176 (Schuster and Krizek, 1978). This assumed six fundamental types of movement: fall, topple, slumps, rotational sliding, lateral spreading, and flows.

Figure A1-57. Examples of how natural processes of weathering, erosion, and mass wasting can grind up and disaggregate consolidated bedrock into loose particles bereft of any appreciable cohesion in a manner of seconds (left, Corbis via Getty Images-USC; right, AGU Blogosphere. Federal Housing Administration).

realization can be seen by viewing videotapes of embankment failures (like levees or earth dams) and slope failures on natural slopes.

So, everyone who works with landslides probably agrees that the operative material properties can change significantly during a mass-wasting event, but we cannot always predict when these things will occur, unless we have a significant amount of instrumentation (like the creep measurements preceding the reactivation of the dormant Monte Toc Landslide into Vaiont Reservoir in October 1963).

Hungr et al. (2014) also advanced the case for establishing a landslide velocity scale (their Table 2; reproduced here in Figure A1-58). This was long overdue and very much needed in establishing meaningful databases from which to validate dynamic evaluations. Anyone can videotape a fast-moving flow slide with their smart phone. Velocity scales are long overdue.

Velocity class	Description	Velocity (mm/s)	Typical velocity	Response[a]
7	Extremely rapid	5×10^{3}	5 m/s	Nil
6	Very rapid	5×10^{1}	3 m/min	Nil
5	Rapid	5×10^{-1}	1.8 m/h	Evacuation
4	Moderate	5×10^{-3}	13 m/month	Evacuation
3	Slow	5×10^{-5}	1.6 m/year	Maintenance
2	Very slow	5×10^{-7}	16 mm/year	Maintenance
1	Extremely Slow			Nil

Figure A1-58. Recommended landslide velocity scale (Table 2 from Hungr et al., 2014).

Downloaded from http://pubs.geoscienceworld.org/aeg/eeg/article-pdf/31/1/i/6130855/i1558-9161-31-1-i.pdf
by AEG RBAC user

This landslide velocity scale (Figure A1-59) was initially proposed in 1995–96 (IGS-UNESCO WP/WLI, 1995; and by Cruden and Varnes, 1996).

Figure A1-60 reproduces Table 3 from Hungr et al. (2014), which summarizes the suggested landslide-forming material types.

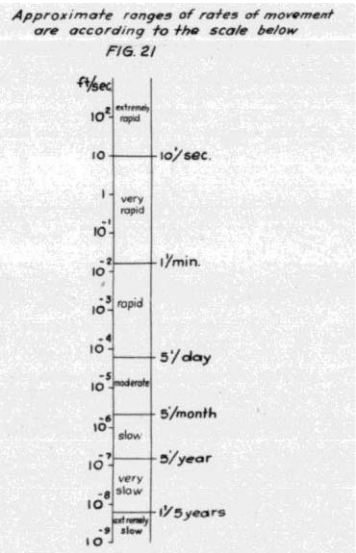

Figure A1-59. It is of some interest to note that similar ranges in the velocity of slides have been advanced by the various HRB-TRB committees dating back to their earliest days, almost 70 years ago. While constructing their 1953 questionnaire, the HRB Committee on Landslides included seven descriptors or suggested modifiers based on average velocities of movement. These were included on Plate 1 of the 1953 HRB Landslide Committee's questionnaire (shown at left), and later reproduced on Plate 1 of HRB SR 29 in 1958 (Eckel, 1958) and in oversize Figure 2.1 of TRB SR 176 in 1978 (Schuster and Krizek, 1978). Note how the rates of movement scale vary between "extremely slow" (10^{-9} ft/s, $3.05*10^{-11}$ m/s), which is about 1 ft in 5 years, up to "extremely rapid" (10^{2} ft/s or 100 ft/s [about 68 mph, or 30.48m/s]). The landslide velocity scale proposed in Table 2 of Hungr et al. (2014) is similar, with their "extremely rapid" threshold >16.4 ft/s (5 m/s or 11 mph).

The first column of Table 3 presents common material names: (1) rock, (2) clay, (3) mud, (4) silt, sand, gravel, and boulders, (5) debris, (6) peat, and (7) ice. These terms were intended to replace the threefold material classes proposed by Varnes (rock, debris, soil).

Physical characteristics listed in the second column were intended to serve as "supplementary terms" or "textural classes." Two terms could be applied to any situation, with the more important aspect mentioned before another that is subordinate.

The term "debris" is rather over-used in relation to mass wasting. It tends to be a catch-all term for mixtures of sand, gravel, cobbles, and boulders, with varying proportions of silt, clay, and organic matter. Debris has also been used to connote any material displaced or transported by landslides or debris flows, exclusive of alluvial flow.

The authors pointed out that Varnes' somewhat arbitrary criterion for "debris" was any material containing more than 20 percent fraction coarser than sand. The particle diameters of medium-grained sands lie between 0.425 mm (#40 sieve) and 1.18 mm (#16 sieve). Hungr et al. (2014) felt this figure was "probably too restrictive," in so far that it could be applied to either plastic or non-plastic materials. They argued that the term "mud" should be applied to remolded mixed clayey soils in which the matrix (sand and finer fraction) exhibits a plasticity index >5 percent and in which the liquidity index (I_p) is >0.5 (close to a liquid state).

Hungr et al. (2014) did not say how they would obtain such samples, only that the conversion of desiccated cohesive soil at a dormant landslide, where the transformation would necessitate "rapid mixing with surface water" and "increase in porosity," is a combination that is "seldom available in nature" (likely along ephemeral channels of some sort).

The descriptive term "earth" does not have an established meaning in geologic or geotechnical description schemes. However, "earthflows" connote a semi-cohesive mass of plastic soils in which the liquidity index (I_p) is <0.5. For material with higher clay content, the material flows slower.

Hungr et al. (2014) also noted that Sharpe (1938b) included ice as a landslide-forming material, likely because of the latter's field observations made in Canada during his landslide reconnaissance field trips in the 1930s (describer earlier). Hungr et al. (2014) felt that ice and snow should be added to the list of landslide-forming materials because they aid in soil saturation, which is an important trigger for the rapid velocity of several types of landslides.

Material name	Character descriptors (if important)	Simplified field description for the purposes of classification	Corresponding unified soil classes	Laboratory indices (if available)
Rock	Strong	Strong—broken with a hammer		UCS>25 MPa
	Weak	Weak—peeled with a knife		2<UCS<25 MPa
Clay	Stiff	Plastic, can be molded into standard thread when moist, has dry strength	GC, SC, CL, MH, CH, OL, and OH	I_p> 0.05
	Soft			
	Sensitive			
Mud	Liquid	Plastic, unsorted remolded, and close to Liquid Limit	CL, CH, and CM	I_p>0.05 and I_l>0.5
Silt, sand, gravel, and boulders	Dry	Nonplastic (or very low plasticity), granular, sorted. Silt particles cannot be seen by eye	ML	I_p<0.05
	Saturated		SW, SP, and SM	
	Partly saturated		GW, GP, and GM	
Debris	Dry	Low plasticity, unsorted and mixed	SW-GW	I_p<0.05
	Saturated		SM-GM	
	Partly saturated		CL, CH, and CM	
Peat		Organic		
Ice		Glacier		

Figure A1-60. Landslide material forming types (Table 3 from Hungr et al., 2014).

Downloaded from http://pubs.geoscienceworld.org/aeg/eeg/article-pdf/31/1/i/6130855/i1558-9161-31-1-i.pdf
by AEG RBAC user

Figure A1-61 is an excerpt from that table, which presents supplementary material terms based on geomorphic analyses (Table 4 of Hungr et al., 2014). These include the most common soil and rock materials normally observed to be comprising much of the landslide debris. Some of the argillaceous materials are often susceptible to slaking, so they tend to lose mass as they disintegrate into smaller pieces and particles, which are usually more soil-like, often comprised of saprolites.

Here, we list some examples of the ways in which assumed supplementary terms could be applied to the names of some common types of landslides using the assumed supplementary/modifier terms that Hungr et al. suggested in their 2014 article (shown within parentheses).

Examples of landslide names with assumed supplementary terms:

- Debris slide (residual soil)
- Rock compound slide (weak sedimentary rock)
- Silt flowslide (eolian silt)
- Clay rotational slide (soft lacustrine clay)
- Clay flowslide (sensitive marine clay)
- Earthflow
- Sand flow (dry fluvial sand)
- Debris flow
- Mudflow
- Debris avalanche (volcaniclastic debris)
- Rock avalanche (strong igneous rock)

Proposed Definitions of Landslide Types

In their 2014 article, Hungr et al. indicated that their suggestions were based on those of Varnes (1978), Hutchinson (1988), and Hungr et al. (2001). They also acknowledged a group of supplementary terms proposed by Cruden and Varnes (1996) that describe post-failure activity of the landslide. These included the terms "reactivated," "dormant," and "relict."

The recommendations proposed would increase the number of landslide types that would be formally defined from 29 to 32 types. The 32 types of landslides were listed in Table 5 by Hungr et al. in their 2014 article in the journal *Landslides* (reproduced here as Figure A1-62).

Some examples of the proposed landslide type classes (from Hungr et al., 2014) are shown in Figure A1-63.

Figure A1-64 shows the slow spreading of sandstone blocks due to deep deformation of a weak shale substrate underlain by phyllite, in Prague, Czech Republic (Zaruba and Mencl, 1969).

Translational and rotational slides are shown in Figure A1-65, and ridge-top spreading on Mission Ridge, southern British Columbia, Canada, is shown in Figure A1-66.

Rock	Intrusive, volcanic, metamorphic, strong sedimentary, (carbonatic or arenaceous) and weak sedimentary (argillaceous)
Soil	Residual, colluvial, alluvial, lacustrine, marine, aeolian, glacial, volcanic, organic, random anthropogenic fills, engineered anthropogenic fills, mine tailings, and sanitary waste

Figure A1-61. Supplementary material terms based on geomorphological analysis (Table 4 from Hungr et al., 2014).

Type of movement	Rock	Soil
Fall	1. *Rock/ice* fall[a]	2. *Boulder/debris/silt* fall[a]
Topple	3. Rock block topple[a]	5. *Gravel/sand/silt* topple[a]
	4. Rock flexural topple	
Slide	6. Rock rotational slide	11. *Clay/silt* rotational slide
	7. Rock planar slide[a]	12. *Clay/silt* planar slide
	8. Rock wedge slide[a]	13. *Gravel/sand/debris* slide[a]
	9. Rock compound slide	14. *Clay/silt* compound slide
	10. Rock irregular slide[a]	
Spread	15. Rock slope spread	16. *Sand/silt* liquefaction spread[a]
		17. Sensitive clay spread[a]
Flow	18. *Rock/ice* avalanche[a]	19. *Sand/silt/debris* dry flow
		20. *Sand/silt/debris* flowslide[a]
		21. Sensitive clay flowslide[a]
		22. Debris flow[a]
		23. Mud flow[a]
		24. Debris flood
		25. Debris avalanche[a]
		26. Earthflow
		27. Peat flow
Slope deformation	28. Mountain slope deformation	30. Soil slope deformation
	29. Rock slope deformation	31. Soil creep
		32. Solifluction

For formal definitions of the landslide types, see text of the paper.

[a] Movement types that usually reach extremely rapid velocities as defined by Cruden and Varnes (1996). The other landslide types are most often (but not always) extremely slow to very rapid

Figure A1-62. Summary of the proposed version of Varnes' landslide type classes in use since 1978 (Table 5 from Hungr et al., 2014).

Downloaded from http://pubs.geoscienceworld.org/aeg/eeg/article-pdf/31/1/i/6130855/i1558-9161-31-1-i.pdf
by AEG RBAC user

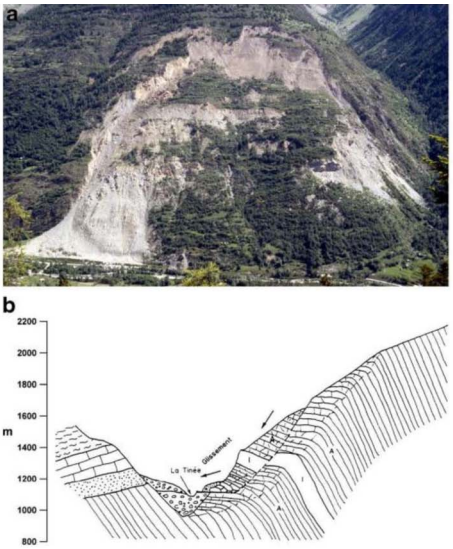

Fig. 5 a Large flexural topple, in the process of converting into a rotational slide. La Clapiére, France (photo, O. Hungr). b Schematic cross-section of the Clapiére flexural topple by Follacci (1987). A micaceous gneiss, I quartzitic gneiss

Large flexural toppling failure beginning to transition into a rotational slide.

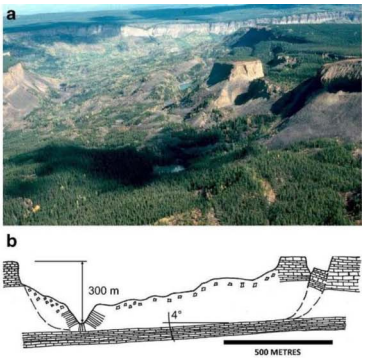

Fig. 9 a A compound slide in Cretaceous shale, Liard Plateau, British Columbia. b Schematic cross-section (Gerath and Hungr 1993). The valley is an ancient meltwater channel, occupied by a grossly underfit stream

Compound slide in Cretaceous shale on Liard Plateau in British Columbia, Canada

Figure A1-63. Examples of proposed landslide type classes (Figures 5 and 9 from Hungr et al., 2014).

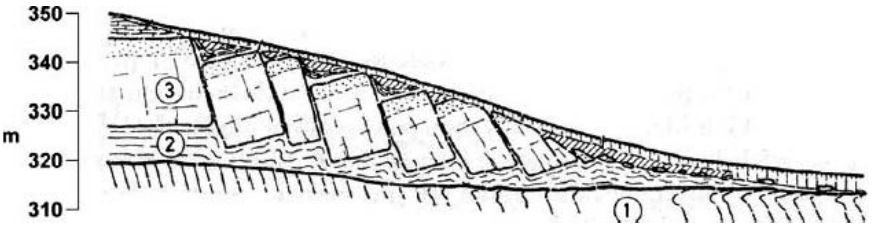

Figure A1-64. Slow spreading of sandstone block (Zaruba and Mencl, 1969).

Figure A1-65a. Translational slide on Tertiary clay shale in northern Italy.

Figure A1-65b. Rotational slide in Cretaceous shale along Liard Plateau in Canada.

Downloaded from http://pubs.geoscienceworld.org/aeg/eeg/article-pdf/31/1/i/6130855/i1558-9161-31-1-i.pdf
by AEG RBAC user

Figure A1-66. Ridge-top spreading on Mission Ridge, southern British Columbia, Canada.

Figure A1-67 shows lateral spreads triggered by multiple retrogressive compound sliding of glacio-lacustrine clay over Cretaceous shale with bentonite seams.

Figure A1-68 shows debris avalanches and debris flows.

Figure A1-69 shows a compound slide in glacio-lacustrine deposits, Churn Creek, Interior British Columbia. Note the plethora of internal scarps in normal and anti-slope inclinations, suggestive of toppling drag or seasonal thawing of the upper few meters (slide is 1 km wide).

Figure A1-70 shows multiple retrogressive flow slides in ice-rich permafrost (known as a "thaw flow"), Mackenzie Region, Northwest Territories, Canada.

Figure A1-71 shows a rock avalanche.

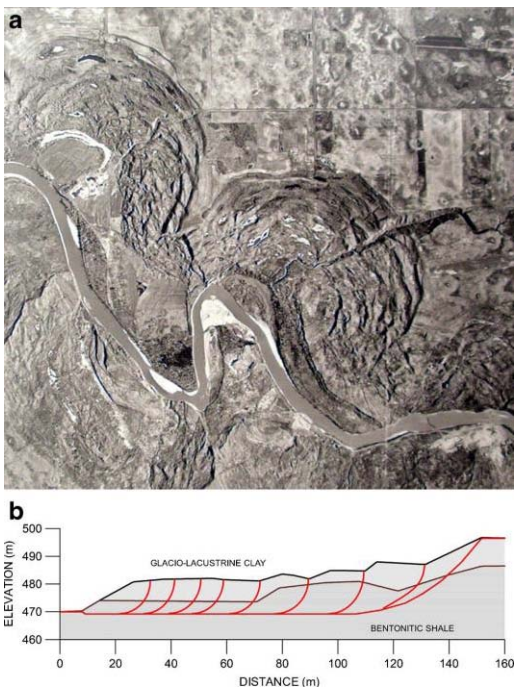

Figure A1-67. Lateral spreads.

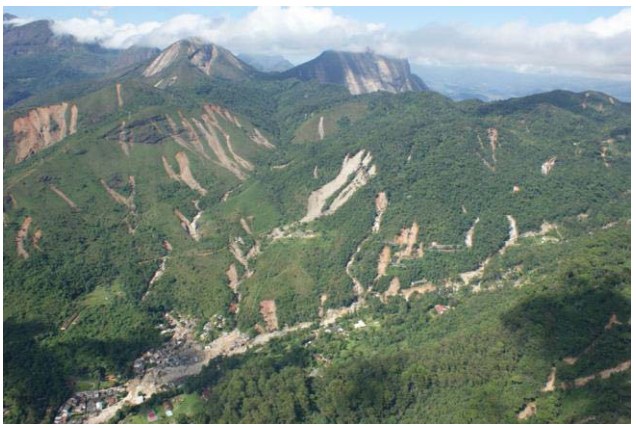

Figure A1-68. Debris avalanches and debris flows of January 2010 in the Serrana region of Brazil.

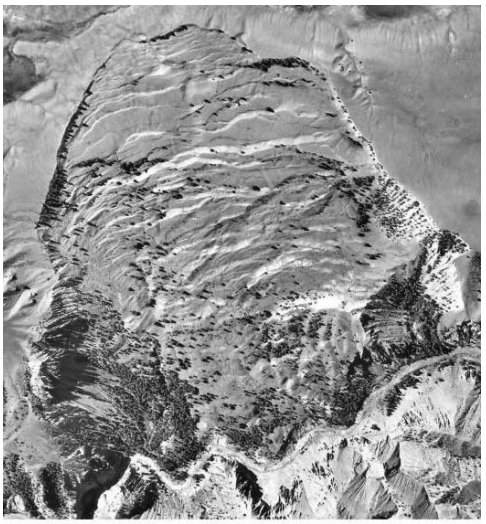

Fig. 13 Vertical aerial photo of a compound slide in glacio-lacustrine deposits, Churn Creek, British Columbia Interior. B.C. Government Airphoto BC7721. The frame is approximately 1 km wide. Note that internal shears form scarps both in normal and anti-slope directions

Figure A1-69. Compound slide in glacio-lacustrine deposits.

Figure A1-70. Multiple retrogressive flow slide.

Downloaded from http://pubs.geoscienceworld.org/aeg/eeg/article-pdf/31/1/i/6130855/i1558-9161-31-1-i.pdf
by AEG RBAC user

Fig. 21 The 1999 rock avalanche deposited on a glacier surface, Mt. Munday, British Columbia, Canada (Delaney and Evans 2013). (Topography and ortho-photo courtesy of MacElhanney, Ltd., Vancouver and image courtesy S.G. Evans, University of Waterloo)

Figure A1-71. Rock avalanche.

REFERENCES CITED IN APPENDIX 1

Collin, A., 1846, *Recherches Expérimentales sur les Glissements Spontanés des Terrains Argileux Accompagnées de Considérations sur Quelques Principes de la Mécanique Terrestre*: Carilion-Goeury, Paris.

Collin, A. (translated by W. R. Schriever), 1956, *Landslides in Clays by Alexandre Collin (1846*): University of Toronto Press, Toronto, Ontario, Canada, 161 p., 21 plates.

Cornforth, D. H., 2005, *Landslides in Practice: Investigation, Analysis and Remediation/Preventative Options in Soils*: John Wiley & Sons, Inc., New York, 596 p.

Cruden, D. M. and Lefebvre, G., 1994, *Final Administrative Report of ISSMFE Technical Committee 11, Landslides 1989–1994*. In XIII ISSMFE, New Delhi, pp. 217–219.

Cruden, D. M. and Varnes, D. J., 1996, Landslide types and processes, Chapter 3. In Turner, A. K. and Schuster, R. L. (Editors), *Landslides: Investigation and Mitigation*: Transportation Research Board Special Report 247, National Academy of Sciences, Washington, D.C., pp. 36–75.

Eckel, E. B. (Editor), 1958, *Landslides and Engineering Practice*: Highway Research Board Special Report 29, National Academy of Sciences/National Research Council, Washington, D.C., 232 p.

Effland, A. B. W. and Effland, W. R., 1994, Soil geomorphology studies in the U.S. Soil Survey program: *Agricultural History*, Vol. 66, No. 2, pp. 189–212.

Eisbacher, G. H. and Clague, J. J., 1984, *Destructive Mass Movements in High Mountains: Hazard and Management*: Paper 84-16, Geological Survey of Canada, Ottawa, Ontario, Canada, 230 p.

Fox, C. S., 1935, *A Comprehensive Treatise on Engineering Geology*: The Technical Press, Ltd., London, 471 p.

Giraud, A.; Rochet, L.; and Antoine, P., 1990, Process of slope failure in crystallophyllian formations: *Engineering Geology*, Vol. 29, No. 3, pp. 241–253.

Hansen, W. R., 1965, Effects of the earthquake of March 27, 1964, at Anchorage, Alaska: U.S. Geological Survey Professional Paper 542-A, 68 p.

Harrison, J. V. and Falcon, N. L., 1936, Gravity collapse structures and mountain ranges as exemplified in south-western Persia: *Quarterly Journal of the Geological Society of London*, Vol. 92, pp. 91–102.

Horner, S. E. and McNeal, J. D., 1950, Application of geology to highway engineering: *Colorado School Mines Quarterly Review*, Vol. 45, No. 1B, pp. 155–186.

Hungr, O.; Evans, S. G.; Bovis, M. J.; and Hutchinson, J. B., 2001, A review of the classification of landslides of the flow type: *Environmental & Engineering Geoscience*, Vol. VII, No. 3, pp. 221–238.

Downloaded from http://pubs.geoscienceworld.org/aeg/eeg/article-pdf/31/1/i/6130855/i1558-9161-31-1-i.pdf
by AEG RBAC user

Hungr, O.; Leroueil, S.; and Picarelli, L., 2014, The Varnes classification of landslide types, an update: *Landslides*, Vol. 11, No. 2, pp. 167–194.

IAEG (International Association of Engineering Geology) Commission on Landslides, 1990, Suggested nomenclature for landslides: *Bulletin of the International Association of Engineering Geology*, Vol. 41, pp. 13–16.

IGS UNESCO WP/WLI (International Geotechnical Societies' UNESCO Working Party on World Landslide Inventory), 1990, A suggested method for reporting a landslide: *Bulletin of the International Association of Engineering Geology*, Vol. 41, pp. 5–12.

IGS UNESCO WP/WLI (International Geotechnical Societies' UNESCO Working Party on World Landslide Inventory), 1991, A suggested method for a landslide summary: *Bulletin of the International Association of Engineering Geology*, Vol. 43, pp. 101–110.

IGS UNESCO WP/WLI (International Geotechnical Societies' UNESCO Working Party on World Landslide Inventory), 1993, A suggested method for describing the activity of a landslide: *Bulletin of the International Association of Engineering Geology*, Vol. 47, pp. 53–57.

IGS UNESCO WP/WLI (International Geotechnical Societies' UNESCO Working Party on World Landslide Inventory), 1994a, A suggested method for reporting landslide causes: *Bulletin of the International Association of Engineering Geology*, Vol. 50, pp. 71–74.

IGS UNESCO WP/WLI (International Geotechnical Societies' UNESCO Working Party on World Landslide Inventory), 1994b, *Multilingual Landslide Glossary*: BiTech Publishers Ltd., Richmond, British Columbia, Canada, 32 p.

IGS UNESCO WP/WLI (International Geotechnical Societies' UNESCO Working Party on World Landslide Inventory), 1995, A suggested method for describing the rate of movement of a landslide: *Bulletin of the International Association of Engineering Geology*, Vol. 52, pp. 75–78.

ISSMFE (International Society for Soil Mechanics and Foundation Engineering), Technical Committee 11, 1993, *Landslide Illustrations: A Collection of 26 Slides*: Department of Engineering, Cambridge University, Cambridge, U.K.

Iverson, R. M., 2003, How should mathematical models of geomorphic processes be judged? In Wilcock, P. R. and Iverson, R. M. (Editors), *Prediction in Geomorphology*: Geophysical Monograph 135, American Geophysical Union, Washington, D.C., p83–94

Iverson, R. M., 2006, Forecasting runout of rock and debris avalanches: *Landslides*, Vol. 49, pp. 197–209.

Keefer, D. K., 1984, Rock avalanches caused by earthquakes: Source characteristics: *Science*, Vol. 223, pp. 1288–1290.

Keene, P. and Horner, S. E. (Editors), 1951, *Present Practice in Subsurface Drainage for Highways and Airports, A Report of the Committee on Subsurface Drainage*: Highway Research Board Bulletin 45, National Research Council, Washington, D.C., 20 p.

Legros, F., 2002, The mobility of long-runout landslides: *Engineering Geology*, Vol. 63, pp. 301–331.

Neuendorf, K. K. E.; Mehl, J. P., Jr.; and Jackson, J. A., 2005, *Glossary of Geology*, 5th ed: American Geological Institute, Alexandria, VA, 779 p.

Ostaficzuk, S., 1973, Large-scale landslides in north-western Libya: *Acta Geologica Polonica*, Vol. 23, No. 2, pp. 231–244.

Pierson, T. C., 1986, Flow behavior of channelized debris flows, Mount St. Helens, Washington. In Abrahams, A. D. (Editor), *Hillslope Processes*: Allen & Unwin, Boston, MA, pp. 269–296.

Rendulic, L., 1936, Relation between void ratio and effective principal stress for a remolded silty clay. In *Proceedings of the 1st International Conference on Soil Mechanics and Foundation Engineering*: Harvard Printing Office, Cambridge, MA, pp. 48–51.

Rogers, J. D., 2022, The Alcan pioneer road and discovery of permafrost. In *Proceedings of the Canadian Society of Civil Engineers Annual Conference 2022*, Whistler, British Columbia, pp. GEN 151-1 to GEN 151-15.

Schuster, R. L., 1978a, Introduction, Chapter 1. In Schuster, R. L. and Krizek, R. J. (Editors), *Landslides: Analysis and Control*: Transportation Research Board/National Research Council Special Report 176, National Academy of Sciences, Washington, D.C., pp. 1–10.

Schuster, R. L., 1978b, Socioeconomic significance of landslides in landslides investigation and mitigation. In Schuster, R. L. and Krizek, R. J. (Editors), *Landslides: Analysis and Control*: Transportation Research Board/National Research Council Special Report 176, National Academy of Sciences, Washington, D.C., pp. 12–31.

Schuster, R. L. and Krizek, R. J. (Editors), 1978, *Landslides: Analysis and Control*: Transportation Research Board/National Research Council Special Report 176, National Academy of Sciences, Washington, D.C., 234 p.

Sharpe, C. F. S., 1938a, *What is Soil Erosion?*: U.S. Department of Agriculture Miscellaneous Publication 286, 84 p.

Sharpe, C. F. S., 1938b, *Landslides and Related Phenomena*: Columbia University Press, New York, 137 p.

Skermer, N. A. (translator), 1989, *Landslides and Human Lives*: Bi-Tech, Vancouver, British Columbia, Canada, p. 55–137.

Suarez Diaz, J., 1998, Deslizamientos y Estabilidad de Taludes en Zonas Tropicales: Instituto de Investigaciones sobre Erosion y Deslizamientos, Bucaramanga, Colombia.

Tompkin, J. M. and Britt, S. H., 1951, *Landslides: A Selected Annotated Bibliography*: Highway Research Board Bibliography 10, 53 p.

Van Gassen, W. and Cruden, D. M., 1989, Momentum transfer and friction in the debris of rock avalanches: *Canadian Geotechnical Journal*, Vol. 26, pp. 623–628.

Varnes, H. D., 1949, *Landslide Problems of Southwestern Colorado*: U.S. Geological Survey Circular 31, 13 p.

Varnes, D. J., 1958, Landslide types and processes, Chapter. 3. In Eckel, E. B. (Editor), *Landslides and Engineering Practice*: Highway Research Board Special Report 29, National Academy of Sciences/National Research Council, Washington, D. C., pp. 20–47.

Varnes, D. J., 1963, *Geology and Ore Deposits of the South Silverton Mining Area*: U.S. Geological Survey Professional Paper 378-A.

Varnes, D. J., 1969, *Stability of the West Slope of Government Hill Port Area of Anchorage, Alaska*: U.S. Geological Survey Bulletin 1258-D.

Varnes, D. J., 1974, *The Logic of Geological Maps, with Reference to their Interpretation and Use for Engineering Purposes*: U.S. Geological Survey Professional Paper 837, 3 plates, 48 p.

Varnes, D. J., 1978, Slope movement types and processes, Chapter 2. In Schuster, R. L. and Krizek, R. J. (Editors), *Landslide Analysis and Control*: Transportation Research Board Special Report 176, National Academy of Sciences, Washington, D.C., pp. 12–33.

Varnes, D. J., 1990, Memorial to Edwin B. Eckel 1906–1989: *Bulletin of the Association of Engineering Geologists*, Vol. 27, No. 1, pp. 123–124.

Varnes, D. J., 1997, personal communication, October 3, 1997, U.S. Geological Survey Engineering Geology Branch (retired).

Zaruba, Q. and Mencl, V., 1969, *Engineering Geology*: Elsevier Scientific Publishing Co., New York, 503 p.

Downloaded from http://pubs.geoscienceworld.org/aeg/eeg/article-pdf/31/1/i/6130855/i1558-9161-31-1-i.pdf
by AEG RBAC user

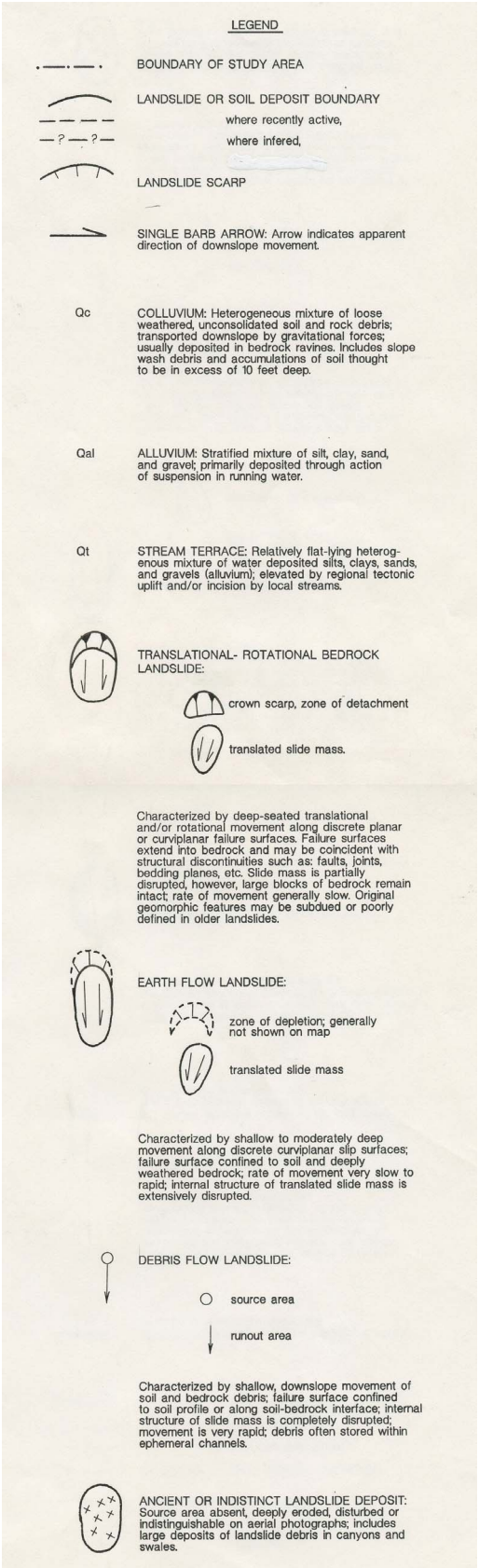

Figure A2-1. Legend of interpreted landslide features.

APPENDIX 2—LANDSLIDE HAZARD MAPPING ON PARCEL MAPS

These colored parcel maps are 1:7,200 in scale (1 in. = 600 ft [1 cm = 72.0 m]), based on parcel maps provided by the City of Orinda in 1991.

The ocher color represents colluvium of unknown depth. The light-yellow color represents alluvium deposits. The light pink represents youthful landslide deposits. The vermilion color (with "x") represents ancient/indistinct landslide deposits. The dark pink represents weathered landslide deposits. The dashed lines represent the inferred boundaries of interpreted areas.

Figure A2-1 presents the legend of interpreted landslide features overlain on the Contra Costa County Assessor's Parcel Map of 1991. Figure A2-2 presents an overview of the orthophototopographic map tile locations.

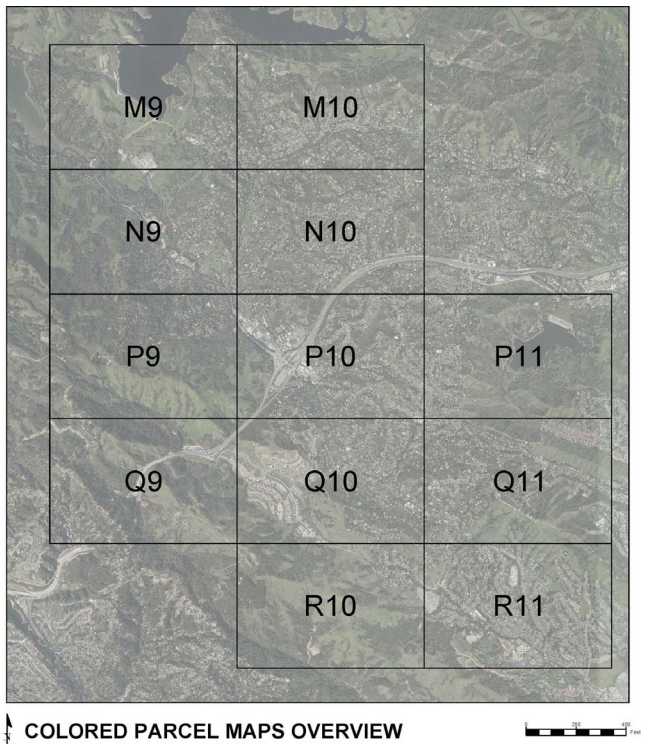

Figure A2-2. Overview map of the individual presented parcel map tiles.

Downloaded from http://pubs.geoscienceworld.org/aeg/eeg/article-pdf/31/1/i/6130855/i1558-9161-31-1-i.pdf
by AEG RBAC user

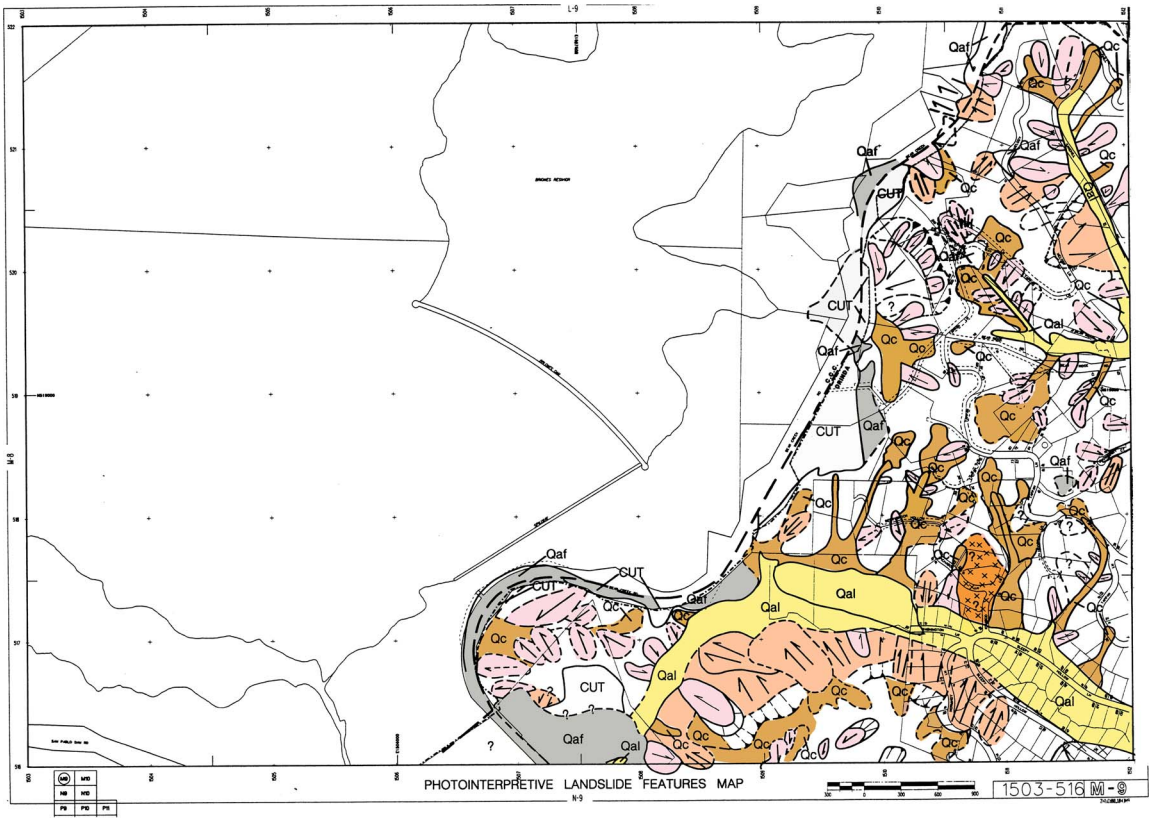

Figure A2-3. Map (color).

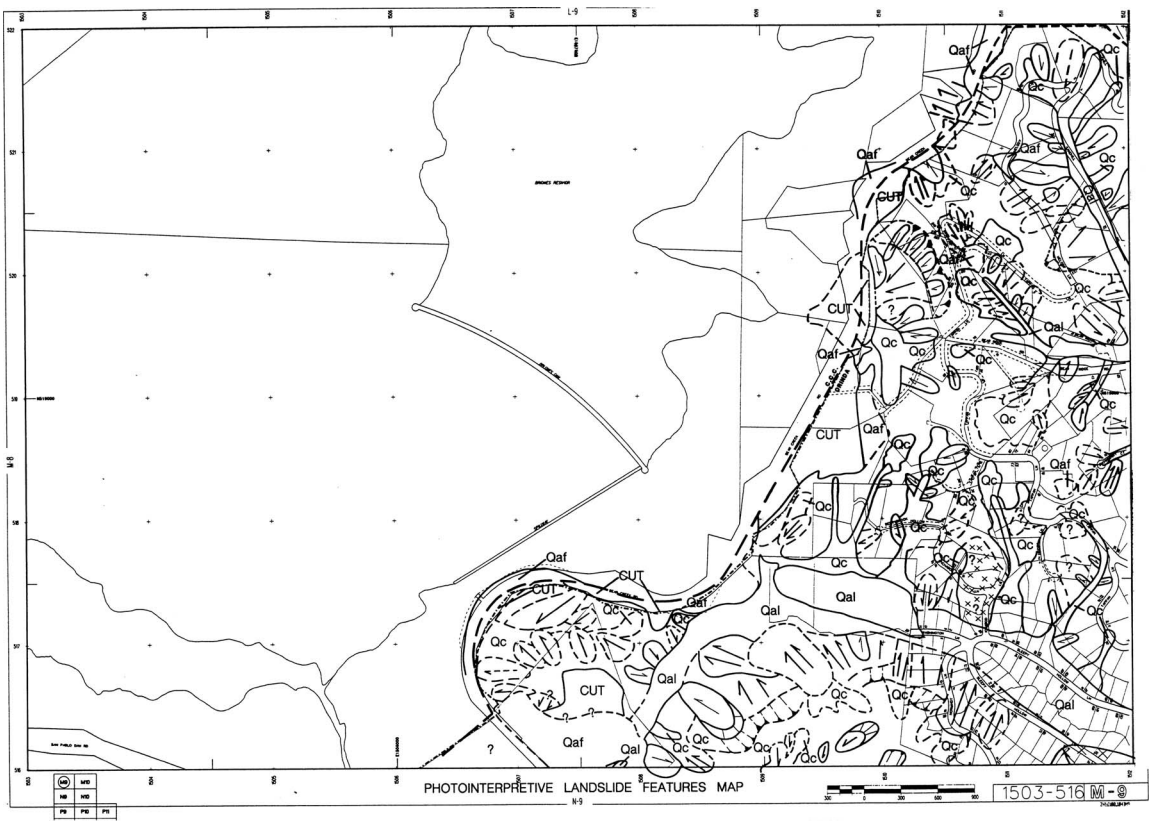

Figure A2-3. Map (black and white).

Downloaded from http://pubs.geoscienceworld.org/aeg/eeg/article-pdf/31/1/i/6130855/i1558-9161-31-1-i.pdf
by AEG RBAC user

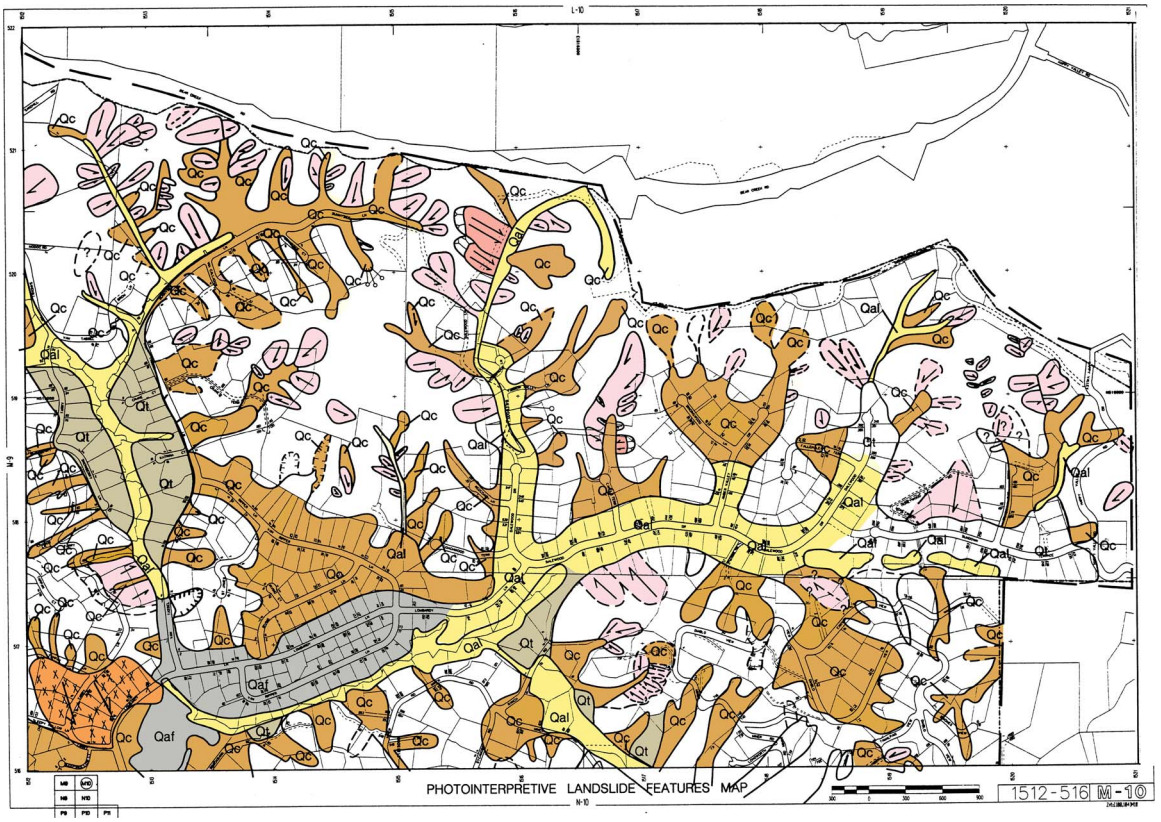

Figure A2-4. Map (color).

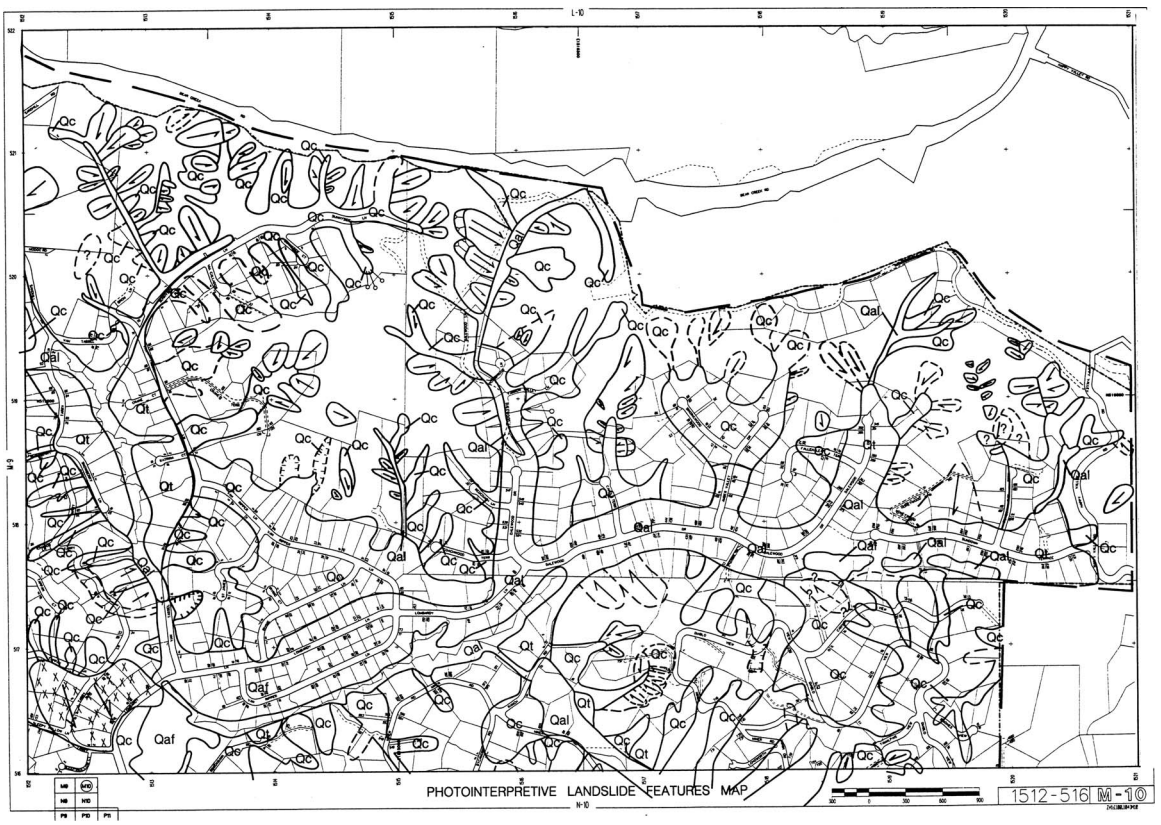

Figure A2-4. Map (black and white).

Downloaded from http://pubs.geoscienceworld.org/aeg/eeg/article-pdf/31/1/i/6130855/i1558-9161-31-1-i.pdf
by AEG RBAC user

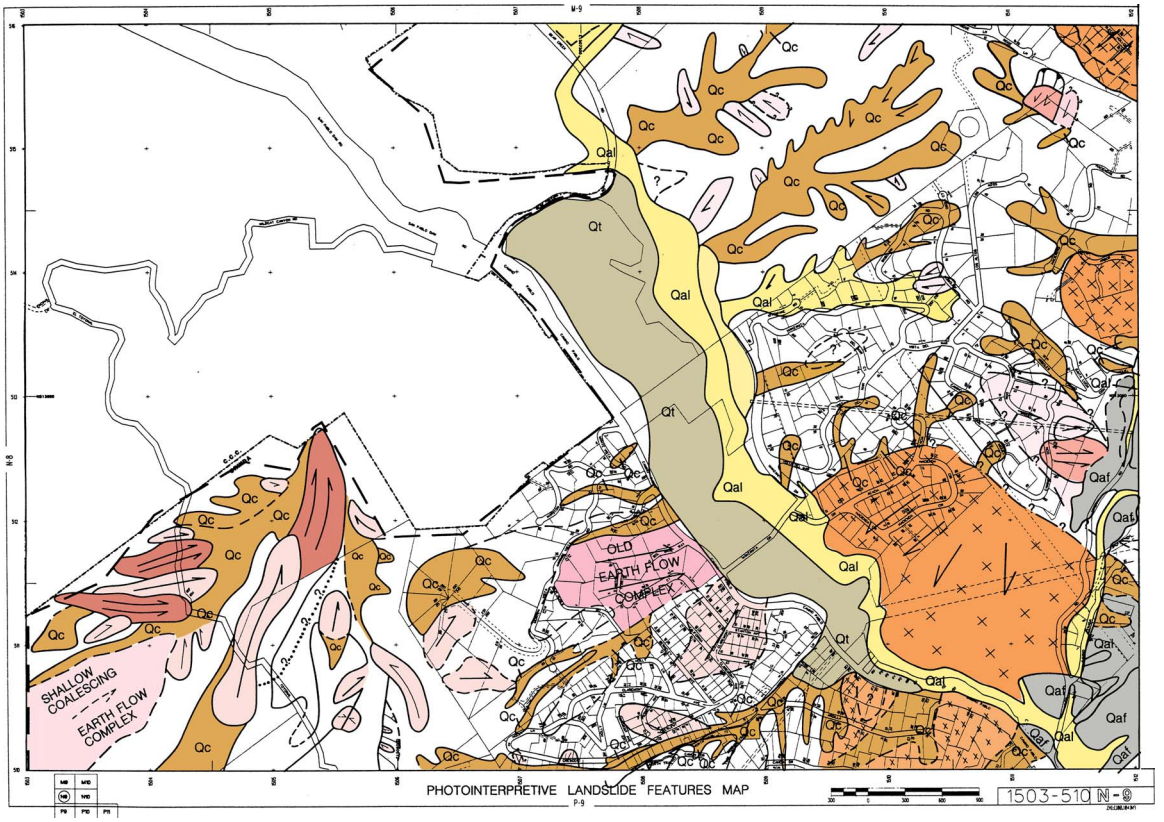

Figure A2-5. Map (color).

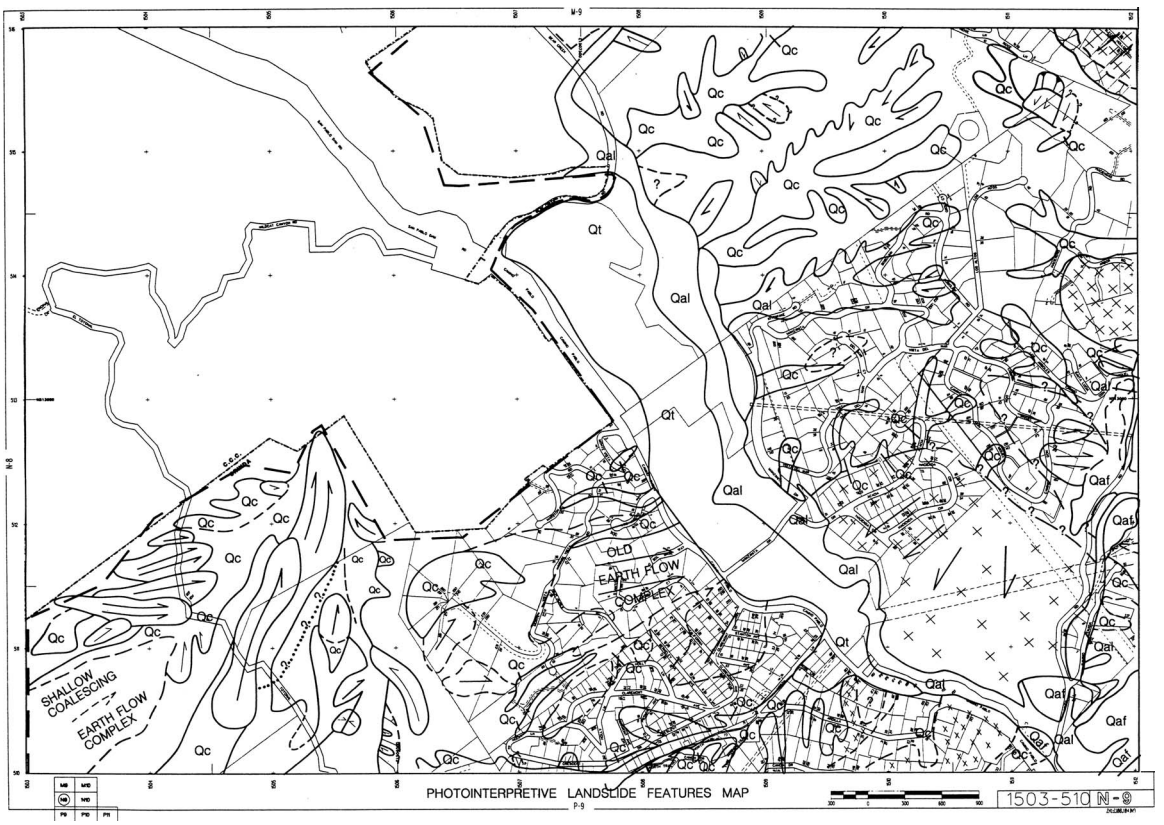

Figure A2-5. Map (black and white).

Downloaded from http://pubs.geoscienceworld.org/aeg/eeg/article-pdf/31/1/i/6130855/i1558-9161-31-1-i.pdf
by AEG RBAC user

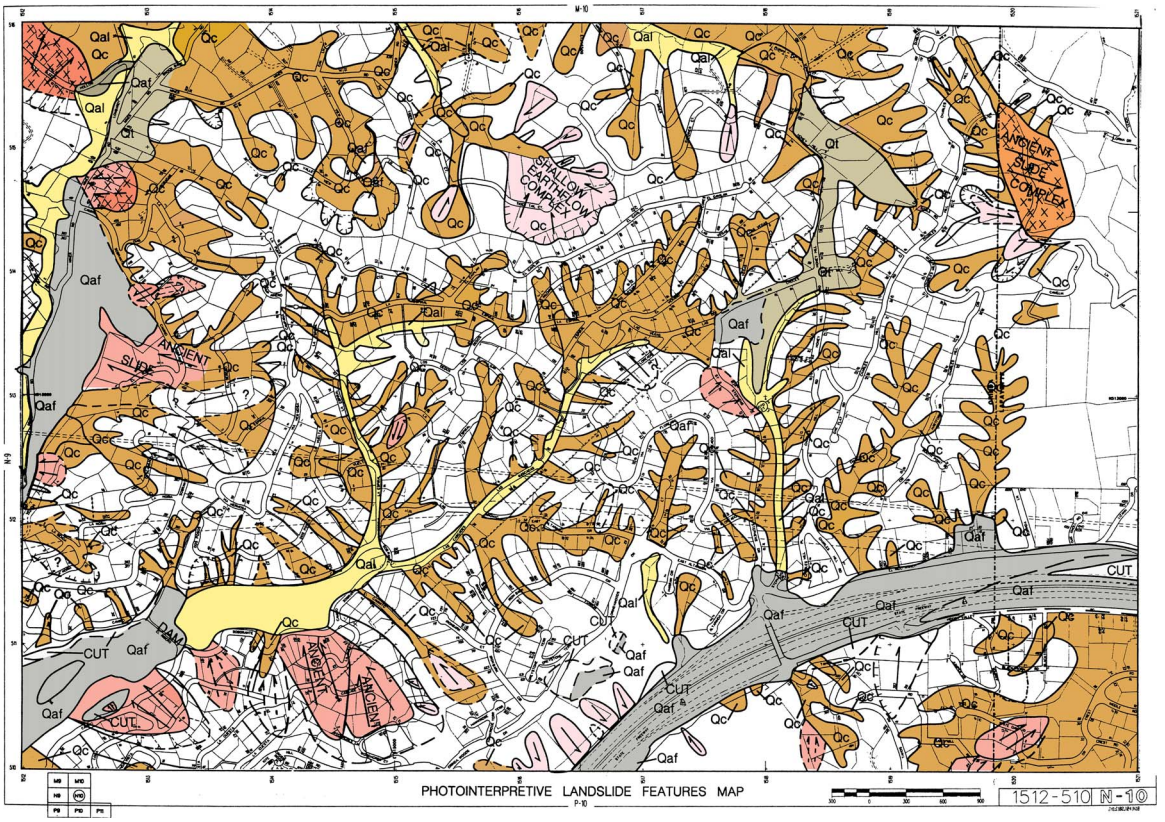

Figure A2-6. Map (color).

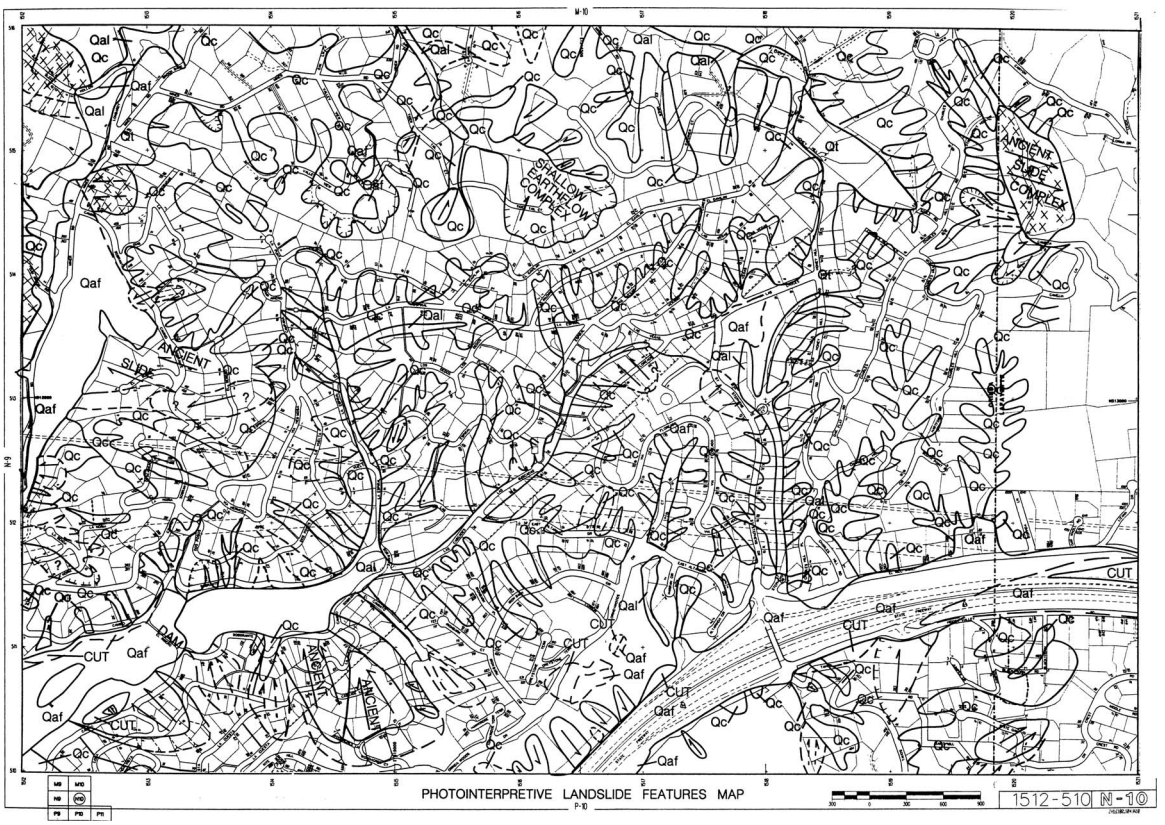

Figure A2-6. Map (black and white).

Downloaded from http://pubs.geoscienceworld.org/aeg/eeg/article-pdf/31/1/i/6130855/i1558-9161-31-1-i.pdf
by AEG RBAC user

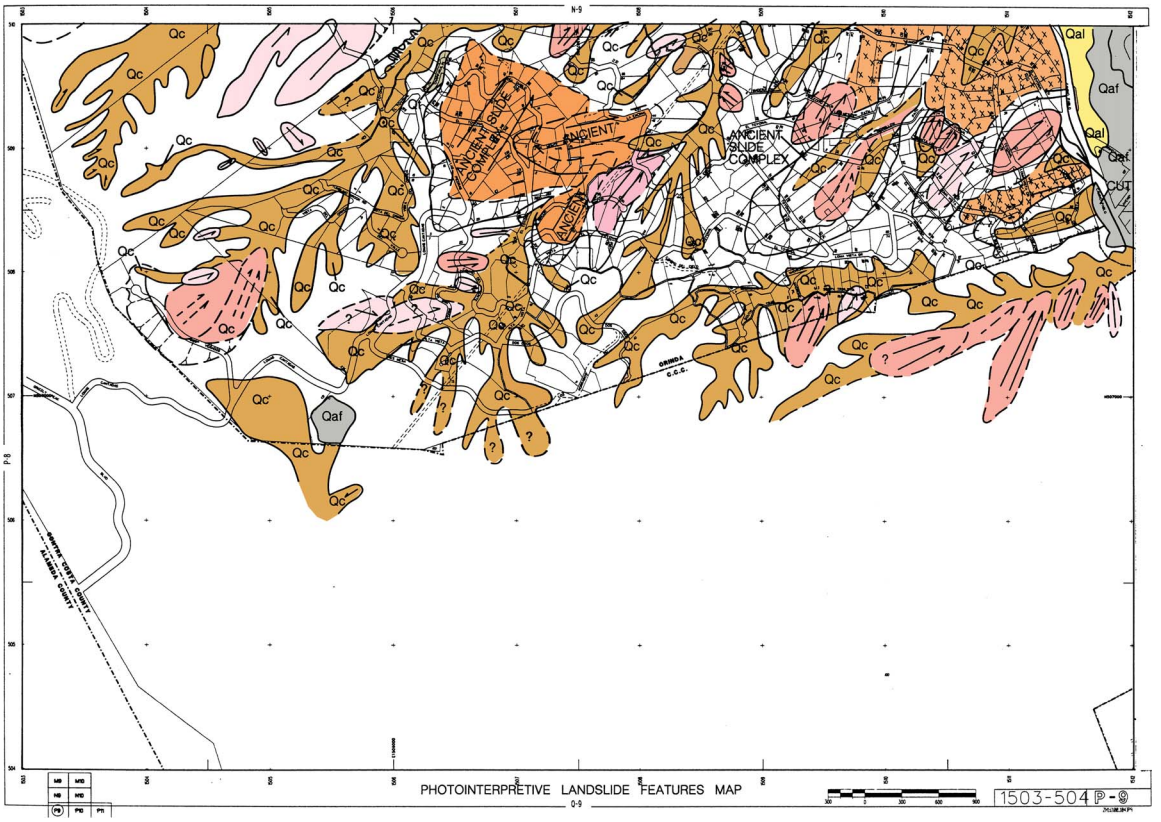

Figure A2-7. Map (color).

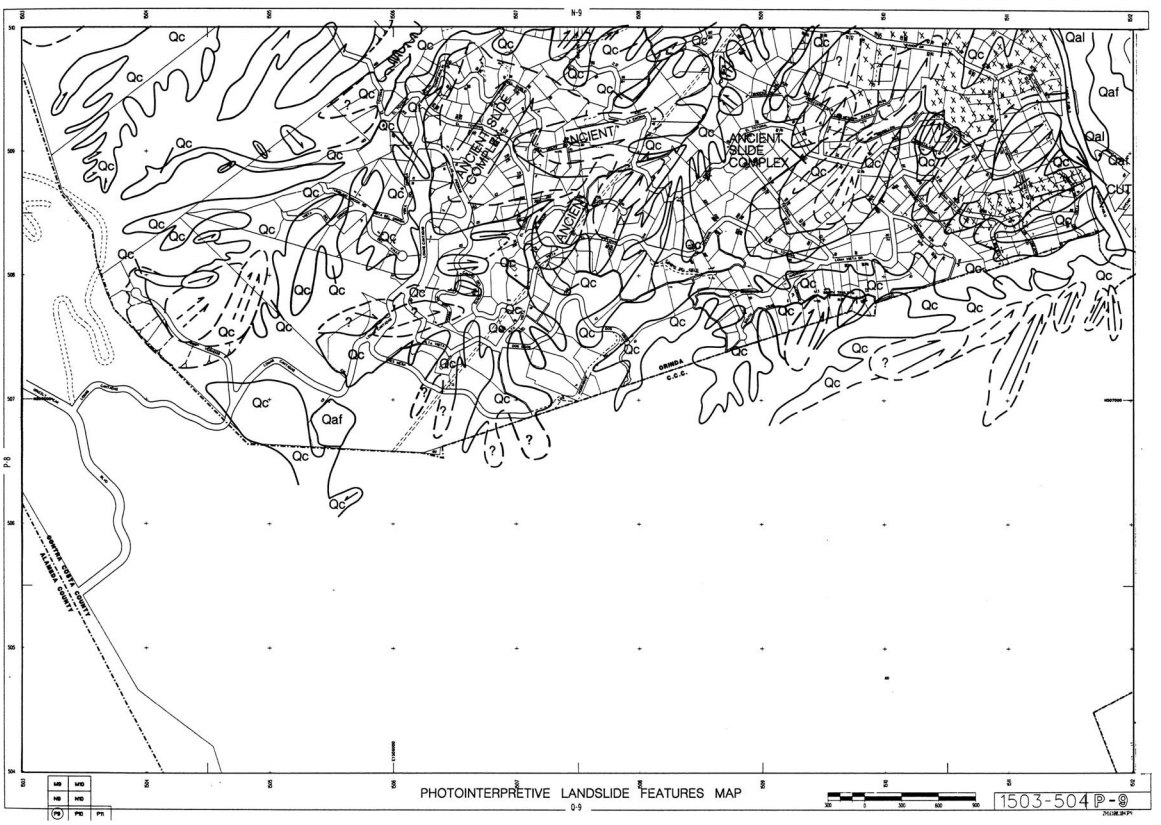

Figure A2-7. Map (black and white).

Downloaded from http://pubs.geoscienceworld.org/aeg/eeg/article-pdf/31/1/i/6130855/i1558-9161-31-1-i.pdf
by AEG RBAC user

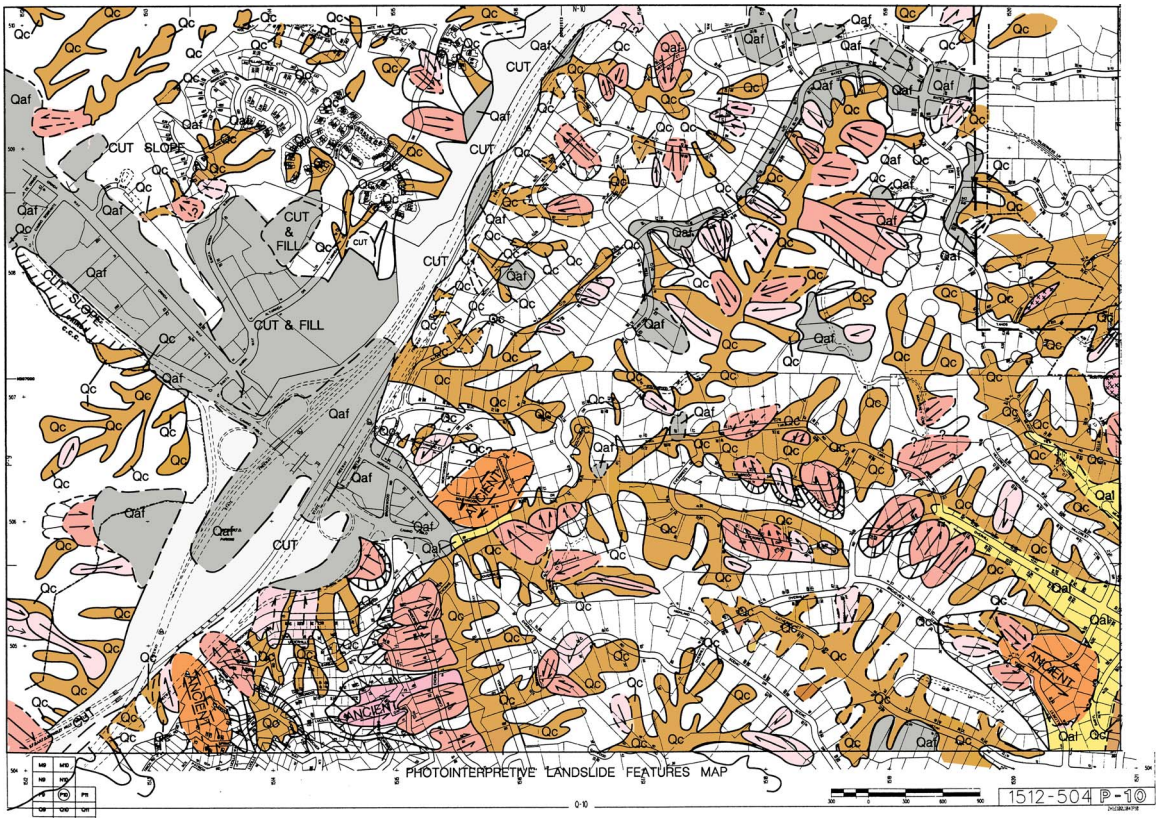

Figure A2-8. Map (color).

Figure A2-8. Map (black and white).

Downloaded from http://pubs.geoscienceworld.org/aeg/eeg/article-pdf/31/1/i/6130855/i1558-9161-31-1-i.pdf
by AEG RBAC user

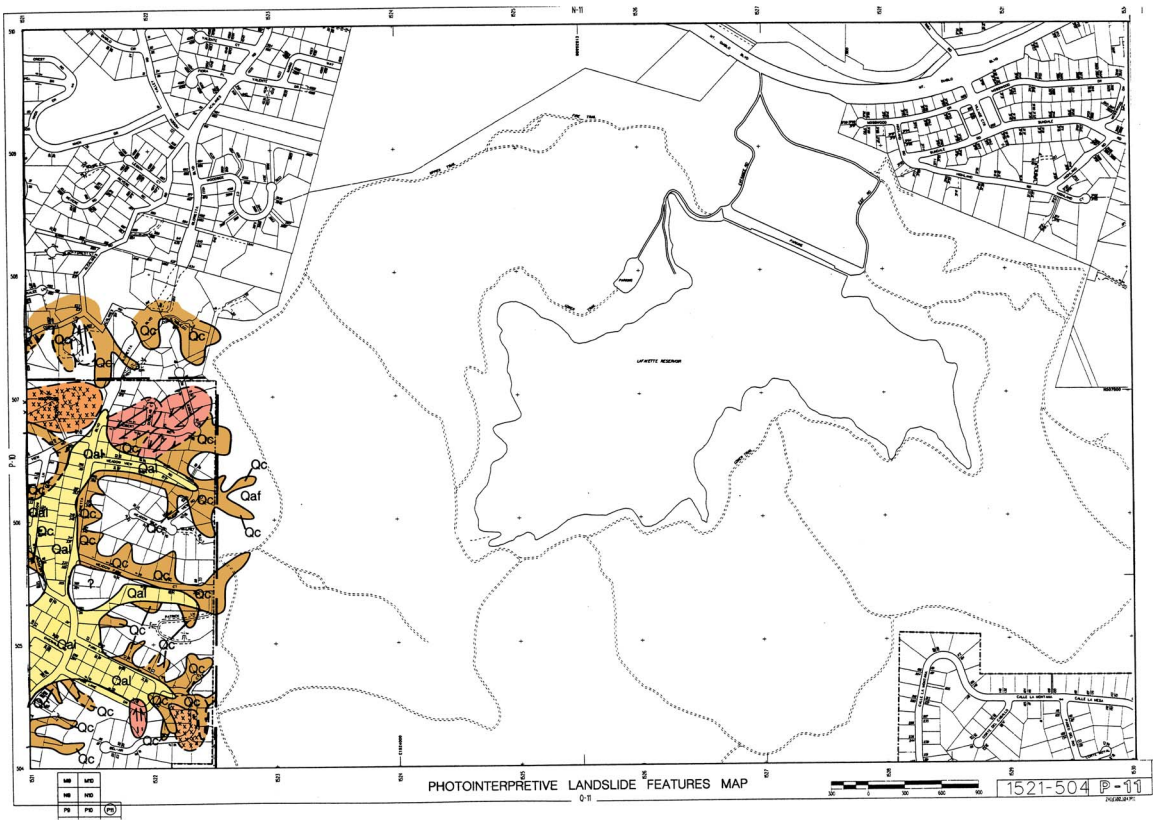

Figure A2-9. Map (color).

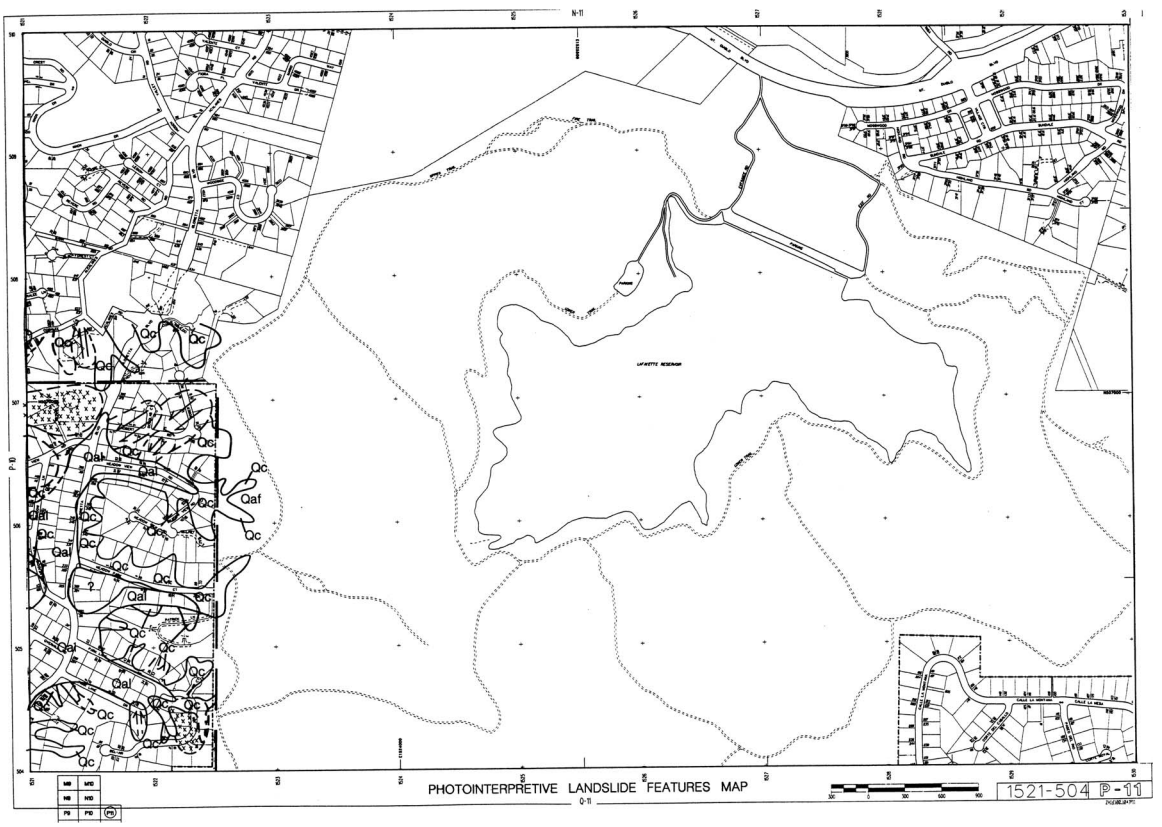

Figure A2-9. Map (black and white).

Downloaded from http://pubs.geoscienceworld.org/aeg/eeg/article-pdf/31/1/i/6130855/i1558-9161-31-1-i.pdf
by AEG RBAC user

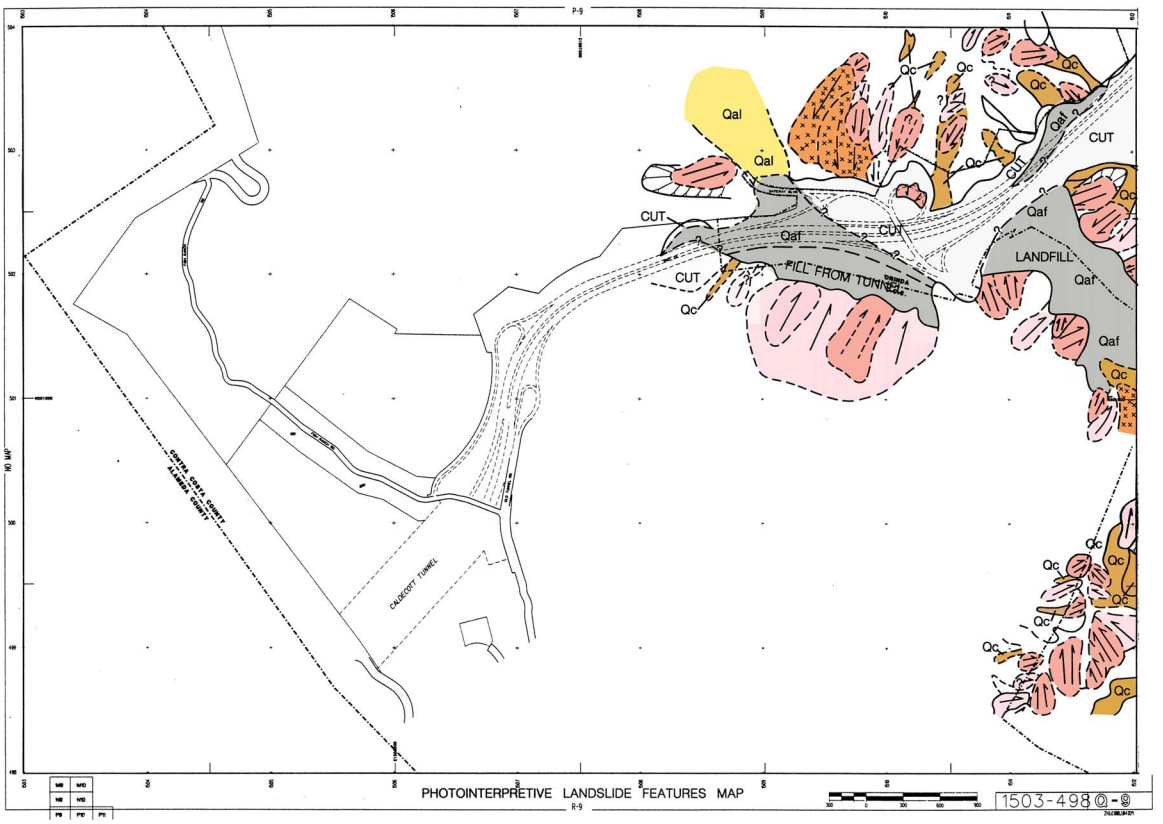

Figure A2-10. Map (color).

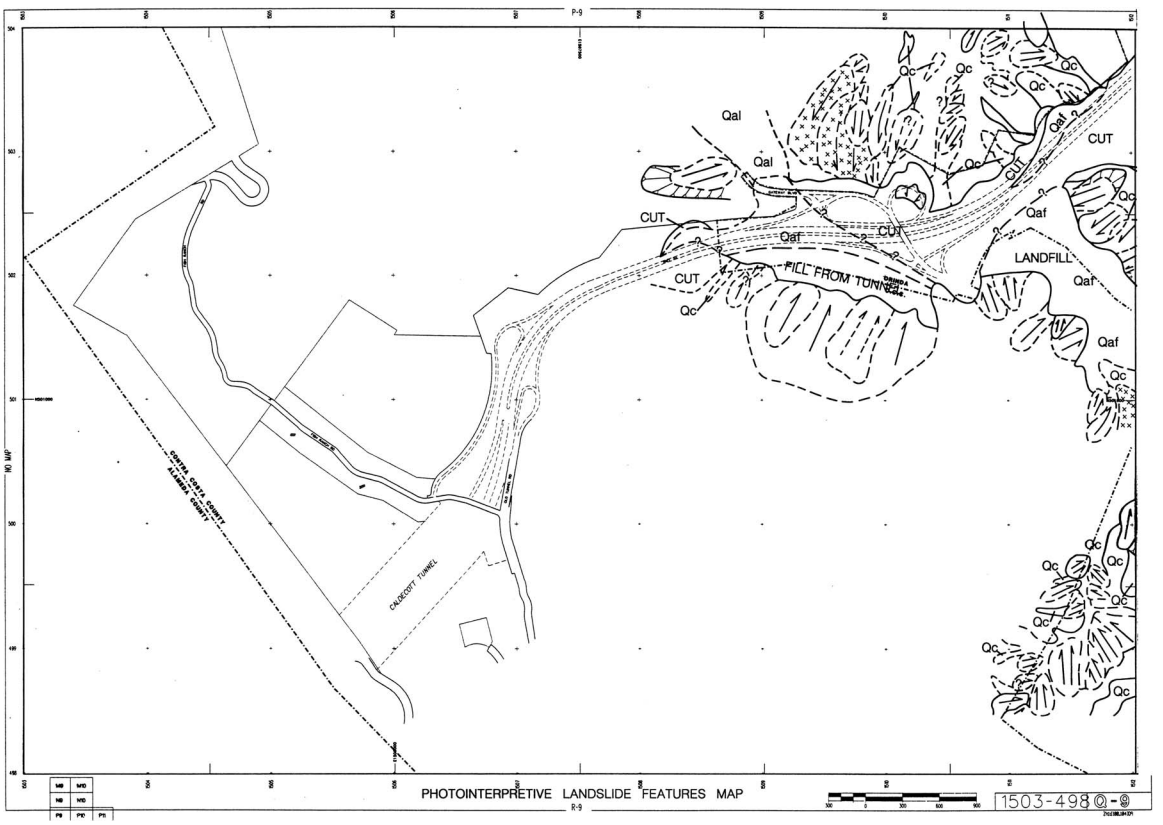

Figure A2-10. Map (black and white).

Downloaded from http://pubs.geoscienceworld.org/aeg/eeg/article-pdf/31/1/i/6130855/i1558-9161-31-1-i.pdf
by AEG RBAC user

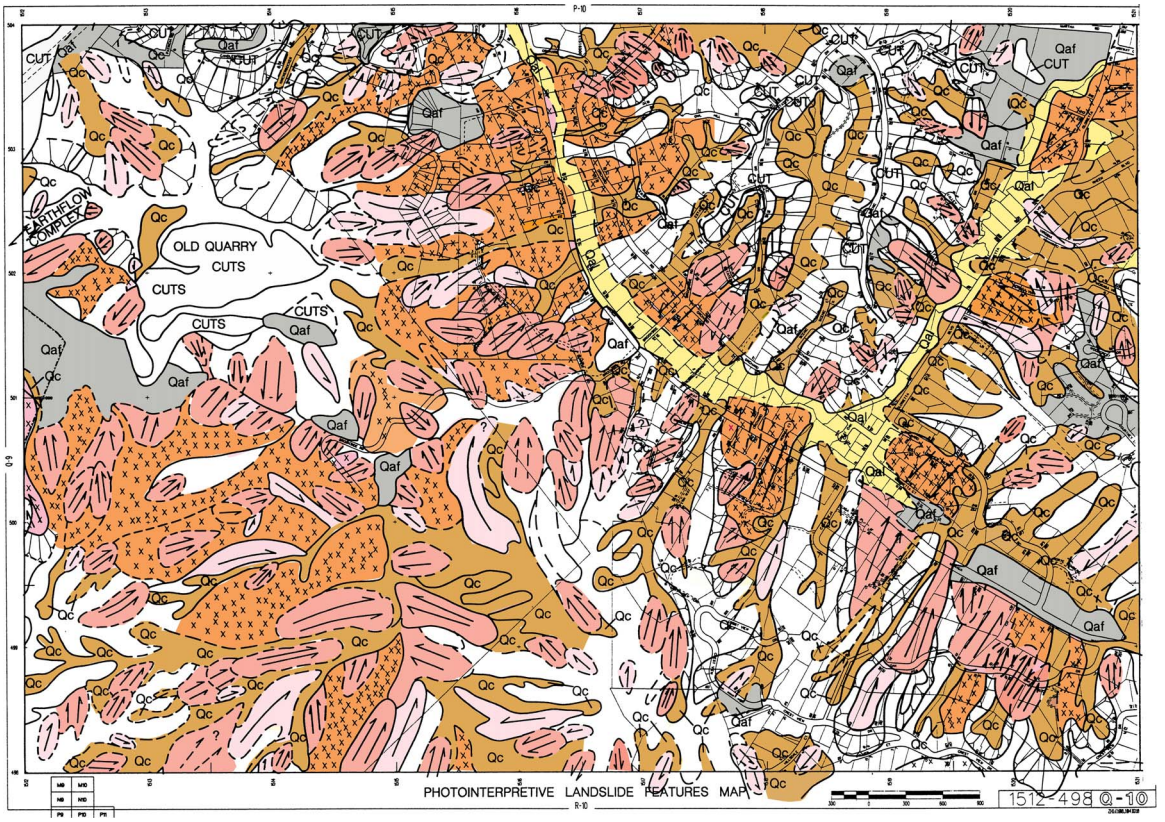

Figure A2-11. Map (color).

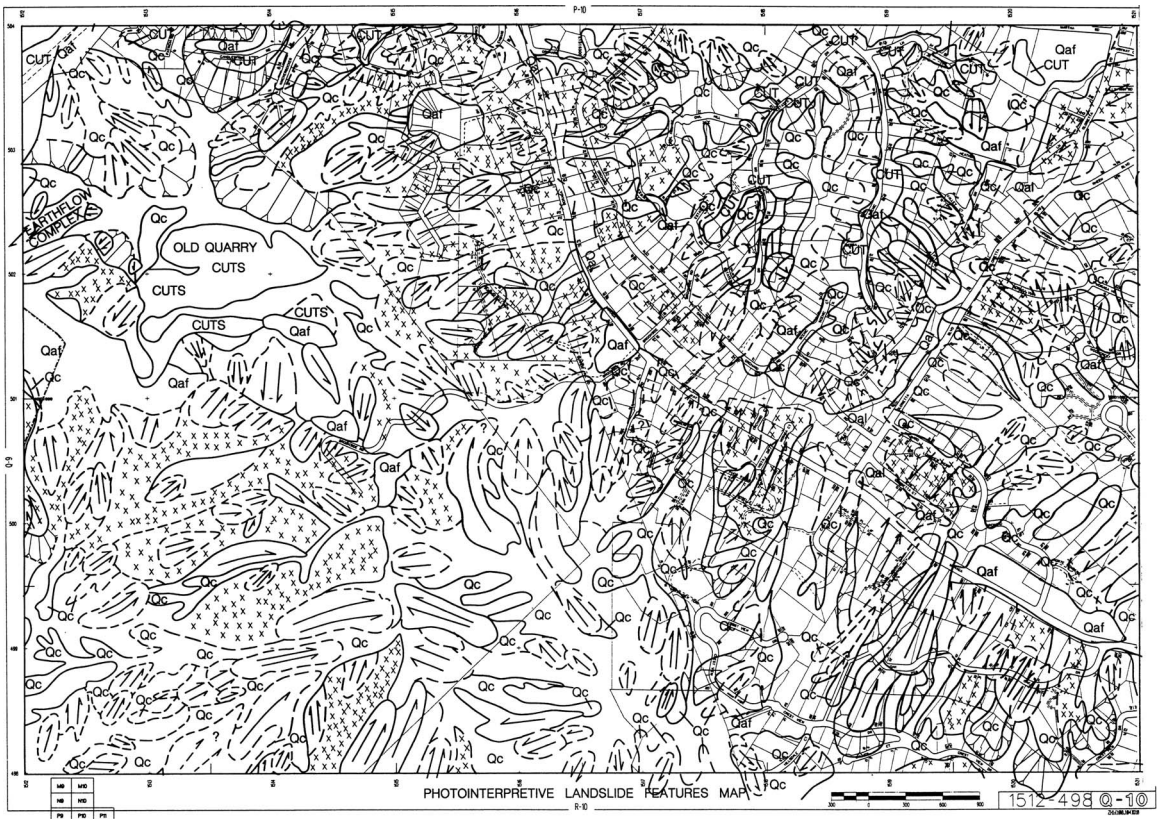

Figure A2-11. Map (black and white).

Downloaded from http://pubs.geoscienceworld.org/aeg/eeg/article-pdf/31/1/i/6130855/i1558-9161-31-1-i.pdf
by AEG RBAC user

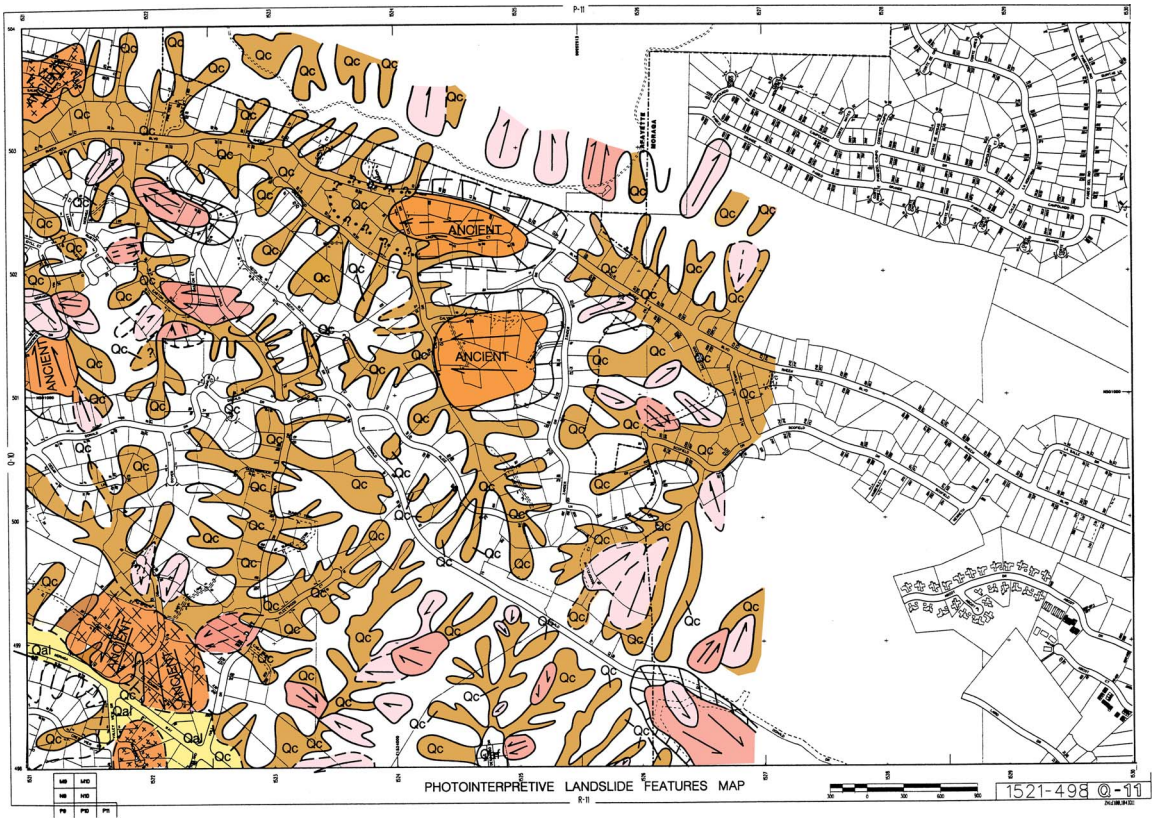

Figure A2-12. Map (color).

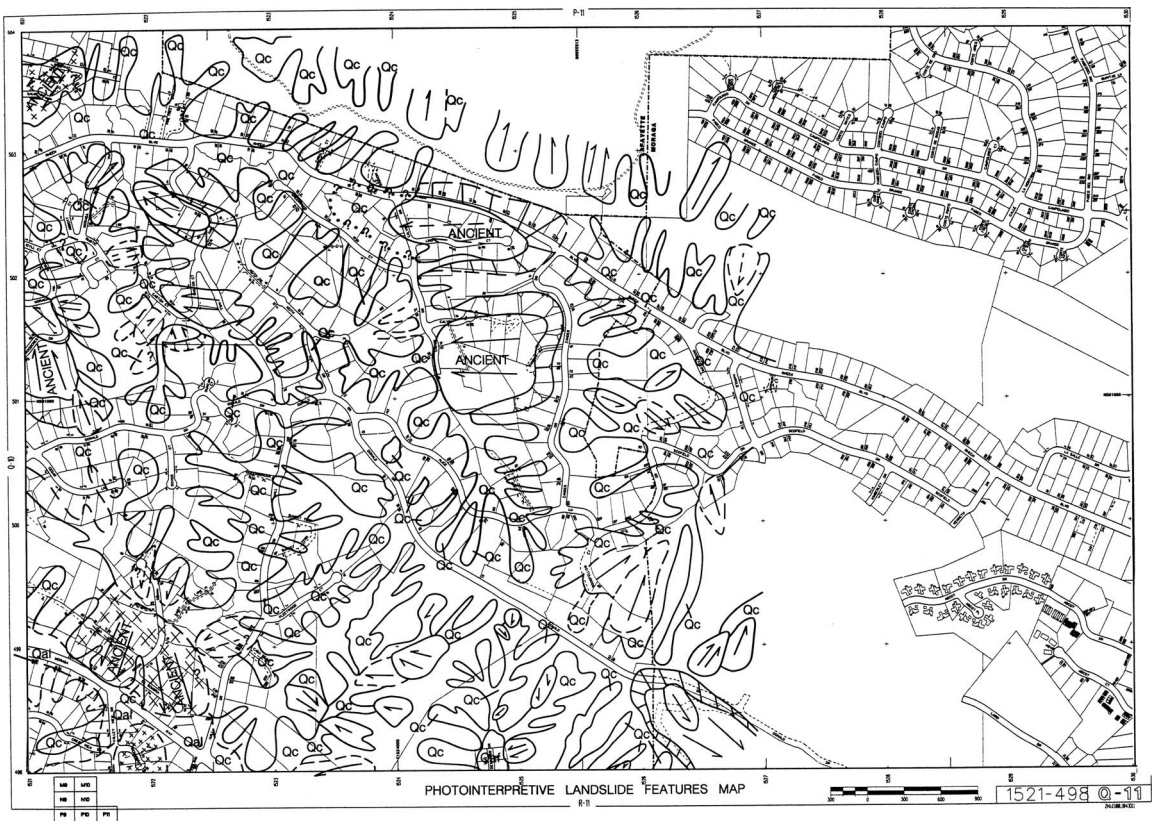

Figure A2-12. Map (black and white).

Downloaded from http://pubs.geoscienceworld.org/aeg/eeg/article-pdf/31/1/i/6130855/i1558-9161-31-1-i.pdf
by AEG RBAC user

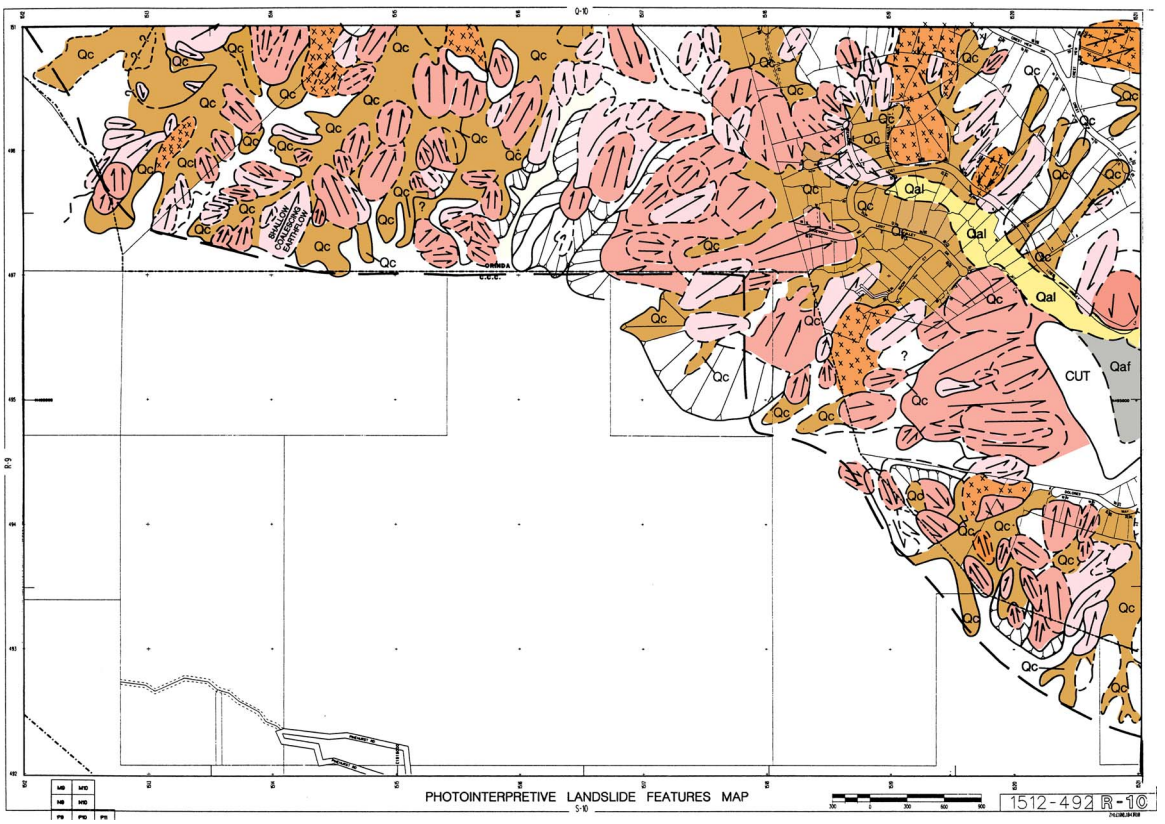

Figure A2-13. Map (color).

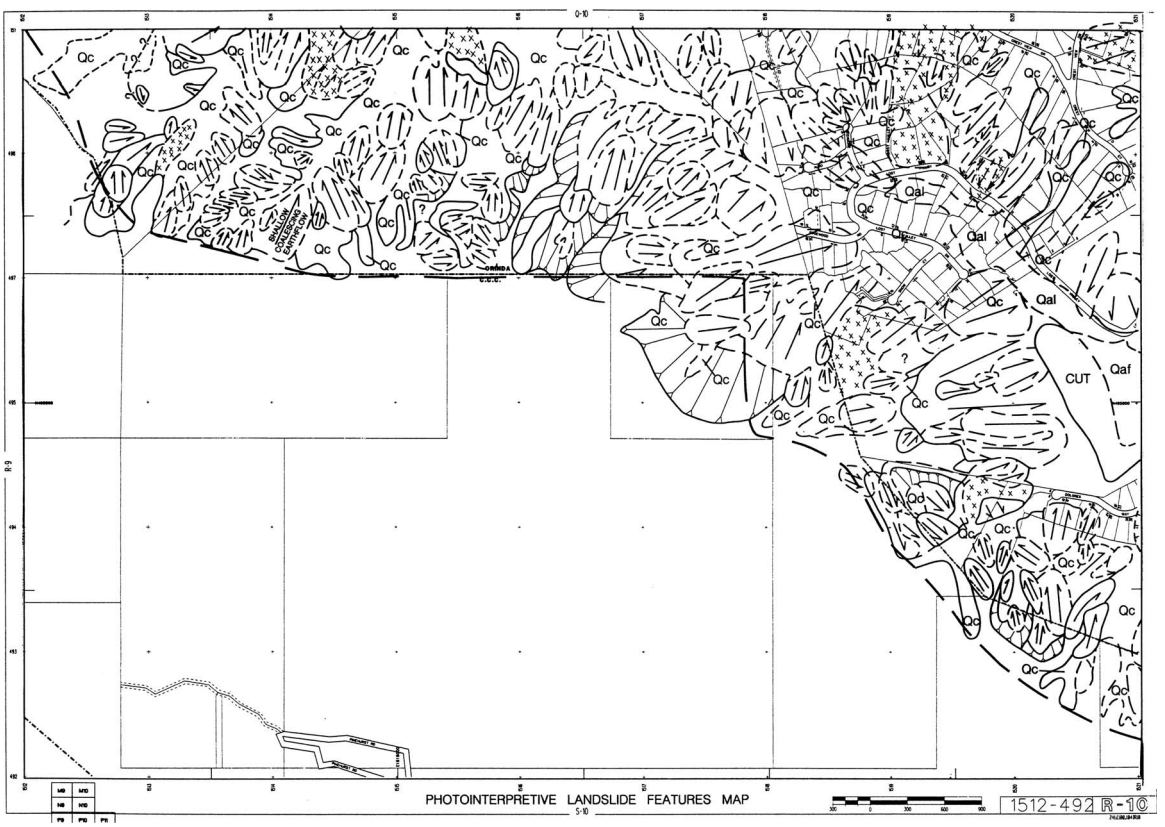

Figure A2-13. Map (black and white).

Downloaded from http://pubs.geoscienceworld.org/aeg/eeg/article-pdf/31/1/i/6130855/i1558-9161-31-1-i.pdf
by AEG RBAC user

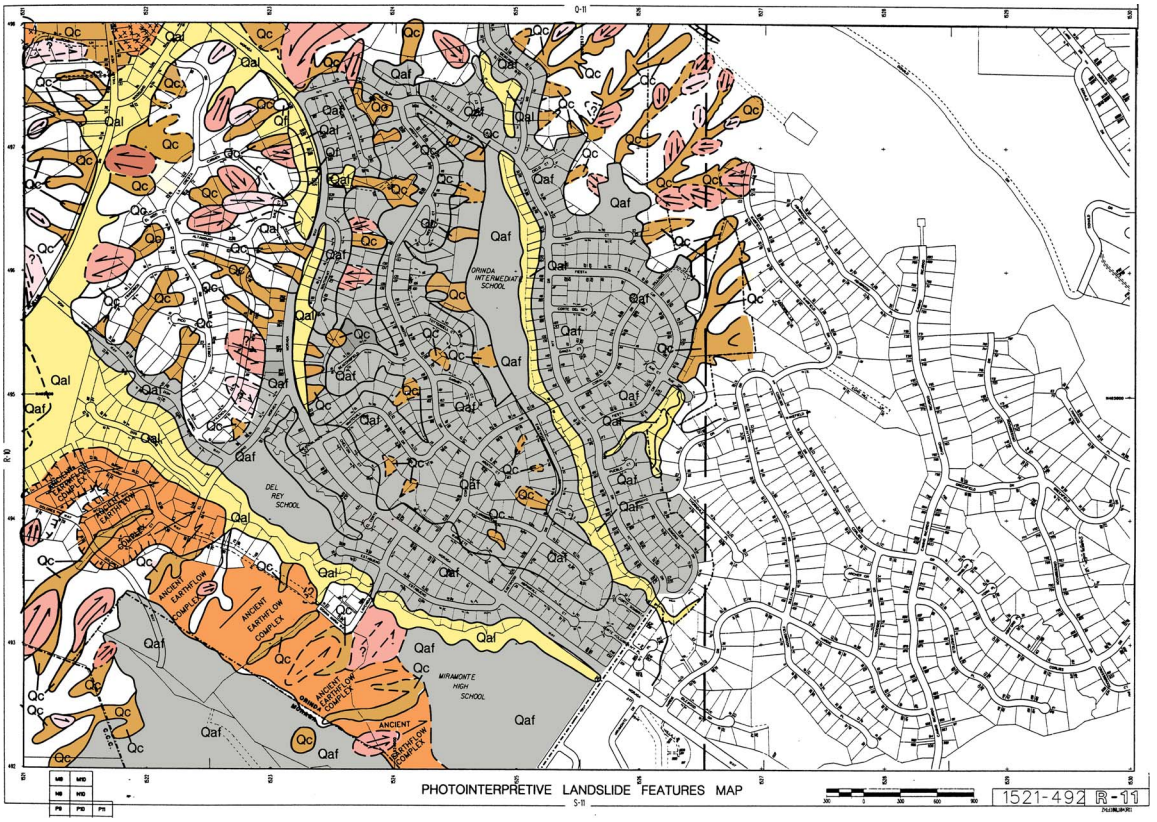

Figure A2-14. Map (color).

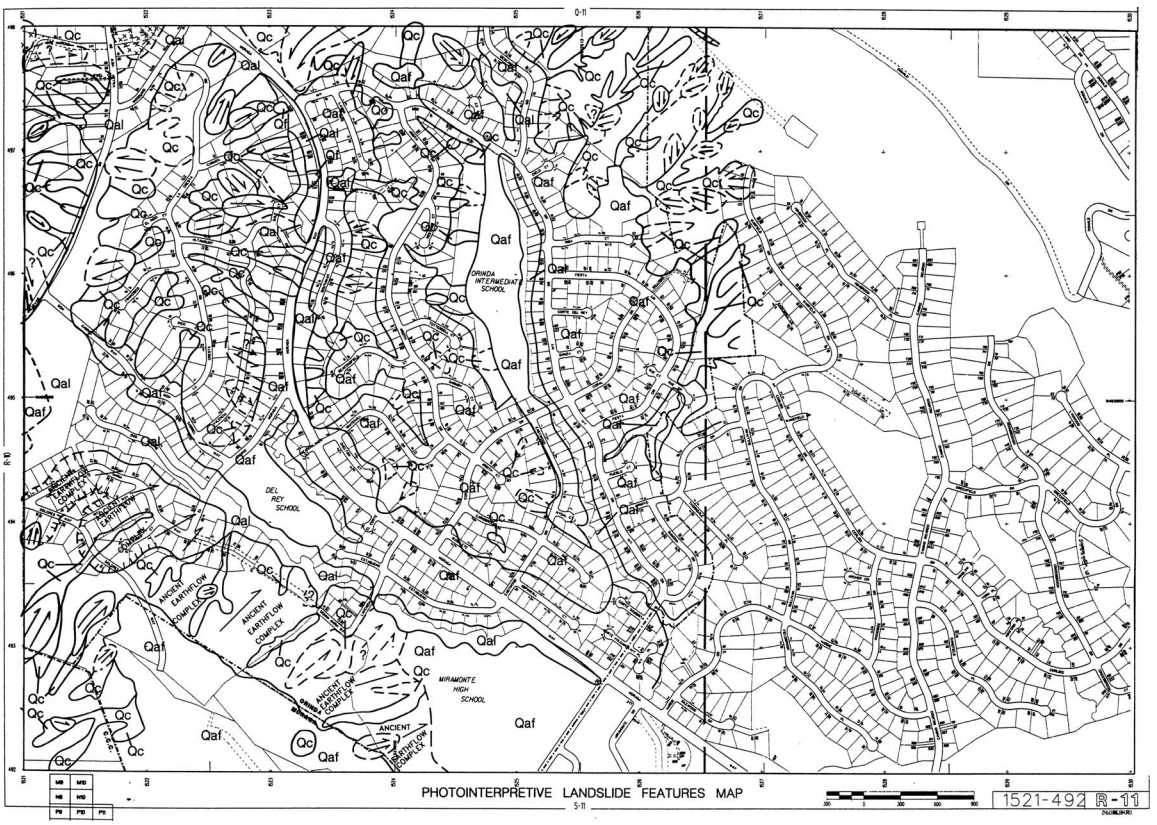

Figure A2-14. Map (black and white).

Downloaded from http://pubs.geoscienceworld.org/aeg/eeg/article-pdf/31/1/i/6130855/i1558-9161-31-1-i.pdf
by AEG RBAC user

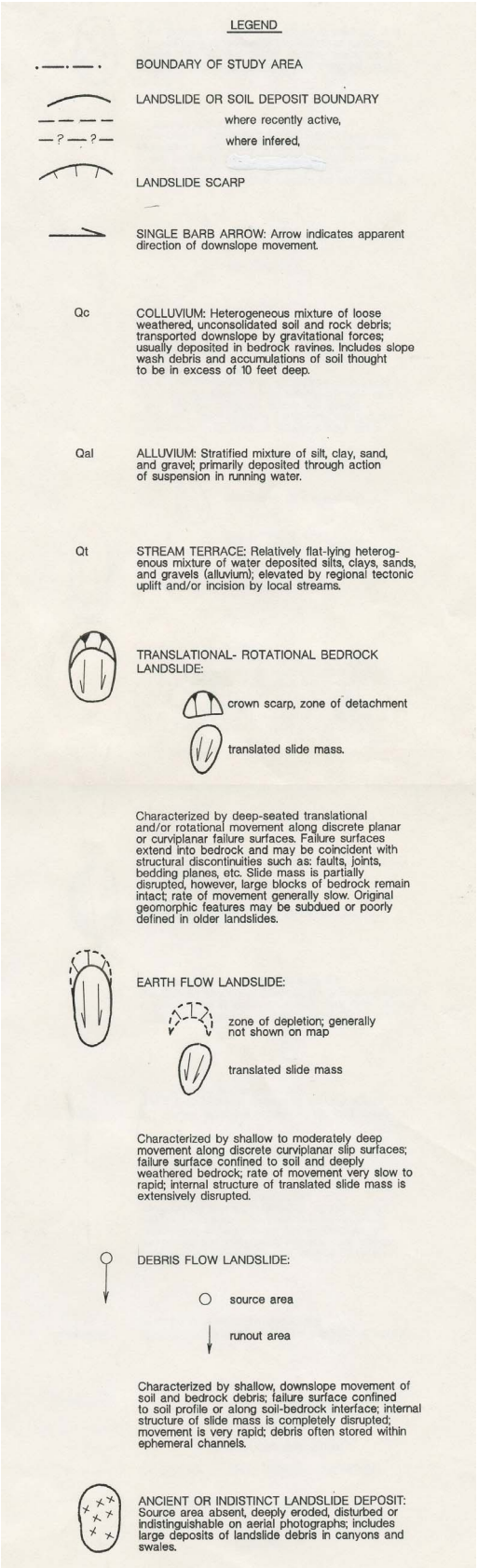

Figure A3-1. Legend of interpreted landslide features.

APPENDIX 3—LANDSLIDE HAZARD MAPPING ON ORTHOPHOTO-TOPOGRAPHIC MAPS

The orthophoto maps were photogrammetrically prepared by Hammond, Jenson, Wallen & Associates (Oakland, CA) for Rogers/Pacific, Inc. (Pleasant Hill, CA), using aerial photography dated March 8, 1991. Images of objects above ground level may be displaced. Horizontal and vertical control was based on the California Coordinate System Zone III and the National Geodetic Vertical Datum of 1929.

The information contained in these maps has been compiled from sources believed to be reliable. However, the information should not be relied upon unless the information is independently verified by the user. The authors assume no liability for the use of these maps.

Figure A3-1 presents the legend of interpreted landslide features overlain on the orthophoto-topographic maps. Figure A3-2 presents an overview of the orthophoto-topographic map tile locations.

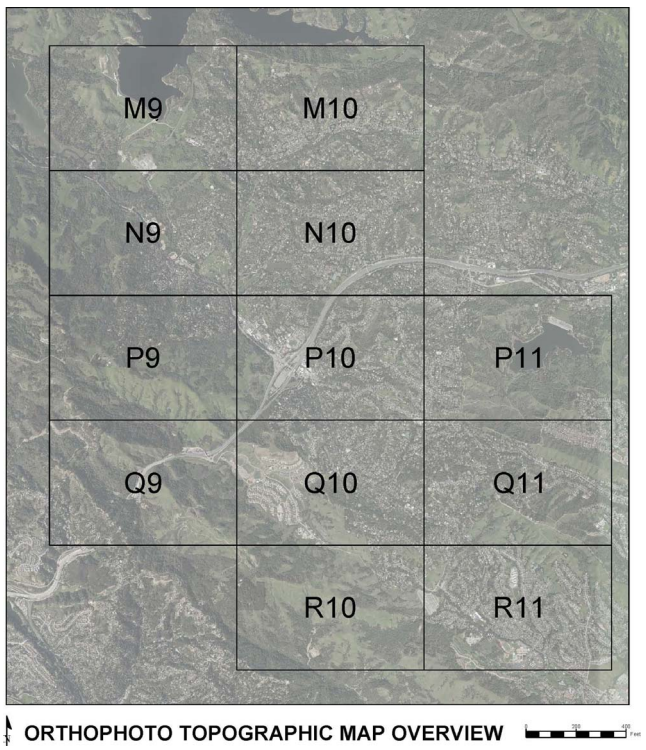

Figure A3-2. Overview map of the individual orthophoto-topographic map tiles.

Downloaded from http://pubs.geoscienceworld.org/aeg/eeg/article-pdf/31/1/i/6130855/i1558-9161-31-1-i.pdf
by AEG RBAC user

Figure A3-3.

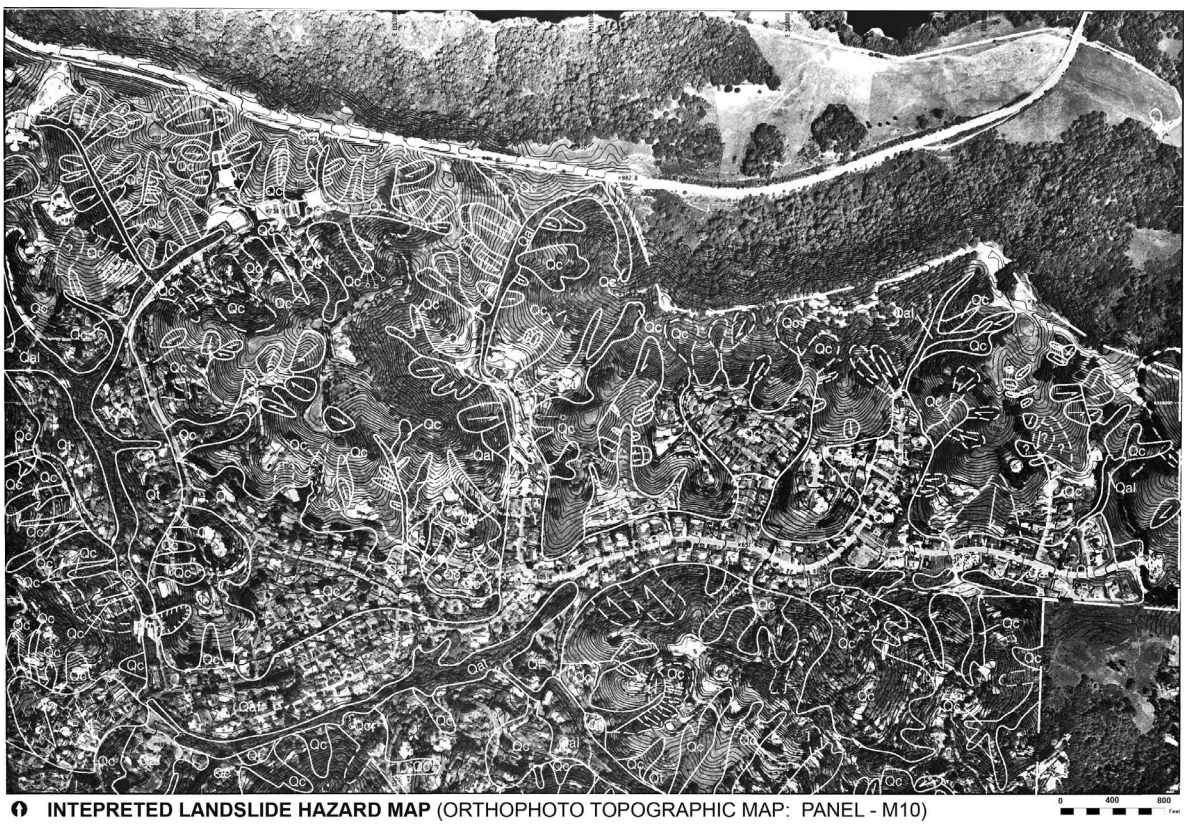

Figure A3-4.

Downloaded from http://pubs.geoscienceworld.org/aeg/eeg/article-pdf/31/1/i/6130855/i1558-9161-31-1-i.pdf
by AEG RBAC user

Figure A3-5.

Figure A3-6.

Downloaded from http://pubs.geoscienceworld.org/aeg/eeg/article-pdf/31/1/i/6130855/i1558-9161-31-1-i.pdf
by AEG RBAC user

INTEPRETED LANDSLIDE HAZARD MAP (ORTHOPHOTO TOPOGRAPHIC MAP: PANEL - P09)

0 400 800 Feet

Figure A3-7.

INTEPRETED LANDSLIDE HAZARD MAP (ORTHOPHOTO TOPOGRAPHIC MAP: PANEL - P10)

0 400 800 Feet

Figure A3-8.

Downloaded from http://pubs.geoscienceworld.org/aeg/eeg/article-pdf/31/1/i/6130855/i1558-9161-31-1-i.pdf
by AEG RBAC user

INTEPRETED LANDSLIDE HAZARD MAP (ORTHOPHOTO TOPOGRAPHIC MAP: PANEL - P11)

Figure A3-9.

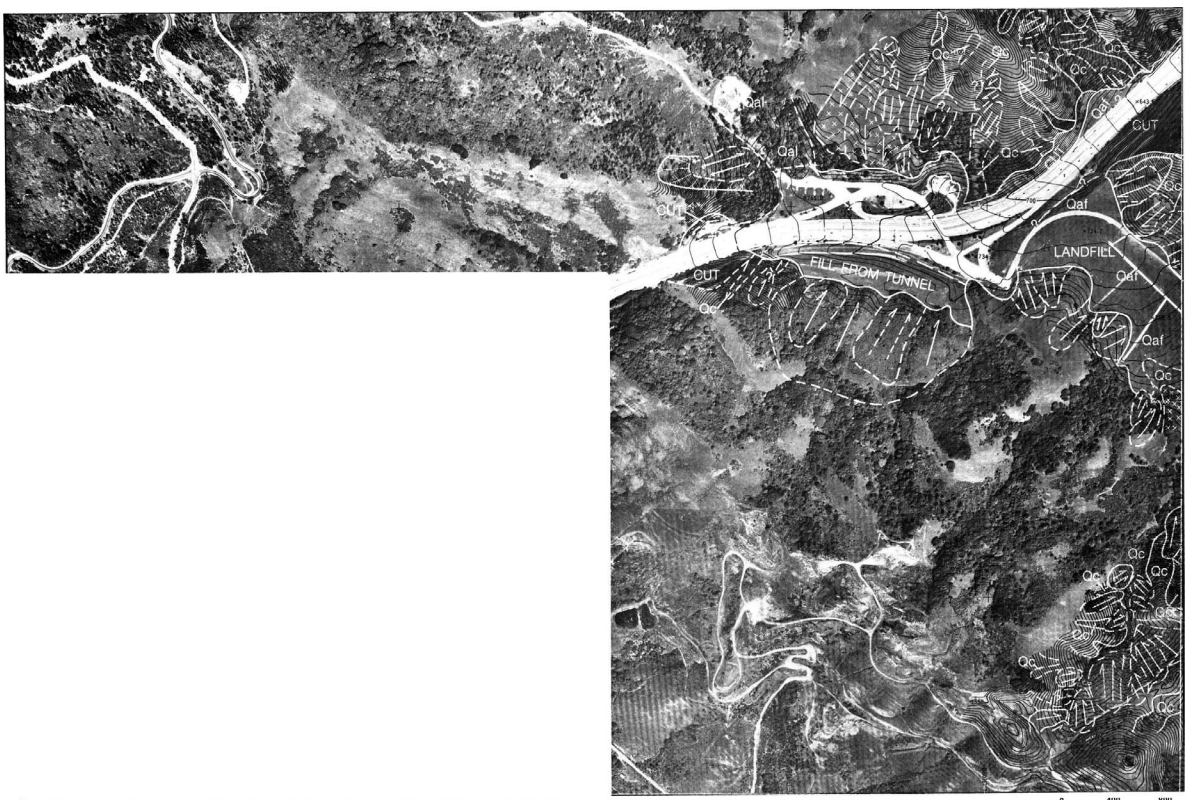

INTEPRETED LANDSLIDE HAZARD MAP (ORTHOPHOTO TOPOGRAPHIC MAP: PANEL - Q09)

Figure A3-10.

Downloaded from http://pubs.geoscienceworld.org/aeg/eeg/article-pdf/31/1/i/6130855/i1558-9161-31-1-i.pdf
by AEG RBAC user

INTEPRETED LANDSLIDE HAZARD MAP (ORTHOPHOTO TOPOGRAPHIC MAP: PANEL - Q10)

0 400 800 Feet

Figure A3-11.

INTEPRETED LANDSLIDE HAZARD MAP (ORTHOPHOTO TOPOGRAPHIC MAP: PANEL - Q11)

0 400 800 Feet

Figure A3-12.

Downloaded from http://pubs.geoscienceworld.org/aeg/eeg/article-pdf/31/1/i/6130855/i1558-9161-31-1-i.pdf
by AEG RBAC user

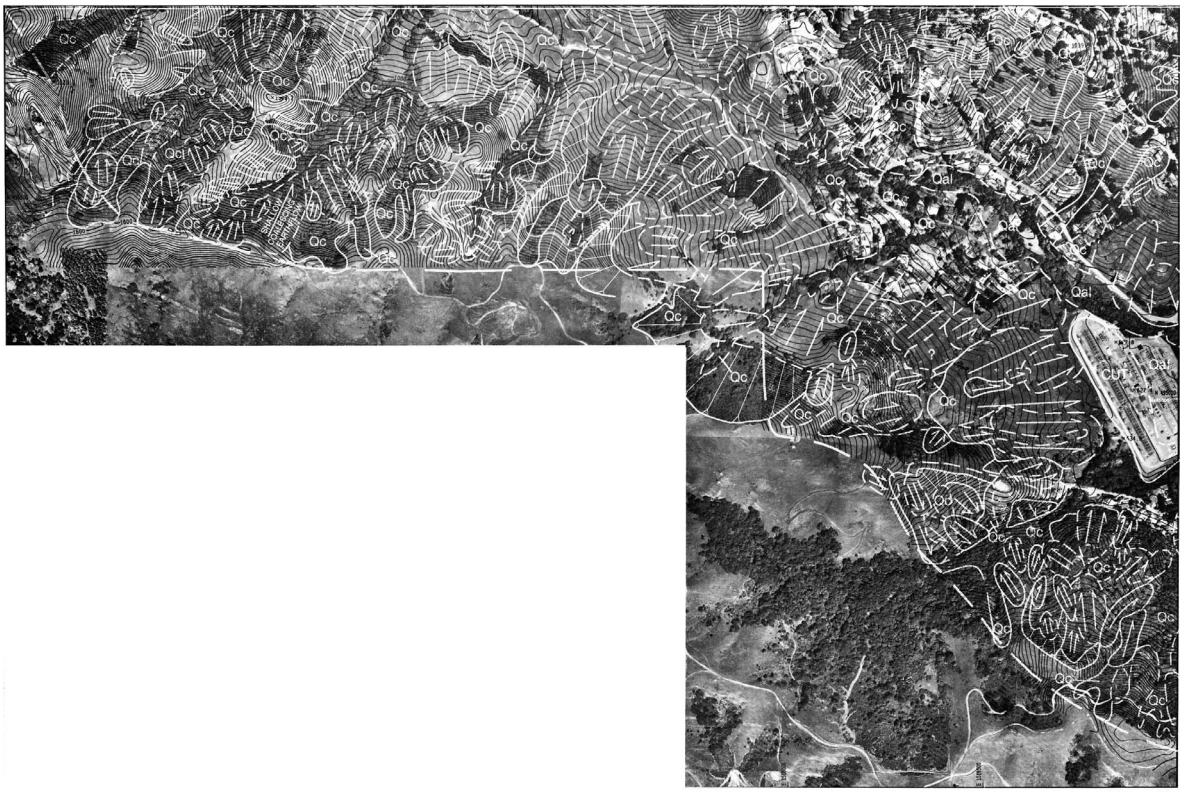

INTEPRETED LANDSLIDE HAZARD MAP (ORTHOPHOTO TOPOGRAPHIC MAP: PANEL - R10)

Figure A3-13.

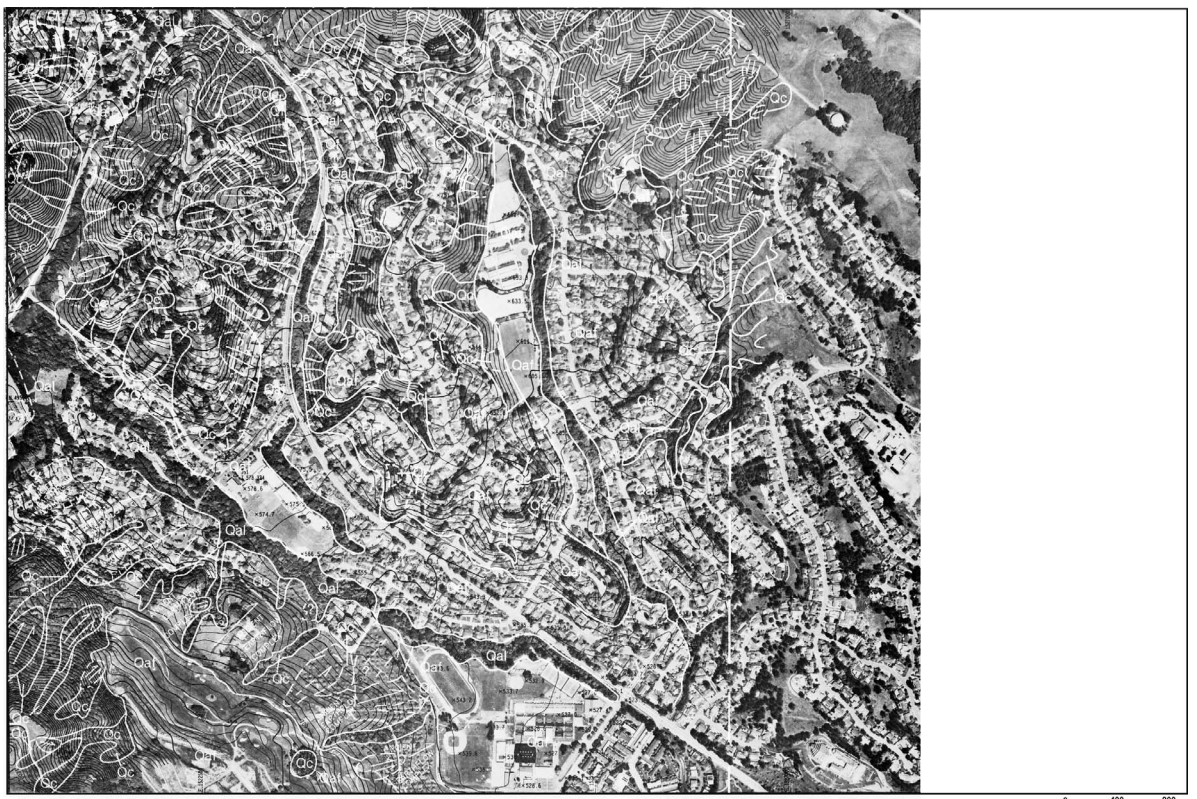

INTEPRETED LANDSLIDE HAZARD MAP (ORTHOPHOTO TOPOGRAPHIC MAP: PANEL - R11)

Figure A3-14.

Downloaded from http://pubs.geoscienceworld.org/aeg/eeg/article-pdf/31/1/i/6130855/i1558-9161-31-1-i.pdf
by AEG RBAC user

SUPPLEMENTAL MATERIAL—PRECIPITATION DATA

Precipitation analyses were based on data presented by the PRISM Climate Group, part of the Northwest Alliance for Computational Science and Engineering.[5] The PRISM Climate Group gathers climate observations from a wide range of monitoring networks, applies sophisticated quality-control measures, and develops spatial climate data sets to reveal short- and long-term climate patterns. The resulting data sets incorporate a variety of modeling techniques and are available at multiple spatial/temporal resolutions, covering the period from 1895 to the present.

PRISM offers an interactive tool for analyzing time-series data for a single location.[6] The user specifies the location by entering either the State & County or geographic coordinates. Next, the desired data return types are checked (precipitation). Next, the data type is selected (30-year normal, annual values, single month values, monthly values over a range, or daily values). The units for the output data are then specified (English or SI). The user then "retrieves" the time series, from which a download can then be initiated.

The monthly values were downloaded from PRISM for the period 1895 (January) to 2020 (December). The running 1-month, 3-month, 6-month, 12-month, 18-month, 24-month, 36-month, 48-month, and 60-month cumulative precipitation amounts were calculated by summing the monthly totals over the running average period.

[5] Website: https://prism.oregonstate.edu/

[6] Website: https://prism.oregonstate.edu/explorer/

AUTHOR BIOGRAPHIES

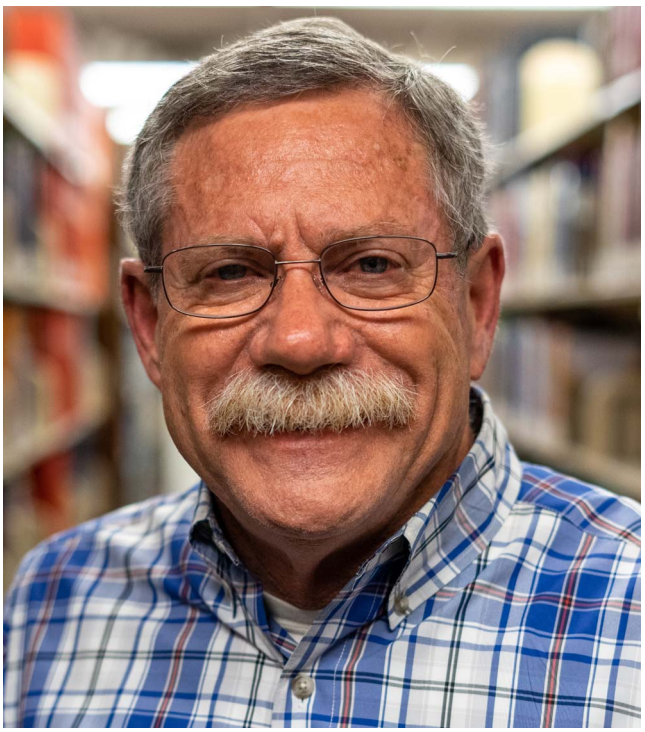

J. David Rogers is a professor and the Karl F. Hasselmann Chair in Geological Engineering at the Missouri University of Science & Technology. Rogers received his B.S. degree in geology from California State Polytechnic University at Pomona (1976), his M.S. degree in civil engineering (1979), and Ph.D. degree (1982) in geological and geotechnical engineering from the University of California at Berkeley. From 1984 to 2001, he founded consulting firms with offices in northern and southern California and Hawaii. From 1994 to 2001, he served as a lecturer at the University of California at Berkeley. He taught undergraduate courses in engineering geology and a graduate course in environmental geology for planners prior to accepting his current position in 2001.

His research has focused on the identification of landslide dams and catastrophic outbreak flood terraces, slope morphology of landslide features, high-tech downhole sensor systems, earthquake site response, lateral spread features, dams, levees, and flood-control systems, fluvial geomorphology, geohydrology, virtual geotechnical databases, and evolution of geotechnics in professional practice.

Rogers is most known for his work on regional landslide hazard evaluations and the recognition of prehistoric landslide dams on five continents (North America, South America, Africa, Australia, and Central and Southwestern Asia), where he has supervised landslide

Downloaded from http://pubs.geoscienceworld.org/aeg/eeg/article-pdf/31/1/i/6130855/i1558-9161-31-1-i.pdf
by AEG RBAC user

reconnaissance studies of approximately 465,000 km^2 (180,000 $miles^2$). In September 2022, Rogers received the Schuster Medal from the Canadian Geotechnical Society (CGS) and the Association of Environmental and Engineering Geologists (AEG).

Dr. Rogers is a registered civil engineer, geologist, engineering geologist, and hydrogeologist in California, as well as a Fellow of the Geological Society of America and the American Society of Civil Engineers. In 2011–13, he served on a National Academy of Engineering panel on levees and the National Flood Insurance Program: Improving Policies and Practices. In 2022, Rogers was named the Third Legacy Lecturer for the U.S. Society on Dams in recognition of his efforts in raising consciousness about landslide dams as a new potential failure mode (PFM) for dam safety review boards and expert panels to consider during scheduled safety reviews.

The first author used Orinda as a study area for his graduate research at the University of California Berkeley funded by the U.S. Geological Survey.

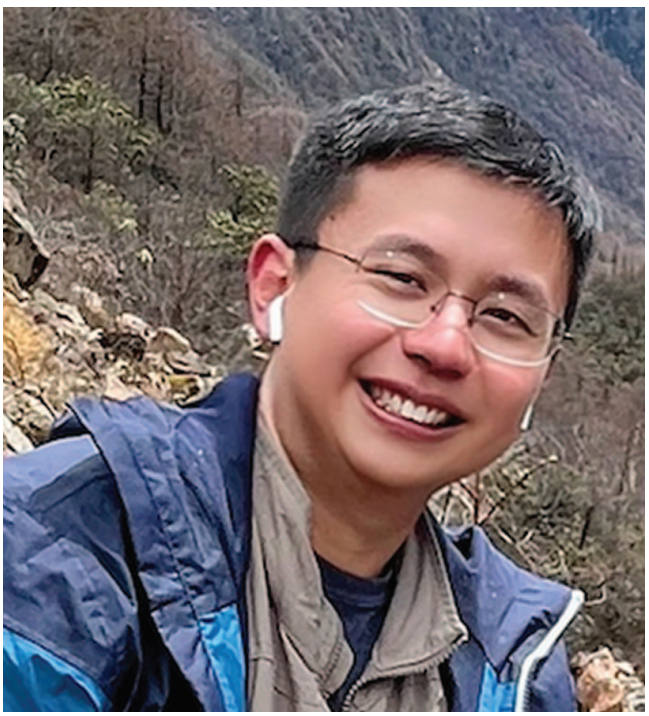

Dan Wang is an assistant professor in geological engineering at Chengdu University of Technology. His research interests are related to observational seismology, engineering geophysics, and early warning of geohazards. His most recent research has been mapping the internal structure of glaciers in the southeast Tibetan Plateau using seismic signals generated by geohazard events to provide insights on the dynamic behavior of the fluvial-glacial geohazard masses.

Dan received his B.S. degree in geology and geophysics from the Missouri University of Science and Technology (2014), his B.Eng. degree in exploration geophysics from China University of Petroleum (2014), and his Ph.D. degree in Seismology and Geophysics from the Missouri University of Science and Technology (2020). After graduation, he served as a postdoctoral scholar with Dr. J. David Rogers in the geological engineering program at Missouri University of Science and Technology studying landslide mapping techniques. In 2021, Dan accepted his current position at the Chengdu University of Technology.

The first two authors contributed equally to this book, both in the big picture overview and by detailed technical analyses of areas prone to landslides. The first author wrote in English and the second author championed the translation into Chinese, another major language of the world in an area with a lot of landslides.

Rune Storesund is a consulting geotechnical & civil engineer in the San Francisco Bay area. He provides consulting services in all aspects of civil, geotechnical, water resources, ecological, restoration, and sustainability engineering projects. His expertise is on the application of reliability and risk-based approaches to engineering projects in order to effectively manage project uncertainties. He provides expert forensic engineering services for geotechnical and civil infrastructure systems. In addition to being a consulting engineer, he is the CEO/president of Storesund Construction, Inc. (a heavy civil construction

Downloaded from http://pubs.geoscienceworld.org/aeg/eeg/article-pdf/31/1/i/6130855/i1558-9161-31-1-i.pdf
by AEG RBAC user

firm focusing on construction of water storage and water distribution systems), and CEO/president of NextGen Mapping, Inc. (a software development company designed to advance and enhance civil works data collection, analysis, and dissemination). He is an American Society of Civil Engineers Fellow and a Board-Certified Forensic Engineer through the National Academy of Forensic Engineers (NAFE).

Rune received a B.A. degree in anthropology from the University of California at Santa Cruz (2000) and a B.S. degree in civil engineering (2000) from the University of California at Berkeley. He obtained an M.S. degree in geotechnical engineering (2002) and a doctorate of engineering (D.Eng.) degree in civil engineering systems (2009), both from the University of California at Berkeley. He serves as the executive director for the Center for Catastrophic Risk Management (CCRM) at the University of California at Berkeley, where his research is focused on safe and reliable critical infrastructures. He is also CEO/president of SafeR3, a non-profit risk and crisis management education and technology development organization that disseminates state-of-the-art and innovative enterprise risk management to state-of-the-practice via pragmatic tools and education that increase safety, resilience, and reliability as well as measurable risk reduction.

The third author provided invaluable technology transfer using Geographical Information Systems (GIS) which were not known or used when this Orinda landslide study began in the 1990's.

About Missouri University of Science and Technology

Missouri University of Science and Technology (Missouri S&T) is a STEM-focused research university of over 7,000 students. Part of the four-campus University of Missouri System and located in Rolla, Missouri. Missouri S&T offers 101 degrees in 40 areas of study and is among the nation's top 10 universities for return on investment, according to Business Insider. For more information about Missouri S&T, visit www.mst.edu

Downloaded from http://pubs.geoscienceworld.org/aeg/eeg/article-pdf/31/1/i/6130855/i1558-9161-31-1-i.pdf
by AEG RBAC user